ISOTOPE AND GEOCHRONOLOGIC STUDIES OF SPELEOTHEM

PLEISTOCENE CLIMATES DETERMINED FROM STABLE ISOTOPE AND GEOCHRONOLOGIC STUDIES OF SPELEOTHEM

By

MELVYN GASCOYNE, B.A., M.Sc.

A Thesis
Submitted to the School of Graduate Studies
in Partial Fulfilment of the Requirements
for the Degree
Doctor of Philosophy

McMaster University
December 1979

DOCTOR OF PHILOSOPHY (1979)
(Geology)

McMASTER UNIVERSITY
Hamilton, Ontario

TITLE: Pleistocene Climates determined from Stable Isotope and Geochronologic Studies of Speleothem

AUTHOR: Melvyn Gascoyne, B.A. (Lancaster University, England)
M.Sc.(Lancaster University, England)

SUPERVISORS: Professor Henry P. Schwarcz and
Professor Derek C. Ford.

NUMBER OF PAGES: xxxi, 467.

ABSTRACT

Speleothems are calcium carbonate deposits, such as stalagmites, stalactites and flowstones, formed in a cave environment by loss of carbon dioxide from saturated groundwaters. Variations in the $^{18}O/^{16}O$ ratio of calcite speleothems are related to changes in depositional temperature provided that the speleothem formed in isotopic equilibrium with its seepage water (conditions characterised by slow CO_2 loss and no evaporation of seepage water). Variations in $^{18}O/^{16}O$ of the seepage water will also be reproduced in the calcite but allowance for this effect can be made if $^{18}O/^{16}O$ ratio of the source (ocean water) can be estimated (from deep sea sediment cores) and if the influence of temperature on $^{18}O/^{16}O$ ratio of precipitation at the site can be determined. Because cave temperatures closely approximate mean annual surface temperature, the axial $^{18}O/^{16}O$ record of a speleothem is therefore an indication of paleoclimate and of temperature change over the period of its growth.

The frequency distribution of age measurements for several speleothems from an area may also be used as a paleoclimatic indicator because cold or glacial conditions above the cave will inhibit speleothem growth by freezing water at the surface and removing vegetation and soil cover, the main source of CO_2 for the limestone dissolution-reprecipitation process.

Pure, non-porous calcite speleothems from several limestone regions have been dated in this study by the $^{230}Th/^{234}U$ method, and in cases of uranium-rich speleothems, by the $^{231}Pa/^{230}Th$ method also. For ten such cases examined, good agreement of ages determined by both dating methods was found.

Relatively few deposits however, have shown deposition under isotopic equilibrium conditions, due probably to the well-ventilated nature of the caves studied.

The age distribution for speleothem from Cascade Cave on Vancouver Island , B.C., indicates growth during the mid-Wisconsin interstadial dated as 65 - 30,000 yrs. B.P. Stable isotope profiles for two speleothems which grew over this period both show values of $^{18}O/^{16}O$ ratios of calcite which are significantly lower than calcite growing in the cave today. This is the first clearly-defined record of such an occurence (in previous work, $^{18}O/^{16}O$ of fossil speleothem was generally greater than modern). Using estimates of the change in $^{18}O/^{16}O$ of ocean water from a Pacific deep sea core, and the value determined by Dansgaard (1964) for the temperature dependence of $^{18}O/^{16}O$ of precipitation for oceanic sites, a realistic paleotemperature record is derived. The results indicate that temperatures at the Cascade Cave site were about 4.0°C , 64,000 yrs. ago and gradually declined to 0°C by 35,000 yrs. ago. These data are consistent with the findings of Canadian workers from ^{14}C and palynological studies of fossil organic matter in the area, and do not support the proposal by some American workers of a major glaciation occurring between 35 - 40,000 yrs. B.P.

The age distribution for 140 analyses of 82 speleothems collected from caves in north-west England show abundant deposition during the periods 130 - 90,000 yrs. B.P. and 13,000 yrs. B.P. to present, with limited growth over the periods > 350 - 170,000 yrs. B.P. and 70 - 35,000 yrs. B.P. No ages were found to lie within the periods 170 - 140,000 yrs. B.P. and 35 - 15,000 yrs. B.P. These intervals are correlated to the Wolstonian and Devensian glaciations respectively.

Only four speleothems were found to have grown in isotopic equilibrium with their seepage waters, and one of these showed periods of non-equilibrium deposition. In contrast to the Vancouver Island results, all $^{18}O/^{16}O$ ratios were found to be greater than or equal to modern, indicating that the apparent oceanic location of this site is not expressed in the value for temperature dependence of $^{18}O/^{16}O$ of precipitation.

An oxygen isotope profile for a flowstone dated between 126,000 and 109,000 yrs. B.P. shows $^{18}O/^{16}O$ ratios commencing at values slightly lower than for modern calcite, and shifting to still lower values at about 112,000 yrs. B.P. This shift may indicate a cooling event perhaps correlative with the isotope stage 5e - 5d transition seen in the deep sea core record. A profile for a flowstone over the period 290 - 190,000 yrs. B.P. shows excellent correlation to interglacial stages 9e and 7c seen in the deep sea core record, and a pronounced growth hiatus dated at about 250 - 210,000 yrs. B.P. correlates with glacial stage 8. These are the first speleothem results to show a climatic record beyond 200,000 yrs. B.P.

The differences in $^{18}O/^{16}O$ behaviour for speleothems from the two locations (N.E. Pacific and N.E. Atlantic) are interpreted in terms of their relative proximity to the ocean, potential for exchange of water vapour and 'rainout' by airmasses moving towards the cave sites, and possibility of change in meteorological conditions (principally storm track) over the periods studied.

In a subsidiary study, evidence for major sea level lowering during the Illinoian glaciation is recognised by age determinations on the calcite core of speleothems collected at 45m below present sea level from a 'blue hole' near Andros Island in the Bahamas.

The possibility of applying the $^{234}U/^{238}U$ dating method to speleothem is also investigated in this work, by the analysis of modern calcites and their seepage waters, using a new method for uranium extraction from groundwater. However the variations in $^{234}U/^{238}U$ ratios observed over short distances in the same cave demonstrate that estimation of initial fossil $^{234}U/^{238}U$ in the speleothem cannot simply be made by averaging modern ratios for the cave.

Consideration is also given to the temperature dependent distribution of trace elements in calcite, particularly magnesium and strontium. Analyses of modern calcites and waters show that Mg incorporation is strongly temperature dependent whereas Sr is not. The possibility of using Mg variations in fossil speleothem as indication of temperature change is briefly examined but the results for one sample are found to be inconclusive.

ACKNOWLEDGEMENTS

I would like to acknowledge the following people for their assistance during the development of this thesis:

Dr. Derek C.Ford and Dr. Henry P. Schwarcz who initiated speleothem research at McMaster and allowed me to come over from England to begin this work, and who have constantly offered their support and advice during it.

Ada Dixon, Jan Burns and Marija Mureika who have helped in the analytical work and injected some humour into the business.

Dr. Tony Fallick for his mastery of the problems which curse mass spectrometers ; without his early work in renovation and repair, no reliable stable isotope results would have been obtained.

Alf Latham, Tony Fallick, Chas Yonge, Fred Longstaffe and John Fish for many technical discussions, criticisms and constant friendship.

Dr. Russell Harmon who introduced me to the dating techniques used here and was a constant source of advice and enthusiasm.

Dick Glover, whose support, enthusiasm and friendship have been invaluable over the years.

Dr. Klaus Fritze of the Chemistry Department, McMaster University for advice in chemical extraction techniques, Dr. R. Brown of AECL, Chalk River, Ontario, for initial analyses of cave waters and Dr. N.J. Shackleton of Cambridge University for making available deep sea core results and helpful discussions.

I would especially like to thank the many caving friends in England, Canada and Jamaica who have either provided samples for analysis or who have helped in their collection; in order of the chapter sequence they include :

The Parks Branch, British Columbia, and Phil Whitfield, Pat Shaw and and members of VICEG for permission and help in sampling Vancouver Island caves; Alan King, Thomas Lord for permission and help in sampling Victoria Cave, Settle; Dr. John Farrer, Alf Hurworth and Bob Jarman for permission to sample Gaping Gill and Ingleborough Cave systems; Julian Barker and Mr. A.F. Bagshaw for permission to sample White Scar Cave; Danny Ellwood, Dick Glover, John Gardner, Ben Lyon and Whernside Manor cavers, and countless Lancaster University Speleological Society members for help in other Craven caves; Dr. George J. Benjamin for permission to date speleothem from the Bahama Blue Holes and his constant enthusiasm and support of the project; Alan Fincham, members of the Jamaica Caving Club and Dr. Pete Smart for help in sampling Jamaican caves; Jean Roberge, Daniel Caron, members of the Société Québecoise de Spéléologie and the people of St-Elzéar, Québec, for permission and help in sampling speleothems from La Grotte de St-Elzéar.

Jack Whorwood and Bob Bignell have helped in the preparation of photographic work in this thesis.

Finally, my sincere thanks go to Simcha Stroes for typing the final text, her insight in discussing problems related to this research and her personal support.

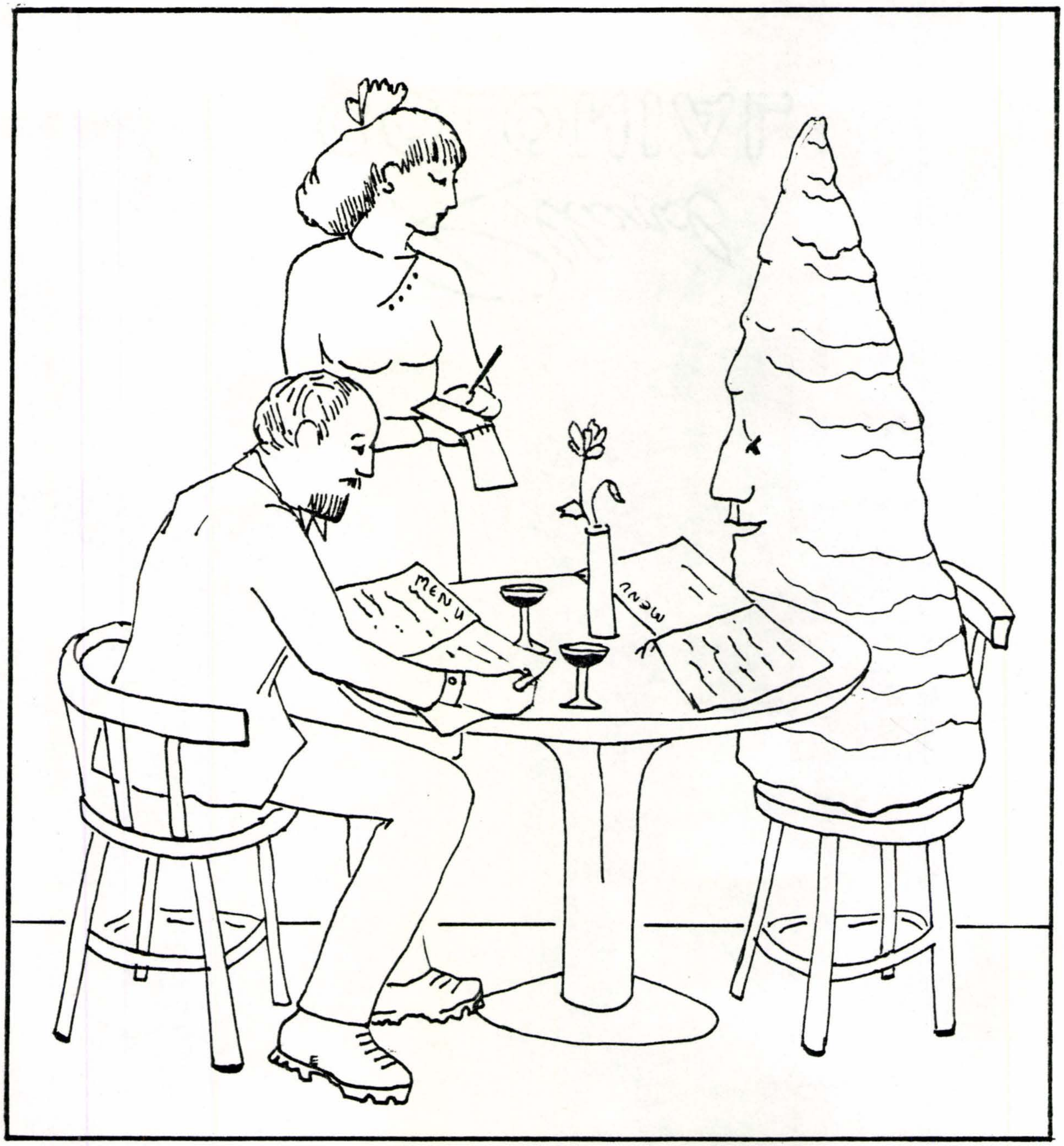

It's nice to take a break from dating stalagmites.

TABLE OF CONTENTS

Page

CHAPTER 1 THE TIME SCALE AND INTENSITY OF QUATERNARY EVENTS : GEOLOGICAL EVIDENCE AND THE ROLE OF SPELEOTHEM

CHAPTER 2 URANIUM SERIES DATING OF SPELEOTHEM

CHAPTER 3 STABLE ISOTOPE GEOCHEMISTRY OF SPELEOTHEM

CHAPTER 4 AGE DETERMINATION AND STABLE ISOTOPE ANALYSIS OF SPELEOTHEM FROM VANCOUVER ISLAND

Page

CHAPTER 6 DATING OF SPELEOTHEM FROM THE BAHAMA BLUE HOLES

CHAPTER 7 APPLICATION OF DATING AND STABLE ISOTOPE TECHNIQUES TO SPELEOTHEM FROM OTHER AREAS

Page

Page

CHAPTER 8 URANIUM ISOTOPIC DISEQUILIBRIUM IN SPELEOTHEM AND KARST GROUNDWATERS

CHAPTER 9 TRACE ELEMENT GEOCHEMISTRY OF SPELEOTHEM

CHAPTER 10 CONCLUDING REMARKS

LIST OF FIGURES

Page

Page

LIST OF TABLES

CHAPTER 1

THE TIME SCALE AND INTENSITY OF QUATERNARY EVENTS : GEOLOGICAL EVIDENCE AND THE ROLE OF SPELEOTHEM

Introduction

The most recent period of the earth's geological past is known as the Quaternary. It has been variously estimated as describing an interval ranging from the last 350 Ka (1 Ka = 1000 years) (Emiliani 1955), to 3 million years (Flint 1971) but is now thought to have begun about 1.6 to 2 million years ago (Shotton 1977, Bowen 1978). Its base is defined by the substantial faunal change in the marine succession of the Calabrian Formation in Italy, and it is a period characterised by animals and plants of predominantly modern types. It is also considered to be a period of fluctuating climate marked by several major ice advances in the northern hemisphere. The Quaternary is sub-divided into the Recent (or Holocene) epoch comprising the last 10 Ka (a warm period following the last glaciation), and the Pleistocene which corresponds to the remainder of Quaternary time. The Pleistocene is defined primarily in terms of glacial-interglacial climatic cycles (Flint 1971). Recently, glacial events have been recognised in the Pliocene period, so that now the term 'Late Cenozoic glacial ages' is considered to more correctly describe the succession of ice ages attributed to the Pleistocene (Turekian 1971).

Early studies of the Quaternary deposits of a region subdivided the period into several stages, each named according to the type locality of a characteristic geological deposit (usually a glacial till, lake or river sediment deposit). The result was the creation of a confusing array of stage names for glaciated regions, few of which could be inter-correlated satisfactorily.

Table 1.1 illustrates the present nomenclature for glacial and interglacial stages characterising the Late Quaternary deposits of N. America, Britain, N.Europe and the Alps. Inter-correlation of stages within the two most recent glacial/interglacial cycles of Europe and Britain has been proposed on biostratigraphic and thermal evidence (Mitchell et al. 1973), but correlation between these and the Alpine or N.American sequence is so far not proven.

The last twenty years has seen a fervour of activity aimed at obtaining a detailed record of Quaternary climate. An important motive has been determination of the cause of rapid changes, so that future climatic events might be predicted. This work has shown that the most consistently reliable and globally extensive results are obtained from deep sea sediment cores. A continuous paleoclimatic record extending back into the Pliocene has now been constructed from studies of deep sea cores and tested against theories and models of climatic change. Deep sea cores however, by virtue of their slow accumulation rate and environment of deposition, are difficult to date accurately and are unable to record sudden fluctuations in climate lasting 1 - 2 Ka or less. For these reasons they cannot precisely define or predict the speed and timing of continental climate change, and this is the type of change in which mankind is most interested. Alternative methods must therefore be used to

CLIMATE	N.AMERICA	ALPS	N.EUROPE	BRITAIN
Interglacial	PRESENT	HOLOCENE	HOLOCENE	FLANDRIAN
Glacial	WISCONSIN	WÜRM	WEICHSEL	DEVENSIAN
Interglacial	SANGAMON	RISS/WÜRM	EEMIAN	IPSWICHIAN
Glacial	ILLINOIAN	RISS	SAALE	WOLSTONIAN
Interglacial	YARMOUTH	MINDEL/RISS	HOLSTEIN	HOXNIAN
Glacial	KANSAN	MINDEL	ELSTER	ANGLIAN
Interglacial	AFTONIAN	GÜNZ/MINDEL	CROMER	CROMERIAN
Glacial	NEBRASKAN	GÜNZ	MENAP	BEESTONIAN

Table 1.1 Nomenclature for glacial and interglacial stages for the Late Quaternary of North America, the Alps, Northern Europe and Britain.

determine the 'fine structure' of the earth's climate. This thesis describes the application of one such method, isotopic analysis of speleothem, to determine paleoclimate changes in several maritime areas of N.America and Europe.

This chapter briefly describes other techniques used in Quaternary studies and contains a summary of ice core and deep sea core evidence. The role of speleothem in determining a continental record of climate change is then described.

1.1 Evidence of Climatic Change

Table 1.2 summarizes the types of geological feature or deposit which can give paleoclimate information. Some deposits or formations only indicate the climatic regime in which they were formed, (eg. till, submerged beaches and pollen deposits) while others are characteristic of the prevailing climate and can be dated by a radiometric or other absolute technique (eg. fossil organic matter, uplifted reef terraces). Others again can both be dated and yield information of change in absolute temperature or climate by the presence of a component in the deposit which is sensitive to such change (eg. $^{18}O/^{16}O$ ratios in deep sea cores and D/H ratios in ice cores).

Construction of a reliable paleoclimate or paleotemperature record for the Quaternary requires good preservation and continuity of the geological evidence, a factor seldom seen in most of the deposits listed in Table 1.2. However, correlation between records of the same type of formation (eg. tree rings, pollen zones) for overlapping time periods, has permitted the synthesis of several detailed paleoclimate curves.

Table 1.2 Evidence for climatic change during the Quaternary.

Type	Feature	Selected References
1) Climate-characteristic deposits	- till, fluvioglacial deposits	Flint (1971)
	- erratics, glacial striae, periglacial features, U-valleys etc.	
	- pluvial lakes (in presently arid regions)	
	- presently-submerged beaches, shorelines and caves	Heezen et al. (1959) Gascoyne et al. (1979)
	- coastal sedimentary cycles	Butzer (1975)
	- river terraces	Zeuner (1959) Clayton (1977)
	- deep sea sedimentation rate	Broecker et al. (1958) Heath et al. (1976)
	- mineralogy of deep sea sediments	Bostrom (1970) Broecker (1971)
	- faunal distributions in the terrestrial zone	Coope (1977a) Stuart (1977) Butzer and Isaacs (1975)
	- pollen record in bog and sediment cores	van der Hammen et al. (1971)
	- faunal zones in the marine foraminiferal record	Ericson et al. (1961)
	- statistical comparison of faunal assemblages, temperatures and salinities in pelagic sediments	Imbrie and Kipp (1971) Kipp (1976)
2) Datable climate-characteristic deposits	- lake sediments	Kaufman and Broecker (1965)
	- soils and paleosols	Ruhe (1965) Valentine and Dalrymple (1976)
	- loess	Kukla (1975)
	- well-preserved fauna, wood, peat etc.	Coope (1977a,b) Clague (1976)
	- archeological sites	Butzer and Isaacs (1975) Schwarcz (1979)
	- varves	Tauber (1970) Flint (1971)
	- caliche	Ku et al.(in press)
	- till (when interbedded with datable strata, e.g volcanic rocks)	Porter (1979)
3) Datable deposits containing climate- or temperature-sensitive component (eg. isotopic ratio)	- deep sea carbonate cores	Emiliani (1955, 1966,1978) Shackleton and Opdyke (1973) Ninkovitch and Shackleton (1975)
	- groundwater	Evans et al. (1978)
	- coral reef terraces	Fairbanks and Matthews (1978)
	- tree rings	Yapp and Epstein (1977)
	- ice cores	Dansgaard et al. (1969) Epstein et al. (1970)
	- speleothem	Hendy and Wilson (1968) Thompson et al. (1976) Schwarcz et al. (1976) Harmon et al. (1978a)

Nevertheless, the terrestrial records are usually incomplete and frequently disagree with one another, even for the same locality. It is also questionable to what extent the marine records can be extrapolated onto the continents because extremes of climate and rapidity of change are seldom experienced in the deep sea environment.

1.1.1 The Ice Core Record

Ice cores may help to bridge the gap between continental and marine paleoclimate records. For instance, Dansgaard et al. (1971) have shown how the upper 280m portion of the Camp Century ice core (N.Greenland) contains climatic details in the form of secular variations in $^{18}O/^{16}O$ ratio of ice for the last 800 years (Figure 1.1a). Beyond this time however, only longer period climatic oscillations are recorded (Figure 1.1b), due to molecular diffusion and thinning of ice layers. Shorter period warming events (interstadials) can be seen superimposed on the Late and Early Wisconsin glacial periods, but Dansgaard et al. have perhaps been overambitious in correlating these directly to the continental records of N.America and Europe. These interstadials may only be local phenomena and so far, insufficient precise data are available to permit intercorrelation of such events over large distances.

1.1.2 The Deep Sea Core Record

Deep sea cores contain several components and characteristics which are capable of giving a continuous paleoclimate record for all of the Quaternary (Table 1.2). They can be dated by ^{14}C and uranium series methods in their upper parts (0 - 200 Ka), by dated ash layers and faunal

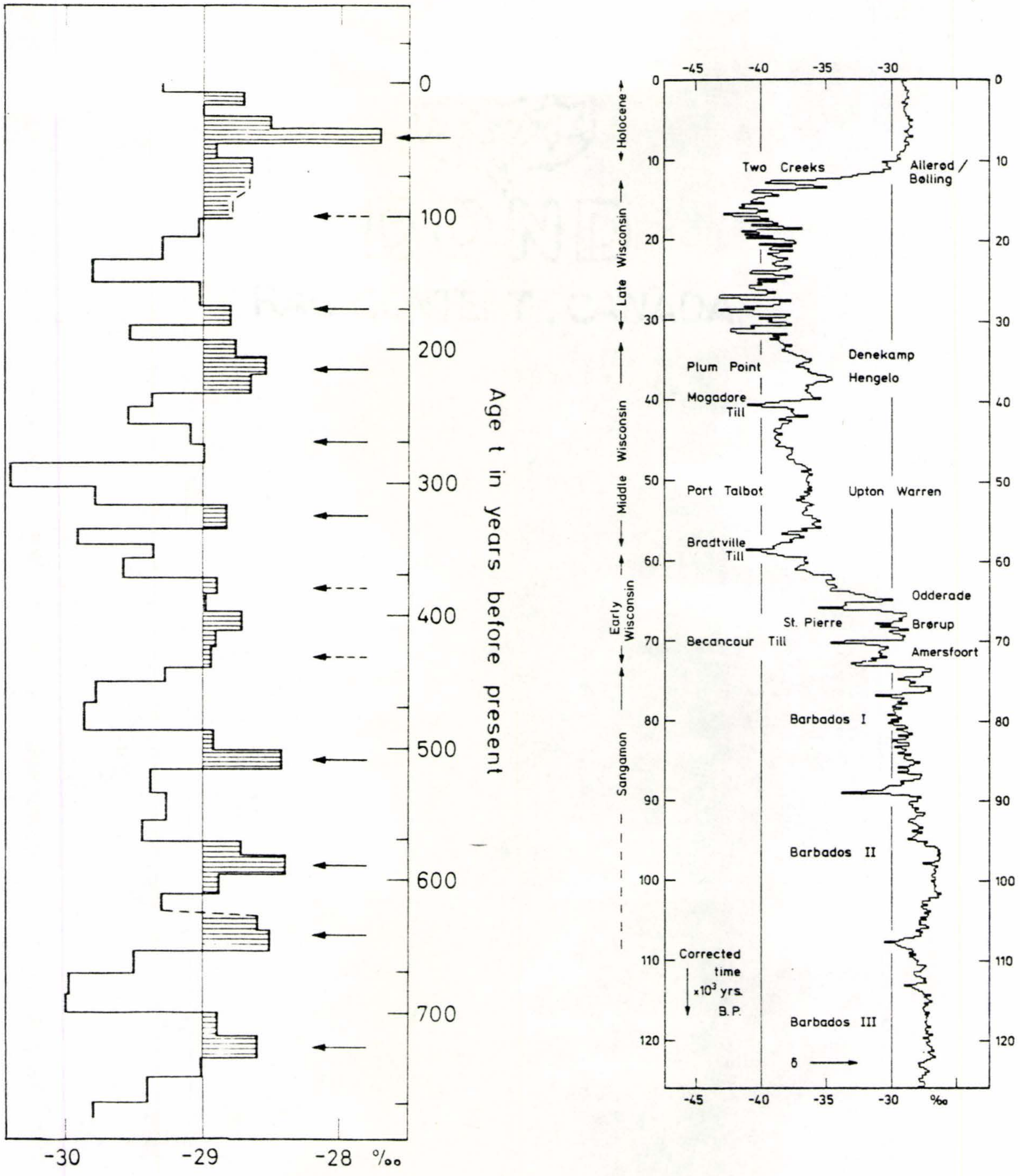

(a) (b)

Figure 1.1 a) Variations in $^{18}O/^{16}O$ ratio of the upper part of an ice core from Camp Century, Greenland, showing secular variations due to changes in recent climate (from Dansgaard et al. 1971)

b) Variations in $^{18}O/^{16}O$ ratio for the remainder of the Camp Century core showing correlation with N.American and European climatic events, (from Dansgaard et al. 1971).

For both figures, time scales are determined from the dynamics of ice flow and frequencies of climate oscillations.

extinctions in middle parts and by the presence of dated paleomagnetic reversals in their lower parts (>700 Ka). Ages of intermediate horizons are then obtained by assumption of constant sedimentation rate from a 'dated' zone. Alternatively they can be dated by correlation of stable isotopic maxima and minima (notably stage 5e of the last interglacial) to climatic events which have been dated by other means.

Shackleton and Opdyke (1973) have shown that the oxygen isotopic variation of foraminifera in deep sea cores is directly related to the oxygen isotopic composition of the oceans. The latter in turn, is a function of the amount of ice accumulated on the continents, and therefore is an indicator of eustatic sea level and global paleoclimate during the Quaternary. This interpretation is in contrast to that proposed by Emiliani (1955), wherein most of the oxygen isotope variations in deep sea cores (in the Caribbean) were attributed to a change in surface ocean temperature, with only a small change (∿20%) due to the ocean isotopic composition.

Many deep sea cores have now been analysed (Shackleton alone has studied over 60 cores) and some workers have constructed a composite core record representing changes in global ice volume and paleoclimate over the last 500 Ka or more (Hays et al. 1976; Emiliani 1978). Typical records from long cores and composite cores are shown in Figure 1.2. Prominent peaks (warm periods) are assigned odd stage numbers, and troughs (cold periods) are assigned even stage numbers as initially proposed by Emiliani (1955). Isotopic sub-stages are assigned letters (a, c, e = warm; b,d = cold) after Shackleton and Opdyke (1973). The alternative nomenclature of 'terminations' (transition from glacial to

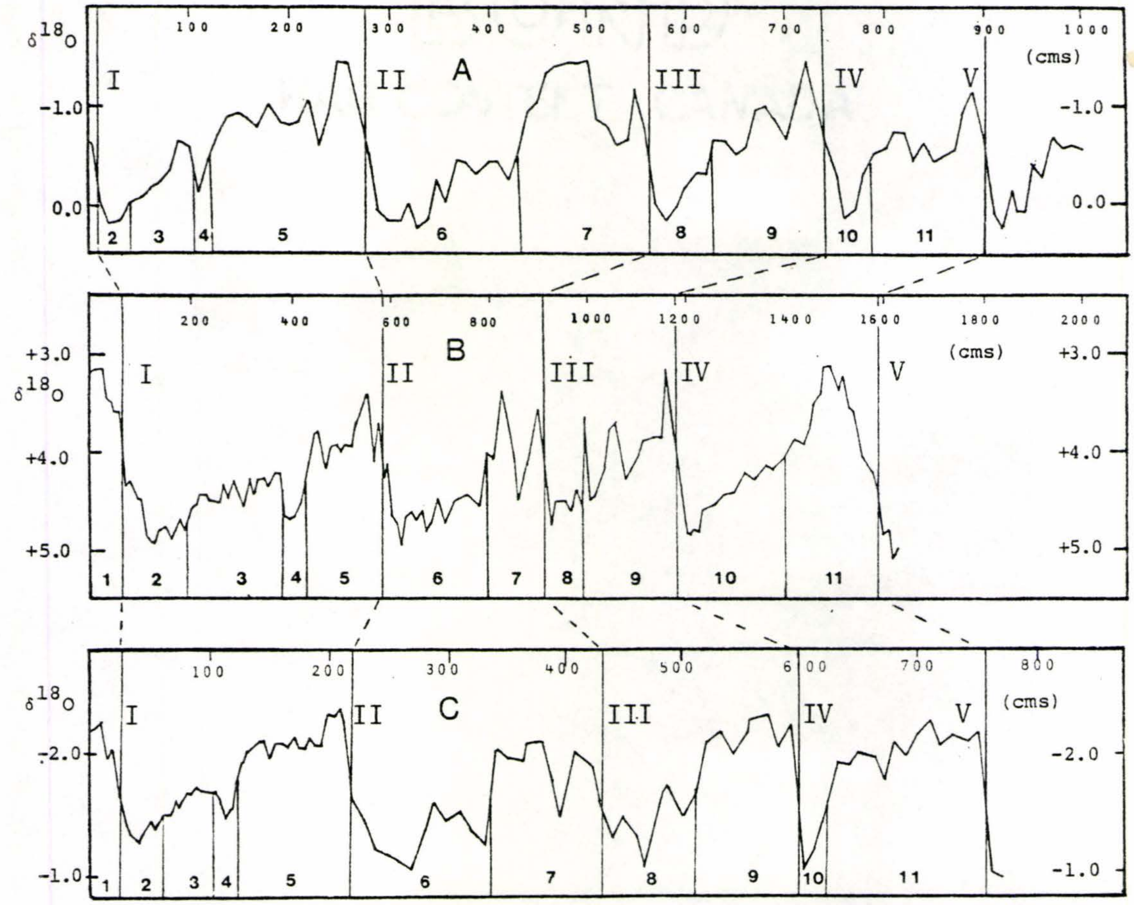

Figure 1.2 Correlation of isotopic peaks and troughs (interglacial and glacial stages) for three deep sea cores from different areas : A. P6408-9 from the Caribbean (Emiliani 1978); B. V19-28 from the eastern Pacific (Ninkovitch and Shackleton 1975); C. V28-238 from the western Pacific (Shackleton and Opdyke 1973). Good correlation between isotope stages (Arabic numerals) and terminations (vertical lines with Roman numerals) can be seen between cores.

interglacial; Broecker and van Donk 1970) is also shown. An excellent correlation of stages and isotopic detail is seen in Figure 1.2 between all cores irrespective of locality.

The study of faunal assemblages in deep sea cores has permitted both qualitative and quantitative distinction between cold and warm periods in the past. Ericson et al. (1964) have used variations in species abundance and coiling directions of foraminifera to obtain paleoclimate curves for the Pleistocene. A more quantitative approach, taken by Imbrie and Kipp (1971), is to mathematically relate present faunal assemblages and distributions, from deep sea core tops taken around the world, to the physical state of the overlying surface water (ie. temperature, salinity). Faunal variations down a core may then be interpreted in terms of paleoenvironments.

Recently, Hays et al. (1976) have combined isotopic and faunal methods in spectral analysis of the variations in a composite deep sea core of $\delta^{18}O$ of foraminifera, temperature (from statistical analysis of radiolarian assemblages) and abundance of C.davisiana (a radiolaria whose abundance is not directly temperature controlled but is a function of surface salinity and thermal gradient). Time- and frequency-domain spectra derived from these parameters has shown excellent correlation with the record of the variations in the earth's orbital geometry (obliquity, precession, eccentricity), thus indicating that changes in orbit geometry are the fundamental causes of the succession of the Quaternary ice ages.

1.2 The Role of Speleothem

1.2.1 Speleothem Deposition and Morphology

The term 'speleothem' describes any mineral deposit formed within a cave (Moore 1952), and is generally used to describe the familiar stalactites, stalagmites and flowstones which are formed when seepage waters enter a cave. A glossary of cave and speleothem-related terms is given in Table 1.3.

The solution of limestone bedrock by CO_2-rich groundwater, followed by re-precipitation as speleothems in a cave is described by the composite reaction:

$$CaCO_3 + H_2O + CO_2 \rightleftharpoons Ca^{2+} + 2HCO_3^- \qquad (1.1)$$

Several processes combine to control the growth of speleothem in a cave (Pitty 1966, Picknett 1976):

1) meteoric water containing atmospheric CO_2 enters the soil zone and dissolves more CO_2 produced by the respiration of plants and by decaying vegetation,
2) if the soil zone contains limestone fragments ($CaCO_3$) then these are dissolved concurrent to CO_2 uptake (the open system process); alternatively dissolution of the underlying limestone bedrock occurs after the water has left the soil zone so that no further CO_2 uptake is possible (the closed system process). In practice, these processes represent extremes and most systems are a mixture of open and closed dissolution mechanisms. Open system solution generally leads to

Table 1.3 Glossary of terms and abbreviations used in this thesis

aven	- a vertical extension from a cave chamber or passage, either closed at the top or leading to an upper passage.
choke	- complete blockage of a pre-existing cave passage by sediments.
duck	- a short section of cave passage containing water at or near roof level.
fissure	- a narrow vertical cave passage (usually formed entirely under vadose conditions).
flowstone	- defined in text.
karst	- now a general term describing special erosional features associated with limestone regions (originally an area of N.W.Yugoslavia).
limestone pavement	- an area with a limestone bedding plane exposed on the surface and usually weathered along joint planes.
master cave	- usually a large stream passage carrying water collected from several passages draining a large area.
phreatic	- implies cave development below the water table (in the saturated zone) such that solution takes place equally in all directions resulting in roughly circular cross-section passages, often known as phreatic 'tubes'.
pitch	- a vertical or near-vertical descent requiring artificial aids (eg. ladders or ropes).
pothole	- either a vertical pitch open to the surface or a cave system containing several pitches.
shakehole	- a surface depression in limestones and overburden caused by collapse of a cave roof.
siphon	- see sump
soda-straw	- defined in text.
stalactite	- " " "
stalagmite	- " " "
sump	- a pool of water encountered in a cave passage which has a submerged extension (also known as a siphon).
vadose	- refers to the permeable zone above a water table and implies the presence of a free water surface in a cave passage. Solution can therefore occur only laterally and downwards so that vadose passages are commonly trench-shaped.

Symbols and Abbreviations

δ = 'del' or 'delta' defined in Chapter 3

δ suffices: c = calcite, w = water, sw = sea water, p = precipitation
f = foraminifera.

‰ = 'permil' or 'per mille' (= parts per thousand)

λ = radioactive decay constant $t_{\frac{1}{2}}$ = radioactive half-life

Ka = Ka B.P. = 'kilo annum' (1000 years), before present.

higher Ca^{2+} and HCO_3^- concentrations in solution than the closed system.

3) on entering a cave containing a lower partial pressure of CO_2 than that in solution, the seepage water will lose CO_2 and calcium carbonate will precipitate either as calcite or aragonite. Aragonite speleothems are comparatively rare and are usually found only in tropical and sub-tropical environments where high temperatures induce precipitation rapid enough to form the more soluble polymorph, aragonite (Moore 1956). High concentrations of other ions in solution (eg. Mg) will also cause aragonite to precipitate preferentially (Picknett 1976).

Seepage water dripping from the cave roof deposits $CaCO_3$ around itself and gradually constructs a tubular stalactite which extends downwards with time. Slow continuous growth in this way may result in 'straw' stalactites longer than 2m. More often though, blockage of the central hole by $CaCO_3$ precipitation will divert the water flow to the outside, and the stalactite assumes a conical shape. Stalagmites are columnar deposits which grow upwards from the floor towards the drip source. Because the water splashes and flows outwards when it lands, the diameter of stalagmites is usually greater than the stalactite above and is fairly constant over its length. The size difference between a stalactite and stalagmite pair depends on the rate of calcite precipitation, drip rate, and potential for evaporation of the water droplet. Flowstones are thinly-laminated deposits formed from seepage water flowing down cave walls or along floors.

In all three types of speleothem, crystal orientation is usually perpendicular to the growth surface (Kendall and Broughton 1978). Their internal morphology is characterised by a series of growth layers which can be distinguished from one another by changes in colour, texture and impurity content. The layers have been attributed to annual deposition in some stalagmites (Broecker and Olson 1960) but Hendy (1969) has determined from ^{14}C dating that, in a speleothem from New Zealand, they each represent at least 10 Ka.

Clastic sediments such as quartz sand, clays and limestone fragments are sometimes deposited onto a growing speleothem by flood waters. They are then cemented in place by a fresh layer of calcite, once deposition resumes. Deposits formed mainly by evaporation and/or rapid outgassing of CO_2 are usually found in draughty cave passages or at the cave entrance where humidity is low. They are often porous and contain detritus distributed throughout the entire speleothem. Because of their bulk and smooth profile, flowstones are most likely to survive destructive events such as roof-collapse, invasion of sediment-bearing streams and intrusion of glacial ice and sediments.

1.2.2 Depositional Hiatuses

As described above, speleothem growth may temporarily cease due to flooding of the cave and this may be seen as a detrital horizon in the growth layers. Growth may cease or slow down for longer periods either because of local hydrological changes (re-routing of the seepage water due to blockage of the bedrock fissure or stalactite tube) or because of the influence of climate. For instance, arid conditions will reduce or stop the supply of groundwater to the cave; glacial or periglacial conditions will prevent groundwater flow due to a frozen overburden and ice blockage at the drainage outlets. Arctic conditions will also prevent speleothem growth by removing soil and vegetation cover, the main sources of CO_2 in limestone dissolution (and hence in speleothem formation by outgassing).

If deposition resumes at a later date, then the break in growth is often clearly seen either as a thin layer of detritus (from airborne dust or flood events) or as a sudden change in colour or texture of the calcite growth layers. Figure 1.3 shows examples of a stalagmite and a flowstone containing several hiatuses. In the stalagmite, all three hiatuses are clearly marked by a thin detrital horizon whereas the lower two hiatuses in the flowstone are seen only as abrupt colour changes. They are distinct from growth layer differences because crystal continuity ends at the hiatus. Without radiometric dating and stable isotope information from either side of the hiatus it is impossible to determine whether the cause of the break in growth was simply a flood event, a change in the 'plumbing', or one influenced by climate.

1.2.3 The Significance of Speleothem Growth and Paleoclimate Analysis

The presence of fossil speleothem in a cave indicates that at the time of growth, conditions were such that they permitted speleothem development, ie. perma-frost was absent and groundwater could drain freely through the cave without ponding due to ice blockage at the outlet. These inferences, together with isotopic analyses of the speleothem have the following applications:

1) speleogenetic significance: radiometric ages of speleothems stratigraphically related to cave sediments or from several levels in the cave system can indicate maximum average cut-down rates of passages,

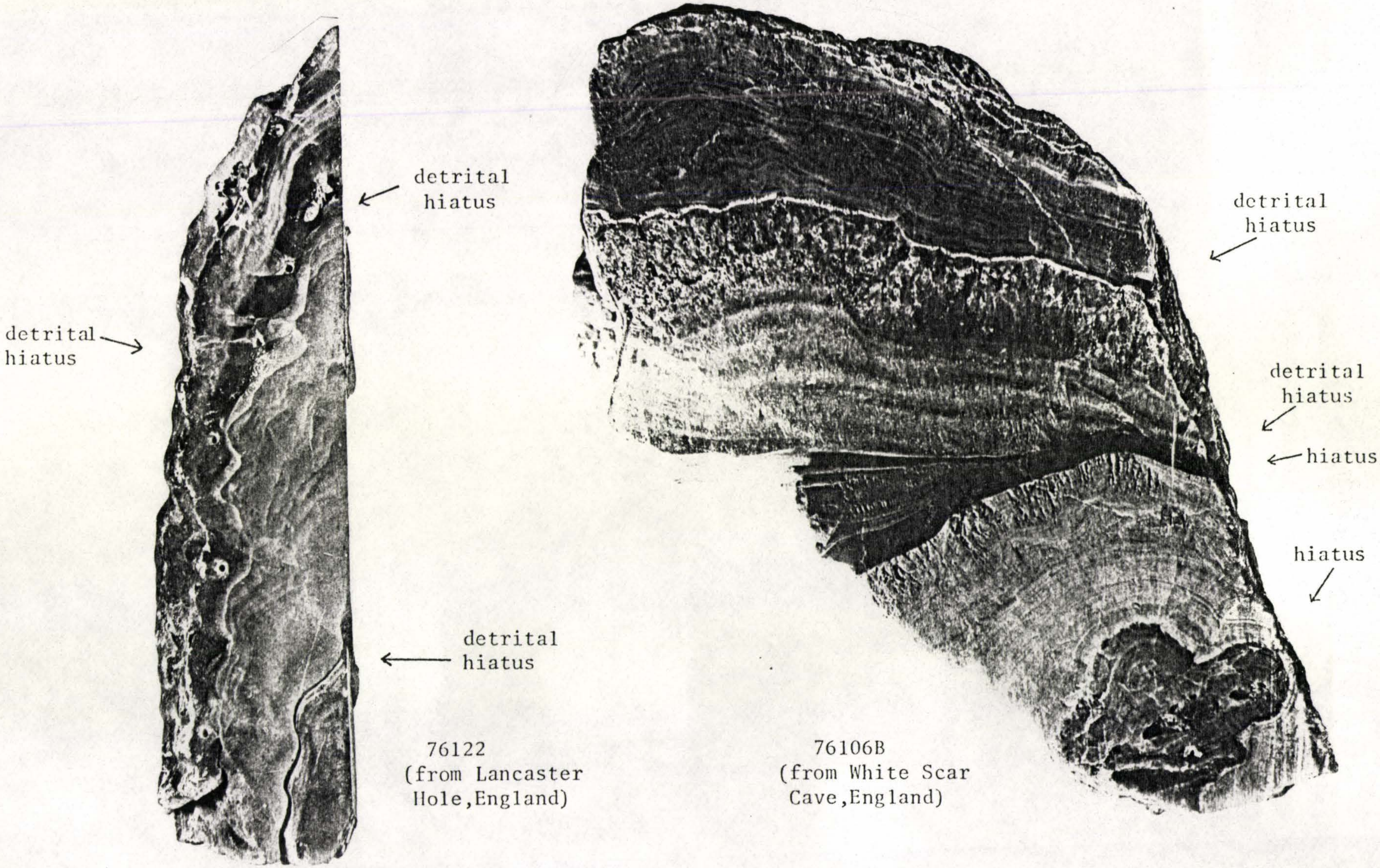

76122
(from Lancaster
Hole,England)

76106B
(from White Scar
Cave,England)

Figure 1.3 Sections through the growth layers of a stalagmite (half-section,left) and a flowstone (right) showing growth hiatuses marked either by detrital horizons or sudden colour change and crystal termination.

relative ages of levels of cave development and minimum ages of dewatering of the passage (the types of speleothem described above cannot be formed underwater).

2) geomorphic and hydrologic significance: speleothem ages may be used to determine the age of local geomorphic and hydrologic events such as the age of cave resurgence levels and localised water tables, the relation of valley floor levels to cave development, valley downcutting rates etc.

3) paleoclimate determination:

   i) from frequency of age distribution: periods of abundant speleothem growth may indicate warm conditions with good soil and vegetation cover (presently applicable to most low to mid-latitude, temperate caves); conversely, absence of speleothem growth may indicate an arid environment or glacial or periglacial conditions during that period.

   ii) from oxygen isotope ratios: variations in the $^{18}O/^{16}O$ ratio of the speleothem calcite if deposited in equilibrium with its drip water indicate changes either in temperature of deposition and/or variation in $^{18}O/^{16}O$ ratio of the water with time. There are several factors which affect the isotopic composition of the drip water, but in certain situations, as will be shown in this thesis, their effects can be estimated and the temperature variation at the site of deposition can be determined. If this is not possible then oxygen isotopic variations must be explained in terms of climate variation (ie. as a combination of changing temperature and precipitation characteristics).

   iii) from the isotopic composition of fluid inclusions: the speleothem calcite sometimes contains small amounts of fluid inclusions which are thought to be representative of the drip water at the time of deposition (Schwarcz et al. 1976). For a speleothem in isotopic equilibrium the difference in isotopic composition between these inclusions and the surrounding calcite is a function of temperature alone.

Speleothems can be used in two other ways as indicators of paleoclimate. Carbon isotopic composition in speleothem calcite is in part a function of the presence and type of vegetation growing above the cave. A change in climate may introduce vegetation with a different carbon isotopic composition which would in turn alter that of the speleothem below. However, the carbon isotopic composition of speleothem is also a function of dissolution-precipitation processes occurring in the system before speleothem formation occurs (Wigley et al. 1978) and the kinetics of isotopic equilibration in solution and isotopic exchange with cave atmosphere CO_2 during speleothem formation (Hendy 1971). These mechanisms are not directly influenced by climate change.

Variations of trace element concentrations in calcite also holds potential for paleoclimate determination but the complexity of the chemical processes involved in the distribution of trace elements between drip water and calcite has so far prevented their variations to be interpreted in terms of climate or temperature change.

1.2.4 Speleothem vs. Deep Sea Cores in Paleoclimate Analysis

Speleothem has several advantages over deep sea cores in paleoclimate studies :

1) Speleothems are usually very pure, consisting entirely of $CaCO_3$; deep sea cores need to be carefully dissected and cleaned to extract the foraminiferal species of interest.
2) Cave temperature has been found to be approximately equal to mean annual surface temperature (Wigley and Brown 1976) and therefore isotopic paleotemperature records obtained from fossil speleothems should closely parallel variations in surface conditions with little distortion; far less temperature variation is experienced by the animals whose tests are found in deep sea cores because of the thermal damping effect of the ocean.
3) Because speleothems record surface temperature they are therefore a direct indicator of continental paleoclimate; the isotopic composition of animal tests in deep sea cores is mainly influenced by changes in the isotopic composition of sea water which in turn measures continental ice volume and therefore paleoclimate. Only benthonic foraminifera can be used to determine ice volume; planktonic species contain an additional temperature-related change.
4) The isotopic composition of speleothem carbonate rapidly responds to changes in mean annual surface temperature and the isotopic composition of drip water, and speleothems often grow rapidly enough in some situations to permit sampling to within 10 or even 1 year growth increments; the amplitude of variation in the isotopic composition of deep sea cores, however, is attenuated by the finite time required for global mixing of ocean waters (~ 1 Ka), and by the action of burrowing animals (known as bioturbation). Speleothem is never affected by bioturbation.

5) Speleothems generally do not undergo recrystallization and effects of re-solution by unsaturated groundwater are usually confined to the surface of the speleothem; deep sea sediments however, often suffer from differential solution or complete re-solution as the planktonic debris descends into depth where seawater becomes unsaturated with respect to calcite and the higher Mg-calcites are preferentially dissolved.
6) Certain species of forams found in deep sea cores are known to exist out of isotopic equilibrium with sea water during their life cycle (Duplessy et al.1970a) and many are subject to influences of salinity, osmotic pressure and sea water density which in turn affects their isotopic compositions (Savin and Stehli 1974). These 'vital' effects are not found in speleothem because it is entirely formed by inorganic processes.

The main disadvantages of speleothem over deep sea cores are:

1) accessibility: speleothems cannot be sampled by 'remote' techniques as can deep sea cores. The most suitable speleothems are often found in the more inaccessible parts of a cave and therefore can be collected only by persons experienced in cave exploration.
2) The aesthetic value of speleothems imposes a strong conservation ethic amongst cave explorers which creates sampling problems because their age cannot be easily estimated before removal to the laboratory. Deep sea cores suffer no such limitations.
3) Similarly, prior to collection and analysis, it is not always possible to identify speleothems formed in isotopic equilibrium with their drip waters and which are therefore useful for paleoclimate analysis.

4) Speleothem growth may not occur throughout the whole year but may be a function of water and HCO_3^- supply which are seasonally controlled. A bias towards recording a seasonal temperature may therefore be found. Benthonic foraminifera in deep sea cores experience no seasonal effects and grow all year round.
5) Speleothems are deposited sporadically and several deposits may be required in order to construct a continuous paleoclimate record. Deep sea cores are usually chronologically continuous, although the core top may be lost during sampling and certain horizons may be compacted or altered.

The ability to date precisely speleothems as old as 350 Ka and obtain excellent isotopic resolution outweighs many of the above disadvantages. Previous speleothem results are reviewed where relevant in the following chapters and are compared and contrasted with the results described in this thesis in Chapter 10.

1.3 Thesis Objective

Speleothems from caves in several maritime limestone regions in N.America and N.W.Europe were collected in this study in order to compare the paleoclimates of N.E.Pacific and N.E.Atlantic environments. This thesis describes the results of dating selected speleothems by the $^{230}Th/^{234}U$ and $^{231}Pa/^{230}Th$ methods and the application of stable isotope analysis to several of the dated samples. It has not been possible to fulfil the objective described above mainly because of the lack of deposits, in both regions, which have comparable growth periods and which are suitable for isotopic analysis.

The results, instead, are interpreted in terms of their speleogenetic and geomorphic significance and implications for Quaternary chronology in the areas studied. Results on topics of related interest are also described, including the disequilibrium of uranium isotopes in groundwater and speleothem, and trace elements in speleothem and their application to paleotemperature determination.

CHAPTER 2

URANIUM SERIES DATING OF SPELEOTHEM

Introduction

Within the three decay series of the naturally-occurring, long-lived actinides, ^{238}U, ^{235}U and ^{232}Th, are several shorter-lived nuclides which can be applied to dating recent geological deposits. The three decay series are described in Figure 2.1 showing mode of decay and half-lives of intermediate nuclides.

To use any of these methods requires a knowledge of some or all of the following :

1) initial conditions; ie. the amount of radionuclide present, or its ratio relative to some other nuclide,
2) present nuclide concentrations (or more usually, radioactivities, here simply referred to as 'activities'),
3) absence of daughter product at the time of initiation, or the possibility of estimating the amount initially present,
4) the decay scheme and nuclide half-lives.

In addition, there is a general requirement of 'closed system' conditions following formation or emplacement of the deposit, ie. no migration or addition of parent, daughter and intermediate nuclides.

The methods of particular relevance to speleothem work are those which permit deposits at least one million years old to be dated.

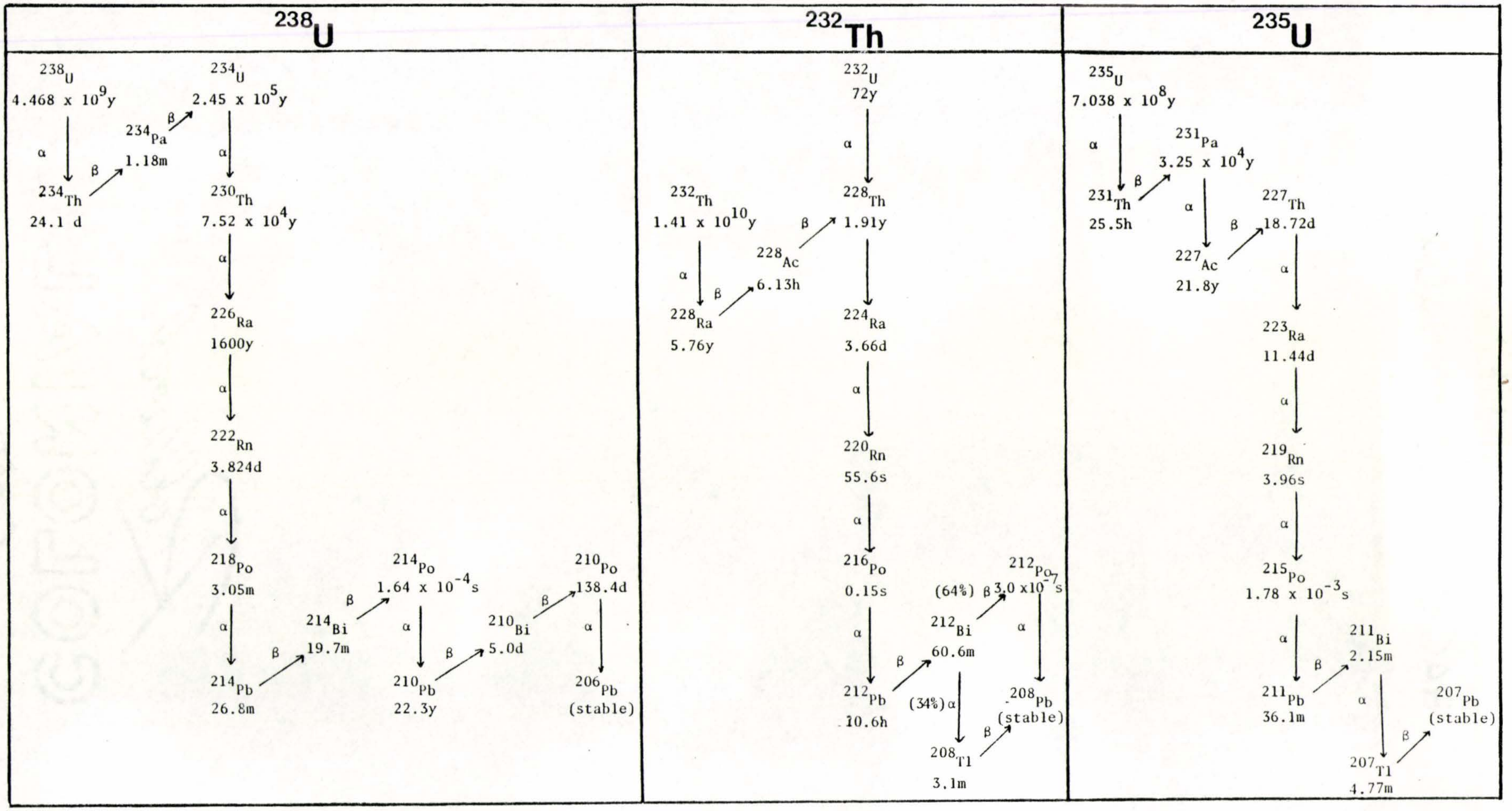

Figure 2.1 The uranium and thorium decay series (after Lederer et al. 1978, with amendments to $t_{1/2}$ ^{230}Th from Attree et al.(1962) and $t_{1/2}$ ^{231}Pa from Kirby (1961)).

The longest of the intermediate decay sequences, $^{238}U \rightarrow ^{234}U$, is best suited for this. Unfortunately, it requires precise knowledge of the initial $^{234}U/^{238}U$ ratio in the speleothem, a parameter which is not easily predicted or determined by other means, and so the method has so far found little use in speleothem work. It is discussed in more detail in Chapter 8 together with measurements of variations of this ratio in young speleothem and groundwater.

Speleothem and other carbonates have mainly been dated by techniques involving measurement of the amount of daughter nuclide, initially absent from the system, that has grown towards equilibrium with the parent nuclide. In particular, the 'ionium' method ($^{230}Th/^{234}U$) is most useful because of the large differences in the chemical properties of each nuclide. A related method, involving the ingrowth of ^{231}Pa towards equilibrium with parent ^{235}U is applicable to speleothem containing high uranium concentrations. These methods are described in the following pages, with emphasis on their application to dating speleothem.

2.1 Decay Theory

During the radioactive decay of a parent nuclide, the number of atoms of daughter nuclide (N_2) present at any time t after formation of the deposit is a function of 1) the rate of its own decay and 2) the rate of production by decay of the parent, ie. :

$$\frac{dN_2}{dt} = \lambda_1 N_1 - \lambda_2 N_2 \qquad (2.1)$$

where λ_i is the decay probability of the nuclide i.

N_1 is related to the initial concentration N_1^o by :

$$N_1 = N_1^o \, e^{-\lambda_1 t} \tag{2.2}$$

Therefore (2.1) can be rewritten as :

$$\frac{dN_2}{dt} = \lambda_1 N_1^o \, e^{-\lambda_1 t} - \lambda_2 N_2 \tag{2.3}$$

and integration gives the concentration of daughter nuclide presently remaining :

$$N_2 = \frac{\lambda_1}{\lambda_2 - \lambda_1} \, . \, N_1^o \, (e^{-\lambda_1 t} - e^{-\lambda_2 t}) + N_2^o \, e^{-\lambda_2 t} \tag{2.4}$$

The second term refers to the daughter nuclide initially present in the system, ie. co-deposited with parent. For most carbonate deposits this is found to be zero and so the term is omitted. Equation 2.4 can be rewritten in terms of the ratio of daughter to initial parent concentrations :

$$\frac{N_2}{N_1^o} = \frac{\lambda_1}{\lambda_2 - \lambda_1} \, . \, (e^{-\lambda_1 t} - e^{-\lambda_2 t}) \tag{2.5}$$

This equation forms the basis of most U-series dating applications.

It should be noted that all references to nuclides in this thesis refer to their 'activity', not concentration, eg. $^{230}Th = N_{230}\lambda_{230}$ in the above nomenclature.

2.2 The Geochemistry of Uranium and Thorium

The geochemical cycles of U and Th are very different from one another. U forms a number of soluble complexes in the natural environment, particularly with bicarbonate, phosphate and fluoride ions, so that it is easily weathered from source rocks and transported in solution. Th is from 100 to 1000 times less soluble, forms few complexes, and on weathering from a parent rock, is usually removed as an insoluble particulate rather than a dissolved ion. For these reasons, although Th is four times more abundant in crustal rocks than U, its concentration in seawater is less than 1/200 that of U (Koczy 1954). The U/Th ratio in freshwater is less well-known and may be influenced by the presence of organic complexing agents in solution. In general though, Th is almost completely excluded from groundwater owing to its very low solubility and ease of adsorption onto clays and other detrital particles. The geochemical cycle of U is more complex and is discussed in greater detail in Chapter 8. Protactinium (Pa) behaves like Th in the groundwater cycle and is also precipitated.

It is a prerequisite of speleothem dating that during the precipitation of calcite in a cave, Th and Pa are not co-precipitated with U in any appreciable quantity. Results of dating modern speleothem from N. American caves (Thompson 1973a, Harmon 1975) and English caves (this study) generally indicate that this is the case. A few results showing the presence of excess ^{228}Th in dripwater or speleothem (Thompson 1973a) and some non-zero ages for modern speleothems from Vancouver Island (Chapter 4, this study) suggest that under certain conditions Th may become mobile, possibly as an organic complex. An additional requirement is that Th or Pa are not included as particulate detrital matter in the speleothem calcite because they may then be available for leaching during the analytical procedure. This aspect is discussed in more detail later on.

The U concentration of speleothem is dependent on factors such as U content of overlying bedrock, residence time of groundwater, availability of HCO_3^- or other ligands, rate of degassing in the cave etc. For these reasons U concentration in a speleothem is likely to vary considerably both parallel to and normal to its growth direction. Variations in U concentration are found locally, from one speleothem to the next in the same cave, and regionally, between limestone formations. U concentrations are found to vary between < 0.01ppm and about 90ppm.

2.3 The $^{230}Th/^{234}U$ Dating Technique

2.3.1 Principle

This technique relies on the precipitation of small quantities of uranium in a growing speleothem, in the absence of thorium. After deposition there is a gradual increase in the concentration of ^{230}Th in the speleothem produced by radioactive decay of ^{234}U (Figure 2.1). The ratio $^{230}Th/^{234}U$ is a function of the age of the speleothem and may be determined by chemically isolating ^{230}Th and ^{234}U from each other and from the calcium carbonate, and measuring the activity of each nuclide by alpha spectrometry. An artificial tracer or 'spike' is added at the outset to permit correction of the measured activities for chemical yield.

In early studies of U series dating techniques (eg. Barnes et al. 1956) the ratio $^{230}Th/^{238}U$ was used as a dating method :

$$\frac{^{230}Th}{^{238}U} = 1 - e^{-\lambda_{230}t} \qquad (2.6)$$

with the implicit assumption that $^{234}U/^{238}U = 1.00$.
However, Cherdyntsev (1955) clearly showed that ^{234}U was seldom in radioactive equilibrium with parent ^{238}U. Equation (2.6) must therefore be modified as follows :

$$\frac{^{230}Th}{^{234}U} = \frac{1 - e^{-\lambda_{230}t}}{^{234}U/^{238}U} + \left(\frac{\lambda_{230}}{\lambda_{230} - \lambda_{234}}\right) . \left(1 - \frac{1}{^{234}U/^{238}U}\right) .$$

$$\left(1 - e^{-(\lambda_{230} - \lambda_{234})t}\right) \qquad (2.7)$$

where λ_{230} and λ_{234} are the decay constants of ^{230}Th and ^{234}U respectively. Solutions of this equation are expressed as an isochron diagram in Figure 2.2. For low ^{234}U excesses the method is restricted to an upper limit of about 300 Ka. In speleothem of high U concentration (> 2ppm) and high initial $^{234}U/^{238}U$ ratio (> 2), it is possible to resolve ages as high as 400 Ka. The limits of the technique are discussed in greater detail at the end of this chapter.

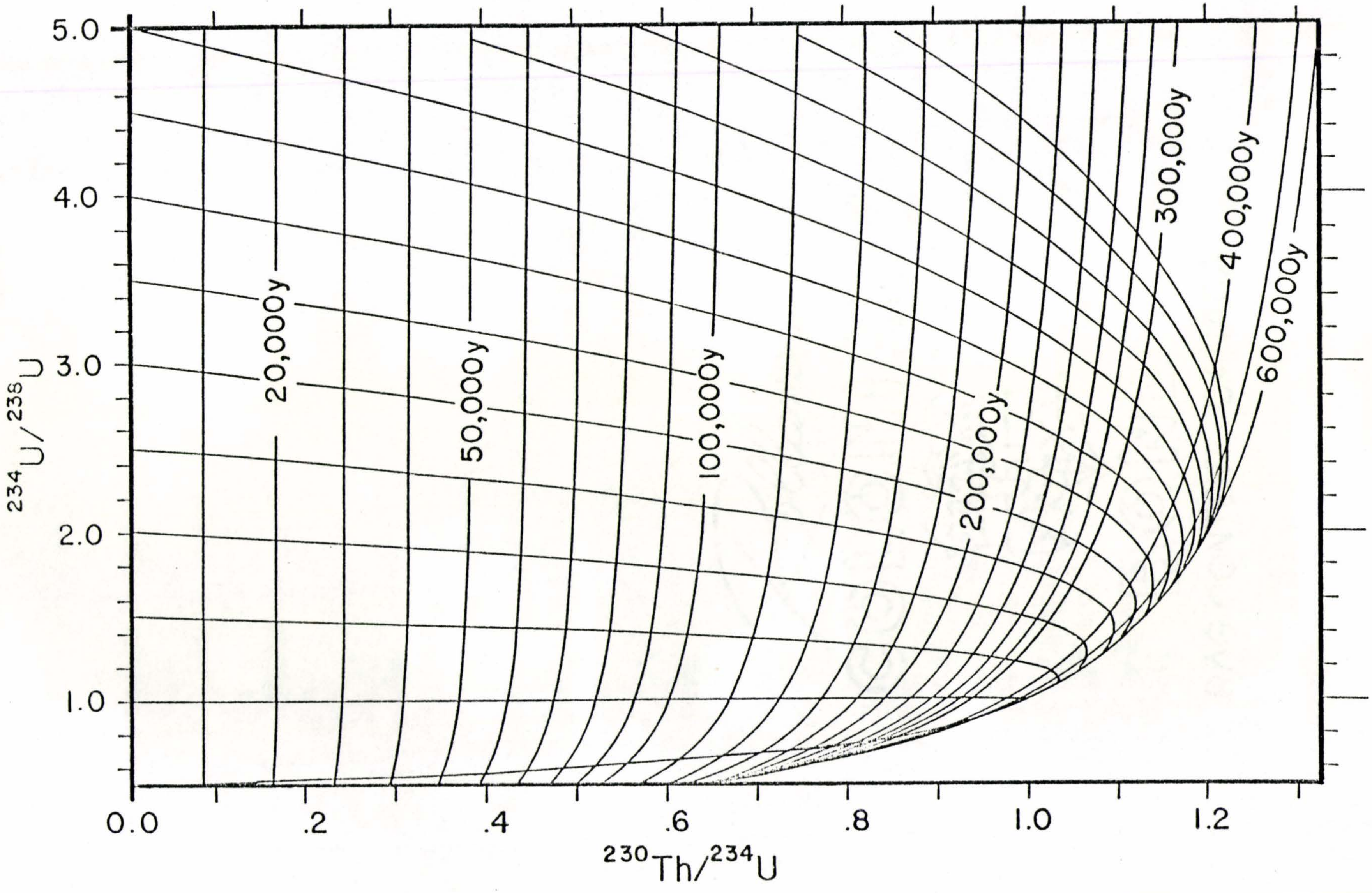

Figure 2.2 Relation between activity ratios $^{230}Th/^{234}U$ and $^{234}U/^{238}U$ for closed systems. Steeply-inclined curves are isochrons, near horizontal curves are growth curves for systems of fixed initial $^{234}U/^{238}U$ ratio, (after Schwarcz, 1979).

2.3.2 Detrital Contaminants

The dating method requires that ^{230}Th is not co-precipitated with uranium or included in detrital grains (sand or clay) during the growth of the speleothem. The presence of detritus itself does not affect the precision or accuracy of the determined age, but if Th and U are leached from it by acid during sample dissolution, then it becomes necessary to correct for the presence of authigenic and detrital ^{230}Th, ^{234}U and ^{238}U in the final spectra. The presence of detrital Th can be seen by the appearance of ^{232}Th in the Th spectrum, but the amount of accompanying ^{230}Th will differ from one sample to the next due to varying amounts of adsorbed and resistate Th in detrital minerals and the time elapsed since deposition of the surface-adsorbed Th. In the latter case ^{230}Th is unsupported and decays away with a 75 Ka half-life, such that in a closed system, the older the speleothem, the less the effect detrital ^{230}Th has on its calculated age.

Previous studies of speleothem have tended to reject ages based on analyses where measured ^{230}Th/^{232}Th ratio is < 20 (eg. Harmon et al. 1978a). Alternatively, ages have been 'corrected' for detrital Th (Thompson 1973a) assuming :

1) detrital ^{230}Th is always accompanied by ^{232}Th and vice-versa,
2) the initial ^{230}Th/^{232}Th ratio of detritus, $(^{230}\text{Th}/^{232}\text{Th})_0$, can be estimated,
3) closed-system conditions have persisted since deposition, ie. the detritus was included in the calcite only during speleothem deposition and no U or Th has entered or left since.

The last assumption is generally true for 'clean' speleothem and can be reasonably extended to cover detrital inclusions. The first and second assumptions are more tenuous; in particular the problem of determining $(^{230}\mathrm{Th}/^{232}\mathrm{Th})_o$ of the detritus and whether this is appropriate to correcting speleothem age, because differential amounts of each isotope may be leached during the dissolution of speleothem for analysis. Furthermore the possibility of leaching $^{234}\mathrm{U}$ and $^{238}\mathrm{U}$ from the detritus will also affect the calculated age, and there is no simple way to determine the magnitude of this effect.

In previous attempts to correct for detrital contamination, it has generally been assumed that preferential leaching and isotope fractionation are negligible and a correction need only be made for $^{230}\mathrm{Th}$ introduced with $^{232}\mathrm{Th}$ during the time of deposition. Three methods have been used to determine this correction :

1) comparison with $^{14}\mathrm{C}$ ages of the same samples to determine the amount of $^{230}\mathrm{Th}$ in excess of that required to give comparable $^{230}\mathrm{Th}/^{234}\mathrm{U}$ ages, (Kaufman and Broecker 1965). These workers found an initial detrital $^{230}\mathrm{Th}/^{232}\mathrm{Th}$ ratio of 1.7 best applied to the sediments of the Pleistocene Lakes Bonneville and Lahontan in the western U.S.
2) isochron plots can be used for contemporaneous samples of differing detrital content. A plot of $^{230}\mathrm{Th}/^{234}\mathrm{U}$ vs. $^{232}\mathrm{Th}/^{234}\mathrm{U}$ gives the corrected $^{230}\mathrm{Th}/^{234}\mathrm{U}$ ratio at $^{232}\mathrm{Th}/^{234}\mathrm{U} = 0$. By this means Osmond et al. (1970) found a $(^{230}\mathrm{Th}/^{232}\mathrm{Th})_o$ value of 5 for modern shells and beachrock in Florida, and Kaufman (1971) a value of 2 for lake sediments in the Dead Sea basin. Turekian and Nelson (1976) used a more simple procedure to date travertine layers in a cave by assuming that all samples have the same age and detrital $^{230}\mathrm{Th}$

activity. Plotting ^{230}Th against ^{234}U gave a straight line, the slope of which, (^{230}Th/^{234}U), was then corrected by subtraction of the ^{230}Th intercept at ^{234}U = 0. Schwarcz (1979) has suggested an improvement to this which only requires that (^{230}Th/^{232}Th)$_o$ is constant in the layers, and then he uses Turekian and Nelson's data to derive a slightly greater age for the deposit. However this age may in part be an artefact of differences in techniques used by the two workers in determining an age from the calculated ratios.

3) Ku et al. (1979) analysed carbonate and detritus content separately and corrected the carbonate age for ^{230}Th leached from the detritus, knowing its ^{230}Th/^{232}Th ratio.

Thompson (1973a) has corrected some speleothem ages for detrital Th by assuming Kaufman's initial ^{230}Th/^{232}Th ratio of 1.7.

Schwarcz (1979) has considered other aspects of detrital contamination including preferential leaching of U isotopes and has distinguished between ^{230}Th adsorbed onto detrital grains and ^{230}Th in secular equilibrium in resistate minerals. He considered model systems for partial leaching and total dissolution of a detrital phase, but concluded that without multiple analyses of the same sample, the complexity of effects prevents satisfactory correction of ages of contaminated samples.

2.3.3 Previous Work

The ^{230}Th/^{234}U dating method has been used to date many types of secondary carbonate including reef limestones, shells, caliches, lake sediments, travertines and speleothems. A comprehensive review of this and related methods has recently been given by Ku (1976). Speleothem was first investigated about ten years after its initial application to marine carbonates, by Rosholt and Antal (1962). They analysed stalagmites from European caves but found evidence of appreciable U loss resulting in excess ^{230}Th and ^{231}Pa. Cherdyntsev et al. (1965) were more fortunate in using speleothems that were not U-leached and they found good agreement between the ionium and protactinium dating methods, in spite of considerable detrital Th contamination. Fornaca-Rinaldi (1968) used the ratio ^{230}Th/^{238}U to date speleothems from Italian caves, but did not allow for ^{234}U excess in the samples, and so the ages obtained were probably too young. Duplessy et al. (1970b) obtained good stratigraphic ordering of ages for a long stalagmite from southern France. No detrital Th was detected in the inner parts of the speleothem but U concentration was generally low (0.06 to 0.12ppm). The speleothem was found to have grown from 130 to 90 Ka and a stable isotope profile for this period was also determined.

G.Thompson et al. (1975) dated a long stalagmite from a Missouri cave by ^{230}Th/^{234}U and ^{234}U/^{238}U methods and argued for accepting the latter ages as more valid. This result was strongly critisized by Harmon et al. (1978c) who re-interpreted G.Thompson's results to indicate that the ^{230}Th/^{234}U ages were more reliable. Aspects of this work are discussed in more detail in Chapter 8.

P.Thompson (1973a) and Harmon (1975) have contributed most to dating speleothem over the last decade, principally for North American caves. In general their results have shown (Harmon et al. 1975, 1977, 1978a, b; P.Thompson et al. 1976) :

1) old speleothems (> 200 Ka) have been found almost exclusively in the Canadian Rockies and the N.W.T.; areas such as north-central USA, Bermuda, Texas and Mexico appear to contain younger speleothems only.
2) U concentrations vary widely between areas (eg. 5 - 100ppm in the N.W.T., 0.02 - 1ppm in Bermuda),
3) $(^{234}U/^{238}U)_o$ ratios range from 0.8 to 2.6 and generally show little relation to either U concentration or age of sample,
4) almost all speleothems were calcite and appeared not to be recrystallized. Only one from Mexico was thought to be recrystallized, presumably from aragonite,
5) most speleothems showed correct stratigraphic ordering for measured ages and showed little detrital Th contamination and no U or Th migration.
6) periods of speleothem deposition were found to correlate quite well with known warm events in the Pleistocene (determined from deep sea cores and reef terraces). Periods of almost zero growth for northern latitude caves existed from 15 - 30 Ka, 60 - 80 Ka, 130 - 160 Ka, and 235 - 260 Ka, indicating times of cold or glacial climate. Pronounced warm events were marked by the abundance of speleothem ages about 0 - 10 Ka, 90 - 150 Ka, 185 - 235 Ka and 275 - 320 Ka.

2.4 The ^{231}Pa/^{230}Th Dating Technique

2.4.1 Principle

This technique, referred to here as the 'protactinium' method is based on the decay of ^{235}U to ^{231}Pa via a short-lived intermediate ^{231}Th (Figure 2.1). Rather than detecting the activity of ^{231}Pa by alpha counting (its α energies are multiple and lie within the ^{232}U region, and it is difficult to chemically isolate free of U and Th) it is easier to either count the β decay of its daughter ^{227}Ac or to monitor the α activity of its granddaughter ^{227}Th and assume that radioactive equilibrium exists between all intermediates and their parents. The age of the sample is given by :

$$\left(\frac{^{231}Pa}{^{235}U}\right)_t = \left(\frac{^{227}Th}{^{235}U}\right)_t = 1 - e^{-\lambda_{231}t} \qquad (2.8)$$

where λ_{231} is the decay constant of ^{231}Pa.

Used in this form, the range of the method is about 200 Ka, governed only by the half-life of ^{231}Pa (32.5 Ka). However, this equation may be combined with the fact that the $^{235}U/^{238}U$ activity ratio in the environment is a constant (1 : 21.7), and that the amount of ^{230}Th grown into equilibrium with ^{234}U is also a function of time; therefore dividing equation (2.8) by equation (2.7) gives :

$$\frac{^{231}Pa}{^{230}Th} = \frac{1-e^{-\lambda_{231}t}}{21.7(1-e^{-\lambda_{230}t}) + \{((^{234}U/^{238}U)_t - 1).(\lambda_{230}/(\lambda_{230} - \lambda_{234})).(1-e^{-(\lambda_{230}-\lambda_{234})t}\}} \qquad (2.9)$$

solutions to this age equation are shown in Figure 2.3 and it can be

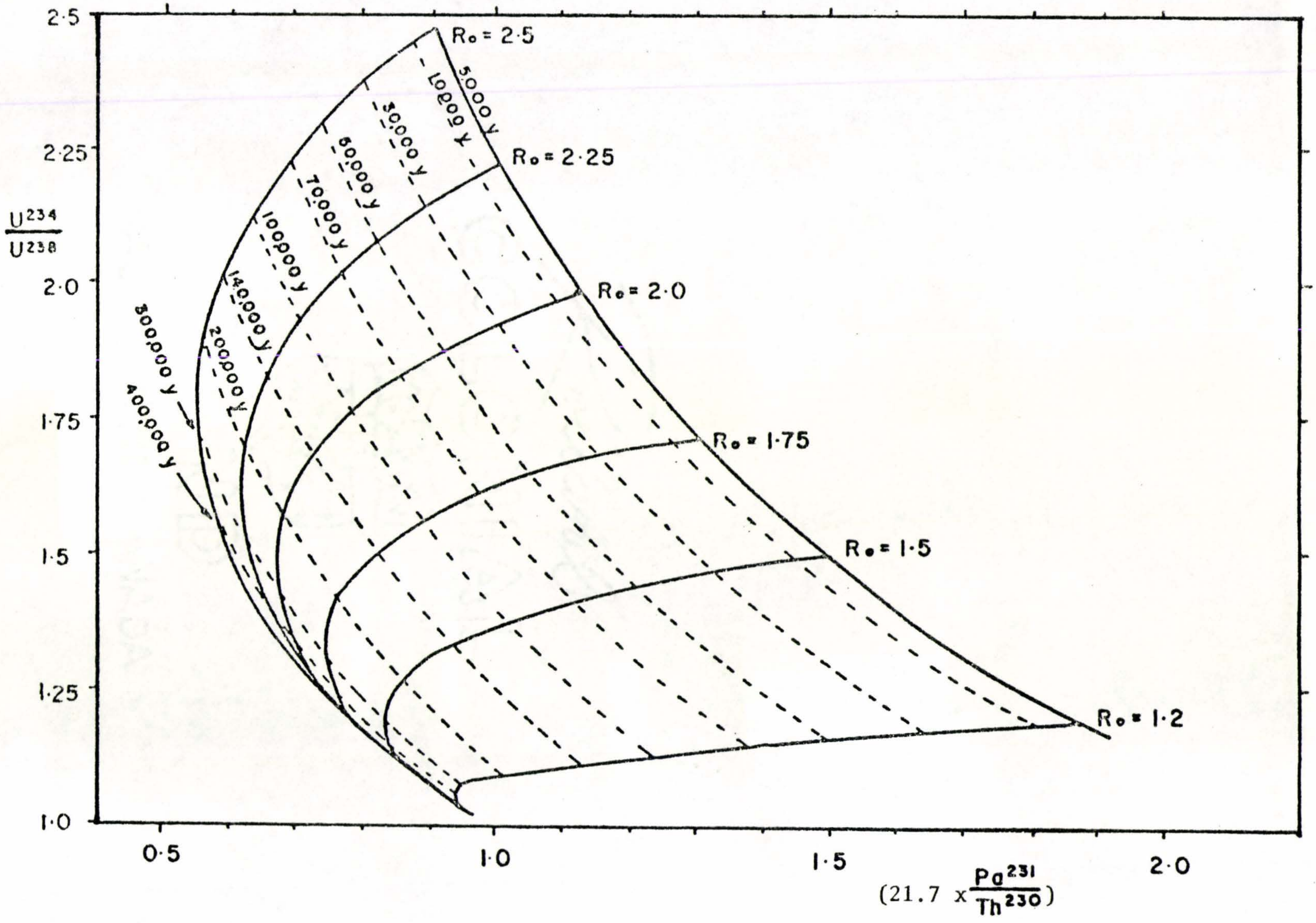

Figure 2.3 Graphical representation of the changing $^{231}Pa/^{230}Th$ ratio in a closed system. The dashed lines are isochrons, the solid lines are for systems of fixed initial $^{234}U/^{238}U$ ratio, (from Thompson 1973a).

seen that the maximum limit of resolution of the method is about 300 Ka. The advantages with this modification are that ^{227}Th activity may be compared directly to ^{230}Th in the same spectrum and therefore no spikes are needed to monitor chemical yields. Addition of a ^{232}U-^{228}Th spike only complicates the technique because daughters of ^{228}Th grow in rapidly enough to mask ^{227}Th. The assumptions and corrections that must be made are :

1) assumption of radioactive equilibrium between ^{231}Pa, ^{227}Ac and ^{227}Th, ie. strict closed-system conditions.
2) correction for decay of ^{227}Th once it becomes unsupported during chemical extraction.
3) correction of ingrowth of daughter ^{223}Ra after plating out.
4) correction for ingrowth of daughters of ^{228}Th which may be present in detritally contaminated samples or if detector background is high in this region.

These factors are discussed in greater detail towards the end of this chapter.

2.4.2 Previous Work

The ^{231}Pa/^{235}U method, using a double spiking technique and α and β counting has been successfully applied to the dating of coral reef terraces by Ku (1968). From this study Ku found that a value of 34.3 Ka for the half-life of ^{231}Pa better fitted ionium ages in the same samples, than the original value of 32.5 Ka determined by Kirby (1961). This was further substantiated by results of dating corals and shells from the Ryukyu Islands (Komura and Sakanoue 1967) and Taiwan corals

(Konishi et al. 1968). The method has also been applied to dating terrestrial carbonates but was thought to be limited by the problem of U leaching after deposition (Rosholt and Antal 1962).

The ^{227}Th/^{230}Th method is less well known than the ^{231}Pa/^{235}U method, but has been used to date cave travertines (Cherdyntsev et al.1965), molluscs (Rosholt 1967), and fossil corals (Moore and Somayajulu 1974) with varying success. The latter workers found good agreement between ionium and protactinium ages but they failed to state which half-life of ^{231}Pa they used. They also did not apparently make a correction for ^{227}Th decay between separation on the anion column and plating out for counting.

In recent speleothem work, P.Thompson (1973a) used the protactinium method to date a small number of samples from caves in West Virginia and the Rockies. In general, he found good agreement with ionium dates for the same samples but observed that the method was restricted to higher U speleothems.

2.5 Analytical Techniques

The initial analytical procedure was developed by Thompson (1973a) and used by Harmon (1975) with minor modifications. It has often suffered from large or occasionally total losses of uranium and thorium. An investigation of aspects of the method was undertaken during the course of this study to determine the cause of these losses. Other aspects have also received attention, such as the determination of reagent blank, background activity levels, true spike activity ratio and correction of errors present in the data processing stage.

Precision and relative accuracy of the dating method were also determined from results of replicate analyses of homogenised standards, interlaboratory calibration experiments and replicate dating of an important speleothem from an earlier study.

Results of these investigations up to June 1977 have been described by Gascoyne (1977a) and are summarized and updated in this chapter. Aspects of the ^{231}Pa/^{230}Th dating technique, developed by Thompson (1973a) are also considered here.

Figure 2.4 summarizes the method of extraction of U and Th from calcite and their separation from each other and purification by co-precipitation, ion exchange and organic solvent extraction. The method is detailed in Appendix 1a. The major changes to the method as used by Thompson and Harmon have been :

1) to reduce the volumes of solutions handled so as to keep reagent usage low, reduce extraction times etc.,
2) to change from anion to cation exchange resin in the extraction of Th, because of the apparent variability of quality of the anion resin used,
3) use of disposable stainless steel discs in the plating-out and counting procedure to reduce magnitude and variability of background activity levels,
4) attention to detail throughout the chemical procedure to maximize yields, eg. rinsing the speleothem residue and all vessel walls, especially in the latter stages of the extraction, to remove adsorbed nuclides.

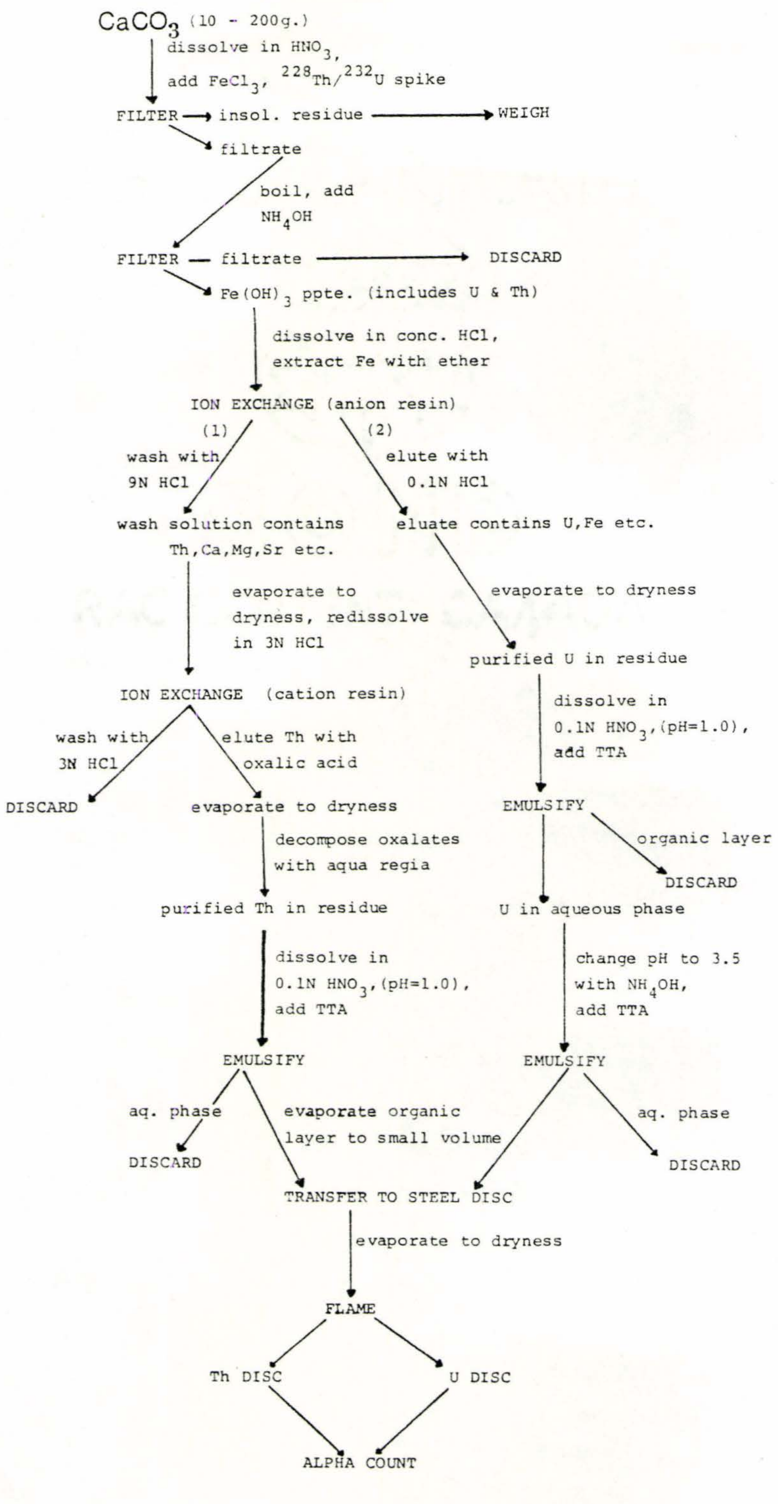

TTA = 2-thenoyltrifluoroacetone

Figure 2.4 Flow chart showing the technique of extraction and purification of uranium and thorium from speleothem (detailed in Appendix 1a).

2.5.1 Aspects of the Chemistry of the Extraction Process

2.5.1.1 Dissolution of Sample

Previous workers have used low strength HNO_3 or HCl in this process to avoid leaching U or Th from detritus present in the calcite. However, it is doubtful whether even dilute acid completely avoids this hazard (Kaufman 1964; Thompson 1973a) and instead, the alternative problem of adsorption of authigenic or spike nuclides onto detritus or glassware may occur at low acid strengths. The procedure adopted here involves adding conc. HNO_3 to the sample standing in distilled water. On filtering off insolubles, a wash of 2N HNO_3 is used at the end to remove any adsorbed and available nuclides from the residue. HNO_3 is preferred over HCl to ensure all U is present as U(VI) and can be homogenized with spike U.

2.5.1.2 Co-precipitation with $Fe(OH)_3$

This stage is one of the most critical in the method with respect to influence on chemical yield. In it, pH changes from <1 to about 8 by addition of ammonia to the boiling solution. Ferric hydroxide begins to form about pH 3.5 and rapidly flocculates in the presence of a slight excess of ammonia. U and Th co-precipitate with the $Fe(OH)_3$ along with a number of other trace elements present in the calcite.

2.5.1.3 Influence of CO_2

If not totally removed by boiling, CO_2 can interfere since it forms a soluble U complex at about pH 7. Several experiments have been run to gauge the effect of presence of CO_2 on U yield.

i) <u>Reprecipitation</u> - after filtering off the first precipitate, more $FeCl_3$ was added to the stirred filtrate causing more $Fe(OH)_3$ to form. This precipitate was then treated in the same way as the first, and subsequently plated out and counted. The results for two speleothem samples showed that about 12% of U escaped the first precipitation, but no additional Th was recovered. This could be explained by the absorption of CO_2 by the solution after precipitation which then dissolved some U, or, by failure to remove all CO_2 when boiling.

ii) <u>CO_2 absorbed after precipitation</u> - allowing the hot solution to stand open to the air after precipitation may permit CO_2 absorption and re-solution of precipitated U. A cabinet was constructed to store samples after precipitation in a CO_2-free atmosphere. CO_2-free air was bled into the cabinet to maintain a slight positive pressure. Gloves in a side-wall allowed all filtration and washing of precipitates to be done in this atmosphere. Seven such experiments showed no increase in yield of either U or Th and the method was abandoned.

iii) <u>Use of new ammonia</u> - CO_2 may be introduced to the precipitate by use of ammonium hydroxide which had previously been exposed to the air (it absorbs CO_2 very rapidly). Yields were therefore compared between analyses using NH_4OH from an unopened bottle and that remaining in a partly-used bottle, (see Gascoyne 1977a). No difference was seen between the two methods. However, a similar experiment to that described in i) above in which new ammonia had been initially used, showed no further U to be scavenged by a second precipitation. An attempt to increase U yield by using CO_2-free ammonia gas also gave no measurable improvement.

iv) The 'white ring' - after precipitation, when solutions have cooled, a white ring is often seen at meniscus level around the inside of the precipitation beakers. It was found to effervesce in acid and atomic absorption analysis showed a high Ca content. No activity was seen on plating it out and counting. It is probably $CaCO_3$ formed by interaction of Ca^{2+} with CO_2 at the surface.

These results show conflicting evidence concerning the effect of CO_2 on U yields. Reference to Chapter 8 describing extraction of U from cave drip waters by co-precipitation in situ shows that U yields can still be quite acceptable even in the presence of excessive amounts of CO_2 (the large volume of water collected in these studies is of high HCO_3^- content, and cannot be boiled before precipitation to remove CO_2). Yields of between 4 and 38% were obtained from 7 such samples.

2.5.1.4 Ether Extraction

This stage of the procedure can give many problems which eventually contribute to U or Th loss, eg. incomplete extraction of iron, generation of three or more phases, variable solubility of aqueous and ethereal phases in one another, gelled organic layers, and a critical dependence on acid strength. These troubles are especially prevalent in the analysis of samples contaminated by clays and organic substances. Some useful observations are :

i) the $Fe(OH)_3$ precipitate is best dissolved in concentrated HCl

(12N) and the filter paper washed afterwards with 9N HCl, because if only 9N is used, the resulting acid strength after reaction with the precipitate may drop below 7N so that incomplete iron extraction with ether occurs.

ii) if too much conc. HCl is used, the resulting solution becomes less ionized and acid solubility in the ether rises significantly so that much of the added ether 'disappears' during the extraction, only to reappear as a separate layer during the boiling off stage. Addition of more water usually overcomes this problem.

iii) if the iron concentration in the aqueous layer is initially high, the first extraction may give three layers instead of two, the middle being deep green iron-chloride-ether compound ($Fe(Et_2O)_2Cl_4^-$, $Et = C_2H_5$). It should be discarded along with the top layer.

iv) sometimes, no matter what is done, the iron will not extract completely into the ether. In this case either the aqueous layer can be boiled to dryness, treated with aqua regia (conc. HCl/HNO_3) to remove organics and re-extracted from 9N HCl or the iron can be extracted at a later stage after elution (along with U) from the anion exchange column. Except where much iron is present, the latter is the better alternative.

Loss of U or Th into the ether layer has been checked by directly plating out and counting a small aliquot of the ethereal layer. Only a small α activity (~ 2% yield) was measured during the analysis of a U-rich speleothem. The presence of at least 3% Th was found in the ether layer in a second experiment using ^{234}Th as a β spike. Ada Dixon (pers. comm.) has found comparable results in similar experiments).

A low activity might be expected however, since Th or U would be carried by acid in the discarded ether.

2.5.1.5 Anion Extraction of U and Th

Until April 1976 Bio-Rad AG 1-X8 100-200 mesh resin was used in the extraction of both U and Th in the Cl^- and NO_3^- forms respectively. Little problem was ever experienced with U extraction but highly variable Th yields were commonly found. Selectivity coefficients for adsorption of U and Th and other trace metals, have been published by Korkisch (1969) and show that Zn^{II}, Cd^{II}, Sn^{II}, Sn^{IV} and Bi^{III} remain adsorbed on anion exchange resin at all concentrations of HCl, and many others adsorb in strong HCl; hence the possibility exists that sufficient amounts of these elements may block exchange sites on the resin causing U to pass through. Elution characteristics of U and Th for a high U speleothem sample have been determined for anion exchange resins to ascertain :

i) whether washing of the U column with 9N HCl removed any U,
ii) the relative efficiency of 9N and 12N HCl in retaining U on the resin column,
iii) the rate of washing of Th from the U column,
iv) the rate of elution of U and Th from their respective columns using 0.1N HCl,
v) whether Th was washed off the anion nitrate column by 8N HNO_3.

Results showed that :

i) U was not leached from the anion resin by either 9N or 12N HCl (up to 6 column volumes),

ii) Th was most rapidly removed from the resin by 9N HCl (about 2 column volumes),

iii) U was eluted within 2 column volumes and Th within about 4 volumes of 0.1N HCl from their respective resins and

iv) Th was not removed by the 8N HNO_3 washes from the anion column in one analysis.

Using anion exchange resin for U and Th extraction generally gave good U yields but variable Th yields, especially in early 1976. It was thought that some substance in the speleothem itself might be the cause since repeatedly low or zero Th yields were obtained for certain samples. Poor Th yields were eventually attributed to variable properties of the anion resin used in the Th purification step. Experiments using spike alone showed complete adsorption of Th by the resin, without release on elution with 0.1N HCl. A different batch number of resin however, gave good Th yields. It was concluded that the anion exchange resin was either of variable quality or suffered degradation (oxidation) in some situations but not in others. The latter would account for the sporadic nature of the Th loss. From April 1976 the cation exchange technique was used in all Th extractions, and yields improved considerably; means of 12% before and 37% after the change have been calculated for over 50 analyses (Gascoyne 1977a).

2.5.1.6 TTA Extraction of U and Th

This step, the third purification phase, further frees U and Th from radioactive daughters, calcium, magnesium and other trace elements that may still be present in the column eluates. Often iron which has not been fully removed is extracted into TTA but if present in trace quantities causes no problem or significant loss of resolution in counting. In fact, it acts as a useful indicator of the progress of the TTA extraction by its characteristic red-brown colour. A preliminary extraction at pH 1 for U samples serves to remove Th that has eluded the exchange resin stage (this can happen if the U columns are inadequately washed with 9N HCl) and to remove Pa which follows U through the extraction procedure. Kaufman (1964) examined the results of separately plating out and counting this phase on 20 samples but found no significant activity in any due to Th or Pa and so abandoned the step. In the present work, the results of counting 5 such samples showed some activity due to the small quantity of U that will extract at this pH, but none due to Th or Pa. However, Pa contamination may become significant when insufficient spike is added to match the ^{238}U (and hence ^{231}Pa) activity. In this case the ^{231}Pa will contribute appreciably to the ^{232}U signal. For this reason, and for the occasions when Th removal is incomplete, the pH 1 step has been retained in the extraction procedure.

2.5.1.7 Additional Notes

i) Th adsorption

Vycor (silica) beakers were used in the ion exchange procedures and for storage prior to counting, to reduce Th adsorption and exchange with Na on glass walls. Addition of about 100mg $LaCL_3$ to the oxalate eluate to inhibit Th adsorption onto vessel walls was not found to significantly increase yields.

ii) Electroplating

A.G.Latham has recently investigated electroplating as a means of preparing a thin source, with the added advantage that the stronger (?) metal-metal bonds so created (rather than metal-oxide bonds as in the TTA method) on the planchet, will reduce the contamination of the detector due to recoil atoms. Results so far indicate that good yields and thinner sources can be prepared in this way thus giving better resolution, but if done without prior TTA extraction, significant contamination of the spectrum by other nuclides is found, eg. Po, Pa.

2.5.1.8 Other Methods of U-Th Extraction

i) The method used by G.Thompson et al. (1973) in U and Th extraction from speleothem omits the carrier iron stage and directly isolates Th by dissolving the sample in 8N HNO_3 and passing through an anion column in nitrate form, ($^{234}U/^{238}U$ was determined by mass spectrometry). This method was tried on a number of occasions, but although it worked well on one sample, others still gave low yields (presumably due to the variable resin quality). It was also unsatisfactory because of the long time taken for the large volume of fairly syrupy acid solution to pass through the resin, and the probable degradation effects that would have occurred during this time.

ii) A variation on the above technique employing a double column procedure was used with limited success. The sample, after dissolving and spiking, was brought up to 8N with nitric acid and passed through an anion column which led into a column of TBP (tributyl phosphate) adsorbed on Fluoropak 80 (trifluorochloroethylene polymer). U extracts into the TBP and can be eluted by 0.1N HNO_3 (Huff 1965). Slow flow-through times and generally poor yields were again obtained.

iii) An alternative to the above methods was to dissolve the sample in in HCl, omit the co-precipitation step and remove U by passage through an anion column in 9N HCl followed by dilution to 3N HCl and extraction of Th on a cation column. This again suffered from the problem of handling large volumes and long passage times.

iv) The method presently in use is a compromise between the method in Figure 2.4 and (iii) above. After the co-precipitation and 9N HCl anion exchange steps, the 9N solution containing Th is diluted to 3N which will then pass fairly rapidly through a cation column, without the problems of destruction of organics and re-solution of the residue found in the original method.

2.5.2 Determination of U and Th Activities

2.5.2.1 Equipment

Three alpha spectrometers are used for pulse height analysis (PHA) of U and Th samples plated onto stainless steel discs. Thompson (1973a) has described the equipment in detail. The method involves capture and measurement of the energy of emitted α particles by a charged surface barrier detector. Pulses are then amplified, energies discriminated and stored in a memory. Visual display of the stored spectrum is available through an oscilloscope and a teletype is used for retrieval. Detectors are used in a vacuum and are set at fixed distances (about 1cm) from the sources. Poor spectrum resolution has occurred often during this study due, in part, to high temperatures in the counting room, (the detectors and pre-amplifiers operate with least noise below 25°C). A remarkable improvement in resolution has recently been obtained by enclosing the detectors, chambers and pre-amplifiers in an air-conditioned hood operating at 15°C.

2.5.2.2 Counting Procedure

A sample is generally counted either for up to 5 days or until 10,000 counts per isotope peak have been accumulated. About once a month, a blank disc is counted to determine background activity, to monitor the slowly-increasing number of recoil atoms that become embedded in the detector. Precise knowledge of this background activity is essential when low activity samples are being counted.

2.5.2.3 Data Retrieval and Processing

Before 1975 the spectrum was retrieved by teletype printout and tape readout. The tape data were then converted by two computer programs to a set of running means and totals from which the counts per isotope peak were extracted. A third program was then used to determine radiometric age. This lengthy procedure was replaced by manual summation of counts directly from the printout by desk calculator.

All counts were re-summed until a constant value was obtained and all subsequent operations were checked afterwards by a different person to minimize the possibility of human error. All ages determined in this study have been checked this way. Increased accuracy by this method is seen in the re-dating of speleothem NB 10 described later on.

i) Determination of count rates

The Th and U of a sample are generally counted on the same unit because of differences in counting efficiency and background activity levels. Interpretation of the spectra is an important but somewhat subjective step in finally determining an age. The use of a second person to check calculations and spectral interpretations as described above helps to standardize this procedure. In this study channel widths for U and Th peaks are kept approximately equal and in the same regions, so that one set of background corrections applies to both spectra. Typical U and Th spectra are shown in Figure 2.5 and printouts are given in Appendix 1b showing nuclide channel widths, count times and calculated activities. In a well-resolved spectrum, (Figure 2.5), ^{235}U is easily recognised in the ^{234}U tail region and omitted during peak integration, but in poorly resolved spectra with larger tails, it is better to include it in the ^{234}U count and then subtract 1/21.7 of the ^{238}U activity from it (the natural activity abundance ratio of ^{235}U to ^{238}U).

ii) Age Calculation

Raw count rates, current background activities, spike activity

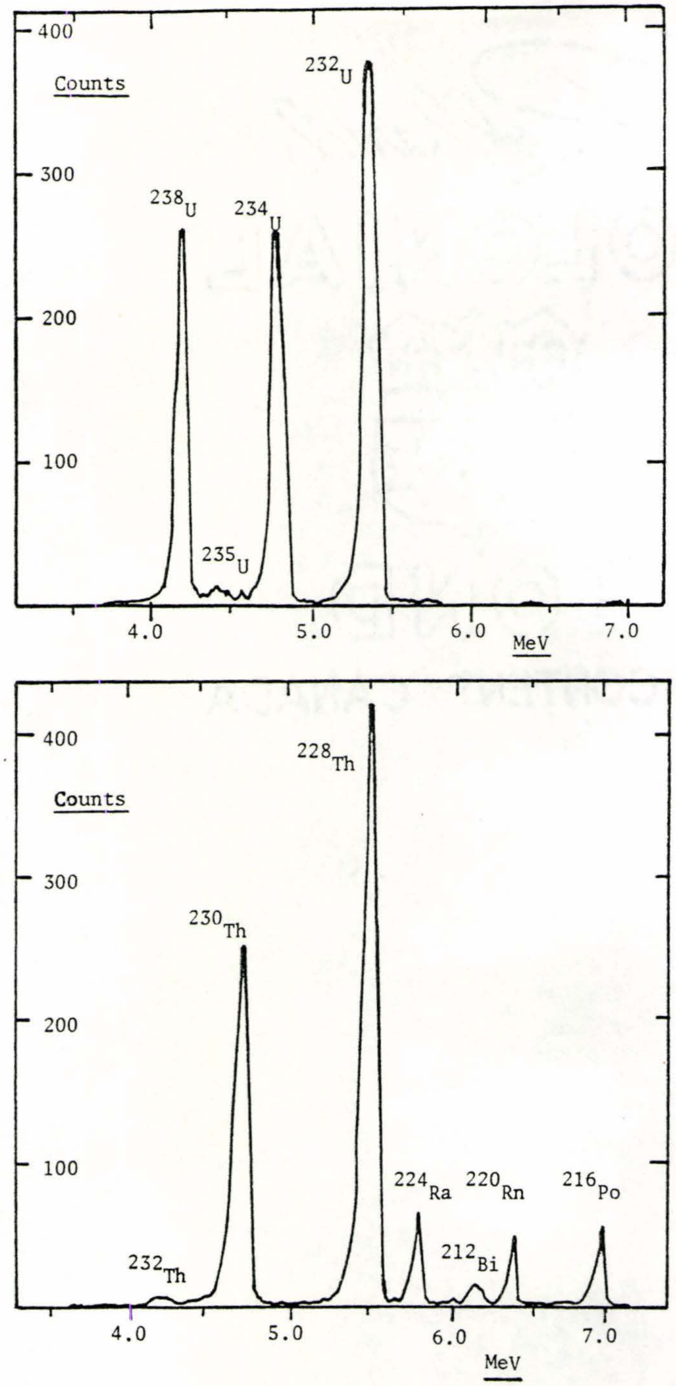

Figure 2.5 Typical uranium and thorium alpha spectra showing speleothem nuclides ^{238}U, ^{234}U ^{232}Th, ^{230}Th and spike nuclides ^{232}U, ^{228}Th and daughters (Ra, Rn etc.).

ratio, sample weight, count times and counter unit calibration factors to determine U concentration and yields are put into a dating program to obtain a radiometric age with associated 1σ error. A prior estimate of the age can be obtained by correcting the measured $^{230}Th/^{234}U$ ratio for yields thus :

$$\frac{^{230}Th}{^{234}U}(\text{true}) = \frac{^{230}Th}{^{234}U}(\text{meas.}) \times R_s \times \frac{^{232}U}{^{228}Th}(\text{meas.}) \qquad (2.10)$$

where R_s is the spike activity ratio ($^{228}Th/^{232}U$), and with the $^{234}U/^{238}U$ ratio, using the isochron plot in Figure 2.2.

The computer program to determine precise ages and error limits was written by Thompson (1973a) and has been extensively checked and modified in this work (several errors have been eliminated). The program is listed in Appendix 1c. Briefly, the routine :

1) determines corrected count rates for each nuclide, allowing where necessary for natural contamination (eg. ^{228}Th from ^{232}Th),
2) corrects ^{228}Th for ingrowth of ^{224}Ra since plating out and for decay since separation from parent ^{232}U,
3) uses equation 2.10 to determine true $^{230}Th/^{234}U$ ratio,
4) calculates sample age (t) using this ratio and the measured $^{234}U/^{238}U$ ratio by an iterative procedure using equation 2.7, its derivative and an estimated value of the age,
5) count rate errors (1σ) are determined and then used as upper and lower limits in the subroutine to find the standard deviation of the age,
6) using this age, a value for initial ratio, $(^{234}U/^{238}U)_o$, is deter-

mined by a second subroutine based on the age equation 8.1.

2.5.3 Correction Factors and Sources of Error

2.5.3.1 Background Activity

Background activity is determined by counting a 'blank disc' at regular intervals. This activity has three sources: i) natural activity from trace actinides in the vacuum housing and detector materials - this is usually negligible, ii) recoil nuclides (from previous sources) adhering to the walls of the chamber, source support and detector rim - these can all be removed by periodic cleaning with an acid solution, iii) recoil nuclides embedded in the detector surface - these can generally not be removed without damaging the detector surface. Those most likely to be present are daughters of extremely short-lived parents (high α energy) and those whose concentration in the sample has been the highest. For these reasons, spike ^{228}Th and its daughters have the highest background activity, but decay away more rapidly. There is often a significant activity in the 'parent' region (^{238}U, ^{232}Th), possibly due to ejection from the source by disintegration of a near-neighbour or contamination in dust, pump-oil vapour etc. When background activity reaches about 0.1 cpm in any one region of interest the detector is 'retired'.

Before October 1975, it was normal practice to re-use the stainless steel planchets, after first removing the old sample with emery paper. However at the start of this study, such a disc was counted to monitor background activity and its very high count rate (~ 5 cpm ^{238}U) indicated that sufficient sample from the previous analysis remained on the edges to appreciably contaminate it. Accordingly, a change to disposable discs was made and a more consistent background activity has since been found.

2.5.3.2 Reagent Blank

Thompson (1973a) showed the presence of a finite amount of U and Th in the reagents used in the extraction process. From six spiked runs he derived a mean activity level for each nuclide and then corrected for yield and included these values into the dating program ready to be subtracted from measured activities of a given sample. Harmon (1975), in apparently similar runs found a negligible reagent blank but continued using the program embodying these corrections.

Table 2.1 summarizes the results of 29 analyses of reagent blank activity over the period Nov. '75 to June '79. Of these, 18 were spiked to allow determination of RB for 100% chemical yields and 11 were unspiked to check for memory effects (nuclides from a previous analysis adsorbed onto glassware and not removed during cleaning, but available for leaching during subsequent analyses). Spiked runs prior to RB 16 were used to determine U and Th reagent blank values for inclusion in the dating program. All dates in this work incorporate these corrections and associated error limits. They are : $^{238}U = 0.016 \pm 0.007$ cpm and $^{234}U = 0.050 \pm 0.043$ cpm for 100% yield. At the time, no ^{232}Th blank was found and the significant but highly variable ^{230}Th activities were attributed to memory effect alone, reasoning that a true reagent blank would show comparable ^{232}Th and

SPIKED ANALYSES

Analysis No.	Date	U count rates (cpm) ^{238}U	^{234}U	Yield (%)	Th count rates (cpm) ^{232}Th	^{230}Th	Yield (%)	Comments
RB 1	Nov'75	-0.009	0.009	39	0.003	0.036	20	resins were re-used
2	Nov'75	0.006	0.009	40	-0.023	-0.002	18	
3	Feb'76	0.014	0.015	59	0.005	0.029	24	
4	Mar'76	0.010	0.040	31	-0.015	0.108	18	
6	Apr'76	0.019	0.010	74	0.004	0.010	44	
7	Apr'76	-0.003	0.020	42	0.002	-0.003	42	resins were re-used
11	Aug'76	0.005	0.034	32	0.017	0.015	38	acid bath in use
12	Feb'77	0.009	0.015	54	0.009	0.013	34	
15	May'77	0.007	-	46	0.020	0.033	67	large ^{232}U tail
17	Nov'77	0.009	0.030	11	0.028	0.040	23	*
18	Jan'78	0.019	0.023	41	0.039	0.015	56	
21	Jul'78	-0.001	0.005	40	0.003	-0.001	68	
22	Jul'78	0.002	-0.011	58	0.003	-0.001	39	using spec-pure acids
23	Oct'78	0.014	0.032	53	0.026	0.031	32	using residual TTA + HNO_3
26	Nov'78	-0.007	0.018	23	-0.007	-0.002	13	*
27	May'79	-0.007	-0.002	11	0.025	-0.006	49	*
28	Jun'79	0.006	0.003	24	0.009	0.049	16	*
29	Jun'79	-0.003	0.013	9	-0.007	0.060	35	
means**		0.009	0.059		0.014	0.099		

UNSPIKED ANALYSES

Analysis No.	Date	U count rates (cpm) ^{238}U	^{234}U	^{232}U	Th count rates (cpm) ^{232}Th	^{230}Th	^{228}Th	Comments
RB 5	Apr'76	0.004	0.005	0.142	0.003	0.007	0.190	resins were re-used
8	Apr'76	0.020	0.029	0.051	-0.004	-0.008	-0.004	
9	May'76	0.006	0.008	0.002	-0.001	0.027	0.027	acid bath in use
10	Aug'76	0.037	0.068	0.021	-0.004	0.031	0.038	
13	Feb'77	0.004	0.012	0.002	0.005	0.027	0.024	
14	May'77	0.000	0.000	-0.010	0.000	0.002	0.015	
16	Nov'77	0.009	0.014	-0.002	0.016	0.013	0.002	* known low U yield
19	Jan'78	0.003	-0.015	0.000	0.000	0.033	0.026	
20	Jul'78	-0.002	-0.024	0.002	-0.008	-0.004	0.051	
24	Oct'78	0.013	0.008	0.005	0.017	0.014	0.001	using residual TTA + HNO_3
25	Nov'78	-0.008	-0.007	0.009	0.000	0.005	0.008	*
means		0.008	0.009	0.020	0.002	0.013	0.034	

* analyses by B.Blackwell

** corrected for yield

Table 2.1 Summary of reagent blank determinations in spiked and unspiked analyses.

^{230}Th activities, whereas a memory effect would only show ^{230}Th activity (Gascoyne 1977a). This assumption was substantiated by the results of unspiked runs in which similar appreciable and variable activities of ^{228}Th were seen. It was therefore considered impossible to define correction factors for Th reagent blank because the amount of residual nuclides picked up from the glassware during the extraction procedure will vary between runs depending on activity of the previous sample, cleanliness and age of glassware, strength of leaching solutions and contact time.

These findings can be extended by examination of all the results in Table 2.1. It can now be seen that :

i) from the spiked runs ^{238}U activity (0.009 ± 0.034 cpm) is far less than that of ^{234}U (0.059 ± 0.074) but in the unspiked runs ^{238}U and ^{234}U levels are comparable. This could be due to the presence of ^{233}U in the spike (formed as a by-product in the neutron activation of ^{231}Pa to produce ^{232}U) whose α energy falls within the ^{234}U region. It may also be due to ^{232}U spike tail. Without counting in an extremely high resolution system it is impossible to differentiate between these effects.

ii) ^{230}Th activities show a larger variability than those of ^{234}U, due probably to greater fluctuations in memory effect.

iii) the reagent blank activities of ^{238}U and ^{232}Th in the spiked runs are comparable (0.009 and 0.014 cpm respectively) suggesting that there are small but detectable levels of U and Th in the reagents. However, negligible ^{232}Th activity is seen in the unspiked runs and so it may be concluded that U is present in small amounts but

^{232}Th is generally absent.

iv) chemical yields are often low in spite of the purity of the system. The fluctuations induced by memory effect, particularly in Th spectra are usually well above levels of activity contributed by the reagents, and therefore for this work, the reagent blank correction stated above has been retained and no Th correction has been used. The ^{234}U correction may be too large if due only to ^{232}U tail but even this becomes negligible for most cases where speleothem ^{234}U activity is between one and three orders of magnitude larger. The adjustments for reagent blank however assume great importance when young, low U speleothem is analysed (eg. post-glacial samples from Vancouver Island, see Chapter 4). Fluctuations in memory effect in particular, will easily lead to spurious results.

2.5.3.3 Spike Activity Ratio

i) 'Old Thompson Spike'

An aliquot of 10 μC of ^{232}U in 3N HCl was purchased from Amersham, England around 1968. The spike was sold as 'in equilibrium' with its daughters above ^{220}Rn but addition of distilled water to the vial by Thompson caused Th to plate out on the glass walls. Acidification partially rectified the disequilibrium but the theoretical equilibrium isotope activity ratio (R_s) could no longer be assumed. A working stock solution was prepared in October 1970, referred to here as 'old Thompson spike'. From 1974 to 1978 this solution (^{232}U activity = 145 dpm/ml) was used in this study.

Growth back into equilibrium was monitored by Thompson using a high resolution detector to separate nuclide α energy peaks. This activity ratio was calculated directly from the spike spectrum (see Thompson 1973b, Gascoyne 1977a). Harmon (1975) continued monitoring growth using this method, and found it to be essentially attained by 1974 with $R_s = 0.99$.

For transient equilibrium between a short-lived daughter (B) and a longer-lived parent (A), the equilibrium activity ratio is given by :

$$R_{B/A} = \frac{t_{\frac{1}{2}}(A)}{t_{\frac{1}{2}}(A) - t_{\frac{1}{2}}(B)} \qquad (2.11)$$

$R_{A/B} = 1.027$ for the ^{232}U - ^{228}Th pair, not 0.99. In the present study, early attempts to determine R_s by the method of Thompson (1973b) have been unsuccessful because of poor resolution of spike peaks. Values of R_s obtained by this method ranged from 0.80 to 1.09.

More precise determinations of spike activity ratio was performed in two ways: 1) by isotope dilution analysis using U and Th standards made up from metal and metal salts, and 2) by calibration against an 'infinite age' uraninite (ie. $^{230}Th/^{234}U$ ratio = 1.000) supplied by J.N.Rosholt. The former method is fully described in Gascoyne (1977a) and was found to give ratios near the true equilibrium value but with a high standard deviation. The uraninite technique, also described in Gascoyne (1977a), was used to calibrate the old Thompson spike in 6 determinations (Table 2.2). Results show a mean R_s of about

Date	Analysis No.	Uraninite Standard Used		$R_s \pm 1\sigma$
pre-July '78	SC 1	1		0.975 ± 0.021
"	2	1		0.996 ± 0.017
"	3	2		0.977 ± 0.016
"	4	2		1.004 ± 0.021
"	5	1		0.997 ± 0.017
"	6	2		0.981 ± 0.013
			mean	0.988 ± 0.012 (1s)
July '78	SC 7	2		0.963 ± 0.010
"	9	2		0.941 ± 0.014
"	10	1		0.950 ± 0.010
"				
			mean ∿	0.95
post-July '78*	SC 11	2		1.0415 ± 0.007
"	12	1		1.019 ± 0.010 **
"	13	2		1.0465 ± 0.017
"	14	1		0.980 ± 0.012 **
"	18	3		1.034 ± 0.013
"	19	3		1.0195 ± 0.016
"	20	1		1.036 ± 0.015
"	21	1		1.007 ± 0.019
"	22	3		0.989 ± 0.014
			mean	1.0298 ± 0.0135 (1s)

* analyses 11 to 22 calculated using mean of $^{230}Th/^{234}U$ and $^{230}Th/^{238}U$ ratios

** not used in determining mean (see text)

1 = ∿ 0.5 g/l Uraninite prepared without HF

2 = ∿ 0.2 g/l Uraninite prepared with HF

3 = ∿ 0.1 g/l Uraninite prepared with HF by A.G.Latham

Table 2.2 Summary of spike calibration results using a uraninite in isotopic equilibrium.

0.99 ± 0.01, fortuitously in agreement with the 'equilibrium' value used by Harmon (1975).

For a short period during this study, before determining the above value precisely, the true equilibrium value of 1.027 was assumed and all speleothems were dated on this basis. However, the results of Phase I of USIP (the U-series Interlaboratory Calibration Project, described later) showed that 0.99 would give better age agreement with the other laboratories, and this was subsequently confirmed by the uraninite analyses described above. All age results were then corrected to this result.

ii) New 'Fortified' Spike

The old Thompson spike was almost completely used up by July 1978, and so a further aliquot from the vial was diluted to give approximately the same activity. However, three calibrations of this spike (Table 2.2) showed it to be more out of equilibrium than the old spike ($R_s \cong 0.95$). A 5 litre volume of a dilute version was then made up (~ 17 dpm/ml) and a calculated aliquot of this passed through an anion column to remove ^{232}U. The ^{228}Th eluate was returned to the 5 l reservoir thus 'fortifying' it to a spike ratio of 1.027, (calculations were based on the 3 analyses in Table 2.2).

This fortified spike was then re-calibrated in 9 subsequent determinations using 3 different preparations of the same uraninite powder standard. Results are shown in Table 2.2. Mean R_s for 7 of these determinations was 1.0298 ± 0.0135 (1s), very close to the equilibrium value. Two analyses were rejected from this calculation because they involved a uraninite standard which was not prepared with HF (to dissolve silicates) so that the standard contained some insoluble residue. Measurements of R_s using this standard were low (Table 2.2) and suggested that some nuclides were preferentially adsorbing with time on the residue, throwing the solution out of equilibrium. Even if these two results are included, R_s (mean) becomes 1.023 which is still within one standard deviation of the equilibrium value.

2.5.3.4 Measurement of U Concentration

In previous work (Thompson 1973a), U concentration of a speleothem was determined from the U spectrum using the equation :

$$\text{U (ppm)} = \left(\frac{^{238}\text{U}}{^{232}\text{U}}\right)_{\text{obs.}} \times \frac{B}{W} \qquad (2.12)$$

where B is the weight of ^{238}U (μg) that has an equivalent activity to the ^{232}U contained in 1ml of spike solution, and W is the weight of speleothem used (g). If greater or less then 1ml of spike was used, the numerator should have been multiplied by V_s, the volume of spike used. This practice was often overlooked during the period 1973 - 1975, giving erroneous U concentrations and many of the speleothem U concentrations given by Harmon (1975) and in Harmon et al. 1975, 1977) are too high by up to a factor of 5. B was determined by counting standard U samples and comparing them to ^{232}U activity determined from direct counting of a spike aliquot.

More precise determination of B is given by isotope dilution analysis. This technique was used by Gascoyne (1977a)and the ^{232}U activity of the old Thompson spike was found to be 144.6 ± 1.6 dpm/ml in October 1976. U concentration is therefore :

$$U(\mathrm{ppm}) = \left(\frac{^{238}\mathrm{U}}{^{232}\mathrm{U}}\right)_{\mathrm{obs.}} \times \frac{144.6 \times V_s}{W \times {}^{238}\mathrm{A}} = \left(\frac{^{238}\mathrm{U}}{^{232}\mathrm{U}}\right)_{\mathrm{obs.}} \times \frac{V_s}{W} \times 195.5 \qquad (2.13)$$

where ^{238}A is the activity of 1μg ^{238}U (= 0.73965 dpm), and the value 195.5 is exactly equivalent to the factor B. An earlier value of about 220 was determined using a less precise method in this work (Gascoyne 1977a) but this was found to be too high during comparison of the Phase I USIP results. The original value measured by Thompson (1973a) and assumed by Harmon (1975) was 136.5. The increase in apparent activity of the spike since then is probably due to partial evaporation of the spike solution, and is a further source of inaccuracy in speleothem U concentrations quoted by Harmon.

2.5.3.5 Detector Calibration and Yield Determination

The yield of ^{238}U and ^{230}Th in the extractions is given by the ratio of the observed ^{232}U and ^{228}Th activities ($A_{\mathrm{obs.}}$) to their true activities (A_{true}). The 'geometric' efficiency (E) of the detector must be known in order to make this calculation, where :

$$E = \frac{A_{\mathrm{obs.}}(\mathrm{cpm})}{A_{\mathrm{true}}(\mathrm{dpm})} \times 100\% \qquad (2.14)$$

E has been determined in three ways in this study : 1) by counting an aliquot of spike solution directly plated out, and determining ^{232}U activity as described by Gascoyne (1977a) 2) by plating out (with assumed 100% TTA efficiency) and counting an aliquot of a U or Th standard solution, and 3) by counting a disc previously calibrated in a known geometry (eg. the 4π geometry of a gridded ionization chamber). The latter is the most precise method and has recently been made possible by calibration of a relatively 'hot' U disc ('# 11') by Simon Webster at Harwell, England.

Yield is calculated as :

$$Y_U = \frac{^{232}U_{obs.}}{^{232}U_s \times E \times V_s} \times 100\ \% \qquad (2.15)$$

and

$$Y_{Th} = \frac{^{228}Th_{obs.}}{^{232}U_s \times E \times V_s \times R_s} \times 100\ \% \qquad (2.16)$$

where $^{232}U_s$ is the ^{232}U activity (dpm) of 1ml spike solution. Detector efficiency E depends on 1) the area and depletion depth of the detector, 2) the area of the disc covered by sample and 3) the spacing between detector and sample disc. Initially, different source-detector spacings were used in the two counters available, but the same efficiency value was used for both. This resulted in one unit grossly underestimating the yield of U and Th. Both units were set to a 2cm spacing in October 1975 and detector efficiency (for the 900mm^2 size) was determined at about 14% using methods 1) and 2) above. The distance was shortened to 1cm in June 1976 increasing detector efficiency to about 28% with no apparent loss in resolution. The Harwell calibration subsequently showed that efficiencies for the three counting systems used ranged between 24 and 34%.

2.5.3.6 Amendments to the Dating Program

A number of errors have been found in the ^{230}Th/^{234}U dating program as used by Thompson (1973a) and Harmon (1975). Two affect sample age, another can substantially alter U concentration in the sample (already described) and others affect error limits associated with the age. In order of significance, the changes made and their effects are:

i) correction of the true ^{228}Th count rate equation in the program to also allow for background activity, ie. $TN6 = N6 - B3 - N4 \underline{\underline{+ B1}}$ This omission only became important when Th yields were low.

ii) a routine was included to correct the measured ^{228}Th count rate for ingrowth of ^{224}Ra over the period of counting and for the time elapsed between plating out and counting. This correction is necessary because approximately 5% of ^{224}Ra energy occurs under the ^{228}Th peak.

iii) re-definition of the reagent blank values originally introduced by Thompson (1973a), a Th reagent blank is no longer included.

iv) reagent blank error limits, already fixed in the program, were found to apply only to 100% yield of nuclide, but they were in fact added on to values that were not adjusted for yield. The effect was to create very large 1σ errors on samples of either low age or low Th yield. This effect was probably the cause of the large errors determined by Harmon (in Atkinson et al. 1978) for young English speleothem samples (eg. GB1A in their paper has 23.6ppm U, an age of 11 Ka but an error of ± 6 Ka; with such a high U concentration, the error should be less than 1 Ka). The error limits for reagent blank analyses determined in this study were ^{238}U = ± 0.007, ^{234}U = ± 0.043, ^{232}Th = ± 0.005, ^{230}Th = ± 0.005, all for 100% yield.

v) a full error propagation equation was used in place of the simplified version in the existing program, ie. contributions from errors associated with reagent blank and background count rates and times have been included (Gascoyne 1977a).

vi) although not an error in the program, frequent failure to activate a routine which corrects for decay of ^{228}Th spike has been noted in some previous work. The parameter DECT (delay in counting Th) allows for decay of unsupported ^{228}Th between separation from its parent (^{232}U) on the anion column and its time of counting. The effect of omission of DECT increases with age of sample, eg. if DECT = 7 days, an age increase of $\leqslant$ 1% is seen below 100 Ka and $\leqslant$ 3% up to 300 Ka.

2.5.3.7 Error in Spike Activity

To the author's knowledge, the error quoted in all radiometric age measurements is based only on counting statistics. Most laboratories dating carbonates by the $^{230}Th/^{234}U$ (ionium) method use a ^{232}U-^{228}Th spike in this work, whose activity ratio is either taken as the equilibrium value 1.027, (often wrongly shortened to 1.03 - since excepting chemical interference 1.02725 is the maximum value attainable) or an intermediate value determined by calibration. It has already been shown that determination of the activity ratio is difficult and unlikely to result in a precision better than ± 0.01. For this reason, even in the case of a spike expected to be in equilibrium, the age error quoted should also reflect uncertainty in the spike activity ratio. Table 2.3 shows that this error can be quite substantial in the case of older samples. However, because ages of speleothem and paleotemperature data obtained here are ultimately to be compared with deep sea core data and other terrestrial results in which no correction for spike error is at present made, it is logical that this error should not be included in speleothem work either.

2.5.3.8 Correction for Detrital Thorium

Most speleothems analysed in this study have consisted of pure calcite free of detrital impurities. Some however contain appreciable amounts of residue which is insoluble in dilute acid, and often a small activity due to ^{232}Th is seen in the thorium spectrum. In the present study, ages showing ^{230}Th/^{232}Th ratios of < 20 have been 'corrected' by assuming $(^{230}\text{Th}/^{232}\text{Th})_o = 1.5$. This value is quite arbitrary and will not necessarily be obtained if sediments in any of the caves studied are leached with acid. It is slightly less than the value used by Thompson (1973a) to correct speleothem ages (1.7) and may therefore be only a minimum correction to the ages presented here. In some respect it serves to test itself by permitting comparison of corrected ages of contaminated speleothem with those of uncontaminated speleothem

Spike Ratios

Sample No.	1.027	1.017	1.007
	Calculated ^{230}Th/^{234}U ages (Ka)		
76001-22	45.0 ± 1.7	44.5 ± 1.7	43.9 ± 1.7
79001-1	$105.2 \pm^{6.3}_{6.0}$	$103.6 \pm^{6.2}_{5.8}$	$101.9 \pm^{6.0}_{5.7}$
77242-1	$300.4 \pm^{69.6}_{43.3}$	$285.8 \pm^{59.7}_{58.4}$	$273.0 \pm^{50.6}_{34.5}$

Table 2.3 The effect of spike ratio on speleothem age

from the same area or cave. Results are discussed individually in the following chapters and general conclusions are drawn in the final chapter.

2.5.4 Determination of Precision and Accuracy

2.5.4.1 Internal Laboratory Standards

To determine if the calculated 1σ error in an age measurement is realistic, a number of replicate dates must be obtained for the same sample. The standard deviation of these results σ_r should be comparable to the mean standard deviation $\overline{\sigma}_c$ calculated from the analysis of propagation of analytical errors as described above, and computed in the dating program.

Three standards have been prepared at McMaster. The first (RHN), prepared by P.Thompson, was from a U-rich speleothem from the N.W.T., Canada. Ten determinations quoted by Harmon (1975, p.61) show the standard to lie outside the dating range (ie. > 350 Ka) and to be essentially in isotopic equilibrium. Mean $^{230}Th/^{234}U$ was 1.05 ± 0.051 (σ_r) while σ_c for each determination varied between 0.01 and 0.02. These results suggest that σ_c is inadequate to describe the observed variation in ratio. RHN is a rather unsatisfactory standard because it does not express variation in terms of age and is atypical of most speleothem dated at McMaster due to its high U content (~ 5ppm).

In the present work, two standards have been prepared. The first was from some remaining pieces of NB 10, a stalagmite collected and previously dated by Thompson (1973a). 12kg was homogenized by crushing, powdering and drum-rolling but 6 ages obtained from aliquots of the standard show wide variations (between 170 and > 300 Ka). It was later found that a portion of the speleothem had suffered U leaching so that any slight inhomogeneity in the powdered standard would cause a wide variation in ages.

A third standard was prepared from pieces of a flowstone collected from Sumidero Tenejapa, Chiapas, Mexico in January 1976, by the author. This standard was found to have a number of advantages over previous standards:

i) it has a moderately low U concentration (0.8ppm) thus making it comparable to samples typically studied at McMaster,

ii) it lies within the age range of the ^{230}Th/^{234}U method (50 Ka - an ideal age for estimating the precision of dates obtained from Vancouver Island speleothem),

iii) because it is a flowstone, larger quantities are available laterally (ie. of the same age) which therefore reduces the possibility of picking up age heterogeneities in the final powdered standard.

Approximately 10kg of the sample was crushed, powdered and sieved to < 100 mesh and drum-rolled for about 6 hours. Incomplete homogeneity was initially suggested by the result of 64.8 Ka (Table 2.4). The powder was then stirred for two hours in a large mixer (courtesy Mrs. Stevens, Arts III Cafeteria) and redated. The one analysis by B.Blackwell lies well outside 3σ limits of the mean of the author's and A.G.Latham's analyses (47.7 ± 1.7 Ka). The ^{231}Pa/^{230}Th result lies within 2σ of this mean and is discussed towards the end of this chapter.

Date of Analysis	Analysis No.	U conc. (ppm)	$\frac{^{234}U}{^{238}U}$	$(\frac{^{234}U}{^{238}U})_o$	$\frac{^{230}Th}{^{232}Th}$	$\frac{^{230}Th}{^{234}U}$	Yields (%) U	Yields (%) Th	AGE (Ka) ± 1σ(σ_c)	
Mar'76	-4S	0.81	1.824	1.947	31	0.377	54	12	49.4 ± 3.6	←
Jun'76	-6	0.90	1.769	1.885	> 1000	0.382	51	12	50.2 ± 5.2	←
May'76	-H	0.78	1.748	1.850	78	0.353	37	32	45.7 ± 2.1	* ←
Aug'76	-L	0.72	1.970	2.103	31	0.357	61	24	46.1 ± 1.7	* ←
Sep'76	-8	0.68	1.825	1.984	270	0.456	66	47	62.7 ± 2.8	
- -	- -	- -	- Re-homogenised			- -	-	-	- - -	
Nov'76	-11	0.79	1.862	1.989	59	0.375	62	12	49.1 ± 2.2	←
Nov'76	-12	0.82	1.839	1.958	40	0.363	60	27	47.1 ± 1.4	←
Dec'76	-13	0.87	1.923	2.056	79	0.369	45	28	48.0 ± 1.5	←
Jun'77	-14	0.78	1.953	2.088	167	0.364	42	27	47.2 ± 1.8	←
Nov'77	-15	-	1.918	1.966	132	-	23	13	$18.3 \pm^{18.0}_{14.9}$	**
Nov'78	-22	0.84	1.900	2.021	35	0.349	33	17	45.0 ± 1.7	←
Apr'79	-25	0.82	1.847	1.944	> 1000	0.307	38	19	38.6 ± 2.1	***
Apr'79	-26	0.79	1.900	2.027	40	0.363	40	40	47.2 ± 1.3	←
Apr'79	-27	0.79	1.855	1.984	25	0.382	43	34	50.2 ± 1.5	←
means		0.81 ±0.05	1.867 ±0.065	1.986 ±0.071			mean age =		47.7 ± 1.7 (σ_r) ± 2.2 ($\bar{\sigma}_c$)	

* determination by A.G.Latham

** dated by 231Pa/230Th method, yields estimated from weight used, 238U and 230Th count rates and data from other analyses

*** determination by B.Blackwell

← indicates results used in calculations of mean age

Table 2.4 Results of analyses of 76001 speleothem standard.

For the eleven indicated results in Table 2.4, σ_r is slightly less than $\bar{\sigma}_c$ in contrast to Harmon's results above. However if the two anomalous ages (62.7 and 38.6 Ka) are included $\sigma_r = \pm 5.1$ Ka whereas $\bar{\sigma}_c$ remains unchanged. Because of the possibility of inhomogeneity and contamination during analysis contributing to the σ_r and not to $\bar{\sigma}_c$ it is difficult to clearly determine the adequacy of σ_c. It seems however that there is general good agreement between the statistical age error and that determined for several replicate analyses.

2.5.4.2 Interlaboratory Standards

Six powdered carbonate samples (5 corals and 1 speleothem) were distributed as Phase I of an interlaboratory calibration project (USIP) in 1976 (Harmon and Ku, 1976). Nine laboratories analysed them and returned results by Sept. 1976 although one of them failed to determine ages from measured ratios (Matthews, pers.comm.); the variations are shown in Figure 2.6. McMaster was laboratory number 5 and can be seen to lie at the upper end of most age distributions. In addition, McMaster's U concentrations were up to 25% greater than most other laboratories. The analysis for RKM 4 gave only a 4% Th yield and so should be ignored. Of the remainder, the bias to higher ages and U concentrations can be attributed to use of incorrect spike ratio and ^{232}U activity as previously described. The ages have been corrected as shown in Figure 2.6 and a better agreement can generally be seen. If results for samples RKM-1,2 and 3 are representative of the spread that might be expected at these ages for perfectly homogenized samples, the two samples (RKM-4 and RHKL-1) show anomalously large age distributions.

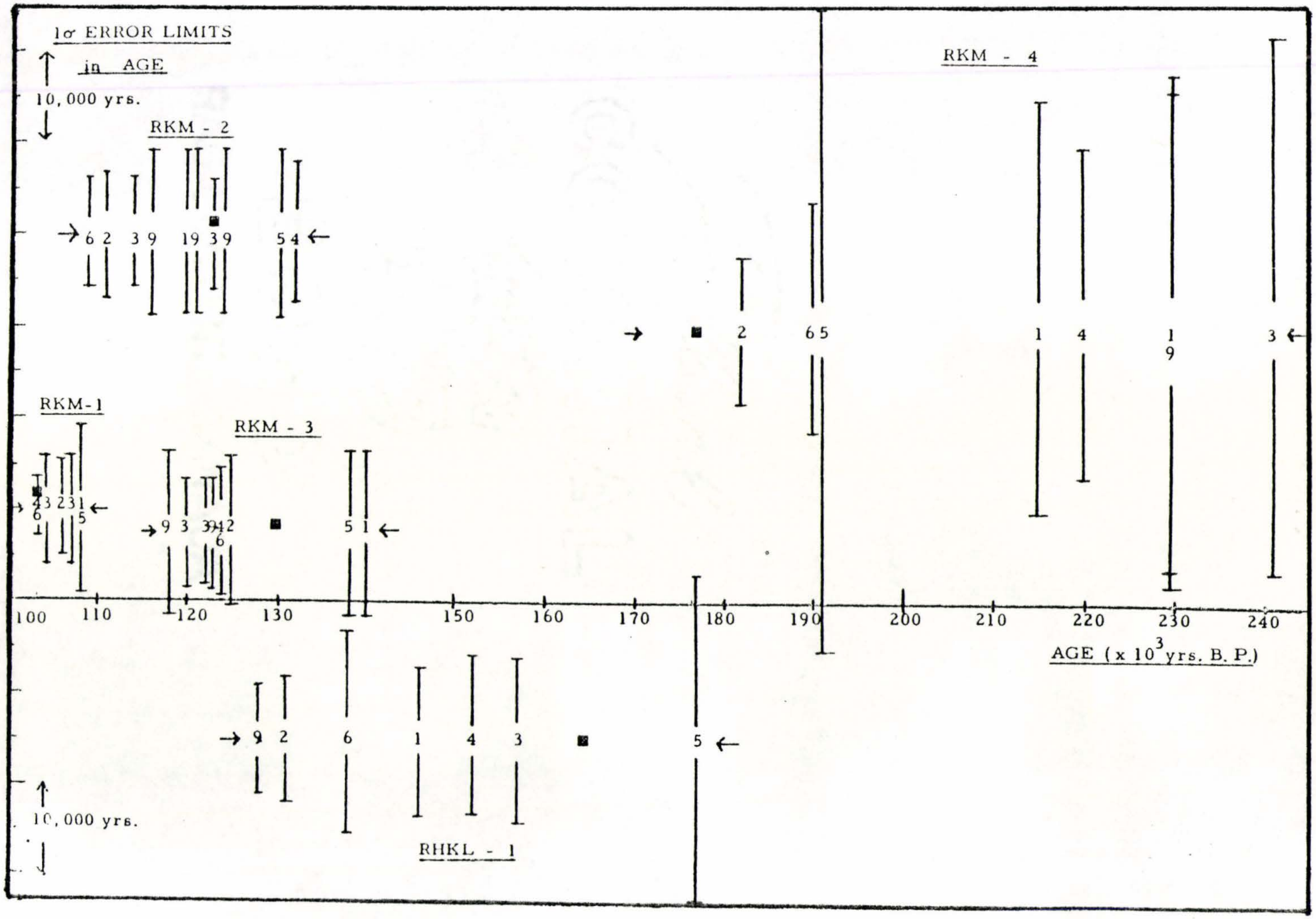

Figure 2.6 Diagrammatic representation of the results of USIP Phase I. Results from individual laboratories (numbered) show age clusters (arrowed) for five carbonate samples within the dating range. Errors (± 1σ) quoted by each lab. are expressed as vertical lines. McMaster is lab.5. Black squares denote McMaster results when corrected for spike ratio (see text).

One explanation may be inhomogeneity of the samples (as previously seen in the NB 10 standard). This is indicated by the fact that RHKL-1 (a coral from Key Largo, Florida) has only " ∿90% aragonite" (Harmon et al.1979a), and is known to have been poorly selected for radiometric dating (Halley, pers.comm.). A coral should be > 98% aragonite; anything less is likely to give variable ages due to differing amounts of re-crystallized portions dated. It is therefore misleading for Harmon et al. to propose a 'best-estimate' age for Florida Key limestone of $139 ^{+18}_{-13}$ Ka based on interlaboratory determinations for this one sample.

In the second part of the project, 3 carbonate powders (2 corals and 1 speleothem - 76001 provided by the McMaster laboratory) were dated with a common spike of ratio 1.027. Results from 9 laboratories have been kindly provided Dr.R.S.Harmon and are shown in Figure 2.7. Many of the laboratories did not report in Phase I so that it is difficult to determine whether an improvement in precision is seen in these results. However, lab 5 (McMaster) is fairly central to all clusters this time.

2.5.4.3 Re-dating NB 10 stalagmite

The speleothem NB 10 from West Virginia has previously been dated by Thompson (1973a) and found to have grown over a period of 45 Ka commencing at 208 Ka. Subsequently it fell over and two smaller stalagmites grew on its side at around 110 Ka. Much of the speleothem paleoclimate record for W.Va. has been based on this sample. As a test of reproducibility in the early part of the present study, portions of it were redated. Eight samples were analysed by the author and ages were determined from the raw spectra by R.S.Harmon. Re-appraisal of the

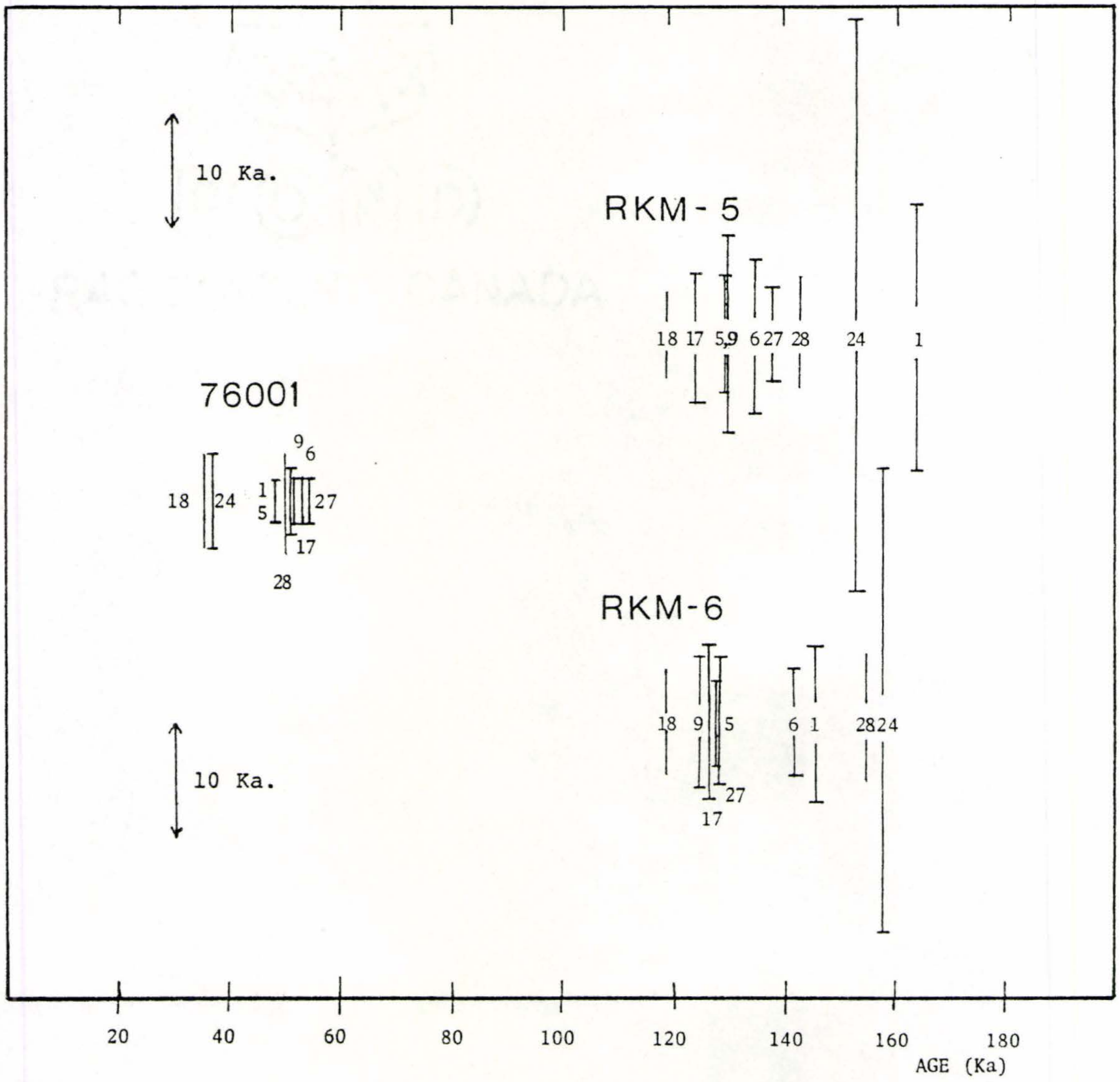

Figure 2.7 Diagrammatic representation of the results of USIP Phase II. Age clusters for three samples dated using interlaboratory spike are shown with ±1σ error limits expressed as vertical lines. McMaster is lab. 5.

original raw results and analysis of two more results by the author and Ada Dixon at a later date revealed some discrepancies. Results are summarized in Figure 2.8. Ages are listed approximately in the correct stratigraphic position although in the re-dating, some doubt existed as to the exact position of the samples with respect to the unbroken stalagmite, because only ill-matching portions of the sample remained. The following can be seen :

i) some leaching of U is evident in the upper and middle parts of the stalagmite, which were largely undated by Thompson (1973a). The leaching is not unexpected because this section contains many re-solution holes,

ii) Ages obtained by Harmon are generally less than Gascoyne/Dixon. This could be explained by the latter workers not knowing the DECT value to correct for decay of ^{228}Th, because no records of it were usually kept. Alternatively, it may be due to differing spectra interpretation between the two groups.

It may be concluded from this project that :

i) double checking of all hand calculations should be done to prevent arithmetic errors,

ii) the agreement between columns 1 (Thompson) and 3 (this work) is generally good because the base date of 246 Ka was obtained on material stratigraphically lower than Thompson's base date, and similarly, Thompson's 163 Ka age was obtained on material that included stratigraphically older layers than those used in sample N (144 Ka),

iii) ages may be quite sensitive to slight differences in spectra interpretation,

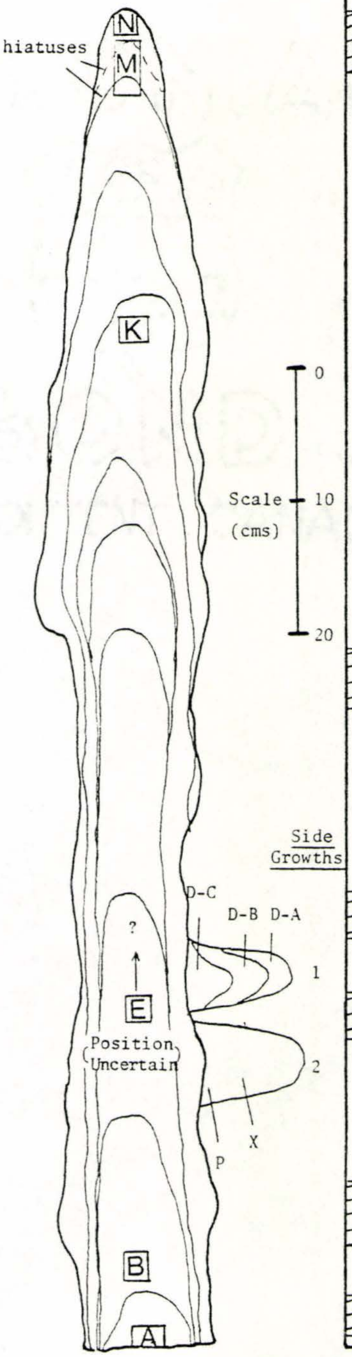

THOMPSON (1973a)	Chemical Extraction by Gascoyne Age calculations by		COMMENTS
	Harmon	Gascoyne/Dixon	
163 ± 7	N = 136 ± 7	N = 144 ± 8	
		M = > 300	U leached ($^{230}Th/^{234}U$ = 4.0)
		K = > 300	U leached ($^{230}Th/^{234}U$ = 2.6)
173 ± 7			
	D-C = 128 ± 8	D-C = 137 ± 9	
		D-B = 123 ± 21**	
183 ± 10	D-A = 132 ± 8	D-A = 129 ± 8	
203 ± 11	E = 218* ± 19	E = > 300	U leached ($^{230}Th/^{234}U$ = 1.15)
X = 105 ± 4 and 115 ± 8 **	P = 97* ± 3	P = 139 ± 6	
195 ± 10			
	B = 184 ± 9	B = 203 ± 9	
200 ± 9	A = 243 ± 20	A = 246 ± 20	

* contains arithmetic error

** $^{231}Pa/^{230}Th$ date

Figure 2.8 Results of replicate analysis of stalagmite NB 10. First column shows Thompson's (1973a) original results and approximate sample locations. Second column shows ages calculated by Harmon from results of chemical analysis by Gascoyne, and third column shows results of checking and re-calculating these ages, with some additional analyses.

iv) NB 10 grew from 245 Ka to 144 Ka, fell over and continued growing side deposits (without a prolonged hiatus), finally stopping growth about 130 Ka,

v) uranium leaching in the upper part of the sample renders this portion undatable. Perhaps the stable isotope data obtained from here (Thompson 1973a, Thompson et al.1976, Harmon et al.1978a) are also invalid.

Summary

A number of problems and errors associated with the $^{230}Th/^{234}U$ dating technique used at McMaster have been identified and solved in this present study, although occasional thorium losses still occur. Preliminary results of using ^{234}Th as a β tracer to detect Th loss, by Ada Dixon, indicate that most of the loss occurs towards the end of the extraction technique, possibly by sublimation of the Th-oxalate compound.

The precision of the technique has been well-established in this work by frequent replicate analysis of internal standards, and more importantly, the ages determined are found to be in good agreement with those determined by other laboratories using different analytical techniques, spikes and data processing methods. Further indication of accuracy is given by the results of $^{231}Pa/^{230}Th$ dating described in the next section.

2.6 The $^{231}Pa/^{235}U$ Dating Method

This alternative dating technique (loosely referred to as the 'protactinium' method) was adapted to speleothem work in the McMaster laboratory and used on a small number of samples by Thompson (1973a) only. Ages were estimated from an isochron plot (Figure 2.3) but no further refinements were made to improve the method, since it relied heavily on the presence of an adequate uranium content in the speleothem. Samples containing $< 1 - 2$ ppm U were regarded as undatable by this method because the natural abundance of the ^{231}Pa parent (^{235}U) is only 0.7% of ^{238}U (the parent in the $^{230}Th/^{234}U$ method). If viable however, this dating method provides an excellent check on the "closed system" assumption, ie. that no nuclide migration has taken place within the speleothem since deposition. Any such change will affect the intermediate nuclides differently because of their different chemistries and half-lives, and therefore, dates obtained by the $^{230}Th/^{234}U$ and $^{231}Pa/^{235}U$ methods on the same sample, will not be concordant.

In the present work, the $^{231}Pa/^{235}U$ technique (or in fact, the more useful $^{227}Th/^{230}Th$ method) has been examined in detail and a computer program written for age determination embodying a number of previously-unused, decay-correction factors.

2.6.1 Chemical Extraction

The extraction procedure is identical to that used in the $^{230}Th/^{234}U$ method (Appendix 1a) except that no spike is added at the dissolution stage and larger amounts of sample are used, depending on U content (usually between 50 and 200g). Since ^{227}Th rapidly decays away once separated from its ^{227}Ac parent, careful note must be taken of the time elapsed between this separation (on the cation column) and the time of plating out (DSPT (hrs.) in the program, Figure 2.9).

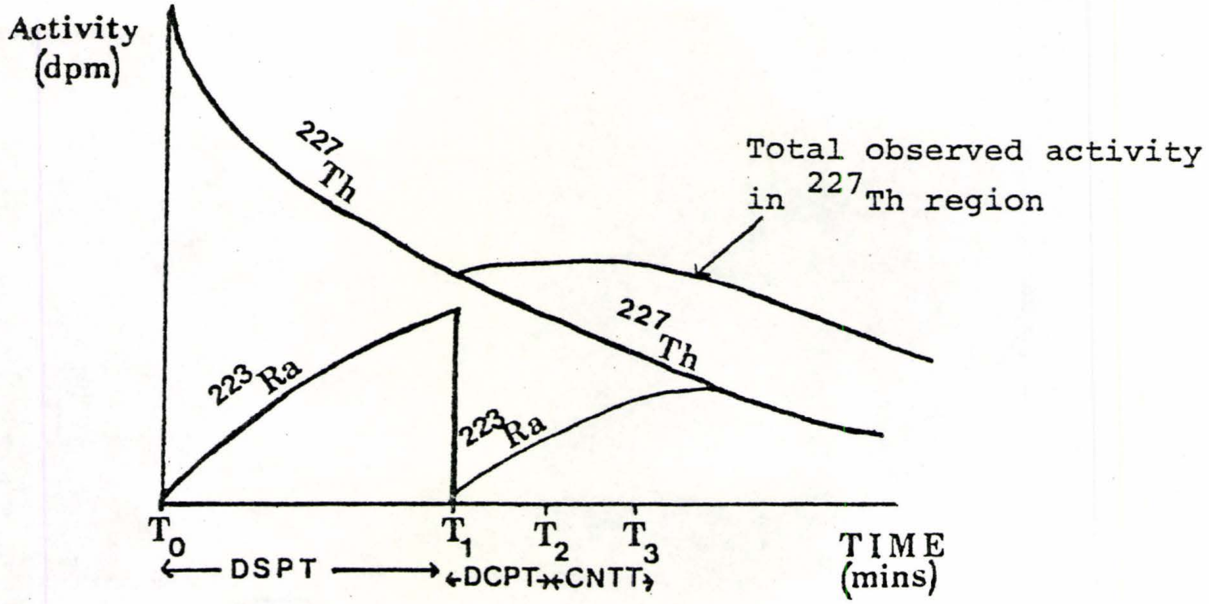

T_0 = time of separation of ^{227}Th from ^{227}Ac parent -- assumed to occur on cation column

T_1 = time of plating out (separation from ^{223}Ra)

T_2 = start of Th count

T_3 = end of Th count

T_1-T_0 = delay between separating and plating Th (DSPT)

T_2-T_1 = delay between counting and plating Th (DCPT)

T_3-T_2 = Th count time (CNTT)

Figure 2.9 Graphical representation of the decay of ^{227}Th and ingrowth of ^{223}Ra after separation from parent ^{227}Ac.

2.6.2 Counting Procedure

To offset the decay effect, the Th sample is counted as soon as possible after ion exchange extraction, and in any event, must be counted immediately after plating out, to minimize ^{223}Ra ingrowth. Note is also made of this latter delay period (DCPT, mins., see Figure 2.9). To minimize background count rates, a new detector is used which has never counted any spiked sample, and whose background activity is measured either immediately before or after counting the Th sample. The U portion is best counted on another detector to measure the ^{234}U/^{238}U ratio, so that contamination of the new detector is not increased.

2.6.3 Data Processing

A typical unspiked U and Th spectrum is shown in Figure 2.10 and printouts are given in Appendix 1b showing calculated count rates and times. Note that a small amount of ^{232}Th is present over background levels, and this gives rise to an approximately equal amount of ^{228}Th, whose ^{224}Ra daughter grows into the combined ^{227}Th-^{223}Ra peak. Corrections to the raw count rates that must be made, in sequence, are therefore :

i) subtract background activity
ii) correct for ingrowth of ^{224}Ra from ^{228}Th over period of counting
iii) correct for ingrowth of ^{223}Ra from ^{227}Th over period of counting
iv) correct this new ^{227}Th activity for decay since separation from the parent at the cation column stage.

Only when these corrections have been made, can the isochron plot be

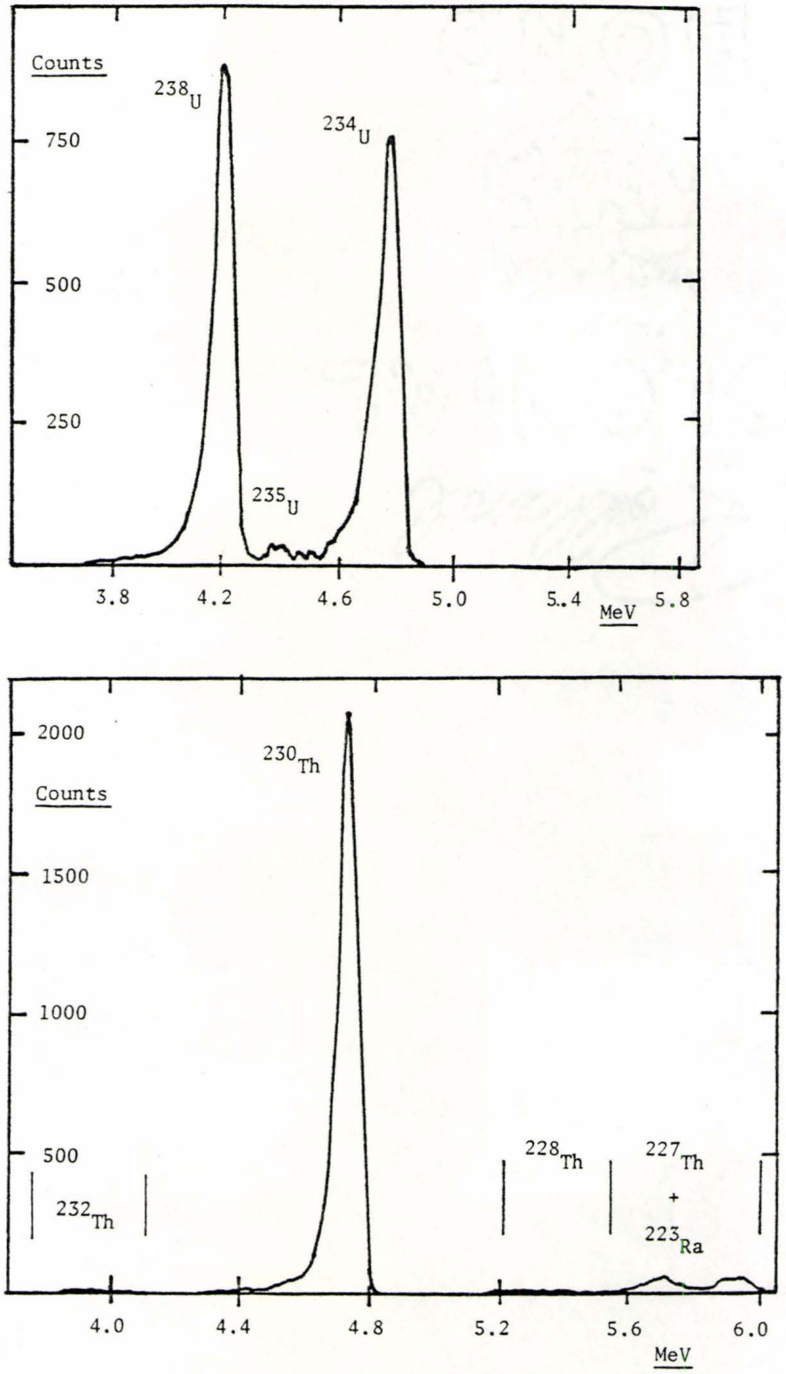

Figure 2.10 Typical unspiked uranium and thorium alpha spectra showing speleothem nuclides ^{238}U, ^{234}U, ^{232}Th, ^{230}Th, ^{228}Th, ^{227}Th and ^{223}Ra daughter.

used (Figure 2.3). Age calculation from the corrected count rates is then a simple procedure involving an iterative step as in the ^{230}Th/^{234}U program. The ^{231}Pa/^{230}Th program is given in Appendix 1c together with a typical printout of the results. Error limits on the age are typically at least twice those of a ^{230}Th/^{234}U date since low count rates are being determined.

2.6.4 Problems

So far, it has been assumed that ^{227}Th is separated from its ^{227}Ac parent at the Th column stage. This is in fact the case only:

i) if Th and Ac chemical yields at that point in the analysis are identical

ii) if the cation column is washed sufficiently to remove all Ac before eluting with oxalic acid.

The first point may be invalid if during the $Fe(OH)_3$ precipitation step more Th is co-precipitated than Ac (quite possible since their hydroxide solubilities differ and the selectivity of surface adsorption on the precipitate may be unequal). In this case ^{227}Th in the resulting ferric chloride solution is in excess of parent ^{227}Ac and decays away without replenishment. The alternative situation of excess Ac is of far less importance due to the longer half-life of ^{227}Ac. The effect is therefore, to make the determined age greater than it really is because the given value for DSPT should be larger.

The second point is very important also, but in the opposite sense to that above. If some ^{227}Ac is eluted with the Th from the cation column, then the decay correction for DSPT is too large, giving an excessively high value for initial ^{227}Th relative to ^{230}Th in the sample. This has the effect of making the age younger than it really is. This problem is probably more acute than hitherto realised because Ac^{3+} and Th^{4+} are strongly retained by cation resin at low strengths when all divalent and most trivalent ions are eluted (Katz and Seaborg 1957). Ac^{3+} is then eluted as acid strength increases (towards 4M).

The amount of washing required to remove all adsorbed Ac could be determined by spiking with a highly active Ac isotope and counting aliquots of the wash solution. It is possible however, that even if Ac were adsorbed, it may not subsequently be eluted by oxalic acid and therefore, would not interfere. The effect of these problems is illustrated in Table 2.5 where the value DSPT is varied from the usual value (for sample 76121 - 3) to cover both cases.

One way to minimize the effect of these situations is to rush the extraction procedures so that the minimum amount of time elapses between the $Fe(OH)_3$ stage and plating out. Even so, this period is probably at least 12 hours and, as can be seen from Table 2.5, this would make a significant difference in extreme cases.

2.6.5 Comparison with ^{230}Th/^{234}U Age Measurements

To clarify some of the problems described above and to serve as a check on the ionium method, a number of speleothems dated in this study have also been dated by the protactinium method. Their results are summarized in this chapter irrespective of speleothem location. Thirteen analyses of 11 carbonates (including 1 coral) have been made (Table 2.6) either by i) taking a stratigraphically-comparable sample or

Sample 76121-3	DSPT (hrs)	Age (Ka)
If ^{227}Ac is eluted with Th	0	$106.4^{+16.9}_{-14.4}$
	11	$100.7^{+16.2}_{-13.9}$
	16	$98.2^{+15.8}_{-13.7}$
"Correct" DSPT value →	21	$95.7^{+15.3}_{-13.2}$
If ^{227}Th becomes unsupported (partially or wholly) prior to the cation column stage	26	$93.2^{+15.2}_{-13.2}$
	31	$90.8^{+15.1}_{-13.0}$
	41	$86.1^{+14.6}_{-12.7}$

Table 2.5 The effect of removal of ^{227}Ac before or after the cation column stage, shown by varying the time between separation and plating of Th (DSPT), expressed in terms of the sample age.

Speleothem No.	Analysis No.	Location	U conc. (ppm)	Yields (%)		$\frac{^{234}U}{^{238}U}$	$\frac{^{230}Th}{^{232}Th}$	$\frac{^{231}Pa}{^{230}Th}$	AGE (Ka) ± 1σ
				U	Th				
76016	-1b[1]	Bahama Blue Holes	-	∼20	∼16	1.031	96	1.324	$122.3\,^{+38.4}_{-27.3}$
	-1a		0.26	33	8	1.028	70	-	$128.8\,^{+12.2}_{-10.9}$
77032	-3[2]	Castleguard Cave Alta.- B.C.	-	∼23	∼42	1.334	430	0.673	> 350
	-2		2.51	71	63	1.362	274	-	$277.8\,^{+26.1}_{-21.6}$
RKM-6	-C[1]	Intercalibration Standard	-	∼83	∼77	1.148	159	1.224	$107.6\,^{+13.8}_{-12.1}$
	-B		3.19	71	54	1.100	31	-	$128.8\,^{+5.9}_{-5.6}$
76001	-15[1]	McMaster Standard	-	∼23	∼13	1.918	132	1.063	$18.3\,^{+18.0}_{-14.9}$
	mean		0.81	variable		1.868	> 20	-	47.7 ± 1.8
76121	-3[1]	Lancaster Hole England	-	> 100[4]	∼82	1.117	160	1.280	$96.4\,^{+15.7}_{-13.5}$
	-2		1.49	76	69	1.130	129	-	$114.0\,^{+7.5}_{-7.1}$
76125	-3[1,3]	" "	-	∼80	∼43	1.569	257	1.042	$54.4\,^{+12.3}_{-11.0}$
	-1		2.01	82	60	1.628	105	-	38.1 ± 1.4
76127	-3[1]	Ease Gill Caverns England	-	∼17	∼19	0.881	89	1.367	$203.4\,^{+27.3}_{-21.1}$
	-1		13.1	46	41	0.878	255	-	$225.2\,^{+24.6}_{-19.7}$
79005	-2[2]	Lancaster Hole England	-	∼21	∼32	1.399	46	1.063	$88.8\,^{+6.8}_{-6.3}$
	-1		0.43	33	34	1.429	11.6	-	$43.3\,^{+3.1}_{-3.0}$ (C) (38.4 ± 4.6)
77126	-3[1]	" "	-	∼47	∼50	1.085	> 1000	1.280	$108.7\,^{+9.5}_{-8.7}$
	-2		3.93	61	37	1.152	240	-	$106.0\,^{+3.6}_{-3.5}$
77162 (top)	-2[2]	Lost John's Cave England	-	∼56	∼63	0.939	199	1.628	$88.8\,^{+6.8}_{-6.3}$
	-1		6.23	48	61	0.944	127	-	$92.0\,^{+4.3}_{-4.1}$
77162 (base)	-3b[2]	" "	-	∼53	∼33	0.882	> 1000	1.445	$165.7\,^{+18.1}_{-15.1}$
	-3		7.21	41	48	0.916	92	-	$112.7\,^{+5.2}_{-5.0}$
78010	Pa dates -8[1]	Warm Mineral Springs Springs, Florida	-	∼61	∼42	1.023	> 1000	3.982	$-92.0\,^{+5.1}_{-5.0}$
	Pa dates -9[1]		-	∼64	∼27	0.963	182	3.539	$-69.3\,^{+10.4}_{-9.5}$
78010	-1		3.47	58	31	0.992	31	-	12.6 ± 0.3
	-2		1.91	52	19	1.006	5.9	-	14.4 ± 0.6 (C) (10.9 ± 1.1)

[1] Pa date, using near-replicate calcite sample

[2] Pa date, exact replicate using solution split

[3] Pa date, chemical extraction by A.G.Latham

[4] approximate yields only for Pa analyses (calculated from U conc. of ionium partner), very approximate in case of near-replicates ([1]) because of different U concs.,eg.76121-3

(C) ages contaminated by detrital Th, corrected age is given

Table 2.6 Data list showing comparison of ages determined by $^{231}Pa/^{230}Th$ and $^{230}Th/^{234}U$ methods for the same speleothem samples.

ii) as a split of a bulk solution of the dissolved speleothem after filtration but before spiking and precipitation. The latter gives more exact comparison to the ionium ages. All results are shown graphically in Figure 2.11.

The results, other than 78010, show agreement within 1σ error limits for 5 ages, 2σ limits for 10 ages and 3σ limits for all ages, and equal bias of above (5 cases) and below (6 cases) ionium ages. With the exception of 78010 (discussed separately below), it may therefore be concluded that:

1) all the samples analysed appear to have remained 'closed' to U and Th migration since deposition,
2) because of the lack of bias between comparisons of ionium and protactinium ages, there is no reason to reject the ^{231}Pa half-life of 32,500 years (Kirby 1961) in favour of that of 34,300 years advocated by Ku (1968),
3) the assumptions, equations and computer routines developed in this study to obtain protactinium ages seem to be correct, or at least, conspire to give credible results,
4) the observed disagreements with ionium ages may be largely explained in terms of counting statistics, but also they may be further influenced by the problem of determining when ^{227}Th becomes unsupported in the extraction process. This time is likely to vary from one extraction to another,
5) within counting error limits, none of the spectra showed excesses of ^{228}Th over ^{232}Th, indicating that closed system conditions had applied at least during the last few years, and that contamination

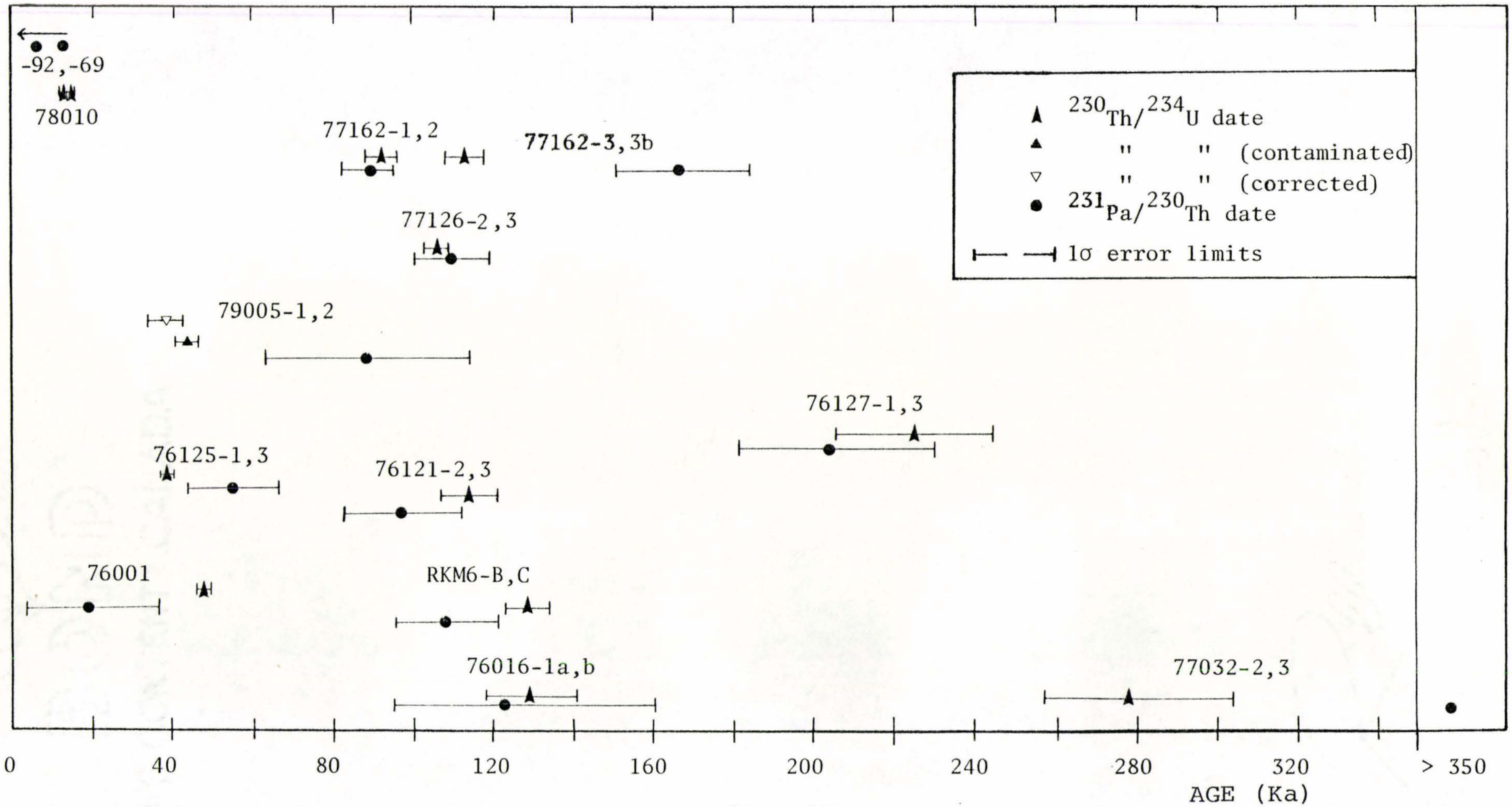

Figure 2.11 Comparison of ages determined by ^{231}Pa/^{230}Th (circles) and ^{230}Th/^{234}U (triangles) methods for the same speleothem samples.

from memory effect on glassware was negligible.

Sample 78010 gives apparent 'negative' ages by this method. This can be explained in two ways - excess of supported ^{227}Th or deficiency of ^{230}Th. 78010 is a porous flowstone which, until about 1977 was located at a depth of 15m in Warm Mineral Springs, Venice, Florida (Chapter 7). Its porosity suggests that it may also give erroneous ionium ages due to variable migration of U and Th. However two different analyses (78010-1,-2,Table 2.6) have given essentially the same ionium age, suggesting that the system either has remained closed since deposition or has been totally and equally influenced by the surrounding water. The former is seen not to be the case by the large disagreement between ages from the two dating methods and therefore, either the spring water chemistry is such that ^{230}Th is removed in preference to uranium (deficiency of ^{230}Th) or supported ^{227}Th is added without any other thorium isotopes (excess of ^{227}Th). It is difficult to conceive of a situation in which ^{230}Th could be removed from the speleothem without also removing some uranium, since the latter is more soluble than thorium in almost all natural systems. It is more likely that there is an excess of ^{227}Th, not due to the addition of ^{231}Pa to the system (because it is equally insoluble) but due to addition of the intermediate ^{227}Ac, a nuclide of greater solubility, of the alkaline earth group. This would lead to a ^{227}Th excess without excess ^{230}Th and bias the age to younger or even negative values.

Because the flowstone was only raised from the spring water during the last two or three years, most of the excess ^{227}Ac still remains in the speleothem. A test of the above hypothesis would be either to look for excess ^{227}Ac with respect to ^{231}Pa or to re-date the sample in 20 years time, when half of the ^{227}Ac will have decayed away.

2.7 Summary and Conclusions

The investigations described in this chapter have shown the following :

1) general improvement and consistency of Th and U chemical yields in the extraction process, largely due to improved analytical techniques and use of cation exchange resins.
2) a reduction in interfering factors in radioactive counting procedures and more precise knowledge of their magnitudes (eg. background and reagent blank activities).
3) precise calibration of the spike by analysis of an infinite age uraninite.
4) correction of computational errors which previously affected sample-U concentration, radiometric age and its error limits.
5) good internal reproducibility when dating a homogenised standard, adequate reproducibility when re-dating a speleothem from a previous study and a fair to excellent correlation with ages obtained by other laboratories on homogenised carbonate samples (some of the disagreement with the latter is likely to be due to their own inaccuracies.
6) the use of ^{227}Th/^{230}Th ratio (in the protactinium dating method) is subject to a number of decay corrections, most of which can be defined precisely. However, the technique is limited to uranium-rich samples, with rapid chemical processing and counting on uncontaminated detectors. Good agreement with ionium ages on the same samples is seen

in these results, over the range 80 to 300 Ka.

More work still needs to be done on chemical aspects of the extraction and separation of U and Th from speleothem. Large Th losses are still occasionally found, sometimes in association with 'dirty' samples, but it remains to be determined why yields are often low in reagent blank analyses where only pure chemicals are present.

Ages that are not in stratigraphic sequence along the growth axis of a speleothem may be biased by nuclide addition or migration from the speleothem since formation. Some parameters can be used to indicate these occurrences: eg. $^{230}Th/^{234}U$ ratios > 1.1 show U leaching (or, less likely, Th addition) and presence of ^{232}Th may indicate addition of non-authigenic ^{230}Th from detritus. However, problems such as partial U migration and addition of ^{228}Th not in equilibrium with ^{232}Th, could occur and would pass unnoticed in a spiked spectrum. The importance of regularly using a second dating method is therefore obvious, concordancy of ages being a major argument for accuracy of the final result.

2.8 The Limits of the Dating Methods

When followed carefully, the ionium dating method is reproducible for detritus-free, non-porous speleothem containing as little as 0.05ppm U, (this corresponds to a ^{238}U count rate of ~0.3 cpm assuming a 50g sample with 50% yield and 30% counting efficiency; ie. a signal to noise ratio of ~5). Below this level, variations in reagent blank, background activity and memory effect reduce the precision to unacceptable values.

Ultimately the accuracy of the dating methods rely heavily on the accuracy with which the decay constants of ^{234}U, ^{231}Pa and particularly ^{230}Th are known (^{230}Th half-life has been variously determined as 80,000 yrs, Hyde 1949; 75,200 yrs, Attree et al. 1962) and a precise re-determination is urgently required . In the same way as uncertainties associated with spike ratio are ignored in the error accompanying a radiometric age, uncertainties in values of decay constants are also omitted. These shortcomings must be given serious consideration when the limits of the dating method are debated.

A lower limit can be easily determined for the ionium method because it relies mainly on the worker's ability to isolate and count small quantities of ^{230}Th. The conclusion in the present study is that ionium ages as low as 200 years can be determined with good precision for high uranium speleothem. This is illustrated by sample 76209 (Appendix 4a) : it contains 9.4ppm U, and its basal age of 0.8 $\pm < 0.1$ Ka was determined from a ^{230}Th activity of 0.2 cpm at 50% yield - an activity that was more than ten times greater than background level.

It is more difficult however, to precisely define an upper age limit. Estimations in the literature and quoted by laboratories in the calibration project include 300 Ka (Thompson 1973a), 350 Ka (Thompson et al. 1976, Harmon et al. 1977), 400 Ka (Schwarcz et al. 1979, Atkinson et al. 1978) and 500 Ka (Schwarcz 1979, in press). To some extent these estimates are based on counting procedure and equipment of the laboratory concerned, but they are also influenced by the zeal of the analyst. Error limits determined solely from counting statistics are seldom less than 10% and more commonly about 15% near the dating limit (say 300 Ka). These limits are only $\pm 1\sigma$ values (68% probability that the true age lies within these limits). A $\pm 2\sigma$ limit would give almost a ± 100 Ka error on a 300 Ka age, representing 95% confidence limits. At this stage the distinction between finite and 'infinite' ages vanishes and only with extremely long count times, excellent instrument stability, low noise levels and high count rates can this distinction be made. Further uncertainty is added if the error limits in spike ratio and decay constants are considered. It is therefore felt that any attempt to push the limit of the dating method back beyond 400 Ka, even for 'ideal' samples and counting conditions, only serves to mislead others who are less familiar with the technique and are therefore unable to judge for themselves.

In the present study a maximum age of 350 Ka has been used, even for the high uranium speleothem analysed from British caves.

CHAPTER 3

STABLE ISOTOPE GEOCHEMISTRY OF SPELEOTHEM

Introduction

The temperature dependent fractionation of light-element stable isotopes in natural processes was first predicted by Urey (1947). In 1951 Epstein et al. calibrated the ^{18}O geothermometer for the $CaCO_3$-H_2O system using differences in ^{18}O content of fresh calcium carbonate growing on shells at different temperatures. Good agreement with McCrea's work (1950) for inorganically-precipitated $CaCO_3$ was subsequently found (Epstein et al. 1953). Since then, new calibrations from theory and experimental work, have been determined for $CaCO_3$-H_2O and numerous other low temperature geothermometers (eg. SO_4-H_2O, PO_4-H_2O, SiO_2-H_2O). The calcite-water system has however been the most important because of the ubiquitous nature of the mineral pair and the relatively large temperature dependence of isotope fractionation. A summary of experimental calibrations and the types of calcium carbonate deposits which have yielded paleotemperature information is given in Table 3.1. Much of the latter work has been done for Tertiary and older continental or marine environments so that relatively little is known from stable isotope studies on recent (Pleistocene) continental paleoclimate. It is here that speleothems help to redress the balance.

Type of study	Description	Author
Experimental calibration	Inorganic precipitation of $CaCO_3$ - as calcite	McCrea et al. (1950)
		Tarutani et al. (1969)
		Clayton (1961)
		O'Neil et al. (1969)
	- as aragonite	Clayton (1961)
		Tarutani et al. (1969)
Calibration from field measurements	Organic precipitation of $CaCO_3$ on marine shells	Epstein et al. (1951, 1953)
	Inorganic precipitation of $CaCO_3$ as calcite in speleothems	Harmon (1975)
Paleotemperature applications of $\delta^{18}O$ of $CaCO_3$ deposits	Jurassic and Upper Cretaceous molluscs	Urey et al. (1951)
	Jurassic ammonites	Stahl and Jordan (1969)
	Cretaceous molluscs	Tourtelot and Rye (1969)
		Spaeth et al. (1971)
	Recent molluscs	Lloyd (1964)
	Recent and fossil brachiopods	Lowenstam (1961)
	Recent and Pleistocene coral	Fairbanks and Matthews (1978)
	Deep sea cores - Pleistocene	Emiliani (1955,1966, 1978)
		Shackleton (1967,1977)
		Shackleton and Opdyke (1973)
		Broecker and van Donk (1970)
	Deep sea cores - Tertiary	Savin et al. (1975)
	Hot-spring travertines	Friedman (1970)
	Speleothem	Hendy and Wilson (1968)
		Duplessy et al.(1970b)
		Thompson et al.(1976)
		Schwarcz et al.(1976)
		Harmon et al. (1978a,d, 1979b)

Table 3.1 Application of various types of carbonate deposit to paleotemperature studies.

3.1 Theory of Isotope Fractionation

Chemical reactions at equilibrium can be described in terms of the equilibrium constant K, the ratio of activities of products to reactants. Every chemical reaction also has a fine structure of isotopic exchange and therefore a second equilibrium constant K' can be defined relating the distribution of isotopic species between products and reactants. For instance, in the exchange reaction:

$$1/3\ \mathrm{CaC^{16}O_3} + \mathrm{H_2{}^{18}O} \rightleftharpoons 1/3\ \mathrm{CaC^{18}O_3} + \mathrm{H_2{}^{16}O} \qquad (3.1)$$

$$K' = \frac{\left[\mathrm{CaC^{18}O_3} \,/\, \mathrm{CaC^{16}O_3}\right]^{1/3}}{\mathrm{H_2{}^{18}O} \,/\, \mathrm{H_2{}^{16}O}} \qquad (3.2)$$

K' can be more conveniently defined in terms of α, the isotope fractionation factor, where

$$\alpha = K^{1/n} \quad (n = \text{number of atoms exchanged}) \qquad (3.3)$$

For the above reaction, only one atom is exchanged and so $\alpha = K$. In this case α can be defined solely in terms of ^{18}O partitioning between the two components; $CaCO_3$ (eg. calcite) and water :

$$\alpha_{c-w} = \frac{^{18}O/^{16}O \ \text{(calcite)}}{^{18}O/^{16}O \ (H_2O)} \qquad (3.4)$$

The distribution of isotopic species between two phases is a function of the distribution of vibrational energy in the crystal lattice. In the exchange of ^{18}O between calcite and water α is therefore temperature dependent and is found to vary as $1/T^2$ over a large temperature range (O'Neil et al. 1969). Theoretical and experimental calibrations of this relationship are shown in Figure 3.1. The agreement between experimental determinations is generally good but theoretical calibrations are significantly different at low temperatures. This is due to problems in determining values for vibrational energies of solids at low temperatures. Calculations by Bottinga (1968) more precisely fit experimental determinations from 0 to 25°C but disagree above 100°C.

For ^{18}O exchange in the calcite-water system at ambient temperatures, α varies by approximately $-0.25‰/^{\circ}C$, ie. as temperature decreases, ^{18}O increasingly concentrates in the calcite.

3.2 Notation and Isotopic Standards

For analytical reasons the $^{18}O/^{16}O$ ratio of a substance is best determined relative to a reference standard. Departures are then referred to in the 'delta' notation:

$$\delta^{18}O_{\text{sample-std.}} = \left(\frac{^{18}O/^{16}O\text{ (sample)} - {}^{18}O/^{16}O\text{ (std)}}{^{18}O/^{16}O\text{ (std)}}\right) 10^3\,‰ \quad (3.5)$$

and the fractionation of ^{18}O between two components (X and Y) is related to the individual δ values by:

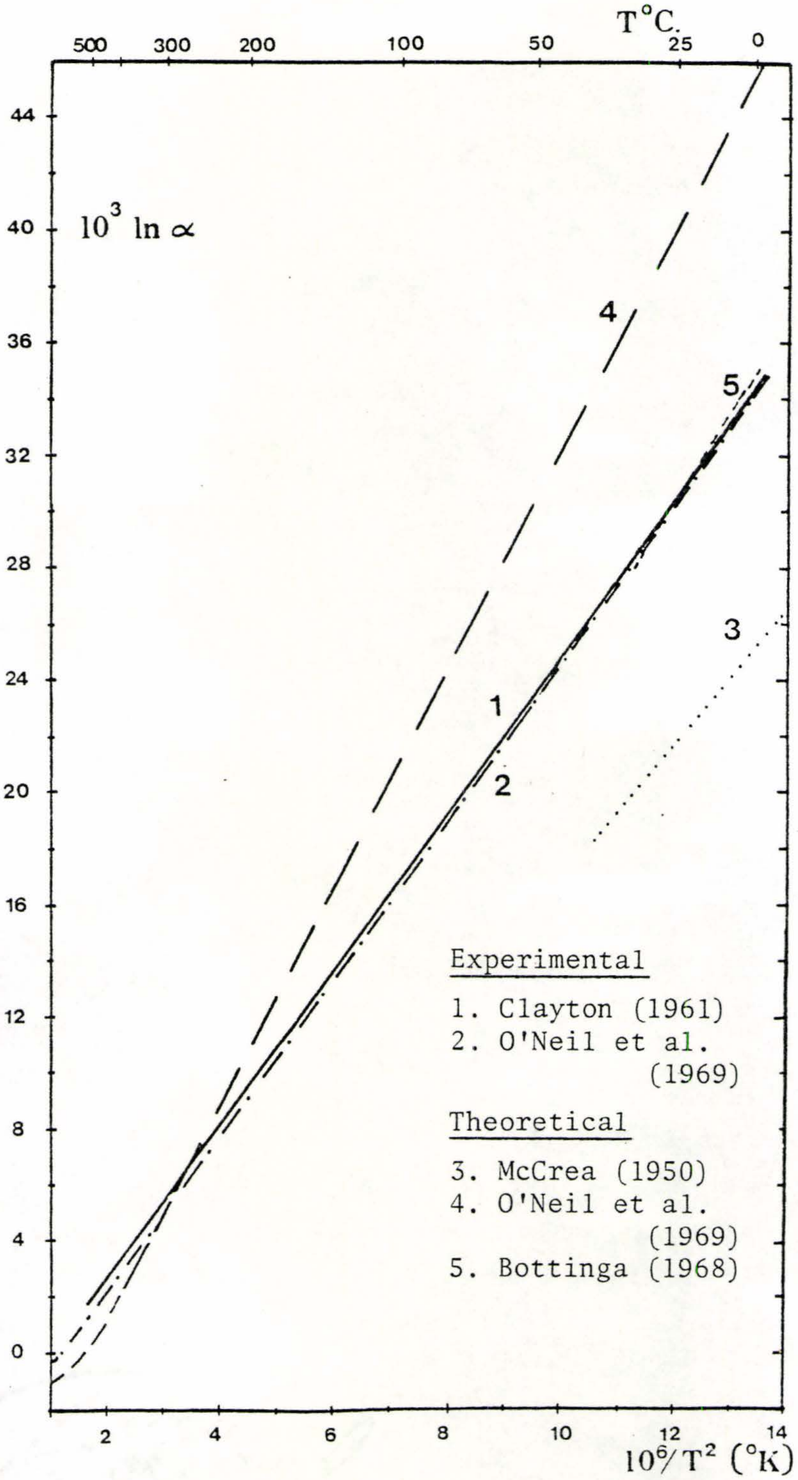

Figure 3.1 Theoretical and experimental calibrations of the calcite-water ^{18}O geothermometer.

$$1000 \ln \alpha \simeq \delta^{18}O_{X\text{-std}} - \delta^{18}O_{Y\text{-std}} \tag{3.6}$$

Hence the difference in δ value for the X-Y system is a measure of the fractionation factor, which uniquely indicates the temperature of the system.

By convention the Chicago standard PDB (a Cretaceous belemnite from the Pee Dee Formation in Southern Carolina) is used as the international primary standard for reporting oxygen and carbon isotope results in low temperature carbonates. SMOW (Standard Mean Ocean Water, a hypothetical standard defined relative to an existing water stored by the National Bureau of Standards) is similarly used as the primary oxygen and deuterium isotope standard (Craig 1961a). Because neither of these are available a series of secondary standards have been made up and their isotopic compositions accurately related to the primary standards. Carbonate standards such as NBS 20 (a sample of finely-ground Solenhofen limestone), TKL-1 and K-2 (two New Zealand carbonates) and water standards such as Vienna-SMOW (of isotopic composition almost identical to the original SMOW), NBS-1 (mid-latitude riverwater), NBS 1a and SLAP (isotopically 'light' waters from snow and ice samples) are now circulated for calibration.

3.3 The $CaCO_3$-H_2O System and Speleothem Isotopic Studies

Large variations in isotopic composition of the elements H, C and O have been found in natural materials. In particular, $\delta^{18}O_c$ of speleothem has been found to vary over 20 ‰ depending on locality, due to:

1) temperature dependence of α_{c-w} (accounting for up to 7‰),

2) variation in $\delta^{18}O$ of the water of formation (up to 20‰).

A similar range of $\delta^{13}C$ of speleothem has also been observed and this is due to:

1) variation in $\delta^{13}C$ of vegetation contributing CO_2 to the system (up to 20‰),

2) the type of limestone solutional process (Chapter 1) prior to the deposition of $CaCO_3$, which affects the amount of limestone carbon incorporated (up to 10‰).

In addition, kinetic isotope fractionation in non-equilibrium situations generally causes an added enrichment of the heavy isotope in the calcium carbonate phase. These aspects are now discussed in greater detail.

3.3.1 Isotopic Equilibrium Deposition and Kinetic Isotope Effects

A number of early studies of variations in $\delta^{18}O$ of speleothem suggested that cave deposits were not suitable for isotopic paleotemperature analysis because of non-equilibrium isotopic fractionation (Labeyrie et al. 1967; Fornaca-Rinaldi et al. 1968; Duplessy et al.1969). As an aid to recognising isotopic equilibrium deposition in a speleothem, Hendy (1971) showed that along any growth layer (or equal time horizon) of the speleothem :

1) there must be no change in $\delta^{18}O$ of the calcite

2) there must be no correlation between $\delta^{18}O$ and $\delta^{13}C$ of the calcite.

Evaporation of water is usually seen as an increase in $\delta^{18}O$ of calcite in the direction of water flow over the speleothem. Rapid loss of CO_2 will cause disequilibrium in isotopic exchange between CO_2 (gas), H_2CO_3,

HCO_3^- and CO_3^{2-}, which affects $\delta^{18}O$ and $\delta^{13}C$ in a similar manner. The problem of kinetic effects was further investigated by Fantidis and Ehhalt (1970). They analysed four speleothems from European caves and in three samples found an enrichment of ^{18}O and ^{13}C in the direction of water flow. In one case however, a depletion was seen in the flow direction (towards the tip of a stalactite). Laboratory simulation of $CaCO_3$ deposition showed that high flow rates gave rise to depletion of heavy isotopes in the direction of flow, changing to enrichment at low flow rates. For reasons of shape, flow down the side of a stalactite is often faster than down a stalagmite and so the simulation results were able to explain the speleothem characteristics.

An additional requirement in the analysis of speleothem growth layers is that analyses must be taken in the direction of flow of water. In the case of a stalagmite or stalactite this presents no problem but in the case of a fossil flowstone which is no longer in its growth position, great difficulty may be experienced in deciding the original direction of water flow. In this study, all flowstones therefore, were analysed along orthogonal directions on the same growth layers. A trend in either set of data, or in both, shows non-equilibrium growth.

Requirements for obtaining paleoclimatic results from the $\delta^{18}O$ of speleothem were set out by Hendy (1969) :

1) average isotopic composition of cave drip water must be the same as the average rain water,
2) temperature at the site of deposition must vary as little as possible (on a diurnal or seasonal basis),
3) sites where there is an appreciable draught should be avoided as this

causes rapid loss of CO_2 from solution and evaporation of water, both causes of kinetic isotope fractionation,

4) speleothem growth and drip rate should be slow.

Ideally therefore, the speleothem location should be deep within a cave, far from any entrance, relatively isolated from the main passages and streamways, the cave humidity should be 100% and the atmosphere of relatively high CO_2 content.

3.3.2 Factors Affecting $\delta^{18}O$ of Speleothem

$\delta^{18}O$ of speleothem deposited in isotopic equilibrium may vary for the following reasons:

1) change in temperature
2) change in $\delta^{18}O$ of seepage water

Factors affecting $\delta^{18}O$ of the water are numerous and complex and are described in the following sections.

3.3.2.1 Temperature Dependence of $\delta^{18}O$ of Precipitation

In the condensation of water from the atmosphere, the distribution of ^{18}O is temperature dependent, and for isotopic equilibrium $d\delta^{18}O/dT$ ranges from 0.14 ‰/°C at -20°C to 0.075 ‰/°C at 40°C (Bottinga and Craig 1969). Measurements of this fractionation are difficult to apply in practice because the condensation is usually a Rayleigh process and the fractionation varies with factors such as atmospheric temperature gradient, amount of back-exchange and re-evaporation etc. Observations of the change in $\delta^{18}O$ of N.Atlantic and Greenland precipitation with increasing latitude (and therefore decreasing surface temperature) have shown a dependence of 0.7‰/°C (Dansgaard 1964). Subsequently other workers have found significantly lower temperature dependence, particularly for continental regions, (see Table 3.2).

3.3.2.2 Speleothem Growth and Variation of $\delta^{18}O$ of Precipitation with Season

Speleothem growth rate may not be constant all year round, but may vary from season to season depending on:

1) rate of supply of water,
2) concentration of $CaCO_3$ in solution (largely dependent on biological production rate of CO_2 in the overburden),
3) changes in cave temperature,
4) periodic flooding of cave passages,
5) changes in barometric pressure gradient through the cave (causing draughts),

etc.

Due primarily to the variation of $\delta^{18}O$ of precipitation ($\delta^{18}O_p$) with temperature, $\delta^{18}O$ of cave drip water may also vary seasonally which, coupled with preferential seasonal growth, may give speleothem with a $\delta^{18}O$ record characteristic of temperatures appreciably different from mean annual cave (or surface air) temperature. Thompson et al. (1976) for West Virginia and Harmon et al. (1978a) for Kentucky, Texas and Bermuda, found that cave seepage waters were slightly enriched in ^{18}O relative to mean annual precipitation. This was explained in terms of a bias towards summer values, probably caused by greater evapotranspiration

Area Studied	$d\delta^{18}O/dT$ (‰/°C)	Reference
Antarctic snow	0.9	Picciotto et al.(1960)
N.Atlantic precipitation and Greenland ice	0.70	Dansgaard (1964)
seasonal Chicago precipitation	0.30	Stuiver (1968)
seasonal West Virginia pptn.	0.28	Thompson (1973a)
Chicago and Edmonton pptn.	0.39	Harmon et al.* (1978a)
Arizona,Texas & Mexico pptn.	0.30 - 0.33	" " "
Yukon and N.W.T. Canada pptn.	0.17 - 0.18	" " "
Bermuda pptn.	0.01	" " "
Kentucky pptn.	0.38	" " "
Maritime Europe pptn.	0.22 - 0.23	Evans et al. (1978)

* using IAEA World Precipitation Survey data for 1969-1970.

Table 3.2 Measurements of the temperature dependence of $\delta^{18}O$ of precipitation.

Method used to determine $\Delta\delta^{18}O_{sw}$	Measured* $\Delta\delta^{18}O_f$ (max) (‰)	Estimated $\Delta\delta^{18}O_{sw}$(max) (‰)	Reference
Planktonic forams. and change in extent and composition of ice sheets	1.8	0.4	Emiliani (1955)
Planktonic forams.	∿1.6	1.2	Shackleton and Opdyke (1973)
Benthonic forams.	1.65	< 1.65	Shackleton (1977)
Composition and extent of ice sheets related to sea level	-	0.9 - 1.3	Olausson (1965)
Benthonic forams.	1.8	> 1.6	Ninkovitch and Shackleton (1975)
Composition and volume of ice sheets	-	> 1.2	Dansgaard and Tauber (1969)
Composition and volume of ice sheets	-	1.6	Craig (1965)
Benthonic-planktonic foram. difference	-	1.6	Shackleton (1967)
Microfaunal assemblages and surface ocean temperatures	-	1.8	Imbrie et al. (1973)
Benthonic and planktonic foram. differences	-	1.0 - 1.5	Duplessy et al. (1970a)
Benthonic forams. in the Antarctic Ocean	0.85	0.85	Savin and Stehli (1974)

* $\Delta\delta^{18}O_f$ (max) = the maximum change in $\delta^{18}O$ of foraminifera analysed

Table 3.3 Estimations of maximum change in $\delta^{18}O$ of seawater ($\Delta\delta^{18}O_{sw}$(max)) from glacial to interglacial times.

effects during summer months. In all cases however, the drip waters showed insignificant seasonal variation and mean annual drip waters were found to be in isotopic equilibrium with calcite forming from them, at the mean cave temperature.

3.3.2.3 Variation with Storm Trajectory

Dansgaard (1964) showed that $\delta^{18}O$ of precipitation was dependent on the distance the airmass had travelled over land, in that the farther it travelled, the lower the $\delta^{18}O$. This was attributed to progressive 'rain-out' of the heavy isotope as well as the effects of exchange with isotopically 'light' freshwater and increasing participation in convective processes where temperature gradients are steeper. During a glacial to interglacial transition, it is very likely that airmass trajectories over continents will change and so affect the mean $\delta^{18}O$ of precipitation at a given site. The CLIMAP project (Gates 1976) has recently modeled atmospheric circulation patterns for the northern hemisphere for July 18,000 years ago (the best estimate for maximum glacial conditions during the Late Wisconsin). For mid-continental North America however, it is thought that precipitation patterns are comparable to those of winter months today and that no appreciable change in $\delta^{18}O_p$ due to this effect would be seen (Harmon et al. 1978a). It is likely that the most important changes in $\delta^{18}O_p$ due to storm trajectory will occur during the actual transition between climatic periods and modeling of this has so far not been attempted.

3.3.2.4 Variation with $\delta^{18}O$ of Source

Early results of $\delta^{18}O$ profiles of deep sea carbonate cores were interpreted as reflecting a change in tropical ocean surface water temperatures of up to 6°C from glacial to interglacial times (Emiliani 1955). This corresponded to about 1.3 ‰ of the observed change of 1.8 ‰ in $\delta^{18}O$ of planktonic foraminifera in the core. These calculations were based on an estimate for the amount of ^{18}O-depleted water stored on the continents as ice during maximum glaciation. Re-calculation of ice volume and average $\delta^{18}O$ of ice by later workers (Olausson 1965, Dansgaard and Tauber 1969) and analyses of benthonic foraminifera in cores from the Caribbean, eastern Pacific and Atlantic Oceans (Shackleton 1967, Duplessy et al. 1970a) have strongly indicated that most of the change in $\delta^{18}O$ of core profiles is due to changes in the isotopic composition of ocean water, not temperature. Various estimates of this change are listed in Table 3.3, and it is presently felt that change due to temperature is at most only about 10% of the total (Ninkovitch and Shackleton 1975).

3.3.3 The Determination of Paleotemperature

The interplay of factors affecting $\delta^{18}O$ of precipitation make it difficult to express variations in $\delta^{18}O$ of speleothem in terms of temperature change. The following approaches have been used.

3.3.3.1 The Oceanic Island Situation

Hendy and Wilson (1968) radiocarbon-dated two speleothems from caves in New Zealand and were first to express a $\delta^{18}O_c$ profile in terms of paleotemperature change. To show that the samples were formed in isotopic equilibrium with dripwater, they used:

1) the constancy of $\delta^{18}O_c$ along three growth layers of one speleothem
2) the lack of correlation between $\delta^{18}O_c$ and $\delta^{13}C_c$ along the three growth layers
3) the finding that isotopic equilibrium deposition exists between modern calcite deposits and groundwater in the same cave.

Because of the proximity to the ocean, Hendy and Wilson argued that the temperature dependence of $\delta^{18}O_p$ should follow Dansgaard's value of 0.69 ‰ /°C, and therefore a change in temperature gradient between the tropical ocean and precipitation site for a given change in climate would affect $\delta^{18}O_c$ of speleothem thus:

$$\Delta\delta^{18}O_c = \Delta\delta^{18}O_{sw} - 0.69\ (T_x - T) + 0.24\ T_x \qquad (3.7)$$

where T_x is the decrease in temperature at the site and T is the decrease in temperature of the tropical ocean surface water. The first and last terms on the right hand side of equation 3.7 act together ($\delta^{18}O_{sw}$ increases when temperature decreases) and the second term runs counter to the other two. Using a maximum of 6°C change in New Zealand's temperature from glacial to interglacial and a measured $\Delta\delta^{18}O_c$ of 0.95‰ for the same period, Hendy and Wilson were able to calibrate their $\delta^{18}O_c$ record in terms of temperature. Re-arrangement of equation 3.7 gives:

$$\Delta\delta^{18}O_c = \Delta\delta^{18}O_{sw} + 0.24\ T - 0.45\ (T_x - T) \qquad (3.8)$$

in which $\Delta\delta^{18}O_{sw} + 0.24\ T = 1.4$ ‰ (the total change of $\delta^{18}O_f$)

Therefore $0.95 = 1.4 - 0.45 (T_x - T)$

and $(T_x - T) = 1$

Therefore the temperature difference between New Zealand and the tropics must have increased by 1°C between the last glacial maximum (20 Ka B.P.) and the present. If the full change in $\delta^{18}O_c$ is used (1.2 ‰ at 26 Ka B.P.) the temperature differential reduces to 0.4°C, a result which is incompatible with current estimates of ocean temperature change and spatial distribution (Gates 1976). Using the estimate of $\Delta\delta^{18}O_{sw}$ from Ninkovitch and Shackleton (1975), Hendy and Wilson's results may be re-calculated;

$$1.2 = 1.8 - 0.45 (T_x - T)$$

$$(T_x - T) = 1.3^{o}C$$

This value is still quite low but may be higher if the temperature dependence of precipitation is less than Dansgaard's value of 0.69 ‰ /°C (as may be the case in precipitation falling at altitudes greater than sea level and inland from the coast).

A less sophisticated approach to paleotemperature interpretation was taken by Labeyrie et al. (1967) and Geyh (1970). Using radiocarbon dating and stable isotope analysis along the axis of two Holocene stalagmites, both groups found correlation between $\delta^{13}C_c$ and $\delta^{18}O_c$ and interpreted the variations in terms of change in climate. A decrease of 0.46 ‰

in $\delta^{18}O_c$ was taken to represent a temperature <u>decrease</u> of 1°C (Labeyrie et al. 1967).

A similar direct relationship was assumed by Duplessy et al. (1970b). In this study uranium series methods were used to date a 2.3m long stalagmite from Aven d'Orgnac, southern France. They assumed that it was deposited in isotopic equilibrium by the absence of air movements in the cave, and by lack of correlation between $\delta^{18}O_c$ and $\delta^{13}C_c$ for points along the growth <u>axis</u>. (As previously noted, the latter is not a criterion for equilibrium deposition). They interpreted $\delta^{18}O_c$ changes in terms of temperature using the relationship

$$\Delta\delta^{18}O_c = 0.69\ \Delta t - 0.24\ \Delta t = 0.45\ \Delta t \tag{3.9}$$

Δt is the variation in surface temperature above the cave.

This relationship ignores:

1) the effect of changes in $\delta^{18}O_{sw}$
2) the change in temperature of tropical ocean surface water (designated 'T' in Hendy and Wilson's work)
3) the possible effect of change in wind trajectory accompanying a climate change

From this, Duplessy et al. proposed a direct relationship of $\delta^{18}O_c$ with temperature, and interpreted the speleothem record as a prolonged warm period from 120 Ka to 97 Ka B.P., sharply bounded on either side by cold periods, with a further warm period terminating growth at about 92 Ka B.P.

3.3.3.2 Use of Modern $\delta^{18}O_c$

Emiliani (1971) was the first to apply the $\delta^{18}O$ of modern cave calcites to the interpretation of $\delta^{18}O_c$ profiles from fossil speleothems. He made the simple assumption that recurrence of modern values in the past indicates deposition under similar conditions to the present. In this way he was able to invert the isotope profile of Duplessy et al. (1970b) and relate the ^{18}O depleted peak at 95 Ka B.P. to the stage 5 interglacial maximum seen in deep sea core records. Further justification for this lies in the fact that speleothem growth rate increased four-fold over this period, as might be expected in warm humid climates.

In more recent detailed studies Thompson et al. (1976) and Harmon et al. (1978a) have used $\delta^{18}O$ of modern speleothem as an indicator of interglacial conditions in their interpretation of $\delta^{18}O_c$ profiles of dated North American speleothems. Good agreement with $\delta^{18}O_c$ (modern) and known warm events in the Late Pleistocene was found in speleothem from West Virginia, Iowa and Bermuda, but a poor to inverse relationship in speleothem from Kentucky and the Canadian Rockies.

3.3.3.3 Allowance for $\delta^{18}O_{sw}$

As previously described, the change in $\delta^{18}O$ of seawater from glacial to interglacial times is now thought to be the dominant factor controlling $\delta^{18}O$ of deep sea carbonate cores. Due to this reversal in thinking, new interpretations have been made concerning the significance of changes in $\delta^{18}O_c$ of speleothem because water vapour from the oceans during glacial times was up to 1.8‰ heavier than in interglacial times. This effect is seen as a concomitant change in speleothem calcite forming in a cave (Harmon et al. 1978a). Analysis of $\delta^{18}O_c$ of speleothem from caves in Iowa and Bermuda have been corrected for change in $\delta^{18}O_{sw}$ by these authors. To do this, the assumption was made that the difference, Δ_t, between $\delta^{18}O$ of foraminiferal tests ($\delta^{18}O_{f(t)}$) at time t and $\delta^{18}O$ of modern tests ($\delta^{18}O_{f(0)}$) was equal to the corresponding change in $\delta^{18}O_{sw}$, ie.

$$\begin{aligned} \Delta_t &\equiv \delta^{18}O_{f(t)} - \delta^{18}O_{f(0)} \\ &= \delta^{18}O_{sw(t)} - \delta^{18}O_{sw(0)} \qquad (3.10) \end{aligned}$$

Values of Δ_t were read off from the data of Ninkovitch and Shackleton (1975) for core V19-29, assuming ages based on constant sedimentation rate and a $\delta^{18}O$ minimum at -820cm in the core, corresponding to isotopic stage 5e (125 Ka). The full range of $\delta^{18}O_f$ (Δ_t = 1.8 ‰) was used without allowance for changes due to temperature. The effect of this correction on the Bermuda data was found to be slight (Figure 3.2) mainly serving to shift $\delta^{18}O_c$ to more negative values. In the Iowa data however, a decrease of about 2‰ in $\delta^{18}O_c$ during the Late Wisconsin deglaciation completely disappeared after correction for $\delta^{18}O_{sw}$. If it can be assumed that temperature increased by 10 to 15°C during this period, then the corresponding change of about - 2.5 to - 3.5‰ in speleothem calcite must have been offset by a similar but opposite change in $\delta^{18}O$ of precipitation ($\delta^{18}O_p$). This order of change is quite acceptable judging from the data in Table 3.2.

Many of these problems associated with interaction of $\delta^{18}O_{sw}$ and $\delta^{18}O_p$ can be circumvented by the direct analysis of the water of deposition preserved as fluid inclusions in the speleothem calcite.

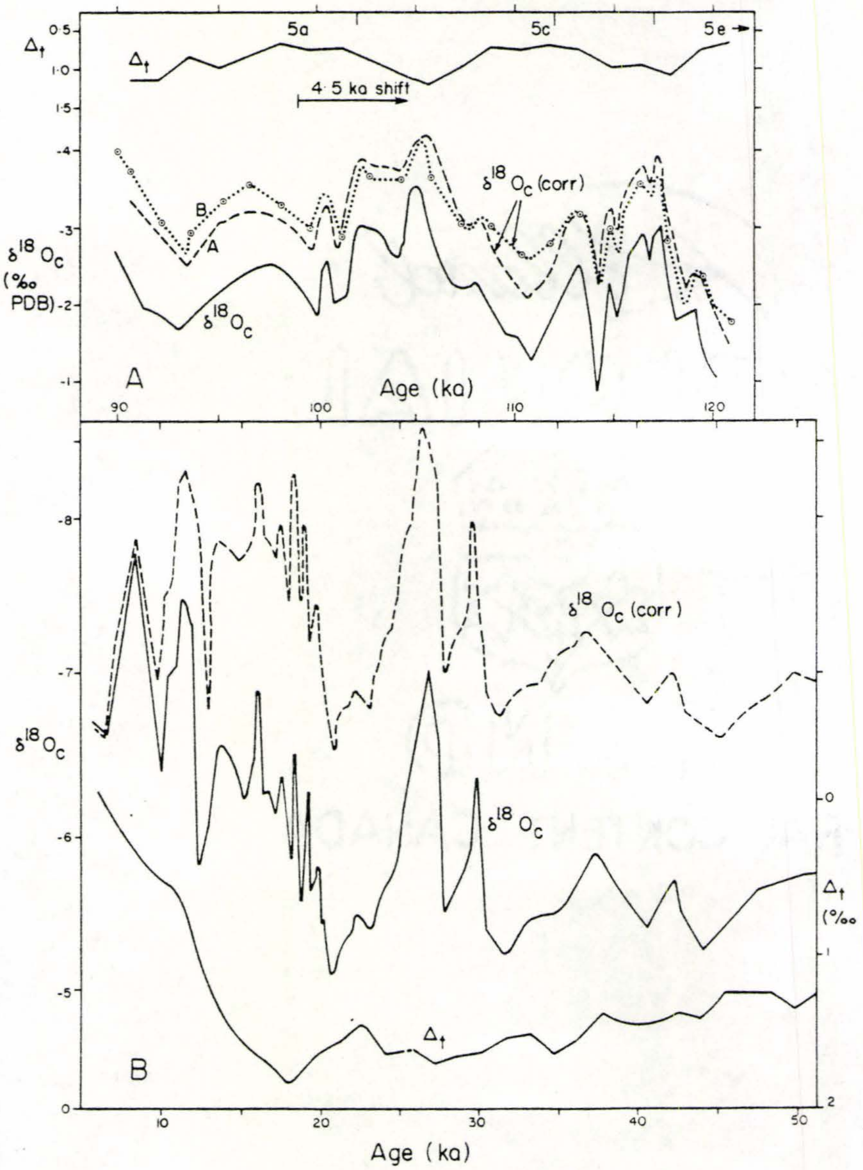

Figure 3.2 Two speleothem $\delta^{18}O_c$ records, from Bermuda (A, upper) and Iowa (B, lower) showing the effect of correcting for change in $\delta^{18}O_{sw}$ (shown as Δ_t, the difference between modern and fossil values of $\delta^{18}O$ of benthic foraminifera in Pacific core V19-29; Ninkovitch and Shackleton 1975). Curve B in upper plot is as curve A but shifted by 4.5 Ka so that stage 5c is coincident with the oldest maximum in the $\delta^{18}O_c$ curve.

3.3.4 Fluid Inclusion Analysis

3.3.4.1 Application to Speleothem

Growing speleothem traps small fluid inclusions (f.i.) of drip water between crystal faces, and this 'paleowater' can be subsequently extracted and analysed isotopically (Schwarcz et al.1976). For speleothem formed in isotopic equilibrium with the drip water, the difference in $\delta^{18}O$ between the two phases is related to the temperature of deposition thus:

$$1000 \ln \alpha_{c-w} = 2.78 \left(\frac{10^6}{T^2}\right) - 2.89 \quad \text{(O'Neil et al. 1969, 1975)} \tag{3.11}$$

where $$1000 \ln \alpha_{c-w} = \frac{1 + 10^{-3}\delta^{18}O_c}{1 + 10^{-3}\delta^{18}O_w} \tag{3.12}$$

Because of the likelihood of subsequent exchange of ^{18}O with host calcite at temperatures different to those during deposition, $\delta^{18}O_{f.i.}$ may be unsuitable for comparison with $\delta^{18}O_c$ for determination of paleotemperatures. The hydrogen component of the inclusion however is not exchangeable since calcite contains no hydrogen, and measurement of the D/H ratio of fluid inclusions can then be related to the original $\delta^{18}O_{f.i.}$ by the meteoric water relationship.

3.3.4.2 The Meteoric Water Relationship

Isotopic analysis of many types of meteoric water (seawater, rivers, lakes, snow and ice) for many different climatic regimes has been shown frequently to give the same empirical relationship (Craig 1961b, Dansgaard 1964) :

$$\delta D = 8\,\delta^{18}O + 10 \qquad (3.13)$$

Using isotopic data from the IAEA-WMO precipitation survey, Dansgaard (1964) recognised certain controlling factors in the determination of isotopic character of precipitation and described a number of locations which did not conform to the above relationship. His findings can be summarized as follows :

1) the δD - $\delta^{18}O$ relationship calculated from known fractionation factors is $\delta D = 8\,\delta^{18}O$ for equilibrium (Rayleigh) condensation and isothermal evaporation processes.
2) non-equilibrium processes affect the slope (m) and introduce an intercept (c) into the relationship, thus: $\delta D = m\,\delta^{18}O + c$
3) non-equilibrium evaporation from i) a limited water body, gives rise to deuterium depletion (ie. negative 'c') and usually $m < 8$; ii) an infinite, well-mixed water body gives a fairly constant and positive c, and $m \cong 8$.
4) non-equilibrium condensation rarely occurs in nature but it can give rise to $m > 8$.

3.3.4.3 Requirements for Paleotemperature Determination in Speleothem

In order to use $\delta D_{f.i.}$ to determine $\delta^{18}O_{f.i.}$ and hence paleotemperature, equation 3.13 or its equivalent, must be shown to be valid over the period of growth of the speleothem. Two approaches to this have been used:

1) analysis of modern calcite and drip waters at the speleothem site. Comparison of mean annual cave temperature with those calculated from fluid inclusions in modern speleothem from West Virginia have shown good agreement (Thompson et al. 1976).
2) examination of isotopic relationships in the ice core record (this would show any variation due to climatic change). Dansgaard et al. (1969) and Epstein et al. (1970) found no change in the δD - $\delta^{18}O$ relationship for polar ice throughout the Late Pleistocene and it has been argued that the same may be true for unglaciated continental North America (Schwarcz et al. 1976). However, in recent determinations of paleotemperatures for the Late Wisconsin in Iowa (Harmon et al. 1979b). use of equation 3.13 gives sub-zero temperatures for part of the growth period of one speleothem. A more realistic paleotemperature record is given by $\delta D = 8\ \delta^{18}O$, suggesting that isotopic characteristics of precipitation may change with climate.

Additional requirements for the use of fluid inclusions in paleotemperature analysis are : 1) the isotopic equivalence of precipitation and cave drip water (this has already been discussed) and 2) the lack of leakage and isotopic fractionation of the inclusions after formation. Calculation of fairly realistic temperatures (between -2 and 20°C) in work done so far is the best testimony that this effect is not important. However a number of temperatures that appear to be too low have been determined for Bermuda (4.5°C), San Luis Potosi, Mexico (6.9°C) and West Virginia (-1.6°C). Possible reasons for this include variation of the δD - $\delta^{18}O$ relationship during the past (as described above) and analytical difficulties. Most of the work was done using soft copper tubing in the crushing operation and subsequent work by Dr.T.Fallick showed the possibility of contamination by appreciable amounts of water present in the tubing which could only be removed by prolonged heat and vacuum treatment before use. Furthermore it was found that after crushing an extraction time of up to 24 hrs was required to completely transfer all liberated inclusions. In previous work, much shorter times were used and so presumably the isotopically lighter fraction would be preferentially collected and this would account for the low calculated paleotemperatures.

In the present work, no fluid inclusion analysis was attempted due to initial problems in $\delta^{18}O$ measurements using the mass spectrometer and the subsequent shortage of suitable isotopic equilibrium deposits in the areas of study.

3.4 Analytical Techniques

3.4.1 Gas Preparation

10 to 25mg of powdered calcium carbonate was taken from an acid-cleaned, dry face of a sectioned speleothem using a low-speed electric drill and 1/16th inch bit. Carbon dioxide was then generated by reaction under vacuum with 100% H_3PO_4 in one of two ways: in individual, isolated reaction vessels at 25°C for 12 - 24 hours (after the method of McCrea (1950) or by reaction of successive aliquots of carbonate in a vat of acid at 50°C for 15 - 30 mins. (a modification of the method used by Shackleton and Opdyke (1973), Shackleton (pers.comm.1979). CO_2 produced in each case was dried by at least 3 passes through dry ice-

$CCl_4/CHCl_3$ traps and yield measured by Hg manometer and checked against expected yield before storage in gas vessels. The 25°C method of preparation has been used in all previous work, although yields were generally not measured. The 50°C method was investigated as a means of speeding up the gas preparation step without incurring additional errors. However the results of tests of

1) reproducibility on 23 preparations (Table 3.4)
2) memory effect using alternate samples of 'light' and 'heavy' calcite (Table 3.5a)
3) variation of $\delta^{18}O_{CO_2}$ with reaction time (Table 3.5 b)

suggest that isotopic exchange with previously generated gases and water could occur and so influence the results.

From Table 3.4 it can be seen that the preparation of CO_2 from $CaCO_3$ using H_3PO_4 is temperature dependent, by about-0.04‰/°C.

3.4.2 Mass Spectrometry

A 6-inch radius, 90° sector, double collecting mass spectrometer was used to determine relative isotopic abundance ratios of CO_2 generated from speleothem carbonate. The mass spectrometer follows the design by Nier (1947) and uses electro-magnetic change-over valves in the inlet system to provide rapid comparison of standard and sample gases (McKinney et al. 1950). In operation, CO_2 from the standard gas reservoir is allowed to 'leak' through narrow-bore capillary tubes into the mass spectrometer where it is ionized by electron bombardment from a tungsten source. The ions are accelerated by a potential drop through a magnetic field, where they are deflected according to their mass. The resulting

Analysis Number	vs.GCSWS number	No. of samples analysed	$^{46}\delta$(raw) (± 1s) (‰)	No. of samples analysed	$^{45}\delta$(raw) (±1s) (‰)
GCS 4* to GCS T6	2	23*	-0.972±0.302**	17*	-0.315±0.294**
GCS W1 to GCS W6	2	5	0.026±0.167	6	-0.097±0.114
GCS C1 to GCS 38	3	10	0.119±0.141	7	-0.096±0.139
GCS 38 to GCS 42	4	5	0.010±0.094	1	-0.13
	CAPILLARIES CRIMPED				
GCS 43 to GCS 49	4	5	-0.176±0.059	6	-0.122±0.091
	NEW FILAMENT				
GCS 51 to GCS 54	5	4	-0.155±0.079	4	-0.078±0.017

* Sample gases prepared at 50°C

** 1σ error

Table 3.4 Summary of results of analysis of same carbonate samples (GCS) on different occasions, against different batches of working standard gas (GCSWS). Standard deviation of the mean is determined for each group.

Carbonate Sample	$^{46}\delta$ (‰)	$^{45}\delta$ (‰)
GCS 10	-0.88	-0.04
NAH 1	-7.07	-6.75
GCS 11	-0.98	-0.20
NAH 2	-7.06	-6.80
GCS 12	-0.91	-0.20
NAH 3	-6.51	-6.11

Table 3.5a Results of test for memory effect using the 50°C carbonate reactor and sequential addition of carbonates (GCS and NAH powdered standards) of differing δ values. NAH 3 can be seen to be appreciably heavier than previous analyses.

Sample No.	Reaction Time (mins.)	Yield (%)	$^{46}\delta$ (‰)	$^{45}\delta$ (‰)
GCS 25	0 - 30	94.4	-1.17	-0.66
	30 - 60	4.1	-0.97	-
	60 - 75	0.7	-1.50	-
	75 - 90	0.2	-0.81	-
	90 - 120	0.2	-2.86	-
	120 - 180	0.2	-4.19	-
GCS 26	0 - 30	-	-1.14	-0.13
	30 - 60	-	-1.75	-0.83
	60 - 180	-	-	-4.41

Table 3.5b The variation of $^{46}\delta$ and $^{45}\delta$ with reaction time using the 50°C carbonate reactor for two carbonate samples. Increasingly light gas is collected throughout the reaction.

ion beams are collected giving ion currents representing masses 44 and 45, or (44 + 45) and 46 depending on the focussing of the mass spectrometer. The ion currents are approximately balanced by a Kelvin-Varley voltage divider and residual current is displayed on a strip-chart recorder. Sample gas at the same pressure is introduced via the change-over valves and analysed in the same manner. After a number of comparisons between sample and standard the relative isotopic abundance ratio of the sample can be determined from the difference in setting of the sample and standard dividers, and recorder trace separations. The value obtained is termed 'δ_{raw}' and must then be corrected for instrumental characteristics and isotope abundance effects, as described later.

3.4.3 Operational Characteristics

A series of problems beset initial mass spectrometer work, in some cases causing the machine to be out of action for months at a time. Problems with magnet supply, source voltage dividers, change-over valve magnets, accelerating voltage supply, source and collector lead-throughs and burnt-out filaments were commonplace. These problems were eventually solved and routine analysis began in early 1977.

3.4.3.1 Standard Gases

The mass spectrometer working standard was carbon dioxide prepared from Grenville marble calcite (GCS). Up to 500mg GCS was used in one reaction to make approximately 0.5 atmospheres in a 250ml reservoir on the mass spectrometer line. Small cuts of this were taken when required. During most runs the same gas sample from a preparation of

NBS 20 (Solenhofen limestone) was analysed to check on machine drift.

3.4.3.2 Isotopic Enrichment of Standard Gas

During the course of routine twin tests (comparison of a fresh cut of working standard with gas already in use) it was discovered that the working standard gas was becoming isotopically enriched during the course of a run. The reason for this was taken to be back-diffusion of gas in the capillary leak allowing preferential retention of the heavier isotope gas molecules. To prevent this, most gas-source mass spectrometers are fitted with crimped capillaries and run at pressures of $\geqslant$ 4cm Hg on the high pressure side of the capillary. Gas flow through the leaks in these conditions becomes viscous and back-mixing does not occur. On the machine used here the capillaries had never been crimped and the inlet pressure was only about 0.5 - 1cm Hg. For the present work, the magnitude of the enrichment effect was measured on each run and, assuming linearity, a time-related correction was added to each raw sample δ value. After each run the machine standard was pumped away. Over the period of measurement the following results were determined :

	no. of cases	range (‰/hr)	mean ± 1σ (‰/hr)
$\Delta^{46}\delta$	56	0.15 to -0.02	0.048 ± 0.029
$\Delta^{45}\delta$	42	0.09 to -0.01	0.025 ± 0.019

The large range of enrichments seen above is probably due to variations in the volume of standard gas in the reservoir and occasional changes in mass spectrometer running pressure. It is interesting to note that mean $\Delta^{46}\delta$ is almost exactly double that of mean $\Delta^{45}\delta$, as might be expected on theoretical grounds. Since a run might last from two to ten hours using the same standard gas, a total enrichment of 0.5 ‰ or more could be seen, and so it was essential to correct for this enrichment first before correcting to the daily secondary gas standard. Longstaffe (1977) also used this procedure for correcting raw δ values and in 25 determinations observed a range of $\Delta^{46}\delta$ = 0.037 to 0.085‰/hr and a mean of 0.069‰/hr. In January 1978, new thick wall capillaries were fitted (I.D. = 0.007") and crimped, so that a 4 - 5cm Hg reservoir pressure of gas gave a pressure at the source of the mass spectrometer of $\sim 5 \times 10^{-7}$ mm Hg. Subsequently, regular checks on the machine standard showed that even after two weeks of daily use of the same aliquot, no measurable enrichment had occurred.

3.4.3.3 Inlet System

With the use of a spiral trap for water vapour in the gas transferring apparatus, it was found unnecessary to use a dry ice trap on the mass spectrometer inlet line. This reduced time spent in gas handling before analysis but because of the higher pressure requirement when the capillaries were crimped, the entire gas sample had to be frozen over into the inlet reservoir. This caused problems of reproducibility of analysis because on warming up, the gas had to be mixed by repeated pumping of the mercury pistons in the reservoir and left for five minutes to completely equilibrate. If this was not done, the measured δ value could be seen to shift during the run. Finally, the volume of the inlet system was reduced sufficiently to allow a cut of the expanded gas to be taken, which when compressed gave sufficient pressure for operation without requiring complete transfer by freezing or use of more carbonate in the preparation stage.

3.4.3.4 Pressure Dependence of δ

It was found that a small change in gas pressure (usually of the sample relative to the standard gas) caused an appreciable change in measured δ value. Using the mass 44 signal displayed on the millivolt meter, a dependence of about -0.07‰/mV was observed from one measurement. This effect is opposite to what might be expected from poor peak shape and larger contributions of 44 tail at higher pressures, and may instead be due to pressure dependent fractionation at the capillaries. Care was taken therefore to exactly match sample and standard mass 44 signals during analysis and each sample was routinely analysed twice for $^{46}\delta$ on different days (and a third time if necessary) until analyses lay within 0.1 ‰ of each other. Usually only one measurement of $^{45}\delta$ was made.

3.4.4 Machine Correction Factors

3.4.4.1 Valve Mixing Correction

Because of the imperfect seal at ground glass joints in the change-over valves, leakage may occur across the valves when closed, thus contaminating the gas being analysed. The measured isotopic difference between sample and standard is therefore less than the true difference and the correction factor is determined as a multiplicative factor (> 1.0) by a method similar to Dienes (1970). The change in mass 44 ion current was measured when a gas was removed from the waste side of the changeover valves. This was expressed as a fraction of the full mass 44 current (f_1) at normal running pressure and was added to the analogous value (f_2) determined when the valves were switched over and gas introduced to the other reservoir. The valve mixing correction is therefore :

$$\mathrm{VMC} = 1 + f_1 + f_2 \tag{3.14}$$

and the raw δ value corrected for valve leakage is :

$$\delta_{c'} = \delta_{raw} \cdot \mathrm{VMC} \tag{3.15}$$

Schwarcz (1971) found that leakage of both valves was negligible and subsequent workers used no correction. In July and October 1978 the mixing correction was redetermined and found to be about 1.007, with one valve accounting for over 80% of this leakage. This value was used to correct all results in this work.

3.4.4.2 Tail Correction

The overlap of the large mass 44 peak tail onto masses 45 and 46 is usually determined graphically and expressed as an 'abundance sensitivity' correction (Deines 1970). The current measured on the narrow collector at a given accelerating voltage is divided by the maximum current of the mass 44 beam, and its inverse, the abundance sensitivity, is plotted against accelerating voltage for a scan over the mass peaks of interest. The mean overlap is measured for each of the minor peaks and

and expressed as a multiplicative correction factor. In July 1978, abundance sensitivity corrections were determined as $ASC^{46} = 1.0082$, $ASC^{45} = 1.0103$. Previous values determined by Schwarcz (1971) were 1.0041 and 1.012 respectively; these were used in most previous work without redetermination.

Raw δ measurements are corrected for the above effects as follows:

$$^{46}\delta_c = {}^{46}\delta_{raw} \;.\; VMC \;.\; ASC^{46} \qquad (3.16)$$

$$^{45}\delta_c = {}^{45}\delta_{raw} \;.\; VMC \;.\; ASC^{45} \qquad (3.17)$$

Other corrections to raw data cited by Deines (1970) include background, difference in voltage dividers and capillary leak fractionations, but these tend to be cancelled out by comparison to a secondary standard analysed in sequence with the samples.

3.5 Precision and Accuracy

Estimation of precision in mass spectrometry can be based on four types of measurements:

1) same gas run on same 'day'
2) same gas run on different 'days'
3) different gas preparations of same sample run on same 'day'
4) different gas preparations of same sample run on different 'days'

where the term 'day' is taken to mean 'period of operation'. Types 2 and 4 usually provide the most information on reproducibility and usually give the largest error limits. Periodic variations (day-to-day or longer term) in mass spectrometer characteristics may also necessitate normalization of all samples to a standard, analysed in sequence with them. The merits of this procedure have also been investigated in this section.

3.5.1 The Effect of Using Crimped Capillary Leaks

Because of the drastic change in operational characteristics after the change-over to crimped capillaries, measurement precision is considered in two parts : before and after crimping.

3.5.1.1 Before Crimping

Analyses made during this period (prior to January 1978) were subject to corrections for time dependent enrichment of the working standard gas as previously described. To determine error limits of type 4 analyses during this period, 43 samples of GCS were prepared over 10 months and means and standard deviations calculated for each group run against the same preparation of working standard or at the same preparation temperature (Table 3.4). Large error limits can be seen for $^{46}\delta$ and $^{45}\delta$ analyses (between ±0.1 ‰ and 0.3 ‰). This range is comparable to that of analyses of the same NBS 20 gas on a different day (type 2) shown in column 5 of Table 3.6. Preparative errors therefore seem to be minor in comparison to those incurred in correcting for time-dependent enrichment of working standard gas.

3.5.1.2 After Crimping

Analyses made after January 1978 were not affected by enrichment of standard gas and accordingly show much better precision. Standard

					5		6	7		8	
Period of Analysis	Preparation Number	Preparation Temperature (^{o}C)	Number of Analyses		Arithmetic Means (±1s)		Working Standard Prepn. No.	Weighted Group Means (±1s)			
			$^{46}\delta$	$^{45}\delta$	$^{46}\delta_{NBS-GCS}$ (‰)	$^{45}\delta_{NBS-GCS}$ (‰)		$^{46}\delta_{NBS-GCS}$ (‰)	$^{45}\delta_{NBS-GCS}$ (‰)	$^{18}\delta_{GCS-PDB}$ (‰)	$^{13}\delta_{GCS-PDB}$ (‰)
29/6/76 to 21/2/77	NBS 20-F	25	3	0	7.523±0.047	-	GCSWS 2	7.550±0.304	-1.367±0.021	-11.750	0.688
	NBS 20-E	25	5	7	7.064±0.205	-1.359±0.058					
	NBS 20-1	25	7	5	7.669±0.124	-1.402±0.036					
	NBS 20-2	25	7	1	7.791±0.110	-1.25					
1/4/77 to 6/7/77	NBS 20-3	50	0	1	-	-1.90	GCSWS 2	6.420±0.049	-1.608±0.031	-10.620	0.911
	NBS 20-4	50	5	7	6.758±0.047	-1.446±0.034					
	NBS 20-5	50	1	2	5.71	-1.910±0.040					
	NBS 20-6	50	3	2	6.093±0.064	-1.725±0.015					
18/7/77 to 12/12/77	NBS 20-MG	25	3	4	7.860±0.243	-1.443±0.057	GCSWS 3	7.953±0.140	-1.370±0.070	-12.149	0.702
	NBS 20-TF	25	2	2	7.905±0.235	-1.385±0.005					
	NBS 20-MG2	25	2	3	7.750±0.080	-1.340±0.197					
	NBS 20-7	25	1	2	8.07	-1.495±0.035					
	NBS 20-8	25	16	4	7.942±0.145	-1.415±0.050					
	NBS 20N-1	25	15	10	8.010±0.115	-1.303±0.046					
14/12/77 to 15/1/78	NBS 20-8	25	3	0	7.713±0.225	-	GCSWS 4	7.698±0.177	-1.37	-11.899	0.693
	NBS 20N-1	25	6	1	7.795±0.237	-1.37					
	NBS 20-9	25	3	0	7.607±0.117						
	NBS 20N-2	25	3	0	7.580±0.122						
CAPILLARIES CRIMPED											
26/1/78 to 25/6/78	NBS 20-8	25	1	1	7.54	-1.47	GCSWS 4	7.489±0.071	-1.393±0.055	-11.690	0.708
	NBS 20N-1	25	10	1	7.530±0.058	-1.34					
	NBS 20N-3	25	7	1	7.470±0.122	-1.42					
	NBS 20N-4	25	23	6	7.470±0.078	-1.365±0.065					
	NBS 20N-5	25	17	7	7.492±0.054	-1.410±0.036					
NEW FILAMENT											
26/6/78 to 6/11/78	NBS 20N-5	25	6	0	7.562±0.087	-	GCSWS 5	7.608±0.079	-1.335±0.057	-11.808	0.652
	NBS 20N-6	25	12	5	7.608±0.088	-1.38 ±0.039					
	NBS 20N-7	25	18	6	7.623±0.071	-1.30 ±0.072					
6/11/78 to 10/12/78	NBS 20N-7	25	15	8	7.604±0.034	-1.347±0.034	GCSWS 5	7.604±0.034	-1.347±0.019	-11.804	0.665
13/12/78 to present	NBS 20N-7	25	22	10	7.566±0.051	-1.381±0.036	GCSWS 6	7.569±0.052	-1.371±0.036	-11.768	0.690
	NBS 20N-8	25	5	1	7.580±0.054	-1.27					

Table 3.6 Means and standard deviations for all analyses of NBS 20 standard gas preparations, determined against different preparations of working standard gas (GCSWS). Derivation of data in columns 7 and 8 are described in text and Appendix 2.

deviations for analyses of 9 preparations of GCS (Table 3.4) show limits of less than ± 0.1 ‰ for both $^{46}\delta$ and $^{45}\delta$, and this is in good agreement with those of 'daily' analyses of 8 preparations of NBS 20 over an 11 month period (column 5, Table 3.6). A slight increase in $^{46}\delta_{NBS-GCS}$ is seen after June 1978, which may be due to use of a new batch of GCS working standard.

3.5.2 Correction to a 'Daily' Secondary Standard

In some previous work with this machine it was thought necessary to correct raw sample results to the 'daily' value for a secondary standard gas (Harmon 1975). However, Olson (1975) found that no improvement in precision was gained by making such a correction; in fact, use of the raw analytical results gave better overall precision, and no normalisation was therefore made. Longstaffe (1977) normalised to an hourly-run secondary standard as a means of correcting for enrichment of standard gas rather than for 'daily' fluctuations. In the present study a comparison was made between the overall mean error of duplicate (post-crimping) analyses of 132 gas samples (the duplicate was run on a different 'day' in all cases) and the overall mean error when each analysis of the pair was corrected to the NBS 20 value for that 'day'. For 132 pairs, overall mean error for uncorrected results is ± 0.045 ‰ and overall mean error for corrected results is ± 0.053 ‰, a value which is nearly 20% larger. It therefore seems that, for this work at least, no improvement in precision can be gained by correcting to 'daily' analyses of a secondary standard.

3.5.3 Conversion to PDB Standard

To permit conversion of raw results to the PDB standard, group means of NBS 20 analyses were determined (column 7, Table 3.6) by averaging 'daily' analyses of NBS 20 preparations which were all run against the same preparation of GCSWS, (column 6, Table 3.6). This was done because the method of preparation of the working standard batches appeared to give slight differences in isotopic content (eg. GCSWS 3 was up to 0.3‰ lighter than other batches). These means were then converted to $\delta^{18}O_{GCS-PDB}$ and $\delta^{13}C_{GCS-PDB}$ (column 8, Table 3.6), using the relationship between NBS 20 and PDB (determined by Craig 1957, later amended by Craig and reported in Blattner and Hulston 1978) :

$$\delta^{18}O_{NBS20-PDB} = -4.18\text{‰} \quad , \quad \delta^{13}C_{NBS20-PDB} = -1.06\text{‰}$$

This conversion, and an example of converting raw sample data to $\delta^{18}O_{X-PDB}$ and $\delta^{13}C_{X-PDB}$ are given in Appendix 2.

3.5.4 Other Secondary Standards

The calcite powders TKL-1 (Te Kuiti Limestone No.1) and K-2 (Kaikoura No.2) were obtained from Dr.P.Blattner (New Zealand Geological Survey). They had previously been circulated to 19 laboratories for measurement of $\delta^{18}O_{PDB}$ of each and hence "explore the likely range and significance of proportional mass spectrometer errors" by calculation of the difference in $\delta^{18}O$ between the two samples. The difference ε was defined as (Blattner and Hulston 1978) :

$$\varepsilon = \frac{\delta^{18}O_{TKL-1-PDB} - \delta^{18}O_{K-2-PDB}}{1 + 10^{-3} \cdot \delta^{18}O_{K-2-PDB}} \qquad (3.18)$$

Results of analyses of two preparations of each standard are shown in Table 3.7 together with means and ranges reported in Blattner and Hulston (1978) for analysts who used PDB as primary reference standard. As can be seen, results from the present work are in excellent agreement with the mean of reported analyses. This indicates that not only are the measurements and data processing methods accurate but that mass spectrometer correction factors (particularly for tail and valve mixing) are also accurate.

Since $\delta^{18}O$ of waters has not been determined as part of this research, no attempt was made to intercalibrate to water standards (eg. SMOW, SLAP).

3.6 Summary and Conclusions

The following comments can be made concerning past and present isotopic measurements in this laboratory:

1) the use of crimped capillaries to increase inlet gas pressure was found to be essential to prevent heavy-isotope enrichment of the working standard gas. The large improvement in precision for $^{46}\delta$ measurements after crimping can be seen in Tables 3.6 and 3.8.
2) The large error limits found by Olson (1975) are not comparable to those given by Harmon (1975) even though both worked concurrently on the same machine (Table 3.8). However a range of 2.9 ‰ for measured

Preparation No.	$\delta^{18}O$ (PDB) (‰)	$\delta^{13}C$ (PDB) (‰)
TKL-1-1	-4.266*	-1.550
K-2-1	-26.943**	-3.654
ε	23.305	2.112
TKL-1-2	-4.120	-1.750
K-2-1	-26.843	-3.657
ε	23.350	1.914

Overall mean ε = 23.33 for $\delta^{18}O$ and ε = 2.013 for $\delta^{13}C$

* mean of four analyses of same gas
** mean of three analyses of same gas

Interlaboratory Comparison Results

	Range of 14 results $\delta^{18}O$ (PDB) (‰)	Mean $\delta^{18}O$ (PDB) (‰)	Mean *** $\delta^{13}C$ (PDB) (‰)
TKL-1	- 4.6 to -3.85	-4.26 ± 0.19	-1.69 ± 0.13
K-2	-27.3 to -26.42	-26.85 ± 0.24	-3.69 ± 0.14
ε	23.00 to 23.60	23.23 ± 0.16	2.023±0.096

*** based on 12 analyses, range not given

Table 3.7 Results of analyses of isotope reference standards TKL-1 and K-2 in this laboratory (upper table) and from other laboratories (lower table). ε is defined in the text. Excellent agreement is seen with other laboratories.

			Quoted Error Limits (‰)			
			Type 2	Type 3	Type 4	
Sample Analysed	Author		(same gas- different days)	(same sample - same day)	(different preparation - different day) normalised	unnormalised
$CaCO_3$	Harmon (1975)		± 0.1	N.D.	'slightly > ±0.1'	N.D.
$BaSO_4$	Olson (1975)		± 0.8*	± 0.25	± 0.55	± 0.35
SiO_2	Longstaffe (1977)		N.D.	± 0.09	± 0.21**	N.D.
$CaCO_3$	This work :	before crimping	± 0.14 (GCS) ± 0.14 (NBS 20)	N.D.	N.D.	± 0.22 (GCS) ± 0.23 (NBS 20)
		after crimping	± 0.04 (GCS) ± 0.08 (NBS 20) ± 0.05 (duplicate analyses)	N.D.	N.D.	± 0.07 (GCS) ± 0.03 (NBS 20)

N.D. = Not Determined

* mean of two sets of analses which were presumable made over a period of greater than one year.

** not clear whether same gas from a number of preparations or just one preparation

All error limits are '1s' for this work and 1σ for other work

Table 3.8 Summary of determinations of analytical precision for isotpic analysis of CO_2 for this work compared to that quoted by previous workers for the same mass spectrometer.

'daily' values of NBS 20 preparations observed by Harmon, is more in keeping with the analytical precision calculated by Olson. During their work the capillaries were not crimped and were of the same material as used in the first part of this work; therefore it is likely that the poor precision found by Olson was due to time-dependent enrichment of the working standard. Normalisation of analyses to a 'daily' standard, as done by Harmon, would not adequately correct for this and, as already noted, Olson found no increase in precision could be gained by such normalisation.

3) from paired measurements of $^{46}\delta$ on 132 samples in this work, better precision was obtained between raw δ results than between results normalised to the 'daily' secondary standard. Normalisation of raw results was therefore not used in this work.
4) all sample gases were analysed at least twice (on different 'days') for $^{46}\delta$ and once for $^{45}\delta$.
5) analytical precision for replicate carbonate analyses before crimping is estimated to be within ± 0.23‰ and after crimping, within ± 0.08‰ for both $^{46}\delta$ and $^{45}\delta$. The latter value is excellent considering the age and operating characteristics of the mass spectrometer, and is comparable to precisions quoted for modern machines.

CHAPTER 4

AGE DETERMINATION AND STABLE ISOTOPE ANALYSIS OF SPELEOTHEM FROM VANCOUVER ISLAND

Introduction

Vancouver Island lies between latitudes 48° and 51° N. on the Pacific coast of Southern British Columbia (Figure 4.1). Today, it enjoys a mild wet climate controlled largely by the warm N. Pacific current. Much of its area is occupied by the Island Mountains whose peaks rise to over 2000m above sea level. Finger lakes are found between north-west trending ridges in the central part of the Island and the west coast is indented by numerous fjords. The lower eastern shore, the Coastal Lowland, borders on the Georgia depression, a submerged valley which separates the Island Mountains from the Coast Range. The depression is known as the Straits of Georgia in the north and the Puget Sound in the south near Seattle. Although densely forested, the southern part of the Island has been cleared and settled for some time, and it is in this region that a number of small, well-decorated cave systems have been found.

This chapter describes the results of dating speleothems from four caves on the Island; stable isotope profiles have been determined for two speleothems. The results are compared to the abundant literature on Quaternary deposits on the Island and the mainland of British Columbia and Washington (USA).

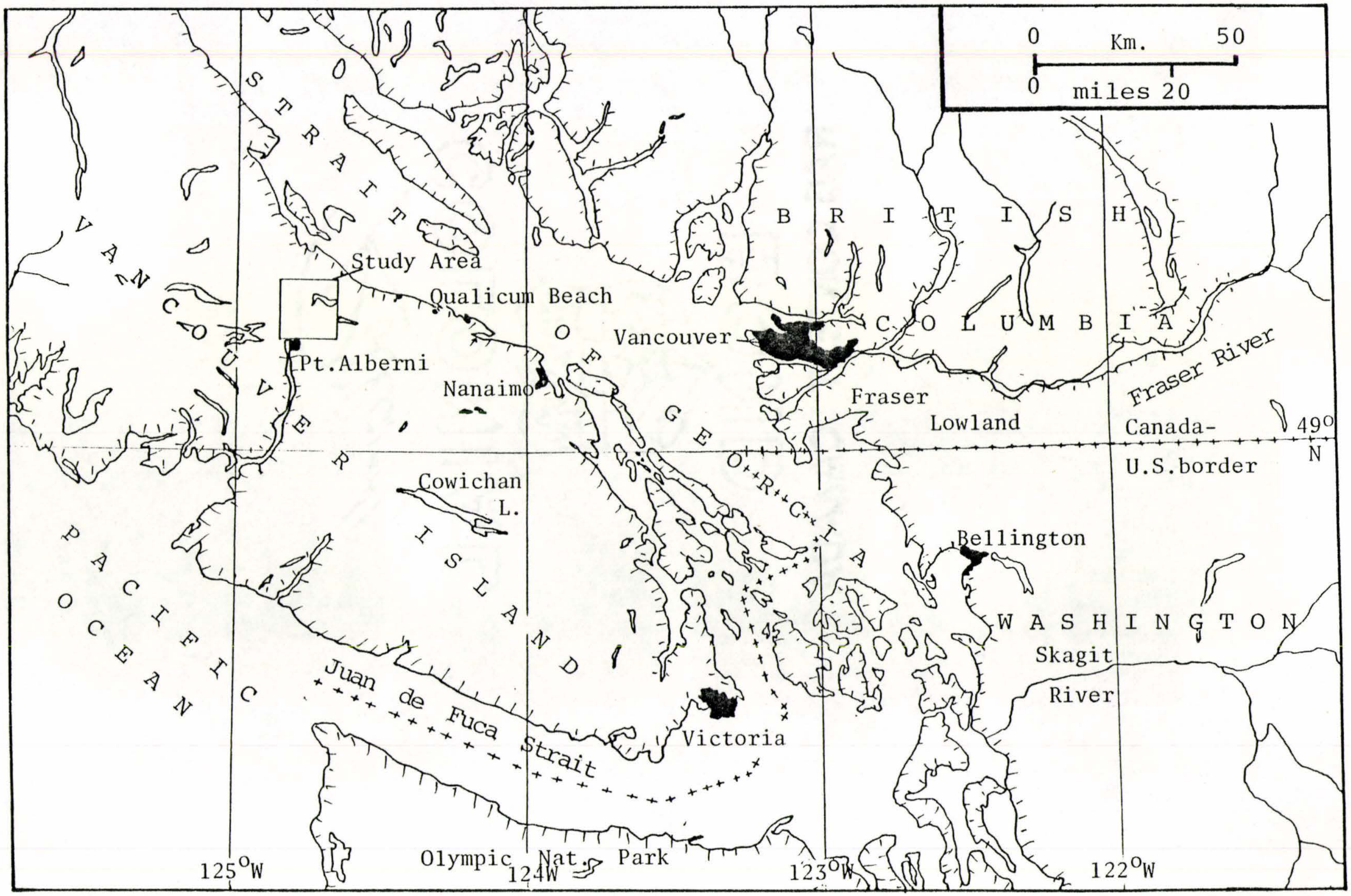

Figure 4.1 Location of study area, Vancouver Island, B.C.

4.1 Geological Setting

The central mountainous part of the Island forms the westernmost extremity of the Canadian Cordillera. The oldest rocks (the Sicker Group) are a metamorphosed complex of basaltic and andesitic volcanics of Triassic age overlying upper Paleozoic limestones and clastic sedimentary rocks (Yole 1969).

Overlying these rocks in the east-central part of the Island are sedimentary rocks of Late Cretaceous age of both marine and non-marine origin. These sediments (the Nanaimo Group) are mainly found in structural basins such as the Alberni Valley and the Coastal Lowland. Post-orogenic, Tertiary clastic deposits fringe the west coast, and on the eastern and southern parts of the Island extensive Pleistocene deposits can be found (Fyles 1963).

4.2 The Quaternary Geology of Vancouver Island and S.W. British Columbia

U-shaped valleys and cirques are abundant in the Island Mountains and demonstrate extensive mountain glaciation during the Pleistocene. Some U-shaped valleys however extend through these mountains instead of originating in them, suggesting that the Cordilleran ice sheet moved across Vancouver Island (with the exception of peaks over 1500m) during the late Wisconsin glacial maximum about 20 Ka B.P. (Fyles 1963). Much evidence exists for local advances and retreats during this period as well as for the existence of previous interstadial, glacial and interglacial climates in the region.

A number of lithostratigraphic units have been recognised in this area and correlated to the Late Pleistocene North American glacial sequence (Table 4.1). The oldest deposits on the Island (the Mapleguard

Table 4.1 Late Pleistocene lithostratigraphic divisions for S.W. British Columbia and Vancouver Island (after Armstrong 1977, Armstrong and Clague 1977, Fulton and Smith 1978).

^{14}C AGE (Ka)	TIME UNIT	GEOLOGIC CLIMATE UNIT	LITHOSTRATIGRAPHIC UNITS (with radiocarbon ages) WESTERN B.C. & FRASER LOWLAND West East	 VANCOUVER ISLAND	UNIT DESCRIPTIONS	
0	HOLOCENE	POSTGLACIAL	SALISH AND FRASER RIVER SEDIMENTS (0.6 - 12.4)			
10	LATE WISCONSIN	GENERAL DEGLACIATION (with local advances and retreats)	SALISH SEDIMENTS CAPILANO SEDIMENTS (10.4-12.8) SUMAS DRIFT (11.4-11.7) FORT LANGLEY FORMATION (11.7-12.9)	CAPILANO SEDIMENTS	Capilano Sediments are glaciomarine and marine sediments formed when sea level was 15m. above present.	Sumas Drift was deposited in the east by the last major Cordilleran advance. The Fort Langley Formation consists of glaciomarine sediments recording at least three local glacier advances and retreats, overridden by Sumas ice in most areas.
13		FRASER	VASHON DRIFT	VASHON DRIFT	The Vashon Drift includes at least three tills and was preceded by fluvial dissection.	
18		GLACIATION	QUADRA SAND ~15 near Seattle COQUITLAM DRIFT ~21 near Vancouver ~ 29 north of V.I.	QUADRA	The Quadra Sediments comprise: 1) an upper unit of white sand with local gravels and plant-bearing silts 2) a middle unit of silty gravel and sand with peat and wood layers 3) a lower unit of shelly marine clay and stony clay with basal lenses of unfossiliferous laminated clay.	Quadra Sand is well-sorted sand with minor gravel and silt, deposited as outwash in front of glaciers advancing southwards in the Georgia depression. Coquitlam Drift represents one advance and retreat of valley ice during this period. The Cowichan Head Formation includes fluvial, estuarine and marine silt, sand and gravels, with abundant organics.
29	MIDDLE WISCONSIN	(OLYMPIA) NON-GLACIAL (INTERSTADIAL)	COWICHAN HEAD FORMATION (25.8-29.6, 32.6-36.2, 40.2-40.5, >37, ~59.)	SEDIMENTS		
>62	EARLY WISCONSIN	SEMIAHOO GLACIATION	SEMIAHOO DRIFT	DASHWOOD DRIFT	Semiahoo Drift contains at least two till units plus glaciofluvial and glaciomarine sediments.	Only one till is recognised in the Dashwood Drift.
	SANGAMON ?	HIGHBURY NON-GLACIAL	HIGHBURY SEDIMENTS ?	MAPLEGUARD SEDIMENTS	Highbury Sediments are cross-bedded rusty sands and silts with wood.	
	Pre-SANGAMON	WESTLYNN GLACIAL	WESTLYNN DRIFT		Impervious cobble gravels, containing angular sands.	

Sediments) are thought to be pre-Early Wisconsin in age, either associated with the Sangamon interglacial or representing the start of the Early Wisconsin glaciation (Fyles 1963). The Dashwood Drift is thought to be derived from the Early Wisconsin ice cover and is usually found underlying basal layers of the Quadra Sediments. The lower and middle units of the Quadra Sediments are collectively termed the Cowichan Head Formation on the mainland (Armstrong and Clague 1977) and represent a cool to warm interstadial phase (the Olympia 'Interglaciation') before onset of the Fraser glaciation. The upper limit of the sediments correlates to the Quadra Sand unit on the mainland. It is a major time-transgressive horizon derived from outwash fans deposited in front of the Fraser ice sheet advancing southwards along the Georgia depression. Radiocarbon ages of wood from Quadra Sand deposits show the Fraser advance to have commenced before 29 Ka in the northern end of the Strait of Georgia, terminating at the southern end of Puget Sound less than 15 Ka (Clague 1976). The Vashon Drift consists of tills from the main part of the Fraser (Late Wisconsin) glaciation. Deglaciation had begun by 13 Ka and rapid eustatic sea level rise caused deposition of the Capilano Sediments on the lower lying shores of the Island. Post-glacial isostatic uplift has since raised these deposits to heights up to 175m above present sea level.

Armstrong (1977) has summarized a number of factors that influence the Quaternary history of the Fraser Lowland area:

1) high mountain ranges surround the area on two sides
2) ice sheets formed by coalescence of piedmont glaciers attained a maximum thickness of 1800m or more, overriding many mountainous

areas and terminating in the sea. They probably filled the Strait of Georgia at their maximum,

3) the area was tectonically active (including sporadic vulcanism) throughout Quaternary time,
4) sea level changes up to 200m or more have occurred due to isostatic, eustatic and tectonic adjustments,
5) in places the thickness of Quaternary deposits exceeds 300m and includes sediments of widely diversified origin and history.

A somewhat different view of the late Quaternary history of the region has come from a study of sediments and peat deposits in northwest Washington (Easterbrook 1969, Hansen and Easterbrook 1974). These authors give stratigraphic and palynological evidence for two glacial advances during the Mid-Wisconsin (known as the Salmon Springs Glaciations). One occurred before 47.6 Ka and the second was younger than 34.9 Ka. These are followed by a cool period (the Olympia 'non-glacial' interval) ending about 22.7 Ka. Heusser (1977) also advocates a late Mid-Wisconsin glaciation, but occurring between 40 and 34 Ka, somewhat older than that proposed by Hansen and Easterbrook. The Olympia interglaciation is placed in the interval 34 - 28 Ka.

The controversy regarding the presence (American workers) or absence (Canadian workers) of a glaciation during the Mid-Wisconsin rests mainly on the validity of three radiocarbon dates for peat interbedded with the Possession Drift of supposedly Salmon Springs glacial origin (Hansen and Easterbrook 1974, Easterbrook 1976), and on two dates for peat interbedded with (glacial ?) clays from sea cliffs in the Olympic Peninsula (Florer 1972, Heusser 1977). Against this evidence is the wealth of radiocarbon dates covering the period > 58 to 28 Ka (Armstrong and Clague 1977) for apparently continuous sequences of the Cowichan Head and Quadra Sands formations. Possibilities of ^{14}C contamination and non-glacial origin of the Possession Drift are discussed in Fulton et al. (1976) and Easterbrook (1976). An interesting point raised by Easterbrook concerns a 6,000 year gap in the Canadian record which coincides with the late Salmon Springs Glaciation (40 to 34 Ka) cited by Heusser (1977).

Recent palynostratigraphical studies, with dating, of organic-rich sediments on the eastern coastal lowland of Vancouver Island, by Alley (1979), have revealed a continuous record of temperate to interglacial climate from > 51 to 29 Ka, with climatic deterioration to tundra-like conditions from 29 to 21 Ka. No indication of glacial conditions is found during the Mid-Wisconsin period, although no reliable finite dates occur in the interval 40 to 34 Ka. In a reconstruction of paleoenvironments of the Mid-Wisconsin for south-central British Columbia, Alley (pers. comm. 1979) has found modern arboreal pollen types present in the Bessette Sediments over the period 41 to 34 Ka, thus indicating the absence of glacial conditions.

The various stratigraphical sequences for the Mid-Wisconsin in these N.E.Pacific environments is shown in Table 4.2 and is further discussed later on in this chapter in light of the speleothem results presented here.

4.3 The Caves of South-central Vancouver Island

Five caves were visited on two separate occasions in 1975 and

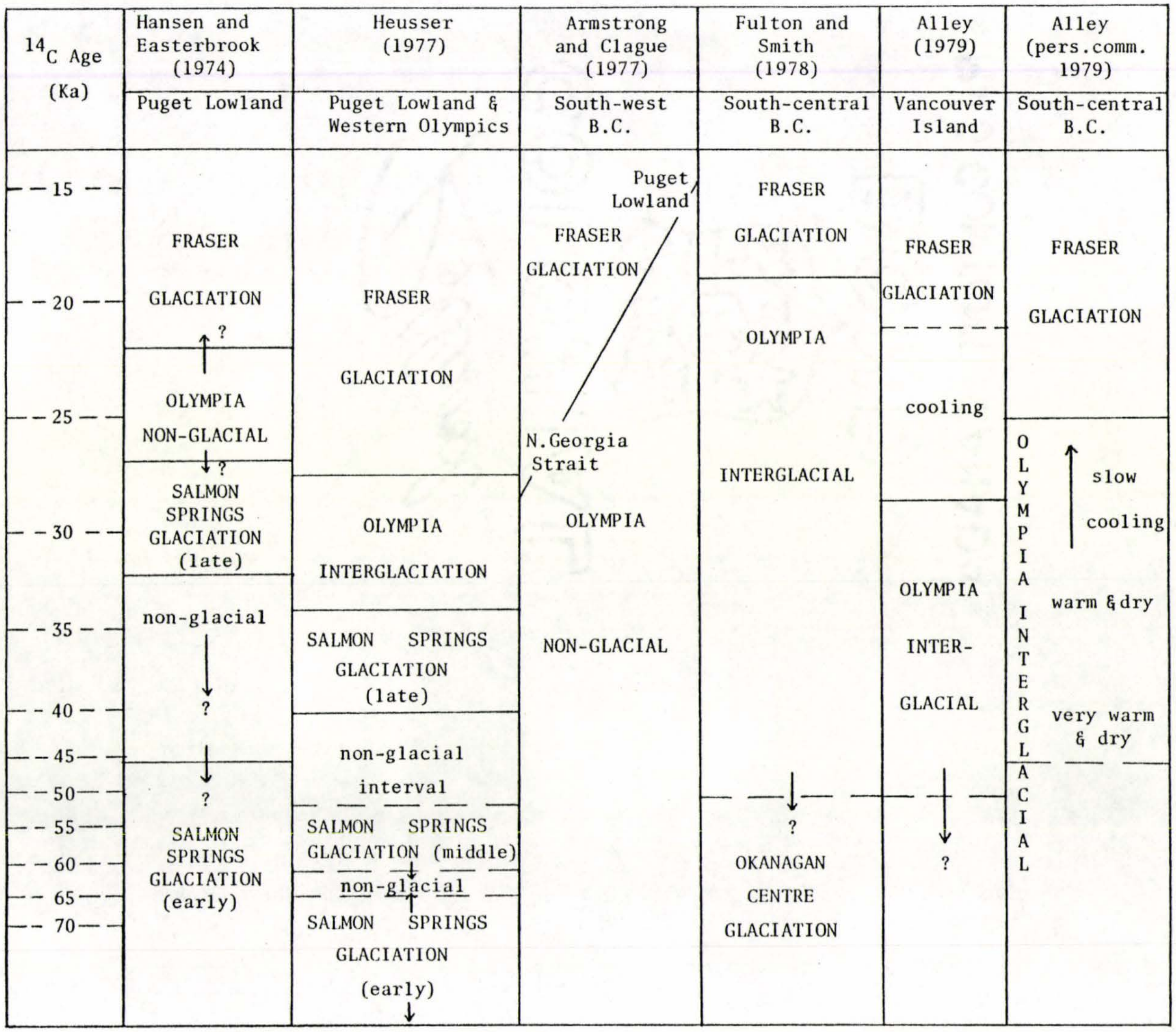

^{14}C Age (Ka)	Hansen and Easterbrook (1974)	Heusser (1977)	Armstrong and Clague (1977)	Fulton and Smith (1978)	Alley (1979)	Alley (pers.comm. 1979)
	Puget Lowland	Puget Lowland & Western Olympics	South-west B.C.	South-central B.C.	Vancouver Island	South-central B.C.
15	FRASER		Puget Lowland FRASER	FRASER GLACIATION	FRASER	FRASER
20	GLACIATION ↑ ?	FRASER	GLACIATION	OLYMPIA	GLACIATION - - - -	GLACIATION
25	OLYMPIA NON-GLACIAL ↓ ?	GLACIATION	N.Georgia Strait	INTERGLACIAL	cooling	OLYMPIA INTERGLACIAL ↑ slow
30	SALMON SPRINGS GLACIATION (late)	OLYMPIA INTERGLACIATION	OLYMPIA			cooling
35	non-glacial ↓	SALMON SPRINGS GLACIATION	NON-GLACIAL		OLYMPIA INTER-	warm & dry
40	?	(late)			GLACIAL	very warm & dry
45	↓	non-glacial interval				- - - -
50	?	- - - -		↓ - - - -	↓ - - - -	
55	SALMON SPRINGS	SALMON SPRINGS GLACIATION (middle)		?		
60	GLACIATION	↓		OKANAGAN	?	
65	(early)	non-glacial ↑		CENTRE		
70		SALMON SPRINGS GLACIATION		GLACIATION		
		(early) ↓				

Table 4.2 Summary of the stratigraphical and chronological sequences proposed for the Wisconsin stage in north-east Pacific environments.

1976. They were: Euclataws Cave, Riverbend Cave, Main Cave and Lower Cave (all in the Horne Lake Caves Provincial Park) and Cascade Cave near Port Alberni. Permission to collect a limited number of speleothems was kindly given by the Parks Branch Authority and the Vancouver Island Cave Exploration Group (VICEG) who control access to Cascade Cave. In 1975 Euclataws, Main, Lower and Cascade were sampled with the help of Dr.D.C.Ford and P.Whitfield (VICEG and Parks Branch) and in 1976 a return was made to Euclataws and Cascade Caves as well as a visit to Riverbend Cave in the company of P.Shaw and others (VICEG) and A.G.Latham (McMaster). The visits had the following objectives:

1) to examine the speleogenesis of the Horne Lake Cave systems,
2) to collect *in situ* speleothem for paleomagnetic measurements,
3) to collect loose speleothem for radiometric dating and stable isotope studies.

The latter part of the project is described in the following pages. The Horne Lake Park caves have been described in detail in two reports (Ford 1976; Latham et al. 1978).

The caves investigated all lie in densely forested areas where thick undergrowth and deadfall obscure the local geology. Fyles (1963) has mapped the surficial geology of the area but has concentrated mainly on the Quaternary sediments of the Coastal Lowland and the Alberni valley (north-west of Pt.Alberni). The cave areas lie in regions of "bedrock outcrop interspersed with patches of thin overburden" (Fyles 1963). Evidence from the mountainous parts of the Island suggest that ice thickness above the caves during the

Late Wisconsin glacial maximum was 1500m or more.

4.4 Cave Descriptions

4.4.1 The Horne Lake Caves

These caves are situated on the southern bench of the Qualicum River Valley just upstream from Horne Lake (Figure 4.2). They lie in deformed crinoidal limestones of the Buttle Lake Formation (part of the Sicker Group) which are of Pennsylvanian to Early Permian age (Yole 1964). In this area the limestones dip WNW at about 40°, and are about 300m thick (Matthews and McCammon 1957). Euclataws Cave at 245m a.s.l. is known to connect to Main Cave (150m), and Riverbend Cave (215m) is hydrologically connected to Lower Cave (145m). These altitudes are only approximate. Euclataws is a fossil engulfment cave, only containing an active streamway in its lowermost passages (Figure 4.3). The entrance series consists of dip- and strike-oriented tubes and crawlways partially filled by dissected fluvial gravels, which are commonly overlain by speleothem deposits. The passage enlarges towards the Dome Room and follows a deep meandering vadose canyon, partially or completely filled with sediments. A series of collapse chambers leads to the 4m Waterfall Pitch and most speleothem formations are in this area. A small stream enters at this point and the passage follows a major joint and ends in a gravel choke at the upper end of Main Cave. A strong draught can be detected in most parts of Euclataws Cave.

In contrast, Riverbend Cave appears to be more recent in origin

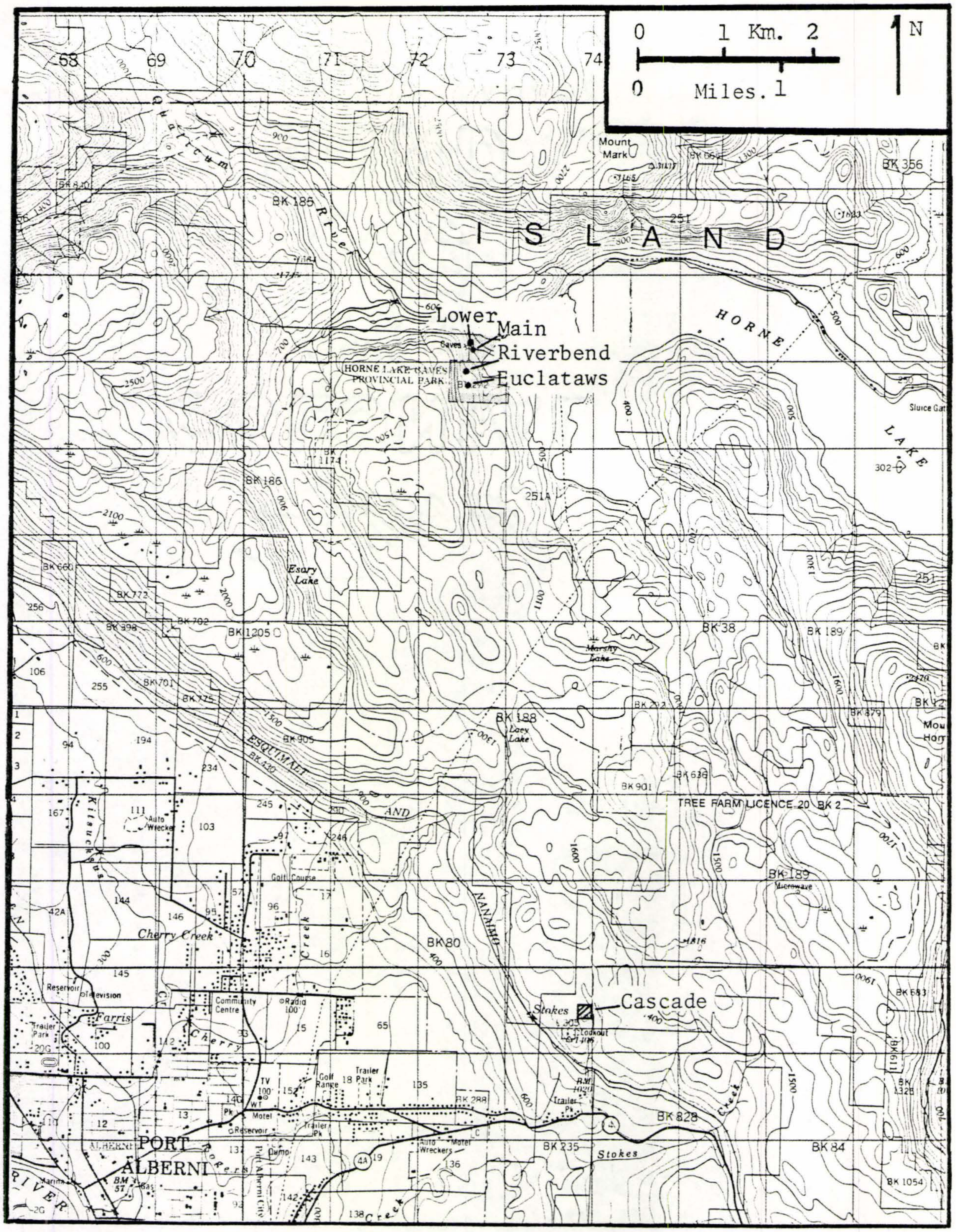

Figure 4.2 Cave location map (reduced from 1:50000 survey sheet 92F/7). Approximate location only for Cascade Cave.

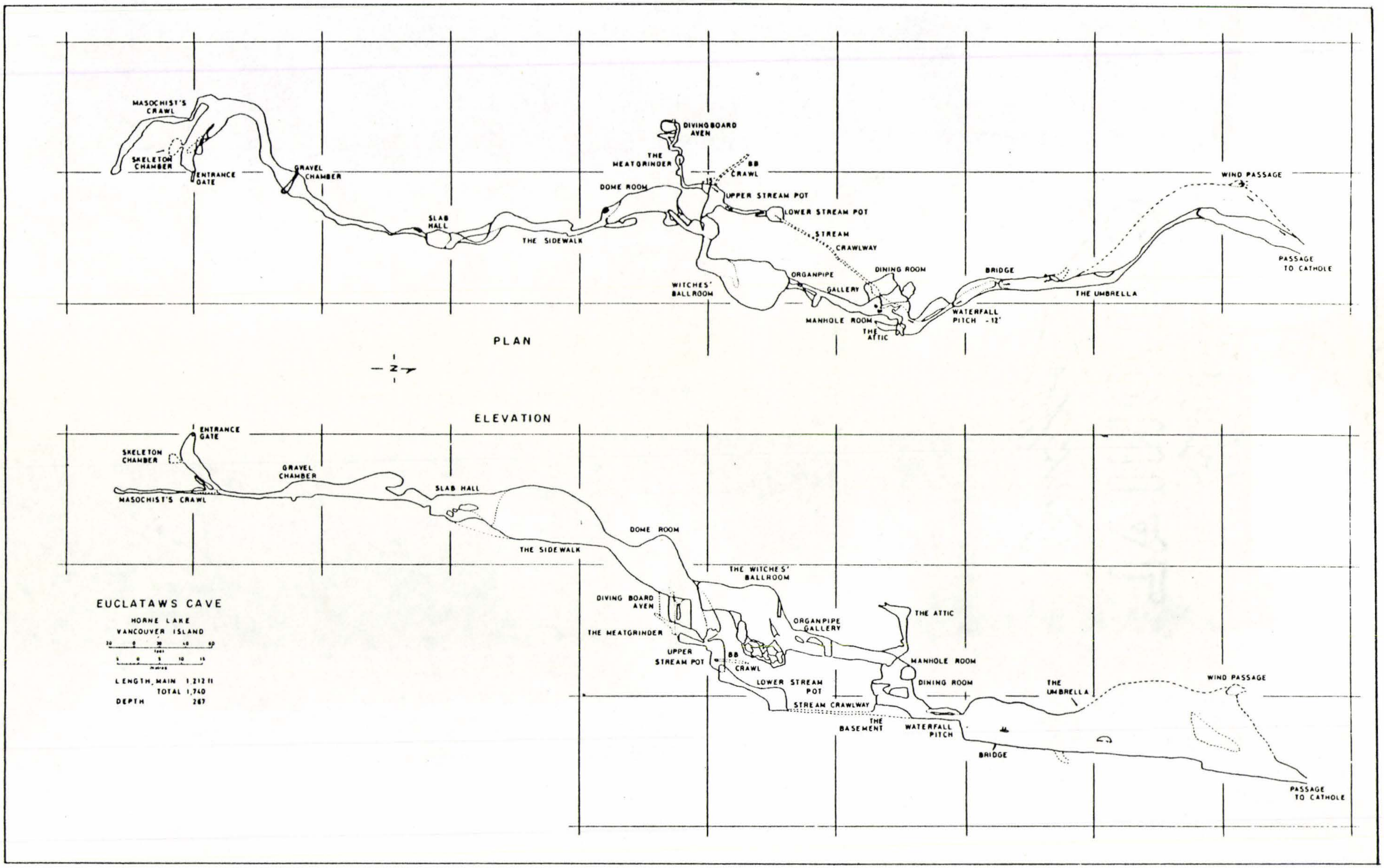

Figure 4.3 Plan and elevation of Euclataws Cave, Vancouver Island (by VICEG, in Thompson 1976).

and contains fewer sections dissected through gravel and almost no fossil (non-active) speleothem (Figure 4.4). The cave develops initially along strike and becomes a low crawlway due to recent aggradation of stream gravels. Beyond this the passage enlarges and a series of vertical drops is met. A number of active flowstone cascades have developed at seepage entry points near roof level above these drops. The gradient reduces after Rainbarrel Pot and a narrow vadose trench finally leads to the sump.

The two resurgence caves, Main and Lower Cave, are 150m and 50m long respectively. They have been known to the public for some time and are now devoid of speleothem.

During the first visit to Euclataws Cave a number of broken speleothems, mainly stalagmites, were collected from inconspicuous sites (under blockfall). On the second visit, a search was made for older deposits but only two small pieces of flowstone were taken. Few samples were available for collecting in Main and Lower Caves and only one small sample was taken from Riverbend, due to the lack of fossil deposits.

4.4.2 Cascade Cave

This cave is one of the most important systems on the Island. It lies to the east of Pt.Alberni at about 365m a.s.l. (Figure 4.2) and its 8m entrance shaft is situated in a stream bed at the end of a small blind valley. The cave is presently over 1km long and over 100m deep, containing a number of vertical drops, low wet crawls and narrow squeezes (Figure 4.5). The entrance and lower series are active vadose passages

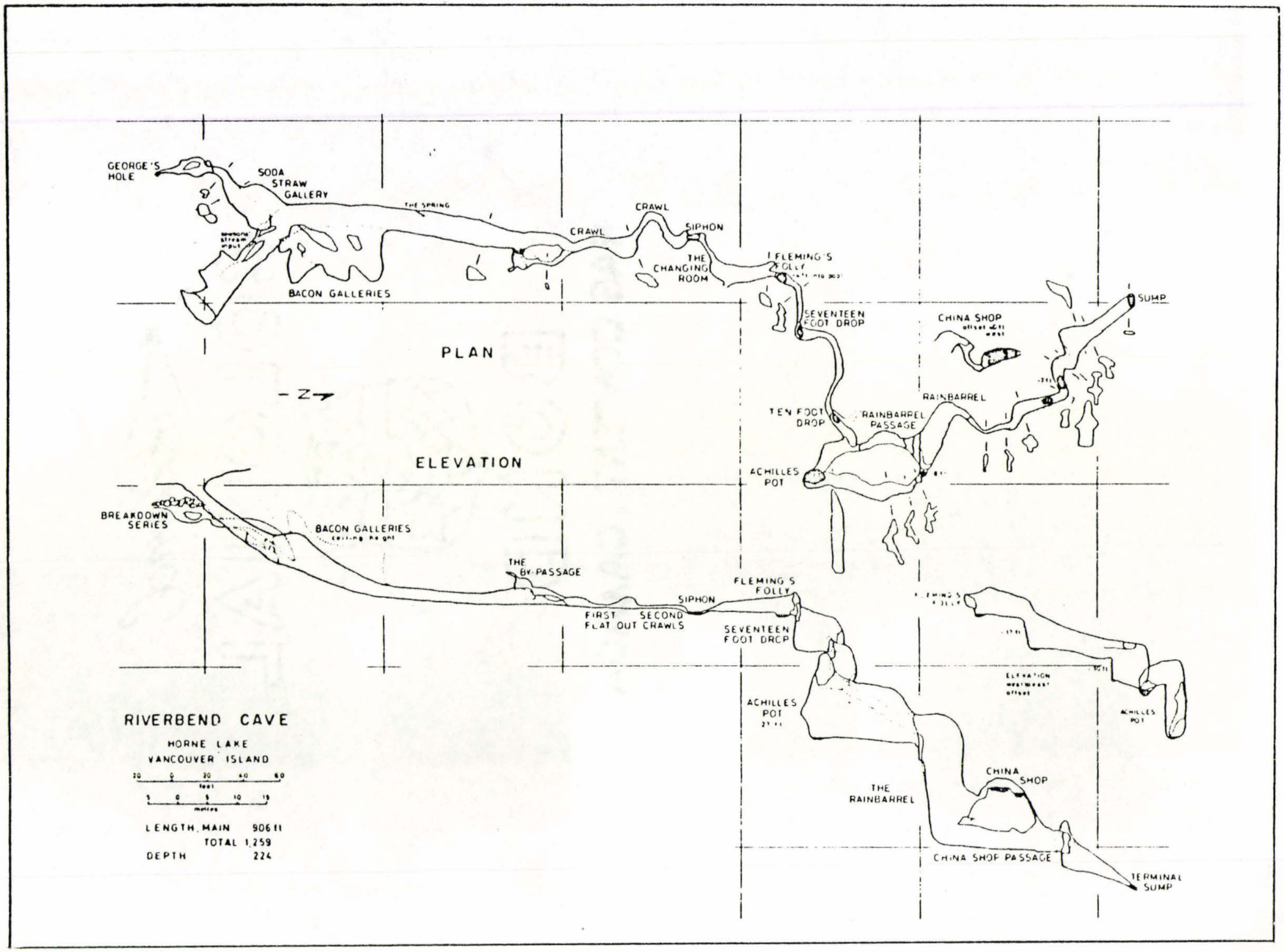

Figure 4.4 Plan and elevation of Riverbend Cave, Vancouver Island (by VICEG, in Thompson 1976).

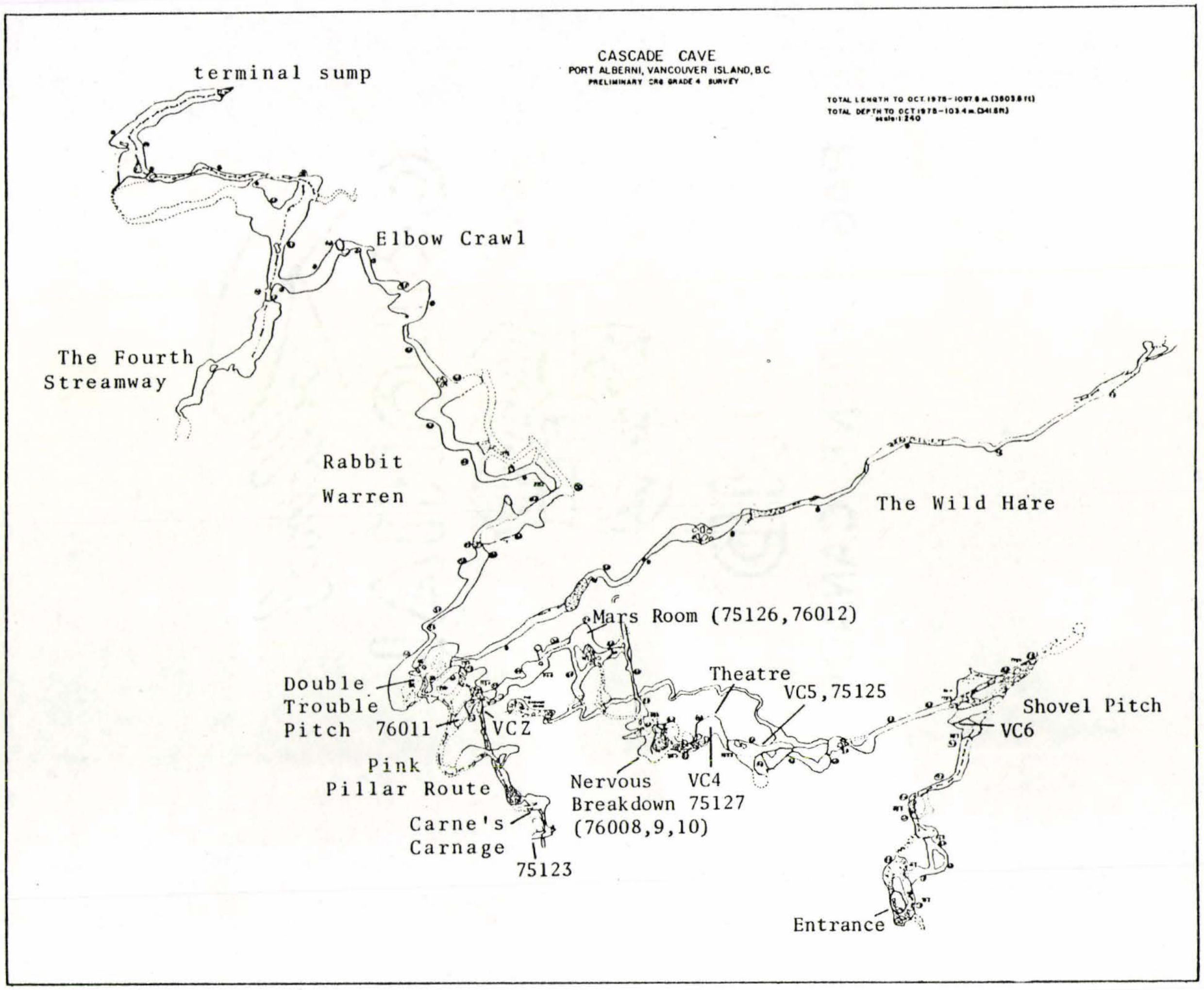

Figure 4.5 Survey of Cascade Cave, Vancouver Island (by VICEG and others, in Thompson 1976), showing location of speleothem samples and dripwater sites.

but below Shovel Pitch the stream sinks in a choke. The continuation is an older vadose fissure into which have collapsed several higher level breakdown chambers. Although the cave is well decorated throughout, the most impressive speleothems are found in these chambers (the Theatre, Mars Room and the Pink Pillar Route). These chambers are about 30m below ground level.

Most speleothem collected from Vancouver Island came from Cascade Cave. Almost all of it consisted of already-broken stalagmites and flowstones from obscure places in passages and chambers as far down as Carne's Carnage. A full description of all samples collected is given in Appendix 3a and in the following pages.

4.5. Results of Speleothem Dating

4.5.1 Horne Lake Caves

Numerous analyses were made of speleothem from Euclataws Cave (Appendix 3a) but low uranium concentrations (< 0.03ppm) were found in all the samples. At these levels of radioactivity, determined 'ages' are dominated by non-statistical errors such as contamination by glassware memory effect or variations in reagent blank contributions (Chapter 2). It was therefore decided to regard all calculated ages for speleothem of < 0.05ppm U as potentially spurious and so they are not reported here. For these reasons and the fact that only an 8% Th yield was obtained on the 'modern' stalagmite 75151 from Main Cave (Appendix 3a), the age of 265 Ka must also be disregarded.

4.5.2 Cascade Cave

Better results were obtained from Cascade speleothem, where U concentration is somewhat higher (0.06 to 0.31ppm). Sample locations and descriptions, isotope ratios and determined ages are given in Appendix 3a and are shown as a bar graph in Figure 4.6.

4.5.2.1 Analyses Showing Detrital Contamination

Many analyses show measurable detrital Th contamination (^{230}Th/^{232}Th < 20). They have been 'corrected' assuming an initial ^{230}Th/^{232}Th ratio of 1.5 (see Chapter 2), and the corrected ages and calculated ^{232}Th concentrations are also given in Appendix 3a . The effect of this correction can be considered in two parts: 1) for speleothem younger than 20 Ka and low in uranium (ie. 75126, 75127, 76011 overgrowth and 76012), the correction drastically shifts the age to younger values, even if only 0.01ppm ^{232}Th is present, 2) for speleothem between 70 and 30 Ka the effect is large only if ^{232}Th concentration is large (say > 0.03ppm). As discussed in Chapter 2, recent dates (< 20 Ka) on low uranium speleothem are based on very low ^{230}Th activities which are comparable to those caused by fluctuations in memory effect or reagent blank levels. Tailing of the ^{228}Th or ^{230}Th peaks into the ^{232}Th region will also add to the measured activity in this region. Agreement with stratigraphy may sometimes be found after age correction (eg. 75126, 75127) but the enlarged error limits reduce the value of this achievement. For these reasons it is possible that both corrected and uncorrected ages are spurious and the only conclusion that can be drawn is that they are all probably post-glacial speleothems

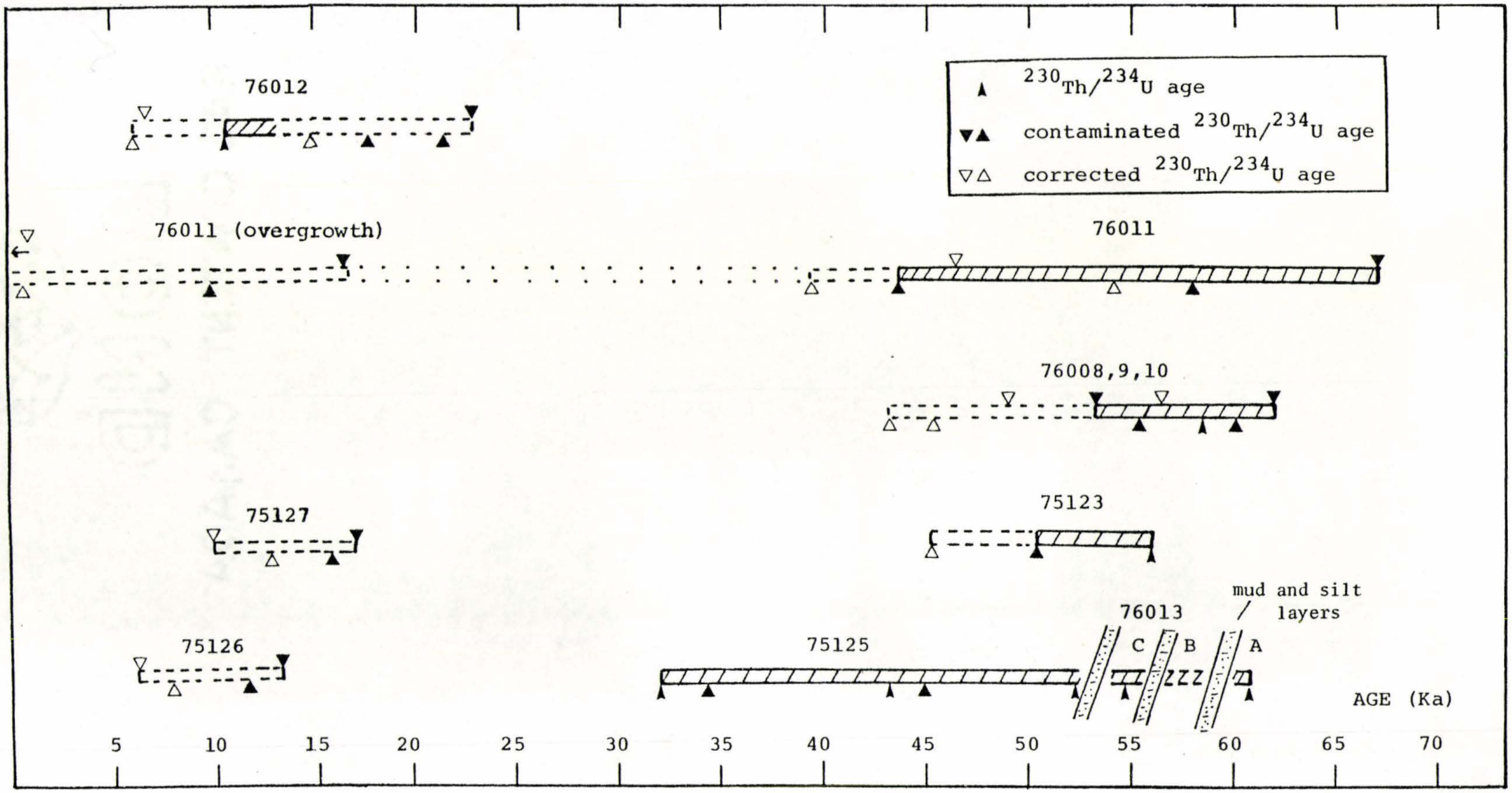

Figure 4.6 Bar graph of ^{230}Th/^{234}U ages of speleothem from Cascade Cave, Vancouver Island. Parallel dotted lines indicate the period represented by a growth hiatus in the speleothem; parallel dashed lines show projection to an age corrected for detrital thorium.

(from about 20 Ka to 0 Ka old).

Evidence for the absence of detrital ^{230}Th, in the presence of measurable ^{232}Th, is seen in the analyses 75125-3 and -4A. Replicate analyses 75125-8 and -7 respectively show no ^{232}Th contamination but still give the same ages within overlapping error limits. In this case therefore, the correction procedure appears to be invalid and the corrected ages are omitted from Figure 4.6.

Many age determinations on young speleothem (< 20 Ka) in this study have been rejected due to the presence of extraneous thorium contamination. Thorium contamination has less impact on age determinations between 70 and 30 Ka such that fewer ages need be rejected.

4.5.2.2 Detritus-free Analyses

Ages determined for speleothem containing negligible amounts of detrital thorium are shown in Figure 4.6. The dates fall into the general period 62 to 32 Ka and one age at 10.7 Ka.

Sample 75125 is a small stalagmite-flowstone formation taken from about 2m up the wall of the passage approaching the Theatre. It was formed on top of three calcite layers (76013) each separated by 3 to 5cms of mud and silt deposits (Figure 4.7). The upper layer C and lower layer A contained sufficient clean calcite for dating. Seven age determinations on these samples show excellent stratigraphic agreement, indicating that the deposit began to grow just prior to 61 Ka. Growth was interrupted by intermittent flood events up to about 55 Ka when continuous slow growth commenced, ending after 32 Ka. A small stalagmite, 75123, grown on a thin flowstone base, was found in a

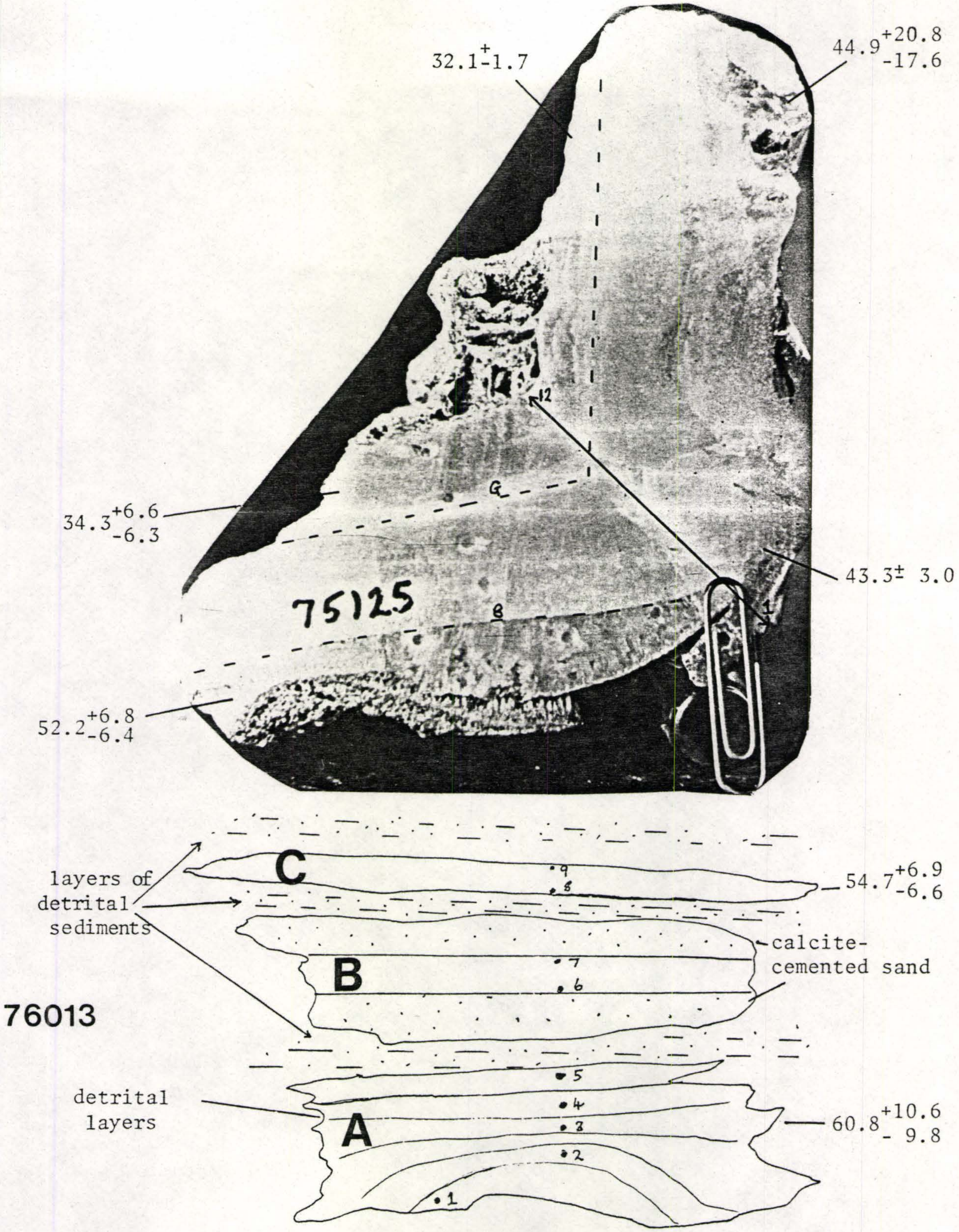

Figure 4.7 Section of stalagmite-flowstone 75125 with sketch of position with respect to underlying calcite layers 76013. Numbered points and line 1-12 show positions of stable isotope samples and dashed lines B and G the growth layers analysed (Appendix 3b). Approximate positions of $^{230}Th/^{234}U$ determinations are shown.

collapsed stream inlet near Carne's Carnage. The speleothem grew continuously from about 56 Ka to 50.5 Ka. Samples 76008, 9 and 10 are blocks from one continuous thickness of flowstone found in a high level boulder collapse zone (the 'Nervous Breakdown') about 10m above the Theatre. Although the three samples were broken when collected, they obviously came from the same flowstone mass and could be stratigraphically related to one another by distinctive growth layers. Dates determined on base and top of each piece show some apparent inversion, but allowing for overlap of 1σ error limits, the speleothem appears to have grown from about 62 to 53 Ka. Sample 76011 was found out of growth position amongst massive breakdown in the waterfall chamber below Carne's Carnage. It consists of a well-laminated, clear brown flowstone base which changes abruptly into porous leached flowstone towards the top. A white, fresh-looking calcite overgrowth thickly coats some areas of the base. Two ages on the brown calcite show growth from about 58 to 43 Ka, followed presumably by further growth which has subsequently been attacked by acidic groundwaters. The white overgrowth appears to be recent and its age is probably less than 16 Ka and 10 Ka as both these results are biased by detrital thorium content.

The top date determined on 76012 (10.7 Ka) is the only analysis of post-glacial age speleothem that is not affected by detrital thorium.

4.6 Stable Isotope Analyses of Cascade Cave Speleothem

$\delta^{18}O_c$ and $\delta^{13}C_c$ have been measured along two growth layers for each of 75123, 75125, 76008 and 76012 (Figure 4.8,Appendix 3b) to determine whether

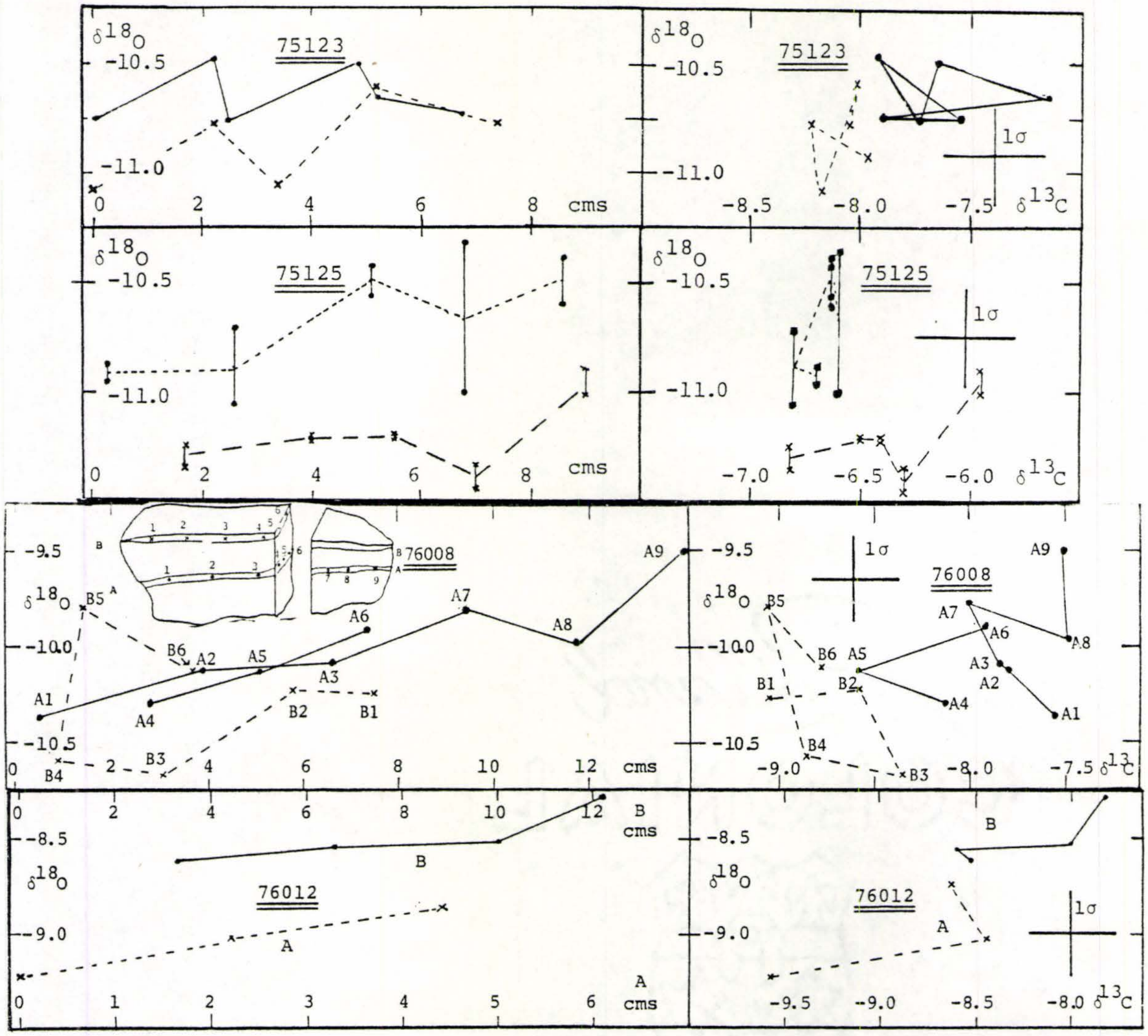

Figure 4.8 Variation of $\delta^{18}O_c$ along individual growth layers and correlation of $\delta^{18}O_c$ with $\delta^{13}C_c$ along growth layers for four speleothems from Cascade Cave, Vancouver Island.

they were formed in isotopic equilibrium. The requirements of constant $\delta^{18}O_c$ and no correlation between $\delta^{18}O_c$ and $\delta^{13}C_c$ along the same growth layer (Hendy 1971) were satisfied by samples 75125 and 75123, although 75125 showed slight tendencies towards increased $\delta^{18}O_c$ along a growth layer (this may have been due to imprecise sampling because growth layers were difficult to see). Samples 76008 (and presumably 76009 and 10) and 76012 showed more obvious trends, although neither sample is strongly fractionated. 76008, 9 and 10 are flowstones and have therefore been analysed for $\delta^{18}O_c$ and $\delta^{13}C_c$ in two dimensions along a growth layer as described in Chapter 3. A sketch diagram showing sample sites is inset in Figure 4.8.

Further evidence that 75125 is essentially an equilibrium deposit comes from its very slow growth rate (0.2cm/Ka) compared to other speleothems (eg. 1.7cm/Ka for 76008, 9, 10), although this may be due to other factors such as rate of water supply, seasonal vs. all year round growth etc.

The $\delta^{18}O_c$ and $\delta^{13}C_c$ profiles along the growth axis of 75125 - 76013 are plotted in Figure 4.9. Superimposed on it are analyses for 75123. Although the latter show large variations , all points scatter about similar $\delta^{18}O_c$ values seen in 75125 and 76013C for the same growth period. The large scatter is mainly due to the lower precision on the 75123 analyses (approximately ± 0.23 ‰ for samples determined pre-crimping). Comparable $\delta^{18}O_c$ results for two speleothems from different parts of the same cave, over the same time range, is good evidence for equilibrium growth.

Also shown in Figure 4.9 and Table 4.3 are analyses of $\delta^{18}O$

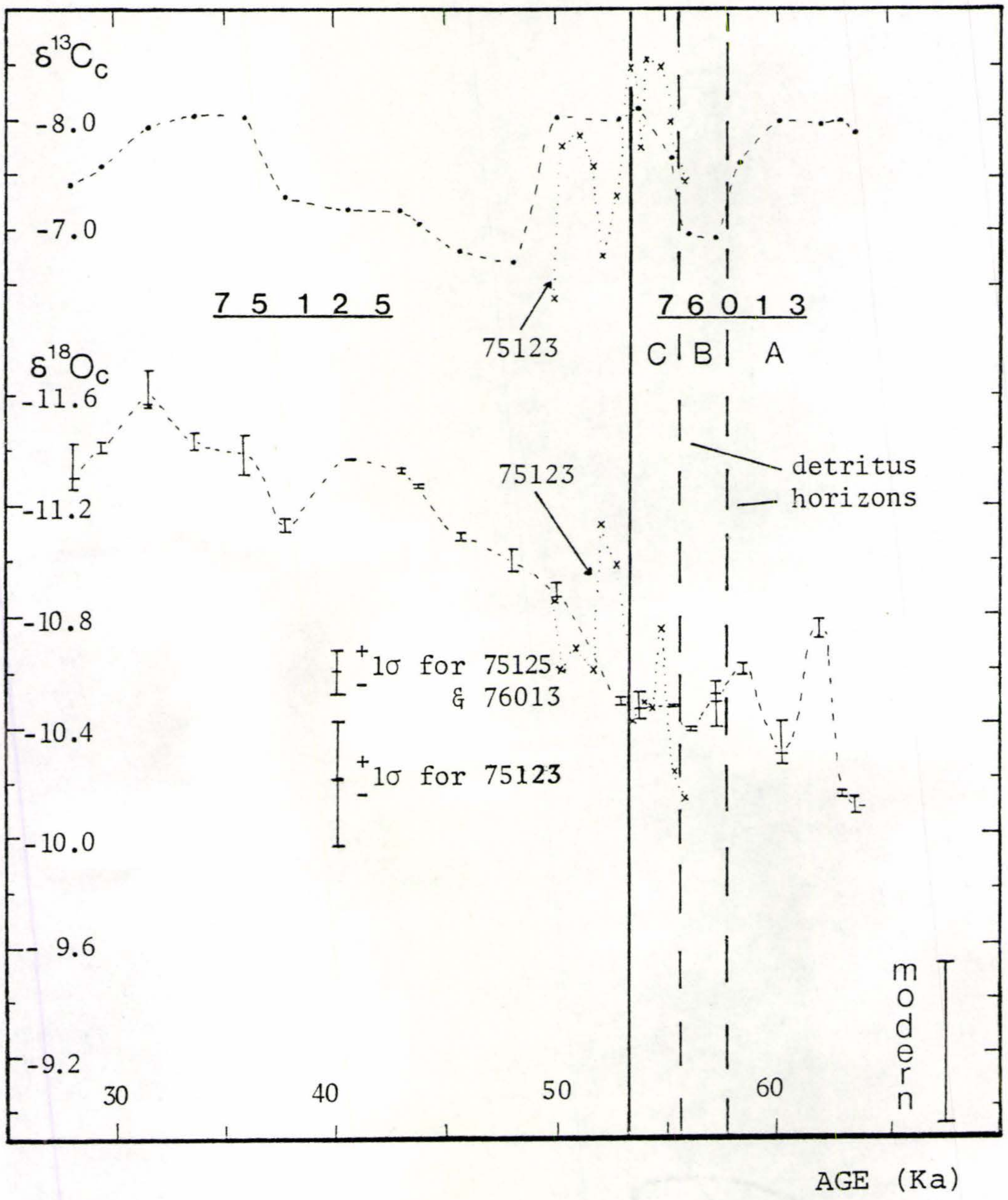

Figure 4.9 Stable isotpe profiles of 75123 (arrowed) and 75125/76013. The range of $\delta^{18}O_c$ (modern) is shown. The time scale is determined as a mean growth rated from dated horizons in each speleothem (Figure 4.6).

Sample No.	Cave	Description	$\delta^{18}O_c$ (‰)	$\delta^{13}C_c$ (‰)	T°C
VC4A	Cascade	red stalactite tip	-9.05 *	-6.49	6.9
VC5B	"	soda-straw tip	-8.94 *	-6.19	N.D.
VC6A	"	soda-straw tip	-9.43 *	-9.65	6.9
VC6C	"	adjacent soda-straw tip	-9.10	-9.25	-
VCZ	"	soda-straw tip	-9.53 *	-10.97	N.D.
VEZ	Euclataws	soda-straw tip	-9.74 *	-10.78	6.7
VE2A	"	soda-straw tip	-10.09 *	-8.56	7.1
VE2B	"	top of stalagmite	-10.14	-8.76	7.1
VEZ1	"	soda-straw tip	-9.30 *	-8.12	N.D.
VM1A	Main	stalactite tip	-9.15 *	-8.70	7.8

* mean of two analyses of same gas

N.D. not determined

Table 4.3 Results of stable isotope analyses of modern calcites (sample locations for Cascade Cave shown in Figure 4.5).

for modern calcite from four different sites in Cascade Cave. For comparison, Table 4.3 also shows data for modern calcite in Euclataws and Main Caves. The range in values is probably due to:

1) local variations in $\delta^{18}O$ of precipitation ($\delta^{18}O_p$) between caves due to differences in temperature, distance inland and altitude,
2) differences in temperature of calcite precipitation between sites (a range of 1.1°C was measured in April 1975, corresponding to a range of 0.4‰ in $\delta^{18}O_c$),
3) Variations in growth period of each sample (some stalactites may only grow during wet seasons while others grow all year round),
4) the finite time range covered by the calcite analysed (changes in $\delta^{18}O_c$ may have occurred during the last hundred years or so due to short term climatic variations),
5) some samples may be more kinetically fractionated than others depending on the cave and location within the cave.

4.7 Discussion

The absence of any dated speleothem older than the early Wisconsin indicates that the development of Cascade Cave may have begun in the Sangamon interglacial (about 130 - 90 Ka). Alternatively, if the cave is older than this, then any pre-Wisconsin speleothems either have not been sampled or were destroyed by the subsequent two glacial events.

Of the four Mid-Wisconsin speleothems dated, three grew in the period 62 - 43 Ka. The fourth (76013/75125) contains three breaks in deposition over the period 61 to 52 Ka, followed by continuous slow growth to 32 Ka. On this evidence alone, it would seem that the Early Wisconsin ice had retreated sufficiently by about 62 Ka to allow speleothem to develop and that the warmest period of Mid-Wisconsin time was during the 20 Ka immediately following this age. The mud layers separating the flowstones of 76013 suggest that this part of the cave was being occasionally used as a flood overflow. The absence of detrital horizons in any other samples indicates that flooding was only occasional and confined to the lower levels of the cave. The lack of speleothem growth in the interval 30 to 15 Ka, correlates with the Late Wisconsin glaciation. Unfortunately the contaminated or stratigraphically inverted ages on post-glacial speleothems preclude an accurate estimate of the time of perma-frost free ground in the area of Cascade Cave, but the data do suggest that speleothem growth began in the period 16 to 12 Ka.

The stable isotope analyses of 76013/75125 show a steadily-decreasing $\delta^{18}O_c$ from the start of growth at about 64 Ka to the end of growth at 28 Ka (both ages are determined by extrapolation of the radiometric ages to the extremities of the speleothem). The data show a range of about 1.5 ‰ with a change from 64 Ka to 28 Ka of about 1.2 ‰. <u>At all times</u>, speleothem $\delta^{18}O_c$ is less than modern $\delta^{18}O_c$ (mean = -9.21 ‰). This observation is <u>opposite</u> to that seen in most previous work (Thompson et al. 1976, Harmon et al. 1978a) where fossil speleothem is usually heavier than modern. The difference may be due to the location of this site at an oceanic margin where changes in α_{c-w} (the fractionation factor for ^{18}O between calcite and water) and $\delta^{18}O$ of seawater ($\delta^{18}O_{sw}$) are more than offset by temperature-dependent change of $\delta^{18}O_p$ as now described.

4.7.1 Determination of Paleotemperatures

In order to interpret these isotopic data in terms of climatic change, the following factors are assumed to influence $\delta^{18}O_c$ of speleothem on Vancouver Island:

1) $d\alpha_{c-w}/dT$ (~-0.27‰ /°C for 0 to 3 °C and ~-0.26‰ /°C for 3 to 6 °C, where T is the temperature of deposition),
2) $d\delta^{18}O_p/dT$ (= +0.7‰ /°C, the value determined from many oceanic precipitation sites by Dansgaard (1964); this assumes that the temperature at the site of evaporation of water vapour (the tropical ocean surface) does not change from glacial to interglacial),
3) $\Delta\delta^{18}O_{sw}$ between time t and the present (this can be determined from deep sea core data such as those from core V19-29 in the Pacific, Lat. 3°35'S, Long 83°56'W, (Ninkovitch and Shackleton, 1975)).

The reasons for choosing core V19-29 are as follows:

1) the benthonic foraminifera analysed (<u>Uvigerina proboscidea</u>) are known to deposit calcite in isotopic equilibrium with seawater and therefore biogenic fractionation should not influence $\Delta\delta^{18}O_f$ (foraminifera) of the core,
2) climatic stages and sub-stages are clearly recognised and well-developed in the core,
3) the core has a high accumulation rate (5.7cm/Ka) and therefore the isotopic record is less likely to be homogenised by bioturbation,

4) ocean bottom temperature at this site (-3091m) is less than 2°C at present and therefore the maximum temperature change contribution to the core record is probably within 0.2 ‰.

Isotopic variations in core V19-29 are plotted in the lower part of Figure 4.10 using data kindly provided by Dr.N.J Shackleton. The time scale is determined by assuming constant sedimentation rate and that the isotopic minimum at -830cm corresponds to stage 5e dated at 125 Ka (Broecker and van Donk 1970). Values of $\delta^{18}O_f$ for the core top are listed below.

depth in core (cm)	interpolated age (Ka)	$\delta^{18}O_f$ (‰)
0	0	N.D.
5	0.76	3.23
10	1.51	3.07
20	3.02	3.34
30	4.53	3.29
40	6.04	3.20 - hypsithermal
50	7.55	3.45
60	9.06	3.63
.	.	.
.	.	.
.	.	.
830	125.3	3.19 - isotope stage 5e

Modern $\delta^{18}O_f$ can be estimated from the following considerations:

1) most deep sea core top results show an increase in $\delta^{18}O_f$ from the

'hypsithermal' (~ 5 Ka B.P.) to the present (eg. 0.05 - 0.25 ‰, Shackleton 1977; ~ 0.1 ‰, Emiliani 1978),

2) isotope stage 5e in most cores is characterised by $\delta^{18}O_f$ equal to, or greater than, both modern and hypsithermal values. Modern $\delta^{18}O_f$ must therefore be $\geqslant$ 3.19 ‰.

A value of 3.35 ± 0.1 ‰ is used as an estimate of $\delta^{18}O_f$ (modern), and $\Delta\delta^{18}O_{sw,t}$ is determined for each speleothem analysis by subtracting this value from the interpolated $\delta^{18}O_f$ value of the same age, (determined from Ninkovitch and Shackleton's data, the lower plot in Figure 4.10).

Using the assumptions previously described, $\delta^{18}O_c$ can be expressed in terms of temperature change ΔT, thus:

$$\Delta\delta^{18}O_{c,t} = \Delta\delta^{18}O_{sw,t} - \frac{d\alpha_{c-w}}{dT} . \Delta T - \frac{d\delta^{18}O_p}{dT} . \Delta T$$

and for the temperature range 0 - 3 ^{o}C,

$$\Delta\delta^{18}O_{sw,t} - \Delta\delta^{18}O_{c,t} = 0.7\ \Delta T - 0.27\ \Delta T$$

therefore,

$$\Delta\delta^{18}O_{sw,t} - \Delta\delta^{18}O_{c,t} = 0.43\ \Delta T \qquad (4.1)$$

and for the range 3 - 6 ^{o}C,

$$\Delta\delta^{18}O_{sw,t} - \Delta\delta^{18}O_{c,t} = 0.44\ \Delta T \qquad (4.2)$$

The temperature change ΔT, between Mid-Wisconsin time and the present is listed in Table 4.4 and plotted at the top of Figure 4.10.

Analysis No.	Assigned Age (Ka)	Mean $\delta^{18}O_c$ (‰)	$\Delta\delta^{18}O_{sw,t}$ (‰)	$\Delta\delta^{18}O_{c,t}$* (‰)	ΔT (°C)
76013-1	63.5	-10.10	0.91	-0.89	4.09
-2	62.9	-10.15	0.95	-0.94	4.30
-3	61.9	-10.75	1.03	-1.54	5.84
-4	60.2	-10.32	1.13	-1.11	5.09
-5	58.4	-10.60	1.16	-1.39	5.80
-6	57.2	-10.49	1.16	-1.28	5.55
-7	56.0	-10.39	1.15	-1.18	5.30
-8	55.2	-10.48	1.07	-1.27	5.32
-9	53.8	-10.48	1.04	-1.27	5.25
75125-1	52.9	-10.49	1.07	-1.28	5.34
-2	50.0	-10.90	1.23	-1.69	6.79
-3	48.1	-10.99	1.13	-1.78	6.77
-4	45.7	-11.09	1.13	-1.88	7.00
-5	43.8	-11.26	1.30	-2.05	7.79
-6	43.0	-11.32	1.27	-2.11	7.86
-7	40.7	-11.36	1.32	-2.15	8.07
-8	37.8	-11.12	1.26	-1.91	7.37
-9	35.9	-11.39	1.48	-2.18	8.51
-10	33.7	-11.43	1.43	-2.22	8.49
-11	31.6	-11.60	1.43	-2.39	8.88
-12	29.5	-11.41	1.52	-2.20	8.65
-13	28.2	-11.33	1.55	-2.12	8.53

↑ using α_{c-w} = 0.26‰/°C

using α_{c-w} = 0.27‰/°C ↓

* using $\delta^{18}O_c$ (modern) = - 9.21‰

Table 4.4 Stable isotope and age data for 76013 and 75125, and estimated changes in $\delta^{18}O_{sw}$ used with Equations 4.1 and 4.2 in constructing Figure 4.10.

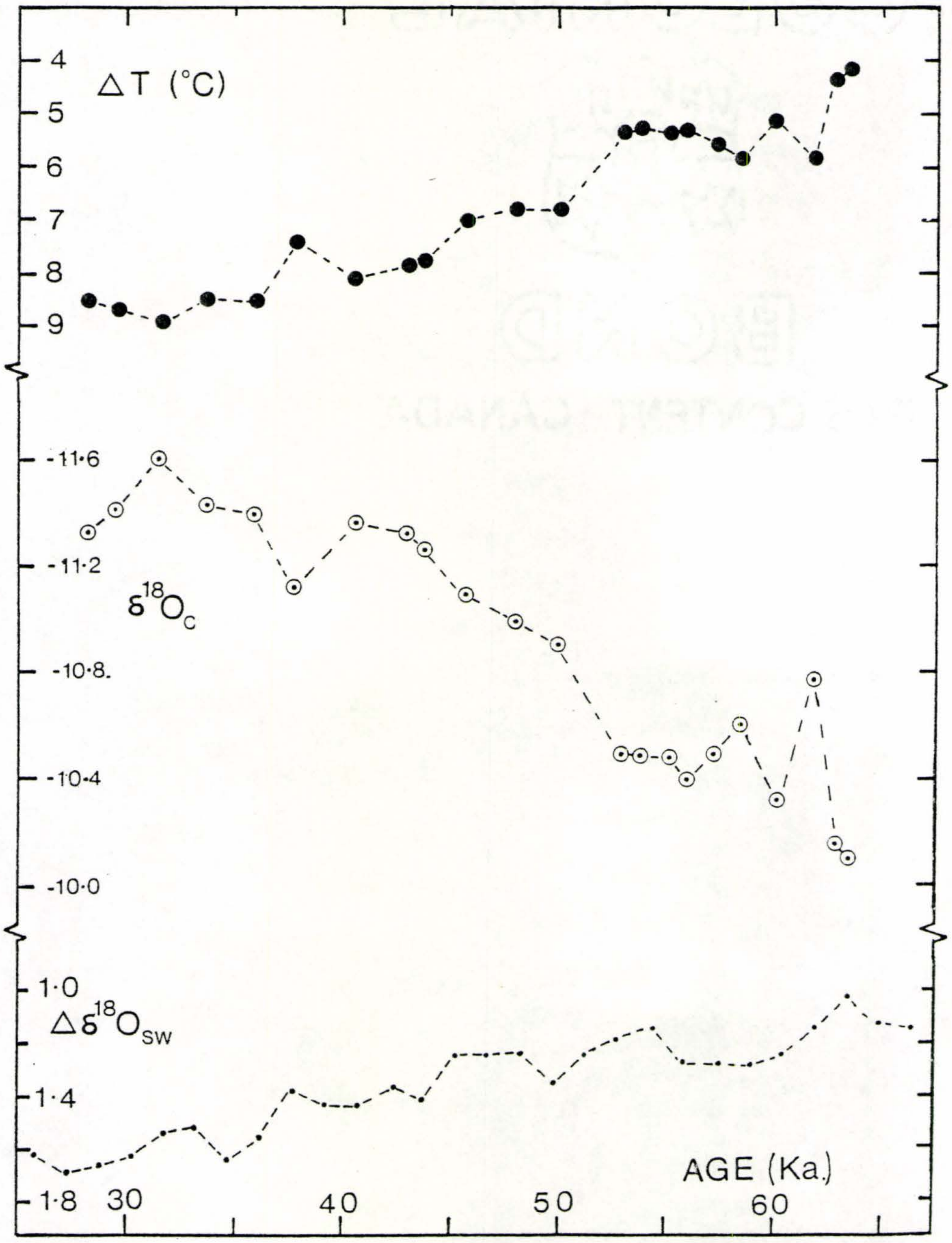

Figure 4.10 Variation of $\delta^{18}O_{sw}$ (lower curve), $\delta^{18}O_{c}$ (middle curve) and calculated difference in temperature (ΔT) between modern and time t (upper curve), over the Mid-Wisconsin period, 64 - 28 Ka. Data for this figure is listed and derived in Table 4.4.

If modern cave temperature can be estimated, absolute temperatures for the Mid-Wisconsin period can be determined. The temperature of two dripwaters in April 1975 from Cascade Cave was 6.9°C but this value may be less than the mean annual cave temperature because of bias of meltwater and the lag effect of winter climates at this time of year (see for instance, Pitty 1974). Mean annual temperatures of observation stations in the area have been determined from Monthly Records of Meteorological Observations in Canada (published by the Atmospheric Environment Service) and these are summarized in Table 4.5 and plotted in Figure 4.11. Moisture-laden winds which rise over this area will cool at approximately 0.6°C/100m (the saturated adiabatic lapse rate for 5°C and 1000 mbar), Berry et al. (1945). At the altitude of Cascade Cave, the mean annual temperature is about $8.0 \pm 0.5^{\circ}$C. Using this value the upper plot in Figure 4.10 has been recalibrated to give a paleotemperature curve for the Mid-Wisconsin in this area (Figure 4.12). This interpretation shows that speleothem growth may have been terminated by cessation of groundwater flow caused by persistence of sub-zero temperatures at the onset of the Late Wisconsin glacial maximum.

The temperature data in Figures 4.10 and 4.12 are affected by the following:

1) A mean value of $\delta^{18}O_c$ (modern) was used in the calculations. If instead, the lowest value given in Table 4.3 is used (least likely to be enriched with ^{18}O due to evaporation), ΔT_{max} in Table 4.4 becomes 8.14°C and therefore the lowest cave temperature from the record is -0.14°C, more in agreement with the requirement of

Station	Location	Map Ref.	Altitude (m a.s.l)	Period of Observations (yrs.)	Mean Annual Temperature (^{o}C)
Alberni Beaver Creek	15 km NNW of Pt.Alberni	4922 12456	91	59	9.3
Alberni Lupsi Cupsi	Pt.Alberni	4915 12449	9	26	9.4
Alberni Robertson Creek	15 km NW of Pt.Alberni	4920 12459	75	15	8.8
Pt.Alberni	as Lupsi Cupsi	4914 12448	60	45	9.8
Pt.Alberni A	airport	4915 12450	3	7	9.2
Qualicum Fish Research Stn.	Qualicum	4924 12437	7.5	14	9.8

Table 4.5 Location and mean annual temperatures for observation stations in the Horne Lake - Alberni region (data from Monthly Records of Meteorological Observations in Canada published by the Atmospheric Environment Service.

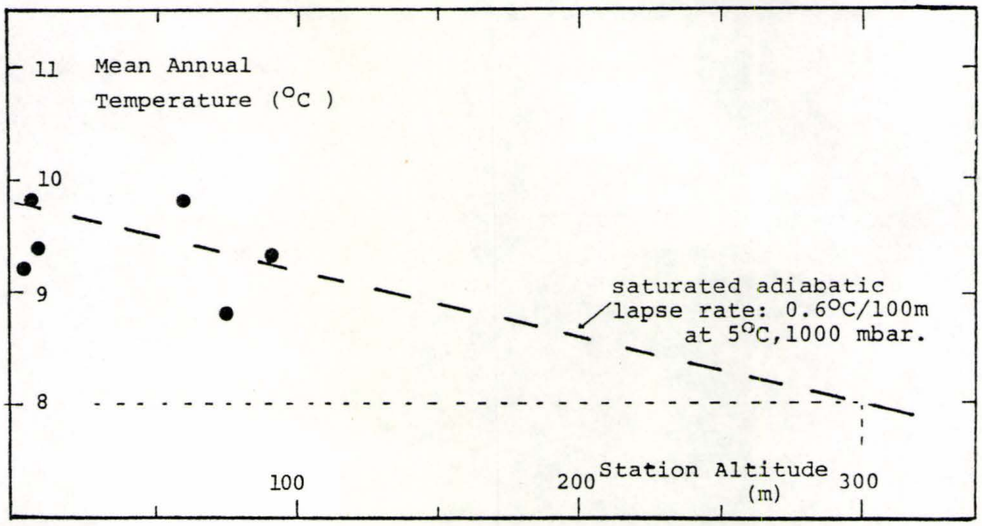

Figure 4.11 Graph of change in mean annual temperature with altitude for data in Table 4.5. Extrapolation at the saturated adiabatic lapse rate gives estimate for Cascade Cave.

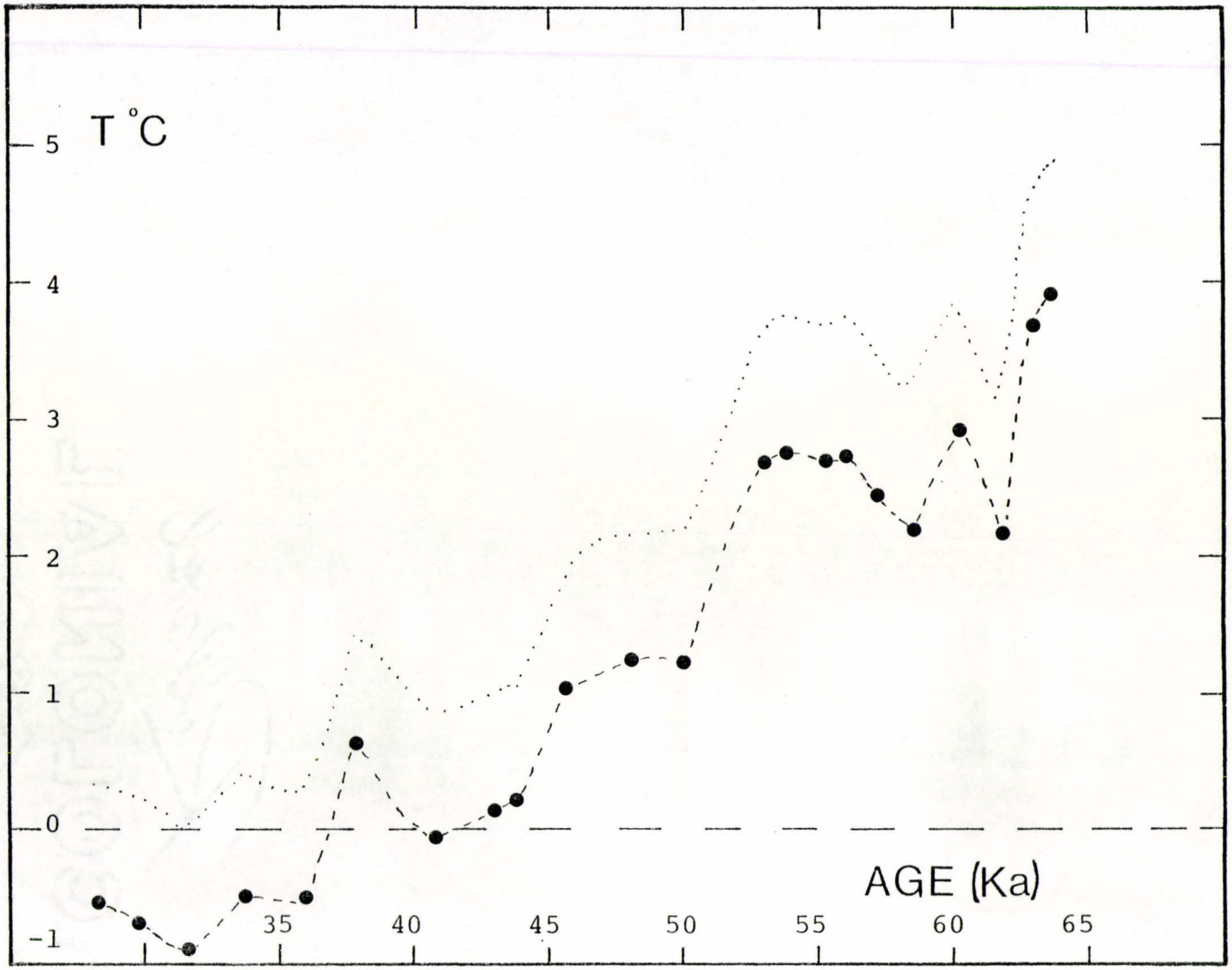

Figure 4.12 Paleotemperature curve for the Mid-Wisconsin period for south-central Vancouver Island at 300m a.s.l. (lower dashed line), from Figure 4.10 using mean value of $\delta^{18}O_c$(modern) and estimate of $\delta^{18}O_f$ (modern) for core V19-28. Upper dotted curve shows allowance for temperature influence on $\delta^{18}O_f$ record and uses minimum $\delta^{18}O_c$ from Cascade Cave, (minimum paleotemperature is $\geqslant 0^{o}$C).

non-freezing conditions for speleothem growth.

2) a further increase of up to 0.4°C in calculated temperatures is obtained if ocean bottom water temperature <u>does</u> vary during glacial/interglacial transitions, causing $\delta^{18}O_f$ to change by up to 0.2 ‰ (Ninkovitch and Shackleton 1975).
3) Dansgaard's temperature coefficient for change of $\delta^{18}O$ of precipitation may be inapplicable at this site. No data are available to test this, but values greater than 0.7 ‰/°C would reduce the calculated range of ΔT as well as generally decreasing its values (and thus raising calculated paleotemperature). The more commonly-observed case of a reduction in the coefficient (ie. < 0.7; Table 3.2) would have the reverse effect, - an unlikely situation because speleothem cannot grow in sub-zero conditions as this case would require.
4) speleothem may change its growth habits as temperature decreases (ie. it may tend to grow more during warmer months) and so $\delta^{18}O_c$ can not be related to mean annual temperature in the same way. This is discussed more fully in Chapter 3.

Errors due to the first two conditions are quantifiable and their maximum effect is shown in Figure 4.12. Combined analytical errors associated with $\delta^{18}O_c$ and $\delta^{18}O_f$ are small by comparison, and correspond to uncertainties of ± 0.4°C. More precise estimates of the present mean annual temperature of the cave will better indicate whether the speleothem terminated growth at or below 0°C.

One striking aspect of the paleotemperature curve in Figure 4.12 is the absence of any obvious interstadial warm 'spike' as seen in mid-continental records of Canada and the U.S.A. (eg. Dreimanis and Karrow 1972). This could be due to the frequency of sampling on the speleothem (approximately one analysis per Ka in 76013 and one per 2 Ka in 75125). However, a more likely reason is that prolonged warm periods did not exist due to the proximity of the ocean, which acted to damp out any sudden thermal fluctuations.

4.8 Summary and Conclusions

This study has shown the following:

1. Caves investigated in south-central Vancouver Island, with the possible exception of Euclataws Cave, appear to be young in comparison to those in the Canadian Rockies. Evidence for this is:
    i) most of the caves are presently undergoing active vadose entrenchment in restricted, precursor (phreatic) passages,
    ii) only Euclataws Cave contains extensive sequences of detrital sediment and re-excavation, followed by deposition of some overlying stalagmite cover. Riverbend and Cascade Caves show little evidence of fill phases,
    iii) in Cascade Cave no speleothem ages older than Early Wisconsin times have been determined, suggesting that the cave may be as young as the Sangamon interglacial. Unfortunately no reliable ages have been determined from the other caves due to low uranium concentrations.
2. In Cascade Cave, a number of speleothem deposits were formed during the period 62 - 43 Ka suggesting that this was the warmest period of

the Mid-Wisconsin interstadial,

3. Two speleothems of Cascade Cave were formed in isotopic equilibrium during the period 64-28 Ka. They show comparable $\delta^{18}O_c$ values over the period of age overlap. At all times, speleothem $\delta^{18}O_c$ was less than modern $\delta^{18}O_c$ by 0.9 to 2.4‰. This is contrary to all results determined for North American caves by previous workers so far. This demonstrates the overriding importance of the dependence of $\delta^{18}O_p$ on temperature for an oceanic environment, causing $\delta^{18}O_c$ to decrease as temperature decreases. At most continental sites $d\delta^{18}O_p/dT$ is considerably smaller, and the inverse relationships of α_{c-w} and $\delta^{18}O_{sw}$ to temperature becomes dominant, such that $\delta^{18}O_c$ increases as temperature decreases. Presumably at some point between these two types of site, $\delta^{18}O_c$ will show no variation with changing temperature.
4. A paleotemperature curve (Figure 4.12) for central Vancouver Island has been determined over the period 64 - 28 Ka before present, using current estimates of change in $\delta^{18}O_{sw}$ and of the temperature dependences of α_{c-w} and $\delta^{18}O_p$. The results show a steady decline in temperature from +4°C at 64 Ka to 0 to -1°C from 36 to 28 Ka. No distinct interstadial or stadial spikes are seen during this time, probably due to the dampening influence of the adjacent ocean. These results are consistent with the views of Clague, Armstrong, Alley and other Canadian workers that there was no widespread glacial advance during Mid-Wisconsin times.

CHAPTER 5

DATING AND STABLE ISOTOPE ANALYSIS OF SPELEOTHEMS FROM CAVES IN N.W.ENGLAND AND ITS CLIMATIC SIGNIFICANCE

Introduction

Karst regions of England and Wales are probably the most intensively studied of any in the world. The main areas, Mendip, South Wales, Derbyshire and north-west England, are shown in the inset of Figure 5.1. They are all characterised by prominent landforms such as tors, gorges, limestone pavements, dolines, potholes and springs, and they are best known for the innumerable caves developed within them. The limestone exposures of north-west England and in particular, the Craven District, immediately north of the road linking Kirby Lonsdale and Settle (Figure 5.1), are the most intensely karstified of all the regions. The Craven District contains a number of deep glaciated valleys known as the Yorkshire Dales, characterised by steep limestone escarpments topped by broad flat expanses of 'pavement' which are formed in the upper beds of the limestone. On these benches rise the steep-sided massifs of Ingleborough, Whernside, Penyghent and other less prominent, impermeable cappings. They act as collecting grounds for surface streams which sink on reaching the limestone and then resurge up to 200m lower down, in the valley bottoms.

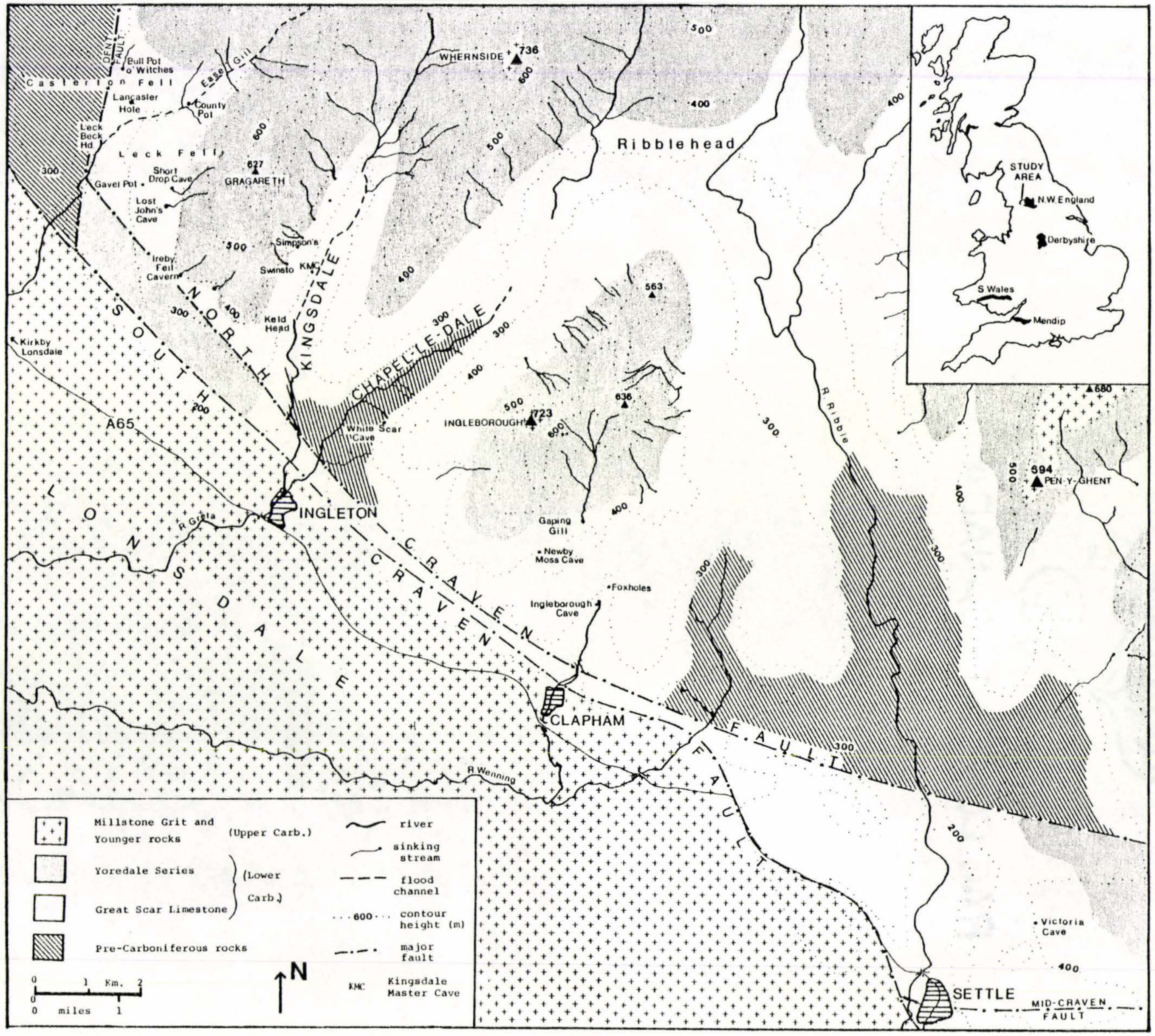

Figure 5.1 Map of Craven District, N.W. England showing location of caves and geology of the area.

Caves formed in this area range from large ancient tunnels situated well above the present water table to low wet crawlways and narrow fissures recently formed by sinking streams. The orientation and distribution of many of the caves bears no resemblance to the surface topography and for this reason exploration and mapping of these systems has frequently yielded surprising information about their origin and development. A detailed description of the area and its major cave systems is given by Waltham (1974).

Until recently, all theories of cavern genesis and enlargement in this region have been described in terms of sequential internal events and there has been little opportunity to relate them to other cave systems or surface phenomena. The relationship of the development of the English karst to Late Pleistocene climatic events has been tentatively outlined in recent literature (Warwick 1956, 1971; Waltham 1974) but much debate continues over the exact timing of cave initiation and periods of enlargement and infilling.

The results presented in this chapter conclusively show that cave and karst development in this region probably began prior to the last three glaciations. Most of the major cave systems have been sampled and the speleogenetic and climatic significance of the radiometric ages is described in this chapter, together with stable isotope data for a few speleothem deposits. These results allow an independent assessment of the time scale and intensity of British Quaternary events.

5.1 The Quaternary Chronology of England

5.1.1 Introduction

With the advent of glacial theory in the early nineteenth century came the realisation that almost all of Britain had been covered by ice at least once during recent times. A number of different tills, often interbedded with non-glacial deposits, were subsequently recognised as evidence for several extensive glaciations interspersed with warm periods. Initially, the classical glacial sequence developed for the Alps by Penck and Brückner (1909) was uncritically applied to the whole of Europe and the general concept of four major glaciations (Würm, Riss, Mindel and Günz) with associated warm interglacials, became firmly established. Stable isotope profiles of deep sea cores have recently shown this concept to be false, and in fact, over 17 glaciations may have occurred during Pleistocene time (Kukla 1977).

Direct evidence of more than three glaciations in England is so far not available, probably due to obliteration of deposits by weathering processes or superposition of more recent deposits. More definitive evidence of Early Pleistocene glaciations is found in the Netherlands, Denmark and parts of the Alps. Radiocarbon dating has shown that the Weichsel of Europe and the Devensian of Britain are contemporaneous with the Würm and that the preceding interglacial is probably of equivalent duration and timing for all regions. Beyond this however, no dating method has been sufficiently used to show synchroneity of earlier events.

A number of techniques have been developed which are capable of interrelating climatic events of the Pleistocene (Chapter 1), but none have the precision that is potentially available from the analysis of speleothems from caves in these areas. For this reason, and the fact that the speleothem results to be described in this chapter cover much of the Upper and Middle Pleistocene period, the status of knowledge of British and European Quaternary history will first be summarized.

5.1.2 Quaternary Stratigraphy

Evidence of climatic regimes and their timing in the British and European Quaternary period has come from many sources :

1) type and age of organic remains (eg. peat, trees, plants)
2) type and age of fossil bones, skeleta, shells (eg. vertebrate fauna, coleoptera, molluscs),
3) pollen sequences (in peat bogs, lake sediments, lacustrine and fluvial deposits),
4) levels of raised beaches, river terraces and wave-cut platforms,
5) presence of tills, fluvioglacial deposits, laminites.

The Alpine, N.European and British Quaternary stratigraphies are summarized in Table 5.1. The general classification proposed by Zeuner (1959) is also included. Correlation of events older than the Wolstonian (Riss, Saale) stage is extremely tenuous and is only shown here for convenience of presentation. Previous estimates of the age of stages older than the Devensian (Würm, Weichselian) have been omitted because of the large variability of values quoted by different authors and because of the conflict between the deep sea core time scale

Table 5.1 Comparison of Alpine, N.European and British Quaternary stratigraphies. Compiled from Zeuner (1959), Penny (1964), Evans (1971), van der Hammen et al. (1971), Coope (1977a,b), Shotton (1977), Funnel and West (1977), Godwin (1977) and Bowen (1977, 1978).

^{14}C and paleomagnetic time scale (Ka)		General terminology (Zeuner)	ALPINE	NORTHERN EUROPE			Pollen Zone	BRITAIN			Human Cultures
			Stage	Stage	Sub-stage	Description		Stage	Sub-stage	Description	
2	BRUNHES	Post - Glacial	RECENT	HOLOCENE			VIII	FLANDRIAN	Sub-Atlantic		Roman
											Iron Age
5							VIIb		Sub-Boreal		Bronze Age
							VIIa		Atlantic		Neolithic
							VI				
9							V		Boreal		Mesolithic
10							IV		Pre-Boreal		
11		Last Glacial	WURM	WEICHSELIAN LATE	Younger Dryas	c	III	DEVENSIAN LATE	Loch Lomond 10.5 (Highland) Re-advance 11.7	c	Upper Paleolithic (Cresswellian)
11.8 12.0					Allerød	w	II		LATE (Scottish Re-advance)	generally	
12.0 12.3					Older Dryas	c	Ic		GLACIAL INTER-	c	Lower Paleolithic
12.7					Bølling	w	Ib		(Windermere) STADIAL	w	
17					Oldest Dryas	c	Ia		Aberdeen - Lammermuir Re-advance	c (polar desert)	
26					Main Weichselian glaciation	c (polar desert)			Main Devensian glaciation	c (polar desert)	
30				MIDDLE	Denekamp I/S (Holl)	w (shrub tundra)		MIDDLE			
39					Hengelo I/S	w (shrub tundra)			Upton 42 Warren I/S Complex 44	w (boreal forest)	Mousterian
43					Moershoofd I/S (Holl)	W (shrub tundra)					
50 58				EARLY	Odderade I/S (Ger)	w (shrub tundra)		EARLY			
61					Brørup I/S (Den)	w (boreal forest)			Chelford I/S	w (boreal forest)	Levalloisan
63.5 65 68					Amersfoort I/S (Holl)	w (boreal forest)			Wretton I/S	w (boreal forest)	
		Last Interglacial	RISS-WURM	EEMIAN		interglacial		IPSWICHIAN		interglacial	Acheulian
		Penultimate Glaciation	RISS	SAALE	Drenthe Treene Warthe	glacial interstadial glacial		WOLSTONIAN	Ilfordian ?	I/S ? glacial	
		Penultimate Interglacial	MINDEL -RISS	HOLSTEIN		interglacial		HOXNIAN		inter-glacial	Clactonian
		Ante-penultimate Glaciation	MINDEL	ELSTER		glacial		ANGLIAN	Lowestoft Stade, Corton I/S Gunton Stade	glacial glacial	
		Ante-penultimate Interglacial	GUNZ-MINDEL	CROMER	III			CROMERIAN	complex	inter-glacial	
					II			BEESTONIAN		c	
690					I			PASTONIAN		w	
890	MATUYAMA Jaramillo	Early Glaciation	GUNZ	MENAP		c		hiatus ?			
950				WAAL		w					
1610				EBURON		c		BAVENTIAN		c	
1790	Olduvai		DONAU ?	TEGELEN		c		ANTIAN		w	
								THURNIAN		c	
2000								LUDHAMIAN		w	
2430			BIBER ?	PRE-TEGELEN				hiatus ?			
	GAUSS							WALTONIAN		c	

PLIOCENE

and that of terrestrial evidence based on K/Ar dates and stratigraphic correlations. However, a time scale based on recent paleomagnetic work (Zagwijn 1975, Bowen 1977) of East Anglian deposits is included in Table 5.1. The N.European succession is presented in Table 5.1 because it contains more detail of climatic events for some stages than the British sequence (particularly in the Devensian) and this will prove useful in the interpretation of speleothem data later on in this chapter.

5.1.3 Early and Middle Pleistocene of Britain

5.1.3.1 'Pre-glacial' Stages

The Crag deposits of Norfolk, Suffolk and Essex are the oldest Pleistocene deposits found in Britain. The Red Crag of Walton-on-the-Naze is thought to be equivalent to the Calabrian of Italy and together, these two formations have been designated as representing the beginning of the Pleistocene period (Mitchell et al. 1973). The stratigraphy of the Early Pleistocene in England has been determined mainly from borehole sections in East Anglia. Examination of pollen and foraminifera in these sediments has shown the presence of alternating cold and temperate conditions, extending up into the warm climate deposits of the Cromerian stage (Sparks and West 1972, p.130). A detailed description of Early Pleistocene deposits and type localities in Britain is given by Funnel and West (1977) and West (1977a). Recent paleomagnetic evidence has shown that a substantial part of the Early Pleistocene is missing from the existing English record (van Montfrans, in Zagwijn 1975; Bowen 1977). About one million years may separate the Pastonian from the

Baventian and 420,000 years between the Ludhamian and Waltonian deposits. This therefore extends the duration of the Quaternary to about 2.5 million years.

5.1.3.2 The Anglian Glaciation

The Cromer till at the base of the Anglian stage is the first evidence of the physical presence of glaciers in England (Figure 5.2). Originally known as the North Sea Drift, the Cromer till contains Scandinavian erratics which suggest an extensive ice cover spreading from the north-east and penetrating as far south as Essex and the Vale of St.Albans (Gibbard 1977). The overlying Corton Sands were deposited in a cold sea and therefore only indicate an interstadial climate. The extensive chalky Lowestoft till forms the west-to-east ice movement, suggestive of a north-westerly origin. It is thought that the Ailsa Craig granite erratics found on the west coast of Britain as far south as the Scilly Isles, were from an Irish Sea ice sheet either of Anglian age (Bowen 1977) or of Wolstonian age (West 1977a).

5.1.3.3 The Hoxnian Interglacial

The last stage that is best represented in East Anglia is the Hoxnian interglacial, a period characterised by a sequence of lacustrine and organic sediments which are frequently found as infillings in deep hollows in the underlying Lowestoft till. A complete succession from cold-climate silts to temperate organics and back into silts is seen in a borehole at Marks Tey, Essex (Shackleton and Turner 1967). Varve counting suggests that the succession was deposited over a period of

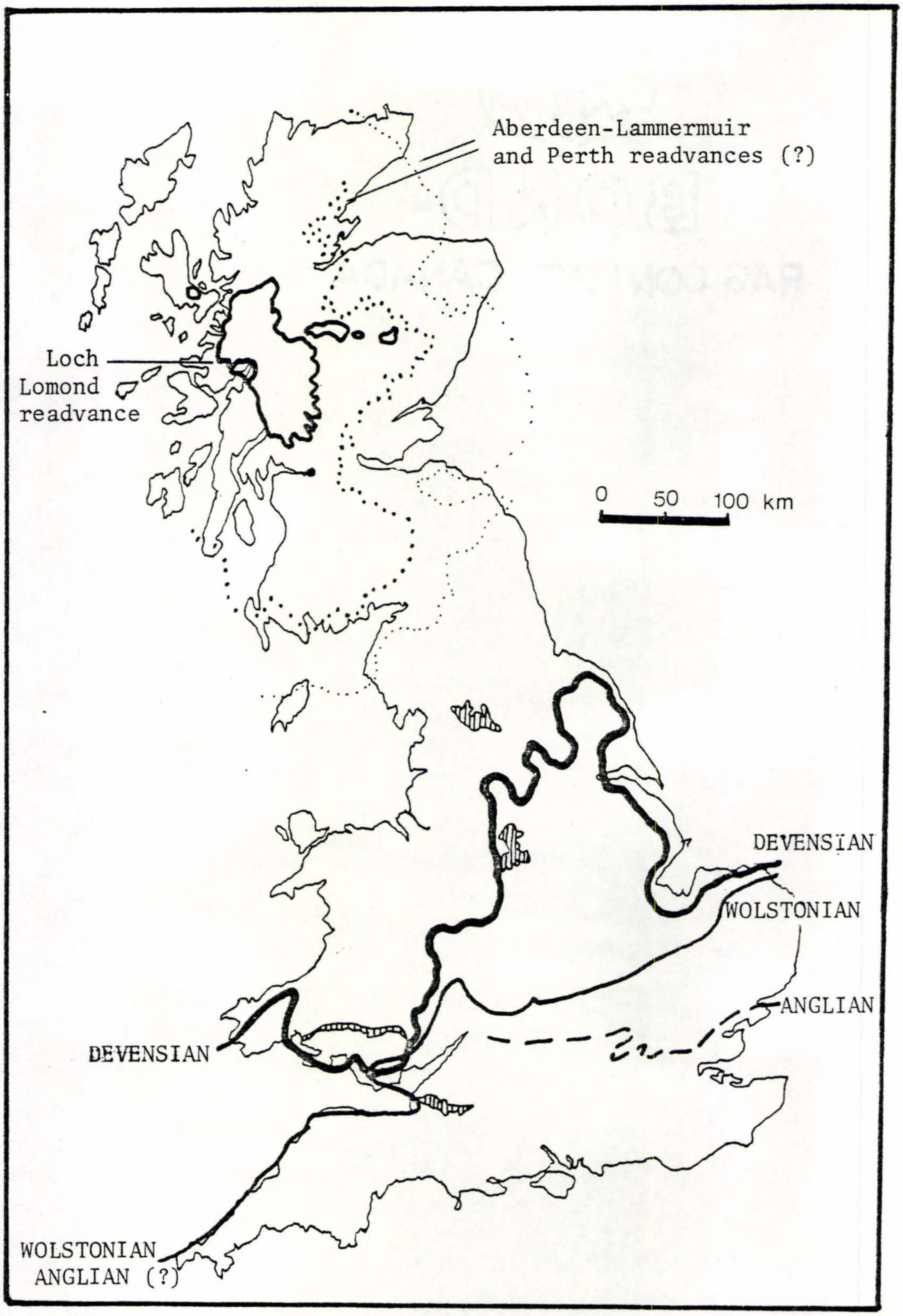

Figure 5.2 Limits of the main glaciations in Britain (after Warwick 1971, West 1977a, Bowen 1978).

30,000 to 50,000 years, thus destroying the previous common belief (deduced from the extent of weathering) of the Hoxnian being a 'Great Interglacial', of duration equal to or greater than 240,000 years (Penck and Brückner 1909).

Marine deposits from several Hoxnian sites have been found at elevations of between 20 and 30m above present sea level and this has been interpreted as a maximum eustatic sea level for the Hoxnian (Sparks and West 1972, p.147; Evans 1971). Using deep sea core isotopic data however, Shackleton and Opdyke (1973) find that sea level did not even reach modern levels at this time and therefore either i) tectonic uplift <u>must</u> have influenced the above sites (this is discounted by Mitchell (1977) because all the strata described are horizontal) or ii) the Hoxnian may not refer to stage 7 of the isotope record but possibly an earlier stage (in which case it becomes substantially older than 250,000 years B.P. - an age inconsistent with some terrestrial evidence). An alternative possibility is that the marine deposits may not in fact be Hoxnian in age but refer either to an earlier (warmer) interglacial or to the Ipswichian when sea level was somewhat higher than today.

Other evidence also suggests that the Hoxnian was a cooler period than the Ipswichian, and that a sea stand of +30m would therefore be unlikely (Shotton et al. 1977) :

i) pine, alder, spruce and fir were abundant in the Hoxnian with little oak,
ii) Mediterranean-type plants were present only in the Ipswichian,
iii) warmer beetle species were present in the Ipswichian,

iv) hippopotamus was only present in the Ipswichian.

5.1.3.4 The Wolstonian Glaciation

This stage was originally defined as the Gipping Glaciation after a till near Ipswich, but it was subsequently shown that the till was of Anglian age (Bristow and Cox 1973). Most Wolstonian till deposits are found in the Midlands although the exact extent of the ice cover remains unclear (see Figure 5.2). European, N.American and deep sea core data all suggest that this glaciation was the most intense, and in Europe, two glacial stages (Drenthe and Warthe) separated by an interstadial (Table 5.1) are thought to be its equivalent. These features are not apparent in most British Quaternary evidence although there is some suggestion that subdivision into two glacial events, enclosing a temperate phase (the Ilfordian) may more realistically define the Wolstonian (Bowen 1977).

5.1.4 Late Pleistocene of Britain

5.1.4.1 The Ipswichian Interglacial

Most deposits of the Ipswichian are found in terraces of river valleys in S.E.England. The type section is a sequence of gyttja (lake deposits) at Bobbitshole, Ipswich. The interglacial is characterised by the presence of hippopotamus, hyena, Mediterranean flora and shell fauna, and sea levels up to 15m above modern (Sparks and West 1972). This evidence suggests that temperatures were appreciably higher than today. Beetle evidence also indicates a warmer climate and one which is distinctly warmer than the preceding Hoxnian interglacial (Coope 1977a). Recently, pollen evidence from the Grande Pile peat bog in France has shown that the equivalent European interglacial (the Eemian) is a complex warm event with up to three temperate periods interspersed with cold, almost glacial, conditions (Woillard 1978). The classical Eemian is ascribed to the first, longest and apparently warmest of the three, and is succeeded by the St.Germain I and II interglacials, and separated from each other by the short Melisey I and II cold periods. These cold periods are correlated by Woillard to the two phases of the Alpine Riss glaciation in the manner proposed by Frenzel (1973) so that the Riss is <u>younger</u> than the Eemian. Deep sea core isotopic data and ages of fossil reef terraces clearly indicate the presence of multiple warm events in the last interglacial. In order of decreasing warmth, the stages 5e, 5c and 5a are dated at about 125, 105 and 80 Ka respectively (Mesolella et al. 1969, Shackleton and Opdyke 1973). However deep sea core data does not indicate a severe cold event during this period, of sufficient intensity and duration to be comparable to the present concept of the Riss glaciation. The problem of correlation rests on the assigning of a time scale to the Grande Pile sequence and on the intensity and duration of the cold periods.

5.1.4.2 The Devensian

1) Early Devensian

Early Devensian time in Britain is variously interpreted as lasting from 115 to 50 Ka (Bowen 1977) or from > 70 Ka to 50 Ka (West 1977a).

Evidence of an early Devensian glaciation is rather scarce in Britain (and in N.Europe), and there are very few British sites which incorporate both Ipswichian and early Devensian deposits. The type locality for the Devensian is the Four Ashes site north of Wolverhampton, in which early Devensian sands and gravels overlie a thin horizon of Ipswichian peat (Morgan 1973). Similar sequences are found at Wretton, Norfolk and Tattershall, Lincs. A cold tundra-like environment is indicated for the Early Devensian from these sites, by the presence of non-arboreal pollen and arctic beetle assemblages, although the total absence of till deposits suggests that ice sheets did not appreciably extend over lowland Britain. The Early Devensian is punctuated by several short climatic ameliorations classified as interstadials (Figure 5.3).

2) The Wretton Interstadial

Organic silt lenses in the sands and gravels overlying Ipswichian deposits at Wretton, Norfolk, have been designated type section for the Wretton Interstadial (West et al. 1974). The predominantly boreal tree pollen assemblage has been tentatively correlated with that of Amersfoort Interstadial in Holland. No radiocarbon dates have so far been obtained from the Wretton deposits, but those at Amersfoort show a duration from 68 to 65 Ka (Shotton 1977).

3) The Chelford Interstadial

Rich organic lenses with beetle species and macrofloral remains characteristic of boreal forest conditions define the interstadial type

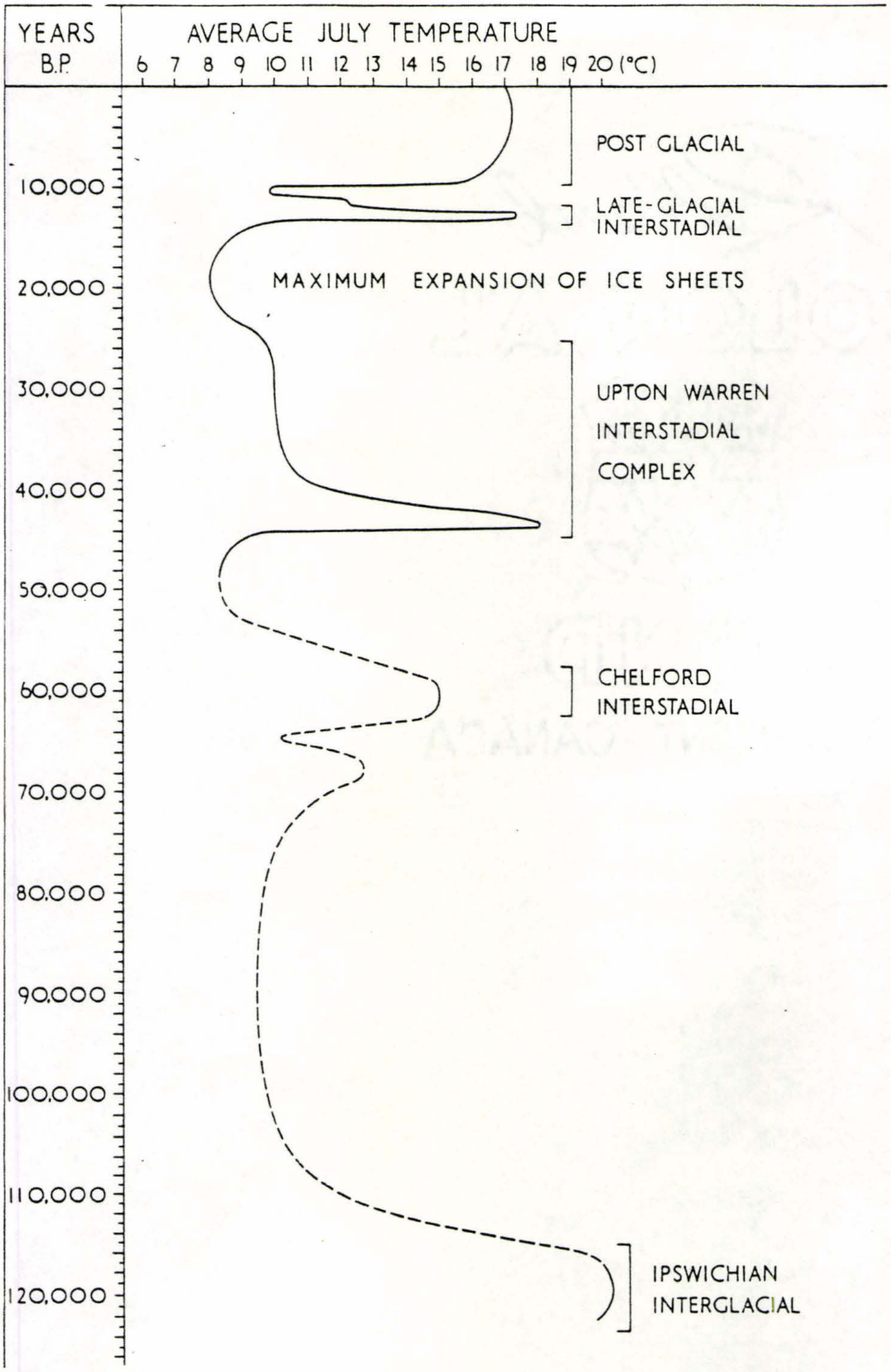

Figure 5.3 Climatic oscillations for the last 120 Ka in Britain, from beetle assemblages (from Coope 1975).

section at Chelford (Simpson and West 1958). An equivalent section is seen at Four Ashes, and possibly at Wretton, overlying the Wretton Interstadial deposits (although here, the beetle fauna suggest full arctic, treeless conditions - Coope 1977b). The Chelford and Brørup Interstadials appear to be equivalent, lasting from 63 to 61 Ka (van der Hammen et al. 1971, Shotton et al. 1977). Further evidence of climatic amelioration about 60 Ka comes from speleothem ages from three caves in Mendip and Yorkshire (Atkinson et al. 1978). Ages of 61 ± 4, 63 ± 11 and 63 ± 19 Ka were determined for three different speleothems, suggesting that permafrost was absent and vegetational activity was present in these areas at that time. Of the three interstadials of Early Devensian, (Early Weichselian), the Chelford (Brørup) seems to have been the warmest.

4) The Odderade Interstadial

This event has only been recognised and dated (58 Ka) at one site: Schleswig-Holstein, Germany, (Shotton 1977), and its existence depends to some extent on the true age of the Brørup found below it. No equivalent has been found in Britain so far.

5) The Upton Warren Interstadial Complex

This complex covers a period between 45 and 25 Ka. Average July temperatures up to 18°C (compared to 15.5°C today) have been determined from beetle assemblages in southern England over the period 44 to 42 Ka (Figure 5.3, Coope 1975). The remaining period was considerably cooler, attaining only 10°C at maximum. The Four Ashes site has also yielded a warm faunal population dated at 42.5 to 38.5 Ka and flora of a silt bed at Earith dates at 42.1 Ka and is known to require a summer mean temperature of about 16°C (in Shotton 1977). In spite of the warmth, the vegetation in Britain appears to have been treeless, suggesting that climate was changing too rapidly to allow the establishment of trees. This rapidity is further demonstrated by the cold-then-warm sequence of beetle horizons at Tattershall which lie within a few centimetres vertically of each other and have overlapping radiocarbon dates in the range 44 - 42 Ka (Girling 1974). Mollusc assemblages indicate continuously cold conditions over this period (Kerney 1977) and this lack of response to the environment may also indicate the short duration of the warming. On the continent, the Moershoofd (50 - 43 Ka) and Hengelo (40 - 37.5 Ka) Interstadials are well-documented events but neither correlate directly with the Upton Warren Interstadial. This apparent anomaly can however be explained in a number of ways, eg. systematic error in age measurement, unique climatic differences between the two areas, bias due to the small number of deposits available etc.

6) Pre-Main Devensian Glaciation

A number of radiocarbon dates have been determined for organic horizons and bones for the period 39 - 26 Ka. All deposits studied indicate an arctic tundra-like environment (Shotton 1977). No equivalent of the Denekamp (30 Ka) Interstadial is clearly seen in Britain, although the present scarcity of dates about that time does not preclude its existance.

7) The Main Devensian Glaciation

Till of Main Devensian age is widespread in Britain, covering most of Ireland and Scotland and terminating in England north of the Midlands (Figure 5.2). The Hunstanton Till in East Anglia, the Marsh Till of Lincolnshire and the Purple and Drab Tills of East Yorkshire were deposited by ice moving southwards in the North Sea (Shotton et al. 1977). The Cheshire Plain in the west is covered by the Irish Sea Till, but it is not yet certain that the North Sea and Irish Sea ice sheets were contemporaneous. Most evidence points to the maximum glaciation occuring about 18 Ka (the Dimlington moss at Holderness was overun by ice shortly after 18.5 Ka, - Penny et al. 1969; and a woolly mammoth bone was sealed in a Welsh cave by till about 18 Ka - Rowlands 1971). Recent work has shown ice thicknesses at maximum glaciation to be 2000m in the Scottish Highlands, 1600m on the Isle of Man and 800m over mid-Wales (Bowen 1977).

8) Deglaciation

Deglaciation of lowland Britain began sometime after 18 Ka, continuing to about 13.5 Ka. A few radiocarbon dates on beetle populations and wood deposits are available from gravels and clays underlying late-glacial and Flandrian deposits in Britain (Coope 1977b). Taxonomy and dating of these deposits indicate ice-free conditions over the period 14.5 to 13.5 Ka but a tundra-like environment with a climate of arctic severity. European evidence suggests an ice re-advance (the Oldest Dryas) between 15 and 12.7 Ka (Penny 1964). Of comparable age is the Aberdeen-Lammermuir re-advance in Scotland (Flint 1971, Jardine and Peacock 1973) with a maximum at about 13.5 Ka. Following the Oldest Dryas in Europe there are two interstadials, the Bølling (~12.7 - 12.0 Ka) and the Allerød (11.8 - 11.0 Ka), separated by a short cold spell, the Older Dryas. British evidence suggests only one warm period existed, the Last Glacial Interstadial from about 13 to 11 Ka. Maximum temperatures were reached at 12.5 - 13 Ka and this period has been recently termed the Windermere Interstadial (Figure 5.4, Coope 1977b). Beetle assemblages from the Windermere type section indicate July temperatures to be warmer than today. Scottish evidence suggests the presence of an ice re-advance (the 'Perth' event) towards the end of the Windermere Interstadial, but its timing and existence are in some doubt (Jardine and Peacock 1973, West 1977a).

A well-defined cooling associated with an ice re-advance occurred between about 11.7 and 10.5 Ka (Sissons 1967). It is known as the Younger Dryas in Europe and the Loch Lomond (or Highland) Re-advance in Britain (Figure 5.4). Beetle evidence has again provided the best insight to temperature changes over this period, showing that arctic tundra conditions were present in Britain at this time (Coope 1977b).

5.1.4.3. The Flandrian Stage

By 9.5 Ka temperatures had increased to today's values and the Flandrian of Britain and Holocene of Europe were marked by complete deglaciation and high sea stands, resulting in raised beaches and shorelines along the coast of Britain. Full isostatic recovery was essentially attained by the time of the 'hypsithermal', a thermal maximum at about 5.5 Ka (Flint 1971). Modern temperatures are thought to be

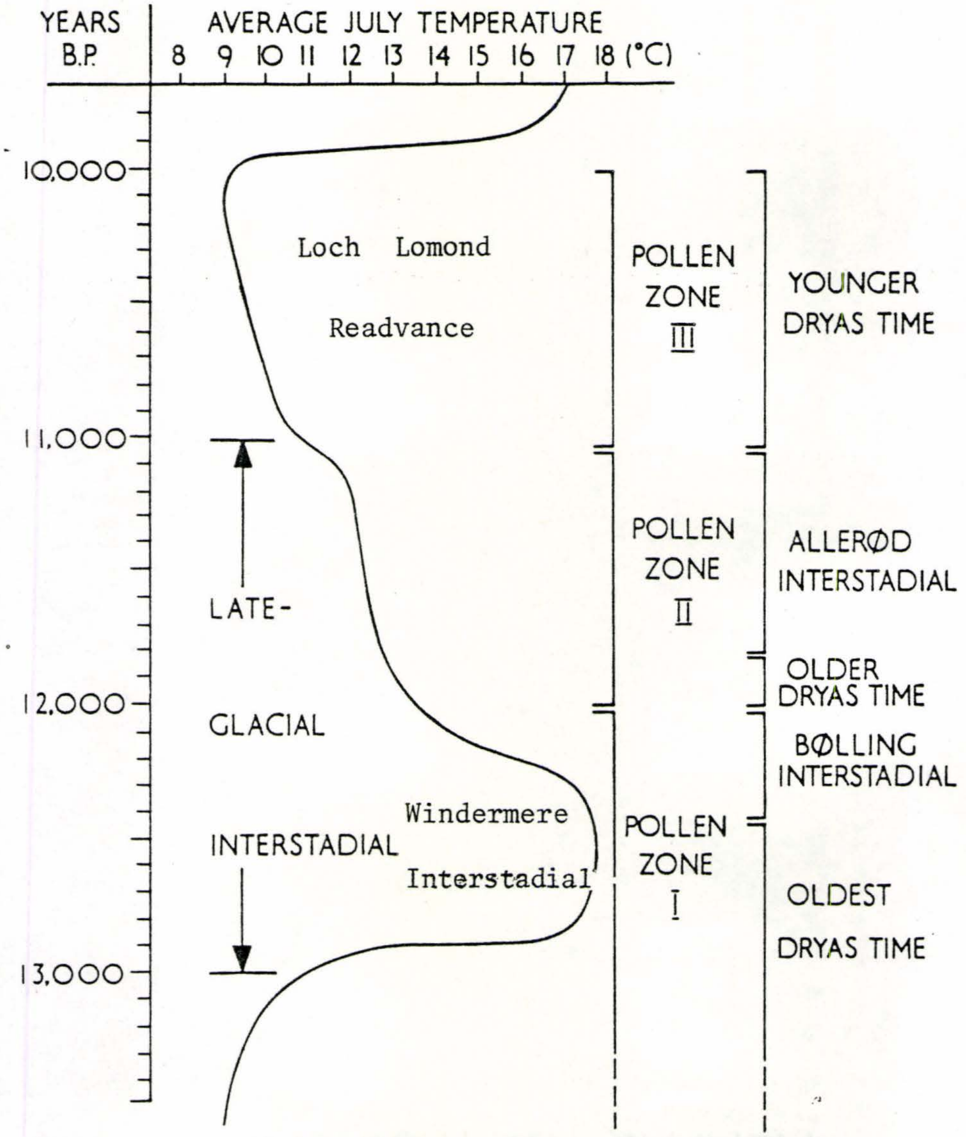

Figure 5.4 Post-glacial climatic fluctuations in lowland Britain showing comparison with the N.European record (after Coope 1975).

somewhat cooler than at this time.

5.1.5 Quaternary Evidence from the Craven District

The oldest glacial sequence recorded in northern England is from boreholes in the Isle of Man where three tills are seen interbedded with sands and gravels (King 1976). The lowest till is thought to be Wolstonian in age, and is occasionally seen in the Pennines and Lake District as deposits of erratics with fines washed out, covered by peat. In the Pennines, this glaciation is known as the Maximum Dales glaciation and the Devensian is known as the Main Dales glaciation, (King 1976).

In the Craven District, pre-Main Devensian deposits are scarce and are mainly restricted to cave earths, usually associated with a datable fauna. During the Main Devensian, ice covered most of the region to altitudes of 670m above sea level (Goodchild 1875). The higher parts of the Yorkshire Dales formed an ice spreading centre as shown by a restriction of Lake District and Scottish erratics to the northern parts only (West 1977a). Glacial erratics found in this region are therefore confined to the local limestones, overlying impervious rocks and the occasional basement slates. Sweeting (1974) has suggested that valley glaciers have caused as much as 60m of overdeepening by direct erosive power. Surrounding limestone benches, particularly in the south, have been scraped clean of cover and may have further been exposed by removal of the overlying Yoredale shales (Figure 5.1). Southward-moving glaciers have left thick deposits of till in the lee of the higher hills (eg. on Newby Moss and East Kingsdale) and a large drumlin field is found at Ribblehead (Warwick 1956).

5.2 The Geological Setting

The major cave systems of north-west England lie towards the southern limb of the Askrigg Block, a major structural feature of the basement rocks. The southern and western boundaries of the Askrigg Block are clearly defined by the Craven and Dent faults respectively and the whole massif dips gently to the north-east (Figure 5.1). Steeply-dipping basement rocks of impervious pre-Carboniferous slates and sandstones outcrop in valley floors near the Craven fault zone, and although not seen at the surface, the Wensleydale granite underlies these formations (Dunham 1974). Most cave development is found in the Lower Carboniferous Great Scar limestone, a pale-grey, massively-bedded unit, up to 200m thick (Figure 5.5). The limestone lies unconformably on the pre-Carboniferous basement. In the Ingleborough area it has been classified into four zones: C_2, S_1, S_2 and D_1 based on fossil content (Dunham et al. 1953; Edwards and Trotter 1968). A number of marker beds are easily recognised in the limestone sequence and these outcrop as distinct horizons in some of the dales (Figure 5.5). Schwarzacher (1958) has classified the upper part of the Great Scar limestone in terms of cyclic horizons of micrite and sparite separated by bedding planes at 10m intervals. Waltham (1971) recognised about 20 shale partings in the Great Scar, many of them of large horizontal extent, but both he and Wilson (1974) found them not to be correlated to the depositional cycles of Schwarzacher and so rejected this method of classification.

Overlying the Great Scar limestone are the Yoredale Series, a cyclic sequence of limestones, shales and sandstones, unconformably capped by the Upper Carboniferous Millstone Grit. In certain areas the lowest Yoredale limestone unit directly overlies the Great Scar limestone with

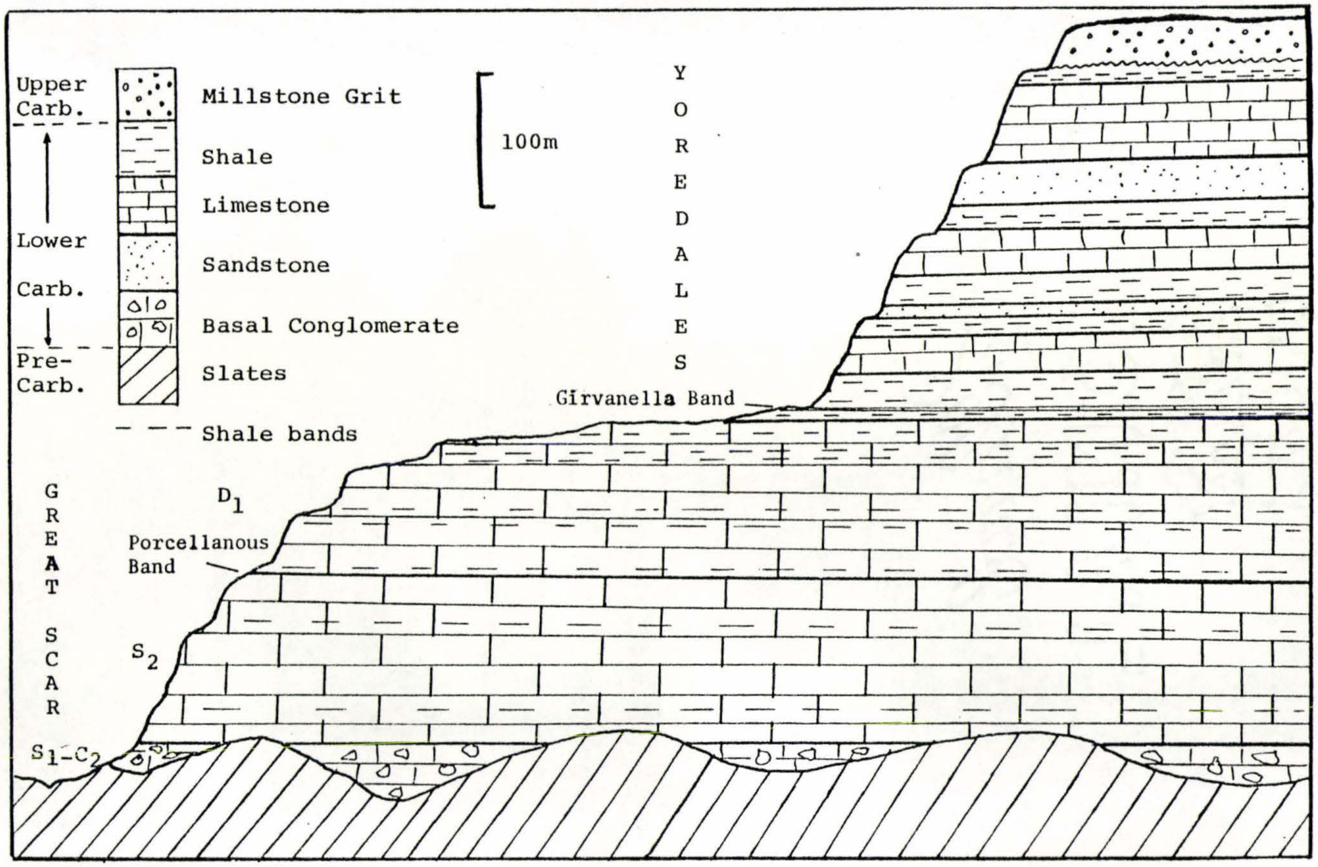

Figure 5.5 Diagrammatic representation of the geological section through Ingleborough.

only a minimal thickness or complete absence of intervening beds, thus giving a greater potential depth for cave development. A thin but extensive bed of blue-black limestone, the Girvanella Band (Figure 5.5) marks the top of the Great Scar limestones.

To the south of the Askrigg Block the Craven faults terminate the exposure of the Great Scar limestone by progressively downfaulting to the south in steps of 300-600m (Waltham 1974). At the Dent fault in the west, the limestones are downthrown about 600m such that they now outcrop against Silurian grits. Within the Askrigg Block, the Carboniferous rocks are relatively undisturbed except for smaller discontinuous faults and several shallow folds whose axes generally run subparallel to the two major fault boundaries.

5.3 Speleogenesis of Caves in the Area

Caves of both phreatic and vadose origin are found in large numbers in the Craven area. The occurrence of several fossil phreatic cave passages at apparently similar levels was initially interpreted by Sweeting (1950) as evidence of a water table origin. Waltham (1974) showed that the following geological controls were far more important in this region:

1) Lithology: The Great Scar Limestone contains both micritic and sparitic members whose relative solubilities and porosities vary. For instance, the Porcellanous Band, at the base of the D_1 limestone is a dense, blue-grey, micritic limestone. Its apparent resistance to solution has caused many passages to develop directly above it, a feature particularly evident in the Gaping Gill system (Glover 1974).

2) Shale Bands: About 20 shale horizons (from 1cm to 2m thick) are found in the D_1 unit of the Great Scar Limestone (Waltham 1971). These tend to be grouped into three zones (Figure 5.5); near the top of the limestone within 25m of the Girvanella Band, about 45m above the Porcellanous Band, and immediately above and below the Porcellanous Band. Although mechanically weak, these shale units are completely insoluble and therefore act as a barrier to downward cave development until stream turbulence is sufficient to cut through them. Waltham (1971,1974) cites many examples of cave passages initiated along the top of these bands.

3) Structure: Gentle folds, joints and small faults in the Great Scar Limestone are important structural controls for the development of phreatic and vadose caves. Although joint density is somewhat affected by lithology, joints are typically spaced between 0.5 and 3m apart (Waltham 1970a). Cave passages frequently follow prominent joints especially if oriented in a down-dip direction. Flooded or phreatic sections of vadose caves are often the result of temporary up-dip development, caused either by following a prominent joint or by the change in dip across a shallow syncline (Waltham 1974). Faults are less frequent, but usually afford easier downward development than joints, such that they characteristically give rise to large high rifts and short, deep cave systems.

In practice Craven caves are probably influenced by all three geological controls described above, and additionally their length, depth and complexity will be affected by the 'local water table level' (usually the valley floor or pre-Carboniferous horizon).

The morphology and speleogenesis of the caves sampled in this study is itself an enormous topic and is considered at length in numerous publications eg. Cullingford(1962); Eyre and Ashmead (1967); Ashmead, Brook, Glover, Lyon and Waltham (in Waltham 1974); Waltham (1977). A short description of the morphology of each of the caves follows and a more detailed consideration of their origin is given later on in this chapter, in light of the radiometric age measurements.

5.4 Cave Descriptions

The caves sampled were (from west to east): The Lancaster Hole-Ease Gill Cavern system, Gavel Pot, Lost John's system, Kingsdale Master Cave, Ibbeth Peril I, White Scar Cave, the Gaping Gill-Ingleborough Cave system, Victoria Cave and Sleets Gill Cave. Locations of most of them are shown in Figure 5.1. Approximately 130 speleothems were collected on two visits to the area in 1976 and 1977. A brief return was made in 1979 to collect several speleothems stratigraphically related to those previously sampled. For reasons of conservation, an effort was made to restrict the collection to loose, broken deposits, but about 15% were from *in situ* fossil flowstone deposits. About seven *in situ* stalagmites and flowstones were collected for paleomagnetic analysis by A.G. Latham. All samples dated are listed, located and described in Appendix 4a . The samples are not located on most of the cave maps included below because of the complexity of most cave systems and large number of samples collected.

5.4.1 The Lancaster Hole - Ease Gill Cavern System

This complex cave system is over 100m deep and is now the longest in Britain (46km) and tenth longest in the world. The entire system underlies Casterton Fell, the westernmost limestone outcrop of the Askrigg Block, and is bounded by the Dent fault in the west and the Craven fault in the south (Figure 5.1). Most of the system's length consists of distributary inlet passages taking water from the main surface stream, Ease Gill (Figure 5.6). The main drainage direction in the cave is from Ease Gill in the east towards Lancaster Hole in the west, whereupon the stream passage (or 'Master Cave') ends in a sump and flow continues under phreatic conditions to the resurgence, Leck Beck Head, about 900m to the southwest. For the most part, the high vadose stream passage runs below a horizontal fossil phreatic tunnel, up to 15m in diameter and about 30m above the stream in the western section (Figure 5.7). Collapse into the stream below has enlarged the tunnel in a number of places thereby connecting the two passages. Numerous other levels of development are found in the west and it is here that connections to Bull Pot of the Witches and other caves to the north may be found. The multi-level passages of Lancaster Hole demonstrate the age and complex development of the system. In addition, a recent connection to the Leck Fell caves via Pippikin Hole on the east side of Ease Gill further indicates its antiquity.

Speleothems were collected from most of the abandoned phreatic tunnels and chambers in the system including Easter Grotto, the main tunnel from Stop Pot to Fall Pot, Bill Taylor's Passage and Bridge Hall.

5.4.2 Gavel Pot

Gavel Pot is one of a number of separate caves on Leck Fell that are genetically related and which drain to the same resurgence, Leck

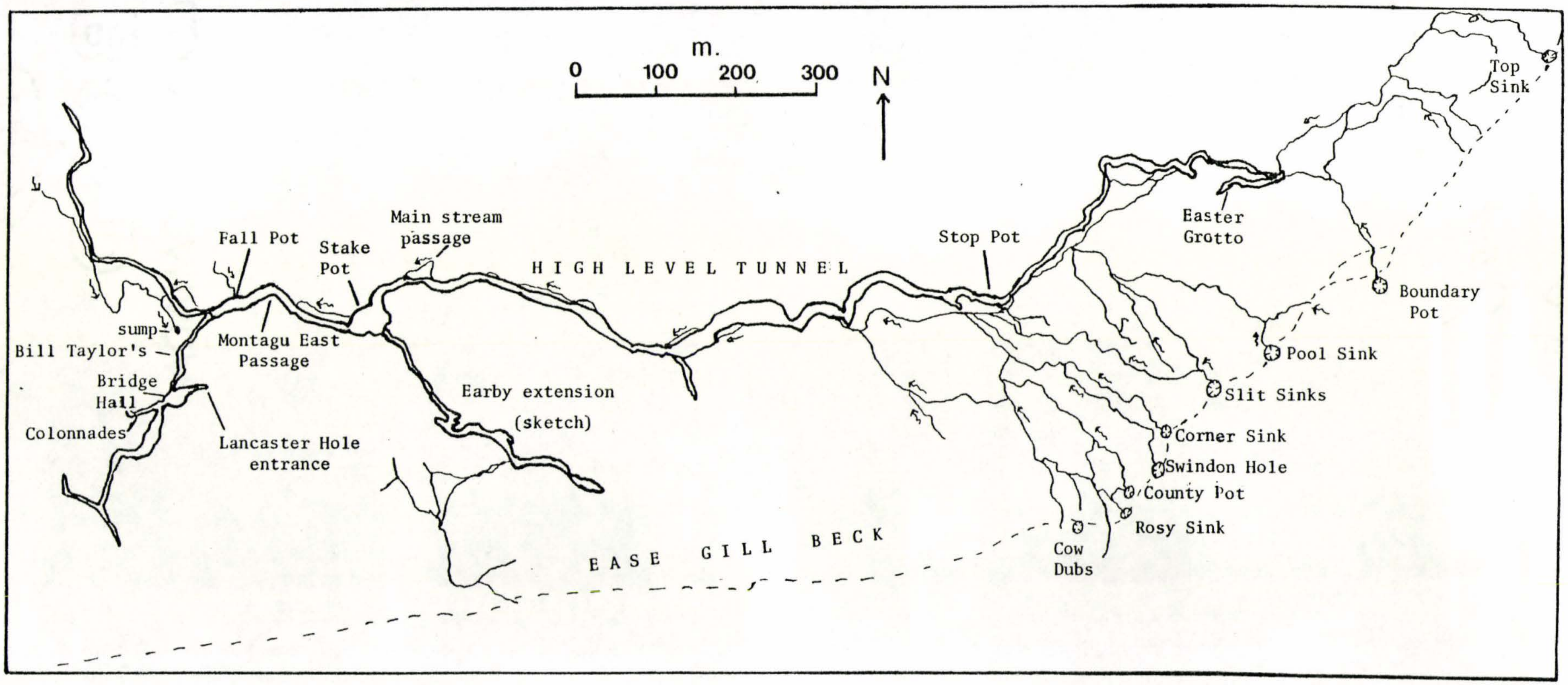

Figure 5.6 Line survey of the Lancaster Hole - Ease Gill Cavern system (after Ashmead 1967).

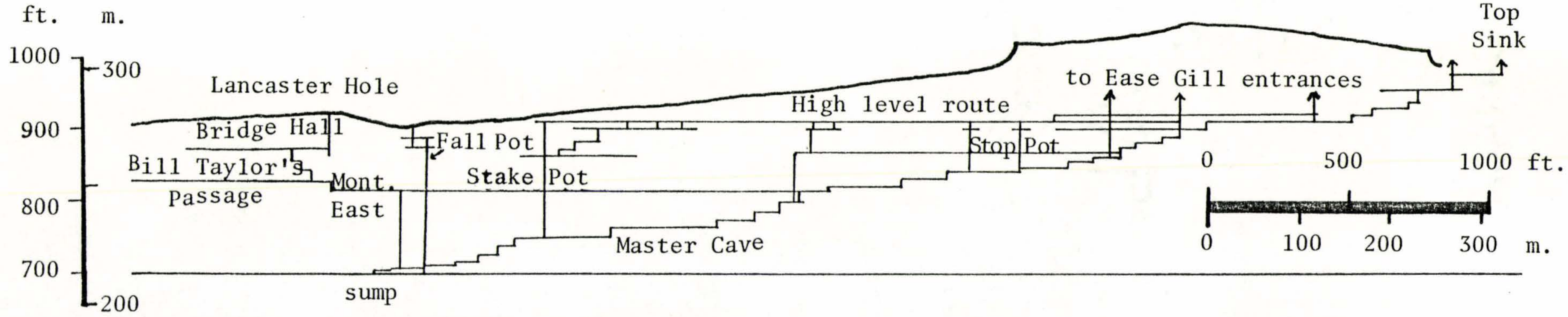

Figure 5.7 Schematic elevation of the Lancaster Hole - Easegill Cavern system (after Ashmead 1974).

Beck Head (Figures 5.1, 5.8). It forms the lower part of the Short Drop Cave drainage route and contains an active vadose streamway which finally drops into a sump via a series of vertical pitches. Above the pitches are two phreatic tube passages : one forms a loop and its arms now act as feeders to the vadose drain, and the second, Glasfurd's Passage, is partially blocked by sediment and contains a number of well-decorated chambers. Broken speleothems were collected from this passage.

5.4.3 Lost John's System

This cave, also on Leck Fell, has a complex series of phreatic rift and active vadose canyon passages in its upper levels, which enter a high meandering streamway (the Main Drain) about 140m below entrance level (Figure 5.8). Now known as the Leck Fell Master Cave, the Main Drain originates upstream at Lyle Cavern, a large collapse chamber whose fossil roof passages show phreatic development with a later stage of vadose modification. They probably represent the original water route from Lost Pot (Figure 5.8). At stream level in Lyle Cavern, the Main Drain can be followed up a low vadose passage to a series of high avens, the present inlets for Lost Pot water. Downstream from Lyle Cavern, the Main Drain continues unbroken for 1500m as a high narrow meandering canyon, comparable to that of the Lancaster Hole-Ease Gill Cavern system, but without the separate high level phreatic tunnel. Tributary streams from Rumbling Hole and Death's Head caves join it below the Lost John's inlet. The passage eventually sumps at about the altitude of the resurgence which lies 1km to the north west.

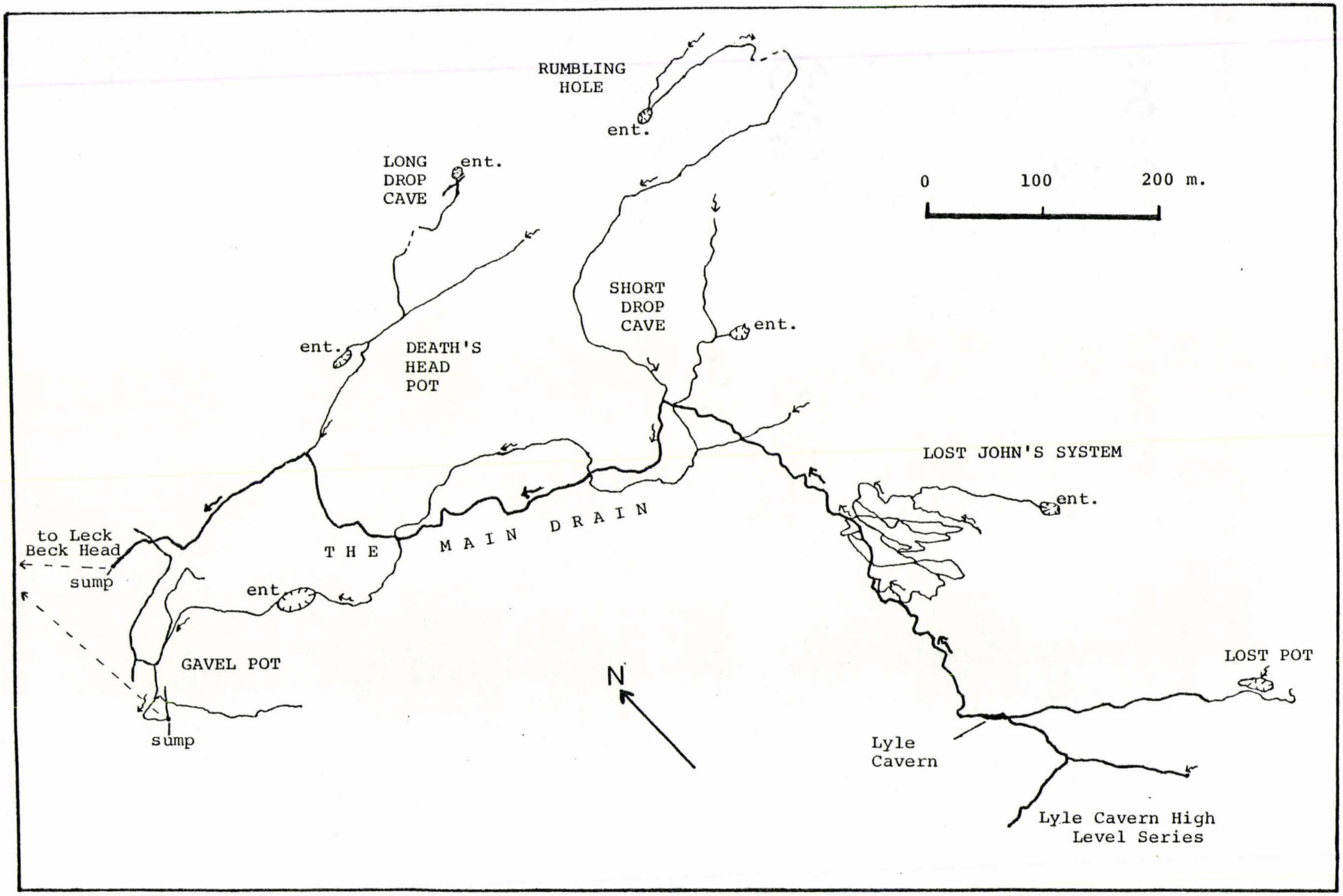

Figure 5.8 Line survey of the Leck Fell cave system (after Waltham 1970b).

The Lost John's system is in general, poorly decorated with speleothem and the only samples collected were from in situ, fossil stalactite curtains and loose eroded flowstone blocks in the Main Drain, and from a boulder choke at the end of the Lyle Cavern high level series.

5.4.4 Kingsdale Master Cave

Kingsdale is a classic hanging valley, partially blocked by moraine at its outlet into Lonsdale. It is unlike most of the other Dales that terminate at the Craven Fault because its floor has not been incised to the impervious basement, but instead is covered by gravels of glacial origin, perhaps 25m thick. The Kingsdale Master Cave (Figure 5.9) is the main drainage route for all active cave systems on the West Kingsdale slopes (recently it has also been found to take some East Kingsdale water). The cave is entered a few meters above valley floor level via a fossil phreatic tube known as the Roof Tunnel. It then splits into two routes, the westerly one leading into a series of complex fossil phreatic crawlways (Milky Way and Carrot Passage) and the northerly route ending abruptly at a 5m drop into the Master Cave. The terminal sump lies immediately downstream but upstream a high wide vadose canyon with roof tube can be followed to a series of low inlets from Simpson's and Swinsto potholes in the west and a low canal section draining caves further up valley. The vadose section has been interpreted as the most recent feature of the cave. Its roof tube originally took water via the Roof Tunnel to resurge at some point higher than Keld Head but which now is blocked by debris. A higher level of phreatic development is seen in Swinsto Hole below the Turbary Inlet

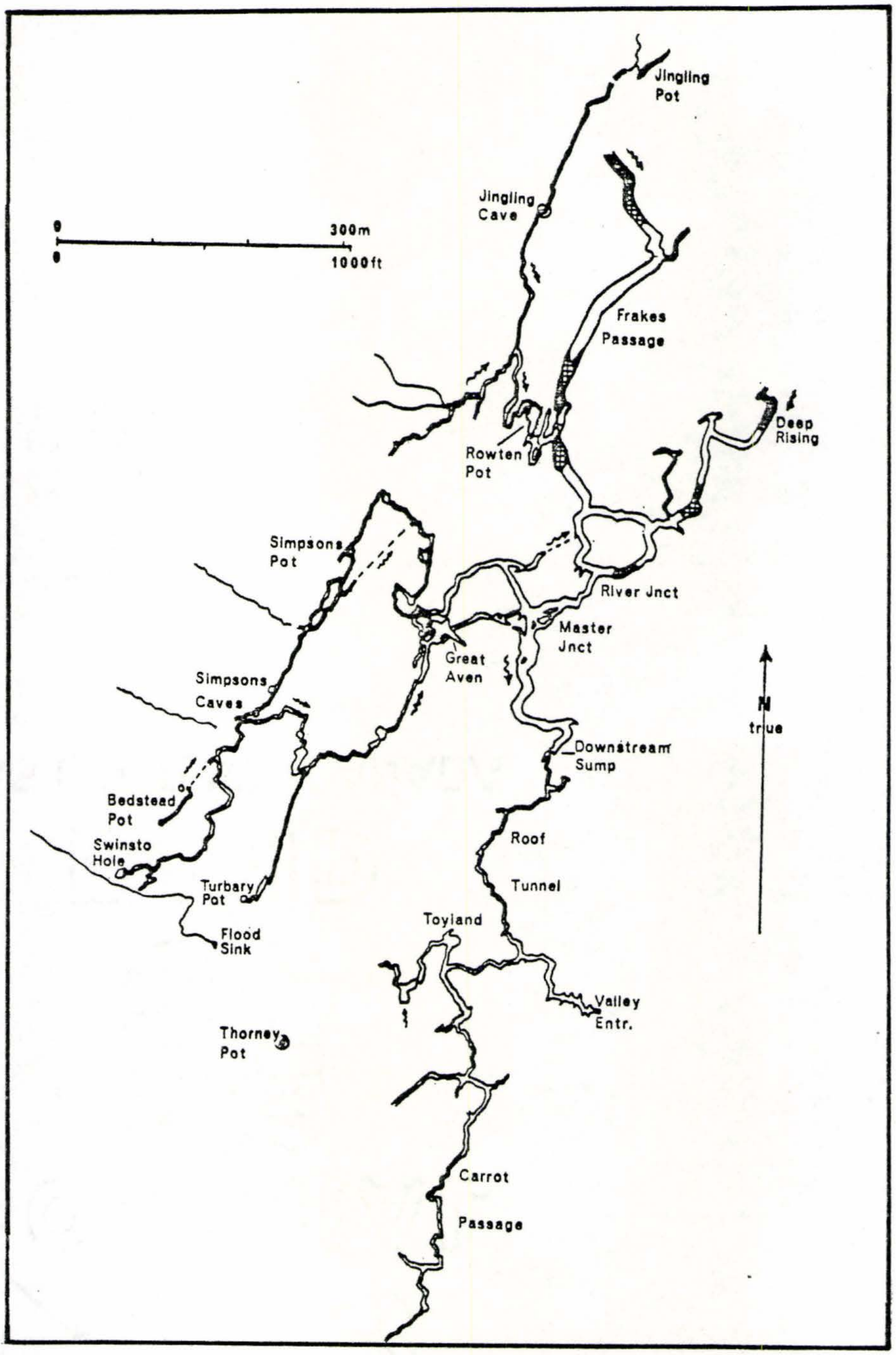

Figure 5.9 Line survey of the caves of the West Kingsdale system (from Brook 1974).

but this is thought to be due to local structural controls as it is not seen in neighbouring systems, (Brook 1974).

Speleothem was collected from sites along the Roof Tunnel and consisted of loose flowstone on the floor and *in situ* scalloped flowstone forming part of the roof.

5.4.5 Ibbeth Peril Caves

Ibbeth Peril I is the most northerly of the caves investigated and is situated in the uppermost beds of the Great Scar Limestone in Upper Dentdale, 5km north of Whernside. The cave is formed at or below the valley floor and is frequently flooded by the River Dee. Its entrance lies behind a 5m waterfall in the river bed and leads downwards through a low passage into a large collapse chamber. A phreatic passage, now containing an entrenching stream enters this chamber and the water sinks in the boulder floor. On the opposite side of the chamber a short fossil tube leads off and contains several flowstones deposited over stream gravels. These flowstones were sampled.

5.4.6 White Scar Cave

This resurgence cave situated part way along Chapel-le-Dale is the major drainage route for the western slopes of Ingleborough (Figure 5.1). Exploration in recent years has penetrated almost as far as the surface sinks known to feed it. At the outlet, the cave is formed along the basal unconformity of the Great Scar Limestone. The main streamway can be followed for almost 2 kms as a meandering vadose passage up to 12m high and 3m wide (Figure 5.10). A large collapse of boulders

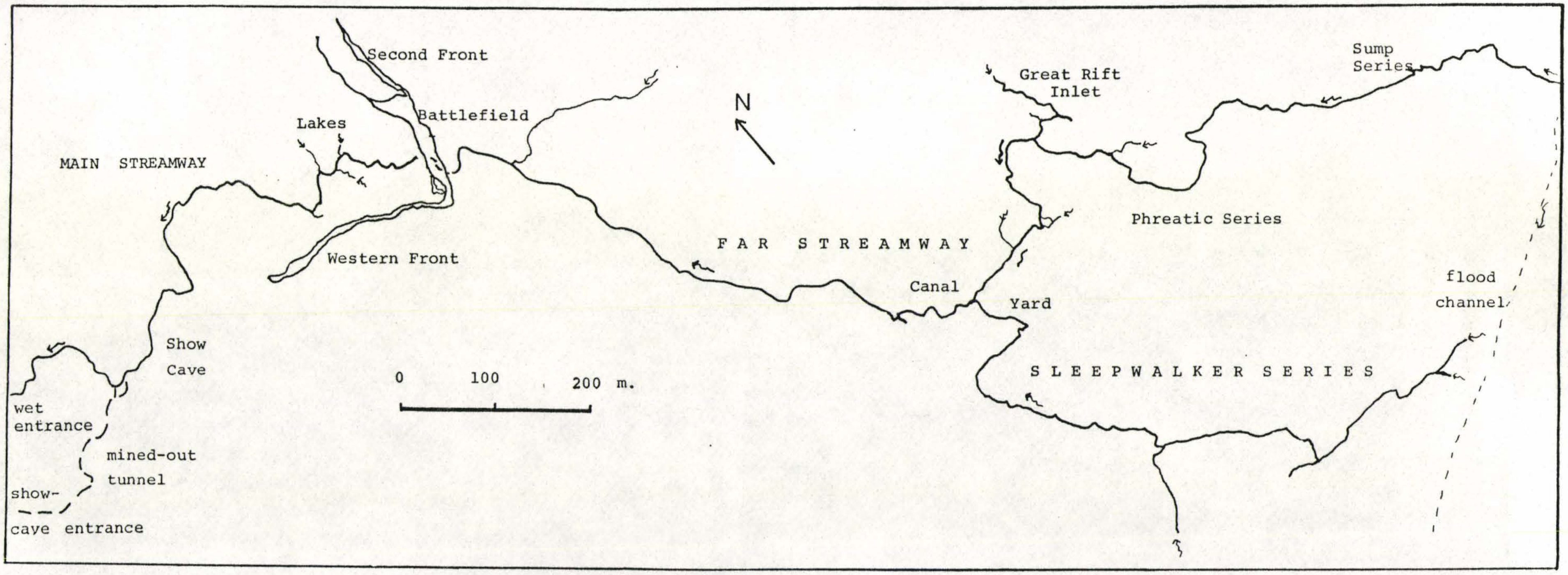

Figure 5.10 Line survey of the White Scar Cave system, Chapel-le-Dale (after Waltham 1977).

(Big Bertha choke) marks the end of Main Streamway and the beginning of Far Streamway. The upstream passages become low and phreatic in form and eventually a series of sumps blocks the way on. Higher level fossil parts of the cave are entered above Big Bertha choke (the Battlefield Series) and towards the end of the Far Streamway (the Sleepwalker Series). The former is an ancient partly-collapsed tunnel known as the Second Front (in the north) and the Western Front, and runs diagonally across the Main Streamway and about 20m above it (Figure 5.10). The Sleepwalker Series is a smaller tube containing much collapse; it forms a tributary to the main roof tube in the Far Streamway. The latter tube emerges from the Great Rift Inlet farther upstream and lies at about the same level as the presently-active phreatic tubes at the end of Far Streamway.

Speleothem has been collected from the Western Front, the first part of the Sleepwalker Series, the roof tunnel above the Far Streamway and from collapse debris in the Main Streamway below the lakes.

5.4.7 The Gaping Gill - Ingleborough Cave System

The Gaping Gill system is one of the best known in the country. It lies on the southern slopes of Ingleborough above the village of Clapham (Figure 5.1) and consists of a series of tributaries (usually active vadose caves) entering a complex, multi-level fossil cave network (Figure 5.11). The system is drained by Ingleborough and Beck Head Caves but so far only the Ingleborough-Beck Head connection has been negotiated by diving. A series of flooded tunnels, wells and fossil passages form the proximal ends of both Ingleborough and Gaping Gill.

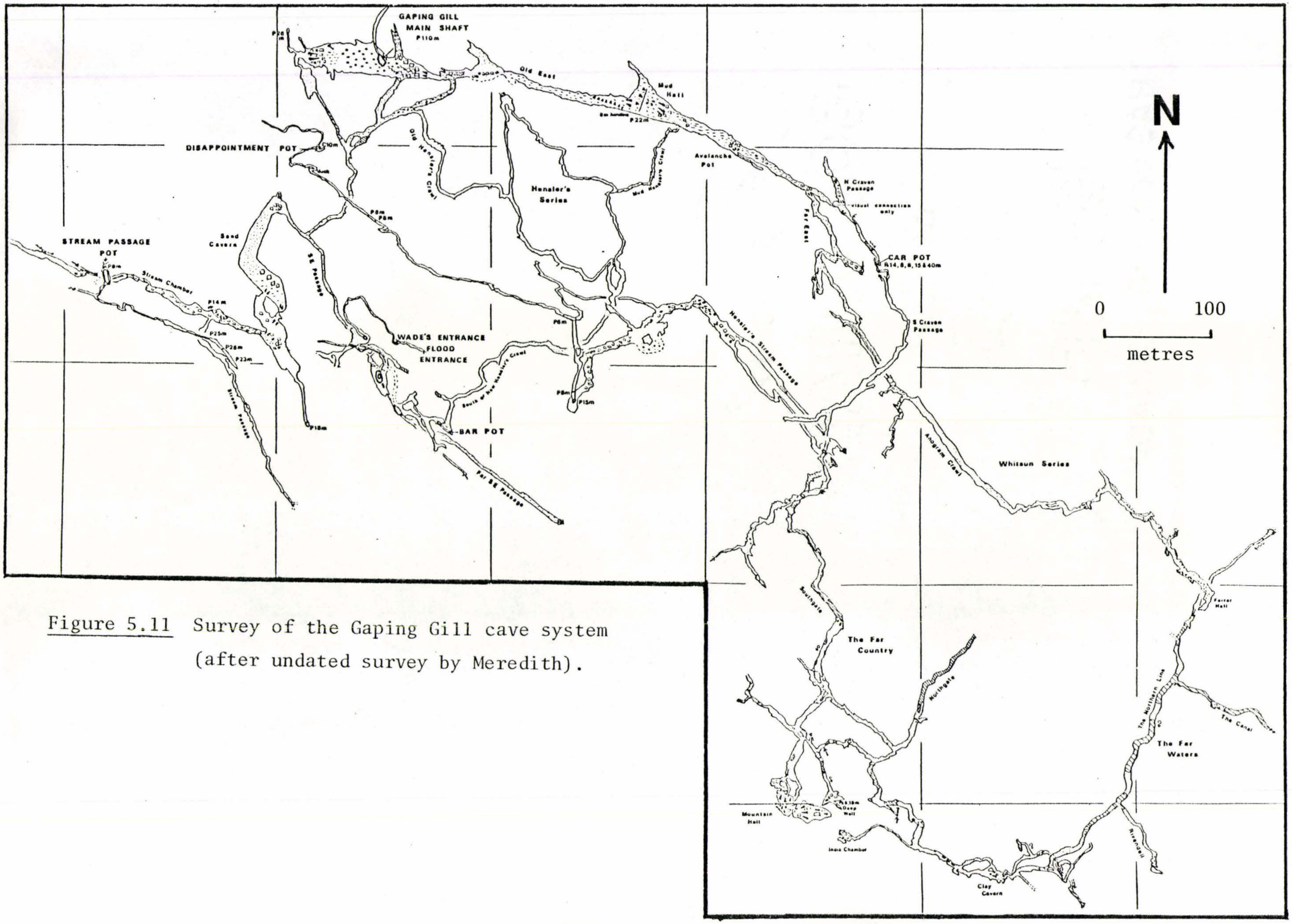

<u>Figure 5.11</u> Survey of the Gaping Gill cave system (after undated survey by Meredith).

Most of the fossil passages of Gaping Gill represent previous routes taken by Fell Beck, the stream which nowadays falls down the 110m entrance shaft, and then immediately disappears in the gravels of the Main Chamber. Apart from apparently static wells at the bottom of some shafts Fell Beck is not seen again until it flows out of Terminal Lake in Ingleborough Cave. The whole of the presently-explored system in Gaping Gill lies above this drainage route, (presumably a phreas). Extensions in recent years bring its total length to over 10km. About four fossil levels of development can be recognised (Figure 5.12); in order of decreasing altitude they are illustrated by:

i) Disappointment Pot streamway, Bar Pot aven bedding planes
ii) Old East, Far East and Craven Passages
iii) Stream Chamber, South-East Passage, Henslers Crawl and the Whitsun Series
iv) Far Country and Far Waters Series

These levels are controlled by shale horizons (i), fault zones (ii) and/or Porcellanous Band (iii), and possibly the proximity of pre-carboniferous basement rocks (iv). Directional control of these passages is determined by faults and major joints (faults control the alignment of Main Chamber to Mud Hall and the Stream Chamber extension to South-West Passage, and joints control much of the linking network of smaller passages). Several large caverns are found at the Porcellanous Band level and are usually associated with faults. They have been enlarged by blockfall and sapping by ephemeral streams.

Ingleborough Cave, by comparison, is a relatively simple system (Figure 5.13), containing two main levels of development only a few

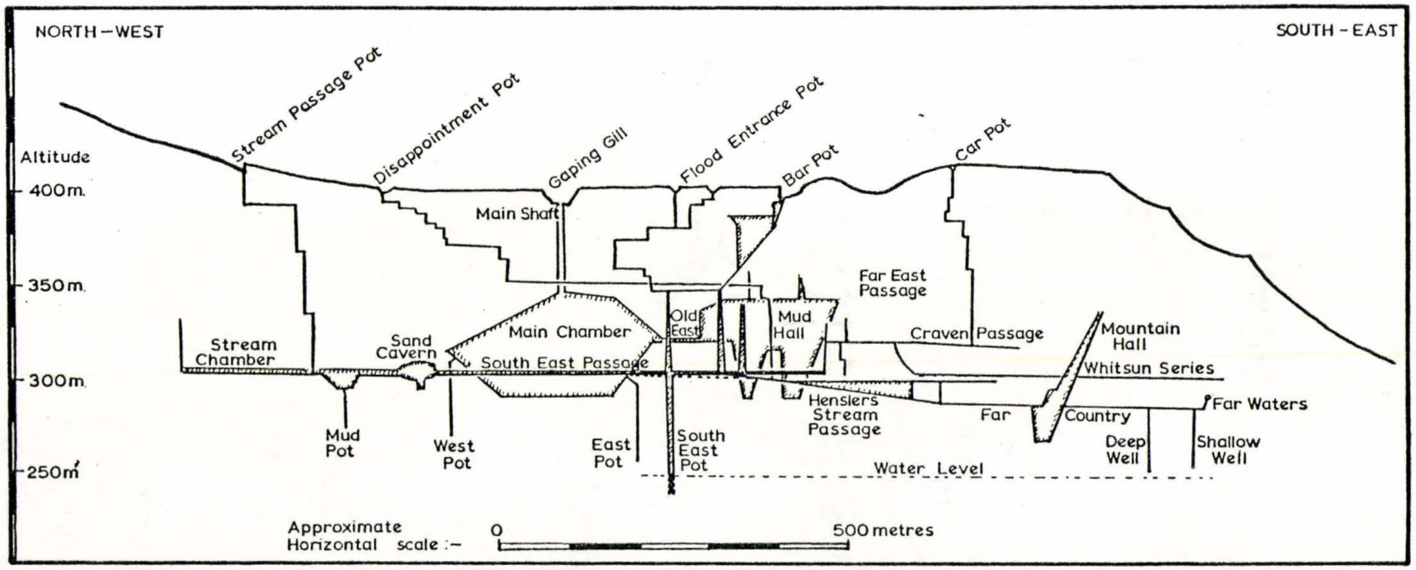

Figure 5.12 Diagrammatic cross-section of Gaping Gill cave system (from Glover 1974).

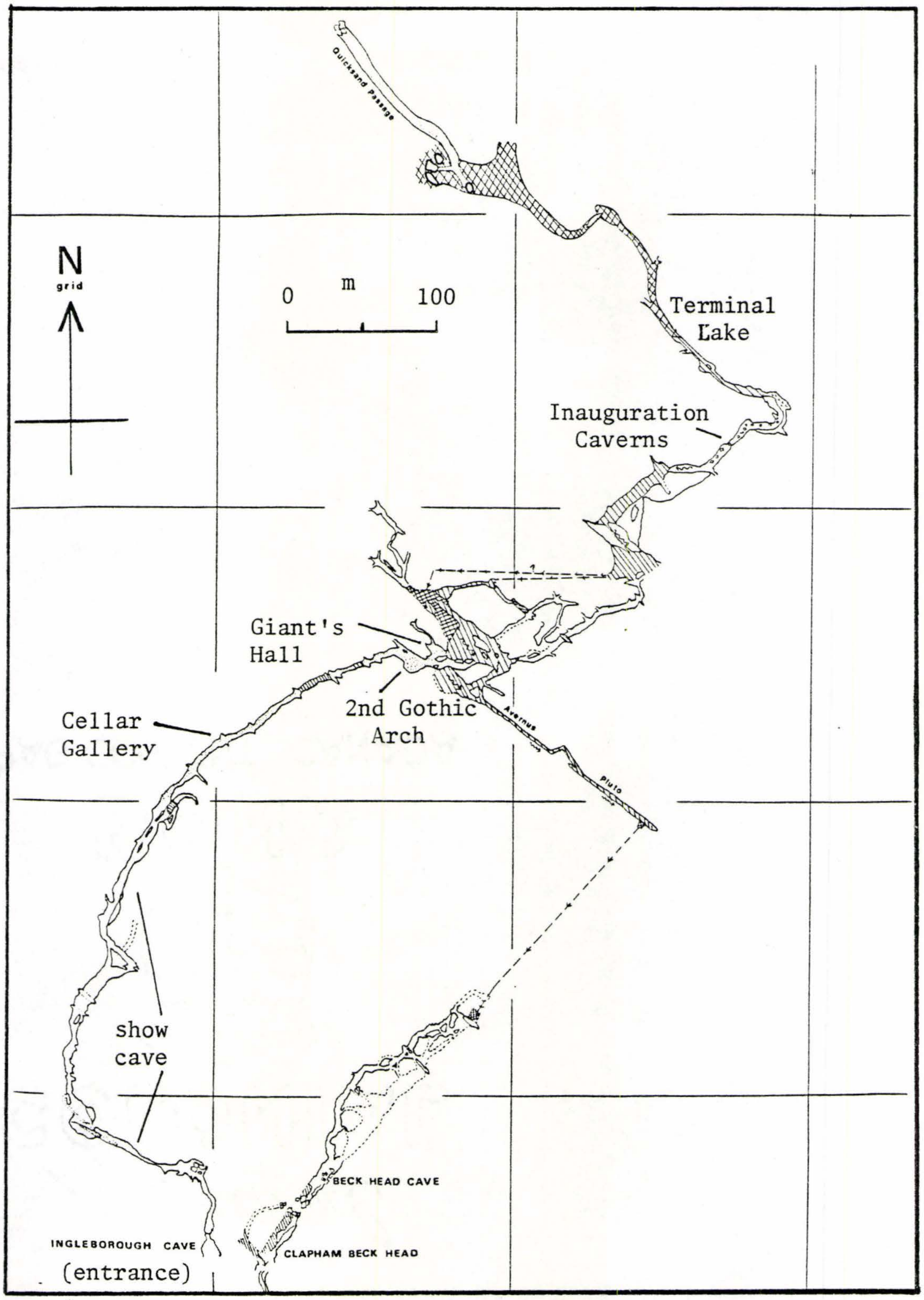

Figure 5.13 Survey of Ingleborough Cave (from an undated survey by Meredith).

meters apart. The show cave and its continuation, Cellar Gallery as far as Giant's Hall, are mainly fossil now and only become streamways in severe floods. In normal flow, water leaves the system via Lakes Avernus and Pluto and the Beck Head Cave passage. Upstream of Giant's Hall, only one course exists : through partially flooded, low, wide bedding planes to a vadose section known as Inauguration Caverns. A complex series of restricted tubes and bedding planes enters here at roof level. The main water resurges out of Terminal Lake at the furthest point upstream.

Speleothem has been collected from many parts of this system of caves: in Gaping Gill, from Old East, Far East, Stalactite Chamber, Henslers Passage and Far Country; and in Ingleborough Cave, from Giant's Hall and the show cave. R.R.Glover has also provided two speleothems from Gaping Gill and one from nearby Newby Moss Cave (Figure 5.1).

5.4.8 Victoria Cave

This is probably one of the oldest caves in the Craven District, as it lies near the upthrust southern limit of the limestone, between the North and South Craven Faults (Figure 5.1). 140 years ago the cave entrance was a very small opening in Langcliffe Scar, but about 1840A.D. excavations of the entrance passage and debris piles outside began, revealing evidence of Romano-British and Upper Paleolithic occupation. These findings overlay laminated clays and bone beds which showed the presence of hyena, deer, bear, rhinoceros and hippopotamus (Warwick 1956, Sutcliffe et al. 1976). The cave was thought to have been a

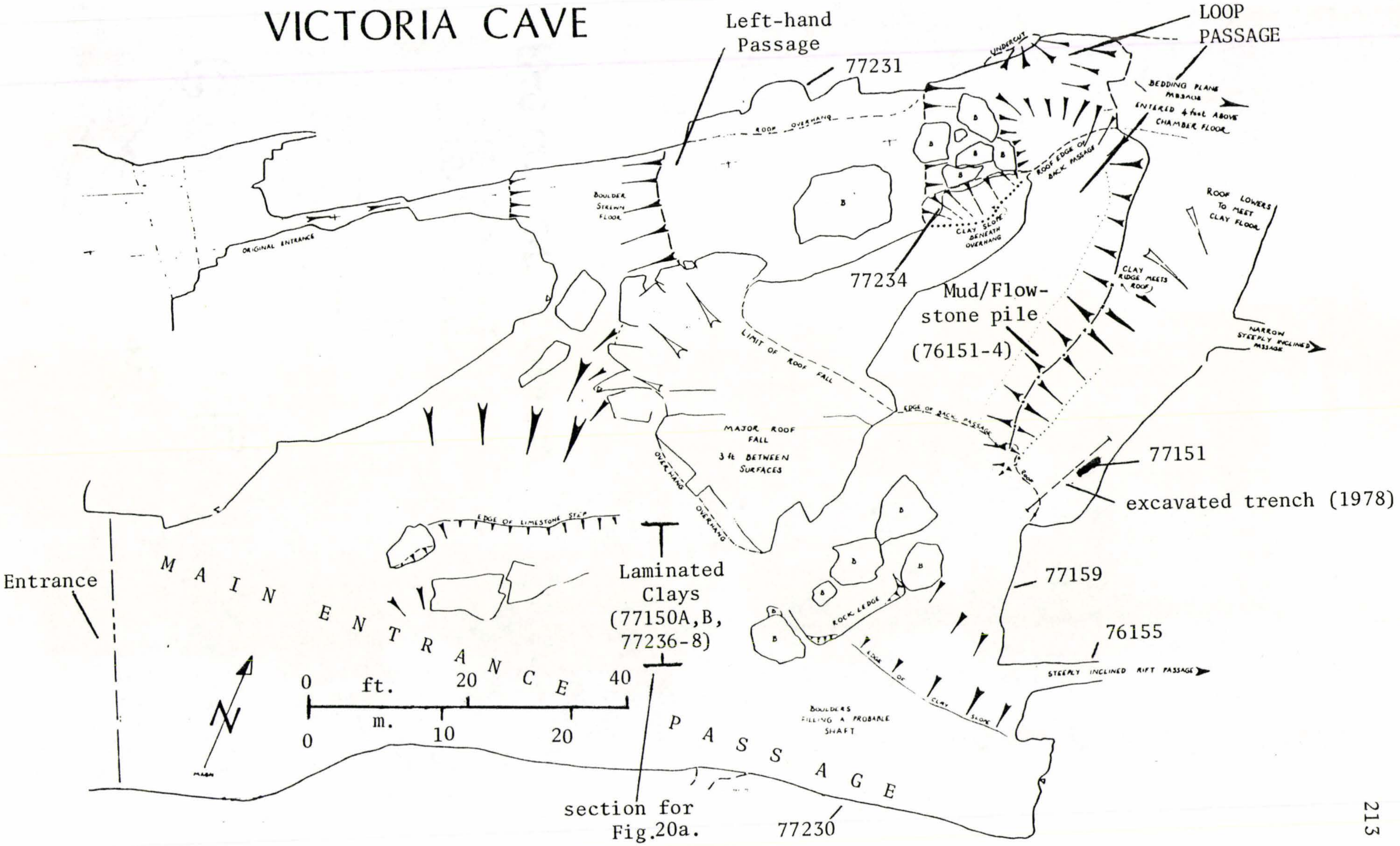

Figure 5.14 Survey of Victoria Cave (drawn by A.King, 1978, unpublished).

hyena den and is now listed as a protected archeological site. Early excavations removed over 5m depth of deposits, revealing a square section tunnel which ends abruptly after about 40m (Figure 5.14). A low-roofed passage continues to the left and loops back round to the entrance. Smaller tubes, climbs and crawlways lead off in several places but all terminate fairly quickly. The cave appears to be the remnants of an extensively truncated and blocked, fossil phreatic system, and little evidence remains to determine its origin and function.

Many speleothem samples were collected from the entrance and loop passages with the aid of archeologist, Alan King, and by permission of the Nature Conservancy. Most of the samples were old flowstones; none were directly associated with archeological finds (mainly because of complete removal by past excavations). Three samples of flowstone containing rhinoceros teeth and part of a jaw bone, and a red deer antler were obtained from Thomas Lord, custodian of the excavated finds, presently held at the Pigyard Museum, Settle. These have also been dated.

5.4.9 Sleets Gill Cave

This cave lies about 60m above valley floor level on the southern slopes of Littondale, about 10km north-east of Settle. A steeply-descending entrance slope leads to a superb phreatic tunnel which penetrates over 450m into the hillside and ends in Hydrophobia Passage (60m of low airspace streamway). Beyond this a large passage continues to a sump, but to the west at this point rises a steep phreatic lift tube, the Ramp, which chokes about 60m above stream level. Most of the cave floods severely at present, probably due to the constricted nature of the downstream continuation of Hydrophobia Passage. However, the phreatic lift passages must date from a time when the entrance discharged at or near valley floor level.

Few speleothems were collected in this cave, and the only one reported in Appendix 4a came from an old eroded stalactite curtain hanging near floor level in the main tunnel.

5.5 Summary

All of the systems investigated contain at least one level of fossil passageway which formed under phreatic conditions. The presence of these passages, often well above modern resurgence level, has been the cause of much debate among Craven speleologists during the last thirty years (Sweeting 1950, Waltham 1970a, Brook 1971). These tunnels were originally flooded drainage routes before downcutting took place, and it is generally accepted that their altitudes were at or below those of the resurgence at that time. A process of rejuvenation to lower levels, truncation of the tunnel by subaerial erosion or glacier action, and infilling with till or fluvioglacial deposits has since occurred such that only segments of the original passage can now be entered.

The abandoned high level tunnels of the cave systems of Leck Fell are an excellent example of this process. Waltham (1974) has interpreted the morphology of these caves in terms of a five-phase sequence of active stream erosion followed by clastic infill and speleothem deposition. He attributes the erosive phases to interglacials and the depositional phases to glacial periods. Two glaciations are recognised by Waltham and to each of these are attributed speleothems found in certain passages of the Leck Fell caves. This interpretation is considered in greater detail later on.

The development of the adjacent Casterton Fell caves was initially related by Eyre and Ashmead (1967) to the European glacial/interglacial chronology of Zeuner (Table 5.1) in terms of infilling and cavern breakdown (glacial), and rejuvenation and downcutting (interglacial). Ashmead (1974) subsequently related the caves instead to erosion surfaces at 320m and 250m a.s.l. and the time scale was shortened to include only the last interglacial and glacial events.

Brook (1974) considers the development of the West Kingsdale cave system in terms of successive glaciations over the last quarter of a million years, each lowering the valley floor by 20 - 50m. Cave systems then developed in accordance with the depth of valley excavation. Brook also suggests that the formation of postglacial lakes in Kingsdale has strongly influenced the development of the passages associated with the Master Cave.

Glover (1974) has discussed the formation of the Gaping Gill-Ingleborough Cave system in some detail with respect to the local geology and lithology but, perhaps wisely, has avoided relating stages in its development to glacial-interglacial events.

In conclusion, this section has shown that previous workers, using stratigraphical, geological and morphological evidence, sometimes pure guesswork, and in the absence of radiometric data, have all concluded that the major cave systems of Craven have seen at least one interglacial-glacial cycle. Most of them also conclude that valley downcutting and removal of the overlying Yoredales by glacial action are essential features of Pleistocene glaciations in this area and that this has caused caves to develop in a series of stages rather than as a continuous process. Whether or not these concepts are correct is considered in conjunction with radiometric data in the following section.

5.6 Speleothem Age Determinations

The ^{230}Th/^{234}U method has been used to obtain 140 ages for 82 speleothem samples. An additional 7 duplicates of ^{230}Th/^{234}U analyses have been made using the ^{231}Pa/^{230}Th dating technique. Details of the methods are given in Chapter 2 and analytical data, ages and sample descriptions are given in Appendix 4a. The ^{231}Pa/^{230}Th ages are not described in this chapter except where they strongly differ from the corresponding ^{230}Th/^{234}U age; they are discussed instead in Chapter 2.

Figure 5.15 summarizes all the results for north-west England. A number of the analyses show appreciable detrital thorium contamination, (^{230}Th/^{232}Th activity ratio < 20; see Chapter 2) and these are indicated in Figure 5.15. They have been corrected by assuming an initial ^{230}Th/^{232}Th activity ratio of 1.5; corrected ages are given in the last column of Appendix 4a. Most analyses of the Ingleborough Cave samples show low ^{230}Th/^{232}Th ratios and very low uranium concentrations. The calculated ages therefore have large error limits (± 30%) and show large shifts when corrected for detrital thorium. They are listed in Appendix 4a but have been omitted from Figure 5.15. Uranium concentrations for the remainder of the Craven speleothem collection are high,

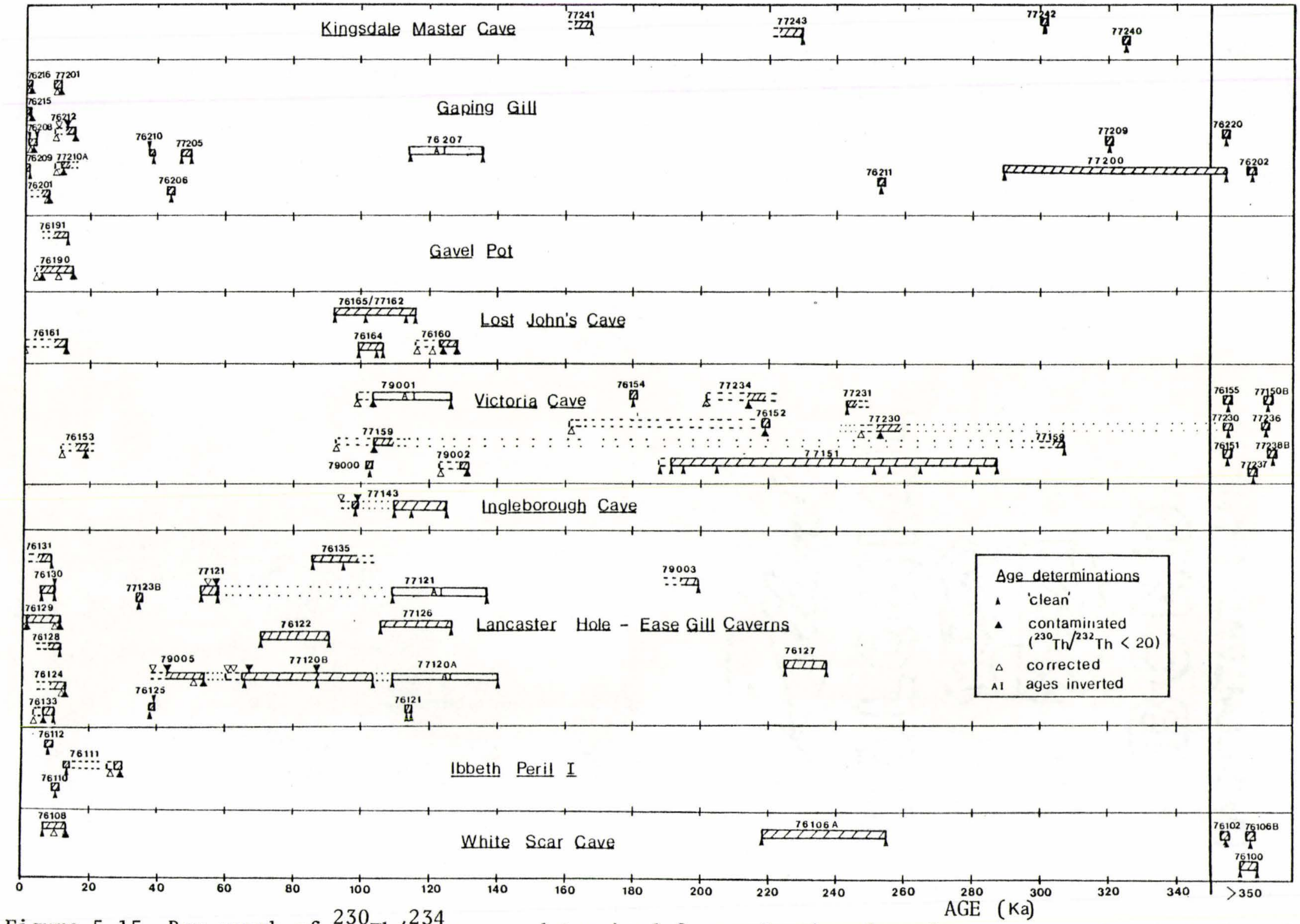

Figure 5.15 Bar graph of ^{230}Th/^{234}U ages determined for speleothem from Craven caves. Parallel dotted lines indicate hiatus(es) between determined ages; parallel dashed lines to open triangles show projection to an age corrected for detrital Th; others indicate continuation of speleothem growth.

between 0.3 and > 20 ppm, such that statistical errors are generally low and within 10% for most ages.

The results will be considered in the following sequence :

1) description of the dating results and discussion of their significance for the speleogenesis of each cave system,
2) their relation to the British Quaternary sequence and implications for its time scale
3) their significance for the development of caves and karst in the Craven area,
4) stable isotope results and their paleoclimatic implications.

5.7 Speleogenesis and Cave Development

5.7.1 Lancaster Hole - Ease Gill Cavern System

Of the samples dated from this system, two sites yielded the most interesting collection of speleothems: 1) samples which were loose, embedded in, or washed out of mud and gravel deposits in Bill Taylor's Passage (the connecting route from Lancaster Hole entrance to Fall Pot), and 2) *in situ* flowstones and recent collapsed blocks from the Colonnade Passage and Bridge Hall near Lancaster Hole entrance.

Three age groupings of speleothem were found at the Bill Taylor's site:

1) stalagmites and flowstones showing surface re-solution features, which grew over the period 126 - 70 Ka. Stalagmite 76122 contains three internal breaks in deposition (seen as detrital horizons) over the period 91 - 71 Ka (Figure 5.16). Intervening layers have not been

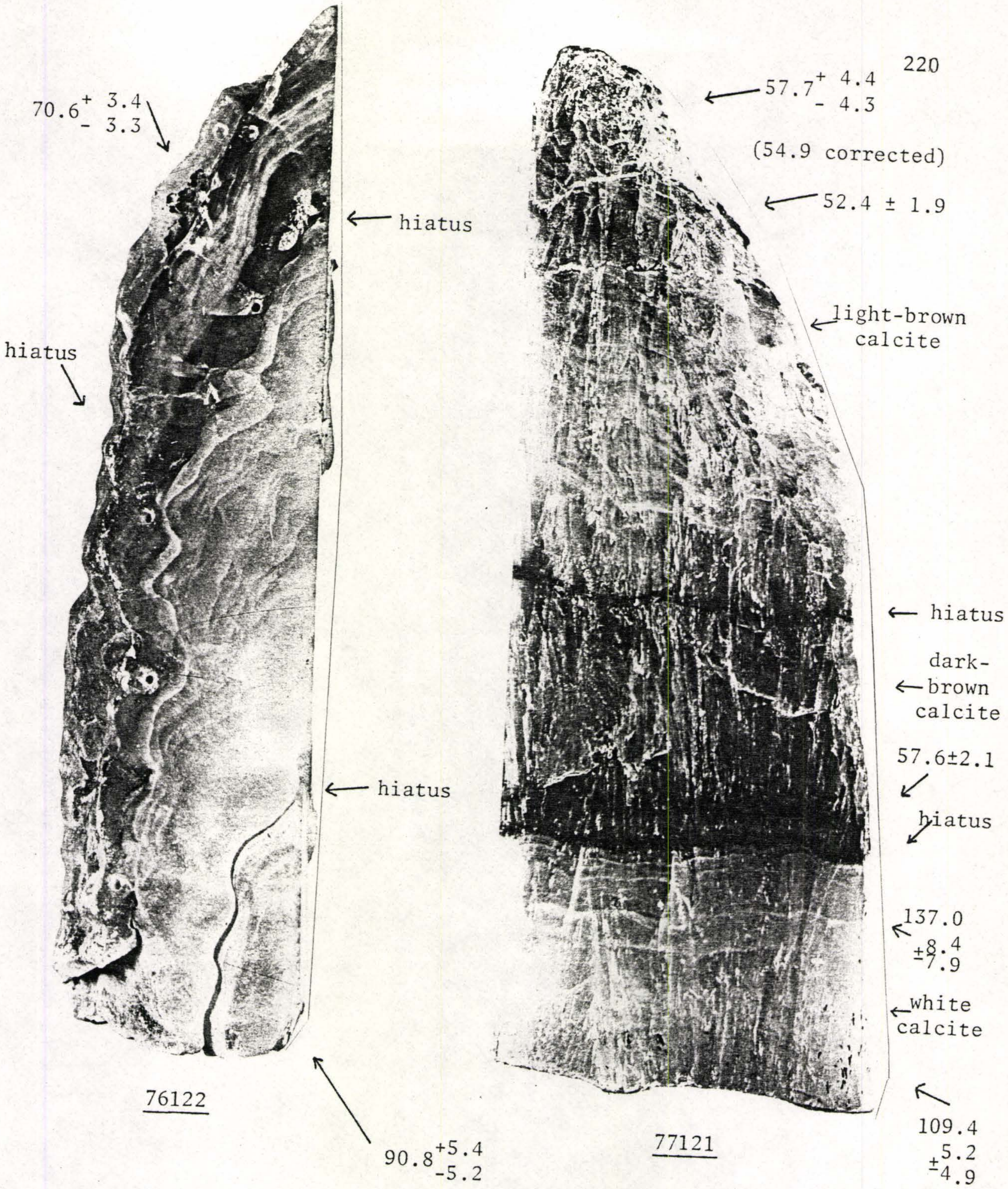

Figure 5.16 Sections of stalagmite 76122 and flowstone 77121 showing growth hiatuses and $^{230}Th/^{234}U$ ages.

dated yet. 76135 is a 1m high flowstone boss in this passage and appears to have been once covered by sediments. It grew from > 95 Ka (centre) to 86 Ka (top). The other samples, 76121 (~ 114 Ka) and 77126 (126 - 106 Ka), show continuous growth. 77120 and 77121 are discussed below.

2) stalagmites and flowstones showing no evidence of surface re-solution, which grew over the short time range 39 - 35 Ka. Stalagmite 76125 has overlapping base and top dates at 39 - 38 Ka and was partly imbedded in sediments when collected. 77123B is from a horizontal, in situ veneer of wall flowstone, perhaps formed as a pool crust, dated at 35 Ka.

3) 77124 is a long thick stalagmite, found loose but with fresh surface features suggesting recent formation. A base date of 13.3 Ka confirmed this (11.9 Ka when corrected for detrital Th).

With the exception of 77124, all the above samples contained > 1 ppm uranium and negligible detrital thorium contamination. The flowstones from the Colonnades Passage site, 77120A and B (two blocks separated by mud), overlain by 79005, show an interesting sequence of deposition occurring over about 100 Ka (Figure 5.17). The base date on the basal block (A) of 140 Ka (9% Th yield) is only 7cms away from the 109 Ka top date, without any apparent hiatus in growth. A.G.Latham (pers. comm.) has obtained a top date of 114 Ka for an equivalent block - in good agreement with this result. For these reasons and the fact that the base consists of porous, macro-crystalline calcite, the 140 Ka age is probably too old. Between blocks A and B is a hiatus representing only about 5 Ka. Correction for detrital thorium in ages determined for the upper part of the centre block (B) shows that the hiatus between

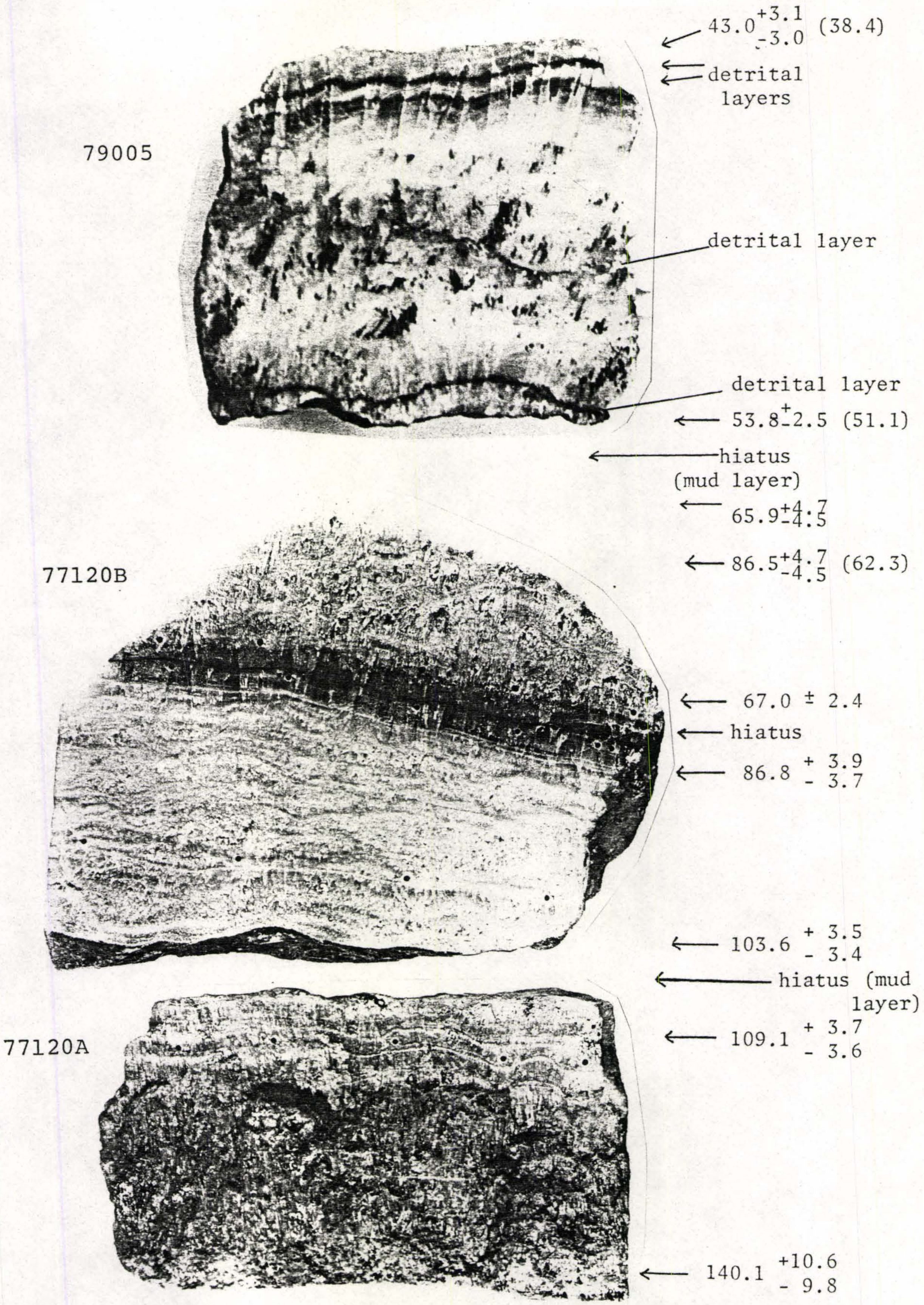

Figure 5.17 Sections of flowstone sequence 77120A/B - 79005 showing growth hiatuses and $^{230}Th/^{234}U$ ages (ages corrected for detrital Th are shown in brackets).

white and brown calcite represents a time gap of about 20 Ka. A 10 Ka time gap is represented by the mud layer between 77120B and 79005. The four internal detrital horizons in 79005 probably result from flooding events over the period 54 to 43 Ka (51 to 38 Ka if corrected for detrital thorium).

The Bridge Hall flowstone (77121) is a complete section from a large slab fallen from its growth position about 10m above present floor level. Contrary to its appearance (Figure 5.16), inspection of the *in situ* parent flowstone showed the brown calcite to be the younger deposit. Ages for the basal white flowstone are inverted with respect to the stratigraphy and no reason for this can be found. The hiatus separating the white and brown calcite layers represents a time gap of between 50 and 70 Ka depending on the basal age used. The brown calcite appears to have grown rapidly over the period 58 to 52 Ka and the second hiatus seen in Figure 5.16 has apparently little time significance.

79003 was collected from a collapsing flowstone boss at a higher level than the parent flowstone of 77121, but in the same rift passage (the Lancaster Hole entrance shaft). Its basal age of 199 (± 20) Ka is one of the oldest obtained for this cave system. The top is as yet undated. The oldest speleothem found is 76127, a small loose block found near the top of the Stop Pot ladder. It dates from 238 (base) to 225 Ka (top); age errors overlap at the 1σ level. An initial basal age determination of > 350 Ka is rejected on the grounds of low U and Th yields and the results of subsequent analyses by both $^{230}Th/^{234}U$ and $^{231}Pa/^{230}Th$ methods (Appendix 4 a).

All other speleothems dated from this system are postglacial with base dates ranging from 11.5 to 9.0 Ka. These include loose stalagmites from Easter Grotto, East Montagu Passage and Eureka Junction and also one in situ stalagmite grown on block fall from the high level passages near Stop Pot.

Large variations in uranium concentration (0.21 to 17.1 ppm) and initial $^{234}U/^{238}U$ ratios (0.74 to 1.74) are found in speleothems from this system. There is some tendency for high U concentration to correlate with low $^{234}U/^{238}U$ ratios but 76121, 76122 and 76129 are exceptions to this (see Appendix 4a). However, there does appear to be a spatial relationship with respect to $^{234}U/^{238}U$ ratios. All Easter Grotto, Eureka Junction and Stop Pot speleothems have initial ratios less than 0.82, while outside of this area ratios range from 1.04 upwards. There is no unusual hydrological, topographical or geological feature in this area that can explain this pronounced ^{234}U depletion in speleothem.

5.7.1.1 Discussion

The following may be inferred:

1) the general lack of speleothem older than the last interglacial (broadly defined here as 140 - 70 Ka) suggests that either little had grown prior to this time, or more likely, prolonged and extensive erosion has removed or obscured most speleothem of greater age,
2) the major high level trunk routes as typified by that at Stop Pot, would appear to be de-watered by at least 240 Ka if sample 76127 originates from this route,

3) the entrance shaft of Lancaster Hole was of vadose character and developed to at least 20m deep, 200 Ka ago,
4) the last interglacial saw the development of many speleothems, particularly in the Lancaster Hole part of the system. It is likely that the Colonnades (5m high stalagmite columns connecting roof to floor) were initiated during this period. Many of the dated samples contain mud layers or internal erosion surfaces due to temporary flooding and sediment deposition or prolonged periods of non-growth. The results suggest that a short period around 105 Ka saw no speleothem growth (Figure 5.15) and there may be at least one common depositional hiatus during the period 90 - 65 Ka. More dating of speleothem adjacent to a hiatus is needed to show this.
5) re-solution features on the surface of interglacial speleothems indicates a period of ponding or full phreatic conditions sometime between 65 and 38 Ka. This may only be a local effect confined to Bill Taylor's Passage because these features are not clearly seen on the Bridge Hall and Colonnades Passage speleothems (although the latter sites are at a higher elevation, Figure 5.7). The ponding is unlikely to relate to the pool crust deposit dated at 35 Ka because this represents a depositional, not solutional, phase.
6) a major erosive period between 38 Ka and the present is indicated by accumulation of loose, broken and buried speleothems older than this in the sediments of Bill Taylor's Passage. Other broken speleothems, not buried in sediments from this passage, East Montagu and Easter Grotto and which are of post-glacial age, are

probably the result of recent vandalism rather than natural processes.

5.7.2 Gavel Pot

The two stalagmites from Glasfurd's Passage were both dated as post-glacial. This was surprising because 76190 was nearly 1m long and lay partially covered by a cemented boulder collapse and 76191 showed calcite-pool encrustation features on its outer surface. This suggests that the cave passage has been post-glacially more active than might have been expected from its location and appearance. The rapid growth rate of 76190 (~ 10cm/Ka) suggests that the passage has taken a strong draught during post-glacial times, causing the speleothem to grow by evaporation and rapid loss of CO_2. A slight air current can be detected in the cave at the present time.

5.7.3 Lost John's System

Three deposits have been dated as last interglacial from the inner reaches of this cave system. A loose flowstone block (76160) containing detrital layers, grew from 128 to 123 Ka (121 to 116 Ka if corrected). It was collected from a boulder choke at the end of the Lyle Cavern High Level Series (Figure 5.8). Another loose block (76164), embedded in mud deposits in a washed-out bedding plane in the Main Drain, grew from 106 to 99 Ka. It contains a prominent hiatus dated on either side at 106.3 and 104.5 Ka. An *in situ*, hanging flowstone, (76165/77162), located near 76164 was sampled about 2.5m above stream level. It appears to have grown continuously from 113 to 92 Ka and no hiatus is seen in the growth layers. Of the two dates determined by the $^{231}Pa/^{230}Th$ method one lies well outside this range ($165.7 \begin{smallmatrix} + 18.1 \\ - 15.1 \end{smallmatrix}$ Ka, Appendix 4a).

This latter deposit is the most significant of those dated from this cave, in terms of its implications for speleogenesis. The ages show that not only was the Main Drain in a vadose condition at that time, but that during the last 115 Ka it has only entrenched a maximum of 2.5m, a rate of $\leqslant$ 2.2cm/Ka.

5.7.4 Kingsdale Master Cave

Four ages have been determined on two loose flowstones and two in situ stalactite-flowstones in the Roof Tunnel. The ages lie between 324 Ka (77240) and 168 Ka (77241). Large error limits (up to ± 100 Ka) accompany the older deposits. Sample 77240 is an indurated flowstone veneer forming the roof of the passage at one point and is a comparable sample to that dated by R.S.Harmon at > 400 Ka (Waltham - pers. comm., reported in Atkinson et al. 1978). A.G.Latham (pers. comm.) has dated an apparently similar sample at 173 Ka. The low weight of the sample used in the present analysis, the fairly low thorium yield (14%) and the low uranium concentration (0.20 ppm) combine to give a large degree of uncertainty to this result. The other in situ speleothem (77241 at 168 Ka) also shows extensive surface re-solution features and collectively, this evidence suggests that:

1) the Roof Tunnel has seen at least one period of ponding or a return to phreas flow since 168 Ka,
2) Vadose conditions in the Tunnel must have existed at least prior to 168 Ka and possibly before 320 Ka for these speleothems to develop,

3) the age quoted by Atkinson et al. is probably too high if the sampling site used by all three workers is the same.

These results show the Master Cave Roof Tunnel to be a surprisingly old feature, for it is only 10 - 15m above the present phreas level. This aspect and its implications for the development of Kingsdale are considered later on.

5.7.5 Ibbeth Peril I

The three samples collected from this cave (76110, 76111 and 76112) are all found to be post-glacial deposits (10.1, 13.7 and 7.6 Ka respectively). An earlier attempt to date a composite sample of 76111 gave an age of 29.4 Ka, (26.9 Ka if corrected) and subsequently, a near replicate gave 13.7 Ka. No reason can be found for the initial result and in view of the replicate age, it should be treated with caution.

In spite of its present proximity to the water table, Ibbeth Peril I appears to have been well-developed sometime before the last glaciation because the dated samples overlay sediments which may have completely filled the passage at one time. The sediments are probably of fluvioglacial origin and those not cemented by calcite have been excavated and removed by flooding some time after the formation of the youngest sample (7.6 Ka ago). The cave was probably formed during or before the last interglacial.

5.7.6 White Scar Cave

Four ages, each > 350 Ka, have been determined on three loose flowstones from this cave as described below. Base and top ages for a large boulder of flowstone (76100) in the main streamway were both beyond the dating limit. The sample was a short distance downstream from the Pulpit, a boulder-strewn passage, partly infilled by collapse from passages above. The flowstone presumably came from a now-blocked branch passage of the Western Front which runs some 20m above and to one side of the streamway (Figure 5.10). A smaller loose flowstone 76102, from near the end of the Western Front also was older than the dating limit. A loose flowstone 76106B, taken from boulders in the Yard, near the beginning of the Sleepwalker Series has a top age of > 350 Ka. This sample is interesting in that it contains at least four internal breaks in growth and each new calcite layer is a different colour (Figure 1.3).

A thin flowstone slab, 76106A, also found loose in the Yard, has finite ages of 255 (base ?) and 218 Ka (top ?), with overlapping error limits. The only other ages within the dating range are from a post-glacial stalagmite, jammed in boulders out of growth position, from the Far Streamway roof tube. Its basal age was 11.6 Ka (9.4 Ka when corrected) and top age was 6.0 Ka.

The ages of > 350 Ka demonstrate the antiquity of the high level passages in this cave, provided that the dated flowstones originate from them. None of the samples appear to have undergone appreciable re-solution, suggesting that the Western Front and Sleepwalker Series were largely de-watered before 350 Ka. Therefore the Main and Far Streamways had developed and were taking the bulk of the water flow by this time. These results reinforce the tentative proposal by Atkinson et al. (1978) based on one speleothem date of 225 (± 60) Ka in the Main Streamway, of early vadose development and downcutting of the stream passage. The significance of these results in terms of the development of Chapel-le-Dale is discussed later.

5.7.7 Gaping Gill

Two samples from Gaping Gill are dated at > 350 Ka. One of them, 76202, is from the base of a large flowstone boulder lodged part-way up the boulder slope in Mud Hall (Figure 5.11). The top has not been dated so far. The second, 77200-2, is from the base (?) of a piece of indurated flowstone taken from a fallen block in the aven of North Craven Passage. The top is dated at 289 (± 22) Ka, and no hiatus is seen in between. 76211 and 77209 are pieces of the scalloped flowstone veneer found on the wall respectively near to, and beneath, a large calcite-cemented cobble shelf in Old East Passage (Figure 5.18). Both samples contain some detritus but are little affected by leaching of detrital thorium (Appendix 4 a). They date at 253 (± 27) Ka and 319 (± > 45) Ka respectively.

Collectively, these speleothems demonstrate the age of the Gaping Gill system and show that the high-level fossil tunnels of Old East and Far East were vadose by at least 300 Ka and probably by > 350 Ka. Re-solution features on 77200 may be a recent effect because the present block sits in spray from the aven waterfall. Scalloping on the Old East flowstones however, appears to be an ancient feature because the scallops themselves are pitted and eroded, suggesting that the cause of the scalloping (fast flowing water), occurred a long time ago. Since deposition of this flowstone, Old East Passage appears to have been filled by sediments at least to the

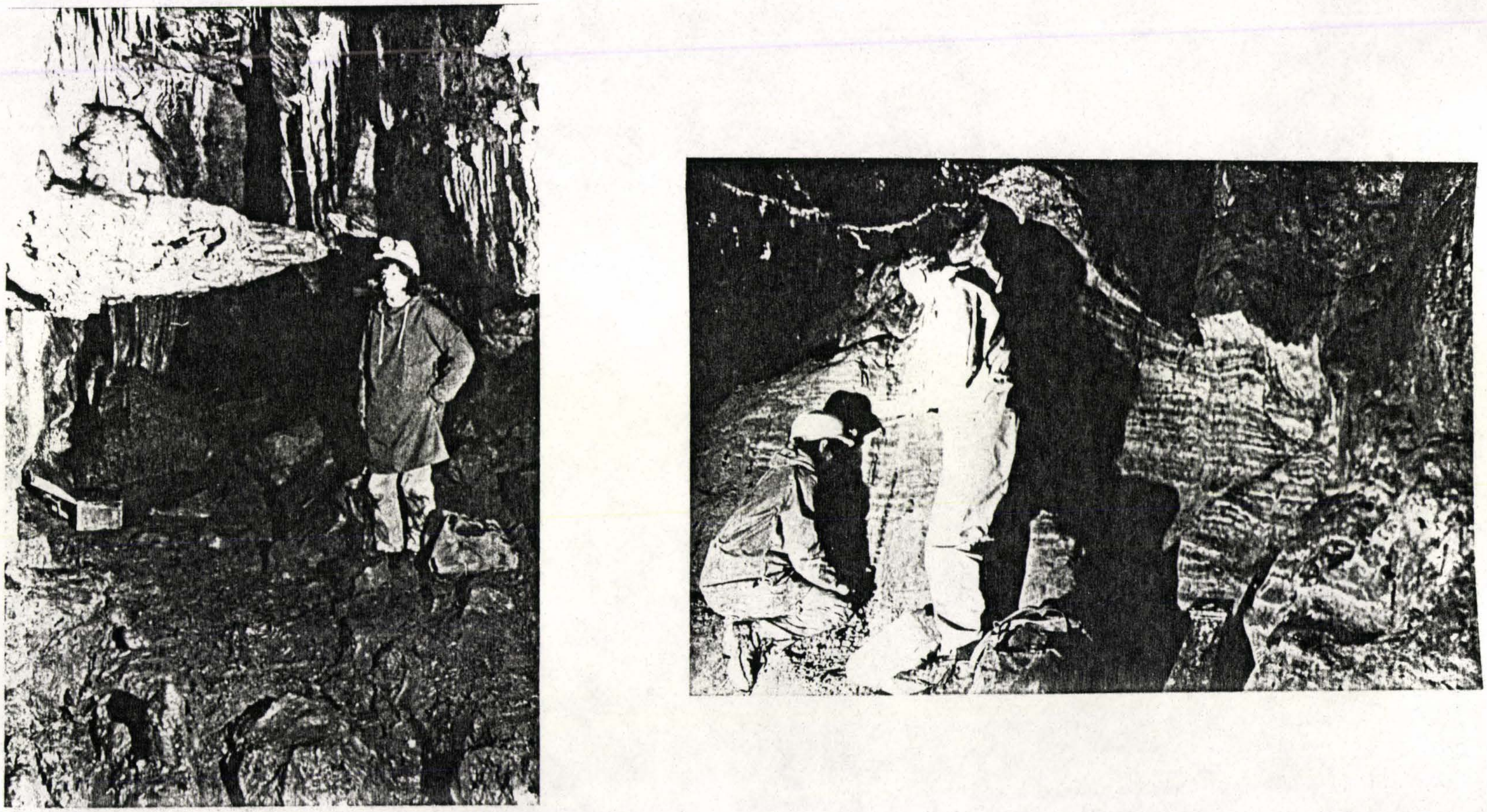

(a)

(b)

Figure 5.18. Two features of speleogenetic and geomorphic significance in the Gaping Gill system:
a) a shelf of calcite-cemented cobbles hanging 2m above modern floor level in Old East Passage,
b) a 4-5m thick sequence of varved sediments in Sand Caverns, overlain by stalagmite 76209.

level of the calcite-cemented shelf and then re-excavated to its present level. It has not been possible to obtain a sample of clean calcite from the shelf itself.

Further evidence of the antiquity of cave development in the Gaping Gill area comes from an age of > 350 Ka on a clean flowstone block, 76220, collected from the entrance series of Newby Moss Cave (Figure 5.1).

Only one speleothem of last interglacial age has so far been dated. 76207 is a loose, eroded stalagmite found on mud a short distance along Nevada Passage in the Far Country Series. The top (135 ± 15 Ka) and bottom ages (114 ± 8 Ka) are inverted with respect to the stratigraphy but overlap at the 1σ level.

Five ages between 50 and 37 Ka, have been determined on three speleothems from Gaping Gill passages. 76206 is a thin flowstone veneer dated at 43.5 Ka which forms the remnants of an old false floor in Henslers Upper Passage. Most of the underlying sediment has been excavated since this time. 76210 is a loose stalagmite found on mud in Old East Passage. It shows rapid growth between 38.5 Ka (base) and 37.7 Ka (top). A prominent hiatus near the top therefore only represents a short time gap. 77205, a loose, eroded stalagmite was collected from the end of Far East Passage and grew during the period 49.7 Ka (top) to 46.4 Ka (base). The ages are stratigraphically inverted but they overlap at the 2σ level. This speleothem also contains a distinct growth hiatus, but it too appears to represent only a small time gap. Both 76210 and 77205 show no significant change in either uranium concentration or $^{234}U/^{238}U$ ratio across the hiatus.

These ages indicate a limited period of speleothem growth comparable to that seen in the Lancaster Hole data.

Half of the dated Gaping Gill collection has proved to be post-glacial (Figure 5.15). Eight speleothems from the high level fossil passages of Old East, Far East, Stalactite Chamber, Sand Caverns and West Chamber are dated over the range 14.6 Ka to 0.8 Ka (the oldest corrected ages all show growth beginning between 10 and 8 Ka). Some speleothems, although lying loose on sediment, were found to be almost modern and were therefore probably broken by vandalism rather than by natural processes. Unfortunately, a short, <u>in situ</u> stalagmite 76209, collected from the top of thick varve deposits in Sand Cavern (Figure 18b) was found to be very young (0.8 Ka basal age), so that no useful upper time limit can be placed on the varves.

5.7.8 Ingleborough Cave

In contrast to the adjacent Gaping Gill system, and to other caves in this study, most of the speleothem dated from Ingleborough Cave grew during the last interglacial, from about 140 to 70 Ka. Almost all of it was collected as loose or <u>in situ</u> flowstones from the upper levels of the Giant's Hall aven (Figure 5.13). Unfortunately most samples have very low uranium concentrations (0.04 - 0.14 ppm) and appreciable levels of detrital thorium (0.01 - 0.08 ppm). As previously shown, (Chapter 2), this situation gives rise to large error limits and large age shifts when correction for detrital thorium is made. For this reason, almost all the determinations have been omitted from Figure 5.15 in order not to suggest equal reliability of these results with others. They are listed instead in Appendix 4a. Two post-glacial speleothems from the show cave have higher uranium concentrations (0.37 to 0.95 ppm) but also contain higher detrital thorium levels (0.05 to 0.12 ppm). They too are only presented in Appendix 4a.

One sample that shows little or no contamination and contains enough uranium for reasonably precise dating is 77143. It comprises an upper block (A) and lower block (B) dated respectively at about 98 Ka and 109 to 125 Ka. The upper block consists entirely of macrocrystalline calcite with indistinct growth layers and numerous pores bounded by crystal faces, and appears to have grown rapidly. The lower block is less porous and is well laminated (Figure 5.19). The three determinations show no contamination and they agree with the stratigraphy. A distinct muddy hiatus separates the two blocks and occurred between about 107 and 99 Ka (determined by extrapolating ages to extreme top and base).

These ages for speleothems which range in height from near floor level to about 10m above it (about 3 to 13m above the modern phreas) generally indicate that vadose conditions at least down to 3m above modern water level existed in the cave over 120 Ka ago. It is probable therefore that the high level chambers and rifts such as Giant's Hall, Second Gothic Arch and Upper Inauguration Series were formed during or previous to the penultimate interglacial (probably the Hoxnian). The re-routing of Gaping Gill water from Cellar Gallery and the show cave to Beck Head Cave may have begun during or before the last interglacial, because the Giant's Hall flowstones show little evidence of surface re-solution from flooding that would have occurred

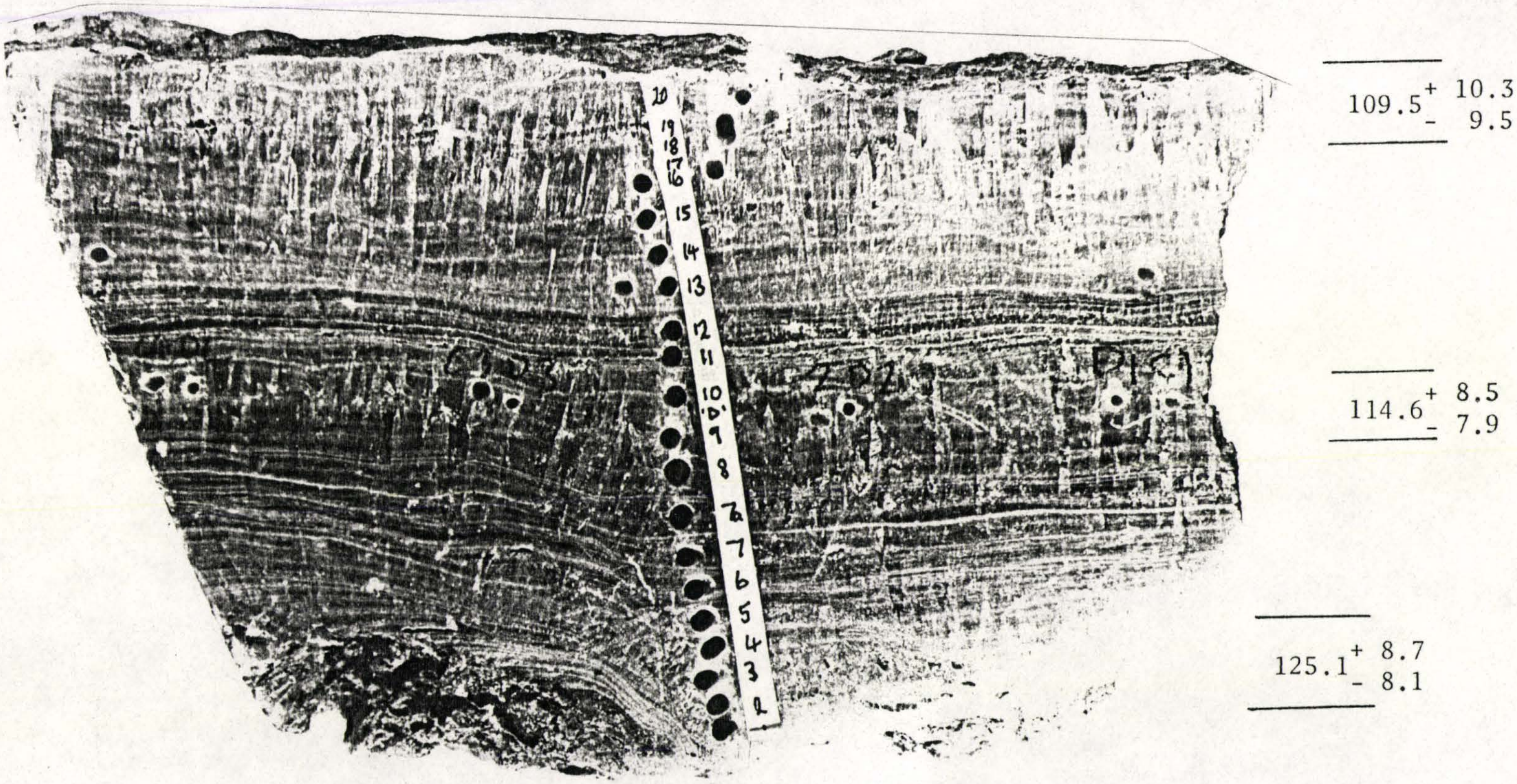

Figure 5.19 Section of flowstone 77143B from Ingleborough Cave, showing $^{230}Th/^{234}U$ ages and sampling locations for stable isotope and trace element analyses.

prior to the opening of this drainage route. It would seem therefore that the present drainage of Gaping Gill to Ingleborough Cave has persisted for at least 200 Ka, and therefore fossil, truncated tubes such as Foxholes (Figure 5.1), upvalley from Ingleborough Cave and possibly connected to the end of the show cave section, would have been active only before this period.

5.7.9 Victoria Cave

Speleothems from this cave have surprisingly yielded the most extensive span of ages of all the caves examined. The addition of data from recently acquired flowstones of archeological interest has fortuitously filled in a gap in the initial set of age data. The results are considered in four parts based on age groupings.

5.7.9.1 > 350 Ka

Seven speleothem samples lie beyond the limit of the dating method although the age of one of these (77236) is in doubt. This rather porous sample has a high $^{230}Th/^{234}U$ ratio (1.156) suggesting preferential uranium leaching. In contrast to all previous speleothems of this age range, six of the seven samples were in situ when collected. 76151 is from a flowstone block, apparently loose, found in a pile of similar blocks, bedrock and mud in the low muddy loop passage near the back of the entrance passage (Figure 5.14). 76155 is taken from a calcite wall veneer and contains a prominent growth hiatus; only the youngest layer has been dated. 77230A is the lowest, and presumably the oldest in a 3m sequence of overhanging flowstones and sediments near the back of the cave. Its age of > 350 Ka may be incorrect because of the low thorium yield obtained (5%) - this is perhaps reflected in the rather high $^{230}Th/^{234}U$ ratio (1.103). The remaining samples of this age were collected in situ from various levels within the excavated mud layers in the cave entrance (see Figure 5.20a).

5.7.9.2 310 - 180 Ka

Many loose and in situ flowstones (including one stalagmite) have ages within this interval. 76152 and 76154 (219 and 180 Ka respectively) are samples of loose flowstone blocks in the loop passage pile (Figure 5.14). 76152 is noteworthy because of its high ^{232}Th content (0.32 ppm), the highest found in this study. Correction for detrital thorium only shifts the age to 161 Ka, thus showing the lessening effect of detrital ^{230}Th, as speleothem age increases. A flowstone layer (F) higher in the sequence of 77230 deposits, dates at 253 Ka; the topmost layer has not been dated yet. A short stalagmite (77231) and an in situ section of flowstone curtain (77234) both from the loop passage, date at 243 and 214 Ka respectively.

77159 shows an interesting internal stratigraphy. It contains four thin layers of flowstone each separated by a detrital horizon representing a break in growth, and each is a different colour. Its basal age is 307 Ka and the top layer dates at 104 Ka (92.5 Ka when corrected). The sample was found in situ on the back wall of the cave, about 5m above the present (excavated) floor and 1m below the roof. It forms part of a continuous horizon on the cave walls and is probably a remnant of a once-continuous cave floor initially formed prior to

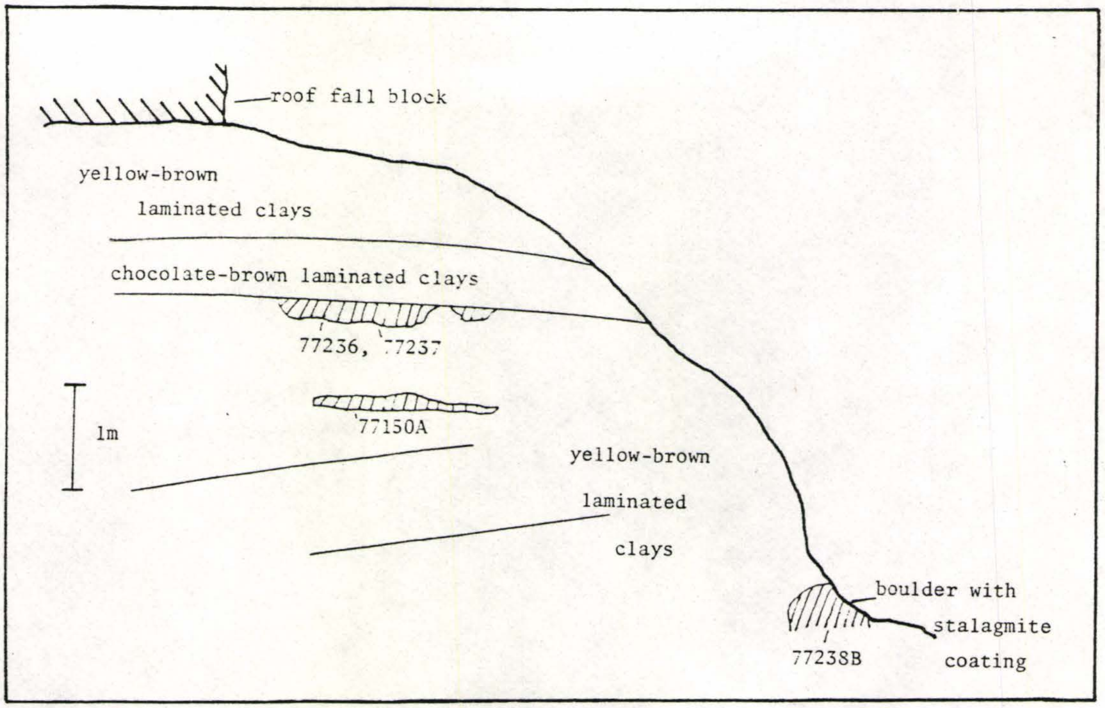

Figure 5.20a Sketch diagram of location of in situ flowstones in mud layers in Victoria Cave (see Figure 5.14).

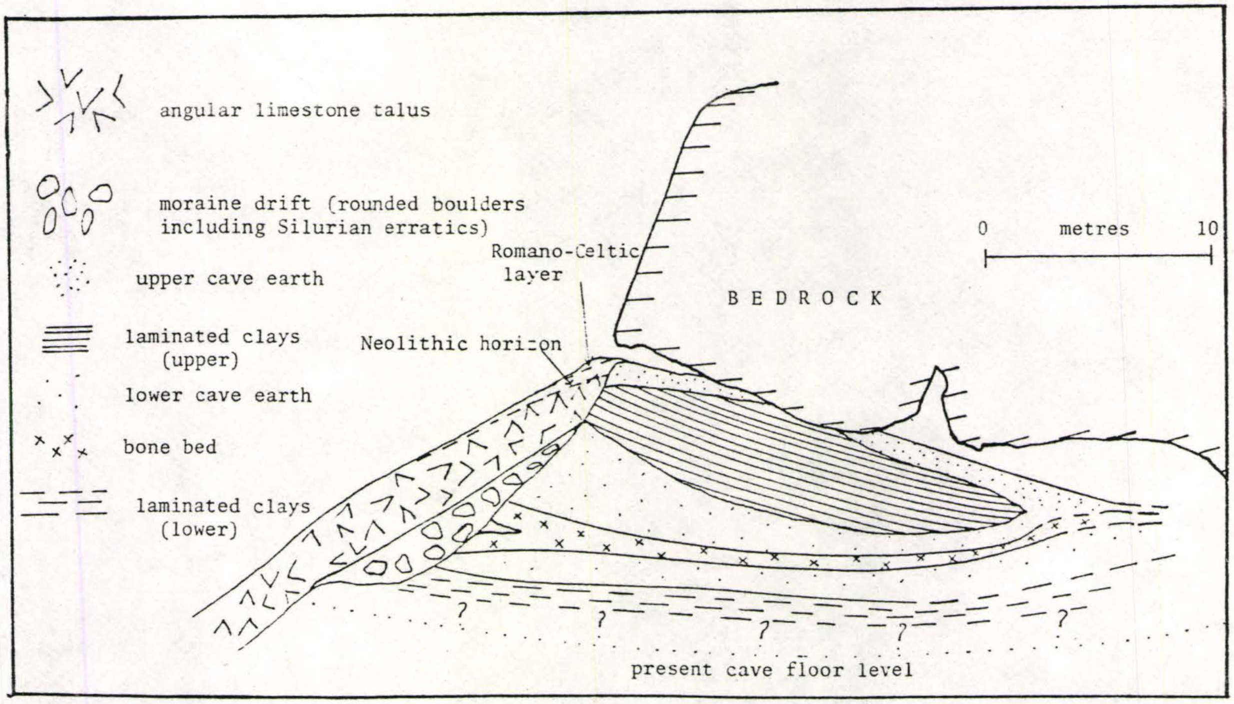

Figure 5.20b Diagrammatic section of Victoria Cave showing original sediment - cave earth sequence, as shown by Tiddeman (1875) with amendments by Lord, King (pers.comm. 1979).

307 Ka. The intermediate layers have not yet been dated.

The most important deposit from Victoria Cave, 77151, is a flowstone taken from an extensive, slumped deposit formed in the loop passage against the cave back wall (Figure 5.14). The flowstone mass was first exposed in a trench excavated in the main chamber for about 9m into the loop passage, by A.King in 1977. The flowstone overlies calcite-cemented angular fragments of clay resting on bedrock. These fragments have been examined for size fraction and mineralogy by Dr. John Catt. Initial results show that the sand-size fraction is almost wholly composed of clay aggregates cemented by iron oxides. In comparison to other sediments analysed in the cave this indicates a fairly cold environment at the time of deposition (Catt 1979, pers. comm.). 77151 contains a small stalagmite in its basal section (Figure 5.21). Breaks in deposition are seen between the lower (A) and middle (B) blocks, and 3cm above the base of the upper block (C). The division between B and C blocks appears to be a natural fracture along growth layers, rather than a depositional hiatus. In total, nine ages have been determined at various levels of this speleothem showing growth over the period 290 - 190 Ka. Agreement with the stratigraphy is seen in all results within error limits, except for one determination on the basal stalagmite. In view of the use of a low weight of sample in this analysis, and the overlying age sequence, this result has been rejected. The speleothem grew almost continuously from about 287 (± 30) Ka to 250 (± 25) Ka with a short break in growth between blocks A and B at about 280 Ka. Two analyses of the top of block C are in excellent agreement and show that growth ceased

Figure 5.21 Section of flowstone blocks comprising 77151 from Victoria Cave, showing growth hiatuses, $^{230}Th/^{234}U$ ages and locations of stable isotope samples.

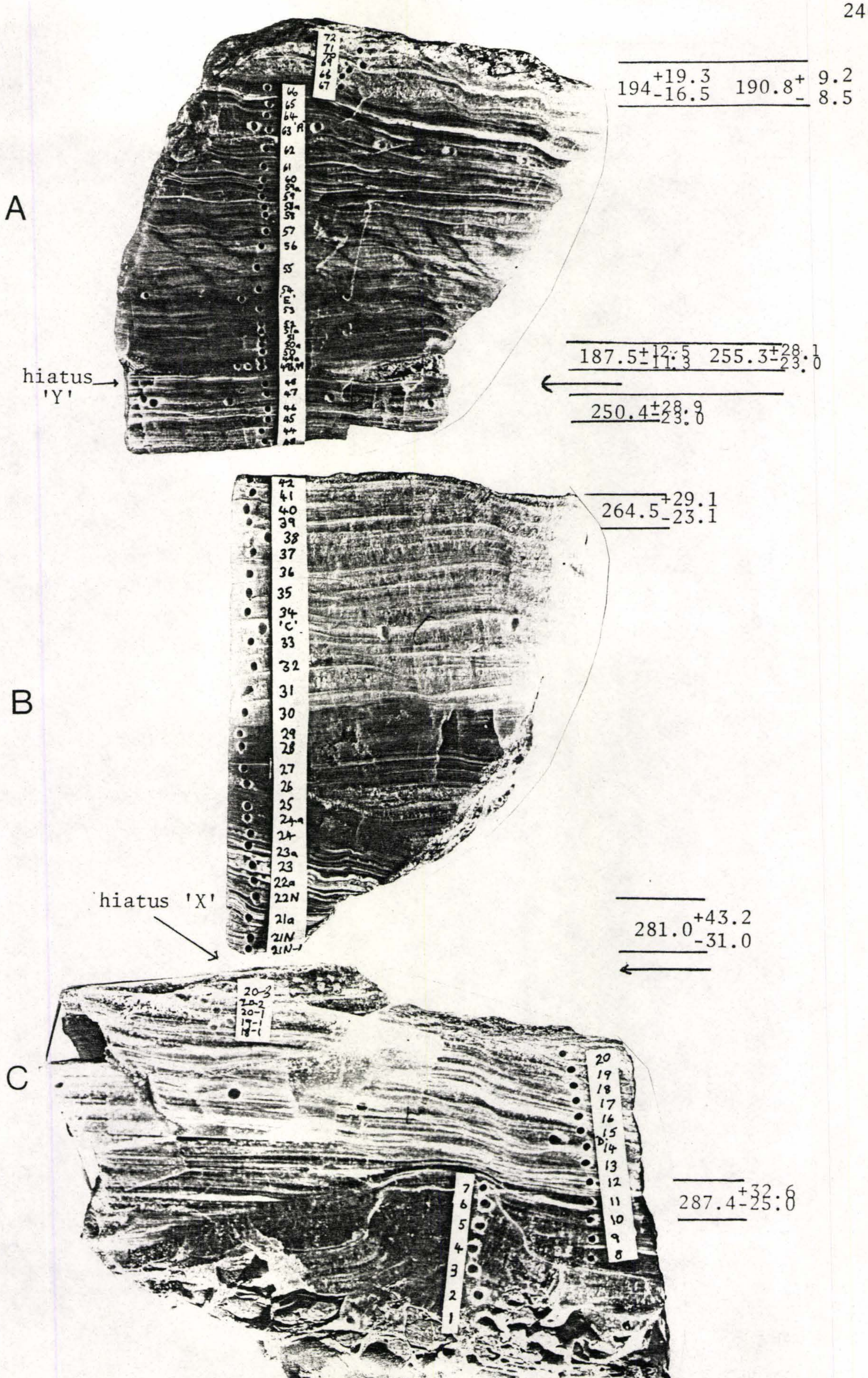
A
B
C
hiatus 'Y'
hiatus 'X'
$194^{+19.3}_{-16.5}$
$190.8^{+9.2}_{-8.5}$
$187.5^{+12.5}_{-11.3}$
$255.3^{+28.1}_{-23.0}$
$250.4^{+28.9}_{-23.0}$
$264.5^{+29.1}_{-23.1}$
$281.0^{+43.2}_{-31.0}$
$287.4^{+32.6}_{-25.0}$
72
71
69
68
67
66
65
64
63 'A'
62
61
60
59a
59
58a
58
57
56
55
54
'E'
53
52
51
50a
49a
47
46
45
44
43
42
41
40
39
38
37
36
35
34
'C'
33
32
31
30
29
28
27
26
25
24a
24
23a
23
22a
22N
21a
21N
21N-1
20-3
20-2
20-1
19-1
18-1
20
19
18
17
16
15
14
13
12
11
10
9
8
7
6
5
4
3
2
1

about 190 Ka. However, the extent of the time gap represented by the hiatus in block C is not made clear by the remaining age determinations. Two analyses above the hiatus give 188 and 255 Ka although their errors overlap at the 2σ level. The stratigraphy is further discussed in conjunction with a stable isotope profile towards the end of this chapter.

5.7.9.3 130 - 90 Ka

Only one age from the last interglacial period has been obtained from speleothem collections made in the cave (77159, previously described). More evidence of speleothem deposition during this interval has come from dating flowstones associated with bone collections presently held in the Pigyard Museum, Settle. These flowstones formed part of the 'lower cave earth' (Figure 5.20b) completely excavated by members of the British Association for the Advancement of Science, and others, since about 1840 A.D. (Tiddeman 1873, Warwick 1956). Exact positions and interrelationships of these samples were not well recorded and much of the archeological history of the cave is therefore inferred from old reports, personal diaries and the bone collection available today. Three samples of flowstone surrounding mammal bones have been dated. 79000 encloses a single rhinoceros molar, 79001 part of a lower rhinoceros jaw with some teeth present, and 79002 a red deer antler. The identifications are provisional at present, but 79000 and 79001 are both thought to be from the narrow-nosed rhinoceros, Dicerorrhinus hemitoechus, (King, Lord, pers. comm.; Sutcliffe et al. 1976).

Because the speleothem deposits form a mould around the bone remains, they must all post-date the bones, and will become younger further away from the bone, given that the flowstone growth layers are conformable to one another. 79000 was dated at 102 (± 7) Ka (6% Th yield) adjacent to the tooth while 79001 gave ages of 104 (± 6) Ka (99 Ka when corrected) nearest to the teeth and 126 (± 9) Ka 2 to 3cm away from the teeth. This apparent stratigraphic inversion of ages in 79001 may be due to the statistical nature of the age determinations (2σ error limits overlap) or due to contamination of calcite adjacent to the bone by uranium-rich bone fragments, although an attempt was made to exclude calcite adjacent to the bone for this reason. Sample 79002, enclosing the deer antler was dated at 131 (± 9) Ka (123 Ka when corrected).

5.7.9.4 20 - 0 Ka

Only one speleothem has been dated within this age range. 76153 is a thin flowstone/stalactite crust found loose on a pile of blocks in the loop passage. It presumably had fallen from the roof. The youngest layer of the flowstone was dated at 19 Ka (11.4 Ka when corrected). The absence of other post-glacial speleothems in the collection is probably due to the accessibility of the cave to visitors and tourists over the last century, so that any fresh, attractive deposits would have been removed for souvenirs. The more ancient deposits have survived because they are difficult to remove and far less attractive.

5.7.9.5 Discussion

The ages determined here indicate the following :

1) the cave is a particularly old feature of the Craven karst region - this has been proposed before from purely geomorphological considerations (Sweeting 1974) and is proved here by the presence of numerous speleothems older than 350 Ka.
2) as judged from the presence of many *in situ* deposits of speleothem, glaciations and fluvial periods since this time have had remarkably little effect on the deposits in the cave. This can be seen, for example, from the age of > 350 Ka for the laminated clay sequence (determined from interbedded *in situ* flowstones) which lies in the entrance passage. The clays may have been formed during times of ponding of water (glacial meltwater ?) caused by blockage of the entrance by moraine and talus (Figure 5.20a, b).
3) the abundance and range of ages of flowstones between 310 and 180 Ka generally indicates a temperate climate without any prolonged glaciation. However, the hiatus in 77151C and the lack of determined ages between 240 - 220 Ka may indicate non-deposition associated with a cold period.
4) the presence of rhinoceros and red deer in the Craven area during the last interglacial is clearly shown by these results. If Ipswichian dates can also be placed on flowstones associated with hippopotamus remains in the Pigyard Museum, then these results are best expressed by Dr. Tony Sutcliffe's comment (in Sutcliffe et al. 1976): "It seems incredible, at the present day, to think of hippos walking across this wild part of the Yorkshire moors"!

5.7.10 Sleets Gill Cave

Only one sample has been analysed from this cave. 77172 is a section of a hanging stalactite curtain in the main tube passage. Because of its porosity, only a thin coarsely-crystalline calcite layer was removed to attempt dating. The result showed a very low uranium concentration (0.02 ppm) and a $^{230}Th/^{234}U$ ratio of 1.715. Both factors are good evidence for extensive uranium migration from this sample and the calculated age of > 350 Ka is not reliable.

5.8 Quaternary Chronology and Classification

5.8.1 Age Frequency Distribution

The frequency distribution of $^{230}Th/^{234}U$ ages for Craven speleothems (with the exception of those with high detrital thorium from Ingleborough Cave, as previously described) over the period 0 to > 350 Ka is given in Figure 5.22 at 1 Ka intervals, corrected and uncorrected for detrital thorium. A second histogram (Figure 5.23) shows the frequency distribution at 5 Ka intervals and by including inferred growth periods (ie. those between a base and top date) better illustrates periods of continuous speleothem growth. Unfortunately, in the selection of samples for dating the tendency has been to determine a basal age first and only later perhaps a top age, with the result that the distribution is biased towards the earlier parts of a growth period. The correction for detrital thorium is seen to 'clean-up' both histograms, and a number of distinct age clusters become apparent. Five periods of abundant speleothem growth can be recognised in Figure 5.22. These periods are

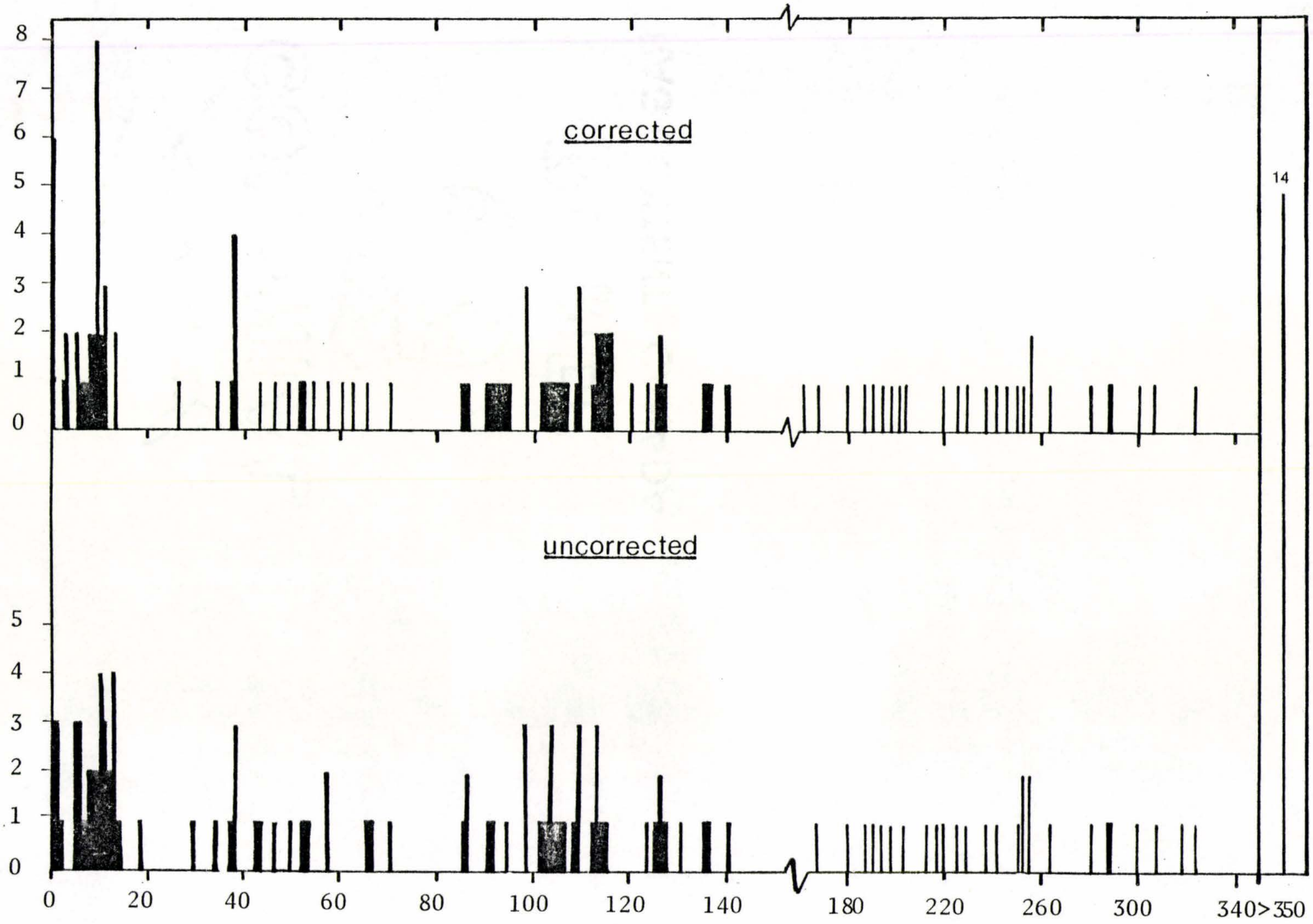

Figure 5.22 Age distribution frequency for all $^{230}Th/^{234}U$ ages shown in Figure 5.15, at intervals of 1 Ka. Distributions corrected and uncorrected for detrital Th are shown.

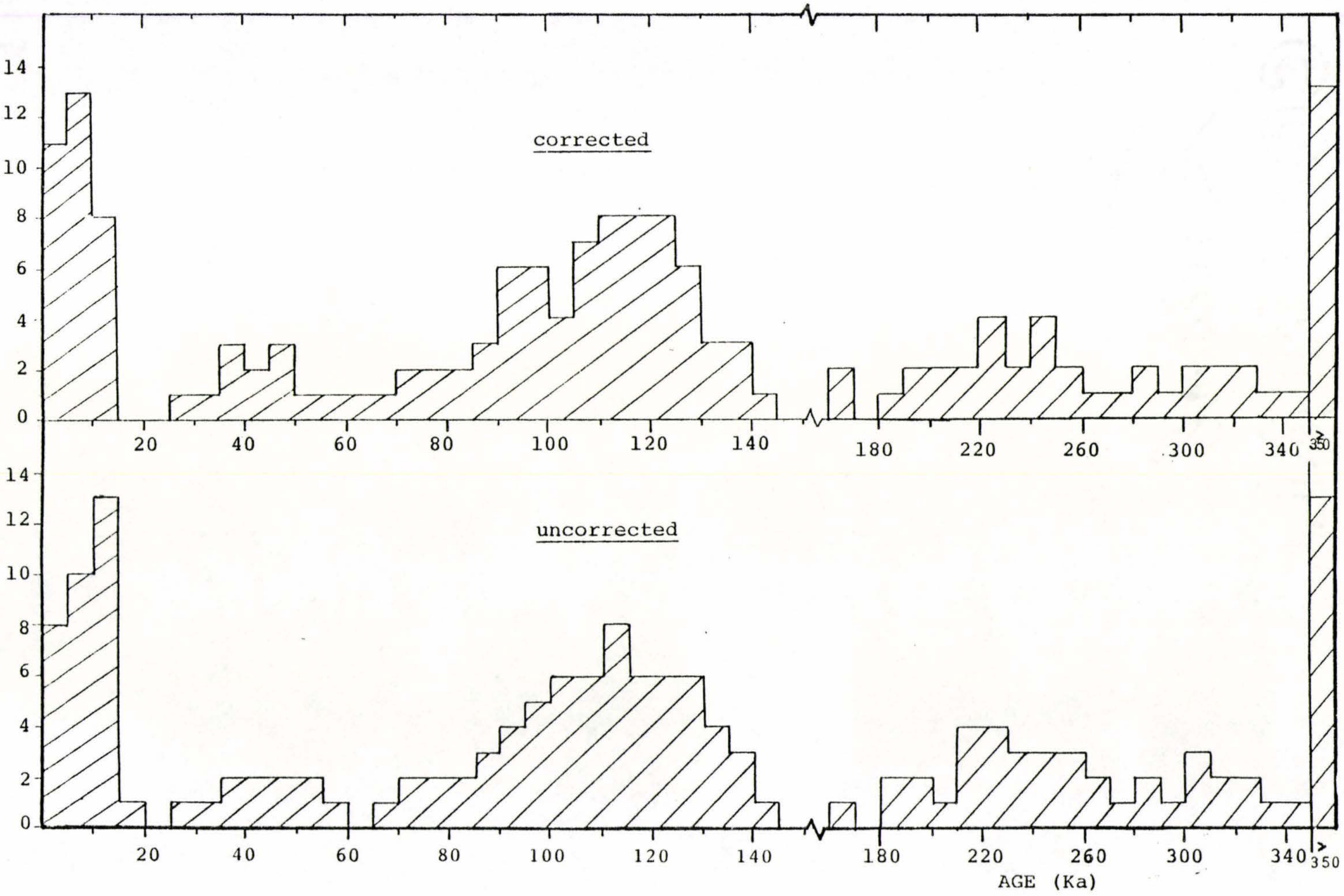

Figure 5.23 Distribution of speleothem growth periods at intervals of 5 Ka. The histograms represent the number of samples whose interpolated growth period lies within the dated range. Distributions for ages uncorrected and corrected for detrital Th are shown.

correlated in Table 5.2 with the British Quaternary record previously described. A detailed analysis follows.

5.8.2 Speleothem Growth

After correction for detrital thorium, no reliable ages are found to lie in the interval 34 - 15 Ka, a period roughly encompassing that of the late Devensian glaciation in England. This strongly supports the contention that speleothem only grows in non-glacierised regions. The periods of speleothem growth seen in Figure 5.22 must therefore be determined by conditions such as lack of perma-frost, open drainage routes etc. as discussed in Chapter 1.

The abundance of ages in any one cluster is unfortunately not simply a direct function of the warmth of a period. Factors such as bias in sampling and selection for analysis, differential preservation of speleothems and changes in local hydrological routing also influence their abundance at any given site. These factors are presumably responsible for one aspect of Craven age data seen in Figure 5.15: Victoria Cave is the only system which contains abundant, well-preserved, in situ speleothem older than 180 Ka, and yet contains almost no Ipswichian speleothem. Lancaster Hole - Ease Gill caverns show the reverse characteristic and Gaping Gill is intermediate between the two.

One main purpose of this study was to obtain speleothems as old as possible in order to date morphological events in these caves. Therefore modern-looking speleothems were not sampled and not dated if later suspected to be modern. Many of the post-glacial ages given

Generalized speleothem age groupings (Ka)	Equivalent British stage		Detailed speleothem age groupings(Ka)	Equivalent British sub-stage
0 - 14	FLANDRIAN post-glacial		-	-
35 - 70	DEVENSIAN	LATE	none	Late Devensian glaciation
		MIDDLE	35 - 45	Upton Warren Interstadial
			50 - 60	none
			none	Chelford
			65 - 70	Wretton ?
		EARLY	~ none	Early Devensian
85 - 130	IPSWICHIAN		85 - ~105 ?	none
			~105 - ~130	Ilfordian ?
none	WOLSTONIAN		none	none
180 - ~220	HOXNIAN		none	none
~250 - ~300	ANGLIAN		none ?	Lowestoft Stadial
			none ?	Corton Interstadial
			?	Cromer Stadial
> 350 ?	CROMERIAN		?	

Table 5.2 Correlation of speleothem growth periods for N.W. England with the British Quaternary record.

here were obtained accidentally while dating what was thought to be older speleothem. Consequently, the distribution frequency of speleothem ages is not necessarily representative (i.e. lower than) its true frequency in the caves studied.

In conclusion, it can be seen that many factors must be considered when making paleoclimatic deductions based only on an age frequency distribution.

5.8.3 Holocene and Post-glacial Speleothem

Speleothem ages younger than 20 Ka are replotted in Figure 5.24. Many are affected by detrital contamination (usually because the base of the speleothem is contaminated by underlying mud and gravel which are incorporated into its lower layers during growth). Most samples began growth during the period 14.5 to 11 Ka (13.5 to 9.0 Ka if corrected). Because the correction method uses a somewhat arbitrary value of initial $^{230}Th/^{232}Th$ ratio (= 1.5) and ignores other influences (Chapter 2), it is best to consider only the uncontaminated results if the time of speleothem initiation is to be determined at all precisely.

Figure 5.25 shows these few results along with present estimates for the timing of British and N.European post-glacial climatic events. The triple cold periods of N.Europe (Dryas events) and the climatic oscillations of England and Scotland (principally the Windermere Interstadial and Loch Lomond Re-advance) do not clearly show their influence on speleothem growth in Figure 5.25. However, allowing for 1σ error limits it is possible that three speleothems (76111, 76128 and 76191) began growing during the Windermere Interstadial. There also

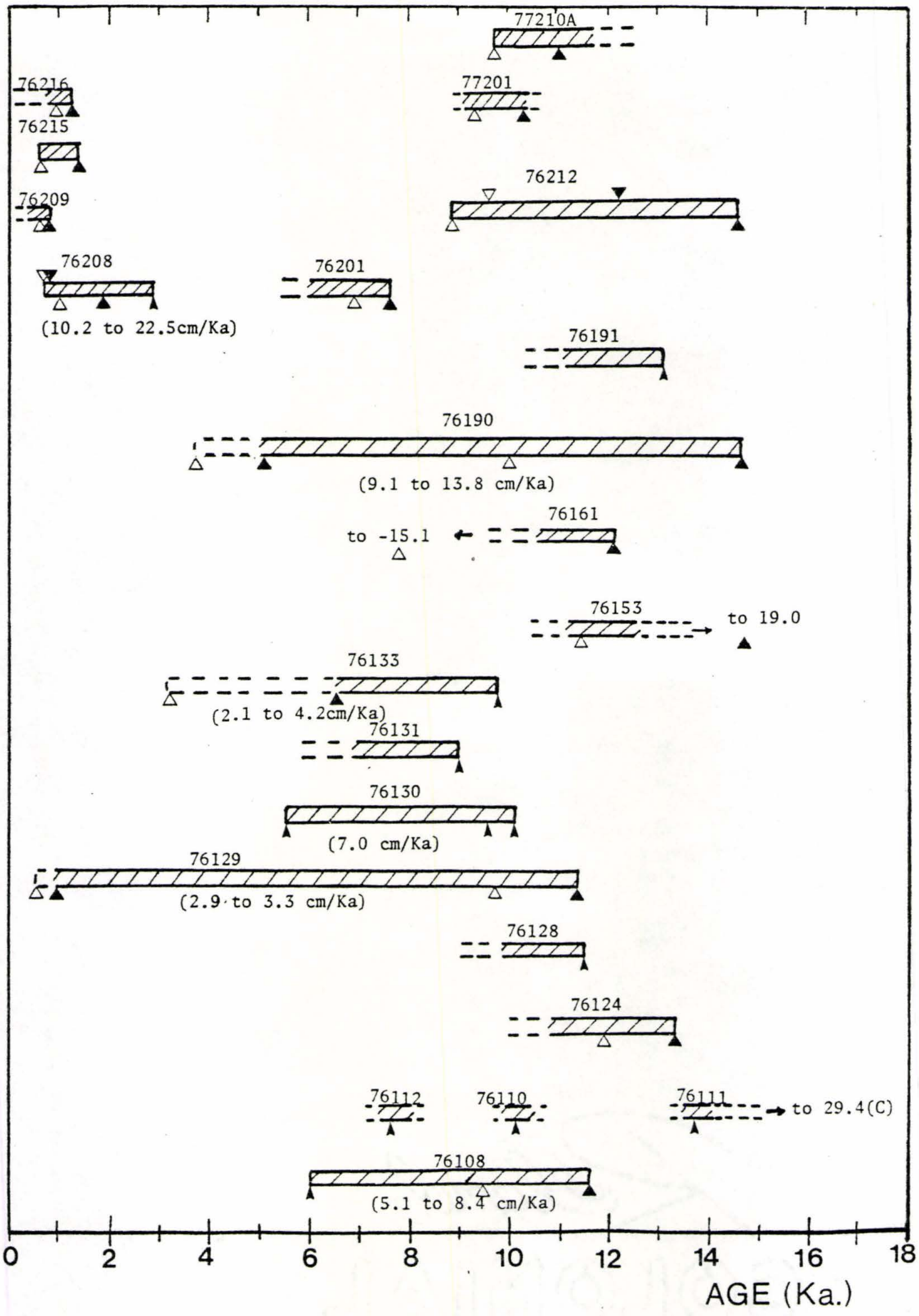

Figure 5.24 Bar graph of all post-glacial and Flandrian $^{230}Th/^{234}U$ ages of speleothem from the Craven District. Calculated growth rates for both corrected and uncorrected ages are shown. (Legend as Figure 5.15).

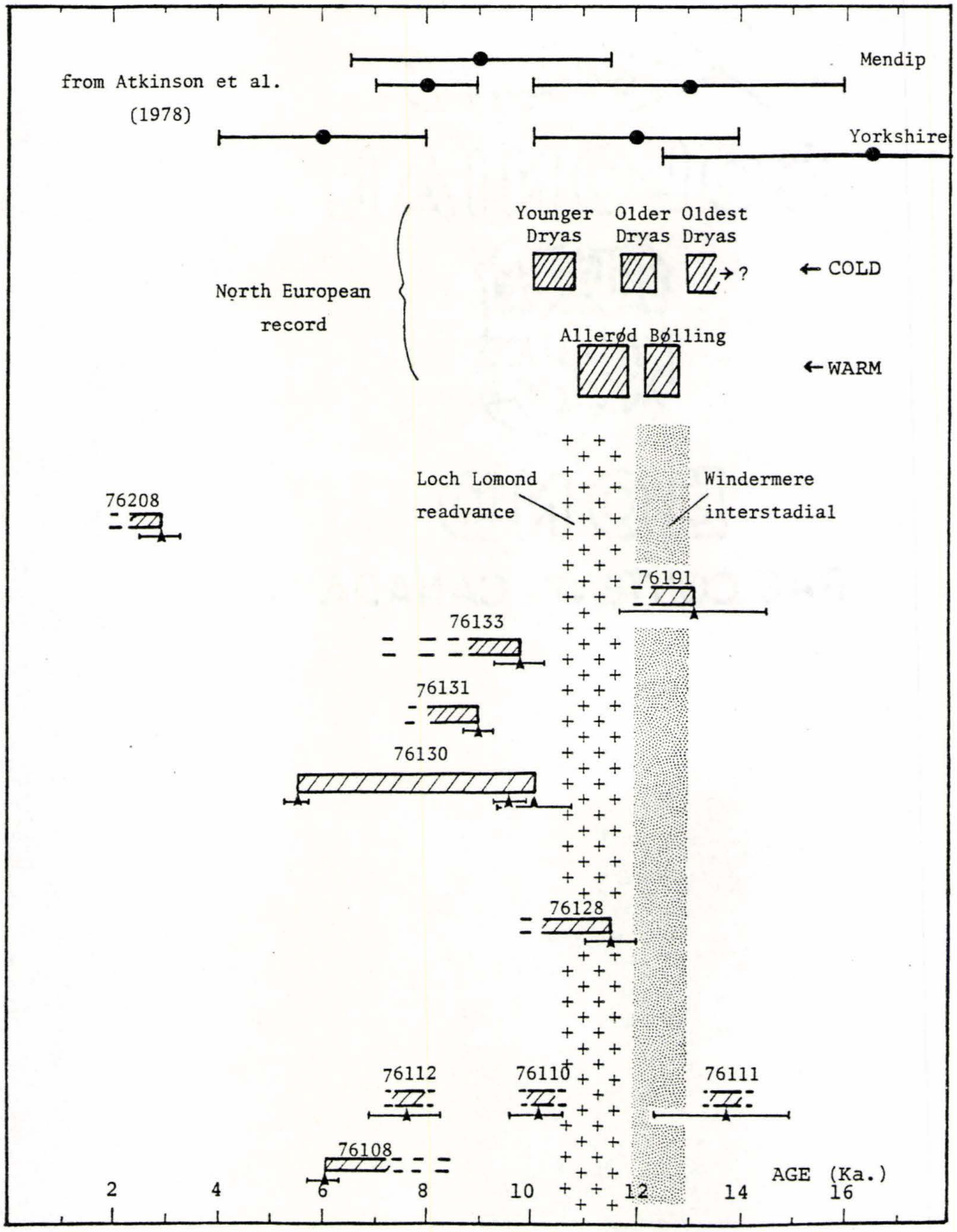

Figure 5.25 Bar graph showing $^{230}Th/^{234}U$ ages and growth periods of post-glacial and Flandrian speleothem which are not contaminated by detrital thorium (ie. $^{230}Th/^{232}Th > 20$). Correlation with the British and N.European records is shown and results are compared to those of Atkinson et al. (1978) for six determinations for Yorkshire and Mendip speleothem at the top of the diagram.

seems to be a sudden surge in growth frequency between 10 and 9 Ka (many of the ages corrected for detrital thorium also fall in this interval). The general lack of ages younger than 5 Ka (regarded as a period of full interglacial warmth) is an artefact of sampling and analysis.

These results neither support nor oppose the possibility of a warm late-glacial interstadial (Windermere) centred on 12.5 Ka as proposed by Coope (1977b). It is possible that insufficient vegetal cover had developed during this short warm spell, to generate enough CO_2 in the sub-surface to cause much speleothem to form in the caves below. In this case it could be argued that speleothem growth lags perma-frost free conditions by as much as 1 Ka, and relies heavily on the rapidity of development of a surface vegetation cover. Only a more detailed study of basal ages of post-glacial speleothem will determine the importance of this.

For comparison, Figure 5.25 also shows six ages determined by Atkinson et al. (1978) on speleothem from Gavel Pot and White Scar Cave, and from G.B. Cave (Mendip). For consistency, only those ages with $^{230}Th/^{232}Th$ ratios > 20 have been plotted. The large errors quoted by these authors are due in part to an error in the computer program used by these authors - see Chapter 2. Their data generally agree with the results presented here, except that one age of 16.5 (± 4) Ka indicates speleothem initiation in the Craven Area much earlier than found in this work.

5.8.4 Devensian Events

5.8.4.1 Late Devensian

No reliable speleothem ages are found in the period 34 - 15 Ka. This correlates well with other data regarding the duration of the Late Devensian glaciation. The scarcity of radiocarbon ages during the early part of this period and the general indication of arctic, tundra-like conditions from faunal evidence (Shotton 1977), suggests that periglacial or glacial conditions prevailed in northern England during this time. The absence of speleothem ages for this interval also indicates perma-frost or full glacial conditions.

5.8.4.2 Mid - Devensian

This period (50 - 26 Ka) shows intermittent speleothem growth from 50 - 35 Ka, with the greatest abundance at about 39 - 38 Ka. These results generally agree with those of Morgan (1973) and Coope (1977b) who place the Upton Warren Interstadial maximum at about 43 Ka based on ages of warm-species beetle assemblages from the Midlands. However the rapid development of warm conditions out of an arctic, tundra-like climate before 45 Ka is not clearly seen from the present results because a few speleothems show intermittent growth well back into Early Devensian times. The detrital horizons in 79005 (Figure 5.17) may indicate sudden warming trends (flood events ?) during 54 - 40 Ka, and sample 77121 indicates a period of rapid growth (Figure 5.16) from 58 - 52 Ka.

5.8.4.3 Early Devensian

Speleothem data provide no clear evidence for either of the two interstadials proposed for Early Devensian time: the Chelford (63 - 61 Ka) and the Wretton (68 - 65 Ka). Only two corrected ages lie in the interval 65 - 60 Ka (Figure 5.22). Instead, intermittent growth of low abundance is found over the entire period 70 - 50 Ka. In complete contrast to this, Atkinson et al. (1978) found three speleothems from Mendip and Yorkshire that grew during the Chelford interval, although the ages have large error limits (± 4 to ± 19 Ka) and apply to low uranium speleothem (0.05 to 0.19 ppm).

The lack of speleothem evidence in this study for these interstadial events may be due to sampling bias or the statistical nature of the ages and associated error limits. It is unlikely however that sampling bias is the cause because two speleothems near to this time period (77121 and 79005/77120) show continuous growth before 66 Ka and after 58 Ka, whereas in each case the period 63 - 61 Ka is one of non-deposition. Only correction of dates of two heavily-contaminated samples of 77120B provide ages within this bracket. These results suggest that the existence of the Chelford and Wretton interstadials as distinct periods of climatic amelioration is in some doubt, and that instead a period of cool but non-arctic conditions may have existed in N.England over the period 70 - 50 Ka.
However, the observed rapidity of these ameliorations and deteriorations of climate may preclude adequate development of a soil and vegetation cover, which in turn will give rise to abundant speleothem growth in the caves below. Only $\delta^{18}O$ variations in these speleothems

have the necessary resolving power to identify these interstadials.

Intermittent periods of speleothem growth from 90 to 70 Ka are seen in two samples (76122, 77120B) but do not appear in Figure 5.22. This is because intermediate ages between base and top dates, particularly in 76122 (Figure 5.16) have not yet been determined; until this is done, little can be said about the climate over this period. It is possible though, that an arctic environment may have persisted sometime between 85 and 70 Ka such that perma-frost would have prevented all speleothem growth.

5.8.5 Ipswichian

The lower end of Ipswichian time is variously cited as ~ 80 to ~ 50 Ka, the difference being most apparent between deep sea core workers and those concerned with the continental record (and therefore restricted by the limit of radiocarbon dating). A period of fairly continuous growth from ~ 130 to ~ 85 Ka is seen in the speleothem record (Figure 5.15). A number of samples end or begin growth, or contain a hiatus during the interval dated at about 105 - 100 Ka. They are summarized in Table 5.3. One notable exception to this is 77162 which shows continuous growth from 113 to 92 Ka. If this depositional break is due to a sudden cooling, then it is quite unsubstantiated by any other paleoclimatic data. In fact, 104 Ka is the age attributed to a high sea stand (and therefore warm period) seen in Barbados and New Guinea reef terrace data (Mesolella et al. 1969; Bloom et al. 1974). An intense cold period has been proposed for a short interval lying between 125 and 105 Ka (Steinen et al. 1973).

Speleothem Number	Cave	Hiatus in growth indicated: (Ka).
77120	Lancaster Hole	between 103.6 and 109.1
77126	" "	< 106.0
77121	" "	< 109.4 ?
76135	" "	> 94.7
77143	Ingleborough Cave	between 109.5 and 98.2
77159	Victoria Cave	~ 100
79000	" "	> 102.1
79001	" "	~ 100
76164	Lost John's Cave	between 106.3 and 104.5

Table 5.3 Summary of speleothems which begin or end growth, or contain a growth hiatus about 105 Ka.

Alternatively it may be possible that the break in growth is not caused by a cooling but rather by the onset of warm arid conditions where speleothem deposition might cease over a large area due to reduction of water supply. This explanation would at least permit isolated growth as seen in 77162.

One prominent feature of all Ipswichian results (Figures 5.15 and 5.22) is the relatively small number of deposits dated at ~ 125 Ka, the supposed interglacial maximum. The period of most intense growth appears to be from 115 to 100 Ka (excepting ~ 105 Ka as described above). This observation has also been made by Harmon (1975) in previous speleothem work. Whether this has any significance is considered further in the last chapter.

5.8.6 Wolstonian

Evidence for the timing, duration and extent of the Wolstonian glaciation is generally scarce in Britain. The speleothem data described here show a complete absence of dates between 167 and 141 Ka (161 - 141 Ka for corrected data). This is a situation comparable to that found for the Late Devensian glaciation, and therefore suggests that periglacial or full-glacial conditions persisted in N.England for at least 20 Ka, between ∿165 - 140 Ka.

5.8.7 Hoxnian and Anglian

Hoxnian interglacial surface deposits are fairly abundant in southern and eastern England. Speleothems dating from pre-Wolstonian times are also quite abundant in Craven caves (Figures 5.15, 5.22), and from these data the Hoxnian interglacial can be seen to end about 180 Ka. The problem is however, at what point in the speleothem record does the Anglian end and the Hoxnian begin, and therefore (presuming no speleothem growth during Anglian stades) which are pre-Anglian deposits ?

Sample 77151 from Victoria Cave shows continuous growth from about 290 Ka to about 250 Ka, followed by a hiatus representing anywhere between 0 and 50 Ka depending on the ages used (Figure 5.21). Growth ended about 190 Ka. The hiatus between 250 and 200 Ka also generally correlates to depositional breaks seen in other speleothems but over this age range, error limits are large. The speleothem thicknesses are also small, so that only short isolated records have been obtained and no clear regional depositional break is indicated. A potentially useful deposit, which so far has only two ages determined for it, is 77230, a complex, 3m deep sequence of flowstones and sediment set high on the southern wall in Victoria Cave. Results so far indicate periods of growth between > 350 and < 250 Ka.

If Shackleton and Turner (1967) are correct in estimating the maximum duration of the Hoxnian to be about 30 - 50 Ka, then the general depositional hiatus at 220 (± 20) Ka in the speleothem data would permit a 40 Ka duration for the Hoxnian (from 220 - 180 Ka) and would place the late Anglian glaciation (the Lowestoft stadial) in the period 250 - 220 Ka. This is somewhat earlier than the time scale proposed by Shackleton and Opdyke (1973) from deep sea core data, where the 7-8 boundary (ie. the warming transition from Anglian to Hoxnian) was put at 251 Ka (Table 5.2). These authors in fact, propose that the classical Hoxnian in England does not correlate to this time period, but to the more-intensely warm event (stage 9), about 100 Ka earlier. However, this proposal is in contrast with results of faunal studies which show that the Hoxnian was not a particularly warm period in England (discussed earlier in this chapter).

The remaining speleothem ages over 250 Ka presumably correspond to middle Anglian times and may extend further into the complex Cromerian period. The relevance of the speleothem results to pre-Wolstonian climatic events is considered in more detail towards the end of this chapter in light of the stable isotope results obtained from 77151 from Victoria Cave.

5.9 Implications for Cave and Karst Development

Three cave systems (White Scar, Gaping Gill with Newby Moss, and Victoria Cave) have been found to contain speleothem older than 350 Ka. Two others, Lancaster Hole - Ease Gill and Kingsdale Master Cave contain speleothem older than 200 Ka. These results and those from Lost John's Cave have the following implications for understanding cave and karst development in the Craven Area.

5.9.1 Erosion Rates of Cave Passages

Two dated sites provide local maximum rates of entrenchment of cave stream channels. The first, in Lost John's, has been shown to give a maximum rate of 2.2cm/Ka for the last 115 Ka. The second, in Kingsdale Master Cave Roof Tunnel shows a maximum average downcutting rate of 5cm/Ka over the last 300 Ka. Both these calculations assume that there is no alternative route that the water may have at one time followed so as to bypass (abandon) the site completely for an unknown interval. This could have happened in the Master Cave, where blocking off the Roof Tunnel above the present sump or water diversion via some parallel phreas may have occurred. The Main Drain in Lost John's is the only known streamway. Very low streamflows and armouring the floor with sediments (as is presently the case) will reduce the downcutting rate to zero.

Other less definite rates of entrenchment come from 1) Stop Pot in Ease Gill Caverns where a downcutting of up to 20m has occurred in at least 240 Ka (< 8cm/Ka), 2) White Scar Cave, where a 20m lowering of the stream level has occurred in > 350 Ka (< 6cm/Ka), 3) Ingleborough Cave, where a lowering of about 3m has occurred in > 120 Ka (~ 2.5 cm/Ka). It should be remembered in the cases of Ease Gill and White Scar that the speleothem dated was not in situ, and if it originated at a higher level, then these rates are only minimum values.

5.9.2 Valley Entrenchment

From this work, the major valleys, Kingsdale and Chapel-le-Dale, were essentially formed to their present dimensions by at least 300,000 years ago. Specifically, the Kingsdale valley floor was no higher than 10m above its present level at about 300 Ka (although it must be remembered that it is presently floored by gravels to perhaps 25m in depth. Chapel-le-Dale could have been up to 70m higher than present > 350 Ka ago, (from bench-top to valley floor, Chapel-le-Dale is about 200m deep). This entrenchment represents an extreme maximum rate of 20cm/Ka. Previous estimates of valley lowering by Sweeting (1974) (up to 60 m caused by glacial scouring) and Brook (1974) (20-

50m per glaciation) can be seen to be high relative to these data.

The speleothem results are consistent with the occurrence of two, and probably three, glaciations in the Craven area in the last 350 Ka. Valley deepening accompanying these, ranges between < 10m to 25m per event. It is perhaps simplistic to think of valley glaciers alone effecting the deepening, given the very long time spans between successive glaciations. If it can be assumed that:

1) the deep sea core record shows up to 20 glacial events in the northern hemisphere during the last 2.5 myrs,
2) valley glaciers occupied the Dales during most of these events,
3) erosive effects of interglacials and interstadials between these events were comparable to those of the last 350 Ka,

then the downcutting of Chapel-le-Dale and Kingsdale into the limestone may have begun between 2 and 0.8 million years ago.

5.9.3 Cave Development

Previous theories of cave development in the Craven area have invoked cave initiation at a stable water table (Sweeting 1950) or up to 55m below it (Waltham 1970a). Ancient, drained phreatic tunnels have been ascribed to a 'pre-glacial' origin (= pre-"Mindel-Riss glaciation") and vadose passages were considered to be post-glacial (Waltham 1970a). This concept was criticized by Brook (1971) who emphasized the presence of several glaciations in the Craven area and the importance of the intervening non-glacial periods in cave development. More recently (Waltham 1974) recognised two glacial events as significant in the development of the Leck Fell caves, but although he retains their importance for valley downcutting they are only marked by speleothem deposition and sediment infill in the caves. The results presented here and in Atkinson et al. (1978) show that Waltham's concept of glacial speleothem growth is wrong.

Eyre and Ashmead (1967) and Ashmead (1974) have variously interpreted the development of the Lancaster Hole - Ease Gill system in terms of glacial/interglacial erosional cycles, or development of erosion surfaces in the area. The earlier work (1967) gave the most ambitious interpretation, and from the age data presented here can be seen to be the more correct in terms of the number of glacial/interglacial cycles the cave has seen, but incorrect in assigning most of the high level tube development to stage 'III', the 'Great' interglacial (= Hoxnian). It is more probable that these tunnels developed in pre-Anglian times.

On the basis of speleothem ages of 225 Ka from the streamway of White Scar Cave and > 400 Ka from Kingsdale Master Cave, Waltham and Harmon (1977) and Atkinson et al. (1978) have proposed a pre-Anglian (probably Cromerian or Pastonian) age for the Dales. However Atkinson et al.(1978) resort to the 'water table concept' to explain the apparently comparable levels of the major fossil phreatic tunnels in the Craven area. They regard the 'ancient water table' to lie between 265m a.s.l. in the west near the Dent fault and at over 300m a.s.l. in the Ingleborough area (Figure 5.26). The lack of vadose entrenchment in most of these tunnels is cited as evidence for rapid rejuvenation from above this level to modern base levels, and

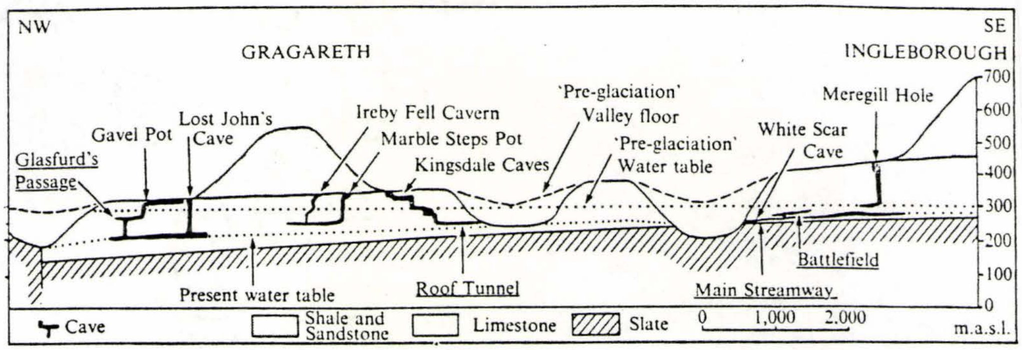

Figure 5.26 Diagrammatic section from Atkinson et al. (1978) proposing a 'pre-glaciation' topography and 'water table' for the area shown.

Cave	Passage	Approximate Mean Passage Altitude (m a.s.l.)	Approximate Altitude of Present resurgence (m a.s.l.)	Reference
Lancaster Hole - Ease Gill Caverns	Montague East to Stop Pot	277	215	Ashmead (1974)
Gavel Pot	Glasfurd's Passage	290	215	Waltham (Leck Fell Survey)
Lost John's Cave	Lyle Cavern High Level Series	260	215	" " "
Ireby Fell Cavern	Duke Street	250	215	Atkinson et al. (1978)
	" "	280		Waltham (1970)
Kingsdale Master Cave	Roof Tunnel	260	253	Brook (East Kingsdale survey, 1967)
White Scar Cave	Western Front Sleepwalker Series	280	247	Waltham (survey 1977)
Gaping Gill	Stream Chamber to S.E. Passage & Whitsun Series	305	251	Glover (1974)
Victoria Cave	Main Passage	440	-	Brook et al. (1976)
Sleets Gill	Main Gallery	265	not known	Brook et al. (1972)

Table 5.4 Approximate mean altitudes of fossil phreatic tunnels in Craven caves and altitude of the present resurgences.

from this they conclude that:

1) the ancient water table caves were 'pre-glacial'
2) the major rejuvenation was due to one glaciation which caused up to 75m of deepening
3) a second rejuvenation, seen in some caves, of 7 - 20m occurred some time later.

The concept of cave formation at or under a water table implies that all the fossil tunnels correlated to it must be approximately contemporaneous and that an upper constraint on the altitude of the water table can be determined from the altitude of the highest tunnel.

Altitudes of a number of fossil phreatic tunnels, most of them sampled for speleothem in this study, are listed in Table 5.4. Although most of the caves have been mapped, their relative altitudes with respect to sea level are not always known precisely, hence the approximate nature of some values. All caves as far east as Gaping Gill are in the same drainage basin and might therefore be interpreted in a regional water table. It is seen that most ancient tunnels west of Ingleborough, lie within the range 280 - 290m a.s.l.. Duke Street and the Roof Tunnel lie at lower levels and the main passages of Gaping Gill at a higher level. Waltham (1974) has previously proposed that all cave systems on Leck and Ireby Fells have at one time drained to a resurgence between 300 and 310m a.s.l. on Leck Fell "obscured by drift at the present". Phreatic features in Ireby Fell Cavern are first seen about 55m above Duke Street (~ 305m a.s.l.) but Brook (1971) has suggested that these may be due to a local, perched phreas and therefore may not indicate that Duke Street was formed at great depth below the water table.

At the moment, it is impossible to conclusively determine whether an ancient resurgence does exist on Leck Fell and whether it took drainage from caves as far away as Kingsdale. It is not relevant here to discuss the many lines of evidence that appear to negate the regional water table concept but it is proper to comment upon the rejuvenation model that Atkinson et al. develop from it. They propose that a downcutting of up to 75m took place in one glacial event prior to 400 Ka. From the present results, maximum valley entrenchment of 25m per glacial/interglacial cycle has been determined for the last 300 Ka. This period included at least two full glaciations, one of which, the Wolstonian, is thought to be the most extensive (and therefore possibly most intensive in an area of generation such as the Dales) known in Britain. It is therefore difficult to envisage how such a large entrenchment could take place in one earlier glaciation, (the 'first' Pleistocene glaciation according to Atkinson et al.). Rather, it is considered that the evidence for rapid de-watering of the system (lack of vadose entrenchment in fossil tubes) and the de-watering process itself, should be re-evaluated. Several of the large tunnels described above contain a vadose entrenchment stage eg. Gavel Pot main streamway, the high level series of Lancaster Hole - Ease Gill Caverns, Lyle Cavern High Level Series and Sand Caverns in Gaping Gill. In many of the other tunnels (White Scar, Duke Street and Glasfurd's Passage) evidence of a vadose phase may be obscured by blockfall and sediments. Dating evidence above, has shown that such trenches can be very slow to form and deepen.

Furthermore, a gradual process of valley downcutting during successive climatic cycles need not give rise to vadose entrenchment of all phreatic tubes. Internal processes of stream diversion by rapid joint opening, blockage by collapse or sediment infill, and flow in the direction of a rising phreatic tube will all prevent the development of vadose features.

It is therefore more probable that valley entrenchment in the Craven area has been a gradual process, occurring in steps of less than 25m per glaciation. This value also includes erosion which occurs during interglacials (there may be appreciable erosion in some circumstances eg. steeper gradient valleys, as seen presently in the River Dee in Dentdale). A logical extension of this gradual process is to anticipate the presence of even higher-level tubes dating from a time when the limestone was only partially exposed and valleys entrenched only into the uppermost beds. Victoria Cave and others in the area may be evidence of this situation, but few are found today probably because of truncation and extensive collapse.

In conclusion, it seems that a series of rejuvenations, or perhaps even one continuous rejuvenation process, can best explain the caves and karst of Craven. The proposal of 'a major rejuvenation' is alien to the continuous glacial/interglacial cycle seen in the Yorkshire Dales during the Late Pleistocene. It is therefore difficult to imagine conditions being stable long enough to permit the development of large phreatic tunnels under a common water table.

5.10 Stable Isotope Results

Several of the dated Yorkshire speleothems have been analysed for $\delta^{18}O_c$ and $\delta^{13}C_c$ along growth layers to determine if they grew in isotopic equilibrium with their waters of deposition. Some samples were flowstones and these have been analysed in two dimensions as described in Chapter 3. Results are shown in Figures 5.27, 5.28 and listed in Appendix 4 b. Three samples from the Lancaster Hole - Ease Gill system, two from Gaping Gill and one from Gavel Pot show kinetic isotope fractionation: $\delta^{18}O_c$ is correlated to $\delta^{13}C_c$, and usually both increase in the direction of water flow. This fractionation is probably due to evaporation of water and rapid outgassing of CO_2, caused by unsaturated air currents in the cave passages.

Four speleothems were found to be deposited in isotopic equilibrium (Figure 5.28). Two come from the Giant's Hall aven in Ingleborough Cave (76142, 77143), one from Stop Pot in Ease Gill Caverns (76127) and one from Victoria Cave (77151). Isotope profiles have been determined for three of these and are discussed individually below and results are given in Appendix 4 b. Sample 76142 was found to be in equilibrium but was difficult to date precisely due to low uranium and high detrital thorium content (Appendix 4 a). It appears to be an Ipswichian deposit and is discussed along with the results for 77143.

5.10.1 Modern Speleothem

Ten modern straw stalactite tips, flowstones and tops of stalagmites have been analysed to determine the range of $\delta^{18}O_c$ in this

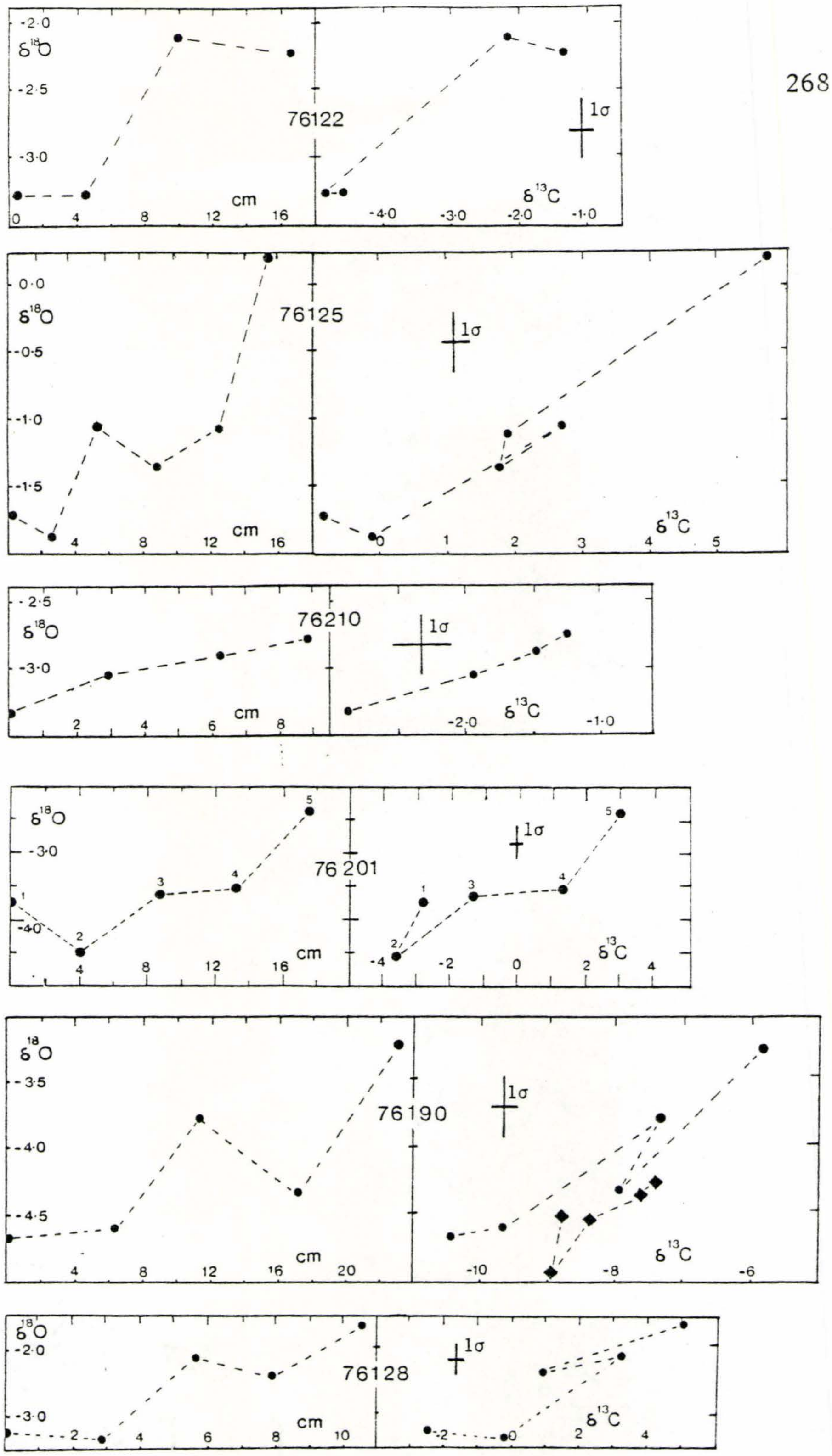

Figure 5.27 Graphs of $\delta^{18}O_c$ versus distance from top of growth layer (on left) and $\delta^{18}O_c$ versus $\delta^{13}C_c$ for growth layers of speleothem from caves in the Craven District. Different growth layers for the same speleothem are shown by letters. Each sample is numbered and joined by vertical lines if analysed more than once (results are listed in Appendix 4b).

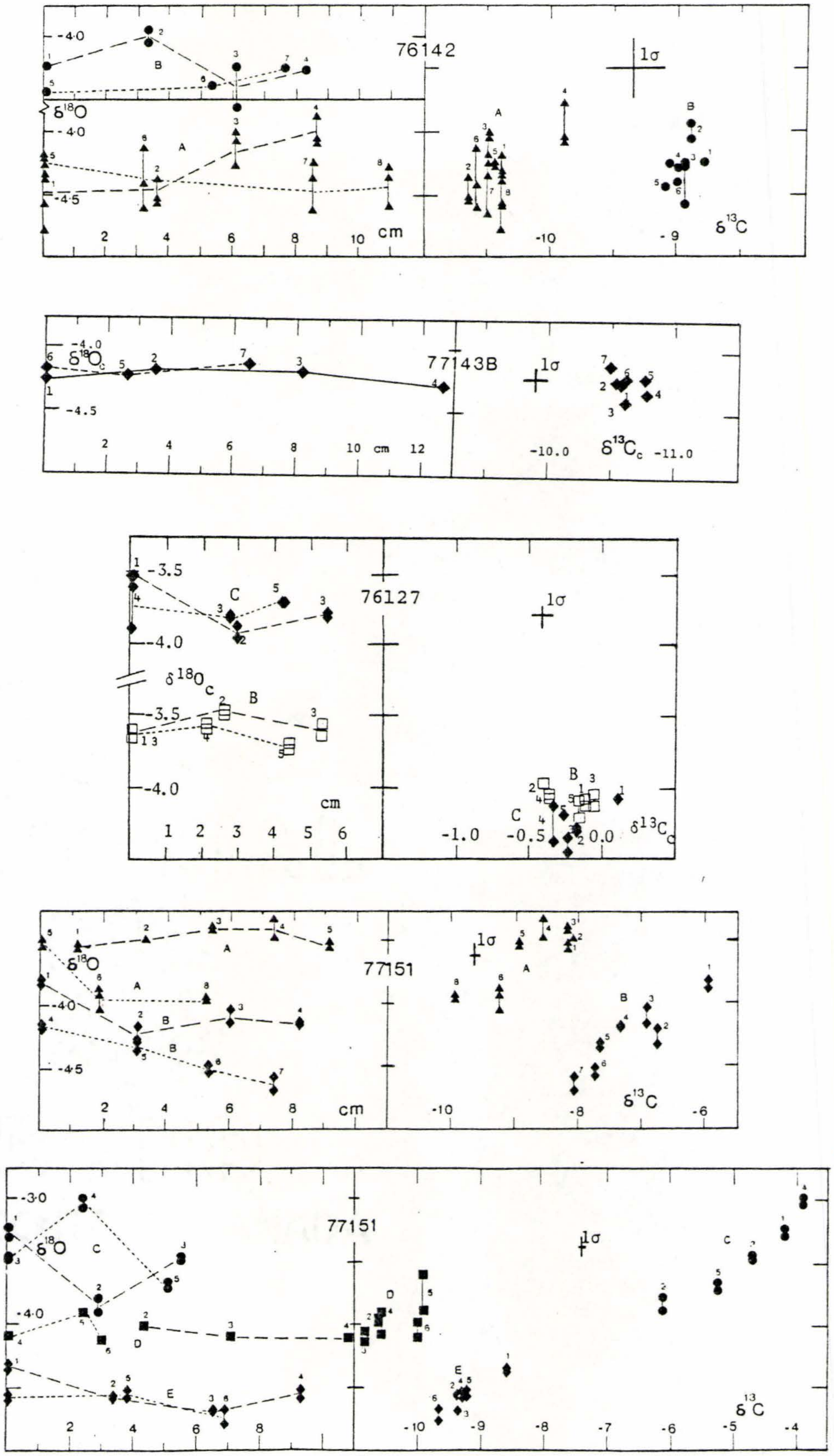

Figure 5.28 Graphs of $\delta^{18}O_c$ vs. distance from top of growth layer (on left) and $\delta^{18}O_c$ vs. $\delta^{13}C_c$ for growth layers of speleothem from caves in the Craven District (as Fig.5.27)

area for growth today. These results are listed in Table 5.5. With one exception (IA 5) all $\delta^{18}O_c$ results lie in the range -5.3 to -4.8‰ IA 5 has $\delta^{18}O_c$ and $\delta^{13}C_c$ values 1‰ heavier than the others and may either represent kinetic isotope fractionation or deposition from an 'evolved' water (see 76127 below). The variations seen here are comparable in magnitude to those of modern speleothem from Vancouver Island, and may be explained in the same manner as in Chapter 4.

5.10.2 76127

This speleothem is a small dense-white flowstone block from Stop Pot in Ease Gill Caverns. It was dated between 238 Ka (near base) and 225 Ka (top). Two growth layer determinations show remarkably consistent values for both $\delta^{18}O_c$ and $\delta^{13}C_c$. The isotope profile is shown in Figure 5.29 on a time scale based on the growth rate between the two dated portions. Modern speleothem is also shown.

It is interesting to note that $\delta^{13}C_c$ values are considerably heavier than seen in modern speleothem, and would either indicate that carbon in solution was predominantly derived from limestone ($\delta^{13}C$ = 0 ‰) or that, more likely, considerable outgassing presumably accompanied by calcite deposition, has already occurred and 76127 is 'residual' calcite. This outgassing (or 'evolution' of the water) may have been an equilibrium or kinetically controlled process, but has ultimately become an equilibrium process in the deposition of 76127. One consequence of this evolution is that kinetic isotope fractionation at an early stage could affect $\delta^{18}O$ of the water by

Sample Number	Cave	Location in cave	Type	$^{18}O_c$ (‰)	$^{13}C_c$ (‰)
IC 2	Ingleborough	near Curtain Range	stalac.	-4.81	-9.70
IC 3	"	behind Mushroom Beds	"	-4.84*	-9.96
IC 4	"	in Abyss	"	-5.01	-9.94
IA 5	"	Giant's Hall	flowst.	-3.91	-7.02
WSA 1	White Scar	200m upstream of show cave	stalac./ flowst.	-4.96*	-10.37
WSC 2	" "	100m upstream of show cave	stalac.	-5.20	-9.77
WSA 5	" "	adjacent to WSC 2	stalac./ flowst.	-5.21*	-8.67
WSWB 1	" "	upstream of show cave	"	-5.31*	-11.69
CPC 1	County Pot, Ease Gill Caverns	Oxford Circus	stalag.	-5.31*	-6.76
IPC 1	Ibbeth Peril I	roof tube	stalac.	-4.92	-10.26

* mean of two analyses of same gas

mean $^{18}O_c$ (excluding IA 5) = -5.06 ± 0.25 ‰

Table 5.5 Results of isotopic analyses of modern speleothem from Craven caves, England.

exist, because the cave is near to the surface (within 30m) and the speleothem is only about 40m from the entrance. In drilling the speleothem for an axis profile, care was taken to avoid the white lines and sample only the clear calcite.

The isotope profile is illustrated in two ways : in Figure 5.31 on an abscissa scale of distance below top with dated segments blocked in and the analytical numbering scheme shown (for ease of comparison to Figure 5.21), and in Figure 5.32 on a time scale determined from dated segments for lower blocks A and B, and a 'floating' time scale whose top is fixed at 190 Ka for block C. The range of values of modern $\delta^{18}O_c$ is shown in both diagrams. Figure 5.31 shows the analytical detail that is lost by scale compression in Figure 5.32 and the floating time scale is necessary because of the difficulty in precisely dating hiatus Y in block C, as discussed previously. The time scale suggested here is determined using the average growth rate of the two lower blocks (0.5 cm/Ka), (there is no textural evidence to indicate that the growth is faster or slower although the general absence of detritus in hiatus Y (Figure 5.21) suggests that the depositional break was not as long as the 40 Ka implied here). The range of $\delta^{18}O_c$ for all growth layers is also shown in Figures 5.31.

The analytical precision obtained for this speleothem is found to be excellent and well within the limit ± 0.08‰ (determined in Chapter 3) for the following reasons : a) 19 analyses of calcites in between already-analysed sites were made some months later to fill in 'gaps' in the record. They are indicated in Figure 5.31. In all

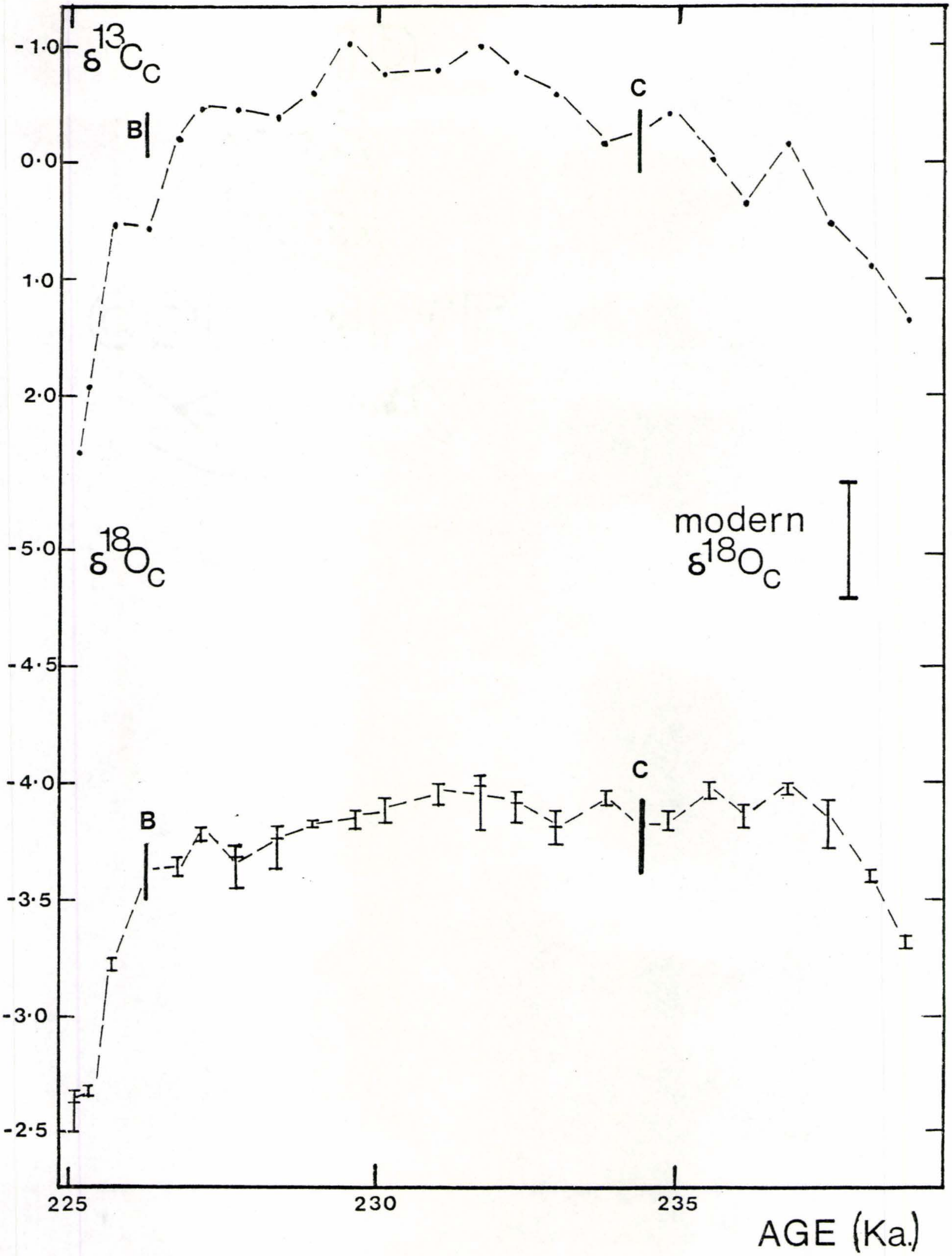

Figure 5.29 Stable isotope profile of flowstone 76127 showing its relation to $\delta^{18}O_c$ of modern calcite. Multiple analyses of the same gas sample are connected by vertical lines. The time scale is determined by interpolation assuming constant growth rate between the dated sections shown. Range in growth layer analyses is shown.

evaporation, and this would consequently give a speleothem with $\delta^{18}O_c$ greater than speleothem deposited from a 'non-evolved' water at the same temperature, in the same area. Therefore, because the amount of evolution may vary over time, fluctuations in the $\delta^{18}O_c$ profile can not simply be related to climatic change.

Good analytical precision is seen in the results of Figure 5.29 by the exact fit in the curve of growth layer analyses at two levels in the flowstone, made some weeks before the isotope profile. A remarkably constant $\delta^{18}O_c$ is seen over the main portion of growth, bounded by ^{18}O - enriched calcite at both ends of the speleothem. This record may be interpreted as follows:

1) the entire period of deposition (240 - 225 Ka) was somewhat cooler than today, giving values of $\delta^{18}O_c$ > 1‰ heavier than modern. This is the 'classical' interpretation of previous speleothem work, where changes in temperature and $\delta^{18}O_{sw}$ override temperature dependent changes in $\delta^{18}O_p$, (Harmon et al. 1978a). 76127 therefore begins growth at the end of a cold period and stops growing at the start of another.
2) the water from which 76127 was deposited had previously evolved in the cave with some enrichment of ^{18}O by evaporation. It is therefore impossible to place any interpretation on the results because the ^{18}O - enrichment at both ends may be due to increased evolution rather than climate change.

It is probable that the second interpretation is more correct because the values of $\delta^{13}C_c$ indicate appreciable loss of the lighter isotope by outgassing, although it is not easy to envisage a situation in which evaporation is occurring upstream but not at the site of deposition.

5.10.3 77143

This flowstone came from a high level bedding-plane passage, not found to be draughting, in Giant's Hall, Ingleborough Cave. Of all the English speleothems collected this situation was most likely to give equilibrium deposition conditions. Two growth layers have been analysed for the lower block of this flowstone (77143B). Unfortunately, by an oversight, $\delta^{13}C_c$ was not determined for one layer, but the $\delta^{18}O_c$ analyses generally showed no change with distance along the growth layer. Complete analyses of a second growth layer in the centre of the block are shown in Figure 5.28. Two growth horizons were analysed in the upper block (A) but because of the general absence of growth layers, its rapid growth (from top and bottom ages), and the porous nature of the calcite, a growth axis profile was not determined. The profile for 77143B and modern speleothem $\delta^{18}O_c$ are shown in Figure 5.30, on a time scale determined by three dates given in Appendix 4a. The change in texture from brown, laminated calcite to clear-white calcite (Figure 5.19) is marked by a step of about 0.2‰ in the $\delta^{18}O_c$ profile. The changes in $\delta^{18}O_c$ are roughly paralled by $\delta^{13}C_c$. 76142 also grew over this general period and growth layer analyses (Figure 5.28) show values of $\delta^{18}O_c$ comparable to those in the centre of 77143B.

Interpretation of the profile of 77143B is made difficult by its relation to modern speleothem calcite. If this speleothem

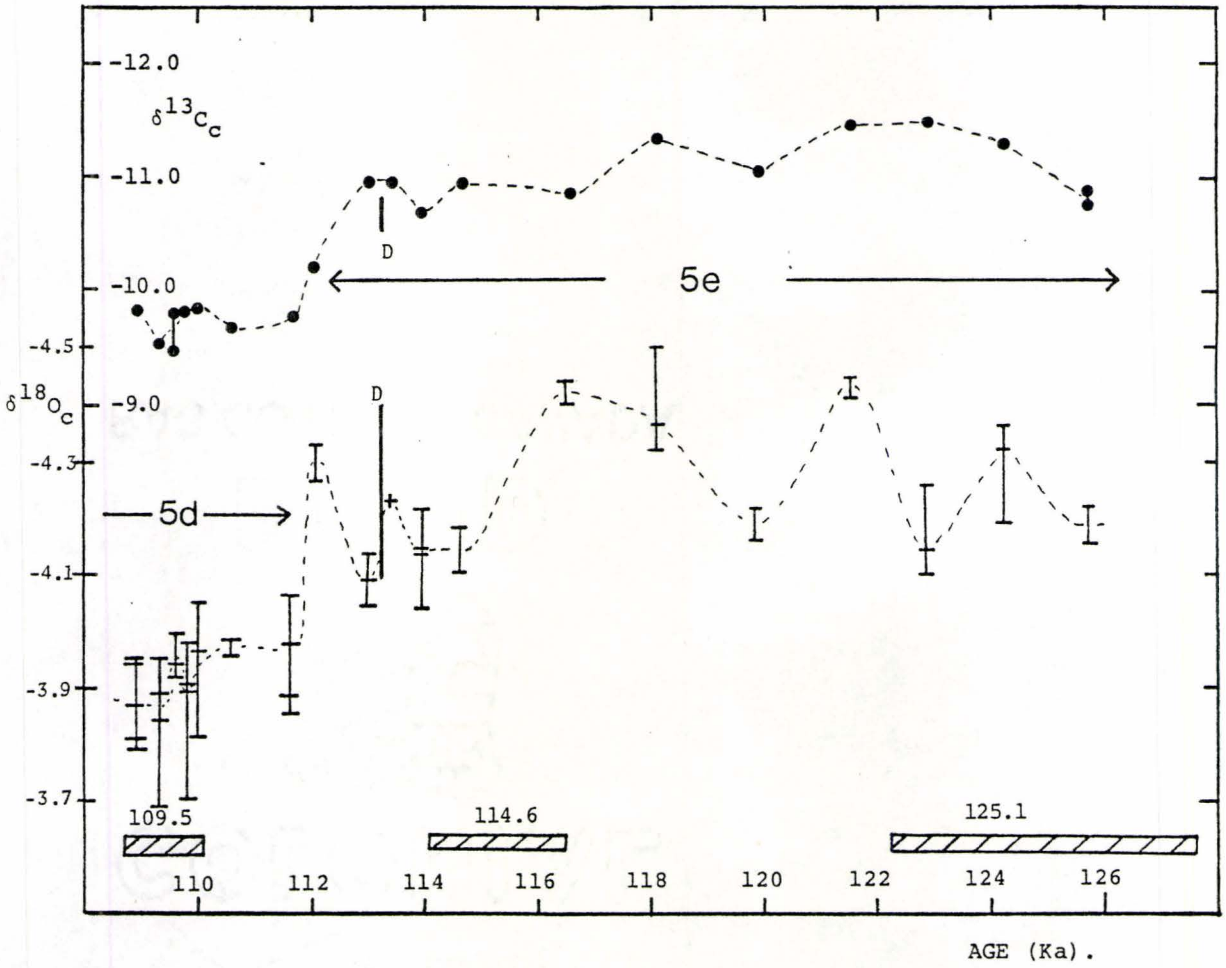

Figure 5.30 Stable isotope profile of flowstone 77143B. Multiple analyses of the same gas sample are connected by vertical lines. The time scale is determined by interpolation assuming constant growth rate between the dated sections shown. $\delta^{18}O_c$ of modern calcite lies at -4.7 to -5.3 ‰. The range of growth layer (D) analyses are shown.

grew from Ipswichian maximum warmth (stage 5e, ~ 125 Ka) towards the warm peak of stage 5c (~ 104 Ka), as the three ages suggest, then the general cooling trend over this period is seen as an increase in $\delta^{18}O_c$ of about 0.5 ‰. This interpetation is comparable to the classical one seen in N.American speleothem (Harmon et al. 1978 a). However at stage 5e the calcite is 0.5 ‰ heavier than modern calcite, a situation incompatible with the concept of the Ipswichian being a warmer period than today, (ie. $\delta^{18}O_c$ values for 77143B should in part, be less than or equal to modern.

An alternative argument might be that, as found in Vancouver Island, $\delta^{18}O_p$ dominates the change in speleothem $\delta^{18}O_c$, therefore explaining why $\delta^{18}O_c$ at about 125 Ka is heavier than modern. However, the record would then appear to indicate that conditions became warmer towards 107 Ka, rather than cooler, as found in most paleoclimate records. Another explanation is that this flowstone is being deposited from an evolved water, one which has seen some evaporation before forming this speleothem. However the values of $\delta^{13}C_c$ are all low and comparable to values expected for equilibrium deposition from a non-evolved water.

These interpretations rely on the assumption that for supposedly comparable temperatures, $\delta^{18}O_p$ at 125 Ka is the same as $\delta^{18}O_p$ today. If it is different, and heavier, then the isotope profile of 77143B indicates a general cooling from 125 Ka to 107 Ka, with peaks and troughs which may correlate to isotope stages 5e and 5d seen in the deep sea core record (Shackleton and Opdyke 1973).

A tentative correlation of the speleothem record with isotope stages is shown in Figure 5.30. If the break in deposition at about 107 Ka is caused by a cold period, as the above interpretation suggests, then it is even more difficult to reconcile the speleothem record (Table 5.3) to that of deep sea cores, which place a maximum warmth (stage 5c) at 104 Ka, as previously described. The depositional hiatus can be interpreted in terms of aridity but only if the speleothem has been deposited from an evolved groundwater (so that $\delta^{18}O_c$ is heavier than modern), or if $\delta^{18}O_p$ dominates the $\delta^{18}O_c$ signal, arguments which have just been rejected.

5.10.4 77151

This flowstone sequence from Victoria Cave has given the longest and most interesting record of all English samples analysed. Its main feature is that it provides a tentative paleoclimate record for the period 290 - 190 Ka, an interval not yet studied in previous speleothem work.

Five growth layers have been analysed in two dimensions for $\delta^{18}O_c$ and $\delta^{13}C_c$ as shown in Figure 5.28. Two of them, B and C, show correlation between $\delta^{18}O_c$ and $\delta^{13}C_c$ indicating kinetic isotope fractionation during deposition, although C shows no trend in $\delta^{18}O_c$ with distance along the growth layer. This indication of non-equilibrium deposition is possibly due to the analysis of calcite which included 'white lines' (desiccation horizons ?) separating clear calcite growth layers. The possibility of varying depositional conditions of isotopic equilibrium and kinetic fractionation may

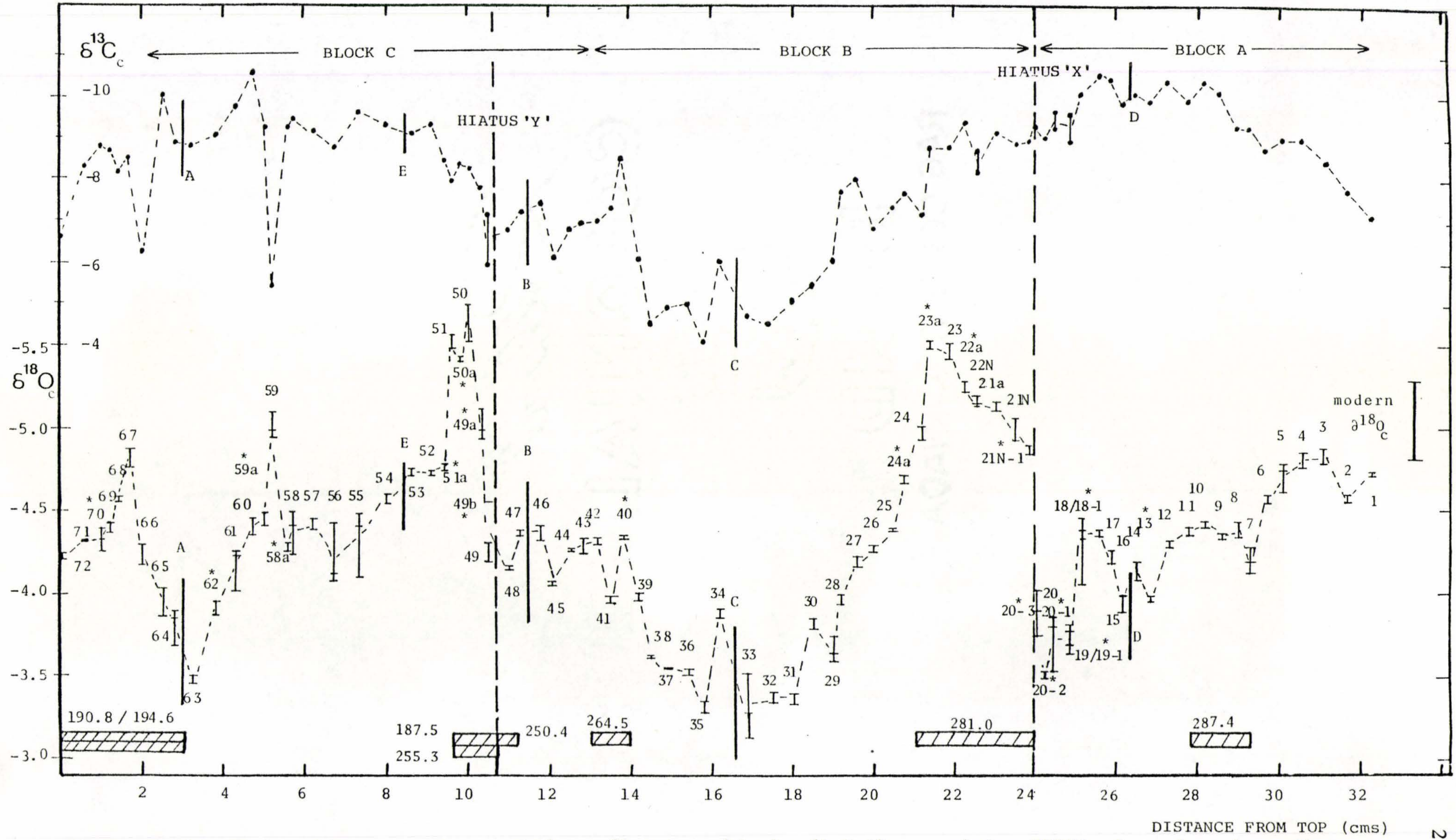

Figure 5.31 Stable isotope analyses of three flowstone blocks (A,B,C) comprising 77151 plotted against distance from top of sample, showing positions of two growth hiatuses (X, Y, see Figure 5.21) and location and $\delta^{18}O_c$ range of growth layer analyses A - E. Sample gas preparations are numbered and multiple analyses of same gas are connected by vertical lines. Asterisks indicate samples analysed at a later date (see text).

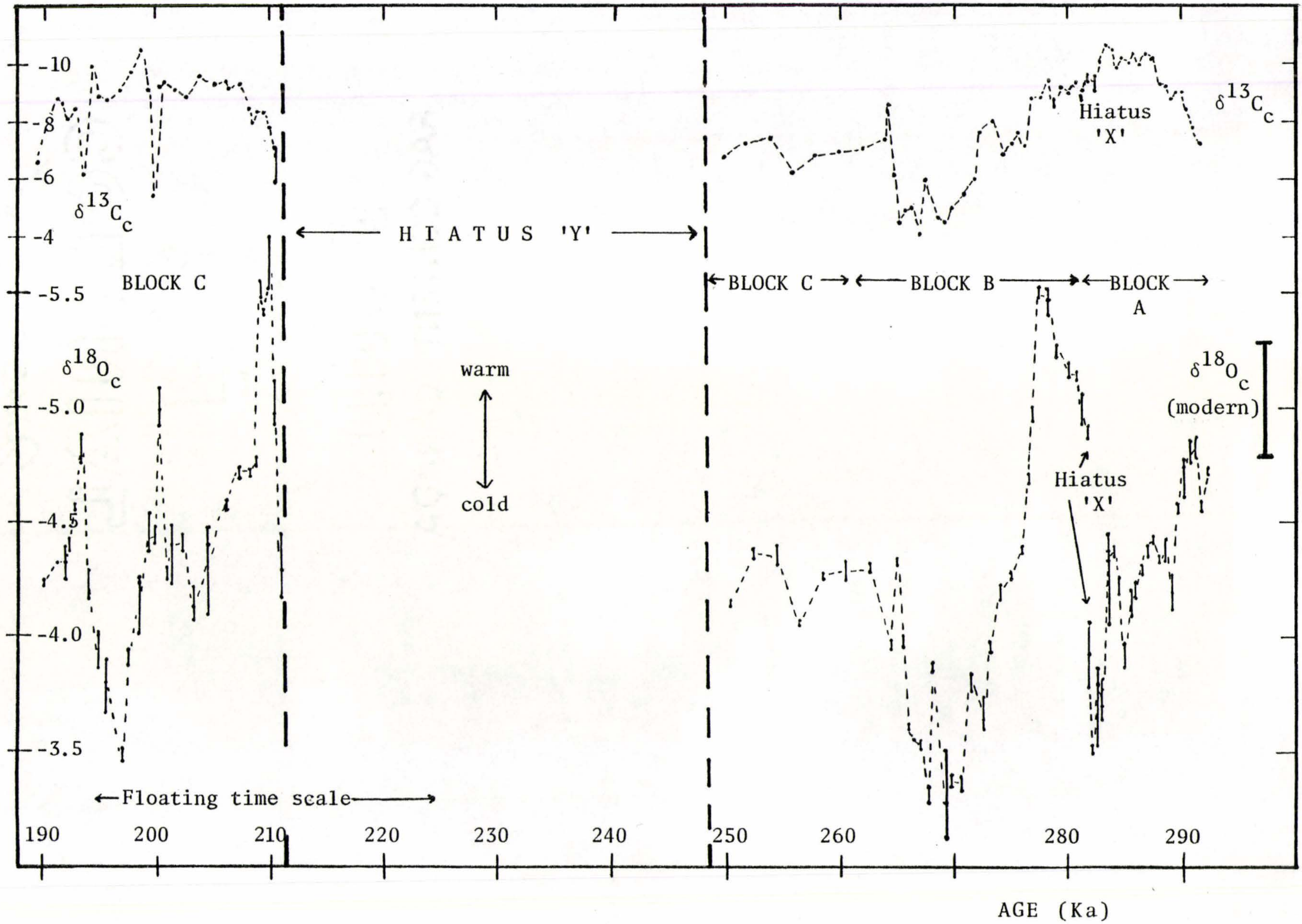

Figure 5.32 Stable isotope profile of 77151. The time scale for blocks A and B is determined assuming constant growth rate between dated sections. The average growth rate for A and B is used to extrapolate the data for block C back from the top ages of 190-195 Ka.

cases the later analyses fit well with their nearest neighbours.

b) 5 sets of growth layer analyses made some time before and during the isotope profile analyses show excellent agreement with the profile.

The following interpretations can be made from the isotope profile of 77151 :

1) The white speleothem surrounding growth layer C may be affected by kinetic isotope fractionation such that values of $\delta^{18}O_c$ are more positive than for equilibrium deposition. This peak is therefore likely to be more subdued than shown in Figure 5.31, 5.32. This reduces the total variation in $\delta^{18}O_c$ for 77151 to about 2‰ .
2) No significant change in $\delta^{18}O_c$ is seen over the sharp colour transition from brown to white calcite in block B between analyses 29 and 30 (Figure 5.21, 5.31).
3) Closely-spaced sampling has shown that most peaks and troughs in the isotope record are real rather than spikes due to analytical error. The spike produced by analysis 59 (Figure 5.31) may not be real as it is not seen in its nearest neighbours. These data indicate the rapidity of change of $\delta^{18}O_c$ and therefore of climate.
4) Most analyses show $\delta^{18}O_c$ of 77151 to be greater than or equal to modern $\delta^{18}O_c$ values, thus suggesting that $\delta^{18}O_c$ is controlled largely by the effect of changes in temperature on α_{c-w} and by changes in $\delta^{18}O_{sw}$.
5) Hiatus X between blocks A and B is marked by a 0.75 ‰ shift in

$\delta^{18}O_c$ whereas that in block C ('Y') has similar values on either side. Both hiatuses occur just prior to intense warm periods.

6) Warm events occurred for short durations of about 5 Ka centred on the ages 278 and ~ 210 ($^{+30}_{-10}$) Ka, temperate conditions existed at about 290, 265 - 250, 200 and 190 Ka, and cold periods (with growth) occurred at about 282, 270 and 195 Ka. Growth was suspended from 250 to about 210 Ka, and for a short period around 280 Ka.
7) $\delta^{13}C_c$ is inversely related to $\delta^{18}O_c$ for the period 295 - 285 Ka but directly related to it during 275 - 265 Ka. At other times there is no obvious correlation. The direct relationship could be due to the observed non-equilibrium deposition seen in growth layer C at this time. Whereas abrupt shifts are seen in the $\delta^{18}O_c$ curve no corresponding breaks are seen in $\delta^{13}C_c$.

5.10.4.1 Discussion

5.10.4.1.1 Factors Affecting Variation of $\delta^{18}O_c$

Evans et al. (1978) have shown that the temperature dependence of $\delta^{18}O_p$ for maritime Europe is as low as 0.22 - 0.23‰ /°C (see Table 3.2). If applicable to this part of England, this dependence almost exactly offsets the temperature effect on α_{c-w} (0.22 - 0.24‰ /°C). Therefore the observed change in $\delta^{18}O_c$ (2‰) should be due only to changes in $\delta^{18}O_p$ caused by the continental ice volume effect on $\delta^{18}O_{sw}$. However the maximum variation of $\delta^{18}O_{sw}$ from glacial to interglacial stages is only about 1.8‰, of which only part would be seen by 77151 because growth of speleothem was probably interrupted during the coldest parts of glacial periods. The following explanations could account for this discrepancy :

1) the temperature dependence of $\delta^{18}O_p$ was less than 0.22 ‰/°C most of the time, varying somewhat with change in climate.
2) a change in storm track from interglacial to glacial conditions (eg. from westerly winds as at present to winds of polar or continental origin during glacials) would cause a decrease in $d\delta^{18}O$ - /dT over and above that due to temperature dependence. (It should be noted that the value of Evans et al. is determined only from seasonal changes for present climatic conditions).
3) all peaks of $\delta^{18}O_c$ may be enhanced by evaporation during deposition (ie. kinetic isotope fractionation) or evolution of the water during colder periods, as previously described.

It is probable that the first two explanations are more realistic than that of evaporation of the groundwater because of the continuous nature of the isotope record (evaporation would tend to be a sporadic process giving more discontinuity to the isotope record than is in fact observed).

5.10.4.1.2 Significance for Quaternary Chronology

The oxygen isotope profile of 77151 is compared to a composite deep sea core for the same time period in Figure 5.33. The core record has been synthesized from three overlapping cores from the eastern Pacific Ocean : V19-28, V19-29 and V19-30 as shown in Figure 5.33 using data from Ninkovitch and Shackleton (1975), Shackleton (1977) and Shackleton (pers. comm. 1979). Cores V19-29, -30 have almost identical average sedimentation rates (~ 5.6cm/Ka, Ninkovitch and

Figure 5.33 Correlation of speleothem (77151) $\delta^{18}O_c$ curve (upper) with composite deep sea core record (lower) for isotope stages 7 to 10 inclusive. The core record is a composite of V19-29 stages 7-9b, (Ninkovitch and Shackleton 1975) and V19-30 stages 9c-10 (unpublished data, Shackleton pers.comm.1979); they are linked as shown. The continuation into stage 10 is interpolated from core V19-28 (Ninkovitch and Shackleton 1975). The speleothem time scale is as shown in Figure 5.32. The core record is fitted to the speleothem time scale assuming constant sedimentation rate and co-incidence of 9e isotope peaks. Stippled areas indicate warm substages and cross areas indicate cold substages.

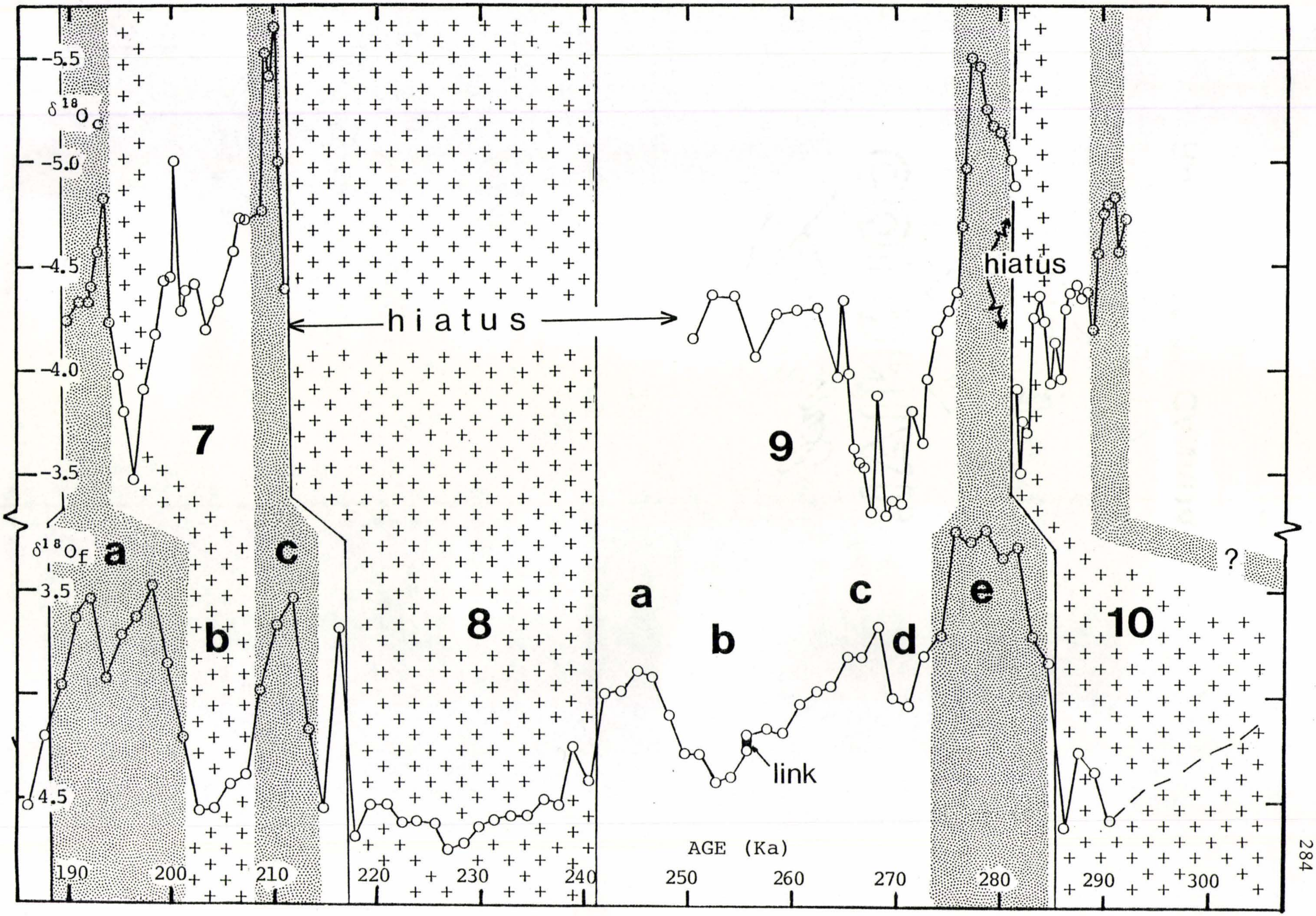
-5.5
-5.0
-4.5
-4.0
-3.5
$\delta^{18}O_c$
$\delta^{18}O_f$
3.5
4.5
7
8
9
10
a
b
c
a
b
c
d
e
hiatus
hiatus
link
?
AGE (Ka)
190
200
210
220
230
240
250
260
270
280
290
300

Shackleton 1975), and V19-28 a lower rate (3.8cm/Ka). The base of V19-29 and a portion of V19-30 are linked as shown in Figure 5.33 by a horizon of similar $\delta^{18}O_f$ and approximately comparable age. V19-28 is used to supplement the record beyond the available analyses of V19-30. Although these cores lie a considerable distance from the region studied here they have previously been shown to best represent changes in oxygen isotope content of the oceans during the Pleistocene (Ninkovitch and Shackleton 1975, Shackleton 1977) and are least affected by bioturbation, calcite re-solution etc. Furthermore they all contain a common dated ash layer 'L' and horizons showing the coccolith minimum 5 and extinction of radiolarian Stylatractus universus, both of which have been dated by other methods. However, comparison of these age determinations and that obtained by assumption of constant sedimentation rate using isotope sub-stage 5e (125 Ka) as a dated horizon, show that there has been some variation in sedimentation rate over the last 250 Ka. Shackleton (pers. comm.,1979) has confirmed this.

A time scale has therefore been fitted to the composite curve by relating the prominent warm peak at about 280 Ka in the speleothem record to isotope sub-stage 9e in the core record and assuming constant sedimentation rate in the core from there to the end of stage 7. The resulting curve is shown in the lower part of Figure 5.33 together with isotope stages and sub-stages (after Emiliani 1955, and Shackleton and Opdyke 1973). The speleothem record is reproduced from Figure 5.32.

An attempt to correlate warm (stippled) and cold (crosses) events in the two records (Figure 5.33) suggests the following :

1) immediately below sub-stage 9e there is a growth hiatus (X) which

may correspond to glacial stage 10. The flowstone below shows progressive cooling from the base towards this hiatus which may represent the deterioration of climate from stages 11 to 10. The speleothem presumably began to grow sometime after the climatic maximum of stage 11.

2) sub-stage 9e is short (~ 5 Ka) and represents climatic conditions comparable to the present. The core record indicates a slightly longer duration of warm climate for 9e.
3) sub-stages 9d and 9c can be seen in the speleothem record although 9d (cool) is probably over-represented due to kinetic isotope effects as described above. 9c is seen as a period of slow growth probably terminating at the start of the colder sub-stage 9b.
4) the hiatus in the upper part of the flowstone (Y) probably corresponds to sub-stages 9b and 9a, and all of stage 8. Isotopic data from several cores (V19-28,-29, Ninkovitch and Shackleton 1975; P6408-9, Emiliani 1978) suggest that stage 8 is of intensity similar to the Early Devensian (stage 4). It has already been concluded from other speleothem evidence that the Early Devensian in Britain was one of cold, tundra-like conditions but with no extensive ice development. If these conditions are also characteristic of stage 8 then this would account for the absence of erosional features or thick detrital layers in this hiatus, (Figure 5.21).
5) speleothem growth resumed at the beginning of stage 7 and climate rapidly ameliorated (within 1 Ka) to a short period of warm conditions comparable to today (sub-stage 7c). In the core record, 7c is apparently of much longer duration (> 10 Ka) and may be broken by a

cold spell, although both the early warming and cold spell are 'one-point' peaks and may be in error.

6) the prominent cooling which is characteristic of stage 7 (sub-stage 7b, Shackleton 1977) is clearly seen in the speleothem record, but at a younger age. This time shift (~ 10 Ka) may be due to more rapid speleothem growth during 7c or variations in core sedimentation rate. A warming event corresponding to stage 7a is seen in the speleothem record just before growth is terminated.

The whole of the above correlation rests on the assumption that the pronounced warm event in the speleothem record is the thermal maximum of sub-stage 9e. Shackleton and Opdyke (1973) have argued that stage 9, and not stage 7, is correlated to the Hoxnian interglacial in Britain because it more closely approaches the minimum $\delta^{18}O_f$ values seen in sub-stage 5e (the Ipswichian). In this present study 7c is seen to be slightly warmer than 9e but of very short duration (~ 2 Ka). This peak would not be seen in the deep sea core record because of the effect of bioturbation etc. (Shackleton 1977).

Shotton et al. (1977) have shown from vegetation and faunal distributions that the Hoxnian was somewhat cooler than the Ipswichian in Britain. Speleothem age distributions and the isotopic evidence from 77151 indicate a period of speleothem growth in conditions slightly cooler than present. These results suggest that it may be incorrect to assign the Hoxnian to stage 9, and that stage 7 best represents the Hoxnian as it is described by floral and faunal evidence. This correlation however, suggests that stage 8 corresponds to the Lowestoft Stadial of the Anglian glaciation - a period when ice covered Britain farther south than the limits reached in Late Devensian times. The absence of erosional features or detritus in hiatus Y of 77151, and the deep sea core isotopic data, suggest that stage 8 cannot represent full glacial conditions in N.England and can therefore not be correlated with either stadial of the Anglian. Alternatively glaciation in Britain may have been more intense than in other regions of the northern hemisphere and so contribute little to the intensity of stage 8 in the core record. The lack of a pronounced speleothem hiatus may simply indicate that the cave was well-sealed from the effect of glaciation. This is indicated by the excellent preservation of the dated mud deposits in the entrance passage. A tentative correlation between speleothem and deep sea core data, and the British Quaternary record is given in Table 5.6, assuming that hiatus Y is correlated to stage 8, and in turn to the Late Anglian period. Comparison of this record to that of 76127 (which indicates a mild period from 240 - 225 Ka, Figure 5.29) shows that the stratigraphic significance of stage 8 is still in some doubt. If the lower boundary of stage 8 is moved forward to 225 Ka, then the whole of the 76127 record correlates to sub-stage 9a (missing from the 77151 record) and stage 8 occurred during 225 - 210 Ka.

It may be possible to resolve the above problems by more detailed analysis of the other deposits in Victoria Cave which have grown over this period.

^{230}Th/^{234}U age (Ka)	Isotopic stage and substage		British Quaternary stage and substage		Climate *
140 170	6	-	WOLSTONIAN		glacial
190-195		a			mild-warm
195-200	7	b	HOXNIAN		cool
~ 210		c			warm
210-220 230-240	8	-	ANGLIAN	Lowestoft Stadial	arctic-glacial
~ 240	9	a		Corton Interstadial	cold
	9	b		Cromer Stadial	cold-arctic
--- 250					
	9	c	CROMERIAN ?	?	mild
--- 270				?	
	9	d		?	cool
--- 275				?	
	9	e		?	warm
— 280					
	10 ?	-			arctic-glacial ?
—> 285					
	11 ?	?	?		mild ?

* the terms used to define climate are based on stable isotope signal of both deep sea cores and speleothem and on presence or absence of speleothem growth as described below:

arctic - generally non-glacial but with presence of perma-frost and tundra
cold - mean annual temperatures about zero because speleothem growth did not occur
cool - mean annual temperatures were > 0 because speleothem growth did not cease
mild - climate somewhat cooler than present
warm - climate comparable to today

Table 5.6 Proposed correlation of British Quaternary events to the stable isotope record of speleothem 77151 and the deep sea core ice volume curve. Radiometric ages are determined from speleothem only.

5.11 Conclusions

Stable isotope analysis of speleothem 77151 has shown remarkable agreement with the deep sea record. Two warm periods (comparable to present conditions) have been recognised and can be correlated to isotope stages 7c and 9e. A correlation between the speleothem record and early British Quaternary stages has been proposed but because of the weaknesses of the stratigraphic record from the Midlands and East Anglia (ie. absence of radiometric ages, limited stratigraphic sections etc.) this correlation is clearly most tentative.

The speleothem record clearly demonstrates the short duration of warm periods in the past : a total of 6 Ka, over a 100 Ka period, was as warm as today. The distribution of speleothem ages has clearly shown the timing and duration of the last two glaciations, the Late Devensian and the Wolstonian. Chronological details of the latter event have been poorly known in England until now. Other than the stable isotope profile for 77143, evidence for the pronounced warmth of the Ipswichian is not seen in speleothem abundance data, and there is some indication that there may be a sudden cooling event at about 105 Ka, not previously indicated by other paleoclimate indices.

More stable isotope profiles, coupled with fluid inclusion analyses, of speleothem (from Victoria Cave in particular) should allow a better correlation to the deep sea core record and permit determination of short-period changes in climate which cannot be seen in the core record. In this way, the study of speleothem deposits should provide a much-needed, independent calibration of events in the Middle to Early Pleistocene of the British Quaternary.

CHAPTER 6

DATING OF SPELEOTHEM FROM THE BAHAMA BLUE HOLES

Introduction

The Bahama blue holes have been known since mediæval times when the first explorers visited the area. Many of the blue holes lie in shallow water off the eastern edge of Andros Island (the largest of the Bahama group) and adjacent to the deep 'Tongue of the Ocean' (Figure 6.1). Regarded with superstitious fear by the island natives, they remained unexplored until about twenty years ago. Their similarity to cave and pothole systems found in continental regions today has led scientists to postulate a freshwater origin, with solutional enlargement during times of lower sea level. Ice accumulation on the continents during glacial periods could cause such a lowering and this in turn would leave much of the Bahama limestone platform exposed to subaerial erosion, so permitting development of an integrated underground drainage system. Proof of this origin has only become available during the last decade, with the finding of freshwater speleothems at depth, in passageways leading off from the bottom of one blue hole.

In this chapter, results are presented of an attempt to verify the relation between blue hole formation and glacial events, by radiometric dating of the speleothem calcite which is preserved in the core

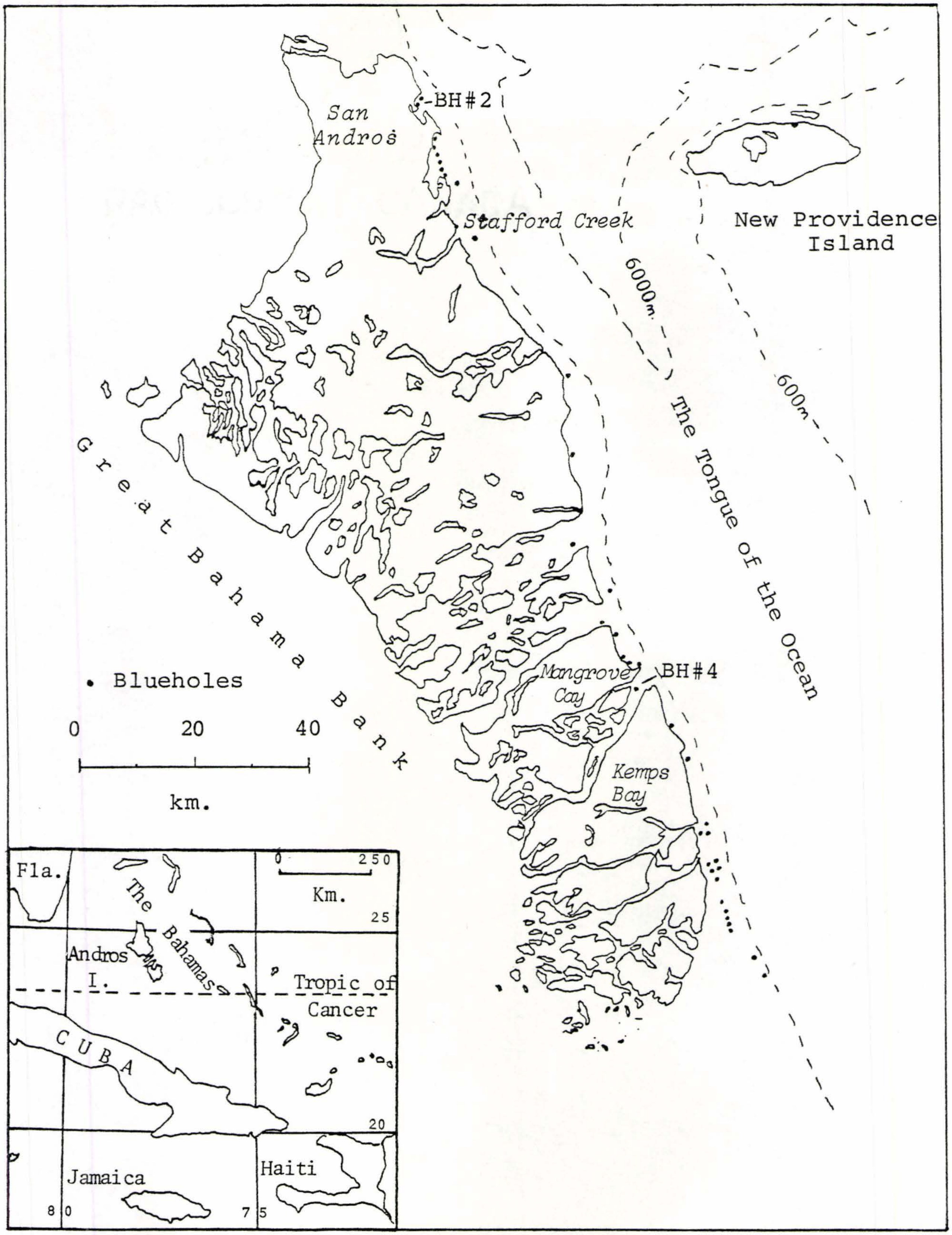

Figure 6.1 Map showing location of Andros Island and blue hole sites (after Benjamin 1970).

of the recovered specimens. A brief review of Pleistocene sea level evidence is given first, followed by description of the area, its geological history and previous speleothem work.

6.1 Pleistocene Sea Level Changes

The Pleistocene epoch is characterised by world-wide changes in sea level due to variations in the size of continental ice sheets. Fossil reef terraces found on tropical coastlines today are evidence of high sea stands which occurred at warm intervals in the past. For these deposits to lie above sea level today requires either platform emergence due to tectonic activity or higher eustatic sea level due to warmer conditions than at present.

In tectonically-active areas such as the island of Barbados (Mesolella et al. 1969) and the Huon Peninsula of New Guinea (Bloom et al. 1974), an excellent record of glacio-eustatic fluctuations is preserved in the form of tiered reef terraces, the oldest generally being at the highest elevations. Islands known to be tectonically stable or slowly subsiding, such as Oahu, Hawaii (Ku et al. 1974), the Bahamas and the Florida Keys (Broecker and Thurber 1965) only show deposits 5 to 10m above present sea level. Ages of these fossil terraces have generally been determined by ^{230}Th/^{234}U dating of corals and the results of dating a number of static and uplifted sites are summarized in Figure 6.2.

The extent and timing of low sea levels cannot be as readily determined because any coral growths associated with a low sea stand are at present submerged. However, by assuming constant uplift rates

Location	^{230}Th/^{234}U Ages (Ka) (+ *relative elevation* -)							Reference
1) <u>Stable or slowly-subsiding sites</u>								
Oahu, Hawaii.					122$^{(+7.6)}$			Ku et al. (1974)
Bahamas					127			Broecker and van Donk (1970)
Bahamas					115 - 130 $^{(+7.8)}$			Neumann and Moore (1975)
Bermuda					124 $^{(+5)}$			Harmon et al. (1978b)
Florida Keys				90	- 140			Broecker and Thurber (1965)
2) <u>Uplifted Sites</u>								
Barbados (1m/Ka)		61 *(-20)*	82 *(-13)*	105 *(-15)*	125	180 - 220	280 - 320	Mesolella et al. (1969) Bender et al. (1979)
Ryukyu Islands (1-2m/Ka)	42 *(-40)*	67						Konishi et al. (1970)
New Guinea (1-2.5m/Ka)	41 *(-38)*	61 *(-28)*	85	107	118 - 142	180 - 190		Bloom et al. (1974)
Loyalty Islands, S.W. Pacific (0.15m/Ka)					117 $^{(+7.5)}$	175 - 190		Marshall and Launay (1978)

Figure 6.2 Summary of radiometric age determinations of Pleistocene reefs and calculated sea level for stable and uplifted sites.

for tectonically-active islands, the amount of sea level change between dated high stands can be determined. Estimates of sea level minima of between -130 and -160m have come from continental shelf terraces of eastern N.America (Heezen et al. 1959), the presence of littoral shells in cores taken off New Jersey and Argentina (Donn et al. 1962), sediment thickness in the Mississippi delta (Fisk and McFarlan 1955) and a submarine delta surface off the Huon Peninsula, New Guinea (Chappell 1974). Variations in the oxygen isotopic composition of deep sea cores is now considered to be primarily a record of changes in oceanic isotopic composition, and this in turn, may be transformed into a record of eustatic sea level for the Late Pleistocene (Shackleton and Opdyke 1973). From these data, a maximum lowering of sea level of between 120 and 150m is indicated for the last 200,000 years.

6.2 Area Description and Geological History

The Bahama platform is one of the largest regions of modern, shallow-water carbonate deposition in the world. It has an area of about 0.3 x 10^6 km^2 and lies up to 12m below the sea surface except for a number of islands which extend to 30m a.s.l. Four deep troughs enter the platform from the ocean side (Figure 6.1) : Grand Bahama Island in the north is separated from the Great Bahama Bank by the Providence Channels, and the Tongue of the Ocean and Exuma Sound penetrate deep into the Great Bahama Bank. These troughs are characterised by near-vertical walls for the first 1000m of depth, followed by shallower gradients to a flat-bottomed floor at 1000 - 3600m depth, depending on location (Newell 1955, Lynts et al. 1973).

Bahamian islands occupy about 7% of the total area of the platform and are generally aligned in a NNW-SSE direction suggesting either tectonic control in their formation or orientation due to prevailing wind and wave action. Near sea level they are underlain by pure oölitic limestones of Pleistocene age but at higher elevations they are covered by well-cemented aeolianites. The shallow-water carbonates of the platform margins comprise an outer barrier rim of oölite on which is built a series of barrier reefs. The central platform contains oölite sand and fæcal pellets in agitated regions, and carbonate ooze in quieter, lagoonal areas.

Two deep drillings on the platform have so far been made. The first, in 1947 at Stafford Creek on Andros Island, penetrated 4446m of wholly carbonate sediments, ending in Lower Cretaceous dolomites and limestones (Goodell and Garman 1969). The second, on the Cay Sal Bank in 1958, encountered carbonates and minor anhydrite to -5600m (Dietz et al.1970). The lack of any large gravity anomalies in the region suggests that this thickness is uniform over all of the platform (Talwani et al. 1960).

The enormous thickness of continuous carbonate sediments shows that the Bahamian platform has been in essentially the same environment over the last 130 million years or more, where slow subsidence keeps pace with carbonate accumulation. Because of the unique morphological and geological character of the platform, much attention has been focussed on its origin and development. Current theory suggests that the platform originated as a small enclosed ocean basin during rifting in the Triassic (Dietz et al. 1970). With further continental drift, the basin infilled with sediments and began to develop outwards and upwards by carbonate accretion directly on top of oceanic crust. It was subsequently carried along as a marginal plateau attached to the North American plate.

The origin of the deep troughs penetrating the platform is more difficult to determine and numerous suggestions have been put forward. These include deepening of the troughs by erosion from current action, steepening of the trough walls by vertical reef growth, and tectonic activity during the Cretaceous, imprinting an early relief which subsequently developed by channel erosion and platform construction (Lynts et al. 1973).

6.3 Platform Submergence Rate

In order to distinguish eustatic sea level changes from changes in elevation of the Bahama Bank, the relative movement of the region due to subsidence, uplift etc., must first be determined. This can be done in two ways; either from the logged depth of stratigraphic units in wells drilled into the bank or by estimation of modern rates of subsidence and sediment accumulation.

Data from the deep well on Andros Island permit correlation of depth with geological age as determined from examination and classification of microfossils in the recovered core (Spencer 1967). Depth versus age are plotted in Figure 6.3. The dashed line is drawn by eye through points that are more clearly defined by Spencer in terms of age, although it is possible that a period of more rapid accumulation

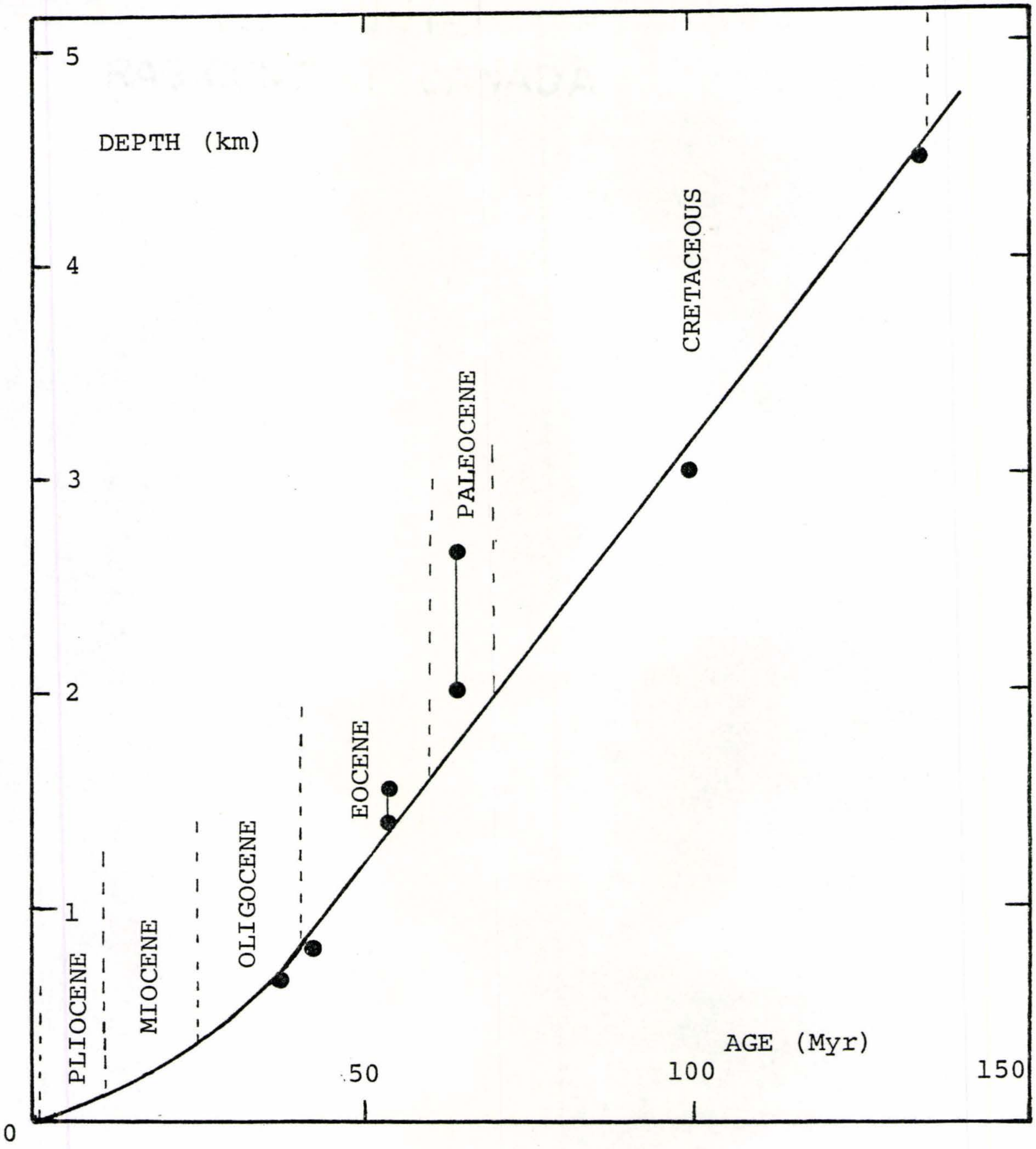

Figure 6.3 Geological age - depth relationship from borehole sediments at Stafford Creek, Andros Island, (data from Spencer1967).

could have occurred during the Paleocene. Two subsidence rates can be calculated :

1) for the Lower Cretaceous to Oligocene periods, an accumulation of 3840m gives a subsidence rate of 0.375m per 10,000 years.
2) for the Oligocene to present periods, an accumulation of 671m gives a rate of 0.18m per 10,000 years.

The difference in rates may be due to periods of subaerial exposure and weathering during the Pleistocene and earlier. This is supported by the fact that much of the limestone and dolomite in the upper section of the well was found to be cavernous, probably due to invasion by circulating freshwater.

The rates determined above are low in comparison to the average rate of sediment accumulation over the Bahama Banks during recent time. Broecker and Takahashi (1966) calculated an average of 1.5m of carbonate mud deposited in 5,000 yrs (3.0m/10,000 yrs) and even low accumulation areas such as the central part of the Tongue of the Ocean (1.0 - 1.2m/ 10,000 yrs, Lynts et al. 1973) show higher values than those above. Unless depositional rates have changed drastically in recent time, it must be assumed that the difference is due to compaction, de-watering, dolomitization and dissolution processes after burial.

6.4 The Blue Holes

Blue holes are thought to be evidence of sea level lowering during Pleistocene glaciations because of their similarity to continental cave and pothole systems found in limestone areas today. Recently a blue hole 40km off the Florida coast was found to be over

145m deep (Kohout et al. 1975) but whether this represents a completely freshwater-formed system or one that penetrated beneath the water table and entered a zone of sea water intrusion has not been determined (ie. the amount of sea level lowering may be substantiallly less than the depth of the hole). Figure 6.4 illustrates the effect of Pleistocene sea level changes on the development of blue holes.

Exploration of the blue holes has only taken place in the last twenty years with the advent of scuba diving. Dr. George Benjamin of Toronto is the best known of blue hole explorers (Benjamin 1970) and has explored and mapped over 60 Bahamian blue holes, and aerially located over one hundred more (Figure 6.1). In addition, his observations of tidal currents through them has given some insight into their structure and length. He has observed that more water discharged from some blue holes than was sucked back into them during the tidal cycle. He suggests that the presence of open tunnels in the face of the vertical wall overlooking the Tongue of the Ocean may allow cold sea water to enter, warm up and emerge through the blue hole, in addition to the tidal flux of water (Figure 6.4).

Conclusive proof of the subaerial origin of Bahamian blue holes was obtained in 1970 when Dr. Benjamin and his son discovered an underwater cavern containing stalagmite columns, some up to 6m long (Figure 6.5) at a depth of about 45m, in blue hole '#4' off Andros Island (Figure 6.1, McKenney 1972). In this system over 2km of passageway was discovered, containing three pits leading down to over 100m depth.

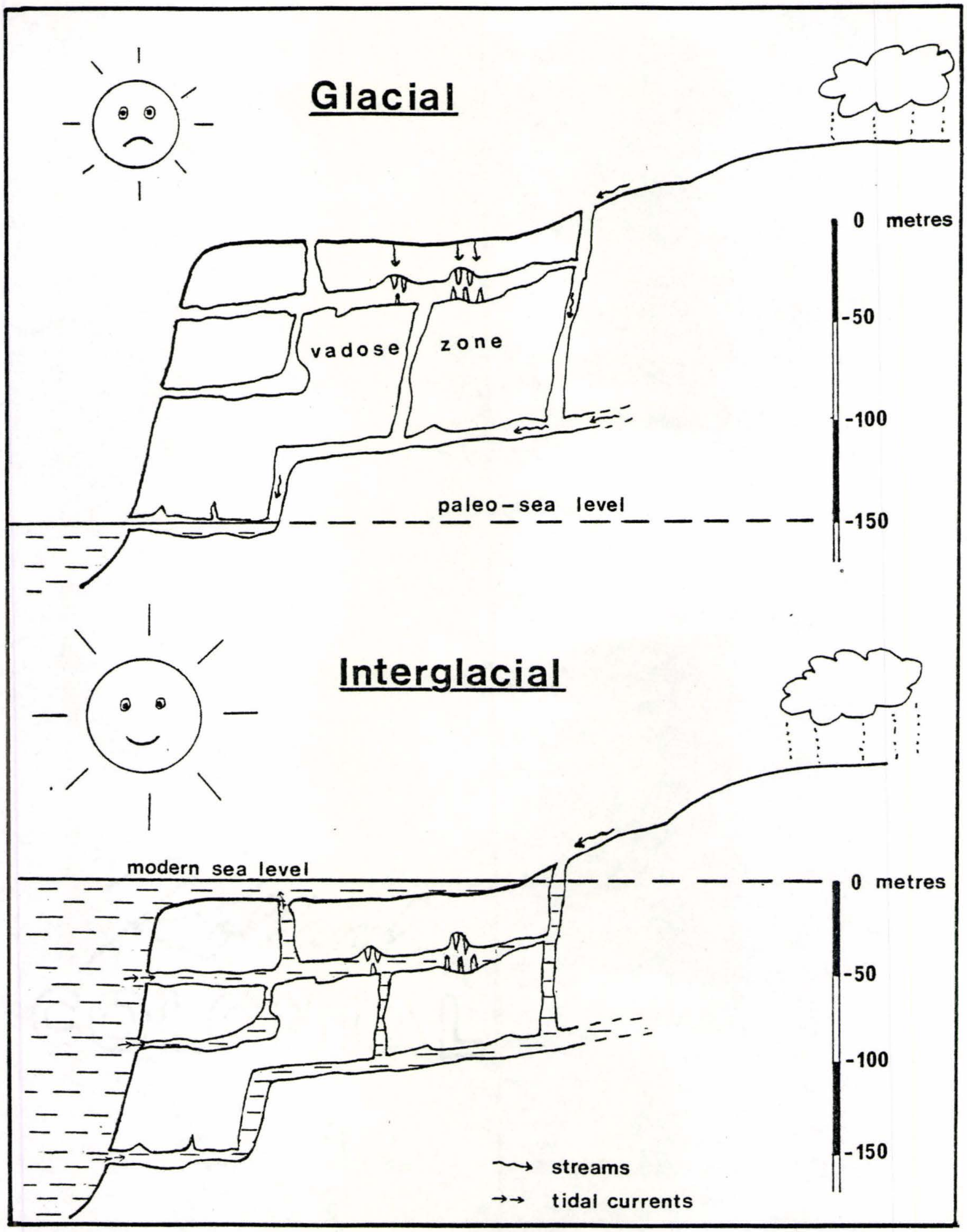

Figure 6.4 Schematic representation of blue hole development in relation to Pleistocene sea level changes.

Figure 6.5 Stalagmite columns found in blue hole '#4', Andros Island,(from a photograph by Dr.G.J.Benjamin in McKenny 1972).

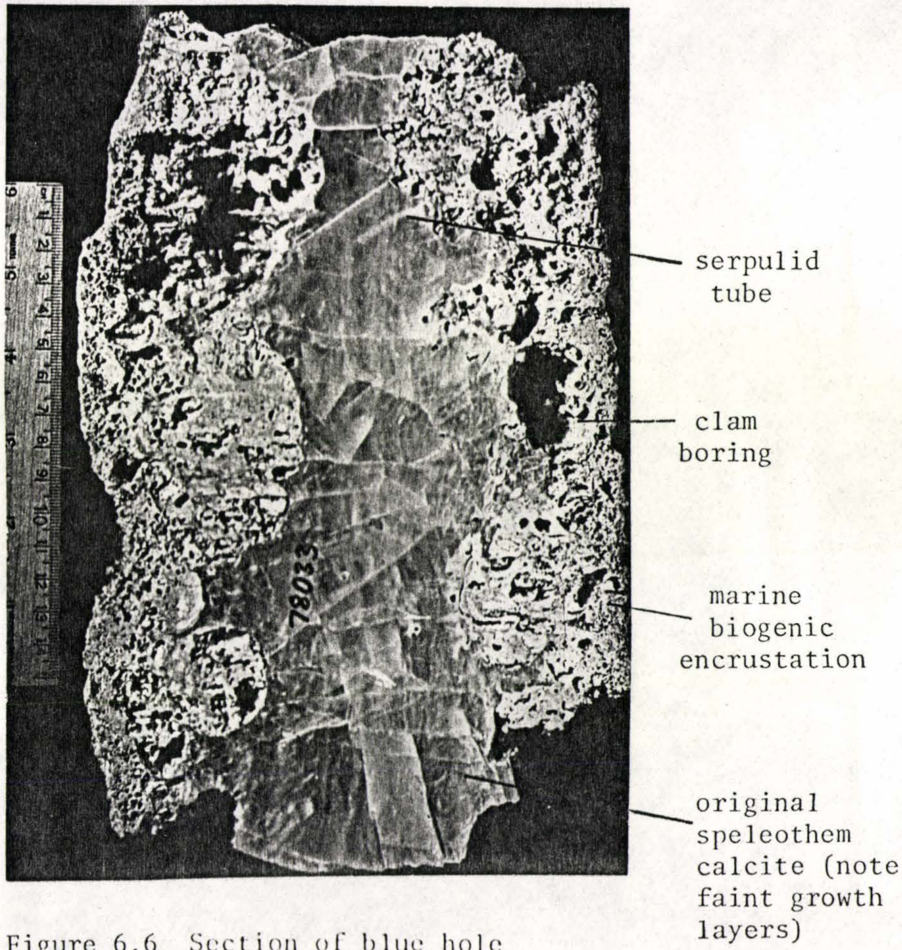

Figure 6.6 Section of blue hole speleothem 78033,showing marine encrustation and borings into speleothem calcite.

6.5 Previous Speleothem Work

Spalding and Matthews (1972) were first to date a submerged speleothem by analysing a stalagmite collected at -12m from a submerged cave on Grand Bahama Island. Ages of 21.9 Ka (^{14}C) and 22.0 Ka ($^{230}Th/^{234}U$) for the same portion were in good agreement although the authors did not indicate whether correction for 'dead' carbon was made for the ^{14}C age. These ages correlated well with estimates of the age of the Late Wisconsin glacial maximum. Harmon et al. (1978b) have dated six in situ speleothems recovered from depths of -11 to -5.7m in Crystal Cave, Bermuda. The results suggest periods of emergence of 195 - 150 Ka, 120 - 100 Ka and 40 - < 10 Ka.

Previous work on submerged speleothem deposits is limited to samples recovered from a maximum of -12m below modern sea level. This depth represents less than 10% of maximum estimated sea level lowering during the Late Pleistocene and therefore may not correspond to maximum glacial periods or even interstadials.

On a recent dive Dr. Benjamin recovered 5 pieces of previously broken stalagmite from blue hole #4 and these have formed the basis of the work described in this chapter. One other sample collected at approximately 10m depth (BH #2, Figure 6.1) has also been analysed.

6.6 Description of Samples

The samples from blue hole #4 (BH, 76015, 76016, 78032, 78033) all form portions of 3 stalagmite columns typified by those shown in Figure 6.5. Their exact stratigraphic relationship (ie. top vs. base and relation to one another) is not known because all were broken off before finding. All however, possess the same general characteristics and can be treated as one for this description.

The stalagmite sections measure between 15 - 25cm long and 12 - 15cm in diameter. Each contains a central core of original calcite whose thickness varies from 10cm to 0cm in intensely eroded portions. The earliest samples received (BH, 76015, 76016) contain no obvious growth layers in the calcite core (Figure 6.6) but distinct layering was subsequently found in the two larger samples (78032, 78033). The calcite core of all the samples appears to be homo-axial (single crystal). The growth layering still preserved in 78032 and 78033 suggests that the speleothems were not recrystallized to this habit but were originally formed as such.

The outer parts of the stalagmites have been intensely bio-eroded into a thick crust of calcite and aragonite (in approximately 1:1 proportions from X-ray diffraction analysis). The crust is mainly micritic (Figure 6.6), but several boring and encrusting organisms can be recognised, including boring clams, serpulids and other polychaetes, bryozoa and fungal filaments (Dr.D.Kobluk, pers.comm.). In the smaller samples, the calcite core is penetrated by many polychaete borings, and the holes contain small but significant quantities of aragonitic micrite.

Sample 76017, from BH #2 is 20cm long and 6cm in diameter at the base. This sample shows very little bio-erosion and the inner calcite is largely free from borings. It also appears to be composed of a single crystal of calcite.

6.7 Results

6.7.1 Initial Work

Samples of the calcite core were chipped out by pneumatic drill and analysed according to the procedure in Appendix 1a. Nine samples of the three speleothems BH, 76015, 76016, showed ages ranging between 162 Ka and 96 Ka (Table 6.1). The lack of stratigraphic ordering of ages for the samples was subsequently thought to be due to incorporation of minor amounts of aragonitic deposits present in the worm tubes that pass through the calcite. In support of this, pieces of the outer crust (76015-7, Table 6.1) were dated and found to be much younger than the core. They were also significantly higher in uranium concentration and had a $(^{234}U/^{238}U)_o$ ratio comparable to seawater. Figure 6.7 indicates a correlation between age, U concentration and isotopic ratio, as might be expected for admixtures of the two end members : pure speleothem calcite and marine deposits.

6.7.2 Leaching Experiments

In an attempt to remove interference due to biogenic infillings, a three-phase leaching experiment was devised using a portion of crushed calcite core (76016-5) in the hope that the softer aragonitic deposits would preferentially dissolve in the initial acid-leach fractions, leaving essentially pure calcite in the last fraction. Each fraction was spiked and dated as usual. The results in Table 6.2a show a progression towards greater ages (maximum 157 Ka), although U concentrations and $(^{234}U/^{238}U)_o$ ratios do not reflect the same trend. U concentrations in

Analysis No.	Location	U (ppm)	Yields (%) U	Yields (%) Th	$\frac{^{234}U}{^{238}U}$	$\left[\frac{^{234}U}{^{238}U}\right]_o$	$\frac{^{230}Th}{^{232}Th}$	$\frac{^{230}Th}{^{234}U}$	AGE (Ka) $\pm 1\sigma$
BH-M	centre portion	0.26	57	13	0.943	0.910	49	0.765	161.6 $^{+23.2}_{-19.0}$
BH-L	lower portion	0.35	78	35	0.987	0.981	54	0.691	127.8 $^{+9.2}_{-8.5}$
76015-3	top of upper (?) block	0.32	45	28	1.019	1.026	26	0.618	104.1 $^{+10.6}_{-9.7}$
76015-1a	replicates of base of upper (?) block	0.29	33	20	0.993	0.990	155	0.678	123.1 $^{+9.5}_{-8.7}$
-1b		0.28	26	14	1.016	1.023	61	0.666	118.5 $^{+9.7}_{-8.9}$
76016-3	top of lower (?) block	0.28	34	15	1.019	1.025	> 1000	0.608	101.1 $^{+7.7}_{-7.2}$
76016-4	middle of lower (?) block	0.31	8	27	1.031	1.040	81	0.591	96.5 $^{+7.0}_{-6.6}$
76016-1a	replicates of base of lower (?) block	0.26	33	8	1.028	1.040	70	0.698	128.8 $^{+12.2}_{-10.9}$
-1b		-	-	-	1.031	1.044	96	-	122.3 $^{+38.4}_{-27.3}$
76015-7	outer aragonitic deposits	1.30	18	5	1.143	1.148	> 1000	0.098	11.1 ± 1.1
76017-1a	basal 4 cm	0.11	44	19	1.000	1.000	11.1	0.350	46.7 $^{+5.1}_{-4.9}$
-1b	replicate of -1a	0.11	30	27	1.022	1.025	120	0.379	51.6 $^{+5.3}_{-5.0}$
-2	top 3cm	0.17	43	34	0.999	0.999	> 1000	0.386	53.0 $^{+4.3}_{-4.2}$

Table 6.1 Results of initial attempts at $^{230}Th/^{234}U$ dating of the inner calcite core of blue hole speleothems. Data for one determination of the outer marine crust (76015-7) is also shown. 76016-1b is a $^{231}Pa/^{230}Th$ date.

this experiment have large error limits (± 50%) because the sample was not re-weighed in between dissolutions; the amount of calcite dissolved was estimated from volumes of acid consumed.

A second leaching experiment (Table 6.2a) showed a similar progression towards older ages but the final age attained was much younger than in the first experiment. A reason for this is found in the magnesium and strontium concentrations of each leach solution. It can be seen that some aragonitic infillings still remained in the final fraction because Mg concentrations were ~ 25% above those determined for the pure calcite core (Table 6.2b). Therefore the final age is still biased towards younger values by incorporation of small quantities of aragonitic deposits. The lines linked by solid and open circles in Figure 6.7 representing change of U concentration and isotopic ratio also indicate that a pure end-member (pure calcite) has not been reached in the leaching sequence. Extrapolation to Mg and Sr values for pure calcite speleothem (Table 6.2b) suggest an age for 76016-9D of about 130 Ka.

6.7.3 Analysis of Pure Calcite

Sufficient pure calcite crystals from two speleothems (76016 and 78032) were hand picked from crushed samples of the speleothem cores to permit analysis. Each sample was rinsed in dilute acid before complete dissolution, to remove adhering powder. Analysis of Sr and Mg for 76016-9 (Table 6.2b) indicated that marine contamination was essentially absent. 78032-5 was not analysed for Mg and Sr after dissolution. Results of the two age determinations are shown in Table 6.2b.

a) LEACHING EXPERIMENTS

		U (ppm)	Yields (%) U	Yields (%) Th	$\frac{^{234}U}{^{238}U}$	$\left[\frac{^{234}U}{^{238}U}\right]_o$	$\frac{^{230}Th}{^{232}Th}$	$\frac{^{230}Th}{^{234}U}$	AGE (Ka) ± 1σ	Mg* (ppm)	Sr** (ppm)
1)	76016-5A	0.17	55	46	0.978	0.977	6	0.129	15.0 ± 2.0	-	-
	-5B	0.20	54	54	0.961	0.958	13	0.254	31.9 ± 2.6	-	-
	-5C	0.36	56	43	1.023	1.035	49	0.767	$156.5 ^{+11.5}_{-10.4}$	-	-
2)	76016-9A	0.59	62	6	1.067	1.073	12	0.235	$28.9 ^{+11.3}_{-10.2}$	9465	1815
	-9B	0.38	49	10	1.030	1.037	28	0.527	$80.8 ^{+8.7}_{-8.1}$	4205	1190
	-9C	0.31	63	32	1.013	1.018	38	0.655	$115.1 ^{+11.5}_{-10.4}$	3505	1100
	-9D	0.27	63	23	1.013	1.018	> 1000	0.658	$115.9 ^{+6.5}_{-6.1}$	1955	1050

b) ANALYSIS OF SELECTED CRYSTALS

	U (ppm)	Yields (%) U	Yields (%) Th	$\frac{^{234}U}{^{238}U}$	$\left[\frac{^{234}U}{^{238}U}\right]_o$	$\frac{^{230}Th}{^{232}Th}$	$\frac{^{230}Th}{^{234}U}$	AGE (Ka) ± 1σ	Mg* (ppm)	Sr** (ppm)
76016-9	0.23	63	83	1.000	1.001	24	0.768	$158.3 ^{+13.3}_{-11.9}$	1377	1080
78032-5	0.26	58	43	0.994	0.992	85	0.722	$139.2 ^{+8.3}_{-7.7}$	-	-
Pure calcite: 76016									1280	990
78032									1200	950
BH									2110	1130
Marine deposit:										
76016									41700	2800
78032									40860	2030
BH									36350	3095

* error ±10% ** error ±20%

Table 6.2 a) Dating results for two leaching experiments on 76016 and analyses of Mg,Sr content of each portion dissolved (for the second experiment only).

b) Dating results for analyses of pure speleothem calcite samples. Sr, Mg contents of the dissolved samples and analyses of pure calcite and marine deposit are shown for comparison.

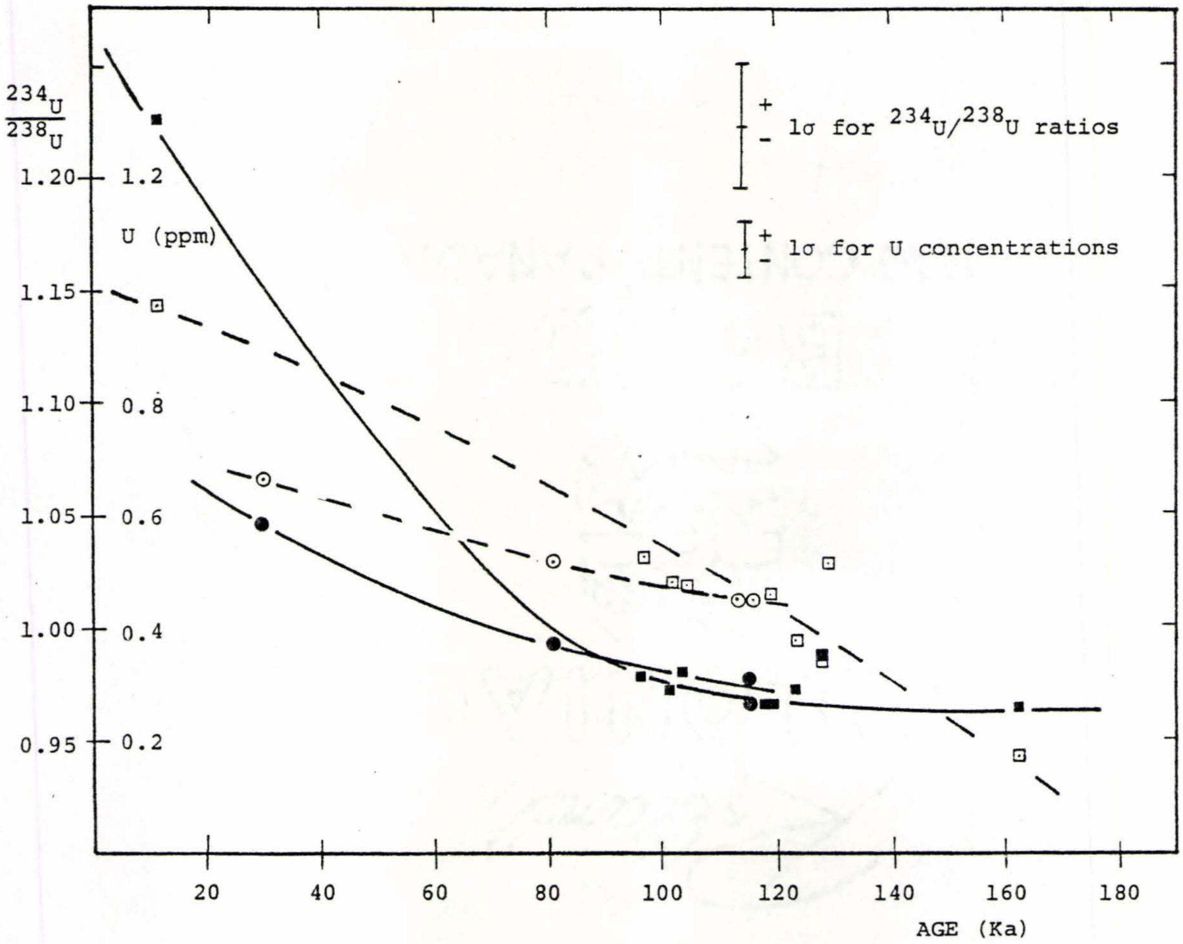

Figure 6.7 Variation of $^{234}U/^{238}U$ ratio (open symbols, dashed lines) and U concentration (solid symbols and lines) with age for initial analyses of BH, 76015 and 76016 (squares) and leaching experiments of 76019-9 (circles). The effect of marine carbonate contamination is seen by younger ages, higher ratios and U concentrations.

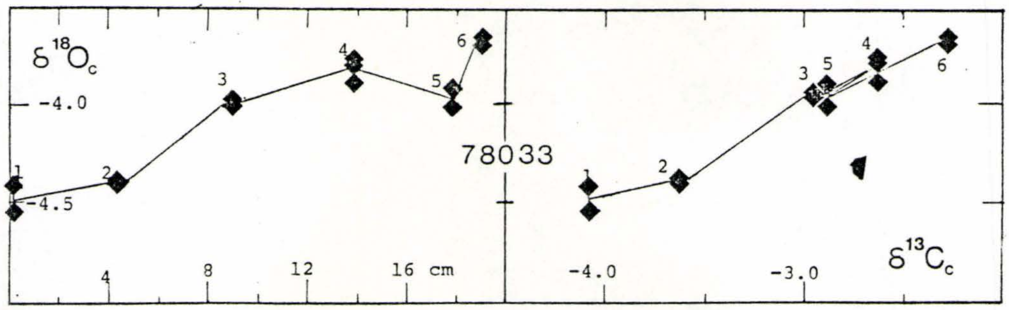

Figure 6.8 Results of analysis of one growth layer in blue hole speleothem 78033 for $\delta^{18}O_c$ variation along growth layer and correlation of $\delta^{18}O_c$ with $\delta^{13}C_c$.

6.8 Stable Isotope Analysis

Analyses of $\delta^{18}O_c$ and $\delta^{13}C_c$ were made along a distinct growth layer in 78033 to determine whether the speleothems were deposited in isotopic equilibrium with their drip waters. Unfortunately, $\delta^{18}O_c$ was found to increase in one direction and was correlated to $\delta^{13}C_c$ thus indicating the deposition was kinetically controlled and therefore useless for paleotemperature analysis. Figure 6.8 shows the analytical results.

6.9 Discussion

These results and the older dates from the initial work on speleothems from BH #4 (presumably corresponding to the least contaminated samples) indicate an age range of 160 - 139 Ka. Although this age range lies within error limits of the individual determinations it may in fact be real because each sample dated has a separate stratigraphic location and stalagmites of these dimensions probably require a period of at least this duration to develop.

The analyses of 76017 show that growth occurred during a period of sea level lowering of over 10m about 50 Ka. Although sea level is known to be lower than present at that time (Bloom et al. 1974), this result gives little indication of the amount of lowering. The deeper speleothems from BH #4 are of much greater significance.

The maximum subsidence rate of the Bahama platform for the period since the Oligocene has been shown to be 0.18m/10,000 years. It may therefore be concluded that speleothems were deposited 150 Ka ago, about 42m below present sea level. It is likely that sea level was even lower than -42m because there was sufficient time for cave

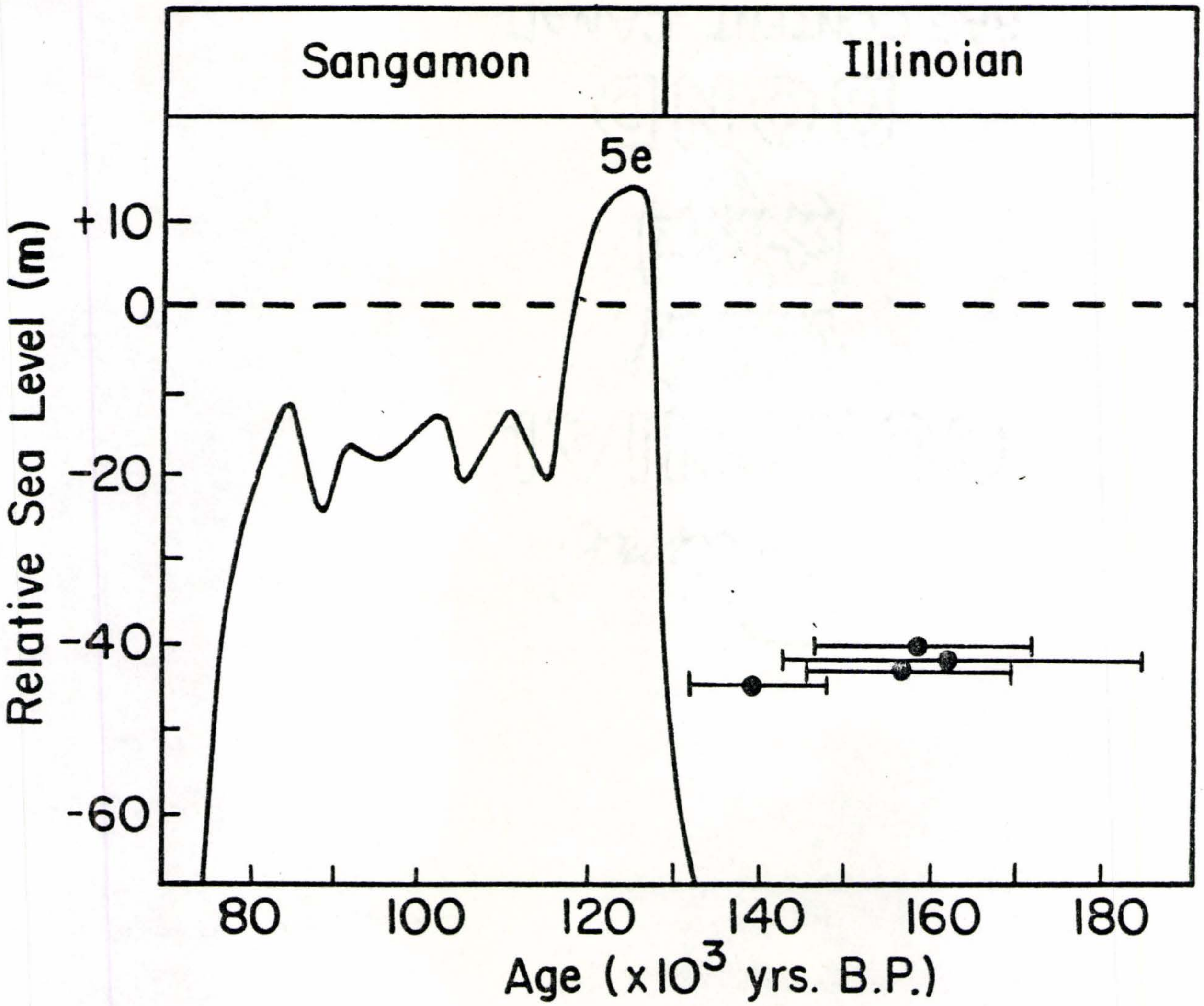

Figure 6.9 Paleosea level, after Shackleton and Opdyke (1973) showing determined ages of blue hole speleothems and inferred depression of sea level. Correlation to the N.American glacial sequence is shown.

passages to develop and integrate and large speleothems to form.

The growth period of these speleothems corresponds to the Illinoian glacial event occurring from approximately 180 - 130 Ka ago. It is tempting to suggest that rising sea level at the end of the Illinoian may have terminated growth of these stalagmites, but unfortunately the younger (outer) layers of the deposits, which might demonstrate this effect have been totally replaced by marine deposits. Correcting for tectonic submergence of the Bahamas platform, sea level must have risen at the end of the Illinoian at no less than 3.2m/Ka.

Figure 6.9 shows the excellent relationship of these results to estimates of sea level lowering obtained from deep sea cores by Shackleton and Opdyke (1973).

6.10 Conclusions

Analysis of speleothems from the deeper chambers of a blue hole near Andros Island have shown that sea level was depressed to at least one-third of its maximum lowering from about 160 - 140 Ka ago, during the Illinoian glaciation. Contamination of speleothem calcite by small amounts of marine carbonates has been found to severely bias ages to younger values due to the higher uranium concentration and younger age of these deposits. Preferential leaching of the marine carbonates during dissolution and analysis of clean, hand-picked calcite crystals has given ages approaching those of the original speleothems.

CHAPTER 7

APPLICATION OF DATING AND STABLE ISOTOPE TECHNIQUES TO SPELEOTHEM FROM OTHER AREAS

Introduction

During the course of this study, the opportunity arose to sample and date speleothem from several areas in North America and the Caribbean, principally in association with speleological expeditions to Jamaica, Gaspé Peninsula (Québec), the Canadian Rockies and North-West Territories. Jamaica was particularly interesting from a paleoclimatological viewpoint because a tropical rain-forest karst region had not been previously investigated for speleothem age distributions and gave the possibility of determining a paleoclimate curve unbroken by local freezing during glaciations. In contrast, the Gaspé Peninsula was ice-covered during most, if not all, North American glaciations and so speleothem age distribution would probably be restricted to non-glacial periods.

Several speleothems from the Canadian Rockies and the Nahanni region, N.W.T., have been dated in the hope of providing new information on cave development and valley incision rates in these areas. Single speleothem samples from other areas have also been dated and the results are briefly described here. The areas include New York State, West Virginia, Florida, Norway and N.Dakota.

7.1 Jamaica

7.1.1 Description of the Area

Jamaica consists of a basement of Cretaceous igneous and meta-sedimentary rocks, overlain by Tertiary limestones (Figure 7.1). The limestones cover almost two-thirds of the island's area and are subdivided into two main groups. The lower group, the Yellow Limestone, is an impure sandy limestone, and outcrops in a narrow band around inliers of the Cretaceous basement rocks. The upper White Limestone group is a sequence of more pure carbonates whose surface exposures are often heavily karstified. The Cockpit Country is a classical example of cone karst (Kegel Karst) - an area of conical limestone hills evenly separated by flat-floored glades, in the west of the island, (Sweeting 1958). The uplifted inliers are impervious to drainage and form the catchment areas for many of the island's large river caves situated at the contact between the basement and the limestones. Most of these caves end abruptly in impenetrable syphons or collapse debris and many have been traced to resurgences, often several kilometers away.

7.1.2 Sampling Areas

Several of the larger river caves and older fossil systems were visited for two weeks in 1975 with members of a Bristol University expedition led by Dr.D.Ingle Smith, and with the help of the Jamaica Caving Club. Speleothems were collected from most of the caves visited and a study of trace element content of freshly-deposited

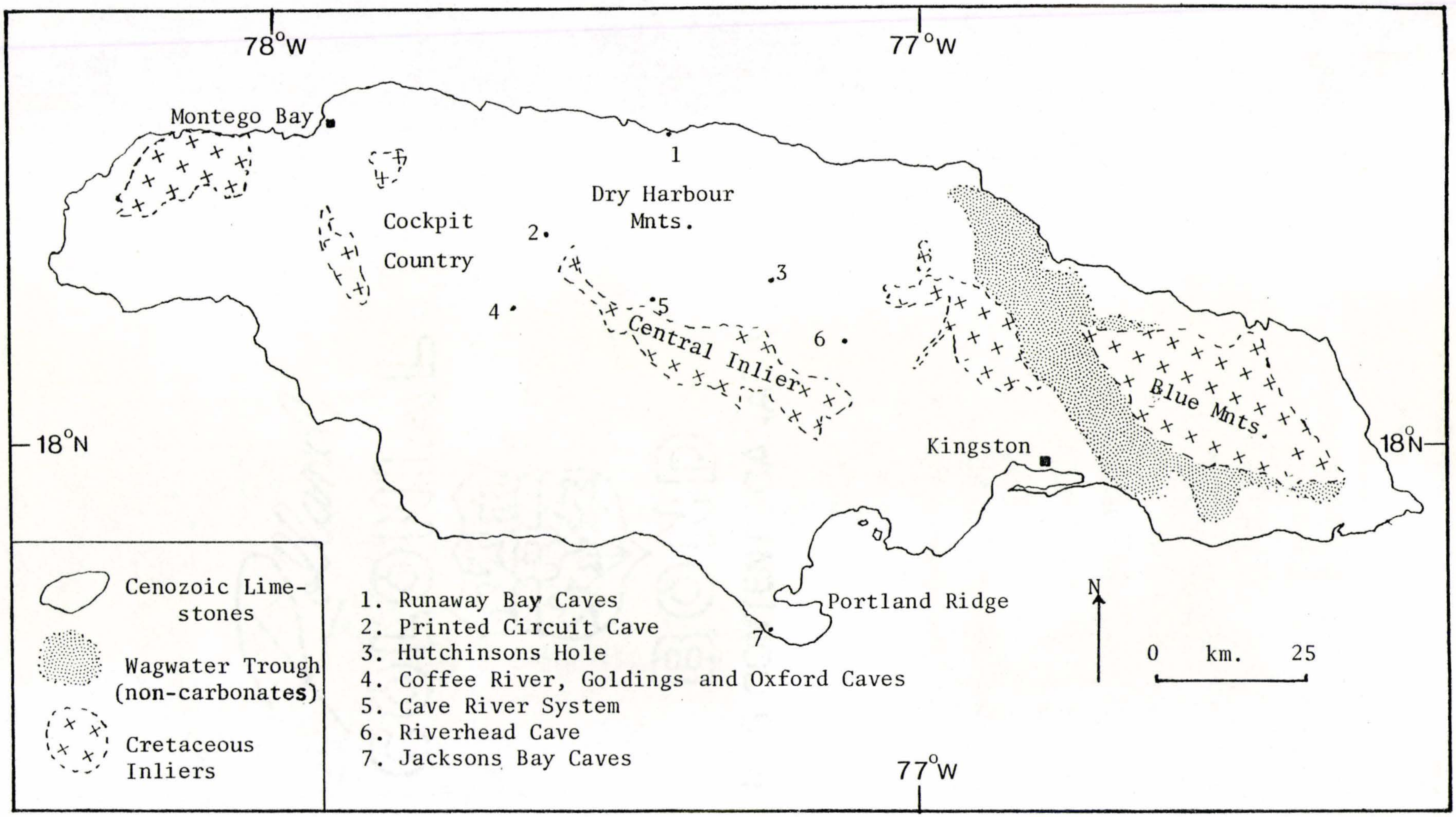

Figure 7.1 Simplified geology and cave location map of Jamaica (after Fincham 1977).

calcite and associated drip water was undertaken in some of the more accessible caves. The results of the trace element study are described in Chapter 9.

Most of the caves sampled were active vadose river systems formed near to the central inlier of the island (Figure 7.1). Some caves however, (Oxford Cave, Jacksons Bay Cave) are fossil high level systems showing phreatic development, followed by periods of clastic infill, speleothem deposition and re-excavation of sediments. A full description of the caves has recently been given by Fincham (1977).

7.1.3 Dating Results

Analytical results are listed in Appendix 5a and shown as a bar graph in Figure 7.2.

7.1.3.1 Detrital Contamination

On sectioning, most of the speleothems collected were found to contain appreciable quantities of detritus, either as horizons between clear calcite layers (presumably representing flood events in the cave) or distributed evenly throughout the speleothem. This has resulted in low $^{230}Th/^{232}Th$ ratios (< 20) for 19 out of the 31 ages determined for 11 speleothems. These results have been corrected for detrital thorium as described in Chapter 2 and are indicated in Figure 7.2. The validity of the correction in light of these and other results is discussed in Chapter 10.

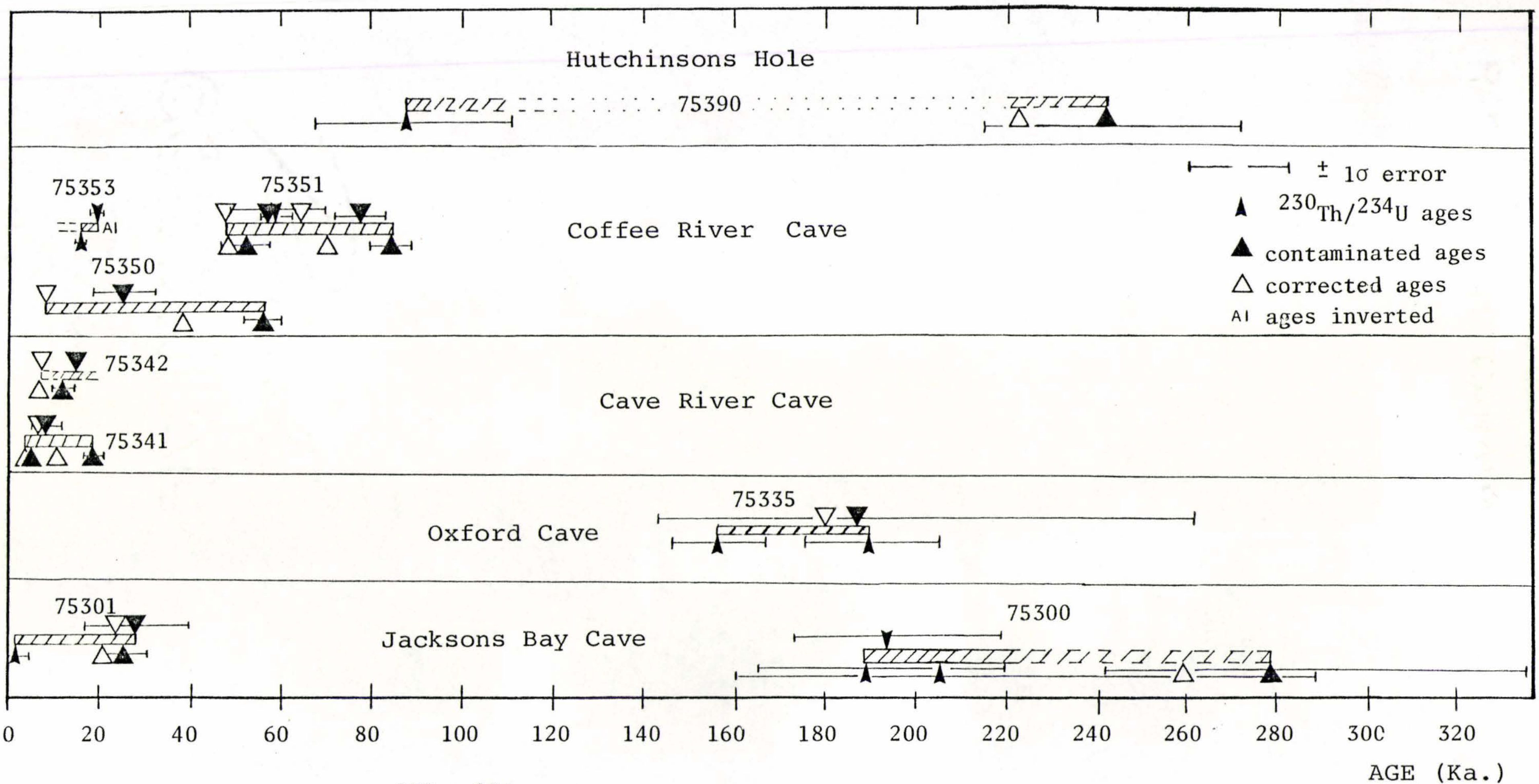

Figure 7.2 Bar graph of $^{230}Th/^{234}U$ ages determined for speleothems from caves in Jamaica. Ages for samples 75320 and 75371 are omitted because of low U and high Th concentrations (data are given instead in Appendix 5a). Parallel dotted lines indicate presence of a growth hiatus between dated portions and parallel dashed lines show projection of growth period to ages corrected for detrital thorium.

7.1.3.2 U Concentrations and $(^{234}U/^{238}U)_o$ Ratios

Only two of the dated speleothems contained more than 1ppm U. The remainder contained less than 0.4ppm. These low concentrations, coupled with the presence of detrital Th in many samples has greatly reduced the precision and reliability of calculated ages. These concentrations presumably reflect the low U content of the Tertiary limestones and absence of U-rich overburden and shale partings in the limestone.

$(^{234}U/^{238}U)_o$ ratios are all close to 1.0 (range 0.75 to 1.3) indicating little preferential enrichment of ^{234}U by groundwater leaching and in some cases, U dissolution from bedrock that is already depleted of ^{234}U (see Chapter 8).

7.1.4 Speleogenetic Significance of Dating Results

A wide range of ages (from 0 to 200 Ka) has been found for Jamaican speleothems (Figure 7.2). Their significance is considered in terms of each cave and the adjoining area.

7.1.4.1 Jacksons Bay Cave

This cave is a complex series of drained and partly-drained phreatic passages whose lowest passages are presently within 1m of sea level (Wadge et al. 1979). In the east the cave shows vertical development up to 70m a.s.l. It has many entrances, some of which contain Arawak petroglyphs carved onto stalagmites. The cave forms the lower level of development in the Portland Ridge (Figure 7.1), a sparsely vegetated limestone hill rising to 180m a.s.l.

Speleothem 75300 was an in situ flowstone projecting from the passage wall in a crawlway connecting two parts of the system. Age determinations show no clear relation to speleothem stratigraphy but growth appears to have been continuous and 1σ error limits for all analyses overlap. This speleothem indicates that the passage was de-watered by at least 200 Ka and therefore that much of the cave system was formed prior to this. Wadge et al. have proposed a complex sequence of development of the caves of Portland Ridge. They consider that karstification of the area began in the Late Pliocene after uplift and folding, and that during subsequent interglacial periods the ridge has often been below sea level. Groundwater ponded above the seawater caused many of these passages to develop under phreatic conditions during these and intervening times. The 20 Ka growth period of 75301, ending about 2 Ka ago, and the abundance of presently-inactive, young-looking speleothems in Jacksons Bay Cave suggest that the Holocene and post-glacial periods were relatively pluvial, the area becoming more arid about 2 Ka ago (it should be remembered however, that this age is based on a 6% Th yield).

Climatic implications of the speleothem data are further discussed in the next section.

7.1.4.2 Oxford Cave

This cave lies about 40m above the Golding River and 20m above the entrances to Golding and Coffee River Caves further upvalley

(Fincham 1977). It is a fossil phreatic tunnel up to 6m in diameter containing much mud, bat guano and stalagmite deposits. The cave may be an abandoned resurgence of the Coffee River, and can be seen to have had a complex genesis, because in places, phreatic flowmarkings are deeply carved into flowstone beds which once occupied much of the cave passage. This feature can only be explained by a second phase of phreatic development followed by rapid de-watering. Younger stalagmite columns then developed and the surface re-solution features of these indicate that a third ponding phase may have occurred.

The only speleothem dated from this cave is a piece of the deeply-scalloped (but non-porous) wall flowstone, 75335. Stratigraphically consistent ages from 190 to 156 Ka indicate that the cave evolved as a phreatic conduit and was dewatered prior to 190 Ka. Two phases of phreatic modification have occurred since 156 Ka, separated by an extensive speleothem depositional phase.

If the initial phreatic development occurred at valley floor level, then the average rate of downcutting of the Golding River valley must be less than 20cm/Ka.

7.1.4.3 Coffee River and Golding's Cave

These caves drain into the same river valley but are hydrologically separate. One stalagmite (75320) was collected from the entrance passage of Golding's Cave and shows extensive surface re-solution features and many internal detrital horizons. Low U and high detrital Th concentrations have made it impossible to date precisely

(Appendix 5 a). Three speleothems from Coffee River Cave have been dated with more success. 75351 was a large stalagmite cemented on a fallen block, but out of growth position (ie. it predates the block fall). It was dated as growing continuously from 84 to 55 Ka but age inversion near the top may be due to detrital Th contamination. Correction for detrital Th removes the age inversion and indicates growth from 70 to 48 Ka. A second stalagmite (75350), collected in situ from near roof level in the streamway, shows discontinuous growth from 56 to 25 Ka (39 to 9 Ka when corrected). A short segment (75353) of a long stalagmite in the streamway was dated at 19 to 15 Ka although its ages are inverted with respect to the stratigraphy.

These ages show that the stream in the cave has entrenched at a rate not exceeding about 15cm/Ka assuming 75351 grew near roof level, about 10m above the present streamway. The many detrital horizons in the lower layers of this speleothem suggest that flooding to roof level was more common about 70 Ka than 50 Ka, a proposal concordant with the concept of an entrenching vadose cave passage.

7.1.4.4 Cave River Cave

This cave consists of a series of passages formed by the sinking and resurging of the Cave River and its tributaries. The part studied here was the section upstream from the Noisy Water entrance containing a well-decorated side passage known as Gour Passage. Two loose stalagmites (75341, 75342) were collected here, each showing surface re-solution features. On sectioning, 75342 was found to contain an inner stalagmite. Attempts to date this inner portion failed due to poor Th yields but the outer deposit was found to be about 15 to 10 Ka in age. 75341 is also a recent deposit showing good age agreement with stratigraphy (19 to 5 Ka, or 11 to 4 Ka if corrected).

7.1.4.5 Hutchinson's Hole

This 90m deep shaft was descended by the author in search of human remains among the debris at the bottom. None were found, but instead a short, *in situ* stalagmite (75390) was collected from the entrance of a low passageway at the bottom of the hole. Its outer surface showed evidence of re-solution and on sectioning it was found to contain an indistinct hiatus near the top. The determined ages indicate a large span of time between base and top (about 150 Ka) which is inconsistent with the size of the speleothem, the apparent insignificance of the hiatus and the lack of pronounced surface erosion features. Only replicate analysis will clarify these results.

7.1.5 Stable Isotope Results

Two speleothems (75341, 75351) show good radiometric age control, internal crystallinity and agreement with stratigraphy, and they were examined for isotopic equilibrium growth. Both samples showed increase of $\delta^{18}O_c$ and correlation between $\delta^{18}O_c$ and $\delta^{13}C_c$ along the growth layers (Figure 7.3), indicating kinetic isotope fractionation during growth. A third speleothem, 75300, (Figure 7.3) was analysed in two dimensions as descibed for flowstones in Chapter 3 and found to have constant $\delta^{18}O_c$ but with correlation between $\delta^{18}O_c$ and $\delta^{13}C_c$

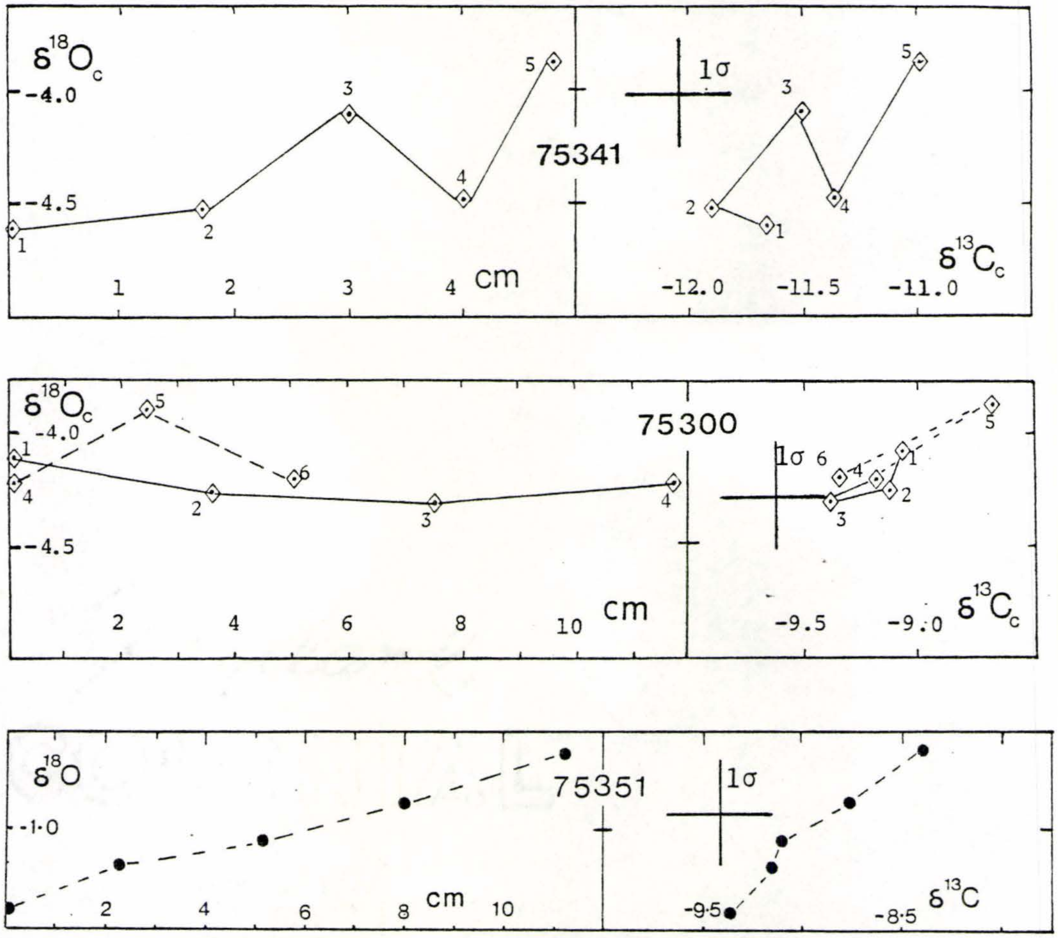

Figure 7.3 Variation of $\delta^{18}O_c$ along growth layers and correlation of $\delta^{18}O_c$ and $\delta^{13}C_c$ along growth layers for three Jamaican speleothems.

along one growth layer, also indicating kinetic isotope fractionation. All three speleothems were collected in passages containing appreciable air currents, which, if present during growth, would account for the observed results. Isotopic analyses are listed in Appendix 5b.

No inferences concerning Jamaican paleoclimate can therefore be made from stable isotope studies on the speleothems dated here.

7.1.6 Age Distributions and Paleoclimatic Significance

It has already been suggested that the abundance of presently-inactive,young speleothem in Jacksons Bay Cave and the dated growth period of one speleothem from 25 to 2 Ka indicates a more pluvial climate in this area during the last glaciation. The remaining speleothem data presented here (Figure 7.2) although infrequent, further indicate depositional periods which coincide with estimated durations of cold or glacial periods in the northern hemisphere, ie. 190 - 160 Ka, 80 - 50 Ka, and 30 - 5 Ka. These results are in contrast to those of Bonatti and Gartner (1973) who propose that glacial periods are marked by increased aridity in the Caribbean, based on changes in the kaolinite (humid) to quartz (dry) ratio of the Caribbean cores. However to justify further comparison and resolve this apparent disagreement, a far greater population of speleothem age determinations is first needed. Stable isotope profiles and comparison of growth rates during dated periods would give additional evidence.

7.1.7 Conclusions

This investigation of speleothem from Jamaican caves has been limited by low uranium and high detrital contents of many of the samples collected. Detrital layers seen in many speleothems probably indicate frequent and intense flooding events in these caves. Valley entrenchment rates, where calculable appear to be high, and these further illustrate the energy of the dynamic processes influencing cave development in a tropical, rain-forest environment. Many of the caves investigated carry air currents which are presumably responsible for kinetic isotope fractionation seen in three of the dated speleothems.

Average growth rates of three dated speleothems (75301, 75341, and 75351) vary between 1.5 and 4cm/Ka. These are rather low for non-equilibrium deposits formed in a tropical environment (compare for instance the rates calculated for English speleothem formed during the Holocene, Figure 5.24).

7.2 Gaspé Peninsula

7.2.1 Location

Limestones of Silurian to Devonian age outcrop in narrow, steeply-dipping belts in southern Gaspésie, the eastern peninsula of Québec (Bourque 1975). The area is covered by Quaternary glacial deposits of Late Wisconsin age and was probably ice-covered during previous glaciations (Flint 1971). Several small caves are known in the region (Beaupré 1975) but one of the most interesting has recently been found in the Silurian Baie-des-Chaleurs limestone group, north of the village of Saint-Elzéar de Bonaventure (see inset, Figure 7.4).

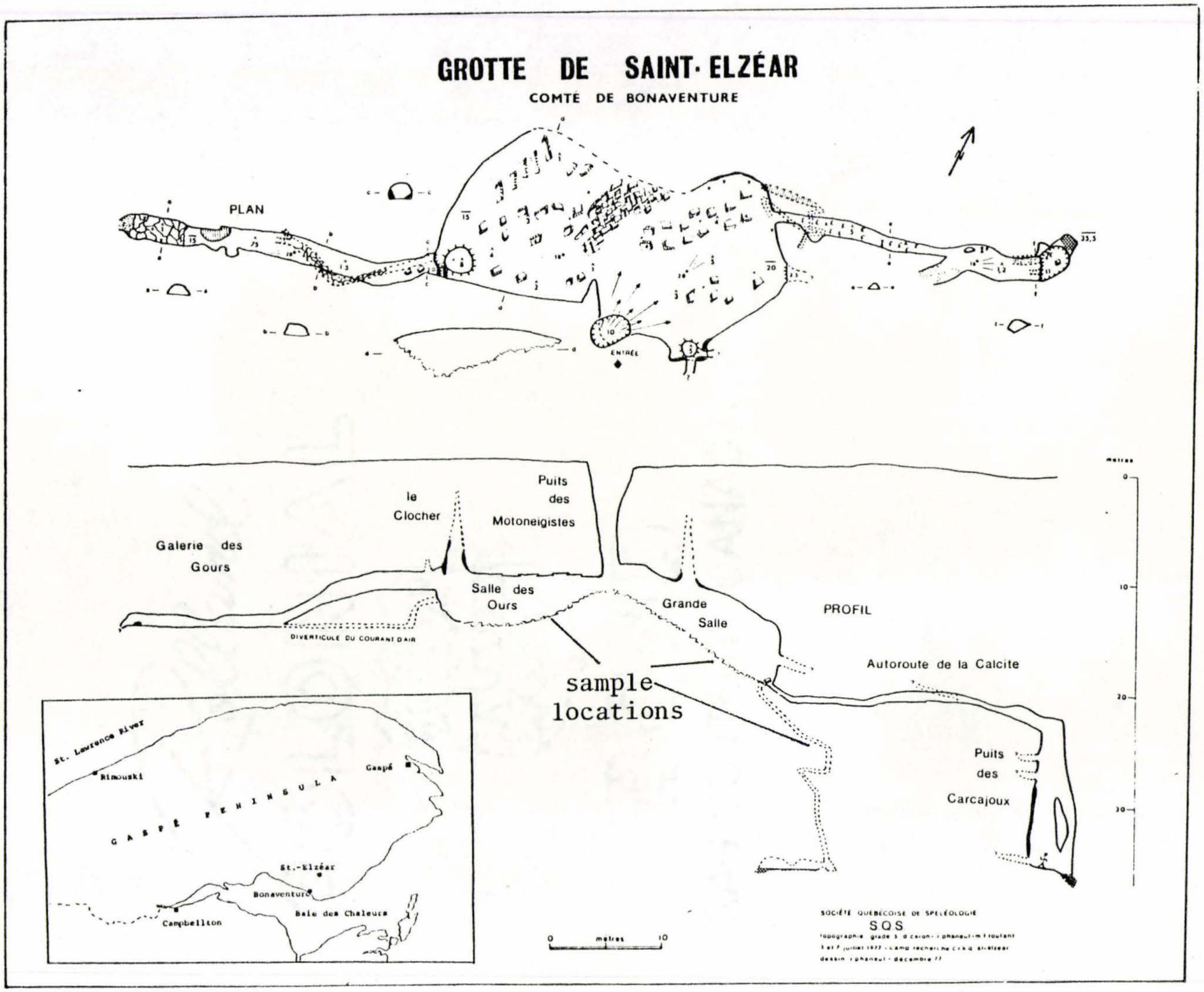

Figure 7.4 Plan and elevation of La Grotte de Saint-Elzéar, Gaspé Peninsula, with location map inset (after Roberge and Gascoyne, 1978).

Discovered by local people early in 1977, La Grotte de Saint-Elzéar attracted much attention because of the enormous quantities of fossilized bear bones found in two chambers at the base of a 10m entrance shaft. The chambers, Salle des Ours and Grande Salle, are separated by a low roof and a debris pile. From each, short fissure passages and fossil phreatic passages lead off (Figure 7.4).

In April 1977, the author was invited to join an expedition by members of the Société Québécoise de Spéléologie in Montréal, to the cave, to collect dripwater for chemical analysis and speleothems for dating. The cave is not well decorated with speleothem but several small stalagmites were found loose or cemented to displaced boulders in breakdown debris in Salle des Ours. Two stalagmites, also cemented to blocks and out of growth position, were collected from La Grande Salle. The cave has been described in detail with initial dating results by Roberge and Gascoyne (1978).

7.2.2 Results

Eight $^{230}Th/^{234}U$ ages have been determined on seven stalagmites from La Grotte de Saint-Elzéar. The results are listed in Appendix 5 c and shown as a bar graph in Figure 7.5. Three speleothems show slight contamination with detrital Th and their ages have been corrected as described in Chapter 2. Some of the ages indicated in Figure 7.5 are less reliable than others because of their low U concentrations (< 0.1ppm). As described in Chapter 2, ages determined for these speleothems may be influenced by random contamination effects not expressed in the standard deviation error of the age.

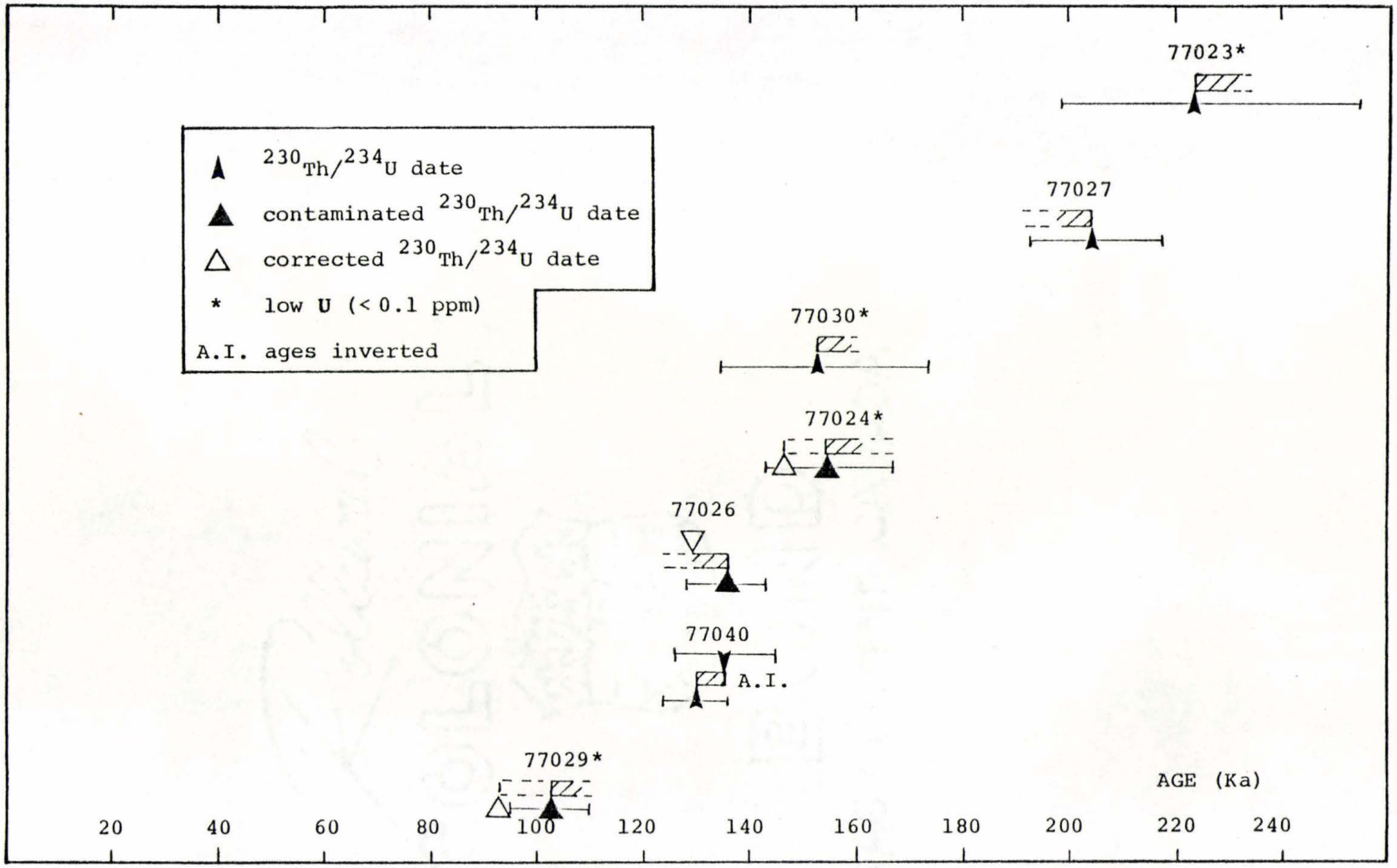

Figure 7.5 Bar graph of $^{230}Th/^{234}U$ ages of speleothems from Grotte de Saint-Elzéar. Parallel dashed lines to open triangles show projection to ages corrected for detrital thorium, others indicate continuation of speleothem growth (undated).

7.2.2.1 U Concentration and Isotopic Ratio

Speleothem U concentration varies by almost an order of magnitude between stalagmites in the same chamber, La Salle des Ours, (range 0.06 to 0.41ppm). $(^{234}U/^{238}U)_o$ ratios are all high, between 2.20 and 3.15. As previously found by Harmon (1975), no distinct relationship can be seen between U concentration, $(^{234}U/^{238}U)_o$ ratio and age (Figure 7.6), although it is possible that higher U samples are formed during interglacial periods, ie. about 200 Ka and 140 - 120 Ka.

7.2.2.2 Speleogenetic and Paleoclimatic Significance

These results indicate that the cave was de-watered prior to about 200 Ka and has remained so since, because no samples show evidence of re-solution. Cave development by solutional enlargement must therefore have occurred more than 200 Ka ago. The ages of all higher U speleothems (> 0.1ppm) lie within proposed interglacial periods for North America, ie. the Yarmouth (~ 230 - 180 Ka) and the Sangamon (~ 140 - 90 Ka), (Harmon et al. 1977). Ages of two low U speleothems (77024, 77030) place them in the Illinoian glacial event (~ 170 - 140 Ka) which, if real, may indicate the presence of an interstadial separating two glacial advances as recognised in deep sea cores taken from seamounts off the Grand Banks, Newfoundland (Alam and Piper 1977), and in Europe (Table 5.1). Alternatively it may be due to a bias caused by minor contamination during analysis (eg. reagent blank fluctuation, memory effect) such that the samples actually belong to one or other of the interglacials described above.

The fact that the Yarmouthian speleothems were found intermingled with Sangamonian speleothems in the debris of La Salle des Ours indicates

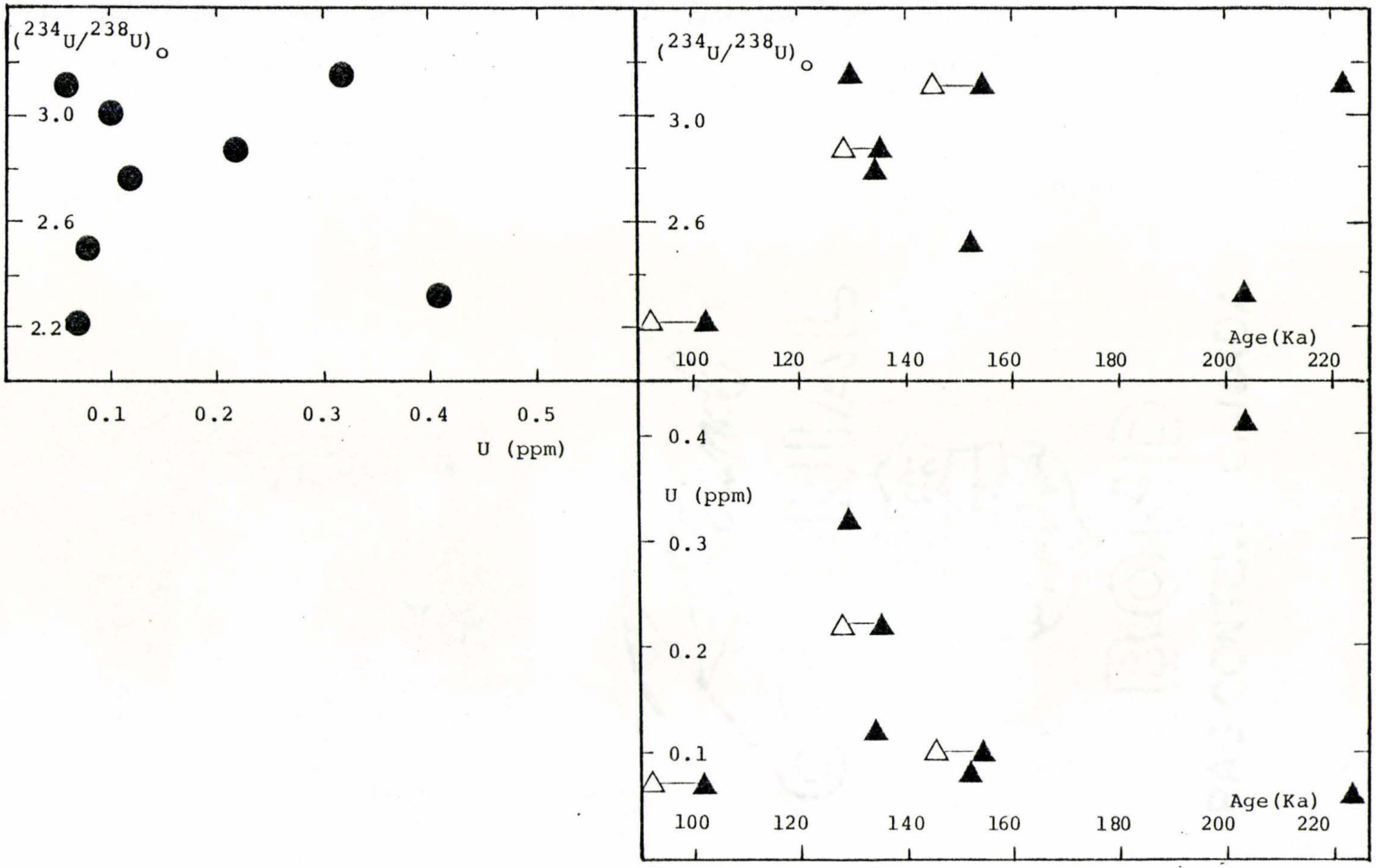

Figure 7.6 Relationships between $(^{234}U/^{238}U)_o$, U concentration and age of speleothems from La Grotte de Saint-Elzéar.

that the intervening Illinoian glaciation contributed little to either the erosional enlargement or clastic infilling of the cave.

7.2.3 Conclusions

This cave is noteworthy for the high $(^{234}U/^{238}U)_o$ ratios, variable U concentrations and relatively high ages of its speleothem deposits. Limited speleothem growth during the last two interglacials is indicated by these results and the absence of Mid-Wisconsin interstadial deposits suggests that cold conditions prevailed throughout this period in this area.

7.3 Canadian Rockies

Two speleothems whose ages have considerable geomorphic significance have been dated from caves in the Canadian Rockies. Sample 77032 from Castleguard Cave, Banff National Park, Alberta-B.C., was collected in 1977 from the bottom of the '80 ft. pitch' in the cave. It was found lying loose on a sediment bank and may have been transported there by persons unknown, as part of a previous collecting trip. Ages for the top and bottom of the stalagmite are 278 and > 350 Ka respectively (Appendix 5 d). This speleothem is the oldest so far obtained from Castleguard Cave (the oldest previously determined was 147 Ka; Harmon et al. 1977) and therefore indicates de-watering of the farther reaches of the cave by at least 350 Ka. This result permits revision of valley entrenchment rates for this region, giving lower, more acceptable values.

The second speleothem, 72025, from Gargantua Cave, Crows Nest Pass area, was initially collected and analysed by Harmon (1975) giving an age of about 219 ± 16 Ka and a U concentration of 18.1ppm (quoted in Harmon et al. 1977). However, this date is known to be based on yields of 2% (U) and 9% (Th). Replicate analysis of an exactly similar piece of the speleothem in the present study has given an age of > 350 Ka and U concentration of 2.91ppm, (Appendix 5d).

7.4 Nahanni Region, N.W.T.

Several analyses have been made of speleothems collected in 1975 from Grotte Valerie in the Nahanni Plateau region and these are reported and used for interpretation in Harmon et al. (1977). However three of these (75029, 75030-1, -2) are based on low yields (< 5%) and were not intended for publication. The influence of the low yields can be seen in the fact that the $^{230}Th/^{234}U$ ratios are all greater than 1.10, giving apparent ages of > 350 Ka. The only reliable $^{230}Th/^{234}U$ age is for flowstone 75037 (> 350 Ka), given in Appendix 5d.

7.5 West Virginia

Two stalagmites (NBL, NBS) were collected in 1975 from the streamway below the Half Way Room in Norman Cave in an effort to add to the age and stable isotope data determined by Thompson (1973a) for West Virginian Caves. On sectioning, both were found to contain re-solution holes and detrital layers. NBL contained a prominent hiatus half way along its length. Analytical data for analyses of the top and bottom of each speleothem are given in Appendix 5d. NBL was found to have grown from 121 to 93 Ka, during the Sangamon interglacial. NBS appears to be considerably older (top date is 221 Ka) but this may be an artefact of partial leaching of uranium as seen in the basal age, ($^{230}Th/^{234}U$ ratio = 1.140). No stable isotope analyses have so far been made for these speleothems.

A small in situ stalagmite (78042) was collected from a fossil phreatic roof tube in part of the Canadian Hole system, W.Va., in 1978. An age on its flowstone edges was 155 Ka. The speleothem showed considerable surface re-solution features indicating that a return to phreatic or vadose conditions, with flooding, has occurred sometime since this date. The stalagmite may have grown just prior to the maximum glacial conditions of the Illinoian event (probably associated with periglacial conditions in this area) and then suffered re-solution by ponding of meltwaters during de-glaciation. Alternatively it may indicate the presence of an interstadial period in the Illinoian, as suggested above.

7.6 New York State

McFails Cave, near Albany, New York, unlike the West Virginian caves, was glaciated during Wisconsin and probably during Illinoian times. Speleothem ages are therefore likely to be confined to interglacial or interstadial times. Two speleothems from McFails, 75032 and MCFA 4, have been dated and are found to have grown during the period 44 - 36 Ka, (Appendix 5d), corresponding approximately to the Port Talbot II interstadial of the Eastern Great Lakes record (Dreimanis and Goldthwait 1973). Another speleothem, 75034, probably grew during the Late Wisconsin de-glaciation, and ended about 8 Ka ago. The base of the sample has not been dated.

7.7 Warm Mineral Springs, Florida

This hot spring, near Venice, Florida, has an average temperature of 30.5°C and its surface lies about 1.5m above sea level. It has recently been the site of several important archeological finds which have been preserved at depth by the anoxic waters (Royal 1978). Royal has located several stalagmites and flowstones at depths up to 55m in the Springs. A sample of a flowstone at -15m (78010) has been dated by both ^{230}Th/^{234}U and ^{231}Pa/^{230}Th methods. The latter results are described at the end of Chapter 2. Ionium ages of 12.6 Ka and 14.4 Ka (10.9 when corrected) have been determined on two different pieces of the flowstone (Appendix 5d). Good agreement is seen between the two ages suggesting that the porosity of the sample either has not permitted differential migration of radioelements, or that the whole speleothem has been equally affected. These alternatives are discussed more fully in Chapter 2. If no migration has occurred, then the ionium ages indicate that the spring level was at least 15m below its present level about 12 Ka ago.

This result is in general agreement with estimates of eustatic sea level by Curray (1965) and Milliman and Emery (1968) which indicate a depression of between 40 and 80m below modern at that time.

7.8 Norway

Two speleothem samples from caves in Norway have been dated in this study. Both were collected by S.E.Lauritzen. The first (78006) was a thin flowstone veneer over clay breccia, thought to be glacial outwash deposits. Two analyses (Appendix 5d) showed high detrital Th contamination but indicated that the flowstone was middle Holocene, in agreement with its location. 78007 was a flowstone block found buried in debris in a cave stream passage. It was low in U and dated at 162 Ka (148 Ka when corrected). This age may indicate that the speleothem grew during the Treene interstadial separating the main phases of the Saale glaciation. Alternatively its age may be biased slightly by contaminants, such that it belongs to the Eemian or Holstein interglacials.

7.9 Wind Cave, S.Dakota

A 1cm thick calcite encrustation on a cobble, collected by T.Miller from Wind Cave, has been dated at > 350 Ka. The date is suspect because of the rather high $^{230}Th/^{234}U$ ratio (1.099) and the low Th yield (5%) in the analysis (Appendix 5d). The high $^{234}U/^{238}U$ ratio however indicates that the sample is not of 'infinite' age and this may account for the apparently high $^{230}Th/^{234}U$ ratio (see isochron plot, Chapter 2). If correct, this date indicates the antiquity of the Wind Cave system.

CHAPTER 8

URANIUM ISOTOPIC DISEQUILIBRIUM IN SPELEOTHEM AND KARST GROUNDWATERS

Introduction

Disequilibrium of the isotopes of uranium, ^{234}U and ^{238}U, in the natural environment was first observed in the USSR by Cherdyntsev (1955). Since then, isotopic disequilibrium has been shown to be the rule rather than the exception, and values of the activity ratio, ^{234}U/^{238}U, ranging from 0.5 to > 12 have been observed in groundwater systems. Studies of disequilibrium have included applications to water tracing and hydrological mass balance, earthquake prediction, uranium prospecting and age dating. The ^{234}U/^{238}U dating method is potentially useful for dating Pleistocene deposits that lie beyond the range of the ^{230}Th/^{234}U method (> 350 Ka). Its main drawback is the difficulty in determining or predicting the initial ^{234}U/^{238}U ratio.

This chapter discusses the theory of U isotope fractionation and briefly reviews relevant literature. Cave drip waters and associated calcite deposits have been analysed to determine the variability, in time and space, of ^{234}U/^{238}U activity ratios. As part of this study, a novel technique for U extraction from groundwater has been developed, which is more compact and portable than that used by previous workers. Analyses have been made of calcites and drip waters collected from caves in West Virginia, Kentucky, the Canadian Rockies and N.W.England.

8.1 Geochemistry of Uranium

Uranium has a number of oxidation states but only U(IV) and U(VI) are important in the natural environment. In its primary source, felsic igneous rocks, it is present almost entirely as U(IV). On weathering in an oxidising environment it becomes the more soluble U(VI). In solution, it forms a number of anionic complexes in preference to the 'free' cations U^{4+} and UO_2^{2+}, eg., $UO_2(CO_3)_2^{2-}$, $UO_2(CO_3)_3^{4-}$, $UO_2(HPO_4)_2^{2-}$. Langmuir and Applin (1977) have shown the dominance of these species in groundwaters between pH 4 and 10. In karst groundwaters, the stability of the carbonate species is dependent on the partial pressure of CO_2; degassing of saturated waters will cause U to co-precipitate with carbonate minerals (eg. calcite). U in limestone groundwaters may be derived from allogenic surface streams but more usually it originates in the limestone and interbedded shale partings. Overlying glacial drift and local mineralizations may be additional sources.

8.2 Uranium Disequilibrium

Until the discovery of unsupported ^{234}U in groundwaters, it was always supposed that isotopes of heavy elements could not be measurably fractionated by chemical means, and only slightly by physical means. It was thought that the half-lives of the intermediate nuclides were short enough to allow the $^{234}U/^{238}U$ activity ratio to be unity (ie. at secular equilibrium) for any geological deposit or deep groundwater system, (the decay sequence of ^{238}U is shown in Figure 8.1).

Some early studies of ^{234}U disequilibrium attempted to simulate

^{238}U DECAY SERIES

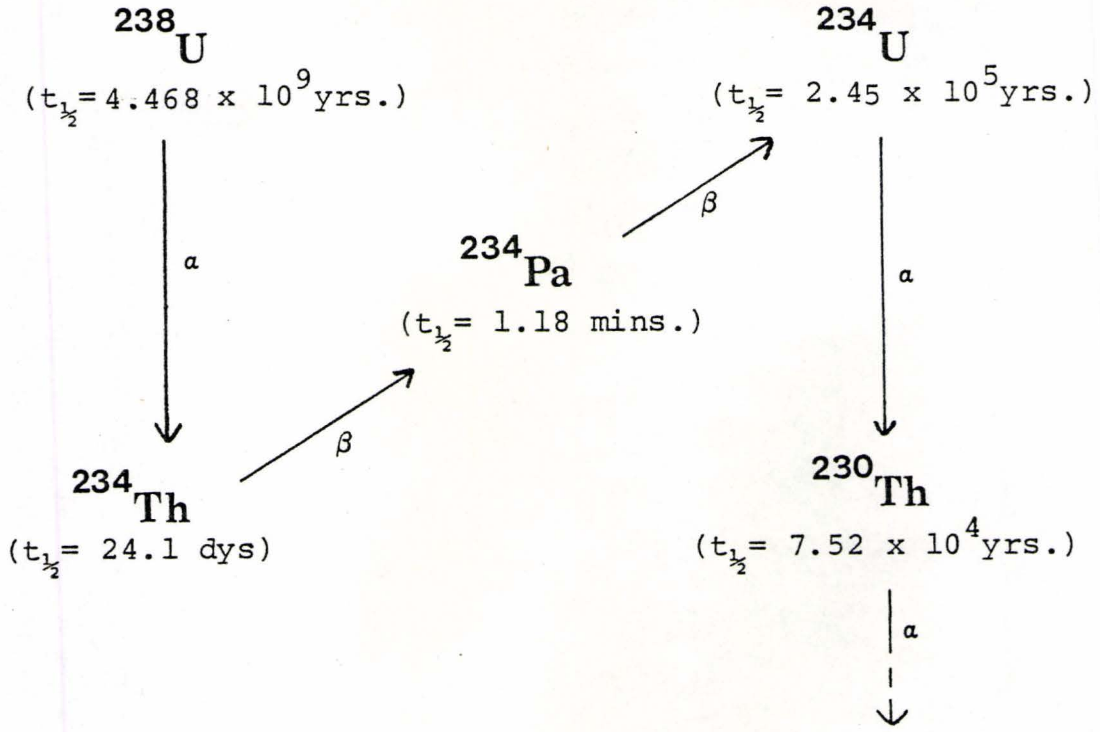

Figure 8.1 Part of the ^{238}U decay series, showing intermediate nuclides before formation of ^{234}U.

its fractionation by leaching experiments on whole rocks and sediments. It was found that ^{234}U preferentially migrated to the aqueous phase leaving the solid phase deficient (Baranov et al. 1958, Starik et al. 1958, Chalov 1959). Many subsequent studies have measured $^{234}U/^{238}U$ ratios in rivers, lakes, groundwater, sediments, bedrock, peat bogs and hot springs. A recent comprehensive review of literature on uranium disequilibrium has been given by Osmond and Cowart (1976). Figure 8.2 illustrates typical ranges of values of $^{234}U/^{238}U$ ratios and uranium concentrations in the weathering cycle. It is significant that only the ocean is known to have a constant isotopic ratio (Ku 1976).

8.3 Mechanisms of Isotopic Fractionation

8.3.1 Leaching Processes

8.3.1.1 'Damaged-site' ^{234}U

Early workers explained natural U isotopic fractionation in terms of lattice dislocation due to emission of high energy particles during the three-stage decay of ^{238}U to ^{234}U. The resulting ^{234}U was therefore more accessible to leaching by groundwater.

8.3.1.2 Change of Oxidation State

During the decay to ^{234}U, the oxidation state of the U atom can be increased from IV to VI due to stripping of electrons from atomic orbitals by the ejected alpha particle. U(VI) is more soluble than U(IV) and therefore is more easily leached from the solid phase.

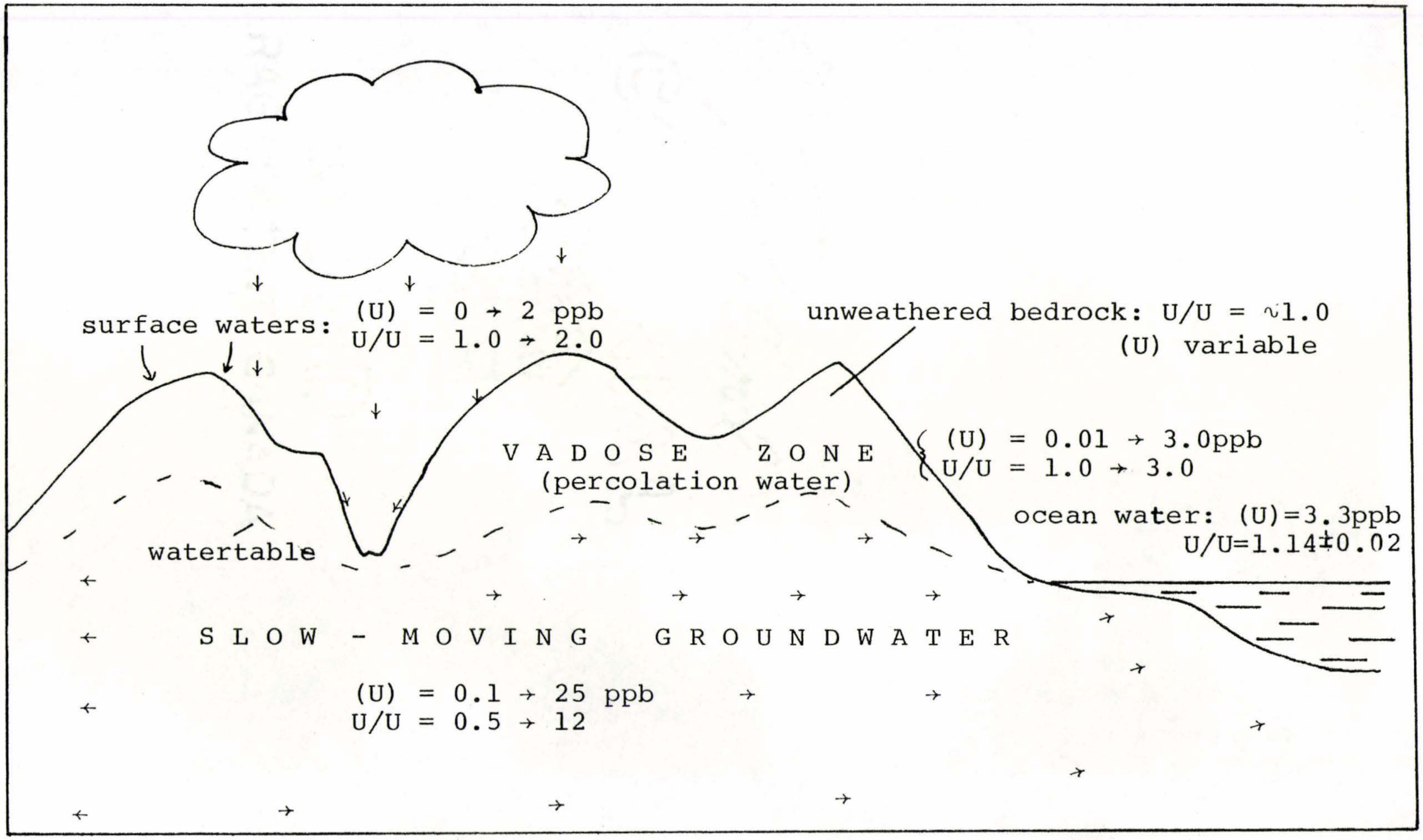

Figure 8.2 Diagrammatic representation showing the range of uranium concentrations (U) and $^{234}U/^{238}U$ (U/U) ratios encountered in the hydrological cycle.

These mechanisms have been experimentally shown to account for disequilibrium ratios of up to 1.3, but very high ratios have been reported by Kronfeld (1974) and these probably involve other mechanisms.

8.3.2 The Alpha-Recoil Mechanism

Kigoshi (1971) suggested a mechanism of ^{234}U enrichment in groundwaters which could explain high values of disequilibrium ratios. Decay by α-emission into the body of the solid phase, from a nuclide at the surface of the grain may cause the daughter to recoil into the adjacent liquid phase. Kigoshi demonstrated this process using a suspension of zircon powder in water. ^{234}Th concentration in the water increased in accordance with calculations based on α-recoil range of ^{234}Th in zircon, surface area and density of the powder and decay constant and concentration of the ^{238}U. Although the ejected ^{234}Th is relatively insoluble, decay to the more soluble ^{234}U takes place soon after formation.

8.4 Additional Effects

8.4.1 ^{234}U Replacement of ^{238}U

Work done on groundwater of the Trinity aquifer of central Texas (Kronfeld 1974) substantiates Kigoshi's mechanism and illustrates a means of enhancing ^{234}U excess in groundwater. In this aquifer, uranium concentration was found to decrease dramatically along the direction of flow (from > 1 ppb to as little as 0.01 ppb) whilst $^{234}U/^{238}U$ ratios increased. The decrease in U concentration was thought to be due to changes in water chemistry, pH and Eh conditions. A uranium-rich precipitate was assumed to coat the aquifer walls and although this was no longer a source of leachable ^{234}U, owing to the chemical conditions, it would continue to supply ^{234}U to the groundwater by α-recoil. Equilibration with the dissolved U would preferentially displace ^{238}U from solution (the more abundant isotope), thereby appreciably increasing the disequilibrium ratio.

8.4.2 Deficient ^{234}U

In water of the Floridan aquifer, Kaufman et al. (1969) also observed that ^{234}U/^{238}U ratios were inversely related to U concentration, but deep groundwaters were enriched in U (up to 25 ppb) with isotopic ratios as low as 0.5. In this case Kaufman et al. proposed that leaching and α-recoil of ^{234}U from the aquifer walls was insignificant because extensive ^{234}U removal had already occurred during times of low sea level in the Pleistocene, leaving a bedrock deficient in ^{234}U. A combination of high permeability, oxidising conditions and an efficient groundwater circulation were now leaching U from bedrock or re-mobilizing precipitated U, in its ^{234}U deficient state.

In summary, the mechanisms of damaged-site leaching and α-recoil for ^{234}U enrichment are applicable to all surface waters and groundwaters, but the methods of selective enrichment of ^{234}U or ^{238}U depend on chemical conditions and previous hydrological history of the area.

8.5 Applications of Uranium Disequilibrium

8.5.1 Hydrological Systems

Characteristic associations of $^{234}U/^{238}U$ activity ratio and uranium concentration have been used to classify aquifer types as follows (after Osmond and Cowart 1976) :

i) $3 > {}^{234}U/^{238}U > 1$ with low U concentration - typically found in oxidised aquifers, open to O_2 and CO_2 exchange with the atmosphere. This is the most common type and is comparable to that of surface waters.

ii) very high $^{234}U/^{238}U$ with low U concentration - one type of reduced aquifer which is closed to atmospheric exchange, usually on the confined portion that lies down-dip from the recharge zone. Water from the higher-level oxidising zone penetrates a 'reducing barrier' causing uranium to precipitate. ^{234}U excess is then increased by α-recoil.

iii) low $^{234}U/^{238}U$ (< 1.0) with high U concentration - another type of closed system aquifer where uranium precipitated during conditions described in ii) is remobilised by lowering of the weathering horizon. Normal denudation processes, or enhancement by change of water levels will cause this.

iv) low $^{234}U/^{238}U$ with low U concentration - a rare type of water only seen so far in geothermal systems where reducing conditions, equilibration with minerals and rapid circulation combine to lower uranium concentration and suppress enrichment of ^{234}U by leaching and α-recoil mechanisms.

The unique characteristics of the groundwaters in this classification allows them to be used as components of mixing model equations to determine discharge contributions to river systems and major karst springs (Osmond et al. 1974).

8.5.2 Age Measurement

The decay of excess ^{234}U in a closed system is described by :

$$\left(\frac{^{234}U}{^{238}U}\right)_t - 1 = \left[\left(\frac{^{234}U}{^{238}U}\right)_o - 1\right] . e^{-\lambda_{234}t} \qquad (8.1)$$

where λ_{234} is the decay constant of ^{234}U and subscripts t and o represent the measured and initial activity ratios for a sample of age t.

Corals were first to be dated by this method (Thurber 1962) but the low ^{234}U initial excess in marine carbonates (14%) gives rise to ages with large error limits (± 35% of the calculated age, Veeh 1966). Attempts have also been made to use the decay of excess ^{234}U to date freshwater and Pleistocene lake sediments (Chalov et al. 1966, 1970; Kaufman and Broecker 1965) and groundwater (Kronfeld and Adams 1974). Results of dating travertine and speleothem by this method are described in a later section.

8.5.3 Other Applications

Isotopic ratios and concentration of U in seawater have been used for calculating U residence time in the oceans. Values of 280 Ka and 500 Ka respectively, have been determined in this way (Osmond and

Cowart 1976). The discrepancy suggests that mean $^{234}U/^{238}U$ ratio and U concentration in runoff are poorly estimated, but Ku (1965) has suggested that ^{234}U mobilization (by α-recoil) after sedimentation in the oceans, may provide an additional source of uranium which is not accounted for in the calculations.

Uranium disequilibrium has been considered for use in prospecting for uranium ore deposits by studying ^{234}U excess in waters and soils. Rosholt et al. (1965) have shown that ore bodies that have been altered by weathering and oxidation, have excess ^{234}U, whereas unaltered ores generally show ^{234}U deficiency. Accumulation zones might also be determined by sudden changes in $^{234}U/^{238}U$ ratio of groundwater as it moves through an aquifer.

Geothermal waters from active volcanic regions and now-dormant (neovolcanic) regions can be recognised by their different $^{234}U/^{238}U$ ratios and U concentrations. In the former, ratios and concentrations are lower than in the latter due presumably to high temperature isotopic equilibration with minerals and U precipitation in a reducing environment. High ratios and a higher U concentration reflect equilibration at depth and enrichment by ^{234}U from α-recoil during the longer residence time of neovolcanic waters.

There is some suggestion that U isotopic ratios may change prior to earth movements, in the same way that Rn and He content of groundwater has been found to vary. Increasing rock strain has the effect of releasing loosely-attached gas bubbles and particles, and dissolution of these particles (presumably enriched in ^{234}U by α-recoil) may be reflected in groundwater. One interesting speculation is that travertines from hot springs located in active zones may record earthquake history by variations in $^{234}U/^{238}U$ ratio (Osmond and Cowart, 1976).

8.6 Uranium in Speleothem

8.6.1 Sources

U is present in limestones at concentrations generally < 1ppm and so dissolution of bedrock limestone by water rich in CO_2 from the soil zone will cause a corresponding uptake of U. Interbedded shales contain more U, especially if organic compounds are present ('black' shales). U may also be present in overlying fluvial deposits and till, and in localised concentrations associated with vein filling. Allogenic surface waters collected on non-carbonate rocks may initially leach considerable amounts of U, although the decrease in CO_2 content when exposed to the atmosphere will reduce the solubility of the carbonate species and so decrease U concentration.

8.6.2 Uranium Species

As already described, U forms stable soluble anionic complexes with bicarbonate and phosphate ions and these complexes are the dominant species in natural waters. Acidic percolation waters entering limestone may have pH values as low as 3, at which UO_2^{2+}, UO_2F^+, $UO_2F_2^o$ and $UO_2SO_4^o$ become important species (Langmuir and Applin 1977). In addition, U forms insoluble complexes with fulvic acids (ph 6 - 8) and humic acids (pH 4 - 6) but the complexes are soluble at other pH values (Manskaya and Drozdova 1968). Because limestone waters lie in the pH range 6 - 8, uranyl fulvates therefore are unlikely to occur in solution. However uranyl humates are soluble in this range and are most likely to be present when limestone dissolution takes place by the open system process, ie. when limestone is dissolved in the presence of a soil-CO_2 atmosphere. In this situation, the pH of the percolation water will rapidly attain the range 6 - 8 in which both humic acids and uranyl humates become soluble. In the closed system process however, (limestone dissolution without replenishment of CO_2 from the soil) the low pH range before contact with the limestone (pH 3 - 6) prohibits solution of either humic acids or uranyl humates with the result that negligible concentrations of organic-U complexes will be found in solution.

It is not clear how uranium becomes incorporated in speleothem. Direct substitution of U^{6+} (ionic radius = 0.80 Å) for Ca^{2+} (i.r. = 0.99 Å) could be possible from size considerations but charge imbalance would prohibit this. Alternatively, the more common UO_2^{2+} ion is the same charge but its large size would reduce its solubility in calcite. Aragonite can accommodate large ions such as UO_2^{2+} , with greater ease (c.f. incorporation of strontium, Chapter 9) and this is reflected in the higher U concentrations found in aragonitic deposits. An alternative to ion-for-ion substitution is the possibility of adsorption onto, or occlusion within the growing calcite lattice.

Several mechanisms exist that induce coprecipitation of U with $CaCO_3$ in the cave environment. Loss of CO_2 causes uranyl carbonate complexes to dissociate. Fluoride and sulphate complexes become less stable with increasing pH (pH increases as $CaCO_3$ precipitates from solution) and may hydrolyse and precipitate as oxides and hydroxides. Evaporation of water would enhance the incorporation of U that is present in the form of sparingly-soluble organic complexes or in a colloidal state. These conditions can be seen in well-ventilated caves with slow drip-rates in the Canadian Rockies and North-West Territories, where speleothems are often coloured brown due to organic content trapped in the calcite by evaporation.

8.6.3 Previous Speleothem Work

Uranium-series dating of speleothem was first attempted by Rosholt and Antal (1962) using the $^{230}Th/^{234}U$ and $^{231}Pa/^{235}U$ methods (Chapter 2). Cherdyntsev et al. (1965) recognised that the $^{234}U/^{238}U$ method could not readily be applied to speleothem because the isotopic ratio at the time of formation, $(^{234}U/^{238}U)_o$, was unlikely to be constant over the period of growth and could not be simply determined by analysing waters at the same site.

Nguyen and Lalou (1969) found $^{234}U/^{238}U$ ratios to be reasonably constant with time for speleothem from caves in southern France and suggested that, in principle, the $^{234}U/^{238}U$ method could be used to date speleothem older than the limit of the $^{230}Th/^{234}U$ method. Most subsequent studies (Duplessy et al. 1970b, Cherdyntsev 1971, P.Thompson et al. 1975) have shown variable initial uranium isotopic ratios in speleothem dated by the $^{230}Th/^{234}U$ method. P.Thompson et al. (1975) analysed modern drip waters and associated calcite deposits from caves in West Virginia and found not only differences in $^{234}U/^{238}U$ ratios between nearby collection sites but also variation with season.

In spite of these observations, G.Thompson et al. (1975) found $^{234}U/^{238}U$ ages for a Missouri speleothem to be more concordant with stratigraphy than $^{230}Th/^{234}U$ ages and they used this to reject the $^{230}Th/^{234}U$ method. Two principal assumptions made in their work were :

i) a mean value of initial $^{234}U/^{238}U$ derived from analyses of 5 waters in the cave could be used as $(^{234}U/^{238}U)_o$ in the age equation (8.1)

ii) this value was constant over the period of growth of the speleothem (estimated at up to 800 Ka).

The authors admit these assumptions to be rather tenuous but still persist in establishing a case for $^{234}U/^{238}U$ speleothem dating by this method. Harmon et al. (1978c) have strongly criticized this paper and suggest an alternative explanation of the data which shows that the $^{230}Th/^{234}U$ ages may be more valid than those of the $^{234}U/^{238}U$ method.

The work described here was done to investigate spatial and temporal variations of $^{234}U/^{238}U$ ratios in modern speleothem and associated calcite, to attempt to resolve more clearly the validity of G.Thompson's work. Practical limitations in obtaining sufficient data were overcome by development of a simple, compact method of extracting uranium from groundwater.

8.7 Extraction and Analytical Techniques

8.7.1 Previous Work

In most previous studies, trace amounts of U have been extracted from water by coprecipitation with an insoluble hydroxide (eg. $Fe(OH)_3$,

$Al(OH)_3$). After filtration, the carrier hydroxide is removed by solvent extraction in strong acid and the U purified by ion exchange separation. A radioactive tracer is added at the beginning to monitor yield and determine U concentration. The coprecipitation method is laborious when applied to cave studies because of the bulky equipment required and the restricted nature of many cave passageways. Large polythene 'garbage can' collectors (Thompson et al. 1975) are awkward and liable to split during transport. When finally in place they are open to dust and other drip waters. Other alternatives include absorption of U directly from the water onto a $Fe(OH)_3$ impregnated sponge (Lal et al. 1964) and adsorption of U from water at pH 5 by wood charcoal (Nguyen and Lalou, 1969). Thompson (1973a) applied these methods in West Virginia caves but found low extraction efficiency and trace metal contamination in the $Fe(OH)_3$ sponge method, and negligible U adsorption by charcoal.

Veselsky (1974) has reviewed methods of U extraction from natural waters and found that the coprecipitation method often gave poor yields (0 - 50%). He also found that U adsorption on charcoal involved prolonged heating to remove all carbon before analysis, as well as being non-specific in trace element uptake. He suggested that the low yields of the coprecipitation method may be due to incomplete removal of CO_2 during boiling. Optimum extraction efficiency was given by a method involving pre-conditioning a water sample to pH 1 for spike equilibration, adjusting to pH 4 and then adsorbing U on cation exchange resin. Uranium was then eluted by concentrated HCl directly onto anion resin and finally purified by electrolytic deposition.

Industrial methods proposed for recovering U from ore-wash water have included the use of anion exchange resins in the carbonate form to adsorb U from water pretreated with sodium carbonate solution (Shankar et al. 1956). An inverse relationship was found for extraction efficiency versus molarity of Na_2CO_3 (Figure 8.3). U was eluted with 5% NaCl.

Most of the above methods involve pretreatment of the water sample and so are not easily applicable to cave studies. A simple, portable method was needed for concentrating U directly from groundwater, which preferably avoided the transportation and use of hazardous chemicals in caves.

8.7.2 Ion Exchange Extraction

Because karst groundwaters represent an extension of the rising limb of the plot in Figure 8.3 (equivalent to $< 0.2g/l\ Na_2CO_3$), it seemed logical that U could be adsorbed onto exchange resin without pretreatment of the water. A laboratory experiment was designed to test this, using carbonated water (CO_2 bubbled continuously through deionised water) and Analar $CaCO_3$ containing a few milligrams of uranium hydroxide. The hydroxide appeared to dissolve fully with prolonged stirring and passage of CO_2 but after passing the solution through preconditioned anion exchange resin and eluting, no uranium was detected in the eluate. Field tests, however, fully substantiated initial expectations. The laboratory experiment probably failed due to the large concentration of HCO_3^- produced by high PCO_2. The field technique eventually used, allowed all equipment and reagents for a number of sites to be carried in

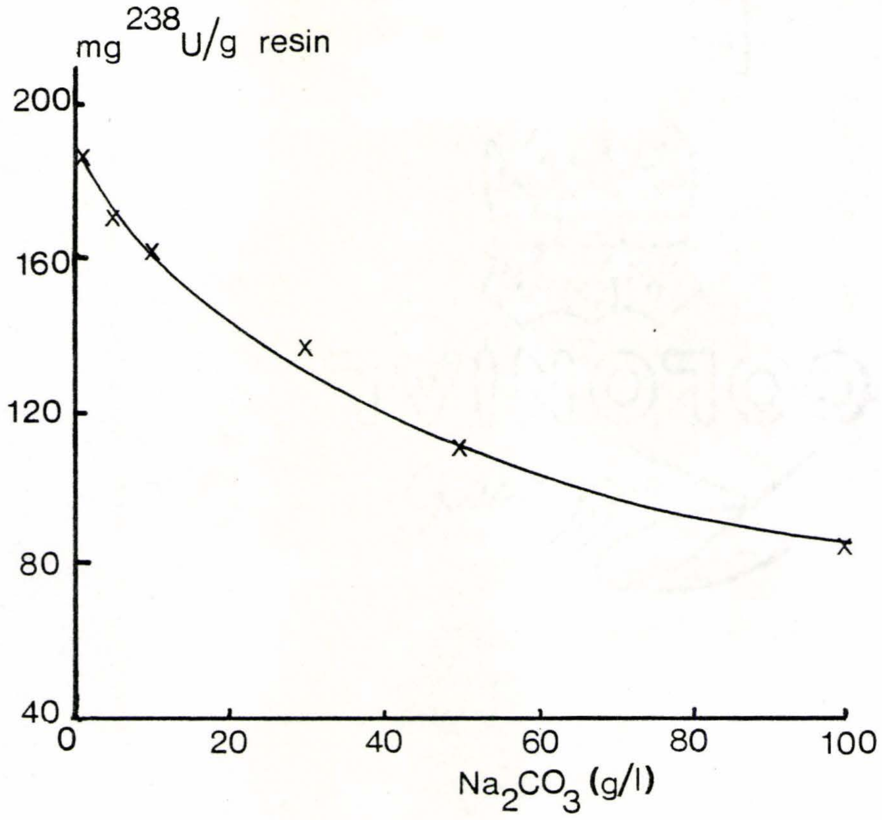

Figure 8.3 Effect of Na_2CO_3 concentration of feed-water on uranium saturation capacity of anion exchange resin (Amberlite IRA-400), from Shankar et al. (1956).

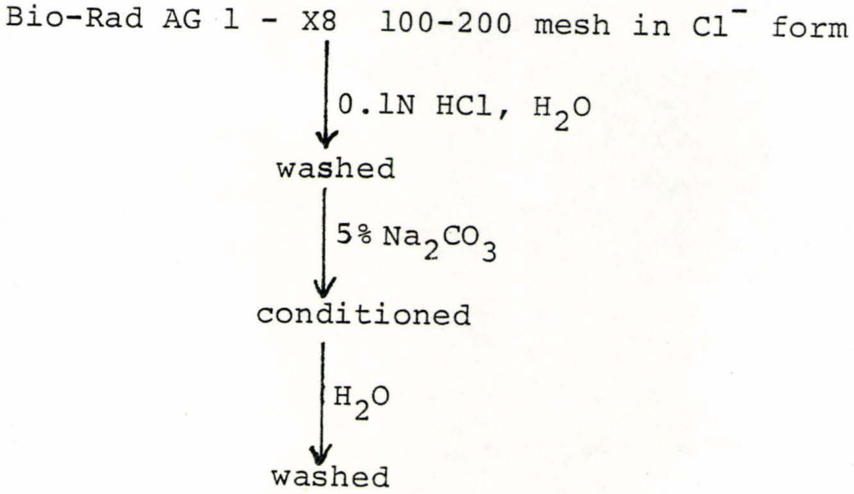

Figure 8.4 Preconditioning procedure for anion exchange resin.

a waterproof metal box, 30cm x 20cm x 10 cm.

8.7.2.1 Procedure and Analytical Details

Anion exchange resins used in this study were preconditioned using the procedure shown in Figure 8.4. During field work, two techniques were used for U extraction from groundwater :

A) to determine $^{234}U/^{238}U$ ratio, U concentration and resin column efficiency: a column was attached to a slowly-dripping stalactite using a clamp and wire hanger (Figures 8.5, 8.6). A rubber tube on the outlet channeled the eluate into a large heavy-gauge polythene bag The volume of water collected was measured and treated as shown in Figure 8.7.

B) to determine $^{234}U/^{238}U$ ratio and approximate U concentration: the ion exchange column alone was suspended under a slowly-dripping stalactite. No attempt was made to collect the water. Drip rates and drip volumes were measured on installation and removal of the column in order to calculate the approximate volume of drip water passed.

When not in use, all columns were stoppered at the top and pinched at the outlet in the presence of some water to prevent the resin from drying out. A 5 - 30g sample of the stalactite or stalagmite was removed for U analysis. Columns were left in place for periods of days to months depending on drip rate and accessibility. The procedure shown in Figure 8.7 was followed for U extraction from the column, effluent water and speleothem. Initially 5% NaCl solution was used for eluting the column but it was found difficult to completely dissolve the

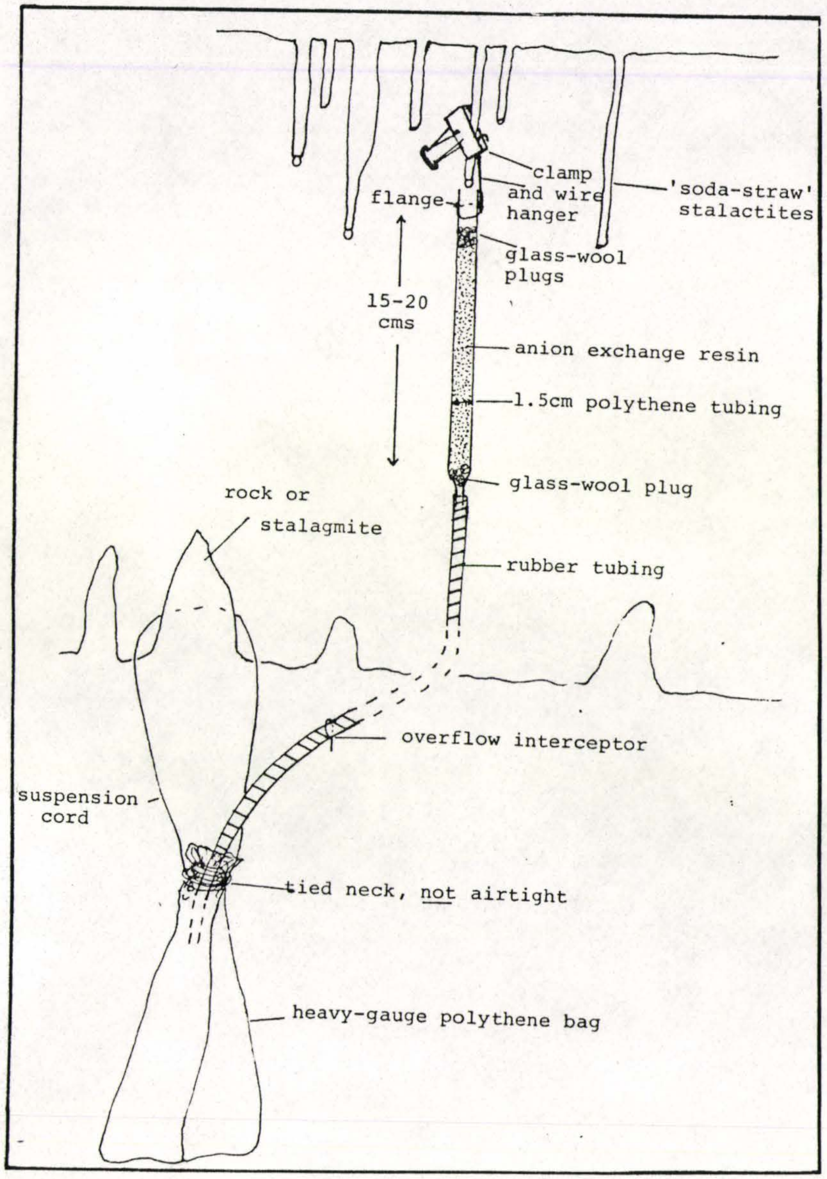

Figure 8.5 Sketch diagram of typical U-sampling apparatus for a stalactite in a cave.

Figure 8.6 Resin column and polythene bag water collector assembly in Castleguard Cave.

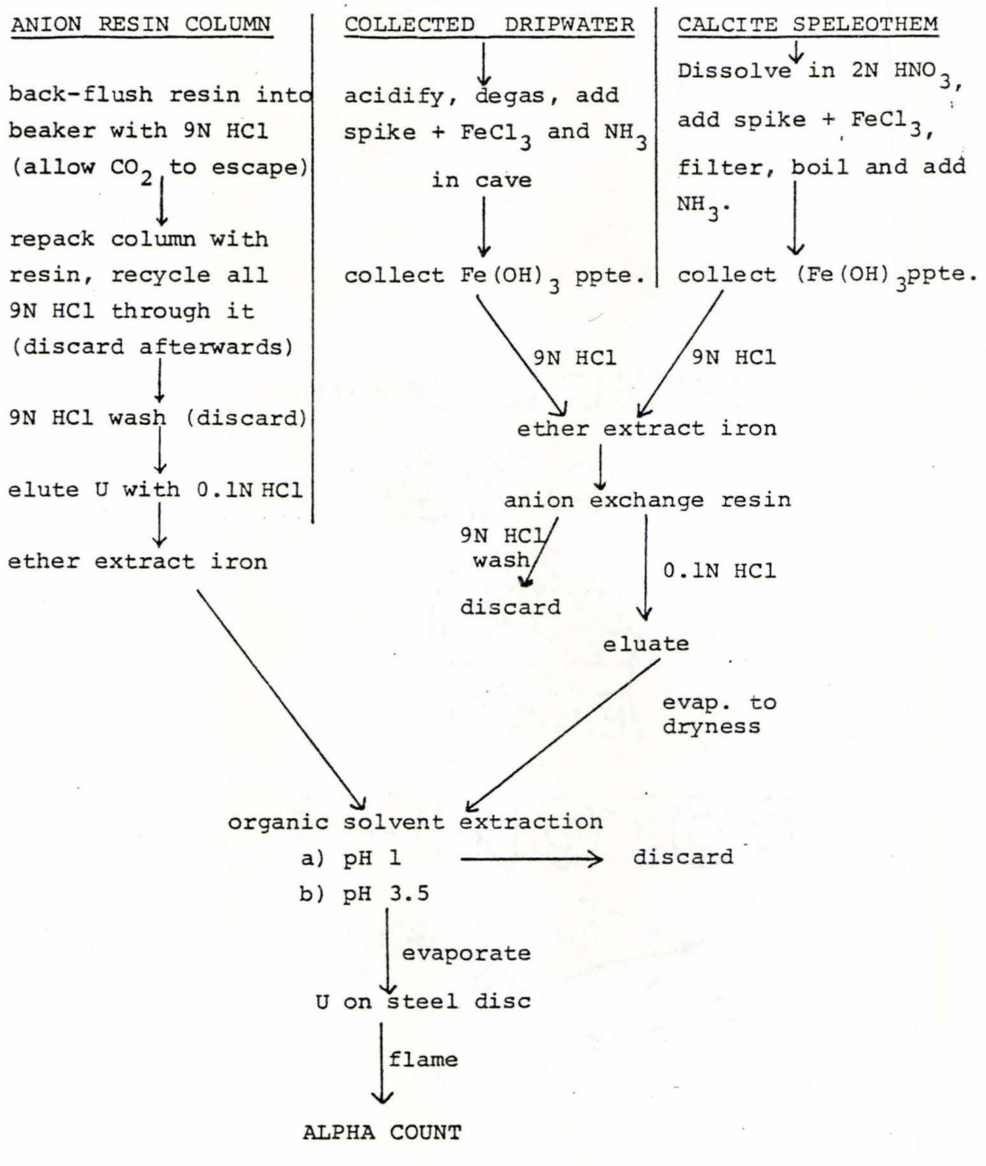

Figure 8.7 Analytical procedure for anion resin, effluent dripwater (collected in bag) and speleothem calcite. Details are given in text and Appendix 1a.

NaCl residue in dilute acid for TTA extraction. Elution with 0.1N HCl avoids this problem because this reagent is completely volatile (Figure 8.7).

However, on occasions a white crystalline residue often remained after evaporating the 0.1N HCl to dryness. X-ray diffraction analysis showed this to be anhydrite. This is difficult to account for because although SO_4^{2-} ions might adsorb on the resin, Ca^{2+} will pass through. One explanation is that the complex $CaSO_4^o$ is retained by the resin owing to its size and dipolar nature. Large quantities of this residue could be removed by further passage through anion exchange resin in 9N HCl.

8.7.2.2 Data Analysis

i) $^{234}U/^{238}U$ ratios are simply determined from the alpha spectra (Chapter 2, Appendix 1b)

ii) U concentration in collected effluent water is :

$$U_e = \frac{^{238}U}{^{232}U} \times B \times \frac{V_s}{V_w} \qquad (8.2)$$

where U_e is the concentration in μg/l of U remaining in the effluent water, ^{238}U and ^{232}U are observed activities, B is the ^{238}U equivalent spike activity constant (Chapter 2), V_s is volume of spike added to effluent (mls) and V_w is volume of collected effluent (litres).
The concentration of U in solution that is extracted by the column (assuming 100% efficient elution and extraction into TTA before

counting) is:

$$U_c = \frac{{}^{238}U}{V_w} \times \frac{1}{E} \times \frac{1}{0.73965} \quad (\mu g/l \text{ of water collected}) \qquad (8.3)$$

where E is α-counting efficiency of the detector (Chapter 2) and 0.73965 dpm is the activity of 1 μg ^{238}U.

Total uranium concentration in the drip water is therefore :

$$U_w = U_c + U_e \qquad \mu g/l \qquad (8.4)$$

Resin column efficiency R is estimated as the relative amounts of U adsorbed on the column and scavenged by coprecipitation :

$$R = \frac{U_c}{U_c + (U_e \times \frac{100}{Y_u})} \times 100\% \qquad (8.5)$$

where Y_u is the yield of U determined from measured ^{232}U spike activity and V_s (Chapter 2). R depends on the presence of other adsorbing ions (Cl^-, SO_4^{2-}, PO_4^{3-} etc.) and whether resin saturation has been reached.

8.7.3 Results

8.7.3.1 Resin Column Extraction Efficiency

Results from seven sites equipped according to procedure 'A' (ie. with collection vessel) are shown in Table 8.1. In most cases

Site No.	Column No.	Location	Duration	Volume of water passed (l)	Uranium Concentrations				$^{234}U/^{238}U$ ratios (±1σ)			Column Efficiency (%)
					column (μg/1)	effluent ppte (μ-/1)	(yield)	calcite (ppm)	column	effluent ppte	calcite	
4	CGA1	Helictite Passage Castleguard Cave Alta.-B.C.	16/4 - 19/4/77	1	1.39	∿ 0	16%	2.3	1.395±0.074	-	1.485±0.046	100
5	CGA2	The Grottos, Castleguard Cave Alta.-B.C.	16/4 - 19/4/77	2	0.74	0.2	38%	0.71	1.502±0.101 **	2.04±0.42 **	1.401±0.035	81
1	AC1	Andy Collins Crystal Onyx Cave, Kentucky.	1/3 - 26/4/76	30	0.43	0.08	25%	0.98	1.213±0.027	2.07±0.31 **	1.094±0.059	84
2	GWC1	Gray's Water Cave, Kentucky	1/3 - 26/4/76	30	0.84	0.34	4%	1.07	1.696±0.028	1.744±0.246 **	1.732±0.032	71
3	GWC2	Gray's Water Cave, Kentucky	1/3 - 26/4/76	10	0.86	0.32	19%	1.12	1.778±0.038	1.232±0.119	1.728±0.044	73
7	N2	Entrance slope Norman Cave W.Va.	5/9 - 13/11/76	25	0.25	0.03	12%	0.48	1.525±0.041	1.164±0.066 **	1.387±0.044	89
10	N5	Mud-floored room Norman Cave W.Va.	5/9 - 13/11/76	∿ 85*	∿ 4.0	0.01	21%	3.19	1.515±0.015	1.459±0.082	1.488±0.018	∿100

* collector overflowed, estimated from drip rate

** < 0.05 μg ^{238}U recovered

Table 8.1 Comparison of U concentrations and $^{234}U/^{238}U$ ratios for U extracted by anion exchange column, $Fe(OH)_3$ precipitate of effluent water from column and calcite speleothem formed from the drip water. Efficiency of U extraction by resin method is given in last data column.

little U is scavenged from the column effluent and the activities measured may be partly due to reagent U. It is difficult to use the reagent blank values determined for age measurements (Table 2.1) to correct for this because the analytical procedures and quantities used are different. In one case however, where > 0.5 μg* U was scavenged, $^{234}U/^{238}U$ ratios are comparable with those found in the speleothem calcite and the resin column eluate.

It can be seen that resin extraction efficiency is high. The quoted figures in Table 8.1 are minimum values for each column because 100% efficiency of all purification processes is assumed in the treatment of the resin column. No measurements of selectivity and breakthrough capacity of the resin for U adsorption have been made but some indication of its efficiency is given in sample N5 which had adsorbed about 250 dpm (= 340μg) ^{238}U for an approximate resin volume of 20mls. Resin capacity is 1.4 meq/ml and if the most abundant U species is $\left[UO_2(CO_3)_3\right]^{4-}$, the resin was approximately 20% saturated with respect to U. A column from the same site (results not reported here) which had been passing drip water for some months was almost 40% saturated with U.

8.7.3.2 U Concentration and Isotopic Ratios

Twenty-eight calcite-water pairs have been collected and analysed from caves in Kentucky, West Virginia, the Canadian Rockies and the Craven area of Northern England. Of these, seven were fitted with collecting bags as described above and the remainder were free-draining columns of

---

* 0.5 μg ^{238}U is the minimum quantity that can be counted with reasonable precision (~ 0.1 cpm).

type B. A sample of the recently deposited carbonate was taken with each column (either stalactite tip or stalagmite top, depending on availability and size). U concentrations and isotopic ratios are listed in Table 8.2 and ratios are represented graphically in Figure 8.8. It was not always possible to determine the volume of water passed because drip rates often varied, drip volume was not always measured (0.1ml/drop was assumed in this case) and with time, swelling of the resin or calcification of the glass wool plug decreased permeability and so caused the column to overtop and lose drip water.

U isotopic ratios were found to range between 0.77 and 1.8 in the caves studied, and in one cave, for samples taken along 1km of passageway, ratios varied between 0.77 and 1.6.

8.7.3.3 Temporal Variation of $^{234}U/^{238}U$ Ratio

Two sites in White Scar Cave (England) had fairly constant drip rates and adequate U concentration in the drip water. Ten columns were placed here over the period August 1976 to September 1977 (with the assistance of Dr.R.Halliwell, University of Hull). They were subsequently eluted and analysed in the McMaster laboratory. The results shown in Figure 8.9 suggest that there may be an asymmetrical annual variation in $^{234}U/^{238}U$ ratio with a late spring low and late summer high. The total observed range in isotopic ratio at both sites is about 0.13. This range may be partly explained by statistical counting error, although the same trend and magnitude of variation is seen at both sites.

Table 8.2 Results of analysis of eluates of anion resin columns (≡ drip waters) and associated speleothem from caves in N.America and England.

				DRIP WATER ANALYSIS				SPELEOTHEM ANALYSIS			
Site No.	Column No.	Location	Duration	Measured drip rates (secs)	Vol. of water passed (l.)	Conc^{n}. of U in water (μg/l)*	$^{234}U/^{238}U$ of drip water	Type**	Chemical Yield (%)	U conc^{n}. (ppm)	$^{234}U/^{238}U$ of calcite
6	CGA3	Grottos, Castleguard Cave.	16/4 - 19/4/77	N.D.	N.D. (low)	-	1.426±0.057	c	32	1.3	1.324±0.072
8	N3	Butterscotch Rm. Norman Cave	5/9 - 13/11/76	1/0.75s	> 100	-	1.559±0.022	c	41	0.44	1.919±0.064
9	N4	1.5m from N3	5/9 - 13/11/76	1/7.5s	35	0.72	1.453±0.027	g	52	0.24	1.375±0.056
11	N6	Mud-floored ch. Norman Cave	5/9 - 13/11/76	1/90s	6.6	1.46	1.463±0.036	c	58	3.4	1.364±0.021
12	CPA1	2nd pitch, County Pot, England	22/7 - 17/8/76	1/13, 18, 15s	14	1.90	1.331±0.025	c	56	1.12	1.171±0.080
13	CPA2	Trident Pass. County Pot, Eng.	22/7 - 17/8/76	variable (<1/60s to dry)	-	-	1.253±0.040	c/f	37	1.94	1.231±0.039
14	CPA3	P.J., County Pot England	26/7 - 17/8/76	1/8.5, 4s	26	0.05	1.467±0.054	g	38	1.97	1.493±0.037
15	IA1	Oxbow, Ingleboro' Cave, Eng.	24/7 - 22/8/76	1/35s	7.2	1.67	0.770±0.025	c	43	0.76	0.831±0.048
16	IAB1	2m from IA1	3/9 - 18/9/77	1/12s	10	0.38	0.855±0.046	c	39	0.84	0.812±0.032
17	IA2	2nd Gothic Arch Ingleboro' Cave	24/7 - 30/7/76	1/2.5s	20.7	0.12	1.367±0.034	c	37	0.15	1.381±0.081
17	IA4	replicate of IA2	30/7 - 22/8/76	1/3.5s	66	0.07	1.335±0.035				
19	IA3	~5m from IA2	24/7 - 22/8/76	1/2.5, 3s	83.5	0.08	1.254±0.030	c	43	0.12	1.224±0,062
18	IA5	Giants Hall, Ingleboro' Cave	30/7 - 22/8/76	1/12, 15s	14.7	0.04	1.595±0.124	f	66	0.08	1.420±0.050
20	IA6	~3m from IA3 ~8m from IA2	30/7 - 22/8/76	1/10, 11s	18.1	0.20	1.484±0.077	c	50	0.17	1.558±0.158
21	IA7	the Abyss, Ingleboro' Cave	9/8 - 22/8/76	1/10, 12s	12.3	0.08	1.596±0.086	c	25	0.07	1.491±0.126
23	WSA2B	~50m upst. of show cave, White Scar Cave, Eng.	27/8 - 31/10/76	1/5.5s & flooded	>100	-	1.035±0.078		< 0.5 μg recovered		
22	WSA3A	~100m upstr. of WSA2B	25/7 - 27/8/76	1/4s	64.2	0.25	1.622±0.023	f	60	0.24	1.484±0.087
22	WSA3B	replicate of WSA3A	27/8 - 31/10/76	1/4, 22s	I	-	1.550±0.021				
22	WSA3C	replicate of WSA3A	31/10- 22/1/77	1/22, 46s	I	-	1.549±0.029				
22	WSA3D	replicate of WSA3A	22/1/77 - not known	1/46s	I	-	1.491±0.029				
24	WSA4A	2nd Lake, White Scar Cave, Eng.	19/7 - 31/10/76 (or22/1/76)	N.D.	-	-	1.749±0.021	c	88	0.33	1.683±0.035
24	WSA4B	replicate of WSA4A	not known - 4/9/77	N.D.	-	-	1.586±0.180				
26	WSA6	~150m upstr. of WSA2B	9/8 - 27/8/76	1/5.5, 6, 8s	26	0.19	1.487±0.039	c	10	0.53	1.683±0.145
25	WSA5A	~100m upstr, of WSA2B	9/8 - 27.8/76	1/4, 5, 7.5s	27.4	1.07	1.397±0.020	g	30	0.77	1.580±0.079
25	WSA5B	replicate of WSA5A	27/8 - 31/10/76	1/7.5, 5.5s	85	0.30	1.494±0.023				
25	WSA5C	replicate of WSA5A	31/10/76- 22/1/77	1/5.5, 2.5s	> 100	< 0.25	1.432±0.028				
25	WSA5D	replicate of WSA5A	22/1 - not known	1/2.5s -	I	-	1.370±0.015				
25	WSA5E	replicate of WSA5A	not known - 4/9/77	- 1/8s	I	-	1.486±0.040				
25	WSAXB	replicate of WSA5A	4/9 - 18/9/77	1/8, 10s	13.5	0.87	1.413±0.036				
27	IPA1	Roof tube, Ibbeth Peril Cave, Eng.	21/7 - 22/8/76	variable	I	-	1.015±0.029	c	47	0.63	0.965±0.022
28	IPA2	20m upstr. IPA1	9/8 - 22/8/76	1/5s	22.5	0.14	1.033±0.033	c	22	0.48	1.045±0.061

N.D. = Not Determined   I = Indeterminate   * assumes 100% efficiency of extraction from column and in plating out

** c = stalactite, g = stalagmite, f = flowstone

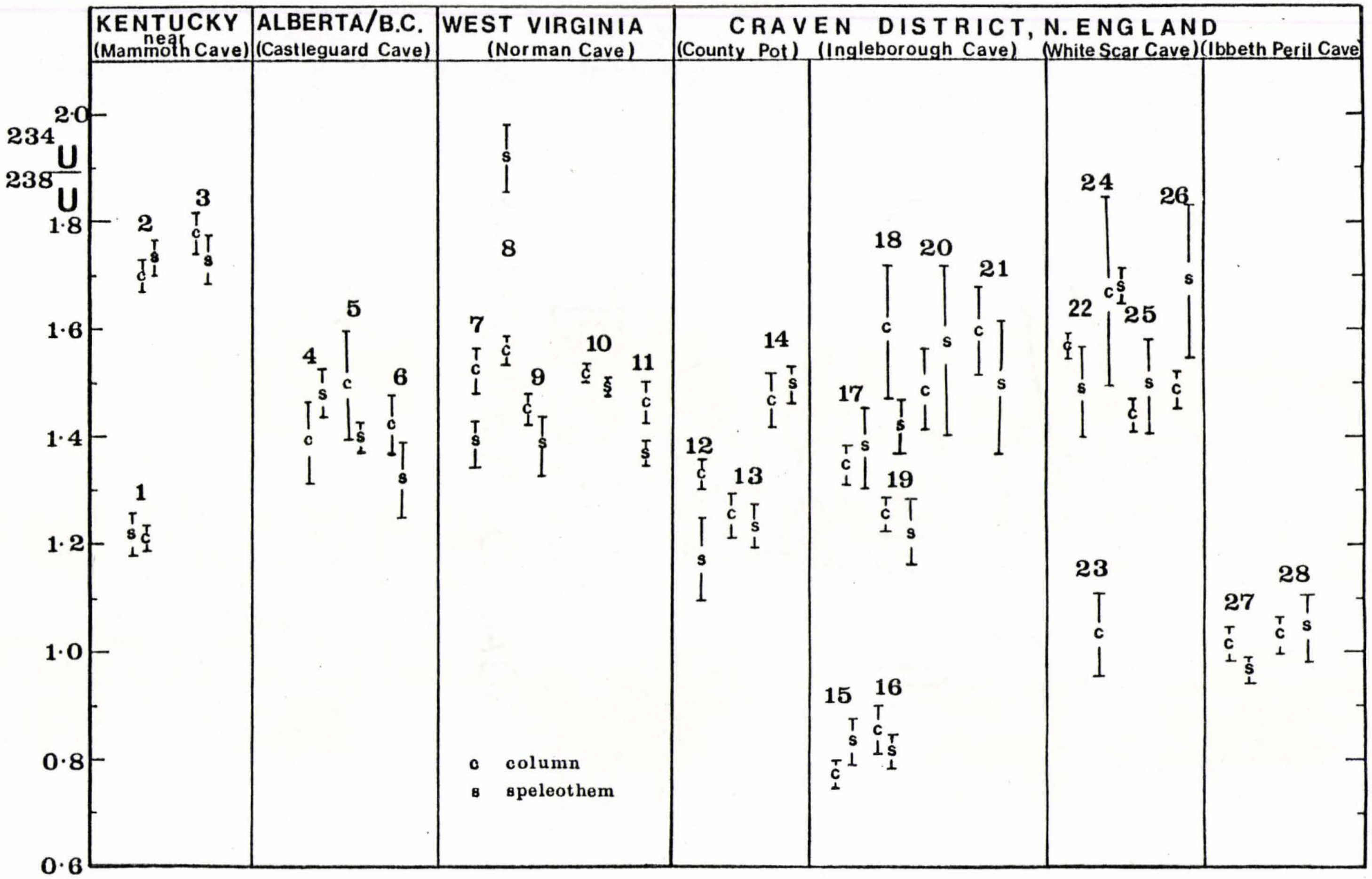

Figure 8.8 Diagrammatic representation of results in Table 8.2 of $^{234}U/^{238}U$ analyses of 28 calcite-water pairs, (with ±1σ error limits as vertical lines) for samples where > 0.5 μg ^{238}U was recovered.

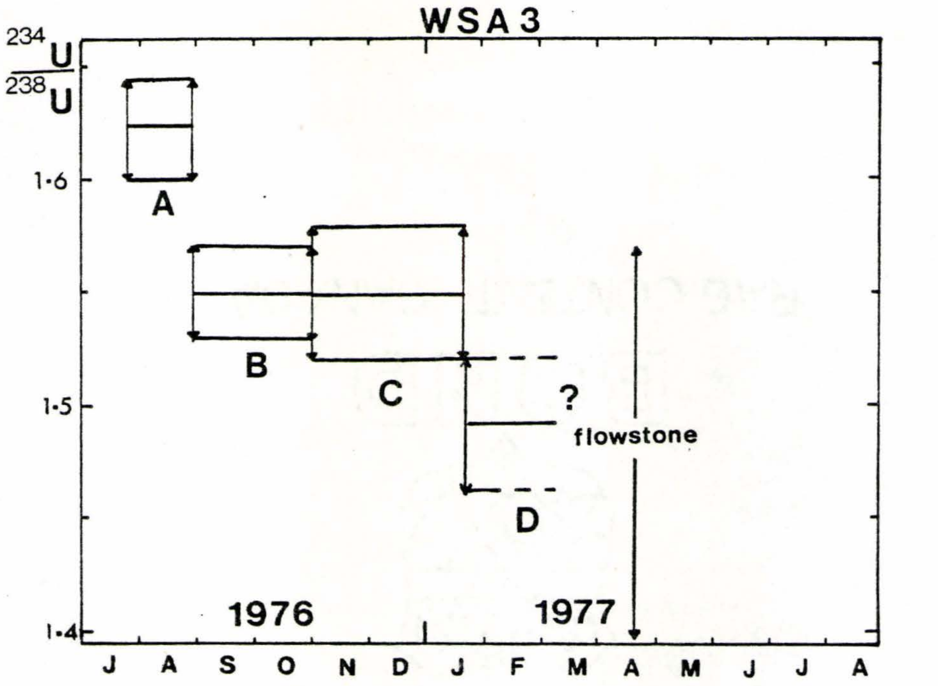

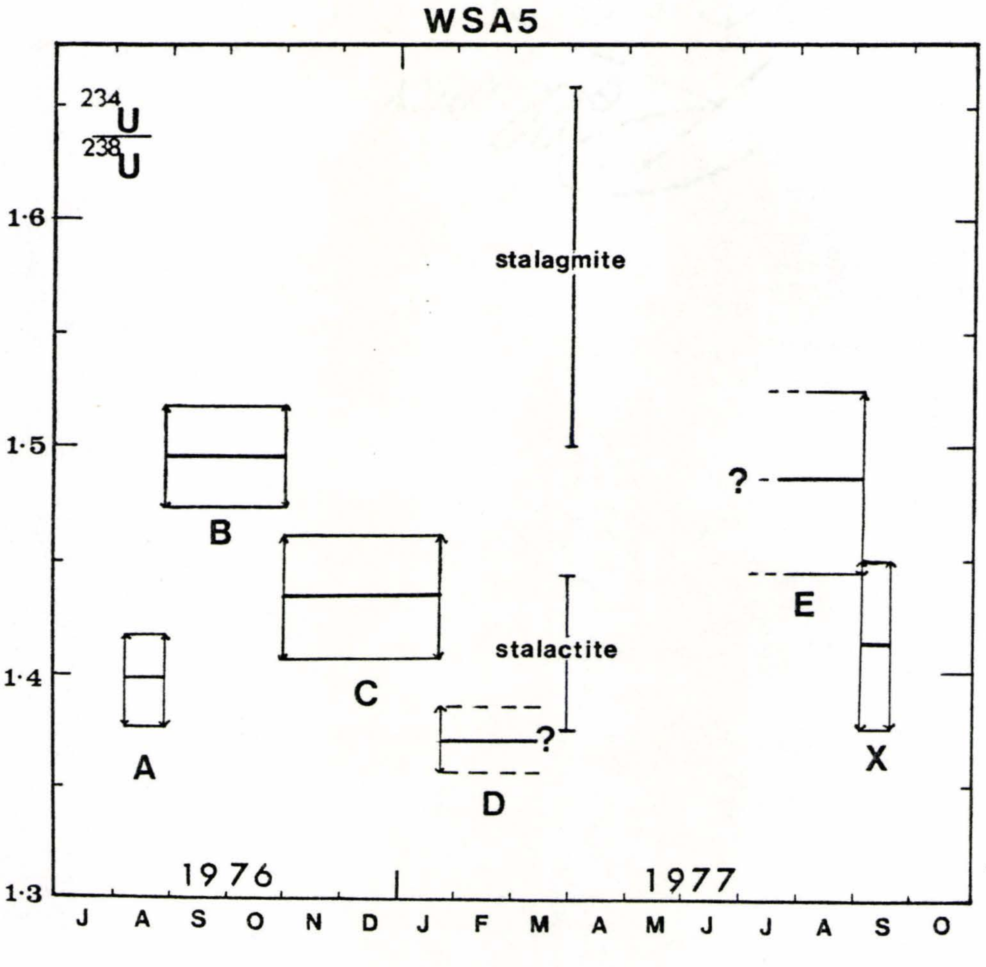

Figure 8.9 Variation of $^{234}U/^{238}U$ ratios with time for two drip sites in White Scar Cave, N.W.England. Data for each are given in Table 8.2.

8.7.3.4 Discussion

Five speleothem-column pairs (nos. 7,8,11,12 and 26) show no overlap of 1σ errors in Figure 8.8. Of these, four overlap within 2σ limits and one lies well outside even 3σ limits (no. 8). This distribution is comparable to that expected for a normal distribution. It is therefore concluded that $^{234}U/^{238}U$ ratios in groundwater (ie. measured from U collected by the above process) are faithfully reproduced in the associated carbonate deposits. To some extent this is a surprising conclusion because :

i) it might be expected that organically-bound U may differ isotopically from inorganic U, and varying proportions of organic and inorganic U may be incorporated in the speleothem depending on the depositional process involved,

ii) the water analysed is collected over relatively short-term periods (up to three months), whereas the piece of speleothem analysed may have taken hundreds of years to grow.

Because of the ability of anion resin to adsorb large dipolar organic molecules as well as anionic species, it is difficult to determine from results described here the relative proportions of organic and inorganic U species present in solution. The close similarity between speleothem and drip water ratios suggests the following possibilities:

i) the same proportion of organic to inorganic U species are adsorbed by the resin as are incorporated in the speleothem,

ii) $^{234}U/^{238}U$ ratios in organic and inorganic species are the same,

iii) inorganic U complexes are the dominant species in most drip waters studied here; organic forms only become significant when organic-rich horizons are drained (eg. peat bogs, black shales etc.).

The most significant finding of this study is the unpredictability of $^{234}U/^{238}U$ ratios over short distances in the same cave. The most striking example of variability, Ingleborough Cave, shows a spread of ratios from 0.77 to 1.6 within 1km of cave passage. Of these, sites 17, 18 and 20 are all within 5m of each other and yet show a range of 1.22 ± 0.06 to 1.48 ± 0.08, values which only overlap at the 2σ limit. However, some results do indicate a general invariance of $^{234}U/^{238}U$ ratio over short distances. Sites 15 and 16 in Ingleborough Cave are about 2m apart yet have comparable calcite and drip water ratios, and sites 27 and 28 in Ibbeth Peril Cave, although about 20m apart, also have similar ratios. Sites 2 and 3 in Gray's Water Cave are $\sim$1m apart and were deliberately set at this distance to check on reproducibility as they appeared to be fed by the same groundwater source. They cannot therefore be considered as evidence for constancy of ratio between sites. The three samples from Castleguard Cave were spread out over about 4kms of passageway and yet all $^{234}U/^{238}U$ ratios overlap within 1σ limits.

The variable nature of these results may be due to a number of factors :

i) all ratios <u>do</u> vary widely from site to site and insufficient analyses have been made to reveal this in all caves,

ii) the proportion of organic to inorganic uranium species in solution may vary from cave to cave,

iii) isotopic ratios may depend on degree of weathering of overlying bedrock or of the uranium source material, and this is likely to vary throughout the cave.

Only a much more detailed study than that presented here will show which factors are significant.

8.8 Conclusions

The small variation of $^{234}U/^{238}U$ in groundwater with season agrees with the general conformity seen between drip water and speleothem analyses. A ratio that varies by large amounts depending on season would give rise to more discrepancies between the 'time-averaged' speleothem value and the spot water analysis.

The groundwaters analysed in this study fall mainly within the first category of Osmond and Cowart (1976) ie. open system, oxidised aquifer water. Those showing deficiency in ^{234}U, from Ingleborough Cave, are more typical of the third category which describes closed-system aquifers, but in this case it is unlikely that the weathering horizon has lowered appreciably to cause remobilization of ^{238}U-enriched deposits. It is more probable that previously weathered bedrock is now being totally removed in solution.

This work indicates that adjacent but hydrologically-distinct drip waters may have considerably different U isotopic ratios. By extension therefore, it is extremely unlikely that $(^{234}U/^{238}U)_o$ ratios of fossil speleothem will bear an *a priori* relationship to ratios in modern drip waters located either in the same cave or at the same site. The observation, by G.Thompson et al. (1975) that this assumption can be made when using the $^{234}U/^{238}U$ dating method, is therefore invalid. The stratigraphic agreement obtained for speleothem ages determined in this way, is probably fortuitous.

CHAPTER 9

TRACE ELEMENT GEOCHEMISTRY OF SPELEOTHEM

Introduction

Trace metals can be incorporated in a calcite speleothem in several ways:

- i) by occlusion of particulates in interstices between growing calcite crystals,
- ii) by adsorption onto the surface of growing crystals,
- iii) by direct substitution for Ca^{2+} ions.

The study of detritus-free speleothems avoids problems of determining trace element contribution from particulate sources. The distinction between adsorbed and substituted trace elements is less clear and becomes very important in the case of cations of limited solubility in limestone groundwaters (eg. Fe, Mn) as described in the previous section. Except **for** rare cases involving occurences of low Eh, low pH groundwater it is probable that Fe and Mn in most speleothem is generally incorporated as adsorbed or detrital oxides, hydroxides, carbonates and organic compounds. Substitution for Ca^{2+} by a trace metal cation is the simplest to understand and quantify and therefore has been the subject of most intense investigation in previous work.

The degree of incorporation of a trace element in a solid phase relative to its concentration in a co-existing liquid phase is known as the partition coefficient. Partition coefficients are often found to be temperature dependent and much work has been done in igneous geochemistry to determine them for trace element partitioning between melt and crystalline phases of magmas and hydrothermal fluids. They can be used to determine temperature of crystallization, initial composition of melt, rate of cooling, magma origin and number of pulses of magma into a magma chamber (McIntyre 1963). There have been relatively few low temperature studies until recently when interest in their use as paleothermometers and salinometers for the surface environment has greatly increased.

In the same way that ^{18}O distribution between calcite and water in speleothem growth can be used as an indicator of past temperature, so might certain trace metals which substitute directly for Ca^{2+} ions and whose partition coefficients are temperature dependent.

Theoretical aspects of trace element substitution are considered in this chapter with emphasis on their application to paleotemperature determination in speleothem. Results of several determinations of distribution coefficients of magnesium and strontium from analysis of growing speleothem and associated drip water are presented and trace element analyses of a fossil speleothem are compared to a stable isotope profile determined previously.

9.1 Theory

9.1.1 Homogeneous Distribution

Substitution of a trace metal M in a calcium carbonate lattice :

$$M^{2+} + CaCO_3 \rightleftharpoons MCO_3 + Ca^{2+} \qquad (9.1)$$

may be described by the partition coefficient k :

$$k = \frac{a_{M^{2+}(\text{solid})}}{a_{M^{2+}(\text{liquid})}} \tag{9.2}$$

where $a_{M^{2+}}$ is the activity of M^{2+} in the relevant phase.
Generally, for very dilute solutions, Henry's Law applies, and the activity is equal to the mole fraction (x) so that

$$k = \frac{x_M(\text{solid})}{x_M(\text{liquid})} \tag{9.3}$$

This is known as the Berthelot-Nernst relationship.
It is generally more useful to normalize k with respect to concentration of the element it is replacing (Ca), and in this case it is referred to as the distribution coefficient D :

$$D = \frac{M_s/Ca_s}{M_l/Ca_l} \tag{9.4}$$

This relationship describes the distribution of trace element between solid and liquid phases for equilibrium deposition. This form of the partition ceofficient is more useful because when $D > 1$, enrichment of M in the solid phase is found, and if $D < 1$, then M preferentially remains in solution. D is analogous to α, the fractionation factor for ^{18}O between calcite and water.

The chemical potential (μ) of trace element M in phases 1 and 2 is given by :

$$\mu_1 = \mu_1^o + RT \ln x_1 \tag{9.5}$$

and

$$\mu_2 = \mu_2^o + RT \ln x_2 \tag{9.6}$$

where μ_i^o is the chemical potential of the trace element in its standard state in phase i (ie. at infinite dilution).

At equilibrium :

$$\mu_1 = \mu_2 \tag{9.7}$$

and therefore :

$$\mu_1^o - \mu_2^o = RT \ln \frac{x_2}{x_1} \tag{9.8}$$

From equation (9.3) :

$$\frac{\mu_1^o - \mu_2^o}{RT} = \ln k \tag{9.9}$$

ie. if there is a finite difference between μ_1^o and μ_2^o then k (or D) will vary with the inverse of temperature.

9.1.2 Heterogeneous (or Logarithmic) Distribution

A special case of trace element partitioning occurs when a crystal is growing in a closed system, rapidly enough that equilibrium between the whole of the crystal and the solution cannot be maintained. In this case the concentration of trace elements in solution and solid will change with time, and is described by the logarithmic Doerner-Hoskins relationship :

$$\ln \frac{(M_l)_i}{(M_l)_f} = \lambda_M \cdot \frac{(Cr_l)_i}{(Cr_l)_f} \qquad (9.10)$$

where i = initial and f = final concentrations in the liquid phase (l) of trace element and (M) major (or carrier) element (Cr). λ_M is the distribution coefficient for logarithmic partitioning. If the initial mole fraction of the cation is unity (ie. $x_i = 1$) then equation (9.10) simplifies to :

$$\ln \frac{1}{x_M} = \lambda_M \cdot \ln \frac{1}{x_{Cr}} \qquad (9.11)$$

For infinitesimally-slow precipitation $\lambda = D$, but if the solution becomes supersaturated the calculated value of λ (referred to as λ') is only an apparent distribution coefficient and λ' is either $> D$ if $D_{TE} < 1$ or λ' is $< D$ if D_{TE} is > 1 (TE = trace element).

Deposition of speleothem tends to follow the logarithmic distribution law because solution volume is not infinite and concentrations of trace and carrier element in solution will change appreciably during the precipitation process. Re-equilibration between the precipitate and the same solution from which it was formed cannot occur because the solution is immediately removed from the precipitate by gravity as the water droplet flows along the speleothem. However some equilibration may take place between the precipitate and the next droplet depending on the relative rates of precipitation (speleothem growth rate) and diffusion of cations in the precipitated calcite.

Factors affecting trace element composition of speleothem are considered in greater detail following a review of determinations of distribution coefficients of trace elements in calcium carbonate.

9.2 Previous Work

9.2.1 Experimental Determination of D

Distribution coefficients have been measured in the laboratory by techniques which involve the precipitation of $CaCO_3$ and coprecipitation of added trace elements. A summary of experimental determinations of D for Mg, Sr, Zn, and Mn is given in Table 9.1. Although many of these results were determined from the logarithmic distribution law (as λ), full equilibrium conditions have been assumed by their authors and they are reported here as D.

9.2.1.1 Strontium

Generally good agreement is seen between results for Sr partition in both calcite and aragonite except for the replacement method of Katz et al. (1972). Here distribution coefficients for calcite are significantly lower than those determined by direct precipitation methods (Holland et al. 1964a, Kinsman and Holland (1969), Klötzer and Levi (1966). Katz argues that his results are more realistic since they are less

EXPERIMENTAL DETERMINATIONS

Author	Trace Element	Method of $CaCO_3$ formation	Temperature (^0C)	Calcite or Aragonite	D_M
Holland et al. (1964a)	Sr	i) CO_2 addition to ammoniacal $CaCl_2$	96 - 100	C	0.076
		ii) CO_2 loss from ammoniacal $CaCl_2$		A	7.8
Kinsman and Holland (1969)	Sr	addition of Na_2CO_3 to $CaCl_2$ solution	16	A	1.17
			80	A	0.88
			96	A	too variable
Klötzer and Levi (1966)	Sr	" "	90	A	0.75
			20	C	0.19
Bodine et al. (1965)	Sr	" "	20	C	0.13
			100	C	0.07
			150	C	0.065
			> 150	C	rises slowly
Katz et al. (1972)	Sr	" "	40	C	0.055
			98	C	0.058
Joshi (1960)	Sr	-	25	C	0.14
Katz (1973)	Mg	recrystallization of aragonite with $CaCl_2$/ $MgCl_2$	25	C	0.057
			35	C	0.068
			50	C	0.078
			70	C	0.097
			90	C	0.116
Winland (1969)	Mg	$NaHCO_3$+ $CaCl_2$ with Mg and degassing of sat. $CaCO_3$ soln.	20	C	0.020
Füchtbauer and Hardie (1976)	Mg	Na_2CO_3 addition to $CaCl_2$/$MgCl_2$mixtures	50	C	0.046
			28	C	0.033
			13.5	C	0.025
Tsusue and Holland (1966)	Zn	hydrolysis of Ca org. salt	167	C	57
			167 (+1M NaCl)	C	1.3
			167 (+4M NaCl)	C	0.11
			250	C	3.1
			90	C	230 - 440
			50 (+4M NaCl)	C	12 - 19
Crocket and Winchester (1966)	Zn	CO_2 degassing of sat. $Ca(HCO_3)_2$	25	C	5.7
			35	C	5.2 - 4.1
			50	C	3.2
Dardenne (1967)	Zn	-	28 - 30	C	5.56
			28 - 30	C	5.50
Bodine et al. (1965)	Mn	hydrolysis of org. salt	40	C	16.2
			325	C	2.0
Michard (1968)	Mn	Ca and Mn + $NaHCO_3$soln.	25	-	5.4
FIELD DETERMINATIONS					
Holland et al. (1964b)	Sr	cave speleothems and waters	25	C	0.13 - 0.22
			25	A	1.00
Michard (1971)	Sr	cold-spring travertines	20	C	0.40
Ichikuni (1973)	Sr	hot-spring travertines	45	C	0.21
			40.5	C	0.27
Michard (1971)	Mg	cold-spring travertines	20	C	0.028
Ichikuni (1973)	Mn	hot-spring travertines	45	C	10
			40.5	C	18
Michard (1971)	Cu	cold-spring travertines	20	C	0.35
	Zn	" "	"	C	3.5
	Ni	" "	"	C	0.65

Table 9.1 Summary of experimental and field determinations of distribution coefficients of trace metals (D_M) with $CaCO_3$.

dependent on the kinetics of precipitation than in the direct method and uses this distribution coefficient to explain the anomalously low concentration of Sr in ancient limestones when compared to that expected from a k_{Sr} value of 0.14 at 25°C. His value of k_{Sr} (of about 0.05) shows that recrystallization of aragonitic limestones can occur in marine conditions without necessarily invoking freshwater diagenesis. The distribution coefficient for aragonite appears to be moderately temperature dependent, but for calcite little temperature dependence seems evident.

9.2.1.2 Magnesium

Mg is often found in high concentrations in calcite although it has a fairly low distribution coefficient. It shows a positive correlation with temperature and appears to be independent of Ca^{2+} and NaCl concentration in solution (Katz, 1973). Windland (1969) determined a value of D_{Mg} of 0.02 at 20°C but Katz (1973) has criticized Windland's assumption of homogeneous distribution and suggests that recrystallization via an aragonite intermediate may have caused this low value of D_{Mg}. Recently however, Füchtbauer and Hardie (1976) have determined values of D_{Mg} comparable to Windland's and with a temperature dependence similar to that of Katz.

9.2.1.3 Zinc

Some conflict in results is seen between the papers published so far. Tsusue and Holland (1966) find D_{Zn} to have a strong negative correlation with temperature whereas Crocket and Winchester (1966) find only a low negative correlation and widely different values of D_{Zn} (calcite) at the same temperature. (Values determined by Dardenne (1967) closely match those of Crocket and Winchester). As a possible explanation for anomalously high D_{Zn} values Crocket and Winchester cited occlusion of Zn by imperfect surface layers formed by rapid precipitation, not given chance to re-equilibrate and slightly recrystallize to remove the excess. Surface occlusion and ion exchange were found to be significant factors in the coprecipitation of Zn with calcite.

9.2.1.4 Manganese

Mn incorporation in calcite appears to exhibit a strong inverse correlation with temperature (Bodine et al. 1965) whereas Michard's result (1968) suggests a direct correlation.

9.2.2 Field Measurements of D

Determinations of D for freshwater carbonate deposits are also shown in Table 9.1. The measurements of D_{Sr} given here are higher than the experimental value given by Katz et al. (1972).Ichikuni (1973) suggests that higher values for D in thermal waters could be explained by the presence of divalent cations smaller than Ca^{2+} (eg. Mn^{2+}), which by their competition "affect the partition of Sr between calcite and solution" and D_{Sr} is "increased by the presence of the smaller cations in a small excess of Sr". Alternatively non-equilibrium deposition from supersaturated solutions could increase the apparent D_{Sr} but this is discounted by the fact that D_{Mn} determined on the same samples is comparable to the (equilibrium) value of Bodine et al. (1965).

Much work has been done on the incorporation of trace elements (especially Sr and Mg) in marine carbonates, particularly with a view to determining paleoenvironmental and diagenetic changes. There is considerable disagreement in the literature as to whether the Mg/Ca ratio of marine carbonates is dependent on water depth, salinity, growth rate, etc. Several authors have indicated the negative correlation of Sr and the positive correlation of Mg with temperature, (Pilkey and Hower 1960, Lerman 1965, Benson and Matthews 1971, Weber 1973, Füchtbauer and Hardie 1976). Kolesar (1978) however, has recently shown that Mg variations in coralline algae are controlled primarily by changes in growth rate, not temperature,due to physiological characteristics of Ca and Mg uptake from seawater. Studies of trace element partitioning in the marine environment are more complex than for freshwater deposits because of the added effects of salinity, individual biogenic characteristics and the problem of recrystallization of aragonite to calcite. For these reasons, trace element content of marine carbonates is seldom applied directly to paleotemperature studies.

9.2.3 Speleothem Work

Holland et al. (1964b) observed that $CaCO_3$,deposited either as calcite or aragonite in a cave environment,contained concentrations of Sr in accordance with their published values of D_{Sr}. Harmon (1975) has analysed variations in Mg, Sr, Fe, Mn, Zn, and Cu for growth axes of two speleothems (one speleothem for Cu) from N.American caves to assess the use of trace elements as paleotemperature indicators. Large fluctuations (up to 10-fold) were observed in trace element abundances but neither profile showed a statistically significant correlation with its oxygen isotope profile. Some trace elements did however show a sympathetic relationship to one another (eg. Mg - Sr).

Johnson (1979) has recently concluded an investigation into variations of Mg and Sr in speleothems and the paleoclimatic significance of these variations. Her study was initiated after some preliminary observations from analyses made as part of this work. Her findings are summarized below :

1) fossil speleothem from England, Vancouver Island and West Virginia showed a range in concentration of Mg from 300 to > 3000 ppm and of Sr from 10 to 400 ppm.

2) Mg usually increases along a growth layer (ie. in the direction of flow of water). Sr is less predictable and in various instances showed increasing, constant or decreasing values along a growth layer. Constancy of Mg/Sr ratio along a growth layer was interpreted as indicating equilibrium deposition of the trace elements from the drip water.

3) Mg concentration at a particular site along a growth layer could be used as an indicator of the maximum amount of Ca precipitated from solution down to that point.

4) speleothems known to have grown over a warming period (eg. 12 to 5 Ka) failed to show any clear trend of Mg, Sr, or Mg/Sr, which might indicate their usefulness as a paleothermometer.

The distribution of trace elements in speleothem is considered in greater detail below.

9.3 Factors Affecting the Trace Element Content of Speleothem

9.3.1 Temperature of Deposition

As shown above, some distribution coefficients are found to be temperature dependent such that their concentration in calcite varies inversely (Zn, Mn) or directly (Mg) with temperature of formation. Zn and Mn are generally of low abundance in speleothem (< 50 ppm, Gascoyne 1977b) and are difficult to determine precisely. Mg however, is one of the most abundant trace elements in calcite (from 0.1% to 6%, Gascoyne 1977b) and can be precisely determined even at concentrations < 0.1%.

The temperature dependence of D_{Mg} has been reported as $0.0009/^{o}C$ (from Katz 1973), which, for a speleothem of 500 ppm Mg at $10^{o}C$, corresponds to an increase of about 10 ppm $Mg/^{o}C$ rise in temperature. Taking into account only the analytical error associated with determination by atomic absorption spectrophotometry (5 - 10%), the precision of temperature determination by this method is about $\pm 3^{o}C$. Even lower precision is likely if Füchtbauer and Hardie's (1976) value of $0.0006/^{o}C$ is used. A glacial/interglacial climatic transition should, however, be clearly seen because Mg concentration ought to vary by up to 100 ppm, assuming no change in the Mg content of drip water.

9.3.2 Variation in Drip Water Chemistry

A change in the concentration ratio of trace element to Ca^{2+} in the incoming seepage water over time, will cause a corresponding change in TE concentration in the speleothem, which cannot be distinguished from a change in D due to temperature change. Variation in TE/Ca ratio in the drip water could be caused by change in the depth of weathering resulting in dissolution of different materials (eg. a dolomitic layer, carbonate clasts in glacial overburden etc.) and this in turn may be climatically influenced. Alternatively, re-equilibration with bedrock after dissolution would cause TE/Ca in solution to change according to the distribution coefficient of the trace element thereby counteracting any temperature signal the final speleothem might have had. For simplification in the present discussion, the dissolution process is considered to be a uni-directional reaction without appreciable re-equilibration with bedrock. This interpretation may become invalid as saturation with respect to $CaCO_3$ is approached during the solution process and reaction rate slows sufficiently to permit some back-exchange with the bedrock. However no evidence has been found (to the author's knowledge) of a trace element-enriched (or depleted) layer at the surface of a limestone which has been in prolonged contact with undersaturated water, which might indicate this.

Variations in the activities of other ions in solution may affect the activities of trace and carrier ions differently (by ion-pairing, complex formation etc.). It is practically impossible to determine whether this has occurred during the formation of a speleothem and can only be assumed to have affected like ions in a similar way. In the case of Mg^{2+} and Sr^{2+}, variation in ionic strength of the drip water, without selective complexation of one ion, will not affect trace metal content in the solid phase. A small divergence between Sr and Mg content may be seen however, because of the different values of effective ion diameter (a_i^o) for each ion in solution. The activity coefficient of each ion (γ_i) is related to a_i^o, the ionic strength (I) and ion charge (z), by the Debye-Hückel relationship :

$$-\log \gamma_i = \frac{A\, z_i^2 \sqrt{I}}{1 + a_i^o B \sqrt{I}} \qquad (9.12)$$

For Mg and Sr, at $20^{o}C$ and $I = 0.001$: $A = 0.5042$, $B = 0.3273 \times 10^{-8}$, $a^o_{Sr^{2+}} = 5 \times 10^{-8}$, $a^o_{Mg^{2+}} = 8 \times 10^{-8}$, so that $\gamma_{Sr^{2+}} = 0.8697$ and $\gamma_{Mg^{2+}} = 0.8732$. Therefore a change in ionic strength of the drip water will only cause a 0.4% lower change in Sr^{2+} activity than Mg^{2+} activity - a divergence that is not detectable in most situations.

9.3.3 Depositional Conditions

Precipitation of an infinitesimal amount of solid from solution will give values of the trace element distribution coefficient λ_{TE} equal to those of D_{TE} (homogeneous distribution). However, in the case where drip rates are slow and differences between P_{CO_2} of the water and the cave atmosphere are high, the amount of calcite lost from solution while flowing over the speleothem may be quite high (up to 80%, calculated from Mg variations in growth layers of English speleothem, Johnson 1979). In this case, trace element concentrations in solution will change according to the logarithmic distribution law. For instance, in the case of Mg and Sr (D_{Mg} and D_{Sr} are both < 1), preferential rejection of the ions at the solid-solution interface results in increasing concentrations of these ions in solution. If crystallization proceeds at a greater rate than trace ions can be rejected at the interface (and can diffuse back into the bulk of the solution) then the solution immediately adjacent to the solid becomes enriched in trace elements and this causes a corresponding enrichment in the new solid phase. In this case the calculated distribution coefficient (λ') will be greater than that for equilibrium and is related to the degree of supersaturation by (Burton et al. 1953, McIntyre 1963) :

$$\lambda' = \frac{\lambda_o \, S \, (\delta_{TE}/\delta_{Cr})}{\lambda_o \, (S-1) + (\delta_{TE}/\delta_{Cr})} \qquad (9.13)$$

where S is defined as $\dfrac{a_{Ca^{2+}} \cdot a_{CO_3^{2-}} \text{ (observed)}}{a_{Ca^{2+}} \cdot a_{CO_3^{2-}} \text{ (at saturation)}}$

and δ_{TE}/δ_{Cr} is the ratio of the diffusion coefficient of trace element to carrier ion (Ca^{2+}) in the solution. It can be seen that as $S \rightarrow 1$, $\lambda' \rightarrow \lambda_o$.

In the case of Mg and Sr whose distribution coefficients are less than unity, an increase in supersaturation causes an increase in λ' and therefore an increase in trace element in the solid phase. This is seen in the graphical expression of equation 9.13 for three cases of δ_{TE}/δ_{Cr}

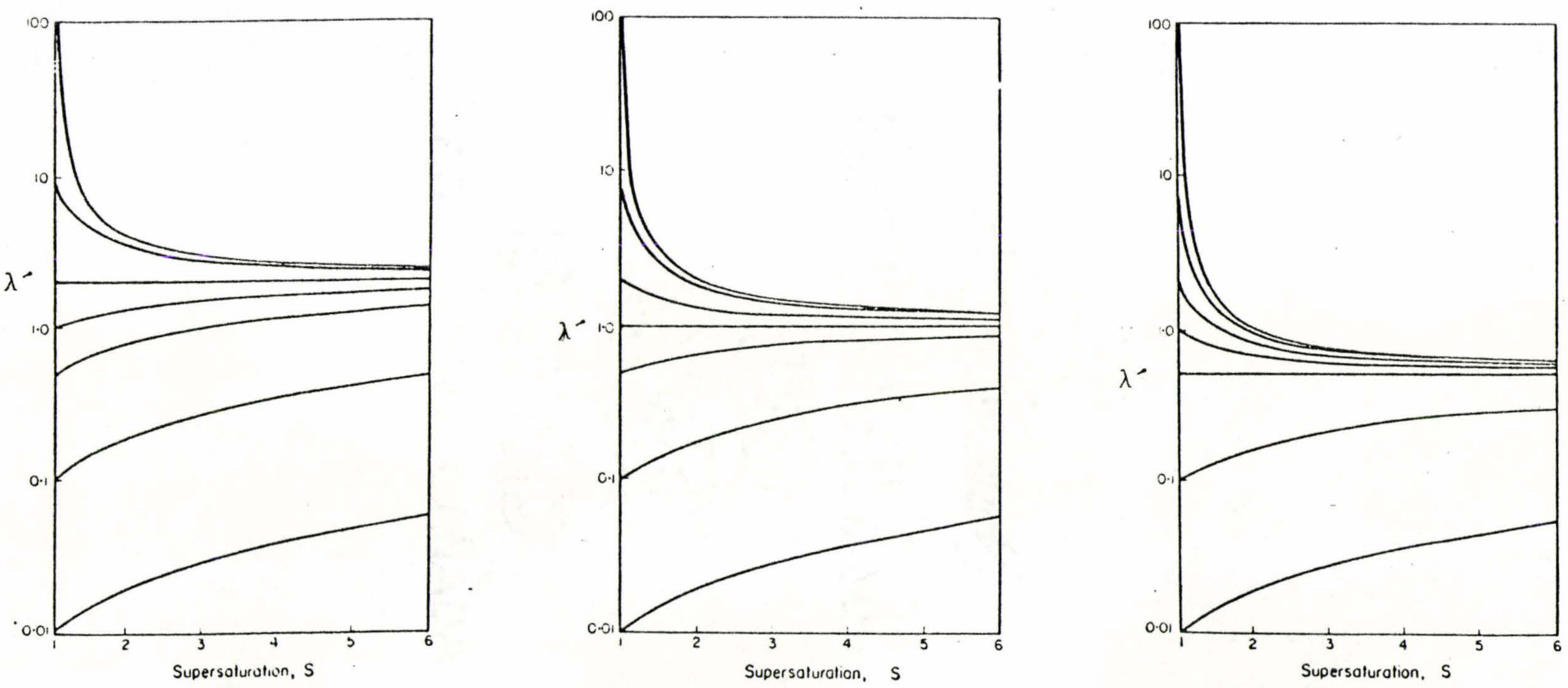

$\delta_{Tr}/\delta_{Cr} = 2{\cdot}0$

(a)

$\delta_{Tr}/\delta_{Cr} = 1{\cdot}0$

(b)

$\delta_{Tr}/\delta_{Cr} = 0{\cdot}5$

(c)

Figure 9.1 Effect of degree of supersaturation (S) on observed logarithmic distribution coefficient λ' for various ratios of diffusion coefficients (δ) of trace (Tr) to carrier (Cr) elements in solution, (from McIntyre, 1963).

in Figure 9.1 (from McIntyre, 1963).

Concentrations of Mg and Sr along a speleothem growth layer, precipitated from a supersaturated solution may vary considerably depending on whether supersaturation is increasing or decreasing in the direction of flow of water. The ratio Mg/Sr in the calcite will not be constant because the change in λ'_{Mg} will be greater than (or less than) λ'_{Sr} for a given supersaturation value (Figure 9.1b) depending on whether D_{Mg} is greater than or less than D_{Sr} (see variation in literature values, Table 9.1).

Equation 9.13 embodies an additional effect which causes enrichment (or depletion) of trace elements in the solid phase depending on the value of the diffusion coefficient ratio in solution (δ_{TE}/δ_{Cr}). The gradient of the λ - S curve will increase (Figure 9.1a) or decrease (Figure 9.1c) depending on whether δ_{TE}/δ_{Cr} is greater than or less than unity.

Johnson (1979) has explained variable Sr behaviour along speleothem growth layers in terms of varying states of supersaturation of the solution which affects λ_{Sr} more than λ_{Mg}. However the calcite samples analysed in her study were not from the same growth horizons at the top and bottom of the stalagmite, (in all cases growth layers thinned considerably towards the bottom so that for the same drill size, a larger number of layers was sampled at the bottom than at the top). This therefore introduces an additional factor of varying trace element content between layers into her measurements, and so may account for the variable behaviour of trace elements along growth layers.

9.3.4 Discussion

Before the trace metal content of speleothem can be interpreted in terms of paleotemperature variation the following conditions must be met:

1) trace metals in the speleothem must have been deposited by direct substitution for Ca^{2+} ions,
2) this substitution must have followed an equilibrium distribution law, (ie. either homogeneous (equation 9.4) or logarithmic (equation 9.10) laws). In either case, $D \cong \lambda$. Appreciable supersaturation of the water will give trace element concentrations that differ from those expected from equilibrium deposition. This situation may perhaps be recognised by variation in the ratio of two trace elements along a growth layer.
3) there must have been no change in drip water chemistry, or at least in the ratio of trace to carrier element over the period of deposition.

It may be possible to eliminate the third requirement if two trace elements, having a similar source and chemistry, can be examined, but whose distribution coefficients have a different dependence on temperature. Changes in drip water chemistry will therefore not cause their concentration ratio to change, but a change in temperature will affect this ratio. Such a case is seen in the trace elements Mg and Sr where D_{Mg} is temperature dependent and D_{Sr} is not (Table 9.1). If it can be assumed that for Mg and Sr, incorporation in the calcite is by the substitution mechanism only (condition 1) then the major problem in interpreting a speleothem trace element profile is in ensuring that condition 2 is met at all times during the speleothem's growth. Unfortunately, as shown above, trace element distribution is sensitive to degree of supersaturation of solution whereas ^{18}O distribution is not, and so an equilibrium speleothem (from an isotopic point of view) may not necessarily be suitable for trace element paleotemperature interpretation.

In an attempt to further assess the use of trace elements (particularly Mg and Sr) as paleotemperature indicators in speleothem, two studies have been undertaken in this work:

1) determination of the distribution coefficients of Mg and Sr and their temperature dependence, from speleothem growth in two regions of different temperature - this permits comparison to published results in Table 9.1 and extension of Katz's work to lower temperatures.
2) examination of Mg and Sr fluctuations in a fossil speleothem which has been found to have grown in isotopic equilibrium with its drip water and which is known to have grown over a warm-cool transitional period.

These studies are described below.

9.4 Determination of D from Modern Speleothem Deposits

Thompson (1973a) and Harmon (1975) have used the precipitation of calcite from seepage water in caves to determine the fractionation factor for ^{18}O partitioning between calcite and water at a given temperature. Their main problems lay in determining at which season of the year speleothem growth occurred, if it was not an all year round process, and what was the average $\delta^{18}O$ composition of the seepage over the growth period. Single samples of drip water collected over a duration of up to one hour were used to calculate average $\delta^{18}O_w$. The non-representative nature of this as a sample of year-round precipitation was commented upon by both authors. The same problem is found in the study of trace element partitioning with the additional problem that the water sample may be insufficient, or too dilute for analysis. Partial solutions to both these problems were developed by use of cation exchange resin to pre-concentrate trace elements from seepage water over a period of several days or weeks, as described below.

9.4.1 Sampling and Analytical Techniques

Bio Rad AG 50 X-8 100-200 mesh cation exchange resin was used to extract double- and triply-charged cations from stalactite drip water in exactly the same manner as anion exchange resin was used to isolate uranium (Chapter 8). The cation resin was packed initially in glass tubes and subsequently in unbreakable polythene tubes, 1.5cm diameter and 15-20cm long. It was pre-conditioned by washes of 6N HCl, de-ionized water and 5% NaCl solution. In the cave the column was suspended under a slowly dripping stalactite and a 12 litre capacity polythene bag was attached to the outlet via a length of rubber tubing, similar to that shown in Figure 8.5.

The volume used and the exchange capacity of the resin (1.7meq/ml) permitted a minimum of 7.5 l.of 'maximum' hardness water to pass (say 100ppm Ca and 10ppm Mg) before the resin capacity was saturated. On collecting the column a small sample of fresh eluate was collected (sample 'C') for Ca and Mg analysis to determine if column saturation had occurred. A sample of the bulk eluate in the bag was taken (sample

'B') and the total volume of eluate was measured using a graduated cylinder. Either before or after fitting the column a sample of the stalactite tip and/or the stalagmite top was taken and the water temperature was measured. The columns were sealed at both ends after use.

In the laboratory particulates above and in the top layer of glass wool were rinsed out with de-ionized water. Two aliquots of 50ml of 6N HCl were allowed to drain slowly through the resin and each eluate was analysed separately to check on complete elution of trace elements from the resin by the first aliquot. Sodium chloride was added to each aliquot to give 5% NaCl solution before analysis. Speleothem samples were dried, weighed and dissolved in varying known volumes of 6N HCl before analysis and NaCl was added as described above.

A Perkin Elmer 303 atomic absorption spectrophotometer was used for analysis of Ca, Mg, Sr, Fe, Mn, Cu, Zn, Cr and Pb. An air-acetylene flame was used throughout. Mixed cation standards containing NaCl were made up from pure metals, metal oxides or metal salts and were given a high Ca base by addition of $CaCO_3$ dissolved in HCl. Use of a Ca-based standard was necessary to equalize the viscosity of sample and standard solutions and cancel out enhancing or suppressing effects due to the presence of high levels of Ca in the sample solutions. Column eluates were run against standards containing 4000ppm Ca (which was diluted to 400ppm if the Ca concentration of the eluate was low) and speleothem samples were matched against standards containing 8000ppm Ca. For determination of Ca and Mg content of the eluate, small aliquots were removed and diluted to the range 0 - 4ppm and run against single metal standards of the same concentration.

It was found that Analar $CaCO_3$ used in preparing the high Ca standards contained appreciable amounts of Sr and some Mg, giving a non-zero blank when analysed. 'Spex' $CaCO_3$ was later used and was found to be essentially free of Sr and Mg.

9.4.2 Results

The procedure described above was used for five drip sites in caves of Vancouver Island and twelve sites in Jamaican caves. The volumes of drip water passed by the resins and the trace element concentrations in first and second 50ml acid eluates are shown combined together in Table 9.2. A third 50ml acid eluate of the Jamaica columns was analysed for Ca but no eluate showed more than 2ppm Ca indicating that elution was essentially complete after 100mls of acid. However the second 50ml eluate was found to be necessary because one eluate (V4) showed higher Cu and Zn concentrations than the first aliquot. Six of the Jamaican columns consisted of three pairs of replicates for the same drip sources. Good agreement can be generally seen for each pair, for Ca, Mg and Sr concentrations in the drip water.

Analyses of Ca and Mg in residual drip water eluates (samples B and C) are also shown in Table 9.2. Distribution coefficients have been determined using equation 9.4 and the means of calcite analyses and of drip water analyses (where duplicated) are shown in Table 9.3. Results for column J8 are not used in this study because the speleothem was found to be aragonitic (by X-ray diffraction). This is reflected in the high Sr and low Mg concentrations in the speleothem (Table 9.2). These analyses demonstrate the following:

Cave	Sample	Duration	Volume of water passed (l)	T (°C)	Sample 'B'		Sample 'C'		TRACE METAL ANALYSES IN < column acid eluates as ppm (or *ppb*) / calcite samples - average given here as ppm								Column efficiency	
					Ca (ppm)	Mg (ppm)	Ca (ppm)	Mg (ppm)	Ca	Mg	Sr	Fe	Mn	Cu	Zn	Pb	from Ca (%)	from Mg
Main	V1	31/5-2/6/75	2.25	7.8	1.6	0.08	-	-	39.70	0.846	*17.92*	*8.08*	*1.6*	*<10.4*	*14.0*	*< 34.0*	96.0	90.5
									-	180.1	28.7	34.5	9.3	3.4	12.5	64.3		
Euclataws	V2	" "	1.23	7.1	2.9	0.09	-	-	52.47	1.39	*39.70*	*17.07*	*2.99*	*< 10.6*	*11.8*	*< 34.0*	94.5	93.5
									-	178.9	56.1	55.2	7.4	107.0	46.3	99.3		
"	V3	" "	0.73	6.9	0.4	0.10	-	-	56.04	0.99	*27.79*	*43.62*	*<10.3*	*<35.7*	*574.7*	*<50.7*	99.3	89.9
									-	163.8	46.1	61.4	6.7	139.2	18.4	53.2		
"	V4	1-2/6/75	0.365	6.9	1.65	0.16	-	-	47.01	6.01	*22.23*	*607.1*	*41.4*	*727.6*	*786.1*	*80.8*	96.5	97.3
									-	869.8	33.0	8.6	2.9	3.0	12.4	42.3		
"	V6	" "	0.13	6.9	1.75	0.12	-	-	61.04	6.44	*<40.54*	*172.2*	*16.3*	*<60.8*	*<230.5*	*302.9*	97.1	98.1
									-	532.7	33.7	19.5	3.6	4.7	10.6	39.6		
Coffee River	J1^{1}	18-21/6/75	2.83	24.0	0.4	0.07	18.0	0.65	40.76	5.68	*5.39*	*12.01*	*1.24*	*2.21*	*37.1*	*11.5*	99.0	98.8
									-	2460	-	-	-	-	-	-		
Printed Circuit	J2	19-24/6/75	3.92	23.5	0.35	0.02	7.0	0.20	6.53	0.33	*42.60*	*10.71*	*1.40*	*3.51*	*72.32*	*14.67*	94.6	93.9
									-	1160	-	-	-	-	-	-		
Oxford	J3	18-24/6/75	2.72	23.2 -23.6	0.5	0.04	5.8	0.25	56.76	3.87	*17.46*	*22.79*	*1.47*	*221.0*	*49.63*	*17.46*	99.1	99.0
									-	1142	22.16	24.31	4.52	12.04	21.16	76.7		
Riverhead	J5^{2}	10-17/6/75	1.60	∿23	1.5	0.08	5.0	0.18	69.53	1.41	*43.44*	*22.19*	*4.06*	*21.09*	*75.0*	*29.69*	97.8	94.3
									-	352	-	-	-	-	-	-		
Cave River	J6^{3}	10-17/6/75	1.725	22.6	0.25	0.07	11.5	1.2	53.79	26.24	*19.13*	*14.49*	*2.61*	*41.3*	*14.5*	*21.7*	99.5	99.7
									-	8925	54.1	15.91	3.54	14.2	11.5	72.5		
Coffee River	J7^{1}	11-18/6/75	7.22	24.2	0.3	0.04	13.0	0.75	43.63	5.86	*6.37*	*3.81*	*0.76*	*1.56*	*5.33*	*9.35*	99.3	96.0
									-	2460	-	-	-	-	-	-		
" "	J8	18-24/6/75	0.68	23.8	0.85	0.14	9.7	0.65	40.40	17.76	*17.06*	*113.0*	*12.5*	*187.6*	*90.6*	*47.8*	97.9	99.2
									-	162.8	542.7	7.47	N.D.	7.7	12.23	72.35		
Cave River	J9^{3}	17-20/6/75	0.796	21.9	1.2	0.07	7.5	1.2	45.34	26.56	*25.82*	*66.12*	*4.41*	*63.0*	*78.7*	*37.8*	97.4	99.7
									-	8925	54.1	15.91	3.54	14.2	11.5	72.5		
Coffee River	J10	18-24/6/75	2.73	23.4	0.25	0.04	5.8	0.32	64.64	13.27	*12.27*	*31.25*	*2.20*	*6.87*	*207.5*	*16.5*	99.6	99.7
									-	3945	19.50	7.14	1.71	1.77	20.27	81.5		
" "	J11	21-24/6/75	1.71	22.6	1.1	0.06	4.0	0.11	45.49	5.58	*8.25*	*63.68*	*4.53*	*48.4*	*93.2*	*46.3*	97.6	98.9
									-	1950	-	-	-	-	-	-		
Printed Circuit	J12	19-24/6/75	7.58	24.0	1.75	0.04	8.8	0.4	56.01	2.73	*59.37*	*7.26*	*1.39*	*20.78*	*15.2*	*12.2*	96.9	98.5
									-	908	37.32	13.5	3.57	4.37	10.92	46.85		
Riverbend	J13^{2}	17-26/6/75	2.31	-	0.95	0.04	∿15	0.35	61.65	1.43	*40.74*	*26.97*	*1.97*	*82.5*	*48.8*	*22.7*	98.4	97.7
									-	352	-	-	-	-	-	-		

Notes
1) suffices ^{1} ^{2} ^{3} indicate duplicate columns, ie. columns attached to the same drip source but at different times.
2) column eluate analyses are in ppm for Ca and Mg (ordinary type) and ppb for the remainder (*italics*), and are determined from the sum of the two acid eluates.
3) speleothem calcite analyses are averages of one to four analyses of different calcite samples (ie. stalactite tips and stalagmite tops).
4) samples 'B' are analyses of the bulk drip water eluate after passing through the column in the cave, samples 'C' are analyses of eluate emerging from the column immediately prior to collection of the apparatus.
5) column efficiency is determined by $E = 100 - (\frac{\text{sample 'B' (ppm)}}{\text{acid eluate (ppm)}} . 100)$ %
6) speleothem J8 is aragonitic.
7) **estimated precision from replicate analysis of the same sample is ± 10% for Ca,Mg, and ± 20% for the remainder.**

Table 9.2 Analyses of drip waters (determined from cation column eluates) and recent calcite growths for five sites in Vancouver Island caves and twelve sites in Jamaican caves.

Column No.	$T^{o}C$	Mg_{l}^{1} (ppm)	Sr_{l}^{2} (ppb)	Ca_{l}^{1} (ppm)	Mg_{s} (ppm)	Sr_{s} (ppm)	λ_{Mg}	λ_{Sr}
V1	7.8	0.935	18.67	41.35	180.1	28.7	0.0199	0.159
V2	7.1	1.49	42.01	55.52	178.9	56.1	0.0167	0.185
V3	6.9	1.10	27.99	56.44	163.8	46.1	0.0210	0.232
V4	6.9	6.18	23.04	48.31	869.8	33.0	0.0170	0.174
V6	6.9	6.56	< 41.75	62.86	532.7	33.7	0.0128	0.127
J1 J7	24.1	5.93	5.93	42.55	2460	N.D.	0.0441	-
J5 J13	∿23	1.48	42.91	66.87	352	N.D.	0.0398	-
J6 J9	22.3	26.48	22.87	50.31	8925	54.1	0.0423	0.298
J2	23.5	0.35	45.03	6.90	1160	N.D.	0.0572	-
J3	23.4	3.91	17.62	57.28	1142	22.16	0.0418	0.180
J10	23.4	13.31	12.32	64.90	3945	19.5	0.0481	0.257
J11	22.6	5.64	8.45	46.61	1950	N.D.	0.0403	-
J12	24.0	2.77	61.27	57.80	908	37.32	0.0474	0.088

[1] corrected for yield (see Table 9.2)

[2] corrected for yield using Ca yields in Table 9.2.

Table 9.3 Average Ca,Mg and Sr concentrations for dripwaters and speleothem, with calculated distribution for Mg and Sr for Vancouver Island and Jamaican cave sites.

Column No.	D_{Fe}	D_{Mn}	D_{Cu}	D_{Zn}
V1	0.424	0.577	0.032	0.089
V2	0.424	0.325	1.324	0.515
V3	0.197	0.091	0.546	0.005
V4	0.002	0.008	0.001	0.002
V6	0.017	0.034	0.012	0.007
J3	0.151	0.436	0.008	0.060
J6	0.148	0.182	0.046	0.107
J9	0.027	0.091	0.026	0.017
J10	0.037	0.126	0.042	0.016
J12	0.260	0.360	0.029	0.101

Table 9.4 Calculated distribution coefficients for Fe,Mn,Cu and Zn for sites in Vancouver Island and Jamaican caves.

1) The close agreement of 8 determinations from different sites in Jamaica and 5 determinations from different sites in Vancouver Island suggest that either i) all sites are depositing Mg under equilibrium conditions (ie. $D_{Mg} = \lambda_{Mg}$) or ii) deposition from supersaturated solutions is occurring at some or all sites but has little influence on D_{Mg}.

2) Values of D_{Mg} determined from speleothem and drip water in 8 caves from two temperature regimes are comparable to those determined in experimental studies (see Table 9.1). The values of D_{Mg} at 24°C and 7°C fall below those predicted by extrapolation of the data of Katz (1973) to lower temperatures (Figure 9.2a). Values given by Winland (1969), Michard (1971) and Füchtbauer and Hardie (1976) fall lower still.

3) Katz's observation that Mg concentration in calcite is strongly temperature dependent is substantiated by this work :

$$\frac{dD_{Mg}}{dT} = +\ 0.0009/^{\circ}\mathrm{C} \qquad \text{(Katz 1973)}$$

$$\frac{dD_{Mg}}{dT} = +\ 0.0017/^{\circ}\mathrm{C} \qquad \text{(this work)}$$

4) Values of D_{Sr} are of similar order of magnitude to those published (Table 9.1, Figure 9.3) but vary considerably over the range 0.09 - 0.30. There is no correlation with temperature, as was also found by Katz et al. (1972).

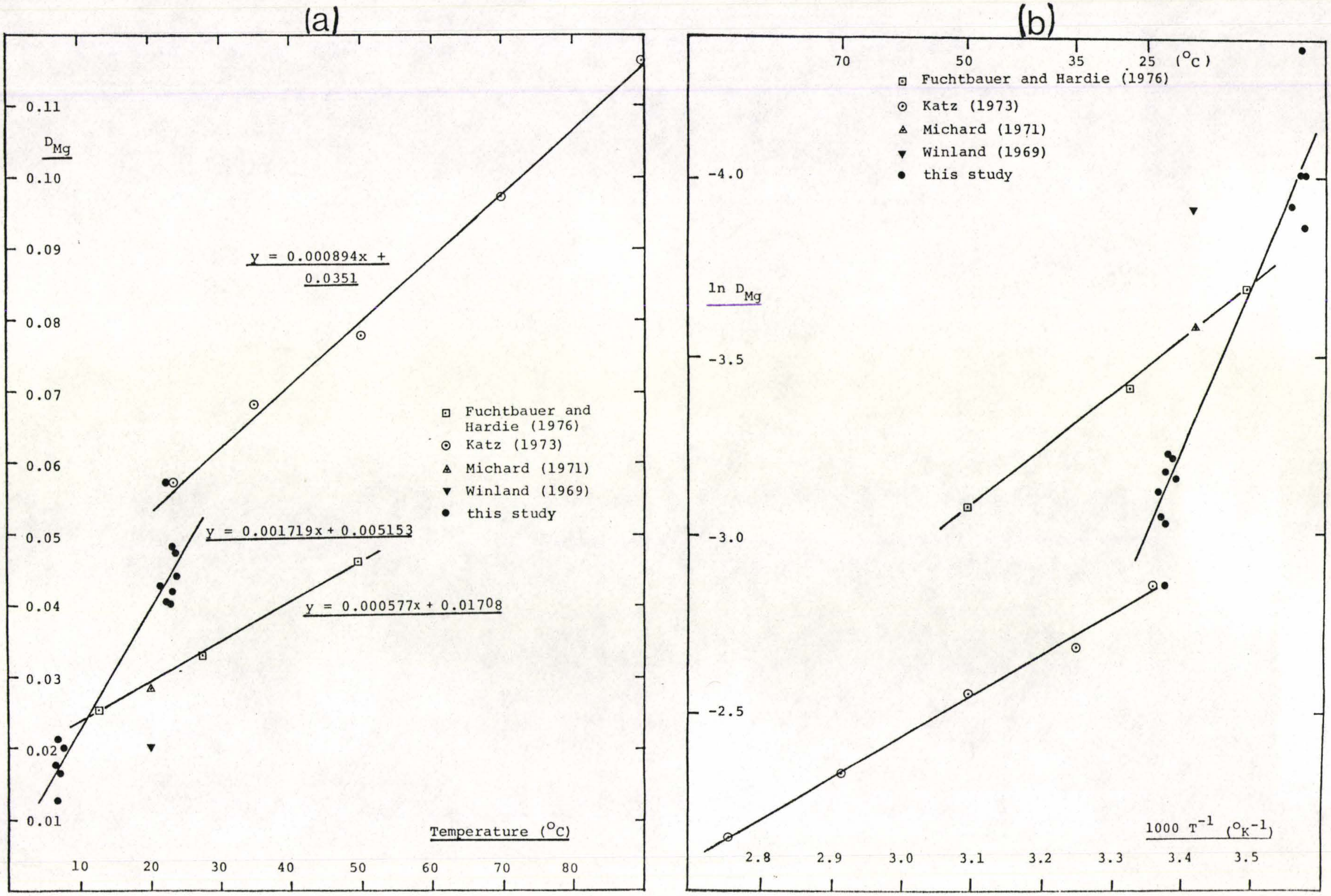

Figure 9.2 a) Variation of D_{Mg} with temperature (T) for this and other studies. Lines are least squares fits.
b) Variation of ln D_{Mg} with 1/T for this and other studies. Lines are fitted by eye.

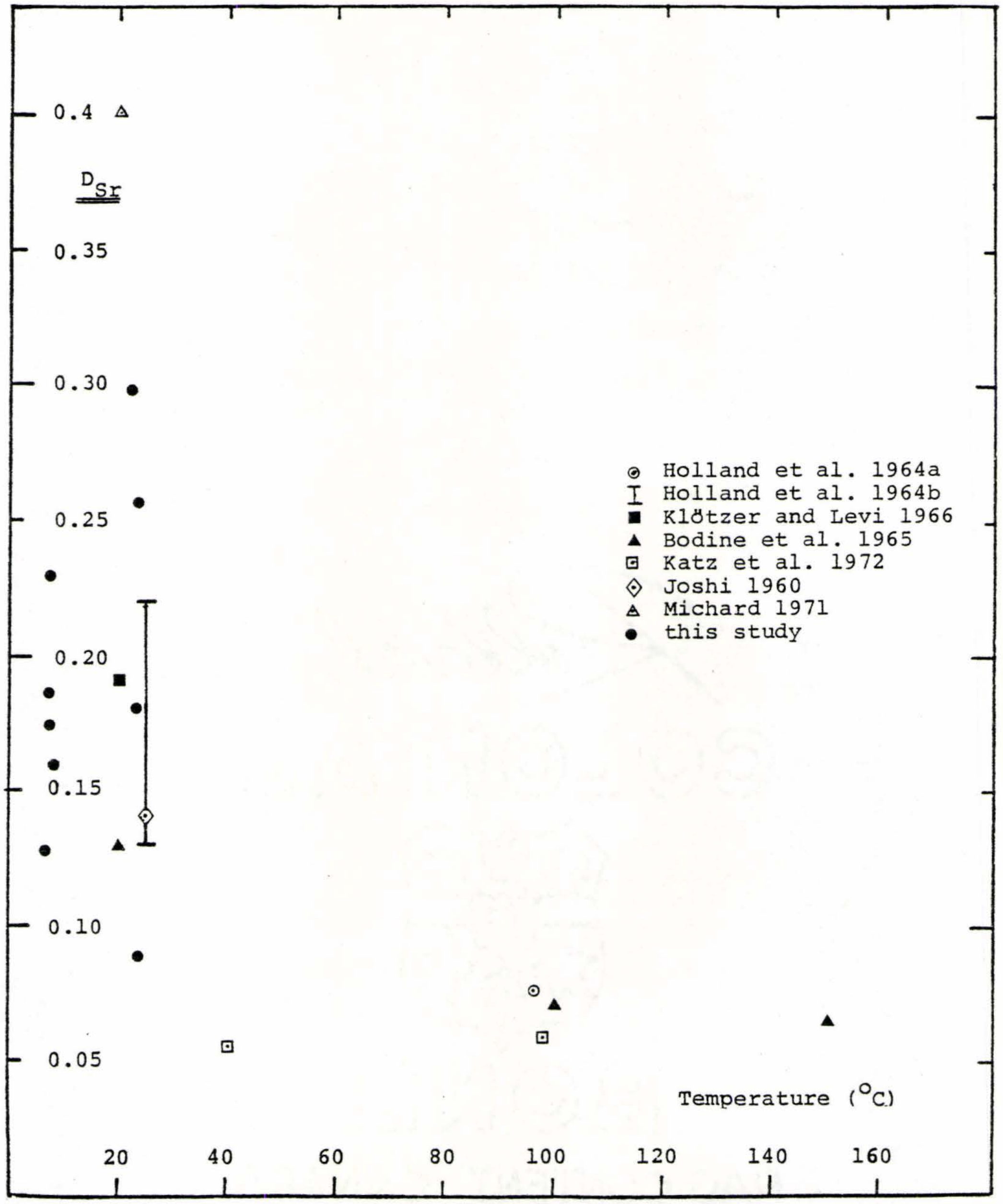

Figure 9.3 Variation of D_{Sr} with temperature for literature values and this study.

9.4.3 Discussion

The results obtained in this study show a temperature dependence of D_{Mg} larger than that obtained by Katz (1973) and Füchtbauer and Hardie (1976), (Figure 9.2a). The discrepancy in absolute values of D_{Mg} could be due to analytical error but the different temperature coefficients indicate a more fundamental discrepancy. It is surprising in fact, that the D_{Mg}-T relationship is linear, because equation 9.9 would lead to a linear relation between ln D and T^{-1}. Unfortunately no intermediate values of D_{Mg} for temperatures between 7 and 24°C have been obtained to test this. Re-plotting the data as ln D vs. 1000 T^{-1} (Figure 9.2b) shows even greater divergence between the three sets of results. It is possible that the system used by Katz and Füchtbauer and Hardie to determine D is not equivalent to that in an natural cave environment as described here and so agreement between distribution coefficients need not be found.

Using the value of dD_{Mg}/dT calculated here, a 1°C decrease in temperature at 10°C would result in a 40ppm decrease in Mg concentration in calcite. If this higher temperature dependence of D_{Mg} is appropriate for cave deposits, then it should be possible to resolve paleotemperature changes to within 1°C using Mg variations in fossil speleothem.

No temperature dependence is immediately apparent for D_{Sr} values determined in this study but comparison of all results shown in Figure 9.3 suggests that either D_{Sr} is non-linearly temperature dependent or is easily influenced by supersaturation conditions at lower temperatures. The latter explanation is more likely in view of the wide range of D_{Sr} values between 0 and 30°C.

The large variation of D_{Sr} and small variation of D_{Mg} at a given temperature in this study is unexpected from consideration of the predicted influence of supersaturation on distribution coefficients. Because D_{Sr} is either equal to or greater than D_{Mg} (from the consensus of results in Table 9.1 and Figures 9.2, 9.3), it should therefore be affected similarly or less than D_{Mg} by changes in supersaturation (as described in section 9.3.3). The greater variations in D_{Sr} may be due to other factors, such as the greater analytical error for Sr determination coupled with its lower abundance, adsorption or occlusion of Sr instead of substitution for Ca, presence of non-ionized or complexed Sr species in solution, etc.

Distribution coefficients for other trace metals (Fe, Mn, Cu, Zn) have been calculated from the data of Table 9.2 and are given in Table 9.4. A variation of over two orders of magnitude can be seen in D for all of the metals, suggesting that they are incorporated in speleothem primarily by processes other than substitution for Ca. They also may be present in the drip water as colloids or particulates. It is doubtful therefore whether these metals can be successfully used as paleotemperature indicators in speleothem deposits.

9.5 Trace Element Variations in a Fossil Speleothem

Speleothem 77143, from Ingleborough Cave, England, has been analysed for Mg and Sr content and compared with $\delta^{18}O_c$ and $\delta^{13}C_c$ variations for the same horizons (described in Chapter 5). In this work, approximately 0.1g of calcite was drilled out, weighed accurately, dissolved in HCl and the volume made up to 50mls by addition of NaCl and deionized water. These samples were analysed as previously described using

Mg and Sr standards of the same Ca concentration (800ppm). Results are shown in Figure 9.4 compared to $\delta^{18}O_c$ and $\delta^{13}C_c$ for the same horizon.

$\delta^{18}O_c$ and $\delta^{13}C_c$ increase appreciably towards the top of the speleothem (ie. towards 108 Ka) and this has been attributed to a cooling period (Chapter 5). This trend is not seen in Mg concentrations but can be observed to some extent in Sr concentrations. Average Mg concentration is 548ppm and the overall range is 270ppm. Therefore from the value of dD_{Mg}/dT determined above for speleothem, this range represents a maximum temperature change of about 7°C, assuming a median cave temperature of 10°C.

It is unlikely that a temperature change as high as 7°C occurred during the growth of this speleothem because it is confined to an interglacial period. Some of the change in Mg concentration must be due therefore either to change in drip water chemistry (this is suggested by the change in Sr concentration) or to variation of supersaturation levels in the water. The latter explanation best accounts for the lack of correlation with $\delta^{18}O_c$.

As previously discussed, the Mg/Sr ratio might be expected to show variation due to temperature without the added effect due to change in absolute ion concentrations. The Mg/Sr ratio in Figure 9.4 suggests however, that a period of relatively stable, cool conditions existed from about 128 - 116 Ka, followed by a warmer period, and with a return to cool conditions at 110 Ka when deposition ceased. This interpretation is in contrast to that deduced from variations in $\delta^{18}O_c$ (Chapter 5) but is more in keeping with the age distribution frequency data of Figure 5.23 showing a period of abundant speleothem growth about 115 - 110 Ka.

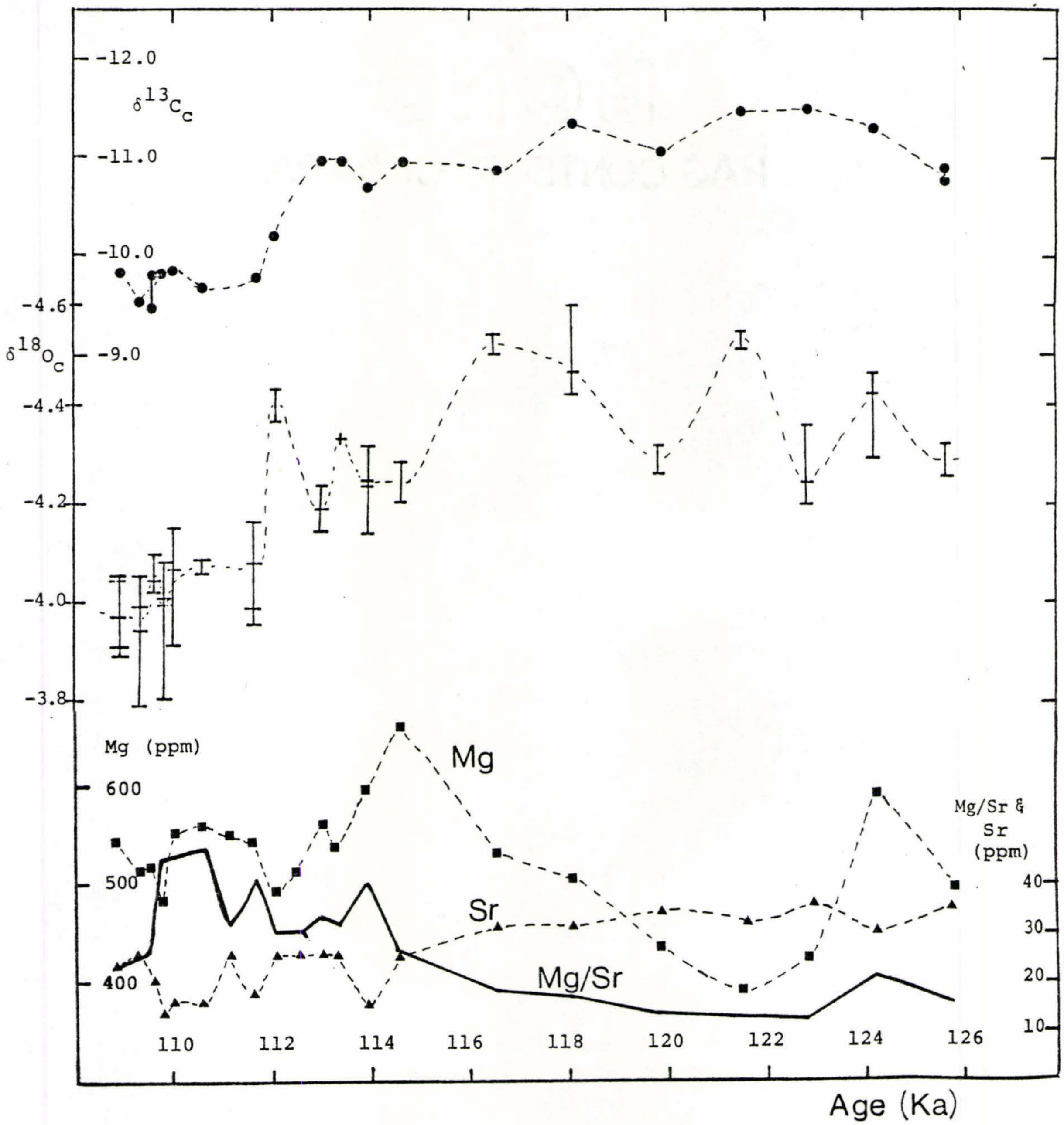

Figure 9.4 Variation of Mg and Sr concentrations (dashed lines) and Mg/Sr ratio (solid line) compared to $\delta^{18}O_c$ and $\delta^{13}C_c$ profiles of speleothem 77143B.

9.6 Conclusions

This study has determined values of the distribution coefficients of Mg and Sr between calcite and water at low temperatures for a natural depositional system. The values of D_{Mg} show good internal consistency but lie in between those predicted by other workers. A greater temperature dependence of D_{Mg} than found in previous results, is indicated in this study and, if correct, greatly increases the potential for resolution of paleotemperatures. No correlation of Mg content and $\delta^{18}O_c$ for a fossil interglacial flowstone has been found due possibly to changes in drip water chemistry. Interpretation of the Mg/Sr profile of the speleothem gives a paleoclimatic record opposite to that indicated by $\delta^{18}O_c$ alone.

Further work on other equilibrium speleothems needs to be done before the potential of Mg and Sr variations in speleothem can be fully assessed.

CHAPTER 10

CONCLUDING REMARKS

Introduction

The foregoing chapters have demonstrated the application of U-series dating techniques and stable isotope analysis to speleothem, from caves in several maritime areas in the northern hemisphere. It was found necessary to undertake some preliminary work on the analytical techniques used because of inadequacies and errors in existing procedures. The purpose of this chapter is collectively to review the results and draw implications from them regarding aspects of dating and stable isotope studies of speleothem and for the paleoclimatic record of the northern hemisphere. These results will also be compared and contrasted to previous speleothem work.

10.1 U-Series Dating of Speleothem

10.1.1 Age Limits and Resolution

The limits of resolution of the $^{230}Th/^{234}U$ method have been discussed at the end of Chapter 2. It was concluded that resolution of a lower age limit of less than 0.5 Ka was possible with a high-U speleothem and a low background detector. Precision of ages near the upper limit was found to be critically dependent on sample activity, counting time and accuracy of spike calibration. With optimum conditions, 400 Ka represents the maximum age to which the $^{230}Th/^{234}U$ method can resolve. For most speleothem, 350 Ka is a more realistic working maximum, although in this and previous work, there has been no deliberate attempt to obtain better precision on ages near the 350 Ka limit (however such precision is implied by Harmon et al. 1977, where distinction is made between speleothem growth periods of 275 - 320 Ka and > 350 Ka). Use of count times in excess of 5 days for medium-high U speleothem (to obtain over 20,000 counts per isotope peak) with good-resolution, low background detectors and stable electronic systems, will be the only means of improving resolution of climatic events in the Middle Pleistocene.

10.1.2 Detrital Thorium Contamination

Throughout this thesis there has been constant use of an arbitrary value for the initial $^{230}Th/^{232}Th$ ratio in speleothem contaminated by detritus. The fact that some ^{230}Th is leached from detritus during sample dissolution is seen by the displacement to older values of ages of apparently recent speleothem from Vancouver Island and England. Correcting with $(^{230}Th/^{232}Th)_o = 1.5$ places some ages at or near zero but also creates some 'negative' ages, an impossible situation. Some idea of the effect of varying choices of $(^{230}Th/^{232}Th)_o$ on the 'corrected' ages can be seen below :

Measured $^{230}\mathrm{Th}/^{232}\mathrm{Th}$	Uncorrected age (Ka)	Corrected ages (Ka) using $(^{230}\mathrm{Th}/^{232}\mathrm{Th})_o$ =		
		1.0	1.5	2.0
1.6	9.9 ± 1.5	4.0±2.8	0.8±3.5	-2.3±4.4

For such a young sample, there is complete overlap of the ages at the ± 1σ level. That such corrections are truly valid is suggested by the observation that ages of contaminated samples are displaced out of intervals which are otherwise characterised by lack of speleothem growth (usually glacial periods). For instance, all of the Vancouver Island speleothems apparently dated at between 23 - 16 Ka (the generally accepted period for the Late Wisconsin glacial maximum) are displaced to ages less than 15 Ka after correction with $(^{230}\mathrm{Th}/^{232}\mathrm{Th})_o = 1.5$. Similarly, some of the Ingleborough Cave speleothems that show appreciable $^{232}\mathrm{Th}$ contamination (Appendix 4a) are displaced from apparent dates in the Wolstonian and Late Devensian glaciations into younger, warmer periods.

In the work on contaminated speleothems so far, the possibility of appreciable contribution of uranium leached from the detritus has been given little consideration. This is due to the difficulty of detecting such an occurrence because of the absence of a characteristic 'detrital' U isotope and the fact that corrected ages of young speleothems would only be made younger and not 'negative' in age if detrital U is added to the system. Better interpretation of contaminated ages can only be made when separate analysis of the detritus is made to determine the amounts of Th and U nuclides that can be leached into solution. Otherwise, all ages for samples with low $^{230}Th/^{232}Th$ analyses (especially for young speleothem) should only be used to give a general indication of age.

10.2 Stable Isotopes in Speleothem

10.2.1 Kinetic Isotope Fractionation

Several speleothems from Vancouver Island, Jamaica and England have clearly shown kinetic isotope fractionation between water and calcite. Ranges of values of $\delta^{18}O_c$ and $\delta^{13}C_c$ and the least squares gradient ($\delta^{13}C_c/\delta^{18}O_c$) for the more strongly fractionated samples are shown in Table 10.1. Hendy (1969) has shown that evaporation alone will cause $\Delta\delta^{13}C_c \cong -2\ \Delta\delta^{18}O_c$ and kinetic loss of CO_2 alone gives $\Delta\delta^{13}C_c \cong 4\ \Delta\delta^{18}O_c$. Measurements along speleothem growth layers by Fantidis and Ehhalt (1970) gave $\Delta\delta^{13}C_c/\Delta\delta^{18}O_c$ values ranging from 2 to 4, and Harmon (1975) obtained values between 1 and 2.3. Table 10.1 shows variation between 0.8 and 3.7, with all English samples lying between 2.5 and 3.7. It would appear therefore that the dominant effect in causing isotopic disequilibrium in the English samples is too rapid loss of CO_2. This suggests that the cave atmospheres are essentially saturated with water vapour but sufficient air currents exist to remove CO_2 rapidly from solution. In the Jamaican caves, evaporation of water seems to play a larger part in causing disequilibrium, possibly due to higher temperatures of the caves.

Location	Speleothem No.	Range in $\delta^{18}O_c$ (‰)	Range in $\delta^{13}C_c$ (‰)	Least squares gradient $\delta^{13}C_c/\delta^{18}O_c$
Jamaica	75351	0.82	0.98	1.22
	75341	0.74	0.92	0.83
Bahamas	78033	0.79	1.82	2.08
N.W.England	76122	1.18	3.23	2.58
	76125	1.64	6.52	2.99
	76210	0.56	1.59	2.88
	76190A	0.59	1.54	2.62
	76190B	1.42	4.63	2.96
	76128	1.74	7.56	3.69
	76201	2.15	6.61	3.24
	77151B	0.79	2.14	2.48
	77151C	0.82	2.19	2.57

Table 10.1 Ranges of $\delta^{18}O_c$ and $\delta^{13}C_c$ in the calcite of growth layers of speleothem showing kinetic isotope fractionation.

10.2.2 Equilibrium Deposition

The present study has been hindered by the difficulty in finding speleothems deposited in isotopic equilibrium. The table below summarizes the results of isotopic analyses for equilibrium speleothem growths.

Location	No. speleothems analysed	No. of kinetically fractionated deposits	No. of equilibrium deposits
Vancouver Island	4	2	2
Jamaica	3	3	0
Bahama Blue Holes	1	1	0
N.W.England	10	6	4*

* includes 77151 of which two growth layers clearly show non-equilibrium deposition

Most of the remaining speleothems that were collected from N.W.England and were dated but not analysed for stable isotopes are probably non-equilibrium deposits because those found to be kinetically fractionated come from the same passages and chambers as the bulk of the collection, and grew over approximately the same time periods. The presence of air currents in these caves at the moment also suggests non-equilibrium deposition in the past. Some deposits, notably 77151, show kinetic and equilibrium isotope fractionation in different growth layers. It has been necessary to allow for this when interpreting the $\delta^{18}O_c$ axial profile (Chapter 5) by assuming that increases in $\delta^{18}O_c$ in the profile may be augmented by non-equilibrium effects.

There are two disadvantages of using flowstone instead of stalagmites for paleotemperature analysis : 1) the water may have travelled some distance in the aerated cave passage before depositing the flowstone analysed; stalagmites however, usually form directly beneath a roof drip source, from water which has just emerged into the cave and 2) the direction of flow of water is not always apparent on a loose fossil flowstone and so growth layers must be analysed in directions normal to one another to detect non-equilibrium deposition. The main advantage of flowstones is that growth layers do not usually 'thin out' away from the water source, as in stalagmites, and therefore larger samples of the same growth layer can be taken for dating and fluid inclusion analysis.

Hendy (1971) has shown how there should be no correlation between $\delta^{13}C_c$ and $\delta^{18}O_c$ if there is isotopic equilibrium between calcite and water during deposition, ie. $\delta^{13}C_c$ may vary along a growth layer but $\delta^{18}O_c$ must not. If a steady increase of $\delta^{13}C_c$ is seen along a growth layer in an equilibrium deposit, then the rate of loss of CO_2 from solution (or the rate of exchange with CO_2 of the cave atmosphere) is sufficiently rapid to be seen in the isotopic composition of the calcite precipitated, but is sufficiently slow as not to disturb equilibrium exchange of ^{13}C (and ^{18}O) between all dissolved carbon species. If the initial pCO_2 of the drip water is low, or the time of outgassing long, then CO_2 exchange with the atmosphere ($\delta^{13}C = \sim -8‰$) becomes significant and $\delta^{13}C_c$ would tend towards ~ + 2 ‰. If such $\delta^{13}C_c$ values are seen in 'equilibrium' speleothem (eg. 76127 in this study) the axial $\delta^{18}O_c$ profile should be interpreted with caution because the prior loss of CO_2 from solution may have been accompanied by some evaporation which would bias all $\delta^{18}O_c$ results to higher values.

It appears from this study, that many more speleothems from deeper parts of caves (in N.W.England) are non-equilibrium deposits than might be expected on the basis of previous work (ie. 33% show equilibrium deposition compared to 80% in Thompson (1973a) and in Harmon (1975)). Many of the cave passages sampled in the present study contain appreciable air currents which may account for this difference. However, the Norman-Bone cave system in West Virginia also takes an air flow but nevertheless yielded three equilibrium speleothems (Thompson et al. 1976). Because of the similar entrance levels of many caves in the flat-lying parts of central U.S.A., pressure differentials are slight and so the systems do not carry strong draughts. These caves therefore often contain chambers and passages with high levels of CO_2 (from the outgassing of groundwater) and maintain high humidities - conditions ideal for isotopic equilibrium deposition). This is especially the case for Cold Water Cave in Iowa and the Flint Ridge system in Kentucky (Harmon et al. 1978a) where CO_2 levels exceed 0.1%. In areas of higher relief, such as N.W.England and the Canadian Rockies, the only places where equilibrium speleothem may occur are in resurgence caves which contain no vadose connection to higher-level systems with separate entrances. Ingleborough

Cave is an example of this type of cave (Chapter 5) and has yielded two flowstones (76142, 77143) which have been found to be equilibrium deposits.

10.2.3 $\delta^{18}O$ of Modern and Fossil Speleothem

Narrow ranges of $\delta^{18}O$ for modern calcite ($\delta^{18}O_c$(m)) have been found in caves in Vancouver Island (-10 to -9 ‰) and N.W.England (-5.3 to -4.8 ‰). This has enabled determination of the factors most important in controlling $\delta^{18}O_c$ for each area, through comparison of glacial age and modern speleothem. In Vancouver Island, $d\delta^{18}O_c/dT$ was found to be positive, showing the overriding importance of change in $\delta^{18}O_p$ with temperature. In N.W.England however, $d\delta^{18}O_c/dT$ was found to be negative, as generally observed by Harmon et al. (1978a).

The use of $\delta^{18}O_c$(m) as a warm climate indicator has only been partially successful in interpreting mid-latitude speleothem results in N.America (Figure 10.1, Harmon et al. 1978a). The lack of agreement between $\delta^{18}O_c$(m) and $\delta^{18}O_c$ for the Alberta record (from Castleguard Cave speleothems) during the last interglacial is probably due to evaporative influences on $\delta^{18}O_c$(m), Atkinson (1979) has shown that speleothem deposition at present in Castleguard Cave is mainly occurring by evaporation rather than CO_2 loss . In Kentucky, $\delta^{18}O_c$(m) also lies central to the observed range of fossil $\delta^{18}O_c$ for one speleothem. This may be due to climatic differences between the present and the period of growth of the speleothem, or the influence of non-equilibrium deposition in parts of the speleothem (only one growth layer was analysed for the 25cm long stalagmite deposit).

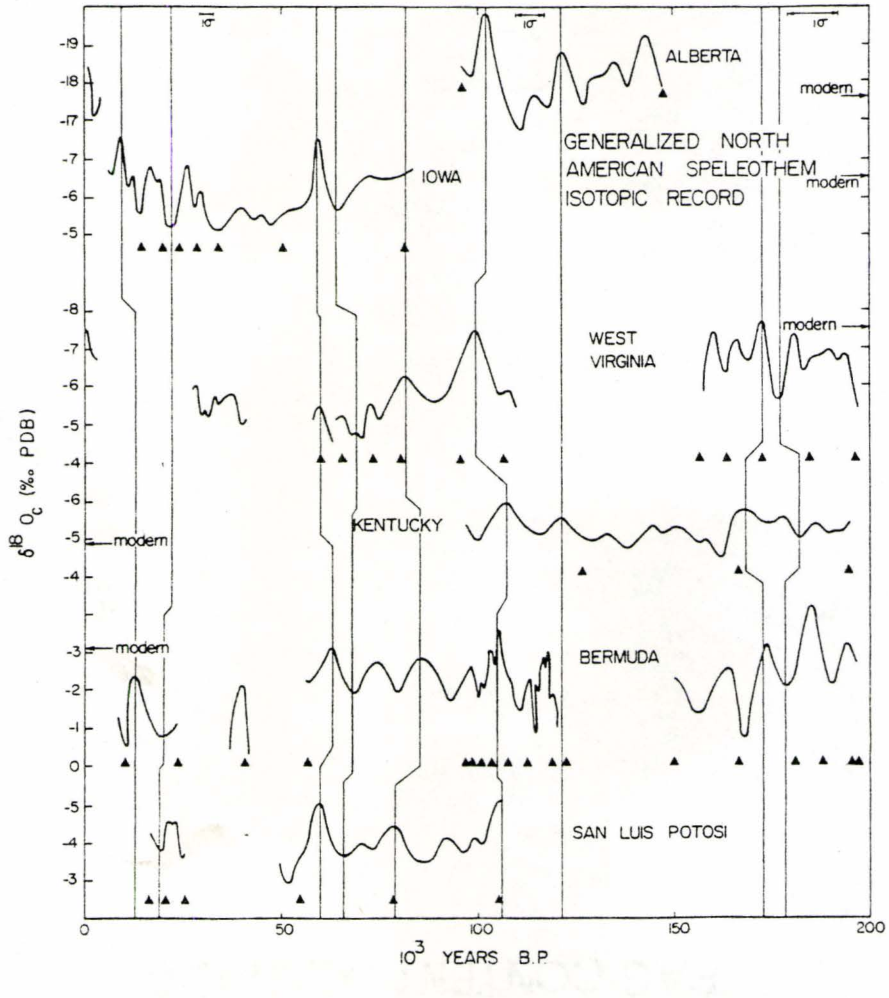

Figure 10.1 Generalised $\delta^{18}O_c$ profile of speleothems from North American caves (from Harmon et al. 1978a). Triangles indicate dated points and $\delta^{18}O_c$ of modern calcite is shown by horizontal arrows. The Bermuda and Iowa records are averaged by two or more contemporaneous records. Vertical lines indicate suggested peak-peak, trough-trough correlation.

10.3 Comparison with Previous Speleothem Results

Several recent papers have published results of speleothem dating and stable isotope studies for caves in N.America (Thompson et al. 1976; Harmon et al. 1977; Harmon et al. 1978a,b,c,d; Harmon et al. 1979b) based on the results in Thompson (1973a) and Harmon (1975). Their general findings have been summarized in Chapter 1 and several important errors and inconsistencies have been pointed out in Chapters 2 and 3 of this thesis. For these reasons, and the difference in localities of research, comparison to the results presented here can only be done in the broadest sense.

General agreement between this and previous work has been found on:

1) the abundance of speleothem ages centred around 105 - 110 Ka. If speleothem growth is most vigorous during warm periods, then 105 - 110 Ka may better describe the peak of the last interglacial, rather than 120 - 125 Ka as obtained from ocean core and reef terrace records.
2) similar amplitude of $\delta^{18}O_c$ in fossil speleothem. In this study 77151 has shown a 2 ‰ maximum variation (limited by cessation of growth during ice advances), while previous results (Figure 10.1), show slightly over 3 ‰ total variation.
3) the negative dependence of $\delta^{18}O_c$ on temperature as described in 10.2.3 above, except for the special case of Vancouver Island.

Previous work (summarized by Figure 10.1) can be criticized for :

1) inadequate time control for slow-growing speleothems - the 50 Ka Alberta record has only two age measurements and the 100 Ka Bermuda record is based on only three ages. In the present work an average

of one age determination per 5 - 10 Ka of growth has been made (eg. 7 measurements on 75125/76013 covering 35 Ka; 9 measurements - 1 rejected - on 77151 for 90 Ka total growth). Although multiple age determinations tend to introduce complications (eg. the one rejected age and the age discrepancies about the upper hiatus in 77151, Figure 5.21) they do enable a more balanced and reliable time framework to be constructed for distribution of stable isotope analyses.

2) insufficient analysis of growth layers to determine whether isotopic equilibrium deposition was continuous throughout the growth period of the speleothem. For instance, of the 20 equilibrium deposits whose axial $\delta^{18}O_c$ profiles make up Figure 10.1, 16 were each based on one growth layer analysis only. All equilibrium speleothems analysed in the present study are based on analyses of at least two growth layers per deposit, and in the case of thicker sections such as 77151, five growth layers have been analysed. The latter speleothem in fact, clearly demonstrates the need for multiple analysis because two growth layers were found to show kinetic isotope fractionation.
In certain instances however, previous workers have been able to demonstrate that isotopic equilibrium conditions exist in the cave today, by analysis of drip waters and their calcite deposits.
Evidence that such conditions existed in the past has come from the determination of concordant $\delta^{18}O_c$ profiles for contemporaneous speleothems from the same cave (Harmon et al. 1978a).

3) the 'spikiness' of the isotopic record. This is probably due to a combination of insufficient closed-spaced analyses giving 'one-point' peaks and troughs, and poor mass spectrometer precision, as discussed

in Chapter 3. Good analytical precision obtained in the present study coupled with close-spaced sampling and analysis of calcite in between two differing results has removed almost all one-point spikes caused by sudden changes in $\delta^{18}O_c$ (ie. deviations of $\geqslant 0.5$ ‰).

Unfortunately, comparison between isotopic records of this and previous speleothem work is limited because two speleothems from this work grew beyond the maximum age for previous equilibrium deposits (~200 Ka). Comparison between the Vancouver Island (Figure 4.10) and Iowa results (Figure 10.1) generally shows agreement for the Mid-Wisconsin in that a slow continuous cooling from 64 to 28 Ka in Vancouver Island compares with cold conditions prevailing in Iowa for the same period, except for the warming around 40 Ka. The two interstadials recognised in the Eastern Great Lakes stratigraphic record (Dreimanis and Goldthwait 1973) and in the Illinoian record (Frye and Willman 1973) are not found in the Vancouver Island record, probably because of the temperature-damping effect of the ocean.

The last interglacial record of 77143B (Ingleborough Cave, N.W. England, Figure 5.30) appears to correlate well with the Alberta record in Figure 10.1 showing decline from maximum warmth at 120 Ka to a cold period at about 110 Ka. However, the position of modern calcite for Alberta in Figure 10.1 suggests that low $\delta^{18}O_c$ may represent cold events and high $\delta^{18}O_c$, warm events, in which case the Alberta record should be inverted. Correlation of this record with other records in Figure 10.1 is generally poor as is also the correlation with the deep sea core record (described in Chapter 5). Only analysis of more deposits over this time period will resolve this problem.

In general, $\delta^{18}O_f$ from the deep sea core record has showed only a fair correlation with $\delta^{18}O_c$ of previous speleothem work, mainly because of the poorly-established synchroneity of events in the two records. In the present work, a good correlation between the core record and $\delta^{18}O_c$ of one speleothem from N.W.England has been found over the period 190 - 280 Ka. Similarly, values of $\delta^{18}O_f$ from a Pacific core have been used to calculate realistic paleotemperatures for the Mid-Wisconsin in Vancouver Island. The implications of these records are further discussed below.

10.4 Implications for the Quaternary Period in the Northern Hemisphere

Age determinations on Vancouver Island and northern England speleothem have clearly shown the absence of growth during two periods in the Late Pleistocene: 30 - 15 Ka and 165 - 140 Ka. These intervals are interpreted as periods of full glacial or arctic conditions, when perma-frost prevented groundwater flow and speleothem deposition. The earlier event is only seen in speleothem from N.W.England and probably correlates with the Wolstonian glaciation. In contrast, the only ages determined for speleothems found at depth in the Bahama blue holes, lie within this period, further indicating full glacial conditions by the lowering of sea level and speleothem formation in the exposed cave systems. The more recent glacial event appears to be approximately synchronous in both N.W.England and Vancouver Island, with speleothem growth ceasing about 35 and 28 Ka respectively and recommencing about 12 and 15 Ka respectively. The differences in timing may indicate the greater warming influence of the ocean for Vancouver Island than for

N.W.England. Alternatively, the shorter period of maximum glacial advance on Vancouver Island may be explained in terms of less ice cover, more rapid melting etc. Similarly, the greater abundance of speleothems for the Mid-Wisconsin Interstadial in Vancouver Island than for the equivalent period in N.W.England may also be due to the proximity of a warm ocean. However, because the number of dated deposits and the number of caves sampled in each area are relatively small, this observation may be based on random chance.

As previously described, in this work and that of Harmon et al. (1978a), there is a strong indication that the last interglacial maximum occurred at 105 - 110 Ka. Speleothem age distributions and stable isotope profiles show the presence of a warm period about 120 - 125 Ka but of lesser intensity than that immediately following. This contrast cannot be further resolved until better stable isotope profiles (with fluid inclusion analyses) are obtained for a suitable speleothem from a non-glaciated area.

The stable isotope record of 77151 has shown the rapidity with which climate change occurs. During the period 290 - 190 Ka there were two transitions from extremely warm to cool conditions and these occurred over a $\sim$2 Ka period as determined from calculated growth rates. It could be argued that kinetic isotope fractionation due to evaporation could induce this result in the profile, but in this case the effect would not be as gradual a change as indicated by the four analyses in the cooling trend from the 280 Ka warm peak. Initiation of air currents in caves has a time period of hours or weeks at the most, whereas these four analyses cover about 1cm of growth - a process requiring centuries to complete.

The 77151 profile demonstrates the potential for obtaining good resolution of climatic change from speleothem. In previous work, insufficient close-spacing of analyses has given resulting profiles a 'spikey' appearance, probably because of jumping from one climatic extreme to another, with the result that some climatic events may be omitted entirely and the peaks and troughs of others may be missed. The two prominent warm peaks in the 77151 record are marked by 7 and 4 analyses each (counting up from the base, for $\delta^{18}O_c < -5.0$ ‰), and the three cold periods are marked by 4, 12 and 4 analyses each ($\delta^{18}O_c > -4.0$‰). In terms of number of analyses per cold or warm event, the resolution obtained in this study is comparable to that seen in high sedimentation rate, deep sea cores. The main difference is that the resolution of rates of climate change is attenuated in core profiles by bioturbation etc. whereas in speleothem it is only a function of the sampling width. It is possible to obtain an order of magnitude better resolution by use of smaller drill bits and closer spacing of sample sites.

10.5 Factors Controlling $\delta^{18}O_c$ in Speleothem

10.5.1 The Vancouver Island and N.W.England Situation

The Vancouver Island results in this study are the first to show dominance of changes in $\delta^{18}O_p$ on $\delta^{18}O_c$ of fossil speleothem. Until now, stable isotope studies of speleothem have consistently found $\delta^{18}O_c$ of fossil speleothem to be similar to or greater than modern $\delta^{18}O_c$, due to the combined dominance of changes of $\delta^{18}O_{sw}$ and α_{c-w} on $\delta^{18}O_c$.

The two main paleoclimatic records obtained in this study, from Vancouver Island and N.W.England, are briefly summarized below in order to clarify the differing interpretations:

Vancouver Island

1. Fossil speleothem calcite is lighter than modern by at least 0.9 ‰.
2. From 64 Ka to 28 Ka, calcite becomes lighter by ∿1.3 ‰.
3. Over the same period, from the deep sea core record, sea water becomes heavier by ∿0.65 ‰; rainwater will therefore show the same enrichment.
4. Because of the oceanic location of Vancouver Island, $\delta^{18}O_p$ is likely to vary with temperature by 0.7 ‰ /°C. The change in $\delta^{18}O_p$ over this time period, due to temperature gradient change alone (ΔT) will therefore be 0.7 ΔT.
5. Speleothem calcite becomes enriched in ^{18}O because of temperature dependent isotopic fractionation (-0.27 ‰/°C), so that $\delta^{18}O_c$ will increase by 0.27ΔT over this period.

Therefore : $$\Delta\delta^{18}O_c = \Delta\delta^{18}O_{sw} + 0.7\ \Delta T - 0.27\ \Delta T \qquad (10.1)$$

or $$-1.3 = 0.65 + 0.43\ \Delta T$$

so that $$\Delta T = -4.5^{\circ}C$$

This change in temperature can be converted to an absolute paleotemperature curve by comparison of fossil and modern $\delta^{18}O_c$ and $\delta^{18}O_{sw}$. A decrease from ~4.0°C, 64 Ka ago, to ~0°C, 28 Ka ago, is found.

N.W.England

1. Fossil speleothem calcite is generally heavier than modern.
2. Over the period ~210 to ~195 Ka (for instance), in the record of 77151 (Figure 5.33) calcite becomes 1.8 ‰ heavier.
3. Using the correlation between isotopic records of speleothem and deep sea cores described in Chapter 5, it can be inferred that sea water (and therefore rainwater becomes heavier by ∿0.8 ‰ over this period.
4. The temperature dependence of $\delta^{18}O_p$ appears to be only ~0.22 ‰/°C. Therefore the change in $\delta^{18}O_p$ due to change in temperature gradient alone for this period is about 0.22 ΔT.
5. Isotopic fractionation again causes a decrease in $\delta^{18}O_c$ of 0.27 ΔT.

Therefore, for the period ~210 to ~195 Ka, the maximum change in temperature is given by (modifying equation 10.1) :

$$1.8 = 0.8 + 0.22\,\Delta T - 0.27\,\Delta T$$

$$\text{so that} \quad \Delta T = -20^{\circ}\mathrm{C}$$

This drop in temperature is too large to maintain speleothem growth throughout. If $d\delta^{18}O_p/dT$ is 0.7 ‰/°C as in Vancouver Island, then temperature is seen to rise by 2°C over this period - clearly inconsistent with the observed relationship between modern and fossil $\delta^{18}O_c$. Reasonable temperature changes can only be obtained if $d\delta^{18}O_p/dT$ is less than 0.22 ‰/°C for this area, or if $\Delta\delta^{18}O_{sw}$ were substantially greater than

0.8 ‰. Here it can be seen that $d\delta^{18}O_p/dT$ is approximately equal and opposite to $d\alpha_{c-w}/dT$, so that change in $\delta^{18}O_c$ of speleothem will only be due to change in $\delta^{18}O_{sw}$ and meteorological effects (eg. variation in storm track).

The interesting question which arises from the above calculations is : 'Why is $d\delta^{18}O_p/dT$ at least 0.7 ‰ /°C in Vancouver Island, yet 0.22 /°C or possibly less in N.W.England ?' Both sites are seemingly equivalent from geographic considerations (Cascade Cave lies about 30km from the Pacific coast at an altitude of ~300m, and the caves of N.W.England lie ~40km from the Irish Sea, at altitudes of about 400m). In addition, the climate of both areas is controlled by proximity to an ocean and the presence of a warm current offshore. Westerly winds prevail in both areas and rainfall is comparable at these altitudes.

10.5.2 Discussion

The calculations outlined above assume that the temperature dependence of $\delta^{18}O_p$ (calculated from seasonal variations in T and $\delta^{18}O_p$ at a site) also can be used to represent secular variations due to climate change. The parameter ΔT represents the secular change in temperature gradient between the site of evaporation (usually latitudes 20°N and S) and the site of precipitation thus :

$$\Delta T = \Delta T_x - \Delta T_o \qquad (10.2)$$

where ΔT_x = change in T at the site of precipitation

and ΔT_o = change in T at the site of evaporation

The results of the CLIMAP study (Hays et al. 1976, Gates 1976) suggest that ΔT_o is small for the Wisconsin and therefore ΔT is due mainly to greater temperature change at the site of precipitation (ΔT_x). This situation is assumed to closely parallel that of seasonal temperature change as described above. Because the value of 0.7 ‰/^{o}C, determined by Dansgaard (1964) for many maritime and polar sites, gives realistic paleotemperatures for Vancouver Island, it would seem that this assumption is valid.

However, in spite of the maritime location of N.W.England speleothem, the value of 0.7‰/^{o}C for $d\delta^{18}O_p/dT$ does not appear to apply to this area, neither for seasonal changes in $\delta^{18}O_p$ at present, nor paleoclimatic changes determined for fossil speleothem. This may be due either to :

1) addition of, or exchange with, water vapour from the Irish Sea, whose temperature varies with season (ie. ΔT_o is no longer small but tends towards ΔT_x), or
2) change in evaporation site and/or storm track, either on a seasonal or secular basis. This will render equation 10.1 invalid because ΔT only refers to change in temperature gradient between fixed evaporation and precipitation sites. For example, a seasonal shift in sites may be seen as summer convective rain originating from local water sources (eg. Irish Sea, North Sea) and winter cyclonic rain derived from Atlantic Ocean water vapour. This shift, probably coupled with a change in the amount of rainout that occurs prior to precipitation at the site (ie. change in storm track) will give a smaller seasonal change in $\delta^{18}O_p$. Similar shifts may occur with climate change.

It is therefore possible that the Dansgaard coefficient of 0.7 may only be experienced within a few km of an open ocean, whose temperature shows minimal changes over a climatic transition, and where there is no shift of storm track over this transition.

In spite of their maritime location, sites such as New Zealand (Hendy and Wilson 1968), S.W.France (Duplessy et al. 1970b, Emiliani 1971) and Bermuda (Harmon et al. 1978a) all show that $d\delta^{18}O_p/dT$ is considerably less than 0.7 ‰/°C, because fossil speleothem is heavier than modern for past cold events. These observations may be explained by changing storm track and/or exchange with an ocean whose temperature varies with climatic change.

It would be interesting to examine speleothem from the karst areas on the west coast of Ireland (particularly County Clare), because here may be seen an exact parallel of the Vancouver Island situation. There are few other comparable areas in the world, but perhaps the South Island of New Zealand may be similar. Tropical oceanic island locations are unlikely to show the same effect because temperature gradients from ocean to site will probably not steepen during a glacial/interglacial transition (ie. ΔT_x is small and $\cong \Delta T_o$). These sites should instead show change in $\delta^{18}O_c$ due only to the ice volume effect on $\delta^{18}O_{sw}$ and give a stable isotope record which exactly parallels the deep sea core record, but without the attenuating and damping effects of bioturbation, re-solution etc. Unfortunately no equilibrium speleothems were found in this study of Jamaican caves, that could be used for stable isotopic analysis.

A good test of many of the hypotheses described above would be to examine equilibrium speleothem from Vancouver Island that have grown during the last interglacial or earlier.

10.6 Conclusions

The results in this thesis have again demonstrated the power of speleothem to date and resolve in detail, events of the Late and Middle Pleistocene. Future work should aim towards obtaining detailed stable isotope profiles with fluid inclusion analyses for continuous growths, in the manner of the results for 77151 from Victoria Cave, England. Frequent replication and good internal precision of isotopic and radiometric measurements is essential to effectively demonstrate the potential and validity of speleothem results. There is no reason why the same cannot be done for the continents using speleothem, as Emiliani and Shackleton have done for the oceans, using deep sea sediment cores. Hopefully, the results presented in this thesis go a small way towards this goal.

REFERENCES

ALAM, M. and D.J.PIPER, 1977. Pre-Wisconsin stratigraphy and paleoclimates off Atlantic Canada, and its bearing on glaciation in Québéc. Géogr. Phys. Quat., 31 15-22.

ALLEY, N.F., 1979. Middle Wisconsin stratigraphy and climatic construction, Southern Vancouver Island, British Columbia., in press, Quat. Res. 11.

ARMSTRONG, J.E., 1977. Quaternary stratigraphy of the Fraser Lowland. Geol. Soc. Amer. Meeting, Field trip no. 6 pamphlet, Seattle.

ARMSTRONG, J.E. and J.J.CLAGUE, 1977. Two major Wisconsin lithostratigraphic units in southwest British Columbia. Can. J. Earth Sci., 14 1471-1480.

ASHMEAD, P.F., 1967. Lancaster Hole - Ease Gill Cavern survey, in Eyre and Ashmead (1967).

ASHMEAD, P.F., 1974. The caves and karst of the Morecambe Bay area, in Limestones and Caves of North-West England, A.C.Waltham ed., David and Charles, Newton Abbot 201-226.

ATKINSON, T.C., 1979. Preliminary Report on meteorological and hydrochemical investigations in Castleguard Cave, April 1979 (unpublished).

ATKINSON, T.C., R.S.HARMON, P.L.SMART and A.C.WALTHAM, 1978. Paleoclimatic and geomorphic implications of ^{230}Th/^{234}U dates on speleothems from Britain. Nature, 272 24-28.

ATTREE, R.W., M.J.CABELL, R.L.CUSHING and J.J.PIERON, 1962. A calorimetric determination of the half-life of ^{230}Th and consequent revision of its neutron capture cross-section. Can. J. Phys., 40 194.

BARANOV, V.I., Yu.A.SURKOV and V.D.VILINSKII, 1958. Isotopic shifts in natural uranium compounds. Geochem. Int., 5 591-599.

BARNES, J.W., E.J.LANG and H.A.POTRATZ, 1956. Ratio of ionium to uranium in coral limestone. Science, 124 175-176.

BEAUPRE, M., 1975. Déscription des régions karstiques du Québec. Spéléo-Québec (Bull. of the Soc. Québécoise de Spéléologie), 2 (2) 31-51.

BENDER, M.L., R.G.FAIRBANKS, F.W.TAYLOR, R.K.MATTHEWS, J.G.GODDARD and W.S.BROECKER, 1979. Uranium-series dating of the Pleistocene reef tracts of Barbados, West Indies. Geol. Soc. Amer. Bull., 90 577-594.

BENJAMIN, G.J., 1970. Diving into the Blue Holes of the Bahamas. Nat. Geogr., 138 347-363.

BENSON, L.V. and R.K.MATTHEWS, 1971. Electron microprobe studies of magnesium distribution in carbonate cements and recrystallized skeletal grainstones from the Pleistocene of Barbados West Indies. J. Sed. Petr., 41 1018-1025.

BERRY, F.A., E.BOLLAY and N.R.BEERS, 1945. Handbook of Meteorology. McGraw-Hill (p.79).

BLATTNER, P. and J.R.HULSTON, 1978. Proportional variations of geochemical $\delta^{18}O$ scales - an interlaboratory comparison. Geochim. Cosmochim. Acta, 42 59-62.

BLOOM, A.L., W.S.BROECKER, J.M.A.CHAPPELL, R.K.MATTHEWS and K.J.MESOLELLA, 1974. Quaternary sea level fluctuations on a tectonic coast : new ^{230}Th/^{234}U dates from the Huon Peninsula, New Guinea. Quat. Res., 4 185-205.

BODINE, M.W., H.D.HOLLAND and M.BORCSIK, 1965. Coprecipitation of manganese and strontium with calcite. In Problems in Postmagmatic Ore Deposition (Symp.), Prague, 2 401-406.

BONATTI, E. and S.GARTNER, 1973. Caribbean climate during Pleistocene Ice Ages. Nature, 244 563-565.

BOSTROM,K., 1970. Deposition of manganese-rich sediments during glacial periods. Nature 226 629-630.

BOTTINGA, Y., 1968. Calculation of fractionation factors for carbon and oxygen isotopic exchange in the system calcite - carbon dioxide water. J. Phys. Chem., 72 800-807.

BOTTINGA, Y. and H.CRAIG, 1969. Oxygen isotope fractionation between CO_2 and water and the isotopic composition of marine atmospheric CO_2. Earth Plan. Sci. Lett., 20 250-256.

BOURQUE, P.A., 1975. Lithostratigraphic framework and unified nomenclature for Silurian and basal Devonian rocks in Eastern Gaspé Peninsula, Québéc. Can. J. Earth Sci., 12 858-872.

BOWEN, D.Q., 1977. Hot and cold climates in pre-historic Britain. Geogr. Magazine, 8 685-698.

BOWEN, D.Q., 1978. Quaternary Geology : A stratigraphic framework for multidisciplinary work. Pergamon Press 221 pp.

BRISTOW, C.R. and F.C.COX, 1973. The Gipping Till : a reappraisal of East Anglian glacial stratigraphy. J. Geol. Soc. Lond., 129 1-37.

BROECKER,W.S., 1971. Calcite accumulation rates and glacial to interglacial changes in oceanic mixing., in Late Cenozoic Glacial Ages, K.K.Turekian ed. Yale Univ.Press 239-266.

BROECKER, W.S., K.K.TUREKIAN and B.C.HEEZEN, 1958. The relation of deep sea sedimentation rates to variations in climate. Amer. J. Sci., 256 503-517.

BROECKER, W.S. and E.A. OLSON, 1960. Radiocarbon measurements and annual rings in cave formations. Nature 185 93-94.

BROECKER, W.S. and D.L.THURBER, 1965. Uranium-series dating of corals and oolites from Bahaman and Florida Key limestones. Science, 149 58-60.

BROECKER, W.S. and T. TAKAHASHI, 1966. Calcium carbonate precipitation on the Bahama Banks. J. Geophys. Res. 71 1575-1602.

BROECKER, W.S. and J.VAN DONK, 1970. Insolation changes, ice volumes, and the ^{18}O record in deep-sea cores. Rev. Geophys. Space Phys., 8 169-198.

BROOK, D., 1971. Cave development in Craven - a comment. Univ. of Leeds Spel. Assoc. Review, (8) 31-34.

BROOK, D., 1974. Cave development in Kingsdale - in Limestones and caves of north-west England, A.C.Waltham ed. David and Charles, Newton Abbot. 310- 334.

BROOK, D., R.G.COE, G.M.DAVIES and M.H.LONG, 1972. Northern Caves, Vol. 1 Wharfedale. Dalesman Pub. Co., Clapham, Yorks.

BROOK, D., A.BROOK, G.M.DAVIES and M.H.LONG, 1976. Northern Caves, Vol 2 Penyghent and Malham. Dalesman Pub. Co., Clapham, Yorks.

BURTON, J.A., R.C.PRIM and W.P.SLICHTER, 1953. The distribution of solute in crystals grown from the melt. Part I Theoretical. Int. Chem. Phys., 21 1987-1991.

BUTZER, K.W., 1975. Pleistocene Littoral-sedimentary cycles of the Mediterranean Basin : A. Mallorquin view. in After the Australopithecines, Butzer and Isaacs eds., Mouton, The Hague. 25-72.

BUTZER, K.W. and G.Ll. ISAACS eds., 1975. After the Australopithecines. Mouton, The Hague, 991pp

CHALOV, P.I., 1959. Isotopic ratio of $^{234}U/^{238}U$ in some secondary minerals. Geochem. Int. 203-210.

CHALOV, P.I., K.I.MERKULOVA and T.V.TUZOVA, 1966. $^{234}U/^{238}U$ ratio in water and bottom sediments of the Aral Sea and the absolute age of the basin. Geochem. Int., 3 1149.

CHALOV, P.I., N.A.SVETLICHNAYA and T.V.TUZOVA, 1970. $^{234}U/^{238}U$ in the waters and bottom sediments of Lake Balkash and the age of the lake. Geochem. Int., 7 604.

CHAPPELL, J., 1974. Geology of coral terraces, Huon Peninsula, New Guinea: A study of Quaternary tectonic movements and sea level changes. Geol. Soc. Amer. Bull., 85 553-570.

CHERDYNTSEV, V.V., 1955. in Transactions of the Third Session of the Commission for Determining the Absolute Age of Geological Formations, (in Russian), Moscow, Izdatel stvo Akad. Nauk. SSSR, 175.

CHERDYNTSEV, V.V., 1971. Uranium-234. Israel Program for Scientific Translations, Monson, Jerusalem 308pp.

CHERDYNTSEV, V.V., I.V.KAZACHEVSKII and E.A.KUZ'MINA, 1965. Dating of Pleistocene carbonate formations by the thorium and uranium isotopes. Geochem. Int., 2 794-801.

CLAGUE, J.J., 1976. Quadra Sand and its relation to the Late Wisconsin glaciation of southwest British Columbia. Can. J. Earth Sci., 13 803-815.

CLAYTON, K.M., 1977. River terraces, in British Quaternary Studies : Recent Advances, F.W.Shotton ed. Clarendon Press, Oxford, 153-168.

CLAYTON,R.N., 1959. Oxygen isotope equilibration in the system calcium carbonate-water. J.Chem.Phys. 30 1246-1250.

CLAYTON, R.N., 1961. Oxygen isotopic fractionation between calcium carbonate and water. J. Chem. Phys. 34 724-726.

COOPE, G.R., 1975. Climatic fluctuations in northwest Europe since the Last Interglacial, indicated by fossil assemblages of Coleoptera., in Ice Ages : Ancient and Modern, A.E.Wright and F. Moseley eds., Liverpool. 153-168.

COOPE, G.R., 1977a. Quaternary Coleoptera as aids in the interpretation of environmental history., in British Quaternary Studies : Recent Advances. F.W.Shotton ed. Clarendon Press, Oxford. 298pp.

COOPE, G.R., 1977b. Fossil coleopteran assemblages as sensitive indicators of climatic changes during the Devensian (Last) cold stage. Phil. Trans. R. Soc. Lond. B280 313-340.

CRAIG, H., 1957. Isotopic standards for carbon and oxygen and correction factors for mass spectrometric analysis of carbon dioxide. Geochim. Cosmochim. Acta 12 133-149.

CRAIG, H., 1961a. Standard for reporting concentrations of deuterium and oxygen-18 in natural waters. Science 133 1833-1834.

CRAIG, H., 1961b. Isotopic variations in meteoric waters. Science 133 1702-1703.

CRAIG, H., 1965. The measurement of oxygen isotope paleotemperatures. Proc. Spoleto Conf. on Stable Isotopes in Oceanographic Studies and Paleotemperatures. 3 3-24.

CROCKET, J.H. and J.W. WINCHESTER, 1966. Coprecipitation of zinc with calcium carbonate. Geochim. Cosmochim. Acta 30 1093-1109.

CULLINGFORD, C.H.D., 1962. British Caving: An introduction to speleology, Routledge and Kegan Paul Ltd. 592 pp.

CURRAY, J.R., 1965. Late Quaternary history, continental shelves of the U.S. in H.E.Wright and D.E.Frey eds. The Quaternary of the United States. Princeton Univ. Press. 723-735.

DANSGAARD, W., 1964. Stable isotopes in precipitation. Tellus 16 436-468.

DANSGAARD, W., S.J. JOHNSEN, J. MØLLER and C.C. LANGWAY Jr. 1969. One thousand centuries of climatic record from Camp Century on the Greenland Ice Sheet. Science 166 377-381.

DANSGAARD, W. and H. TAUBER, 1969. Glacier oxygen-18 content and Pleistocene ocean temperatures. Science 166 499-502.

DANSGAARD, W., S.J. JOHNSEN, H.B. CLAUSEN and C.C. LANGWAY Jr., 1971. Climatic record revealed by the Camp Century ice core, in Late Cenozoic Glacial Ages, K.K. Turekian ed. Yale Univ. Press, New Haven 1971. 37-56.

DARDENNE, M., 1967. Etude expérimentale de la distribution du zinc dans les carbonates de calcium. Bull. Bur. Rech. Geol. Min. 5 75-110.

DEINES, P., 1970. Mass spectrometer correction factors for the determination of small isotopic composition variations of carbon and oxygen. Int. J. Mass Spectrom. Ion Phys. 4 283-295.

DIETZ, R.S., J.C. HOLDEN and W.P. SPROLL, 1970. Geotectonic evolution and subsidence of Bahama platform. Geol. Soc. Amer. Bull. 81 1915-1928.

DONN, W.L., W.R. FARRAND and M. EWING, 1962. Pleistocene ice volumes and sea-level lowering. J. Geol. 70 206-214.

DREIMANIS, A. and R.P. GOLDTHWAIT, 1973. Wisconsin glaciation in the Huron, Erie and Ontario Lobes. Geol. Soc. Amer. Mem. 136 71-105.

DREIMANIS, A. and P.F. KARROW, 1972. Glacial history of the Great Lakes - St. Lawrence region, the classification of the Wisconsin(an) stage and its correlatives. 24th Int. Geol. Cong. Montréal, Canada. Sect. 12, Quat. Geol. 5-15.

DUNHAM, K.C., 1974. Granite beneath the Pennines in North Yorkshire. Proc. Yorks. Geol. Soc. 40 191-194.

DUNHAM, K.C., J.E. HEMINGWAY, H.C. VERSEY and W.H. WILCOCKSON, 1953. A guide to the geology of the district round Ingleborough. Proc. Yorks. Geol. Soc. 29 77-115.

DUPLESSY, J.C., C. LALOU and A.E. GOMES DE AZEVEDO, 1969. Etude des conditions de concretionnement dans les grottes au moyen des isotopes stables de l'oxygen et du carbon. Acad. Sci.,C.R., Ser. D, 268 2327-2330.

DUPLESSY, J.C., C. LALOU and A.C. VINOT, 1970a. Differential isotopic fractionation in benthic foraminifera and paleotemperatures reasssessed. Science 168 250-251.

DUPLESSY, J.C., J. LABEYRIE, C. LALOU and H.V. NGUYEN, 1970b. Continental climatic variations between 130,000 and 90,000 years B.P. Nature 226 631-633.

EASTERBROOK, D.J., 1969. Pleistocene chronology of the Puget Lowland and San Juan Islands, Washington. Geol. Soc. Amer. Bull. 80 2273-2286.

EASTERBROOK, D.J., 1976. Stratigraphy and palynology of late Quaternary sediments in the Puget Lowland, Washington: reply. Geol. Soc. Amer. Bull. 87 155-156.

EDWARDS, W. and F.M. TROTTER, 1968. British Regional Geology : The Pennines and Adjacent Areas. NERC. IGS. pub. 3rd ed. H.M. Stationers 86pp.

EMILIANI, C., 1955. Pleistocene temperatures. J. Geol. 63 538-578.

EMILIANI, C., 1966. Isotopic paleotemperatures. Science 154 851-857.

EMILIANI, C., 1971. The last interglacial : paleotemperatures and chronology. Science 171 571-573

EMILIANI, C., 1978. The cause of the Ice Ages. Earth Plan. Sci. Lett. 37 349-352.

EPSTEIN, S., R. BUCHSBAUM, H. LOWENSTAM and H.C. UREY, 1951. Carbonate-water isotopic temperature scale. Geol. Soc. Amer. Bull. 62 417-426.

EPSTEIN, S., R. BUCHSBAUM, H.A. LOWENSTAM and H.C. UREY, 1953. Revised carbonate-water isotopic temperature scale. Geol. Soc. Amer. Bull. 64 1315-1326.

EPSTEIN, S., R.P. SHARP and A.J. GOW, 1970. Antarctic Ice Sheet : Stable isotope analyses of Byrd Station cores and interhemispheric climatic implications. Science 168 1570-1572.

ERICSON, D.B., M. EWING, G. WOLLIN and B.C. HEEZEN, 1961. Atlantic deep-sea sediment cores. Geol. Soc. Amer. Bull. 72 193-286.

ERICSON, D.B., M. EWING and G. WOLLIN, 1964. The Pleistocene epoch in deep-sea sediments. Science 146 723-732.

EVANS, G.V., R.L. OTLET, R.A. DOWNING, R.A. MONKHOUSE and G.RAE, 1978. Some problems in the interpretation of isotope measurements in British aquifers. IAEA Int. Symp. on Hydrol. Neuherberg. F.R.G.

EVANS, P., 1971. Towards a Pleistocene time-scale, in The Phanerozoic Time-Scale. Spec. Pub. 5 Geol. Soc. Lond. 123-356.

EYRE, J. and P.F. ASHMEAD, 1967. Lancaster Hole and Ease Gill Caverns. Trans. Cave Res. Grp. of G.B. 9 61-123.

FAIRBANKS, R.G. and R.K. MATTHEWS, 1978. The marine oxygen isotopic record in Pleistocene coral, Barbados, West Indies. Quat. Res. 10 181-196.

FANTIDIS, J. and D.H. EHHALT, 1970. Variations of the carbon and oxygen isotopic composition in stalagmites and stalactites : evidence of non-equilibrium isotopic fractionation. Earth Plan. Sci. Lett. 10 136-144.

FINCHAM, A.G., 1977. Jamaica Underground. Geol. Soc. Jamaica publication 247pp.

FISK, H. and E. McFARLAN, 1955. Late Quaternary deltaic deposits of the Mississippi River. Geol. Soc. Amer. Spec. Pap. 62 279-302.

FLINT, R.F., 1971. Glacial and Quaternary Geology. J.Wiley and Sons Inc. N.Y. 892pp.

FLORER, L.E. 1972. Quaternary paleoecology and stratigraphy of the sea cliffs, western Olympic Peninsula, Washington. Quat. Res. 2 202-216.

FORD, D.C., 1976. Report on the Euclataws-Main Cave system of Horne Lake Provincial Park, Vancouver Island. submitted to Min. of Recr. and Cons. Parks Branch, B.C.

FORNACA-RINALDI, G., 1968. Il methodo Th^{230}/U^{238} per la datazione di stalactiti e stalagmiti. Boll. Geofis. Teor. Appl. 10 3-14.

FORNACA-RINALDI, G., C. PANICHI and E. TONGIORGI, 1968. Some causes of the variations of the isotopic composition of carbon and oxygen in cave concretions. Earth. Plan. Sci. Lett. 4 321-324.

FRENZEL, B., 1973. Some remarks on the Pleistocene vegetation. Eiszeitalter und Gegenwart 23/24 281-292.

FRIEDMAN, I., 1970. Some investigations of the deposition of travertine from Hot Springs. I. The isotopic chemistry of a travertine-depositing spring. Geochim. Cosmochim. Acta 34 1303-1315.

FRYE, J.C. and H.B. WILLMAN; 1973. Wisconsinan climatic history interpreted from Lake Michigan lobe deposits and soils. Geol. Soc. Amer. Mem. 136 135-152.

FUCHTBAUER, H. and L.A. HARDIE, 1976. Experimentally determined homogeneous distribution coefficients for precipitated magnesium calcites: Application to marine carbonate cements. Abstr. Geol. Soc. Amer. Ann. Meeting 1976 Colorado.

FULTON, R.J., J.E. ARMSTRONG and J.G. FYLES, 1976. Stratigraphy and palynology of late Quaternary sediments in the Puget Lowland, Washington : Discussion. Geol. Soc. Amer. Bull. 87 153-155.

FULTON, R.F. and G.W. SMITH, 1978. Late Pleistocene stratigraphy of south-central British Columbia. Can. J. Earth Sci. 15 971-980.

FUNNEL, B.M. and R.G. WEST, 1977. Preglacial Pleistocene deposits of East Anglia, in British Quaternary Studies : Recent Advances, F.W.Shotton ed. Clarendon Press, Oxford. 247-266.

FYLES, J.G., 1963. Surficial geology of Horne Lake and Parksville map-areas, Vancouver Island, British Columbia. Geol. Surv. of Can. Mem. 318 142pp.

GASCOYNE, M., 1977a. Uranium series dating of speleothems : an investigation of technique,data processing and precision. Tech. Memo. 77-4 Dept. of Geology, McMaster Univ. Hamilton.

GASCOYNE, M., 1977b. Trace element geochemistry of speleothems. Proc. 7th Int. Speleo. Cong. Sheffield, England, Sept/ 1977. 205-208.

GASCOYNE, M., G.J. BENJAMIN, H.P. SCHWARCZ and D.C. FORD, 1979. Sea-level lowering during the Illinoian glaciation : Evidence from a Bahama 'blue hole'. Science 205 806-808.

GATES, W.L., 1976. Modeling the Ice-Age climate. Science 191 1138-1144.

GEYH, M.A., 1970. Isotopenphysikalische Untersuchungen an Kalksinter, ihre Bedutung für die ^{14}C-altersbestimmung von Grundwasser und die Erforschung des Palaoklimas. Geologisches Jahrbuch. 88 149-158.

GIBBARD, P.C,, 1977. Pleistocene history of the Vale of St.Albans. Phil.Trans.R.Soc.Lond. B280 445-483.

GIRLING, M.A., 1974. Evidence from Lincolnshire of the age and intensity of the mid-Devensian temperate episode. Nature, Lond. 250 270.

GLOVER, R.R., 1974. Cave development in the Gaping Gill system, in Limestones and Caves of North-West England. A.C.Waltham ed. David and Charles, Newton Abbot. 343-384.

GODWIN, H., 1977. Quaternary history of the British flora, in British Quaternary Studies : Recent Advances, F.W.Shotton ed. Clarendon Press, Oxford. 107-118.

GOODCHILD, J.G., 1875. The glacial phenomena of the Eden Valley and the western part of the Yorkshire Dale District. Quart. J. Geol. Soc. 31 65-99.

GOODELL, H.G. and R.K. GARMAN, 1969. Carbonate chemistry of Superior deep test well, Andros Island, Bahamas. Am.Assoc.Petr.Geologists Bull. 53 513-536.

GRAY, J. and P. THOMPSON, 1977. Climatic information from $^{18}O/^{16}O$ analysis of cellulose, lignin and whole wood from tree rings. Nature 270 708-709.

VAN DER HAMMEN, T., T.A. WIJMSTRA and W.H. ZAGWIJN, 1971. The floral record of the Late Cenozoic of Europe, in The Late Cenozoic Glacial Ages, K.K.Turekian ed. Yale Univ. Press 391-424.

HANSEN, B.S. and D.J. EASTERBROOK, 1974. Stratigraphy and palynology of Late Quaternary sediments in the Puget Lowland, Washington. Geol. Soc. Amer. Bull. 85 587-602.

HARMON, R.S., 1975. Late Pleistocene paleoclimates in North America as inferred from isotopic variations in speleothems. PhD Thesis, McMaster Univ., Hamilton, Ontario.

HARMON, R.S., P.THOMPSON, H.P. SCHWARCZ and D.C. FORD, 1975. Uranium-series dating of speleothems Bull. Nat. Speleol. Soc. 37 21-33.

HARMON, R.S. and T-L.KU, 1976. The absolute limits of the $^{230}Th/^{234}U$ dating method: Preliminary results of the Geochronological Interlaboratory Comparison Project. Geol. Soc. Amer. Abs. Ann. Meeting 1976 Colorado. 903-904.

HARMON, R.S., D.C. FORD and H.P. SCHWARCZ, 1977. Interglacial chronology of the Rocky and MacKenzie Mountains based on 230Th/234U dating of calcite speleothems. Can. J. Earth Sci. 14 2543-2552.

HARMON, R.S., P. THOMPSON, H.P. SCHWARCZ and D.C. FORD, 1978a. Late Pleistocene paleoclimates of North America as inferred from stable isotope studies of speleothems. Quat.Res.9 54-70.

HARMON, R.S., H.P. SCHWARCZ and D.C. FORD, 1978b. Late Pleistocene sea level history of Bermuda. Quat. Res. 9 205-218.

HARMON, R.S., H.P. SCHWARCZ, P. THOMPSON and D.C. FORD, 1978c. Critical comment on ' Uranium-series dating of stalagmites from Blanchard Springs Cavern, Arkansas, USA'. Geochim. Cosmochim. Acta 42 433-439.

HARMON, R.S., H.P. SCHWARCZ and D.C. FORD, 1978d. Stable isotope geochemistry of speleothems and cave waters from the Flint Ridge - Mammoth Cave system, Kentucky : Implications for terrestrial climate change during the period 230,000 to 100,000 years B.P. J. Geol. 86 373-384.

HARMON, R.S., T-L KU, R.K. MATTHEWS and P.L. SMART, 1979a. Limits of U-series analysis : Phase 1 results of the uranium-series intercomparison project. Geology 7 405-409.

HARMON, R.S., H.P. SCHWARCZ, D.C. FORD and D.L. KOCH, 1979b. An isotopic paleotemperature record for late Wisconsin time in northeast Iowa. Geology 7 430-433.

HASSAN, F., 1978. Impurity-related centers in a pale-green calcite crystal. Amer. Mineralogist 63 732-736.

HAYS, J.D., J. IMBRIE and N.J. SHACKLETON, 1976. Variations in the earth's orbit : Pacemaker of the Ice Ages. Science 194 1121-1132.

HEATH, G.R., T.C. MOORE Jnr. and J.P. DAUPHIN, 1976. Late Quaternary accumulation rates of opal, quartz, organic carbon and calcium carbonate in the Cascadia Basin area, northeast Pacific. Geol. Soc. Amer. Mem. 145 393-410.

HEEZEN, B., M. THARP and M. EWING, 1959. The floors of the oceans: 1. The North Atlantic. Geol. Soc. Amer. Spec. Pap. 65 122pp.

HENDY, C.H., 1969. The isotopic geochemistry of speleothems and its application to the study of past climates. PhD Dissertation, Victoria Univ., Wellington, New Zealand.

HENDY, C.H., 1971. The isotopic geochemistry of speleothems I. The calculation of the effects of different modes of formation on the isotopic composition of speleothems and their applicability as paleoclimatic indicators. Geochim. Cosmochim. Acta 35 801-824.

HENDY, C.H. and A.T. WILSON, 1968. Palaeoclimatic data from speleothems. Nature 216 48-51.

HEUSSER, C.J., 1977. Quaternary palynology of the Pacific slope of Washington. Quat.Res.2 189-201

HOLLAND, H.D., H.J. HOLLAND and J.L. MUNOZ, 1964a. The coprecipitation of cations with $CaCO_3$. II. The coprecipitation of Sr^{2+} with calcite between 90° and 100°C. Geochim. Cosmochim. Acta 28 1287-1301.

HOLLAND, H.D., T.U. KIRSIPU, T.J. HEUBNER and U.M. OXBURGH, 1964b. On some aspects of the chemical evolution of cave waters. J.Geol. 72 36-67.

HUFF, E.A., 1965. Trace impurity analysis of Th-U and Pu-Th-U alloys by anion exchange - partition chromatography. Anal. Chem. 37 533-536.

HYDE, E.K., 1949. Determination of the half-life of ionium. Natl. Nucl. Energy Series,Div. III, 14b, Transuranic elements Pt. II 1435.

ICHIKUNI, M., 1973. Partition of strontium between calcite and solution : effect of substitution by manganese. Chem. Geol. 11 315-319.

IMBRIE, J. and N.G. KIPP, 1971. A new micropaleontological method for quantitative paleoclimatology : Application to a Late Pleistocene Caribbean core, in The Late Cenozoic Glacial Ages, K.K.Turekian ed. Yale Univ. Press, New Haven. 77-181.

IMBRIE, J., J.van DONK and N.G. KIPP, 1973. Paleoclimatic investigation of a late Pleistocene Caribbean deep-sea core : Comparison of isotopic and faunal methods. Quat. Res. 3 10-38.

JAMES, N.P., E.W. MOUNTJOY and A. OMURA, 1971. An Early Wisconsin reef terrace at Barbados, West Indies, and its climatic implications. Bull. Geol. Soc. Amer. 82 2011-2017.

JARDINE, W.G. and J.D. PEACOCK, 1973. Scotland, in Mitchell et al., A correlation of Quaternary deposits in the British Isles. Geol. Soc. Lond. Spec. Rep. No. 4 99pp.

JOHNSON, J.A., 1979. Investigation of Mg and Sr distribution in speleothem. BSc Thesis.Geology Dept. McMaster Univ. Hamilton, Ontario.

JOSHI, M.S., 1960. Precipitation of carbonates from sea water. Prog. Rep., U.S.A.E.C. Contract No. AT (30-1) - 2266.

KATZ, A., 1973. The interaction of magnesium with calcite during crystal growth at 25-95^{o}C and one atmosphere. Geochim. Cosmochim. Acta 37 1563-1586.

KATZ, A., E. SASS, A. STARINSKY and H.D. HOLLAND, 1972. Strontium behaviour in the aragonite-calcite transformation : an experimental study at 40-98^{o}C. Geochim. Cosmochim. Acta 36 481-496.

KATZ, J.J. and G.T. SEABORG, 1957. The Chemistry of the Actinide Elements. Methuen & Co.508pp.

KAUFMAN, A., 1964. Th^{230}/U^{234} dating of carbonates from Lakes Lahontan and Bonneville. PhD dissertation, Columbia Univ. New York.

KAUFMAN, A., 1971. U-series dating of Dead Sea Basin carbonates. Geochim. Cosmochim. Acta 35 1269.

KAUFMAN, A. and W.S. BROECKER, 1965. Comparison of Th^{230} and C^{14} ages for carbonate materials from Lakes Lahontan and Bonneville. J. Geophys. Res. 70 4039-4054.

KAUFMAN, M.I., H.S. RYDELL and J.K. OSMOND, 1969. ^{234}U/^{238}U disequilibrium as an aid to hydrologic study of the Floridan aquifer. J. of Hydrol. 9 374-386.

KENDALL, A.C. and P.L. BROUGHTON, 1978. Origin of fabrics in speleothems composed of columnar calcite crystals. J.Sed.Petr. 48 519-538.

KERNEY, M.P., 1977. British Quaternary non-marine mollusca: a brief review, in British Quaternary Studies: Recent Advances. F.W. Shotton ed. Clarendon Press, Oxford. 31-42.

KIGOSHI, K., 1971. Alpha-recoil thorium-234 : Dissolution into water and the uranium 234/uranium 238 disequilibrium in nature. Science 173 49.

KING, C.A.M., 1976. The Geomorphology of the British Isles : Northern England. Methuen. 213pp.

KINSMAN, D.J.J. and H.D. HOLLAND, 1969. The co-precipitation of cations with CaCO$_3$ - IV. The co-precipitation of Sr^{2+} with aragonite between 16^{o} and 96^{o}C. Geochim. Cosmochim. Acta 33 1-17.

KIPP, N.G., 1976. New transfer function for estimating past sea-surface conditions from sea-bed distribution of planktonic foraminiferal assemblages in the North Atlantic, in Investigation of Late Quaternary Paleoceanography and paleoclimatology. R.M. Cline and J.D. Hays eds. Geol. Soc. Amer. Mem. 145 3-42.

KIRBY. H.W., 1961. Calorimetric determination of the half-life of protactinium. J. Inorg. Nucl. Chem. 18 8.

KLÖTZER, von D. and H.W. LEVI, 1966. Mitkristallisation im System CaCO$_3$/SrCO$_3$. Radiochim. Acta 6 81-85.

KOCZY, F.F., 1954. Radioactive elements in ocean waters and sediments: Geochemical balance in the Hydrosphere, in Nuclear Geology, H. Faul ed. John Wiley and Sons, N.Y. 120-127.

KOHOUT, F.A., G.W. LEVE and F.T. SMITH, 1975. Red Snapper Sink and groundwater flow, offshore northeastern Florida. 12th Int. Cong. of Int. Assoc. Hydrogeologists. Huntsville. Ala.

KOLESAR, P.T., 1978. Magnesium in calcite from a coralline alga. J. Sed. Petr. 48 815-820.

KOMURA, K. and M. SAKANOUE, 1967. Studies on the dating methods for Quaternary samples by natural alpha-radioactive nuclides. Kanazawa Univ. Fac. Sci. Jap., Sci. Rep., 12 21.

KONISHI, K., A. OMURA and T. KIMURA, 1968. ^{234}U-^{230}Th dating of some Late Quaternary coralline limestones from southern Taiwan (Formosa). Geol. Palaeontol. S.E.Asia 5 211-224.

KONISHI, K., S.O. SCHLANGER and A. OMURA, 1970. Neotectonic rates in the central Ryukyu Islands derived from ^{230}Th coral ages. Marine Geol. 9 225-240.

KORKISCH, J., 1969. Modern Methods for the Separation of Rarer Metal Ions. Pergamon Press 620pp

KRONFELD, J., 1974. Uranium deposition and Th-234 alpha-recoil : An explanation for extreme U-234/U-238 fractionation within the Trinity aquifer. Earth and Plan. Sci. Lett. 21 327-330.

KRONFELD, J. and J.A.S. ADAMS, 1974. Hydrologic investigations of the groundwaters of central Texas using U-234/U-238 disequilibrium. J. Hydrol. 22 77.

KU, T-L., 1965. An evaluation of the U^{234}/U^{238} method as a tool for dating pelagic sediments. J. Geophys. Res. 70 3457-3474.

KU, T-L., 1968. Protactinium 231 method of dating coral from Barbados Island. J. Geophys. Res. 73 2271-2276.

KU, T-L., 1976. The uranium-series methods of age determination. Ann. Rev. Earth Plan. Sci. 4 347-380.

KU, T-L., M.A. KIMMEL, W.H. EASTON and T.J. O'NEIL, 1974. Eustatic sea level 120,000 years ago on Oahu, Hawaii. Science 183 959-962.

KU, T-L., W.G. BULL, S.T. FREEMAN and K.G. KNAUSS, 1979. Th^{230}/U^{234} dating of pedogenic carbonates in gravelly desert soils of Vidal Valley, Southeastern California. Bull. Geol. Soc. Amer. 90 1063-1073.

KUKLA, G.J., 1975. Loess stratigraphy of Central Europe, in After the Australopithecines, K.W. Butzer and G.Ll. Isaac eds. Mouton, The Hague. 99-188.

KUKLA, G.J., 1977. Pleistocene land-sea correlations. 1. Europe. Earth Sci. Rev. 13 307-374.

LABEYRIE, J., J.C. DUPLESSY, G. DELIBRIAS and R. LETOLLE, 1967. Etude des temperatures des climats anciens, par la mesure de l'oxygen-18 du carbone-13 et du carbone-14 dans les concretions des cavernes, in Symposium of Radio-active Dating and Methods of Low Level Counting, Proc. of IAEA Symp., Monaco, 1967, SM-87/5. 153-160.

LAL, D., J.R. ARNOLD and B.L.K. SOMAYAJULU, 1964. A method for the extraction trace elements from sea water. Geochim. Cosmochim. Acta 28 1111-1117.

LANGMUIR, D. and K.APPLIN, 1977. Refinement of the thermodynamic properties of uranium minerals and dissolved species, with application to the chemistry of groundwaters in sandstone-type uranium deposits, in Short Papers of the US Geol. Surv. Uranium - Thorium Symp. Circ. 753, J.A. Campbell ed. 57-60.

LATHAM, A.G., M. GASCOYNE and D.C. FORD, 1978. Report upon the Riverbend Cave system of Horne Lake Caves Provincial Park, Vancouver Island. Min. of Recr. and Conserv. B.C. 9pp

LEDERER, C.M. and V.S. SHIRLEY (eds) 1978. Table of Isotopes. 7th ed. Wiley Intersci. 1523pp.

LERMAN, A., 1965. Paleoecological problems of Mg and Sr in biogenic calcites in light of recent thermodynamic data. Geochim. Cosmochim. Acta 29 977-1002.

LLOYD, M.R., 1964. Variations in the oxygen and carbon isotope ratios of Florida Bay mollusks and their environmental significance. J. Geol. 72 84.

LONGSTAFFE, F.J., 1977. Oxygen isotope and elemental geochemistry of Archean rocks. PhD Thesis Dept. of Geology, McMaster Univ. Hamilton, Ontario.

LOWENSTAM, H.A., 1961. Mineralogy, O-18/O-16 ratios and strontium and magnesium contents of recent and fossil brachiopods and their bearing on the history of the oceans. J. Geol. 69 241-260.

LYNTS, G.W., J.B. JUDD and C.F. STEHMAN, 1973. Late Pleistocene history of the Tongue of the Ocean, Bahamas. Geol. Soc. Amer. Bull. 84 2665-2684.

MANSKAYA, S.M. and T.V. DROZDOVA, 1968. Geochemistry of Organic Substances. Pergamon Press 347pp

MARSHALL, J.F. and J. LAUNAY, 1978. Uplift rates of the Loyalty Islands as determined by 230Th/234U dating of raised coral terraces. Quat. Res. 9 186-192.

MATTHEWS, W.H. and J.W. McCAMMON, 1957. Calcareous deposits of south-west British Columbia. B.C. Dept. of Mines Bull. No. 40.

McCREA, J.M., 1950. On the isotopic chemistry of carbonates and a paleotemperature scale. J. Chem. Phys. 18 849-857.

McINTIRE, W.L., 1963. Trace element partition coefficients - a review of theory and applications to geology. Geochim. Cosmochim. Acta. 27 1209-1264.

McKENNEY, J., 1972. Diving in the world's largest underwater cave. Skin Diver 21 42-49.

McKINNEY, C.R., J.M. McCREA, S. EPSTEIN, H.A. ALLEN and H.C. UREY, 1950. Improvements in mass spectrometers for the measurement of small differences in isotopic abundance ratios. Rev. Sci. Inst. 21 724.

MESOLELLA, K.J., R.K. MATTHEWS, W.S. BROECKER and D.L. THURBER, 1969. The astronomical theory of climate change : Barbados data. J. Geol. 77 250-274.

MICHARD, G., 1968. Coprécipitation de l'ion manganeux avec le carbonate de calcium. Comptes Rendus Acad. Sci. Paris 267 1685-1688.

MICHARD, G., 1971. Contribution à l'étude de l'entrainement des élements traces dans la calcite lors de sa précipitation. Exemple des concrétions de la Fontaine de Reotier (Hautes Alpes, Frances). Chem. Geol. 8 311-327.

MILLIMAN, J.D. and K.O.EMERY, 1968. Sea levels during the past 35,000 years. Science 162 1121-1123.

MITCHELL, G.F., 1977. Raised beaches and sea levels, in British Quaternary Studies : Recent Advances, F.W.Shotton ed. Clarendon Press, Oxford. 169-186.

MITCHELL, G.F., L.F. PENNY, F.W. SHOTTON and R.G. WEST, 1973. A correlation of Quaternary deposits in the British Isles. Geol. Soc. Lond. Spec. Rep. No. 4 99pp.

MOORE, G.W., 1952. Speleothem - a new cave term. Nat. Speleol. Soc. News, 10 2.

MOORE, G.W., 1956. Aragonite speleothems as indicators of paleotemperature. Amer. J. Sci. 254 746-753.

MOORE, W.S. and B.L.K. SOMAYAJULU, 1974. Age determinations of fossil corals using ^{230}Th/^{234}Th and ^{230}Th/^{227}Th. J. Geophys. Res. 79 5065-5068.

MORGAN, A.V., 1973. The Pleistocene geology of the area north and west of Wolverhampton, Staffordshire, England. Phil. Trans. R. Soc. Lond. B265 233-297.

NEUMANN, A.C. and W.S. MOORE, 1975. Sea level events and Pleistocene coral ages in the Northern Bahamas. Quat. Res. 5 215-224.

NEWELL, N.D., 1955. Bahamian Platforms. Geol. Soc. Amer. Spec. Pap. 62 303-316.

NGUYEN, H.V. and C. LALOU, 1969. Comportement geochemique des isotopes des familles de l'uranium et du thorium dans les concrétions des grottes : Application à la datation des stalagmites. Comptes Rendus 269 560-563.

NIER, A.O., 1947. A null method for the comparison of two ion currents in a mass spectrometer: Rev. Sci. Instr., 18 294.

NINKOVITCH, D. and N.J. SHACKLETON, 1975. Distribution, stratigraphic position and age of ash layer 'L' in the Panama Basin. Earth Plan. Sci. Lett., 27 20-34.

OLAUSSON, E., 1965. Evidence of climatic changes in North Atlantic deep sea cores, with remarks on isotopic palaeotemperature analysis. Prog. in Oceanography, 3 221-252.

OLSON, E.R., 1975. Oxygen and sulphur isotope geochemistry of marine evaporites. PhD Thesis, Dept. of Geology, McMaster Univ., Hamilton, Ontario.

O'NEIL, J.R., R.N. CLAYTON and T. MAYEDA, 1969. Oxygen isotope fractionation in divalent metal carbonates. J. Chem. Phys. 51 5547-5558.

O'NEIL, J.R., L.H. ADAMI and S. EPSTEIN, 1975. Revised value for the ^{18}O fractionation factor between CO_2 and H_2O at 25°C. U.S. Geol. Surv. J. Res. 3 623-624.

OSMOND, J.K., J.P. MAY and W.F. TANNER, 1970. Age of the Cape Kennedy barrier and lagoon complex. J. Geophys. Res. 75 469-479.

OSMOND, J.K., M.I. KAUFMAN and J.B. COWART, 1974. Mixing volume calculations, sources and aging trends of Floridan aquifer water by uranium isotopic methods. Geochim. Cosmochim. Acta 38 1083-1100.

OSMOND, J.K. and J.B. COWART, 1976. The theory and uses of natural uranium isotopic variations in hydrology. Atomic Energy Review 14 621-679.

PENCK, A. and E. BRUCKNER, 1909. Die Alpen im Eiszeitalter, Leipzig.

PENG, T-H., J.G. GODDARD and W.S. BROECKER, 1978. A direct comparison of ^{14}C and ^{230}Th ages at Searles Lake, California. Quat. Res. 9 319-329.

PENNY, L.F., 1964. A review of the last glaciation in Great Britain. Proc. Yorks. Geol. Soc. 34 387-411.

PENNY, L.F., G.R. COOPE and J.A. CATT, 1969. Age and insect fauna of the Dimlington Silts, East Yorkshire. Nature Lond. 224 65-67.

PICCIOTTO, E., X. de MAERE and I. FRIEDMAN, 1960. Isotopic composition and temperature of formation of Antarctic snows. Nature 187 857-859.

PICKNETT, R.G., 1976. The chemistry of cave waters, Part II: Advance Discussion, in The Science of Speleology, T.D. Ford and C.H.D. Cullingford eds. Academic Press, London. 225-248.

PILKEY, O.H. and J. HOWER, 1960. Effect of environment on the concentration of skeletal Mg and and Sr in Dendraster . J. Geol. 68 203-216.

PITTY, A.F., 1966. An approach to the study of karst water. Occasional Papers in Geography, No. 5 , University of Hull, England.

PITTY, A.F., 1974. Karst water studies in and around Ingleborough Cavern, in Limestones and Caves of North-West England. A.C. Waltham ed. David and Charles, Newton Abbot. 127-139.

PORTER, S.C., 1979. Quaternary stratigraphy and chronology of Mauna Kea, Hawaii: A 380,000-yr. record of mid-Pacific volcanism and ice-cap glaciation.Summary. Geol. Soc. Amer. Bull. 90 609-611.

ROBERGE, J. and M. GASCOYNE, 1978. Premiers résultats de datations dans la Grotte de Saint-Elzéar, Gaspésie, Québec. Geogr. phys. Quat. 32 281-287.

ROSHOLT, J.N., 1967. Open-system model for U-series dating of Pleistocene samples. Proc. Symp. on Radioactive Dating and Methods of Low-Level Counting, IAEA. 299-310.

ROSHOLT, J.N. and P.S. ANTAL, 1962. Evaluation of the ^{231}Pa/U - ^{230}Th/U method for dating Pleistocene carbonate rocks. U.S. Geol. Surv. Prof. Pap. 450 E108-E111.

ROSHOLT, J.N., A.P. BUTLER, E.L. GARNER and W.R. SHIELDS, 1965. Isotopic fractionation of uranium in sandstone, Powder River Basin, Wyoming and Slick Rock District, Colorado. Econ. Geol. 60 199.

ROWLANDS, B.M., 1971. Radiocarbon evidence of the age of an Irish Sea glaciation in the Vale of Clwyd. Nature Phys. Sci. 230 9-11.

ROYAL, W.R., 1978. The Man who Rode Sharks. Dodd, Mead and Co. N.Y. 254pp.

RUHE, R.V., 1965. Quaternary paleopedology, in The Quaternary of the United States, H.E.Wright and D.G. Frey eds. 755-764.

SAVIN, S.M. and F.G. STEHLI, 1974. Interpretation of oxygen isotope paleotemperature measurements: effect of the $^{18}O/^{16}O$ ratio of sea water, depth stratification of foraminifera and selective solution, in Colloques Internationaux du C.N.R.S. No. 219 183-191.

SAVIN, S.M., R.G. DOUGLAS and F.G. STEHLI, 1975. Tertiary marine paleotemperatures. Geol. Soc. Amer. Bull. 86 1499-1510.

SCHWARCZ, H.P., 1971. Conversion of mass spectrometric data for C, O, S. Tech. Memo. 71-7, Dept. of Geology, McMaster Univ., Hamilton, Ontario.

SCHWARCZ, H.P., 1979. Absolute age determination of archeological sites by uranium series dating of travertines. in press, Archeometry.

SCHWARCZ, H.P., R.S. HARMON, P. THOMPSON and D.C. FORD, 1976. Stable isotope studies of fluid inclusions in speleothems and their paleoclimatic significance. Geochim. Cosmochim. Acta 40 657-665.

SCHWARCZ, H.P., B. BLACKWELL, P. GOLDBERG and A.E. MARKS, 1979. Uranium series dating of travertine from archeological sites, Nahal Zin, Israel. Nature 277 558-560.

SCHWARZACHER, W., 1958. The stratification of the Great Scar limestone in the Settle district of Yorkshire. L'pool. Manchr. geol. J. 2 124-142.

SHACKLETON, N.J., 1967. Oxygen isotope analyses and Pleistocene temperatures re-assessed. Geol. Soc. Amer. Bull. 215 15-17.

SHACKLETON, N.J., 1977. The oxygen isotope stratigraphic record of the Late Pleistocene. Phil. Trans. R. Soc. Lond. B280 169-182.

SHACKLETON, N.J. and C. TURNER, 1967. Correlation between marine and terrestrial Pleistocene successions. Nature 216 1079-1082.

SHACKLETON, N.J. and N.D. OPDYKE, 1973. Oxygen isotope and palaeomagnetic stratigraphy of equatorial Pacific core V28-238 : Oxygen isotope temperatures and ice volumes on a 10^5 year and 10^6 year scale. Quat. Res. 3 39-55.

SHACKLETON, N.J. and N.D. OPDYKE, 1976. Oxygen isotope and paleomagnetic stratigraphy of Pacific core V28-239, Late Pliocene to latest Pleistocene, in Investigation of Late Quaternary Paleoceanography and Paleoclimatology, R.M.Cline and J.D.Hays eds. Geol. Soc. Amer. Mem. 145 449-464.

SHANKAR, J., D.V. BHATNAGAR and T.K.S. MURTHY, 1956. An ion exchange process for the recovery of uranium from carbonate leach solutions. Proc. Int. Conf. on Peaceful Uses of Atomic Energy. Vol. 8 Production Technology of the Materials Used for Nuclear Energy. New York 1956.

SHOTTON, F.W., 1977. Chronology, climate and marine record; The Devensian Stage: its development, limits and substages. Phil. Trans. R. Soc. Lond. B280 107-118.

SHOTTON, F.W., P.H. BANHAM and W.W. BISHOP, 1977. Glacial-interglacial stratigraphy of the Quaternary in Midland and Eastern England, in British Quaternary Studies : Recent Advances, F.W. Shotton ed. Clarendon Press, Oxford. 267-282.

SIMPSON, I.M. and R.G. WEST, 1958. On the stratigraphy and palaeobotany of a late-Pleistocene organic deposit at Chelford, Cheshire. New Phytol. 57 239-250.

SISSONS, J.B., 1967. Glacial stages and radiocarbon dates in Scotland. Scot. J. Geol. 3 375-381.

SPAETH, C., J. HOEFS and U. VETTER, 1971. The isotopic composition of belemnites and related paleotemperatures. Geol. Soc. Amer. Bull. 82 3139-3150.

SPALDING, R.F. and T.D. MATHEWS, 1972. Submerged stalagmites from caves in the Bahamas: Indicators of low sea stand. Quat. Res. 2 470-472.

SPARKS, B.W. and R.G. WEST, 1972. The Ice Age in Britain, Methuen and Co. Ltd. 302pp.

SPENCER, M., 1967. Bahamas deep test. Assoc. Amer. Petr. Geologists Bull. 51 263-268.

STAHL, W. and R. JORDAN, 1969. General considerations on isotopic paleotemperature determinations and analyses on Jurassic ammonites. Earth Plan. Sci. Lett. 6 173-178.

STARIK, I.E., F.E. STARIK and B.A. MIKHAILOV, 1958. Shifts of isotopic ratios in natural materials. Geochemistry. 5 587-590.

STEINEN, R.P., R.S. HARRISON and R.K. MATTHEWS, 1973. Eustatic low stand of sea level between 125,000 and 105,000 B.P. : Evidence from the subsurface of Barbados, West Indies. Geol. Soc. Amer. Bull. 84 63-70.

STUART, A.J., 1977. British Quaternary vertebrates, in British Quaternary Studies : Recent Advances, F.W.Shotton ed. Clarendon Press, Oxford. 69-82.

STUIVER, M., 1968. Oxygen-18 content of atmospheric precipitation during last 11,000 yrs. in the Great Lakes region. Science 162 994-997.

SUTCLIFFE, A.J., D. BRAMWELL, A. KING and M. WALKER, 1976. Cave palaeontology and archaeology, in The Science of Speleology, T.D. Ford and C.H.D. Cullingford eds. Academic Press, London. 495-549.

SWEETING, M.M., 1950. Erosion cycles and limestone caverns in the Ingleborough district. Geogr. J. 115 63.

SWEETING, M.M., 1958. The karstlands of Jamaica. Geogr. J. 124 184-199.

SWEETING, M.M., 1974. Karst geomorphology in North-West England, in Limestones and Caves of North-West England, A.C. Waltham ed. 46-78.

TALWANI, M., J.L. WORZEL and M. EWING, 1960. Gravity anomalies and structure of the Bahamas. 2nd Caribb. Geol. Conf. Trans. Mayaguez, Puerto Rico. 1959. 156-161.

TAUBER, H., 1970. The Scandinavian varve chronology and C-14 dating, in Radiocarbon Variations and Absolute Chronology, I. Olsson ed., Stockholm 173-196.

TARUTANI, T., R.N. CLAYTON and T. MAYEDA, 1969. The affect of polymorphism and magnesium substitution on oxygen isotope fractionation between calcium carbonate and water. Geochim. Cosmochim. Acta 33 987-996.

THOMPSON, G., R.L. WALKER, J.A. CARTER and D.N. LUMSDEN, 1973. Procedures for thorium and uranium extraction from calcite. Radiochem. Radioanal. Lett. 16 53-56.

THOMPSON, G., D.N. LUMSDEN, R.L. WALKER and J.A. CARTER, 1975. Uranium series dating of stalagmites from Blanchard Springs Caverns, USA. Geochim. Cosmochim. Acta 39 1211-1218.

THOMPSON, P., 1973a. Speleochronology and Late Pleistocene climates inferred from O, C, H, U and Th isotopic abundances in speleothems. PhD Thesis, McMaster University, Hamilton, Ont.

THOMPSON, P., 1973b. Procedures for extraction and isotopic analysis of uranium and thorium from speleothem. Tech. Memo. 73-9 Dept. of Geology, McMaster Univ., Hamilton, Ontario.

THOMPSON, P., 1976. Cave Exploration in Canada. Canadian Caver, Univ. of Alberta, Edmonton, 183pp.

THOMPSON, P., D.C. FORD and H.P. SCHWARCZ, 1975. $^{234}U/^{238}U$ ratios in limestone cave seepage waters and speleothems from West Virginia. Geochim. Cosmochim. Acta. 39 661-669.

THOMPSON, P., H.P. SCHWARCZ and D.C. FORD, 1976. Stable isotope geochemistry, geothermometry and geochronology of speleothems from West Virginia. Geol. Soc. Amer. Bull. 87 1730-1738

THURBER, D.L., 1962. Anomalous $^{234}U/^{238}U$ in nature. J. Geophys. Res. 67 4518-4520.

TIDDEMAN, R.H., 1873. The older deposits in the Victoria Cave, Settle, Yorkshire. Geol. Mag. 10 11-16.

TOURTELOT, H.A. and R.O. RYE, 1969. Distribution of oxygen and carbon isotopes in fossils of Late Cretaceous age, Western Interior region of North America. Geol. Soc. Amer. Bull. 80 1903-1922.

TSUSUE, A., and H.D. HOLLAND, 1966. The coprecipitation of cations with $CaCO_3$ - III. The coprecipitation of Zn^{2+} with calcite between 50 and 250°C. Geochim. Cosmochim. Acta 30 439-453.

TUREKIAN, K.K., (ed), 1971. The Late Cenozoic Glacial Ages. New Haven, Yale Univ. Press. Preface.

TUREKIAN, K.K. and E. NELSON, 1976. Uranium decay series dating of the travertines of Caune de l'Arago (France). Proc. UISPP - IX Congrès, 1976 Nice. 171-179.

UREY, H.C., 1947. The thermodynamic properties of isotopic substances. J.Chem. Soc. 562-581.

UREY, H.C., H.A. LOWENSTAM, S. EPSTEIN and C.R. McKINNEY, 1951. Measurement of paleotemperatures and temperatures of the Upper Cretaceous of England, Denmark and the south-east USA. Geol. Soc. Amer. Bull. 62 399-416.

VALENTINE, K.W.G. and J.B. DALRYMPLE, 1976. Quaternary buried paleosols: A critical review. Quat. Res. 6 209-222.

VEEH, H.H., 1966. $^{230}Th/^{238}U$ and $^{234}U/^{238}U$ ages of Pleistocene high sea level stand. J. Geophys. Res. 71 3379-3386.

VESELSKY, J., 1974. An improved method for the determination of the ratio $^{234}U/^{238}U$ in natural waters. Radiochim. Acta 21 151-154.

WADGE, G., A.G. FINCHAM and G. DRAPER, 1979. The caves of Jacksons Bay and the Cainozoic geology of southern Jamaica. Trans. Brit. Cave Res. Assoc. 6 70-84.

WALTHAM, A.C., 1970a. Cave development in the limestone of the Ingleborough District. 136 574-585.

WALTHAM, A.C., 1970b. Survey of the Leck Fell cave system. Priv. Pub.

WALTHAM, A.C., 1971. Shale units in the Great Scar limestone of the southern Askrigg Block. Proc. Yorks. Geol. Soc. 38 285-292.

WALTHAM, A.C., 1974. Geology and geomorphology of the caves of N.W. England, in Limestones and Caves of North-West England, A.C. Waltham ed., David and Charles, Newton Abbot, 25-45, 79-105, 273-309.

WALTHAM, A.C., 1977. White Scar Cave. Trans. Brit. Cave Res. Assoc. 4 345-354.

WALTHAM, A.C. and R.S. HARMON, 1977. Chronology of cave development in the Yorkshire Dales, England. Proc. 7th Int. Speleol. Congr. Sheffield, England 1977. 423-425.

WARWICK, G.T., 1956. Caves and glaciation : 1. Central and Southern Pennines. Trans. Cave Res. Grp. of Great Britain, 4 127-160.

WARWICK, G.T., 1971. Caves and the Ice Age. Trans. Cave Res. Grp. of Great Britain, 13 123-130.

WEBER, J.N., 1973. Incorporation of Sr into reef coral skeletal carbonate. Geochim. Cosmochim. Acta 37 2173-2190.

WEST, R.G., 1977a. Pleistocene Geology and Biology. 2nd ed. Longman, London. 440pp.

WEST, R.G., 1977b. Early and Middle Devensian flora and vegetation. Phil. Trans. R. Soc. Lond. B280 229-246.

WEST, R.G., C.A. DICKSON, J.A. CATT, A.H. WEIR and B.W. SPARKS, 1974. Late Pleistocene deposits at Wretton, Norfolk. II. Devensian deposits. Phil. Trans. R. Soc. Lond. B267 337-420.

WIGLEY, T.M.L. and M.C. BROWN, 1976. The physics of caves, in The Science of Speleology, T.D. Ford and C.H.D. Cullingford eds. Academic Press. 329-358.

WIGLEY, T.M.L., L.N. PLUMMER and F.J. PEARSON Jnr., 1978. Mass transfer and carbon isotope evolution in natural water systems. Geochim. Cosmochim. Acta 42 1117-1140.

WINLAND, D.H., 1969. Stability of calcium carbonate polymorphs in warm, shallow sea water. J. Sed. Petr. 39 1579-1587.

WILSON, A.A., 1974. Developments in limestone geology in the Ingleton-Settle area. Trans. Brit. Cave Res. Assoc. 1 61-64.

WOILLARD, G.M., 1978. Grande Pile peat bog: A continuous pollen record for the last 140,000 years. Quat. Res. 9 1-21.

YAPP, C.J. and S.EPSTEIN, 1977. Climatic implications of D/H ratios of meteoric water over North America (9500 - 22000 B.P.) as inferred from ancient wood cellulose C-H hydrogen. Earth.Plan. Sci. Lett. 34 333-350.

YOLE, R.W., 1964. A faunal and stratigraphic study of Upper Paleozoic rocks of Vancouver Island, British Columbia. Unpub. thesis, Univ. of British Columbia, Vancouver, B.C.

YOLE, R.W., 1969. Upper Paleozoic stratigraphy of Vancouver Island, British Columbia. Geol. Assoc Can. Proc. 20 30-40.

ZAGWIJN, W.H., 1975. Variations in climate as shown by pollen analysis, especially in the Lower Pleistocene of Europe, in Ice Ages: Ancient and Modern, A.E. Wright and F.W. Moseley eds., Seel House Press, Liverpool. 137-152.

ZEUNER, F.E., 1959. The Pleistocene Period. Hutchison, London. 447pp.

APPENDIX 1

a) Radiometric dating analytical technique.

b) Typical raw spectra printouts for ^{230}Th/^{234}U and ^{231}Pa/^{230}Th dating methods showing selection of isotope peaks, determination of count time, count rates etc., and correction for tail, ^{235}U, etc.

c) Dating programs for ^{230}Th/^{234}U and ^{231}Pa/^{230}Th methods, with typical printouts of final results.

a) Extraction and purification technique for thorium and uranium in speleothem

A) Dissolution and Primary Purification Stages

1. Preclean sample of surface detritus either mechanically or by acid action.
2. Stand sample in large beaker (use 5 to 200 g. depending on U content) and add 200-500 mls de-ionised water. Slowly add concentrated HNO_3 while stirring, (100 g. $CaCO_3$ requires about 90 mls conc. HNO_3 for complete dissolution).
3. As dissolution proceeds, add spike and 1 ml $FeCl_3$ solution. Amount of spike added should approximately equal activity of ^{238}U.
4. Filter if necessary either by gravity feed through Whatman 50, or in the case of a large insoluble residue, through Whatman 50 using Buchner funnel and water pump. Wash residue twice with 2N HNO_3.
5. Bring filtrate to boil, boil for about 5 mins. to remove all CO_2, turn off heat and carefully add concentrated ammonium hydroxide while stirring magnetically, until a brown precipitate forms. (U and Th are not amphoteric so a slight excess of ammonia can be tolerated. Addition of ammonia while hot serves to minimize absorption of CO_2 and removes excess ammonia by evaporation.)
6. Cool overnight (or under tap) and filter through Whatman 50. Rinse precipitation vessel with de-ionised water and add to filter paper. Wash precipitate once with de-ionised water to remove NO_3^- which can interfere in the following ether extraction step.

B) Carrier Removal by Ether Extraction

7. Rinse the precipitation vessel with concentrated HCl and add to precipitate. Allow to drain through paper into separating funnel. Dissolve remaining precipitate in minimum amount of conc. HCl and wash paper with a little 9N HCl. Total volume of solution should be 25-50 mls.
8. To remove carrier iron add about 50 mls isopropyl ether (filtered if necessary) to separating funnel, shake well releasing ether vapour pressure, settle and run off lower layer into silica (Vycor) beaker. Discard upper ether layer (if 3 layers form, discard upper 2). Repeat at least once more. Three extractions normally reduce iron content to acceptable levels. After final extraction aqueous layer should be colourless unless contaminated by organics or trace elements other than iron.
9. Heat aqueous layer gently to boil off dissolved ether (layer first becomes cloudy and then clears when all ether is removed). Do not overheat or HCl gas will be preferentially lost, so reducing the normality of the solution.

C) Secondary Purification by Ion Exchange Resin

10. Cool solution, add to anion resin column (12 cm x 0.5 cm) preconditioned by washing with 0.1N HCl and then 9N HCl. Rinse beaker with 9N HCl and add to column. Allow to flow through column at about 0.5 ml/min. (1 drop per 6 secs.). Then wash resin and

reservoir with 3 aliquots of 10 mls 9N HCl. All eluate is collected in a silica beaker. This solution contains the Th.

11. Elute U (and Fe, Co, etc.) from the column with about 15 mls 0.1N HCl and wash twice with two further aliquots of 5 mls each.
12. Evaporate both 9N and 0.1N eluates slowly to dryness.
13. To remove organics derived from the ether or resin, it is best to first boil down the Th residue with 10 ml conc. HNO_3/HCl mixture refluxing the acid by partially covering the beaker with a clean watch glass.
14. Dissolve Th residue in _either_ 25 ml 8N HNO_3 and add to anion resin preconditioned with 0.1N HCl followed by 8N HNO_3 _or_ in 25 ml 3N HCl and add to cation column resin preconditioned by de-ionised water and 3N HCl. Wash beakers and columns as before with appropriate acids.
15. Elute Th from anion column with 30 mls 0.1N HCl and 2 x 10 ml wash aliquots or from the cation column with 20 mls 0.75M oxalic acid and 2 x 10 ml wash aliquots. 1 ml of 100 mg/l. $LaCl_3$ solution can be added to the eluate at this stage as a carrier for Th. Evaporate eluate to dryness.

D) Tertiary Purification by Solvent Extraction

U extraction

16. If U residue appears fairly substantial and brown in colour, boil down under reflux with 2 ml conc. HNO_3/HCl to remove organics derived from ether or decomposed resin. If residue is still brown or red and if the 0.1N eluate was yellow/green in colour, perform one ether extraction by dissolving residue in a little 9N HCl, 'squishing' (emulsify) with IPE, separating off the lower aqueous layer and evaporating again to dryness. This is most conveniently done in a centrifuge tube.
17. When U residue appears small or invisible, dissolve in 0.1N HNO_3 (pH = 1.0) warm gently and 'steep' in the acid if necessary to effect complete solution. Transfer to centrifuge tube, rinse beaker with 2 x 0.5 ml aliquots of acid, transferring also. Add 1 ml 0.5M TTA (2-Thenoyltrifluoroacetone in benzene) and squish for 1 min. with a Pasteur pipette. This extracts any remaining Th, Pa etc. into the organic layer.
18. Centrifuge and discard TTA layer, transfer aqueous layer to a second tube and add dilute ammonia dropwise until pH is 3 to 3.5 (narrow range pH paper is usually adequate). Add 2 mls TTA solution, squish, centrifuge and carefully transfer upper organic

layer to a 10 ml beaker. Repeat the extraction with 1 ml TTA adding this layer to the beaker.

19. The TTA extract is usually coloured brown or red at this stage due to the presence of a little iron. A heavy blood-red coloration will give a thick source and poor α energy resolution. In this case, back extraction of the U and Fe with 3 x 5 ml aliquots of 9N HCl is advisable, followed by ether extraction to remove the iron. A yellow-green coloration of the TTA indicates significant U content and to avoid a thick or excessively 'hot' source it is worthwhile splitting off a measured portion of this solution before continuing.

20. Gently evaporate the benzene from the beaker and reduce the volume to about 0.25 ml by increasing the heat. Take up the solution in a Pasteur pipette and drop slowly onto a clean, new, heated 1" stainless steel planchet. Keep the solution away from the edges while evaporating down and meanwhile add 0.5 ml TTA solution to the beaker and boil down. Transfer this remaining solution to the planchet and allow the final solution to evaporate to dryness in a series of concentric rings.

21. Flame the planchet to bright red heat for 10 secs. and allow to cool. (This step removes the volatile ^{210}Po which would otherwise interfere in the U α spectrum). Count immediately.

<u>Th extraction</u>

22. In the case of anion resin extraction of Th the 0.1N HCl residue should be almost imperceptible and relatively pure. A brown residue may indicate organics and so treatment with HNO_3/HCl should be made as per 16. before continuing. No Fe contamination should be found.

23. For cation resin extraction, the mass of white crystalline oxalic acid remaining after evaporation must first be completely decomposed by 3 treatments with 10 ml conc. HNO_3/HCl, washing down the walls of the beaker at each stage. (It is essential to remove all oxalic acid -- as CO_2 and H_2O -- since it interferes in subsequent TTA extraction and also to remove all mineral acid from the residue since this may displace the pH to < 1.0 during the TTA step. Below pH 1 Th is very poorly extracted. A suitable narrow range pH paper is useful in this step.)

24. Dissolve Th residue in 1 ml 0.1 HNO_3 by heating gently, steep if necessary. Transfer to a centrifuge tube. Wash beaker with 2 x 0.5 ml aliquots of acid and transfer also. pH should be between 1 and 2.

25. Add 2 ml 0.5M TTA solution, squish, centrifuge and transfer top organic layer to 10 ml beaker. Repeat twice with 2 x 1 ml aliquots of TTA solution (the extraction efficiency of TTA for Th is less than that for U). Follow stage 20 for plating out the Th, but

heat the planchet for less time as only organics need be decomposed. Generally all Th samples are thin, pure and give well-resolved spectra.

Notes

i) Both U and Th discs should be counted immediately after plating for the following reasons: a) Bi tends to follow U through the extraction process and some may be incorporated on the disc. Bi itself is not a problem (^{210}Bi is a β emitter, $t_{\frac{1}{2}}$ = 5 days) but its daughter ^{210}Po is an alpha emitter of energy similar to ^{232}U, and slowly grows into equilibrium with its parent. It's presence therefore is only significant in old discs although re-flaming the disc before counting should volatilize most radiogenic Po.
b) For the same reason as above the ^{228}Th count rate is enhanced by development of ^{210}Po from ^{210}Bi which also finds its way in small amounts onto the Th disc.

ii) If refluxing with conc. HNO_3/HCl mixture fails to completely remove all oxalic acid in the Th purification step, conc. $HClO_4/HNO_3$ may be used sparingly and in a specially designed fume-hood.

b) ^{230}Th/^{234}U sample printouts

76125-1 U

on 22·44 11/1/77 unit 1
off 11·49 12/1/77 (Molly Ann)
785 mins.

783 min

$U^{235}: \frac{5768}{21\cdot7}$
$- 266$

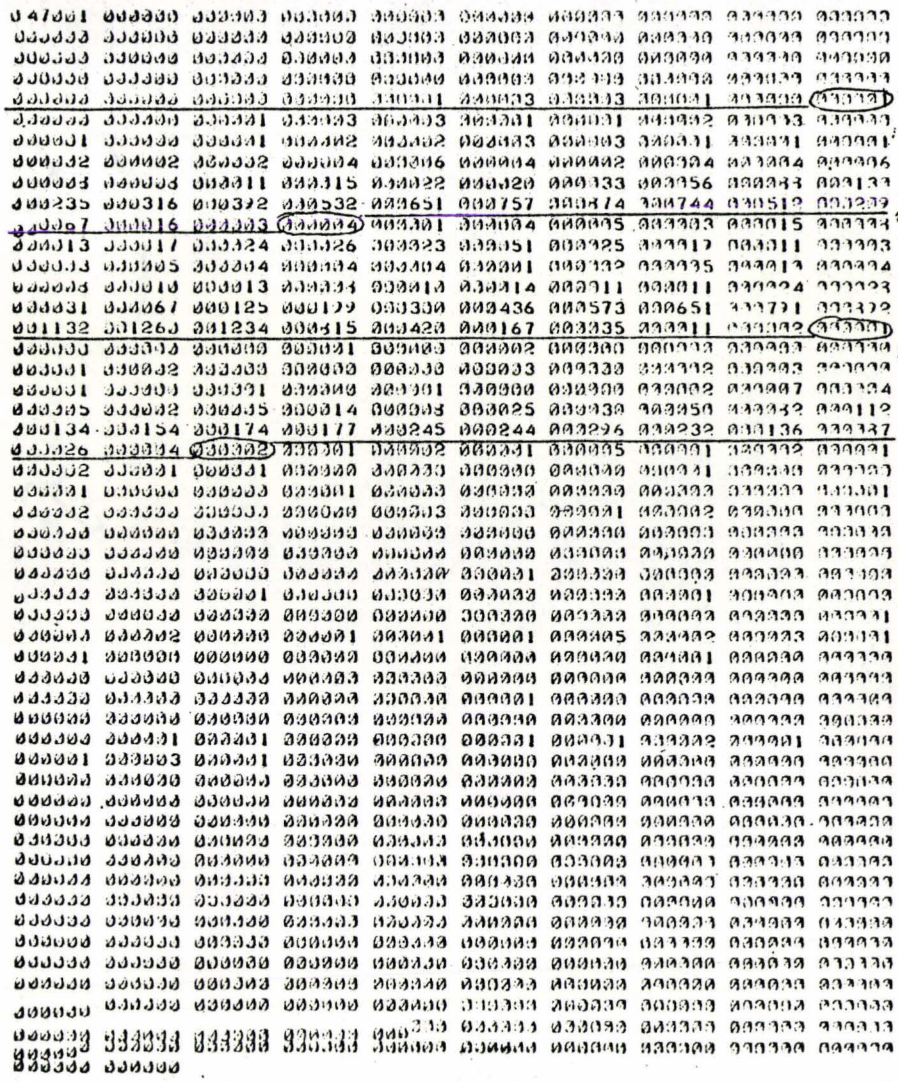

```
047001 000000 000000 000000 000000 000000 000000 000000 000000 000000
000000 000000 000000 000000 000000 000000 000000 000000 000000 000000
000000 000000 000000 000000 000000 000000 000000 000000 000000 000000
000000 000000 000000 000000 000000 000000 000000 000000 000000 000000
000000 000000 000000 000000 000001 000003 000013 000001 000000 000000
000000 000000 000001 000003 000003 000001 000001 000002 000013 000000
000001 000000 000001 000002 000002 000003 000003 000001 000001 000001
000002 000002 000002 000004 000006 000004 000002 000004 000004 000006
000003 000003 000011 000115 000022 000020 000133 000356 000083 000133
000235 000316 000372 000532 000651 000757 000874 000744 000512 000239
000007 000016 000003 000004 000001 000004 000005 000003 000015 000003
000013 000017 000024 000026 000023 000051 000025 000017 000011 000003
000013 000005 000004 000004 000004 000001 000002 000035 000013 000004
000008 000010 000013 000003 000014 000014 000011 000011 000024 000023
000031 000067 000125 000179 000300 000436 000573 000651 000791 000372
001132 001260 001234 000815 000420 000167 000035 000011 000002 000001
000000 000000 000000 000001 000000 000002 000000 000000 000000 000000
000001 000002 000000 000000 000000 000003 000000 000002 000003 000000
000001 000000 000001 000000 000001 000000 000000 000002 000007 000004
000005 000002 000015 000014 000008 000025 000030 000050 000032 000112
000134 000154 000174 000177 000245 000244 000296 000232 000136 000337
000026 000014 000002 000001 000002 000001 000005 000001 000002 000001
000002 000001 000001 000000 000000 000000 000000 000001 000000 000000
000001 000000 000000 000001 000000 000000 000000 000000 000000 000001
000002 000000 000000 000000 000003 000000 000001 000002 000000 000000
000000 000000 000000 000000 000000 000000 000000 000000 000000 000000
000000 000000 000000 000000 000000 000000 000000 000000 000000 000000
000000 000000 000000 000000 000000 000001 000000 000000 000000 000000
000000 000000 000001 000000 000000 000000 000000 000001 000000 000000
000000 000000 000000 000000 000000 000000 000000 000000 000000 000001
000000 000002 000000 000001 000001 000001 000005 000002 000003 000001
000001 000000 000000 000000 000000 000000 000000 000001 000000 000000
000000 000000 000000 000000 000000 000000 000000 000000 000000 000000
000000 000000 000000 000000 000000 000001 000000 000000 000000 000000
000000 000000 000000 000000 000000 000000 000000 000000 000000 000000
000000 000001 000001 000000 000000 000001 000001 000002 000001 000000
000001 000003 000001 000000 000000 000000 000000 000000 000000 000000
000000 000000 000000 000000 000000 000000 000000 000000 000000 000000
000000 000000 000000 000000 000000 000000 000000 000000 000000 000000
000000 000000 000000 000000 000000 000000 000000 000000 000000 000000
000000 000000 000000 000000 000000 000000 000000 000000 000000 000000
000000 000000 000000 000000 000000 000000 000000 000000 000000 000000
000000 000000 000000 000000 000000 000000 000000 000000 000000 000000
000000 000000 000000 000000 000000 000000 000000 000000 000000 000000
000000 000000 000000 000000 000000 000000 000000 000000 000000 000000
000000 000000 000000 000000 000000 000000 000000 000000 000000 000000
000000 000000 000000 000000 000000 000000 000000 000000 000000 000000
000000 000000 000000 000000 000000 000000 000000 000000 000000 000000
000000 000000 000000 000000 000000 000000 000000 000000 000000 000000
000000 000000
```

^{238}U
(5768)
7·363

^{235}U + ^{234}U
(9669)
$- 266$
9403
12·003

^{232}U
(2274)
2903

76125-1 Th

on 22·19 12/1/77 unit 1
off 09·28 14/1/77 (Molly Ann)
2109 mins.

2108 mins

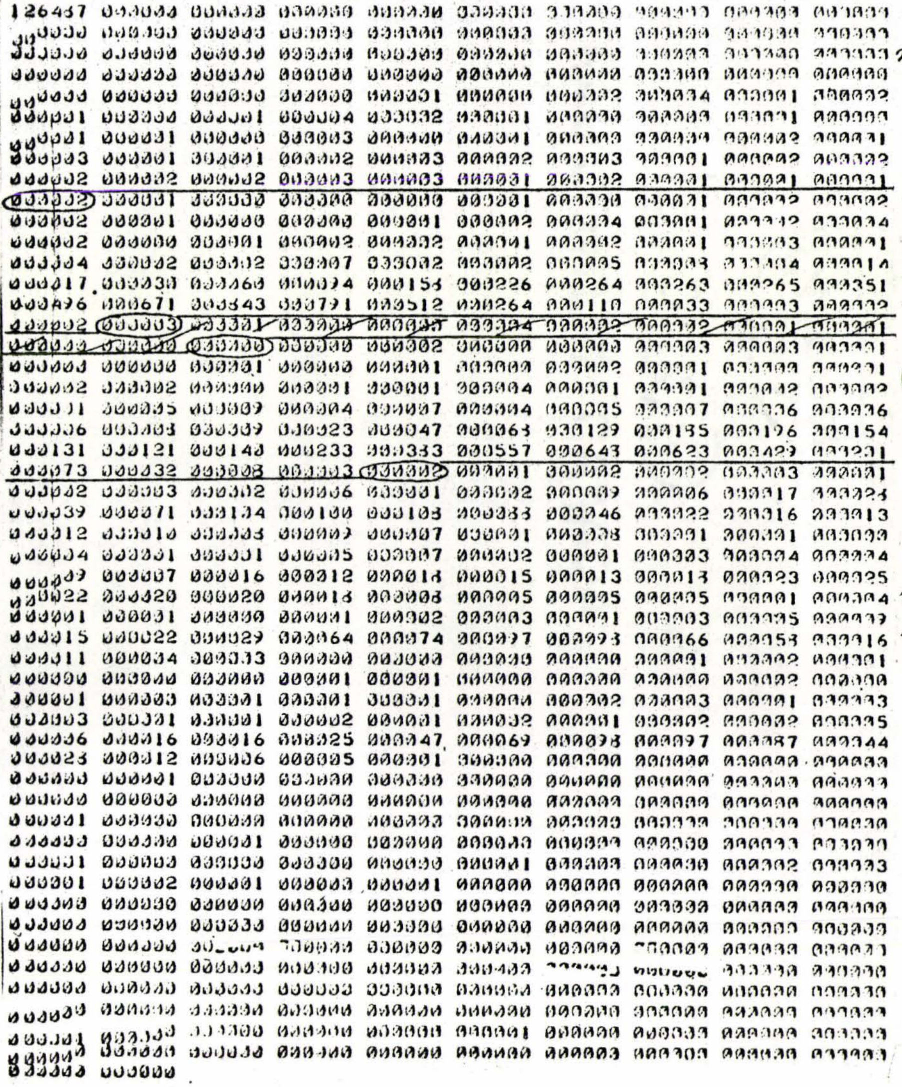

```
126437 000000 000000 000000 000000 000000 000000 000000 000000 000000
000000 000000 000000 000000 000000 000000 000000 000000 000000 000000
000000 000000 000000 000000 000000 000000 000000 000000 000000 000000
000000 000000 000000 000000 000000 000000 000000 000000 000000 000000
000000 000000 000000 000000 000001 000000 000002 000034 000001 000002
000001 000000 000001 000004 000002 000001 000000 000000 000001 000000
000001 000001 000000 000003 000000 000001 000000 000000 000002 000001
000003 000001 000001 000002 000003 000002 000003 000001 000002 000002
000002 000002 000002 000003 000003 000001 000002 000001 000001 000001
000002 000001 000000 000000 000000 000001 000000 000001 000002 000002
000002 000001 000000 000000 000001 000002 000004 000001 000002 000004
000002 000000 000001 000002 000002 000001 000002 000001 000003 000001
000004 000002 000002 000007 000002 000002 000005 000003 000004 000014
000017 000030 000460 000074 000154 000226 000264 000263 000265 000351
000496 000671 000843 000791 000512 000264 000110 000033 000003 000002
000002 000003 000001 000000 000000 000004 000002 000002 000001 000001
000000 000000 000000 000000 000002 000000 000000 000003 000003 000001
000000 000000 000001 000000 000001 000000 000002 000001 000000 000001
000002 000002 000000 000001 000001 000004 000001 000001 000002 000002
000011 000005 000009 000004 000007 000004 000005 000007 000036 000036
000006 000003 000009 000023 000047 000063 000129 000135 000196 000154
000131 000121 000140 000233 000333 000557 000643 000623 000429 000231
000073 000032 000008 000003 000002 000001 000002 000002 000003 000001
000002 000003 000002 000006 000001 000002 000009 000006 000017 000024
000039 000071 000134 000100 000103 000083 000046 000022 000016 000013
000012 000010 000003 000007 000007 000001 000008 000001 000001 000000
000004 000001 000001 000005 000007 000002 000001 000003 000004 000004
000009 000007 000016 000012 000018 000015 000013 000013 000023 000025
000022 000020 000020 000018 000008 000005 000005 000005 000001 000004
000001 000001 000000 000001 000002 000003 000001 000003 000005 000007
000015 000022 000029 000064 000074 000097 000093 000066 000053 000016
000011 000034 000013 000000 000000 000000 000000 000001 000002 000001
000000 000000 000000 000001 000001 000000 000000 000000 000002 000000
000001 000003 000001 000001 000001 000000 000002 000003 000001 000003
000003 000001 000001 000002 000001 000002 000001 000002 000002 000005
000006 000016 000016 000025 000047 000069 000078 000097 000087 000044
000023 000012 000006 000005 000001 000000 000000 000000 000000 000000
000000 000001 000000 000000 000000 000000 000000 000000 000000 000000
000000 000000 000000 000000 000000 000000 000000 000000 000000 000000
000001 000000 000000 000000 000000 000000 000000 000000 000000 000000
000000 000000 000001 000000 000000 000000 000000 000000 000000 000000
000001 000000 000000 000000 000000 000001 000000 000000 000002 000003
000001 000002 000001 000003 000001 000000 000000 000000 000000 000000
000000 000000 000000 000000 000000 000000 000000 000000 000000 000000
000000 000000 000000 000000 000000 000000 000000 000000 000000 000000
000000 000000 000000 000000 000000 000000 000000 000000 000000 000000
000000 000000 000000 000000 000000 000000 000000 000000 000000 000000
000000 000000 000000 000000 000000 000000 000000 000000 000000 000000
000000 000000 000000 000000 000000 000000 000000 000000 000000 000000
000000 000000 000000 000000 000000 000000 000000 000000 000000 000000
000000 000000
```

^{232}Th
(69)
0·033

^{230}Th
(5547)
2·631

^{228}Th.
(4494)
$- 37$
(Ra^{224} corr^n)
4457
2·114

^{224}Ra

^{212}Bi

^{220}Rn

^{216}Po

^{231}Pa/^{230}Th sample printouts

76121-3 U

on 10.20 3/2/77
off 20.13 3/2/77
593 mins
unit 1 (Florence)

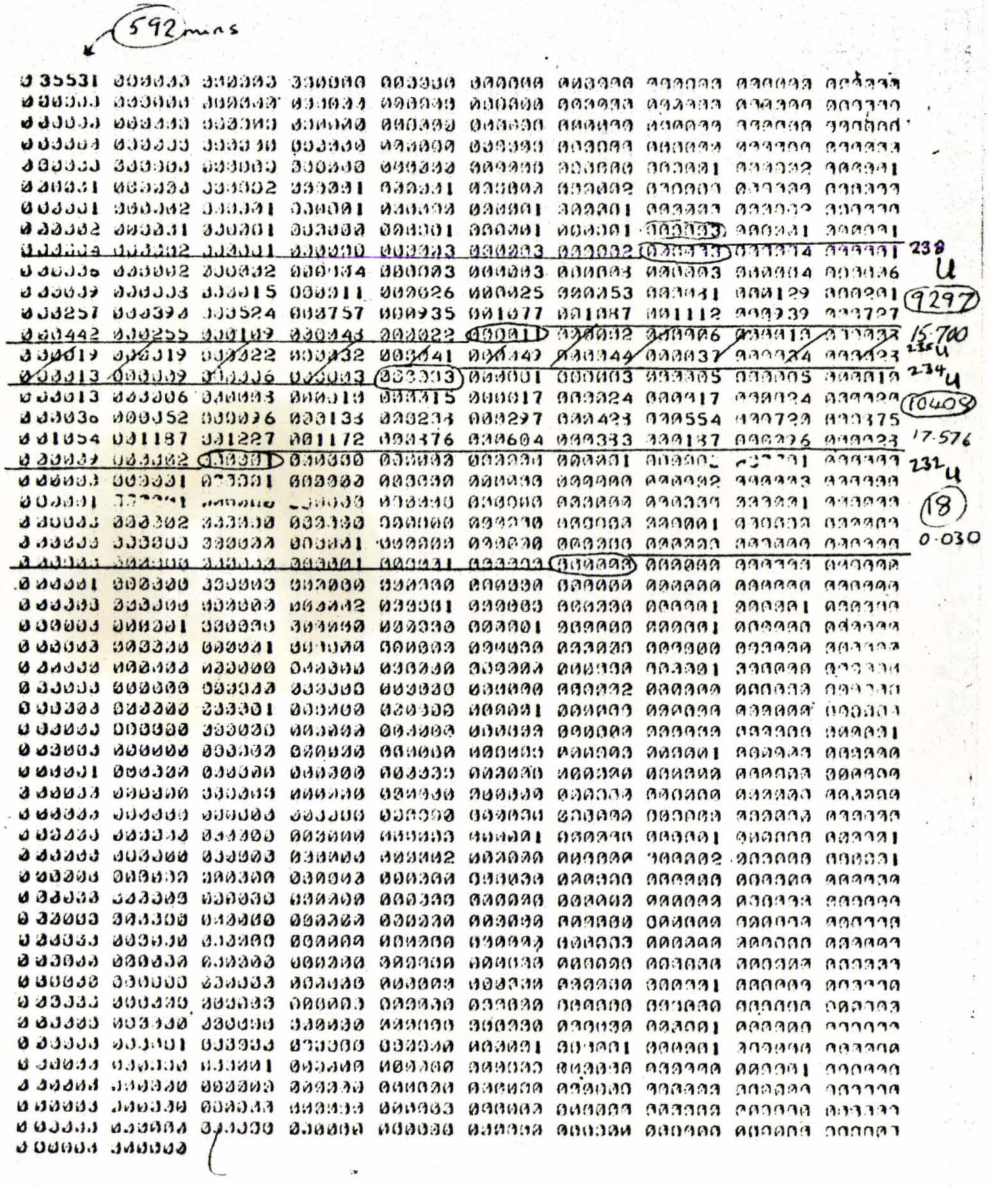

76121-3 Th

on 12.32 2/2/77
off 09.59 3/2/77
1287 mins
unit 1 (Florence)

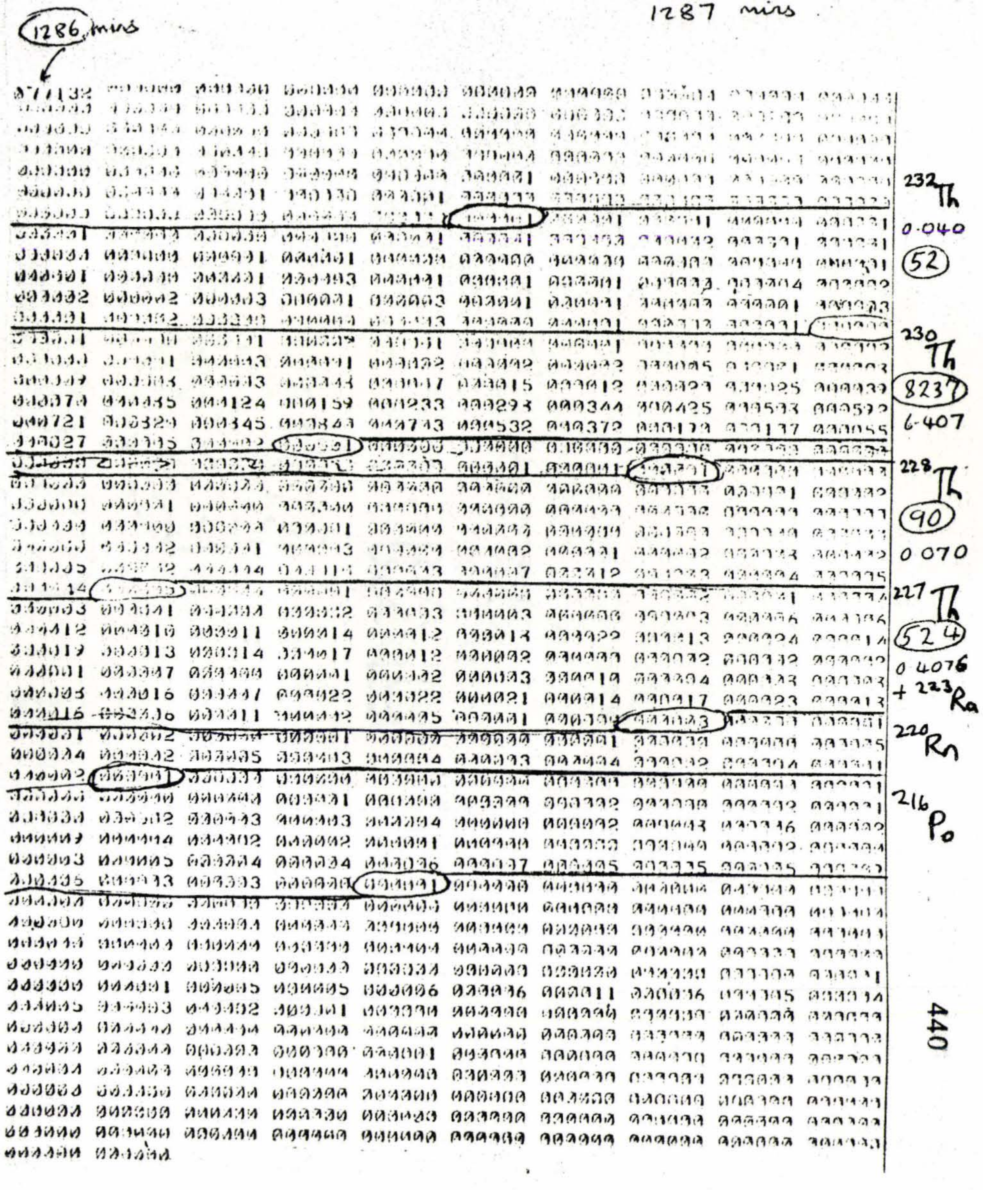

c) ^{230}Th/^{234}U program list and printout

```
C
      PROGRAM TST (INPUT,OUTPUT,PUNCH,TAPE5=INPUT,TAPE6=OUTPUT,TAPE7=PUNCH)
     2CH)
C     ***************************
C     PROGRAM CORRECTS RAW COUNT RATE DATA AND COMPUTES TH-230/U-234
C     U-234/U-238 AND TH-230/TH-232 ISOTOPE RATIOS. THE AGE AND
C     RATIOS
C     N1=U-238 COUNT RATE
C     N2=U-234 COUNT RATE
C     N3=U-232 COUNT RATE
C     N4=TH-232 COUNT RATE
C     N5=TH-230 COUNT RATE
C     N6=TH-228 COUNT RATE
C     SPIKE = TH-228/U-232 OR TH-227/U-232 ACTIVITY RATIO IN SPIKE
C     CNTU = ACCUMULATION TIME FOR U SPECTRUM (MINS)
C     CNTT = ACCUMULATION TIME FOR TH SPECTRUM (MINS)
C     CNBD1= ACCUMULATION TIME FOR BLANK DISC  - U COUNTER  (MIN)
C     CNBD2= ACCUMULATION TIME FOR BLANK DISC  - TH COUNTER (MIN)
C     DECT = DELAY BETWEEN COUNTING TH-228 AND SEPARATION FROM U-232 (DAYS)
C     DCPT = DELAY BETWEEN PLATING OUT AND COUNTING TH (MINS)
C     WEIGHT = WT OF SAMPLE IN GMS
C     B1 = COUNTER BACKGROUND CORRECTION FOR U-238
C     B2 = COUNTER BACKGROUND CORRECTION FOR U-234
C     B3 = COUNTER BACKGROUND CORRECTION FOR U-232
C     B6 = COUNTER BACKGROUND CORRECTION FOR TH-232
C     B7 = COUNTER BACKGROUND CORRECTION FOR TH-230
C     B8 = COUNTER BACKGROUND CORRECTION FOR TH-228
C     B4 = ACTIVITY OF 1.0 ML 232 SPIKE IN CPM/ML  ON THE U COUNTER
C     B9 = ACTIVITY OF 1.0 ML 232 SPIKE IN CPM/ML  ON THE TH COUNTER
C     B5 = VOLUME OF SPIKE USED (MLS)
C     B = WEIGHT OF 238U OF EQUIVALENT ACTIVITY TO 232U IN 1ML SPIKE
C     ***************************
C
      REAL N1,N2,N3,N4,N5,N6,N12,N52,N36,N54,NT52,N42,NT42,N21,NN6,LAM7,
     2LAM3,LAM4
100   READ (5,199) IU
199   FORMAT (1I1)
      IF(IU.EQ.0)GO TO 101
      IF(IU.EQ.1)GO TO 200
      IF(IU.EQ.2) GO TO 301
C
101   READ (5,102) TITLE,TGS,CNTU,CNTT,SPIKE,WEIGHT,DECT,DATE
102   FORMAT(A10,6E10.0,A10)
      IF (TGS.EQ.0.0) GO TO 999
      IF(EOF(5))999,997
997   CONTINUE
103   READ(5,104)N1,N2,N3,N4,N5,N6, THR  ,REPUN2
104   FORMAT(8F10.0)
105   READ (5,106) B1,B2,B3,B,B5,CNBD1,B4,DCPT
106   FORMAT(8F10.4)
      IF (THR.GT.0) GO TO  107
      THR=1.25000
107   B6=B1
      B7=B2
      B8=B3
      B9=B4
      CNBD2=CNBD1
C
310   REPEAT =0.0
      TN3=N3-B3
      YU=100.*TN3/(B4*B5)
C
C        YU = PERCENT YIELD OF URANIUM
C        U-238 REAGENT BLANK EQUALS 0.016 CPM AT 100% U YIELD
C


      TN1=N1-B1-(0.016*YU/100.)
C
C        U-234 REAGENT BLANK EQUALS 0.050 CPM AT 100% U YIELD
C
      TN2=N2-B2-(0.050*YU/100.)
C
C        CORRECT TOTAL TH-228 FOR BACKGROUND
C
      SN6=N6-B8
C
C        DETERMINATION OF AVERAGE RA-224 COUNT RATE OVER CNTT PERIOD
C
      LAM4=1.322+E-4
      RA224=SN6*(1.+((EXP(-LAM4*(CNTT+DCPT))-EXP(-LAM4*DCPT)))/(LAM4
     2*CNTT))
C
C
C        CORRECT TOTAL TH-228 FOR RA-224 INGROWTH
C
      SN6=SN6-(0.055*RA224)
C
C        CORRECT TOTAL TH-228 FOR DETRITAL COMPONENT
C
      SN6=SN6-N4*B1
C
C        CORRECTION FOR TH-228 DECAY
C
      THALF8=9.94E-4
      TN6=SN6*EXP(THALF8*DECT)
C
      YT=(100.*TN6)/(B9*SPIKE*B5)
C
C        TH-232 AND TH-230 REAGENT BLANK IS ZERO
C
      TN4=N4-B6
      IF(TN4.LT.1.E-20)TN4=1.E-20
      TN5=N5-B7
C
C        CONCU = CONCENTRATION OF URANIUM
C
      CONCU=(B5)*(B*TN1)/(TN3*WEIGHT)
C
C
C        CONCTH = CONCENTRATION OF THORIUM-232
C
C        3.0845 IS A UNIVERSAL CONSTANT RELATING T1/2 U238 TO T1/2 TH 232
      CONCTH=(TN4*B5*B*3.0845*SPIKE)/(WEIGHT*TN6)
C
C       CALCULATION OF ISOTOPE RATIOS AND ERRORS IN THESE RATIOS
C        DUE TO STATISTICAL ERRORS IN THE COUNT RATE
C        N21 = MEASURED U-234/U-238 ISOTOPE RATIO
C        N52 = MEASURED TH-230/U-234 ISOTOPE RATIO
C        N54 = MEASURED TH-230/TH-232 ISOTOPE RATIO
C        N36 = MEASURED U-232/TH-228 ISOTOPE RATIO
C        NT52 = ACTUAL TH-230/U-234 ISOTOPE RATIO
C        N42= MEASURED TH-232/U-234 ISOTOPE RATIO
C        NT42= ACTUAL TH-232/U-234 ISOTOPE RATIO
C

      N21=TN2/TN1
      N52=TN5/TN2
      N54=TN5/TN4
      N36=TN3/TN6
      NT52=N52*N36*SPIKE
      N42=TN4/TN2
      NT42=N42*N36*SPIKE
C
C        BR = REAGENT BLANK ERRORS
C
      BR1=(0.007*YU/100.)
      BR2=(0.043*YU/100.)
      BR4=(0.005*YT/100.)
      BR5=(0.005*YT/100.)
C
C        ER = TOTAL ERROR IN U-TH COUNT RATES DERIVED FROM U-TH COUNT RATES
C        , BLANK DISC COUNT RATE FOR U-TH COUNT TIMES
C        , BLANK DISC COUNT RATE FOR BLANK DISC COUNT TIMES AND REAGENT BLANK
C        REAGENT BLANK ERRORS ARE BASED ON S.D. OF RB ANALYSES,
C        NOT ON COUNTING STATS.
C
      ER1=SQRT((TN1/CNTU)+(B1/CNTU)+(B1/CNBD1)+(BR1*BR1))
      ER2=SQRT((TN2/CNTU)+(B2/CNTU)+(B2/CNBD1)+(BR2*BR2))
      ER3=SQRT((TN3/CNTU)+(B3/CNTU)+(B3/CNBD1))
      ER4=SQRT((TN4/CNTT)+(B6/CNTT)+(B6/CNBD2)+(BR4*BR4))
      ER5=SQRT((TN5/CNTT)+(B7/CNTT)+(B7/CNBD2)+(BR5*BR5))
      ER6=SQRT((TN6/CNTT)+(B8/CNTT)+(B8/CNBD2))
C
      ER21=(TN2/TN1)*SQRT(ER1*ER1/(TN1*TN1)+ER2*ER2/(TN2*TN2))
      ER52=(TN5/TN2)*SQRT(ER5*ER5/(TN5*TN5)+ER2*ER2/(TN2*TN2))
      ER36=(TN3/TN6)*SQRT(ER3*ER3/(TN3*TN3)+ER6*ER6/(TN6*TN6))
C
      ER42=(TN4/TN2)*SQRT(ER4*ER4/(TN4*TN4)+ER2*ER2/(TN2*TN2))
      IF(N54.GT.999.9)GO TO 1451
      ER54=(TN5/TN4)*SQRT(ER5*ER5/(TN5*TN5)+ER4*ER4/(TN4*TN4))
1451  ERT52=      NT52*SQRT(ER52*ER52/(N52*N52)+ER36*ER35/(N36*N36))
      ERT42=NT42*SQRT(ER42*ER42/(N42*N42)+ER36*ER36/(N36*N36))
110   CONTINUE
      IF ((NT52.GE.1.1).AND.(N21.LT.1.8)) GO TO 116
112   R52=NT52
      T=TGS
      R42=NT42
      IF(N54.GE.25.0) GO TO 113
      CALL THIDATE(R52,R42,THR,T,TN1,TN2)
C
C     SUBROUTINE THIDAT SOLVES AGE CORRECTED FOR DETRITAL THORIUM
C
      GO TO 114
113   CALL THDATE(R52,N21,T,TN1,TN2)
C
C        SUBROUTINE THDATE SOLVES AGE EQUATION BY AN ITERITIVE METHOD
C
114   IF (T.GE.350000.) GO TO 116
      TL=TGS
      R52=NT52-ERT52
      R42=NT42+ERT42
      IF (N54.GE.25.0) GO TO 115
      CALL THIDATE(R52,R42,THR,TL,TN1,TN2)
      GO TO 1152
115   CALL THDATE(R52,N21,TL,TN1,TN2)
1152  TU=TGS
      R52=NT52+ERT52
      R42=NT42-ERT42
      IF (N54.GE.25.0) GO TO 1153
      CALL THIDATE(R52,R42,THR,TU,TN1,TN2)
      GO TO 1154
1153  CALL THDATE(R52,N21,TU,TN1,TN2)
C
C        RANGE OF AGE VALUES
C
1154  RTL=T-TL
      RTU=TU-T


      I=(T+50.)/100.
      T=I*100
      I=(RTL+50.)/100.
      RTL=I*100
      I=(RTU+50.)/100.
      RTU=I*100
      IF (REPEAT.EQ.1.0) GO TO 1441
C
C        SUBROUTINE UDATE COMPUTES INITIAL U-234/U-238 RATIOS
C        FROM MEASURED U-234/U-238 AND CALCULATED AGE (T)
C
      CALL UDATE(N21,RU0,T)
      R21=N21+ER21
      CALL UDATE (R21,RU0U,TU)
      R21=N21-ER21
      CALL UDATE(R21,RU0L,TL)
      RU0A=ABS((RU0U-RU0L)/2.0)
116    U238= 7HU-238 =
       U234= 7HU-234 =
       U232=7HU-232 =
       TH228=8HTH-228 =
       TH230=8HTH-230 =
       TH232=8HTH-232 =
      CM=3HCPM
      ER=7HERROR =
      PC=7HPERCENT
117   WRITE(6,118)
118   FORMAT(1H1)
      WRITE (6,119) TITLE , DATE
119   FORMAT (* SAMPLE NO. = *,A10,5X,* DATE RUN *,A10)
      WRITE(6,120)
120   FORMAT(1H    )
      WRITE (6,1191) WEIGHT
1191  FORMAT (* SAMPLE WT. = *,F5.1,1X,* G*)
      WRITE (6,120)
      WRITE (6,1192) CNBD1
1192  FORMAT (* BLANK DISC COUNT TIME  ON U COUNTER = *,F6.0,1X,* MIN*)
      WRITE (6,120)
      WRITE (6,1201) CNBD2
1201  FORMAT (* BLANK DISC COUNT TIME ON TH COUNTER = *,F6.0,1X,* MIN*)
      WRITE (6,120)
      WRITE (6,1193) DECT
1193  FORMAT (* DELAY IN COUNTING THORIUM = *,F3.0,1X,* DAYS*)
      WRITE (6,120)
      WRITE (6,1190) DCPT
1190  FORMAT (* DELAY BETWEEN COUNTING AND PLATING THORIUM = *,F6.0,1X,
     2*MIN*)
      WRITE (6,120)
      WRITE (6,1194) B5
1194  FORMAT (* SPIKE USED = *,F4.2,1X,* ML*)
      WRITE (6,120)
      WRITE (6,1195) B4
1195  FORMAT (* ACTIVITY OF 1 ML 232 SPIKE   ON U COUNTER  = *,F5.2,1X
     2,*CPM*)
      WRITE (6,120)
      WRITE (6,1197) B9
1197  FORMAT (* ACTIVITY OF 1 ML 232 SPIKE ON TH  COUNTER  = *,F5.2,1X
     2,*CPM*)
      WRITE (6,120)
      WRITE (6,1196) B
1196  FORMAT (* 238-U OF EQUIVALENT ACTIVITY TO SPIKE = *,F5.1,1X,
     2* MICROGRAMS*)
      WRITE (6,120)
      WRITE (6,124)
124   FORMAT(* RAW DATA*)
```

```
      WRITE(6,125)CNTU,CNTT
125   FORMAT(* U COUNT TIME = *,F6.0,1X,* MIN*,5X,* TH COUNT TIME = *,F
     26.0,1X,* MIN*)
      WRITE(6,126) U238, N1,CM, TH232, N4,CM
      WRITE(6,126) U234, N2,CM, TH230, N5,CM
      WRITE(6,126) U232, N3,CM, TH229, N6,CM
126   FORMAT(1X,A7,F8.3,2X,A3,5X,A8,F8.3,2X,A3)
      WRITE(6,127)
127   FORMAT(20H ********************)
      WRITE(6,128)
128   FORMAT (* BACKGROUND*)
      WRITE (6,126) U238,B1,CM,TH232,B6,CM
      WRITE (6,126) U234,B2,CM,TH230,B7,CM
      WRITE (6,126) U232,B3,CM,TH228,B8,CM
      WRITE(6,127)
      WRITE(6,131)
131   FORMAT(* CORRECTED DATA*)
      WRITE(6,129)
129   FORMAT(*                        ERROR                          ERROR*)
      WRITE(6,132) U238,TN1,ER1,CM,TH232,TN4,ER4,CM
      WRITE(6,132) U234,TN2,ER2,CM,TH230,TN5,ER5,CM
      WRITE(6,132) U232,TN3,ER3,CM,TH228,TN6,ER6,CM
132   FORMAT(1X,A7,F8.3,2X,F5.3,1X,A3,5X,A8,F8.3,2X,F5.3,1X,A3)
      WRITE(6,127)
      WRITE(6,120)
      WRITE(6,135)CONCU
135   FORMAT(* URANIUM CONCENTRATION      =*,F6.2,2X,* P.P.M.*)
      WRITE (6,1355) CONCTH
1355  FORMAT(* THORIUM-232 CONCENTRATION =*,F6.2,2X,* P.P.M.*)
      WRITE(6,136)YU
136   FORMAT(* CHEMICAL YIELD OF URANIUM =*,F6.2,2X,* PERCENT*)
      WRITE(6,137)YT
137   FORMAT(* CHEMICAL YIELD OF THORIUM =*,F6.2,2X,* PERCENT*)
      WRITE(6,138)SPIKE
138   FORMAT(* SPIKE RATIO               =*,F6.3)
      WRITE(6,127)
      WRITE(6,139)
139   FORMAT(9X,*                ERROR*)
      WRITE(6,140) N21,ER21
140   FORMAT(* U-234/U-238 = *,5X,F5.3,2X,F5.3)
      IF (T.GE.350000.) GO TO 1402
      IF((NT52.GE.1.1).AND.(N21.LT.1.8))  GO TO 1402
      WRITE(6,1401) RU0,RU0A
1401  FORMAT(* (U-234/U-238)0 = *,2X,F5.3,2X,F5.3)
1402  WRITE(6,141) NT52,ERT52
141   FORMAT(* TH-230/U-234 = *,4X,F5.3,2X,F5.3)
      IF(N54.GT.999)GO TO 142
      WRITE(6,1411) N54,ER54
1411  FORMAT(* TH-230/TH-232 = *, F8.3,2X,F5.1)
      GO TO 144
142   WRITE(6,143 )
143   FORMAT(* TH-230/TH-232 \   1000.*)
144   WRITE (6,120)
1441  IF (T.GE.350000.) GO TO  163
      IF((NT52.GE.1.1).AND.(N21.LT.1.8))  GO TO  163
145   WRITE (6,146) RTU
146   FORMAT (23X,*+*,1X,F7.0)
      IF (REPEAT.EQ.1.0) GO TO 1481
147   WRITE (6,148) T
148   FORMAT (* THORIUM AGE =*,F7.0,13X,*YEARS*)
      GO TO 149
1481  WRITE (6,1485) T
1485  FORMAT(* UNCORRECTED =*,F7.0,13X,*YEARS*)
149   WRITE (6,150) RTL
150   FORMAT (23X,*-*,1X,F7.0)


      WRITE (6,120)
      IF (N54.GE.25.0) GO TO 151
      WRITE(6,1482)
1482  FORMAT(41H AGE CALCULATED USING THORIUM CORRECTION )
      WRITE (6,120)
      WRITE(6,1483) THR
1483   FORMAT (* CORRECTED AT INITIAL  THORIUM RATIO, R = *,F10.5)
151   WRITE(6,120)
      IF(REPUN2.EQ.0) GO TO  1541
      IF(REPUN2.GT.0) GO TO 1511
      IF(REPUN2.LT.0) GO TO 1531
1511  PUNCH152,N1,N2,N3,N4,N5,N6,SPIKE,TITLE
152   FORMAT(7F10.4,A10)
1521  PUNCH153,ER1,ER2,ER3,ER4,ER5,ER6,YU,YT
153   FORMAT(8F10.4)
      GO TO 1541
1531  PUNCH 154,T,RTU,RTL,YT,TITLE
154   FORMAT(4F10.4,A10)
1541  IF (N54.GE.25.0) GO TO 100
C
C     IN ORDER TO DISCOVER WHAT THE UNCORRECTED AGE WOULD HAVE  BEEN,
C     THIS LOOP RERUNS THE DATA THROUGH THE PROGRAM WITH THE TH-230/TH-232
C     RATIO SET AT 1000.
C
      N54=1000.
      REPEAT=1.0
      GO TO 112
163   WRITE(6,164)
164   FORMAT (* AGE IS \ 350,000 YEARS B.P.*)
      GO TO 100
C
C     THIS SECTION COMPUTES THE U DATA WHEN NO TH YIELD HAS BEEN OBTAINED
C
200   READ(5,201)TITLE,CNTU,WEIGHT,N1,N2,N3
201   FORMAT (A10,5E10.0)
      READ(5,202)B1,B2,B3,B,B5
202   FORMAT(5F10.4)
      TN1=N1-B1
      TN2=N2-B2
      TN3=N3-B3
      ER1=SQRT(TN1/CNTU)
      ER2=SQRT(TN2/CNTU)
      ER3=SQRT(TN3/CNTU)
      N21=TN2/TN1
      ER21=N21*SQRT(ER1*ER1/(TN1*TN1)+ER2*ER2/(TN2*TN2))
      CONCU=(B5)*(B*TN1)/(TN3*WEIGHT)
      U238=7HU-238 =
      U234=7HU-234 =
      U232=7HU-232 =
      CM=3HCPM
      ER=7HERROR =
      WRITE(6,203)
203   FORMAT(1H1)
      WRITE(6,204 )TITLE,WEIGHT
204   FORMAT(*SAMPLE NUMBER = *,A10,5X,* SAMPLE WEIGHT = *,F5.1,2X,* GMS
     2*)
      WRITE(6,120)
      WRITE(6,205 )U238,TN1,CM,ER,ER1,CM
      WRITE(6,205 )U234,TN2,CM,ER,ER2,CM
      WRITE(6,205 )U232,TN3,CM,ER,ER3,CM
205   FORMAT(1X,A7,F7.4,2X,A3,5X,A7 ,F6.4,2X,A3)
      WRITE(6,120)
      WRITE(6,127)
      WRITE(6,206 )CONCU
206   FORMAT(* URANIUM CONCENTRATION = *,F6.2,2X,* P.P.M.*)
```

```
      WRITE(6,207 )N21,ER21
207   FORMAT(* U-234/U-238=*,F5.3,6X,* ERROR=*,F6.4)
      GO TO 100
C
C     THIS SECTION READS SPECIAL INPUT FORMAT FOR THE SAMPLES COUNTED ON
C     DIFFERENT COUNTERS
C
301   READ (5,302) TITLE,TGS,CNTU,CNTT,SPIKE,WEIGHT;DECT,DATE
302   FORMAT(A10,6E10.0,A10)
      IF (TGS.EQ.0.0) GO TO 999
303   READ(5,304)N1,N2,N3,N4,N5,N6,THR,REPUN2
304   FORMAT(8F10.0)
305   READ (5,306) B1,B2,B3,B,B5,CNBD1,B4,DCPT
306   FORMAT(8F10.4)
307   READ (5,308) B6,B7,B8,B9,CNBD2
308   FORMAT (5F10.4)
       GO TO 310
999   STOP
      END
      SUBROUTINE THDATE (NT52,N21,TGS,TN1,TN2)
      REAL NT52,N21,TN1,TN2
      THALF0=9.2173E-6
      THALF4=2.8062E-6
      RLR=THALF0/(THALF0-THALF4)
      TN=TN2/TN1
10    ERLA=EXP(-THALF0*TGS)
      ERLB=EXP(-(THALF0-THALF4)*TGS)
      FUNC=-(NT52)+(1.0-ERLA)/TN+RLR*(1.0-1.0/TN)*(1.0-ERLB)
      DERIV=THALF0*ERLA/TN+THALF0*(1.0-1.0/TN)*ERLB
      DH=FUNC/DERIV
      TGS=TGS-DH
      IF (TGS .GE. 350000.) GO TO 11
      IF(ABS(DH/TGS).GT.0.001)GO TO 10
11    CONTINUE
      RETURN
      END
      SUBROUTINE UDATE (N21,RU0,T)
      REAL N21
      THALF4=2.8062E-6
      RU0=((N21)-1.0)*EXP(THALF4*T)+1.0
      RETURN
      END
      SUBROUTINE THIDATE (NT52,NT42,THR,TGS,TN1,TN2)
      REAL NT52,NT42,TN1,TN2
      THALF0=9.2173E-6
      THALF4=2.8062E-6
      RLR=THALF0/(THALF0-THALF4)
      TN=TN2/TN1
10    ERLA=EXP(-THALF0*TGS)
      ERLB=EXP(-(THALF0-THALF4)*TGS)
      FUNC=-(NT52)+(THR*NT42*ERLA)+((1.0-ERLA)/TN+RLR*(1.0-1.0/TN)*(1.0-
     2ERLB))
      DERIV=-(THALF0*THR*NT42*ERLA)+(THALF0*ERLA/TN+THALF0*(1.0-1.0/TN)*
     2ERLB)
      DH=FUNC/DERIV
      TGS=TGS-DH
      IF (TGS .GE. 350000.) GO TO 11
      IF(ABS(DH/TGS).GT.0.001)GO TO 10
11    CONTINUE
      RETURN
      END
```

```
SAMPLE NO. = 76125-1          DATE RUN JAN 18/77

SAMPLE WT. =  49.7  GMS

BLANK DISC COUNT TIME =  1798.  MINS

DELAY IN COUNTING THORIUM =  1.  DAYS

SPIKE USED =  .20  MLS

ACTIVITY OF 1 ML 232 SPIKE = 17.50  CPM

238-U OF EQUIVALENT ACTIVITY TO SPIKE = 195.5  MICROGRAMS

RAW DATA
U COUNT TIME =    783.  MIN        TH COUNT TIME =  2108.  MIN
U-238 =    7.363  C/M      TH-232 =     .033  C/M
U-234 =   12.003  C/M      TH-230 =    2.631  C/M
U-232 =    2.903  C/M      TH-228 =    2.114  C/M
********************
BACKGROUND
U-238 =     .008  C/M      TH-232 =     .008  C/M
U-234 =     .012  C/M      TH-230 =     .012  C/M
U-232 =     .029  C/M      TH-228 =     .029  C/M
********************
CORRECTED DATA
                   ERROR                               ERROR
U-238 =    7.355   .097 C/M      TH-232 =     .025    .004 C/M
U-234 =   11.991   .124 C/M      TH-230 =    2.619    .035 C/M
U-232 =    2.874   .061 C/M      TH-228 =    2.047    .032 C/M
********************

URANIUM CONCENTRATION      =  2.01   P.P.M.
CHEMICAL YIELD OF URANIUM = 82.11   PERCENT
CHEMICAL YIELD OF THORIUM = 56.96   PERCENT
SPIKE RATIO                = 1.027
********************
                    ERROR                              ERROR
U-234/U-238 = 1.630   .027    (U-234/U-238)0 = 1.705   .033
TH-230/U-234=  .315   .010      TH-230/TH/232 = 104.8   18.8

                      +    1500.
THORIUM AGE = 40000.            YEARS
                      -    1500.
********************
```

^{231}Pa/^{230}Th program list and printout

```
      PROGRAM TST (INPUT,OUTPUT,TAPE5=INPUT,TAPE6=OUTPUT)
C     PROGRAM CORRECTS RAW COUNT RATE DATA AND COMPUTES PA-231/TH-230,
C     U-234/U-238, TH-230/TH-232 AND TH-228/TH-232 ISOTOPE RATIOS AND
C     THE AGE
C     N1=U-238 COUNT RATE
C     N2=U-234 COUNT RATE
C     N3=U-232 COUNT RATE
C     N4=TH-232 COUNT RATE
C     N5=TH-230 COUNT RATE
C     N6=TH-228 COUNT RATE
C     N7=TH-227 COUNT RATE
C     CNTU=ACCUMULATION TIME FOR U SPECTRUM (MINS)
C     CNTT= ACCUMULATION TIME FOR TH SPECTRUM (MINS)
C     CNBD= ACCUMULATION TIME FOR BD SPECTRUM (MINS)
C     DCPT= DELAY BETWEEN PLATING OUT AND COUNTING TH (MINS)
C     DSPT= TIME BETWEEN PLATING OUT AND SEPARATION FROM AC-227 (HRS)
C     WEIGHT = WT OF SAMPLE IN GRAMS
C     B1= COUNTER BACKGROUND CORRECTION FOR U-238 AND TH-232
C     B2= COUNTER BACKGROUND CORRECTION FOR U-234 AND TH-230
C     B3= COUNTER BACKGROUND CORRECTION FOR U-232 AND TH-228
C     B4= COUNTER BACKGROUND CORRECTION FOR TH-227
      REAL N1,N2,N3,N4,N5,N6,N7,LAM3,LAM7,NT75,N21,NT54,LAM4
100   READ (5,101) TITLE,TGS,CNTU,CNTT,CNBD,DCPT,DSPT,DATE
101   FORMAT (A10,6E10.0,A10)
      IF (TGS.EQ.0.) GO TO 999
997   CONTINUE
102   READ (5,103) N1,N2,N3,N4,N5,N6,N7
103   FORMAT (7E10.0)
104   READ (5,105) B1,B2,B3,B4,WEIGHT
105   FORMAT (5E10.0)
      TAPPX=0.0
      NLOOP=0
C
C   . CALCULATION OF COUNT RATES CORRECTED FOR BACKGROUND
C        AND REAGENT BLANK
C
C
C        FOR RB CORRECTION ASSUME U YIELD=50%
C        TH REAGENT BLANK IS ZERO
C
      RB1=0.008
      RB2=0.025
      TN1=N1-B1-RB1
      TN2=N2-B2-RB2
      TN3=N3-B3
      TN4=N4-B1
      TN5=N5-B2
      TN6=N6-B3
      TN7=N7-B4
C        ***************************************************************
C        CORRECTION TO TN7 FOR RA-224 INGROWTH FROM TH-228
C        DETERMINATION OF TOTAL RA-224
      LAM4=1.3224E-4
      RA224=TN6*(1.+((EXP(-LAM4*(CNTT+DCPT))-EXP(-LAM4*DCPT)))/(LAM4
     2*CNTT))
C        CORRECT TH-227FOR RA-224 INGROWTH
      TN7=TN7-(0.945*RA224)
C
C     CORRECTION TO TN7 FOR TH-227 DECAY AND RA-223 GROWTH AFTER PLATING
C
C     TPN7 IS TH-227 COUNT RATE AT TIME OF PLATING OUT
C
      LAM3=4.2113E-5
      LAM7=2.6017E-5
      XA=(1+(LAM3/(LAM3-LAM7)))/(-LAM7)


      XB=(1/(LAM3-LAM7))
      TPN7=(TN7*CNTT)/((XA*(EXP(-LAM7*(CNTT+DCPT))-(EXP(-LAM7*DCPT))))+(
     2XB*(EXP(-LAM3*(CNTT+DCPT))-EXP(-LAM3*DCPT))))
C
C     CORRECTION TO TPN7 FOR TH227 DECAY AFTER SEPARATION FROM AC227 ON
C     TH COLUMN
C     TSN7 IS TH227 COUNT RATE AT TIME OF COLUMN SEPARATION
C
      TSN7=TPN7/EXP(-LAM7*DSPT*60.)
      NT75=TSN7/TN5
      N21=TN2/TN1
      NT54=TN5/TN4
C
C     ER=TOTAL ERROR IN U, TH COUNT RATES DERIVED FROM
C                    1) U,TH COUNT RATE
C                    2) BLANK DISC COUNT RATE FOR U,TH COUNT TIMES
C                    3) BLANK DISC COUNT RATE FOR BLANK DISC COUNT TIME
C                    4) REAGENT BLANK.
C
      BR1=0.004
      BR2=0.022
      BR4=0.000
      BR5=0.000
      ER1=SQRT((TN1/CNTU)+(B1/CNTU)+(B1/CNBD)+(BR1*BR1))
      ER2=SQRT((TN2/CNTU)+(B2/CNTU)+(B2/CNBD)+(BR2*BR2))
      ER4=SQRT((TN4/CNTT)+(B1/CNTT)+(B1/CNBD)+(BR4))
      ER5=SQRT((TN5/CNTT)+(B2/CNTT)+(B2/CNBD)+(BR5))
      ER7=SQRT((TN7/CNTT)+(B4/CNTT)+(B4/CNBD))
      ER21=(TN2/TN1)*SQRT (ER1*ER1/(TN1*TN1)+ER2*ER2/(TN2*TN2))
      ER54=(TN5/TN4)*SQRT (ER5*ER5/(TN5*TN5)+ER4*ER4/(TN4*TN4))
      ERS7=ER7*TSN7/TN7
      ER75=(TSN7/TN5)*SQRT(ERS7*ERS7/(TSN7*TSN7)+ER5*ER5/(TN5*TN5))
      R75=NT75
      T=TGS
      CALL PADATE(R75,N21,T,TN1,TN2)
C
C     SUBROUTINE PA DATE SOLVES AGE EQUATION BY AN ITERATIVE METHOD
C
      IF(TGS.GE.350000.)GO TO 106
      TU=TGS
      R75=NT75-ER75
      CALL PADATE (R75,N21,TU,TN1,TN2)
      TL=TGS
      R75=NT75+ER75
      CALL PADATE (R75,N21,TL,TN1,TN2)
      I=(T+50.)/100.
      T=I*100
      RTL=T-TL
      RTU=TU-T
      I=(RTU+50.)/100.
      RTU=I*100
      I=(RTL+50.)/100.
      RTL=I*100
      CALL UDATE (N21,RUO,T)
C
C     SUBROUTINE UDATE COMPUTES INITIAL U-234/U-238 RATIOS FROM MEASURED
C     U-234/U-238  AND CALCULATED AGE (T)
C
      R21=N21+ER21
      CALL UDATE (R21,RUOU,TU)
      R21=N21-ER21
      CALL UDATE (R21,RUOL,TL)
      RUOA=ABS((RUOU-RUOL)/2.0)
106   U238=7HU-238 =
      U234=7HU-234 =
      U232=7HU-232 =
      TH232=8HTH-232 =
      TH230=8HTH-230 =
      TH228=8HTH-228 =
      TH227=8HTH-227 =
      CM=5HC/MIN
      ER=7HERROR =
107   WRITE (6,108)
108   FORMAT (1H1)
      WRITE (6,109) TITLE, DATE
109   FORMAT (* SAMPLE NO. = *,A10,5X,* DATE RUN *,A10,/)
      WRITE (6,110) CNBD
110   FORMAT (* BLANK DISC COUNT TIME = *,F6.0,1X,* MINS*,/)
      WRITE (6,111) DCPT
111   FORMAT (* DELAY BTWN PLATING AND COUNTING TH = *,F6.0,1X,*MINS*,/)
      WRITE (6,112) DSPT
112   FORMAT (* TIME BTWN PLATING AND SEP"N FROM AC-227 = *,F6.0,1X,
     2* HRS*,/)
      WRITE (6,113)
113   FORMAT (* RAW DATA*,/)
      WRITE (6,114) CNTU,CNTT
114   FORMAT (* U COUNT TIME = *,F6.0,1X,* MINS*,5X,* TH COUNT TIME = *,
     2F6.0,1X,* MINS*)
      WRITE (6,115) U238,N1,CM,TH232,N4,CM
115   FORMAT (1X,A7,F8.3,2X,A3,5X,A8,F8.3,2X,A3)
      WRITE (6,115) U234,N2,CM,TH230,N5,CM
      WRITE (6,115) U232,N3,CM,TH228,N6,CM
      WRITE (6,116) TH227,N7,CM
116   FORMAT (26X,A8,F8.4,2X,A3,/)
      WRITE (6,117)
117   FORMAT (* BACKGROUND*)
      WRITE (6,115) U238,B1,CM,TH232,B1,CM
      WRITE (6,115) U234,B2,CM,TH230,B2,CM
      WRITE (6,115) U232,B3,CM,TH228,B3,CM
      WRITE (6,116) TH227,B4,CM
      WRITE (6,118)
118   FORMAT (* CORRECTED DATA*)
      WRITE (6,119)
119   FORMAT (*                       ERROR*)
      WRITE (6,120) U238,TN1,ER1,CM,TH232,TN4,CM
120   FORMAT (1X,A7,F8.3,2X,F5.3,1X,A3,5X,A8,F8.3,8X,A3)
      WRITE (6,121) U234,TN2,ER2,CM,TH230,TN5,ER5,CM
121   FORMAT (1X,A7,F8.3,2X,F5.3,1X,A3,5X,A8,F8.3,2X,F5.3,1X,A3)
      WRITE (6,122) U232,TN3,CM,TH228,TN6,CM
122   FORMAT (1X,A7,F8.3,8X,A3,5X,A8,F8.3,8X,A3)
      WRITE (6,123) TH227,TSN7,ERS7,CM
123   FORMAT (32X,A8,F8.4,2X,F5.4,1X,A3,/)
      IF (NT54.GT.999.) GO TO 1245
      WRITE (6,125) NT54,ER54
125   FORMAT (* TH-230/TH-232 = *, F7.3,2X,F7.3,/)
      GO TO 1265
1245  WRITE (6,1255)
1255  FORMAT (* TH-230/TH-232 = GT1000*)
1265  WRITE (6,126) NT75,ER75
126   FORMAT (* TH-227/TH-230 = *, F5.3,2X,F5.3,/)
      IF (T.GE.350000.) GO TO 131
      WRITE (6,127)
127   FORMAT (*                                ERROR                        ERROR
     2*)
      WRITE (6,128) N21,ER21,RUO,RUOA
128   FORMAT (* U-234/U-238= *,F5.3,2X,F5.3,2X,*(U-234/U-238)0= *,F5.3,
     22X,F5.3)
144   WRITE (6,120)
145   WRITE (6,146) RTU
146   FORMAT (27X,*+*,1X,F7.0)


147   WRITE (6,148) T
148   FORMAT (* PROTACTINIUM AGE =*,F7.0,12X,*YEARS*)
149   WRITE (6,150) RTL
150   FORMAT (27X,*-*,1X,F7.0)
      GO TO 100
131   WRITE (6,124) N21,ER21
124   FORMAT (* U-234/U-238 = *,F5.3,2X,F5.3,/)
      WRITE (6,132)
132   FORMAT (* AGE IS GREATER THAN 350,000 YEARS B.P.*)
      GO TO 100
999   STOP
      END
      SUBROUTINE PADATE(NT75,N21,TGS,TN1,TN2)
      REAL NT75,N21,TN1,TN2,LAM0,LAM1,LAM4
      LAM0=9.2173E-6
      LAM1=2.1341E-5
      LAM4=2.8062E-6
      TN=TN2/TN1
C
C     SAM AND ROY ARE LAM EXPRESSIONS
C
10    SAM1=EXP(-LAM1*TGS)
      SAM0=EXP(-LAM0*TGS)
      SAM04=EXP(-(LAM0-LAM4)*TGS)
      ROY=(TN-1)*(LAM0/(LAM0-LAM4))
      FUNC=-NT75+((1-SAM1)/(21.7*((1-SAM0)+ROY*(1-SAM04))))
      DERIV=((LAM1*SAM1)*((1-SAM0)+ROY*(1-SAM04))-(1-SAM1)*((LAM0*SAM0)+
     2(TN-1)*LAM0*SAM04))/(21.7*((1-SAM0)+(ROY*(1-SAM04)))**2.)
      ALF=FUNC/DERIV
      TGS=TGS-ALF
      WRITE (6,333) ROY, FUNC, DERIV, ALF, TGS
333   FORMAT (5E18.7)
      IF(TGS.GE.350000.)GO TO 11
      IF(ABS(ALF/TGS).GT.0.001)GO TO 10
11    CONTINUE
      RETURN
      END
      SUBROUTINE UDATE (N21,RUO,T)
      REAL N21
      THALF4=2.8062E-6
      RUO=((N21)-1.0)*EXP(THALF4*T)+1.0
      RETURN
      END
```

```
SAMPLE NO. = 76121-3          DATE RUN MAR21/77

BLANK DISC COUNT TIME =  1261.  MINS

DELAY BTWN PLATING AND COUNTING TH =  2911. MINS

TIME BTWN PLATING AND SEP"N FROM AC-227 =    21.  HRS

RAW DATA

U COUNT TIME =   592.  MINS      TH COUNT TIME =  1286.  MINS
U-238 =  15.700  C/M     TH-232 =    .040  C/M
U-234 =  17.576  C/M     TH-230 =   6.407  C/M
U-232 =    .030  C/M     TH-228 =    .070  C/M
                         TH-227 =   .4076  C/M

BACKGROUND
U-238 =   0.000  C/M     TH-232 =   0.000  C/M
U-234 =   0.000  C/M     TH-230 =   0.000  C/M
U-232 =   0.000  C/M     TH-228 =   0.000  C/M
                         TH-227 =  0.0000  C/M

CORRECTED DATA
                ERROR
U-238 =  15.700  .163 C/M     TH-232 =    .040        C/M
U-234 =  17.576  .172 C/M     TH-230 =   6.407  .072  C/M
U-232 =    .030       C/M     TH-228 =    .070        C/M
                              TH-227 =   .3796  .0171 C/M

TH-230/TH-232 = 160.175   22.402

TH-227/TH-230 =  .059   .003

                  ERROR                                ERROR
U-234/U-238= 1.119   .016  (U-234/U-238)0= 1.159   .025

                          +  15100.
PROTACTINIUM AGE =101000.            YEARS
                          -  13000.
```

APPENDIX 2

Method of correction of raw mass spectrometric data and conversion to PDB standard.

Conversion of Raw δ Results to PDB

This conversion was treated as a three part process:

1) to correct mean NBS 20 analyses (column 7, Table 3.6) for machine characteristics and isotope abundances and so obtain $\delta^{18}O_{NBS-GCSWS}$ and $\delta^{13}C_{NBS-GCSWS}$,
2) to use these values and known relationships of NBS 20 to PDB to determine $\delta^{18}O_{GCSWS-PDB}$ and $\delta^{13}C_{GCSWS-PDB}$,
3) to correct raw sample δ values for machine characteristics and isotope abundances as in 1) and then use the relevant $\delta_{GCSWS-PDB}$ relationships to determine $\delta^{18}O_{X-PDB}$ and $\delta^{13}C_{X-PDB}$, where X = sample.

To illustrate this procedure, the mean values for NBS 20 vs. GCSWS 2 (in column 7, Table 3.6) are used in conjunction with a typical set of sample analyses, also run against GCSWS 2.

1) Correction of mean NBS 20 values

From Table 3.6, mean NBS 20 $^{46}\delta_{raw} = 7.550$, $^{45}\delta_{raw} = -1.37$ and VMC = 1.007, $ASC^{45} = 1.0103$, $ASC^{46} = 1.0082$.

Therefore corrected values for NBS 20 are :

$$^{46}\delta_{corr} = 7.55 \times 1.007 \times 1.0082 = 7.665$$

$$^{45}\delta_{corr} = -1.37 \times 1.007 \times 1.0103 = -1.394$$

To correct for isotpic abundances due to other mass species (eg. $C^{17}O_2$, $^{13}C^{17}O^{16}O$ etc) the relationships derived by Craig (1957) are used :

$$\delta^{18}O_{X-GCS} = 1.0014\ ^{46}\delta_{corr} + 0.0091\ \delta^{13}C_{X-GCS}$$

$$\delta^{13}C_{X-GCS} = 1.0677\ ^{45}\delta_{corr} - 0.0338\ \delta^{18}O_{X-GCS}$$

These equations are solved by successive approximation, initially substituting $^{46}\delta_{corr}$ and $^{45}\delta_{corr}$ for $\delta^{18}O$ and $\delta^{13}C$ and continuing until no values change thus :

$$\delta^{18}O_{NBS-GCSWS\ 2} = 7.660 \quad \text{and} \quad \delta^{13}C_{NBS-GCSWS\ 2} = -1.747$$

2) Determination of $\delta_{GCS-PDB}$

The above relationship can also be expressed as $\delta_{GCSWS\ 2\ -\ NBS\ 20}$ using :

$$\delta_{A-B} = \frac{-\ \delta_{B-A} .\ 1000}{1000 + \delta_{B-A}} \qquad 1)$$

so $\delta^{18}O_{GCSWS2-NBS\ 20} = -7.602$ and $\delta^{13}C_{GCSWS2-NBS\ 20} = 1.750$

Now $\delta^{18}O_{NBS\ 20-PDB} = -4.18‰$ and $\delta^{13}C_{NBS\ 20-PDB} = -1.06‰$ (Craig 1957, Blattner and Hulston 1978)

Since $\delta_{A-C} = \delta_{A-B} + \delta_{B-C} + \delta_{A-B}.\delta_{B-C}.\ 10^{-3}$ 2)

therefore $\delta^{18}O_{GCSWS2-PDB} = -7.602 - 4.18 + (-7.602)(-4.18)$

$= \underline{-11.750}$

and $\delta^{13}C_{GCSWS2-PDB} = 1.75 - 1.06 + (1.75)(-1.06)\ 10^{-3}$

$= \underline{0.688}$

This relationship applies only to GCSWS 2 prepared at 25°C.

3) Determination of δ_{X-PDB}

Raw sample results are $^{46}\delta = 1.07$, $^{45}\delta = -7.55$;

Raw sample values are first corrected for machine characteristics:

$$^{46}\delta_{corr} = 1.07 \times 1.007 \times 1.0082 = 1.086$$

$$^{45}\delta_{corr} = -7.55 \times 1.007 \times 1.0103 = -7.681$$

and then for isotopic abundance as before:

$$\delta^{18}O_{X-GCSWS\ 2} = 1.013 \ , \quad \delta^{13}C_{X-GCSWS\ 2} = -8.235$$

therefore using equation 2) :

$$\underline{\delta^{18}O_{X-PDB} = -10.749‰} \quad \text{and} \quad \underline{\delta^{13}C_{X-PDB} = -7.553‰}$$

APPENDIX 3

a) Sample location, description and radiometric age data for speleothems from Vancouver Island caves (described in Chapter 4)

b) List of stable isotope data for speleothems from Vancouver Island (described in Chapter 4)

abbreviations used :

f/st = flowstone, stalag. = stalagmite

stalac. = stalactite, xilln = crystalline

g.l. = growth layer

* = not recorded, sample lost

** = flowstone, growth layer analysed in two directions

a) Location, description and age data for Vancouver Island speleothems

Cave Name & Location	Speleo-them Number	Location	Speleothem Description	Analysis		U (ppm)	Yields (%)		$\frac{^{234}U}{^{238}U}$	$(\frac{^{234}U}{^{238}U})_o$	$\frac{^{230}Th}{^{232}Th}$	$\frac{^{230}Th}{^{234}U}$	AGE (Ka) ± 1σ	Corrected Age ± 1σ and (^{232}Th (ppm))
				No.	Location		U	Th						
Euclataws Cave	75100	Witches Ballroom	15 cm long stalag. stump	-1	basal 3cm	<0.01	68	34	-	-	-	-	-	
				-2	top 3cm	<0.02	33	25	-	-	-	-	-	
				-3	near base	<0.01	47	53	-	-	-	-	-	
	75101	Dome Chamber	14cm long stalag.	-6	middle	<0.03	35	61	-	-	-	-	-	
	75102	Witches Ballroom	3 broken stalactites	-1	middle of longest	<0.01	38	14	-	-	-	-	-	
	75103		34cm single crystal broken stalag.	-1	top 2cm	<0.01	66	29	-	-	-	-	-	
				-3A	near base	<0.02	35	55	-	-	-	-	-	
	76002	By 12' waterfall	2 small f/sts on fallen block	-1	oldest layer	0.01	34	14	-	-	-	-	-	
Cascade Cave	75123	Carne's Carriage	one of two clear yellow stalags. on common base of f/st. (7cm long)	-1	basal 0.5cm	0.13	46	57	1.505	1.592	29	0.414	$56.1^{+3.8}_{-3.7}$	
				-2A	top 1cm	0.07	46	69	1.765	1.882	12	0.383	$50.5^{+6.9}_{-6.5}$	$45.3^{+9.9}_{-9.6}$ (0.01)
	75125	Upstream of Theatre, ∿2,5m above floor	In situ stalac.-f/st. forming remanants of false floor	-3	top 1cm	0.20	50	11	1.932	2.026	3.6	0.277	$34.3^{+6.6}_{-6.3}$	$21.4^{+13.4}_{-13.1}$ (0.09)
				-4A	upper middle	0.31	31	7	1.192	1.217	1.3	0.342	$44.9^{+20.8}_{-17.6}$	$-7.2^{+46.0}_{-51.9}$ (0.29)
				-6	basal 0.5cm	0.13	62	18	1.775	1.897	21	0.394	$52.7^{+6.8}_{-6.4}$	
				-7	basal ∿ 1.5cm	0.14	59	51	1.758	1.856	24	0.338	43.3± 3.0	
				-8	top 0.5cm	0.20	34	35	1.941	2.030	73	0.261	32.1± 1.7	
	76013	as 75125, directly below it	Three layers of calcite underlying 75125, separated from it and each other by thick mud/sand horizons (up to 1cm deep) From top, order is C,B,A.	C-1	upper layer, 1cm thick	0.11	28	14	1.603	1.703	11	0.407	$54.7^{+6.9}_{-6.6}$	$48.7^{+8.5}_{-8.2}$ (0.02)
				A-2	basal 1cm	0.09	49	8	1.695	1.825	> 1000	0.443	$60.8^{+10.6}_{-9.8}$	
	75126	Mars Room	15cm stalag. on its side, attached to fallen slab	-1	basal 3cm	0.08	51	53	1.526	1.544	4.5	0.102	11.6± 1.8	7.9±3.8 (0.01)
				-2	top 4cm	0.06	63	45	1.631	1.655	2.7	0.119	13.6 ± 2.9	$6.2^{+6.7}_{-6.8}$ (0.01)
	75127	The Theatre	6cm modern red stalag.	-1	basal 2cm	0.09	40	18	1.670	1.701	7.0	0.139	$16.0^{+4.0}_{-3.9}$	12.8±7.3 (0.01)
				-2	middle 2cm	0.08	50	21	1.622	1.652	3.4	0.147	$17.1^{+3.3}_{-3.2}$	$10.0^{+8.0}_{-8.2}$ (0.02)
	76008	Nervous Breakdown	three overlapping flowstones (76008,9,10) from the same block. 76008 is basal(?) block 76009 is middle (?) and 76010 is top(?).	-1	base (?) 1cm	0.07	66	50	1.808	1.952	59	0.431	$58.5^{+4.9}_{-4.7}$	
				-2	top (?) 1cm	0.06	37	40	1.562	1.657	5.5	0.411	$55.5^{+8.2}_{-7.7}$	$43.2^{+11.5}_{-11.1}$ (0.02)
	76009	" "		-1	top (?) 1cm	0.12	10	39	1.228	1.270	4.9	0.432	$60.2^{+18.0}_{-15.6}$	$45.4^{+24.1}_{-22.2}$ (0.04)

Cave Name & Location	Speleothem Number	Location	Speleothem Description	Analysis No.	Analysis Location	U (ppm)	Yields (%) U	Yields (%) Th	$\frac{^{234}U}{^{238}U}$	$(\frac{^{234}U}{^{238}U})_o$	$\frac{^{230}Th}{^{232}Th}$	$\frac{^{230}Th}{^{234}U}$	AGE (Ka) ± 1σ	Corrected Age ± 1σ
Cascade Cave	76010	Nervous Breakdown	as 76008	-2	top (?) 1cm	0.07	40	25	1.694	1.826	13	0.450	$62.0^{+7.2}_{-6.8}$	$56.5^{+9.4}_{-9.1}$(0.01)
				-3	basal (?) 1cm	0.06	14	30	1.633	1.726	15	0.398	$53.2^{+6.3}_{-6.0}$	$49.0^{+8.8}_{-8.6}$(0.01)
	76011	Waterfall Chamber below Carne's Carnage	6cm deep brown f/st (laminated) underlying porous f/st. White f/st overgrowth covers base of brown f/st.	-1	base of brown f/st	0.07	36	22	1.594	1.700	17	0.426	$58.0^{+5.2}_{-5.0}$	$54.1^{+6.2}_{-6.0}$(0.01)
				-2	top of brown f/st	0.08	35	45	1.328	1.395	4	0.471	$67.0^{+11.0}_{-10.0}$	$46.6^{+15.2}_{-14.6}$(0.04)
				-3	overgrowth	0.09	17	30	0.894	0.889	0.7	0.140	$16.4^{+12.6}_{-11.3}$	$-22.1^{+29.2}_{-30.5}$(0.05)
				-4	overgrowth	0.06	39	37	1.424	1.425	1.6	0.088	9.9 ± 1.5	0.8±3.5 (0.01)
				-5	top of brown f/st.	0.08	28	27	1.522	1.584	16	0.338	$43.4^{+3.7}_{-3.6}$	$39.5^{+6.1}_{-6.0}$(0.01)
	76012	Mars Room	15cm long stalag. on its side attached to fallen block.	-1	basal 2cm	0.18	49	36	1.917	1.974	4.6	0.182	21.4 ± 1.6	14.9±2.7(0.04)
				-2	top 1cm	0.16	42	62	1.945	1.993	2.2	0.152	17.7 ± 1.4	$6.2^{+2.7}_{-2.8}$(0.06)
				-3	basal 2cm	0.18	29	26	1.957	1.984	2.1	0.193	22.8 ± 1.2	6.8± 2.3(0.10)
				-5	top 2cm	0.13	36	32	1.965	1.994	114	0.095	10.7 ± 0.7	
Main Cave	75151	High level grotto at end.	small (5cm deep) stalag.(modern)	-1	half of one	0.05	41	8	1.047	1.098	6	0.925	$265.4^{+311.6}_{-152.7}$	$236.9^{+343.5}_{-152.7}$(0.03)

b) Stable isotopic data for Vancouver Island speleothems

Speleothem No.	Analysis No.	Distance along g.l. (cm)	$\delta^{13}C_{c\text{-}PDB}$ (‰)	$\delta^{18}O_{c\text{-}PDB}$ (‰)
75123	123-10	0 (top of g.l.)	-7.55	-10.75
	-10A	2.4	-7.74	-10.76
	-10B	4.8	-7.66	-10.49
	-10C	6.7	-7.89	-10.73
	-10D	2.2	-7.93	-10.47
	-10E	5.2	-7.14	-10.65
	G-1	0 (top of g.l.)	-7.79	-11.08
	G-2	2.2	-8.22	-10.78
	G-3	3.4	-8.17	-11.07
	G-4	5.2	-8.01	-10.60
	G-5	7.4	-8.06	-10.77
75125	125G-1	1.7 from end of g.l.	-8.32	-11.25,-11.35
	G-2	4.0	-8.04	-11.22,-11.23
	G-3	5.5	-7.90	-11.20,-11.22
	G-4	7.0	-7.79	-11.46,-11.34
	G-5	9.0	-7.45	-10.89,-11.02
	125B-1	0.3 from end of g.l.	-6.70	-10.88,-10.96
	B-2	2.6	-6.80	-10.71,-11.06
	B-3	5.1	-6.62	-10.42,-10.56
	B-4	6.8	-6.58	-10.31,-11.01
	B-5	8.6	-6.62	-10.38,-10.60
76012	012A-1	0 (top of g.l.)	-9.59	- 9.23
	A-2	2.2 from A-1	-8.46	- 9.02
	A-3	4.4 " "	-8.63	- 8.74
	012B-1	*	*	*
	B-2	3.3 from B-1	-8.53	- 8.63
	B-3	6.6 " "	-8.51	- 8.56
	B-4	10.0 " "	-8.01	- 8.53
	B-5	12.2 " "	-7.83	- 8.28
76008**	008A-1	0.5 from end of g.l.	-7.56	-10.38
	A-2	3.4 from A-1	-7.81	-10.13
	A-3	5.8 " "	-7.84	-10.09
	A-4	2.8 from A-3	-8.13	-10.30
	A-5	5.1 " "	-8.60	-10.13
	A-6	7.3 " "	-7.92	- 9.90
	A-7	8.1 from A-1	-8.02	- 9.82
	A-8	11.2 " "	-7.48	- 9.97
	A-9	13.5 " "	-7.51	- 9.50

Speleothem No.	Analysis No.	Distance along g.l. (cm)	$\delta^{13}C_{c\text{-}PDB}$ (‰)	$\delta^{18}O_{c\text{-}PDB}$ (‰)
76008**	008B-1	0 to edge	-9.06	-10.27
	B-2	2.3 from B-1	-8.58	-10.23
	B-3	4.4 " "	-8.35	-10.68
	B-4	6.6 " "	-8.85	-10.59
	B-5	1.4 from B-4	-9.07	- 9.79
	B-6	3.7 " "	-8.77	-10.12
		distance from base		
75123	123-1	0.6	-7.44	-10.13
	-2	1.1	-7.95	-10.23
	-3	1.7	-8.49	-10.75
	-4	2.2	-8.54	-10.46
	-5	2.7	-7.74	-10.48
	-6	3.2	-8.47	-10.41
	-7	4.0	-7.31	-10.99
	-8	4.7	-6.77	-11.13
	-9	5.2	-7.58	-10.60
	-10	5.8	-7.85	-10.70
	-11	6.7	-7.74	-10.61
	-12	7.1	-6.37	-10.86
76013	013-1	0.2	-7.88	-10.13,-10.07
	-2	0.3	-7.98	-10.13,-10.16
	-3	0.6	-7.96	-10.78,-10.71
	-4	1.1	-7.99	-10.25,-10.41 -10.29
	-5	~ 1.6	-7.60	-10.58,-10.62
	-6	~ 2.1	-6.93	-10.56,-10.39 -10.48,-10.51
	-7	~ 2.6	-6.96	-10.39,-10.38
	-8	~ 3.1	-7.58	-10.48,-10.48
	-9	~ 3.6	-8.11	-10.52,-10.46
75125	125-1	0.3	-8.00	-10.42,-10.50,-10.47
	-2	0.8	-8.02	-10.87,-10.92
	-3	1.3	-6.71	-11.04,-10.94
	-4	1.8	-6.80	-11.07,-11.10
	-5	2.2	-7.05	-11.26,-11.27
	-6	2.4	-7.17	-11.31,-11.33
	-7	2.9	-7.18	-11.36
	-8	3.5	-7.29	-11.10,-11.15
	-9	3.9	-8.02	-11.45,-11.31
	-10	4.4	-8.03	-11.46,-11.40
	-11	4.8	-7.93	-11.69,-11.55
	-12	~ 5.2	-7.57	-11.43,-11.39
	-13	overgrowth (~ 5.5)	-7.42	-11.26,-11.42,-11.30

APPENDIX 4

a) Speleothem location, description and radiometric age data for caves of N.W.England (described in Chapter 5)

b) List of stable isotope data for speleothems from N.W. England (described in Chapter 5)

abbreviations used :

f/st = flowstone, stalag. = stalagmite
stalac.= stalactite, xilln = crystalline
* = not recorded, sample lost
** = $^{231}\text{Pa}/^{230}\text{Th}$ determinations
*** = flowstone, growth layer analysed in two directions
g.l. = growth layer

a) Location, description and age data for N.W. England speleothems

Cave Name & Location	Speleothem Number	Location	Speleothem Description	Analysis No.	Analysis Location	U (ppm)	Yields (%) U	Yields (%) Th	$\frac{^{234}U}{^{238}U}$	$(\frac{^{234}U}{^{238}U})_o$	$\frac{^{230}Th}{^{232}Th}$	$\frac{^{230}Th}{^{234}U}$	AGE (Ka) ± 1σ	Corrected Age ± 1σ
White Scar Cave, Chapel-le-Dale	76100	Main streamway, downstream from the Pulpit.	26cm deep loose f/st boulder in streamway. Laminated, non-porous, white/yellow calcite	E-1	basal (?) 1cm	1.46	75	16	0.976	-	126	0.976	> 350	
				E-2	top (?) 1cm	0.88	56	18	0.946	-	103	0.956	> 350	
	76102	Gour chamber, Western Front	10cm deep, loose brownish laminated f/st, macro-xilln in centre clay-rich layers towards top and bottom.	-1	top 0.5 cm	0.06	12	65	1.096	-	2.1	1.083	> 350	
	76106A	Sleepwalker Passage, in Yard near top of entrance climb	5 cm deep, clear-brown loose f/st.	-1	top (?) 0.5cm	0.58	16	21	1.018	1.034	36	0.870	$217.9^{+28.9}_{-22.9}$	
				-2	basal(?) 0.5cm	0.61	24	34	0.995	0.989	21	0.903	$255.2^{+62.1}_{-39.2}$	
	76106B	as 76106A	12cm deep multi (4)-hiatus f/st	-1	top 0.5cm	0.80	67	54	0.857	-	37	1.030	> 350	
	76108	In roof tube of Far Streamway above canal	30cm long brown calcite stalag. wedged in by boulder fall, not in growth position.	-1	basal 1cm	1.39	49	44	1.201	1.208	7.4	0.102	11.6 ± 0.7	9.4±1.2
				-2	top 2cm	2.11	57	49	1.082	1.084	23	0.053	6.0 ± 0.3	
Ibbeth Peril Cave (I) Dentdale	76110	Fossil tube near entrance passage	6cm deep 'oily' black-layered f/st, forming false floor	-1	top 2cm	0.72	64	50	0.996	0.996	25	0.089	10.1 ± 0.5	
	76111	Part of f/st boss adjacent to 76110	7cm deep f/st, white upper 4cm, black dirty lower 3cm.	-1	a piece	0.30	58	53	1.067	1.073	15	0.238	29.4 ± 2.2	$26.9^{+3.4}_{-3.3}$
				-2	top 1cm	0.31	74	39	0.947	0.945	> 1000	0.118	13.7 ± 1.3	
	76112	near 76110, f/st bridge across passage	1cm deep f/st forming false floor veneer over gravels	-1	1 cm	1.21	39	48	0.960	0.959	> 1000	0.068	7.6 ± 0.7	
Lancaster Hole (L.H.) – Ease Gill Caverns (E.G.C.) System	76121	Bill Taylor's Passage, L.H.	23cm long, loose, dense-white laminated stalagmite. Shows surface erosion features.	-1	top 1cm	2.42	67	67	1.073	1.100	110	0.656	$113.6^{+7.6}_{-7.1}$	
				-2	basal 2cm	1.49	76	69	1.130	1.179	129	0.661	$114.0^{+7.5}_{-7.1}$	
				-3**	duplicate of -2	-	-	-	1.117	1.153	160	-	96.4** $^{+15.7}_{-13.5}$	
	76122	Bill Taylor's Passage, L.H.	22cm long, multi (3)- hiatus stalag., dense white-yellow calcite	-1	basal 1cm	2.12	44	20	1.203	1.262	54	0.578	$90.8^{+5.4}_{-5.2}$	
				-2	top 0.5cm	2.59	36	25	1.386	1.471	37	0.491	$70.6^{+3.4}_{-3.3}$	
	76124	Bill Taylor's Passage, L.H.	43cm long loose stalag., dense white calcite/	-1	basal 1cm	0.62	36	24	1.229	1.238	13	0.116	13.3 ± 1.0	11.9±1.5
	76125	Bill Taylor's Passage, L.H. overlain by mud deposits near 76135	15cm long, loose stalag., cream-yellow calcite	-1	basal 1cm	2.01	82	60	1.628	1.698	105	0.302	38.1 ± 1.4	
				-3**	duplicate of -1	-	-	-	1.569	1.662	257	-	54.4** $^{+12.3}_{-11.0}$	
				-4	top 0.5cm	1.17	51	32	1.518	1.577	66	0.306	$38.8^{+1.5}_{-1.4}$	

Cave Name & Location	Speleothem Number	Location	Speleothem Description	Analysis		U (ppm)	Yields (%)		$\frac{^{234}U}{^{238}U}$	$(\frac{^{234}U}{^{238}U})_o$	$\frac{^{230}Th}{^{232}Th}$	$\frac{^{230}Th}{^{234}U}$	AGE (Ka) ± 1σ	Corrected Age ± 1σ
				No.	Location		U	Th						
Lancaster Hole (L.H.) - Ease Gill Cavern (E.G.C.) System	76127	Near top of ladder, Stop Pot.	16cm deep loose f/st, non-porous faintly-laminated calcite.	-1	top 0.5cm	13.1	46	41	0.878	0.770	255	0.843	$225.2^{+24.6}_{-19.7}$	
				-2	basal 0.5cm	5.8	12	10	0.911	-	> 1000	0.963	> 350	
				-3**	duplicate of -1	-	-	-	0.881	0.789	89	-	$203.4^{**}{}^{+27.3}_{-21.1}$	
				-4	1 - 1.5cm above base	14.5	64	59	0.848	0.704	> 1000	0.846	$237.7^{+21.8}_{-17.8}$	
	76128	Easter Grotto, (E.G.C.)	51cm long loose stalagmite, clear amber, few growth layers.	-1	basal 3cm	18.3	37	44	0.745	0.736	43	0.745	11.5 ± 0.5	
	76129	Easter Grotto, (E.G.C.)	33cm long loose stalagmite, white non-porous calcite.	-1	top 2cm	3.1	78	51	0.789	0.789	3.2	0.008	0.9 ± 0.1	0.5 ± 0.3
				-2	basal 4cm	1.8	54	33	0.749	0.741	9.8	0.099	11.4 ± 0.6	9.7 ± 1.0
	76130	Montagu East Passage, near Stake Pot, L.H.-E.G.C.	33cm long loose stalagmite	-1	basal 3cm	2.77	44	50	1.222	1.228	72	0.084	9.6 ± 0.3	
				-2	duplicate of -1 (by B.Blackwell)	1.55	22	44	1.244	1.251	8.9	0.089	10.1 ± 0.7	
				-T-2	top 2cm	1.90	53	60	1.232	1.236	153	0.049	5.5 ± 0.2	
	76131	Stop Pot E.G.C. on boulder near ladder	32cm long in situ stalag.	-1	basal 0.5cm	17.1	56	59	0.760	0.754	45	0.080	9.0 ± 0.3	
	76133	Upstream from Eureka Jnc. (E.G.C.)	14cm deep loose stalac/f.st well-laminated orange calcite	-1	top 0.5cm	4.9	63	49	0.820	0.819	2.9	0.054	6.5 ± 0.2	
				-2	basal 0.5cm	9.5	48	17	0.778	0.771	> 1000	0.086	9.8 ± 0.5	
	76135	Large slumped f/st boss in Bill Taylor's Passage, L.H.	∿ 1m deep boss once covered by mud fill. Four samples taken.	-1	top 1cm of central block (∿20cm from top)	0.97	54	49	1.192	1.250	52	0.594	$94.7^{+4.5}_{-4.3}$	
				-2	top 1cm of top block	1.32	65	65	1.240	1.306	> 1000	0.558	$85.7^{+2.6}_{-2.5}$	
	77120	On south side of Colonnade Passage	In situ f/st boss, 3 segments collected, (-A, -B and 79005), each separated by detrital horizon	A-1	basal 1cm	2.71	43	9	1.242	1.358	280	0.750	$140.1^{+10.6}_{-9.8}$	
				A-2	top 1cm	1.90	57	41	1.161	1.219	124	0.647	$109.1^{+3.7}_{-3.6}$	
			A = 8.5cm deep basal segment of yellow, macro-xilln porous calcite.	B-2	basal 1cm	1.64	56	66	1.417	1.558	> 1000	0.640	$103.6^{+3.5}_{-3.4}$	
				B-3	0.5cm below hiatus	0.43	67	51	1.577	1.736	> 1000	0.574	$86.8^{+3.9}_{-3.7}$	
			B = 13cm deep middle segment whose base is clear-white non-porous calcite, and top is yellow macro-xilln, somewhat porous calcite; they are separated by a black detrital line.	B-4	0.5cm above hiatus	0.42	51	49	1.577	1.696	11.1	0.476	67.0 ± 2.4	60.3±3.0
				B-5	1-3cm from top	0.41	43	43	1.380	1.484	4.0	0.567	$86.5^{+4.7}_{-4.5}$	$62.3^{+6.6}_{-6.4}$
				B-1	top 1cm	0.38	44	11	1.473	1.569	> 1000	0.468	$65.9^{+4.7}_{-4.5}$	

Cave Name & Location	Speleothem Number	Location	Speleothem Description	Analysis		U (ppm)	Yields (%)		$\frac{^{234}U}{^{238}U}$	$(\frac{^{234}U}{^{238}U})_o$	$\frac{^{230}Th}{^{232}Th}$	$\frac{^{230}Th}{^{234}U}$	AGE (Ka) ± 1σ	Corrected Age ± 1σ
				No.	Location		U	Th						
Lancaster Hole (L.H.) - Ease Gill Caverns (E.G.C) System	79005	as 77120	Top segment of sequence of f/sts 9.5cm deep, white macro-xilln calcite, contains 4 detrital horizons.	-3	basal 0.5cm	0.57	33	37	1.425	1.490	23	0.399	53.8 ± 2.5	$51.1\pm^{3.5}_{3.4}$
				-1	top 0.5cm	0.43	33	34	1.429	1.477	11.6	0.333	$43.0^{+3.1}_{-3.0}$	38.4±4.6
				-2	duplicate of -1	-	-	-	1.399	1.511	46	-	$88.0^{+34.5}_{-25.2}$	
	77121	Bridge Hall L.H.	18cm deep block from fallen f/st slab, contains 2 detrital lines, brown calcite of upper 13cm contains 1 line and is separated from lower white calcite by 2nd line.	-1	top 2cm	0.22	9	59	1.198	1.233	24	0.418	$57.7^{+4.4}_{-4.3}$	$54.9^{+5.1}_{-4.9}$
				-3	∿2-4cm from top	0.23	51	45	1.314	1.364	44	0.389	52.4 ± 1.9	
				-4	1cm above white/brown hiatus	0.51	33	37	1.518	1.609	47	0.423	57.6 ± 2.1	
				-5	1cm below white/brown hiatus	0.59	41	38	1.178	1.261	547	0.736	$137.0^{+8.4}_{-7.9}$	
				-2	basal 1cm	1.24	68	55	1.313	1.425	73	0.656	$109.4^{+5.2}_{-4.9}$	
	77123B	Bill Taylor's Passage L.H.	2cm thick f/st <u>in situ</u> on wall overlying mud and calcite debris	-1	2cm piece	1.32	69	68	1.565	1.623	75	0.280	34.9 ± 0.9	
	77126	Bill Taylor's Passage	13 cms loose stalag. showing surface re-solution. Dense white laminated calcite.	-1	basal 3cm	6.11	49	36	1.031	1.044	160	0.691	$126.3^{+4.9}_{-4.7}$	
				-2	top 0.5cm	3.93	61	37	1.152	1.205	240	0.635	$106.0^{+3.6}_{-3.5}$	
				-3**	duplicate of -2	-	-	-	1.085	1.115	> 1000	-	$108.7^{**}\,{}^{+9.5}_{-8.7}$	
	79003	On a prominent ledge, ∿15m above base of entrance pitch	4 segments were collected (A-D) from base to top of large slumping f/st boss.	A-1	basal 1cm of basal segment	0.21	48	36	1.117	1.204	62	0.860	$198.6^{+20.5}_{-17.4}$	
Ingleborough Cave	76140	On ledge ∿ 3m above floor in Giant's Hall	9cm long, <u>in situ</u> stalag., macro-xilln containing detritus horizons	-1	basal 2cm	0.10	23	12	1.270	1.413	5.7	0.784	$151.9^{+34.9}_{-26.9}$	$126.9^{+41.7}_{-34.4}$
	76141	In low bedding crawl at top of aven climb in Giant's Hall ∿10m above floor	8cm ~~deep~~ broken f/st. macro-xilln porous calcite - possibly equivalent piece to 77143A	-1	basal 0.5 cm	0.07	66	17	1.462	1.631	10.3	0.668	$110.7^{+11.5}_{-10.5}$	$100.7^{+14.8}_{-14.0}$
				-2	top 1cm	0.10	33	17	1.341	1.412	19.1	0.475	$67.8^{+5.2}_{-5.0}$	$63.9^{+6.3}_{-6.1}$
	76142	∿3m above floor of Giant's Hall on aven climb underlying main f/st boss	11cm deep <u>in situ</u> f/st, macro-xilln porous calcite on one side (base) of prominent hiatus, laminated non-porous calcite on other side (top 3cm).	-1	middle 2cm below hiatus	0.04	81	72	1.306	1.475	14	0.798	$156.4^{+45.4}_{-32.9}$	$147.5^{+49.6}_{-37.5}$
				-2	basal 3cm	0.04	65	67	1.287	1.381	7.5	0.623	$101.0^{+14.3}_{-12.8}$	$87.5^{+18.2}_{-16.9}$
				-3	above hiatus, 0.5-1.5cm from top	0.10	20	9	1.132	1.193	4.0	0.728	$135.8^{+43.3}_{-31.3}$	$103.4^{+56.2}_{-46.3}$

Cave Name & Location	Speleo-them Number	Location	Speleothem Description	Analysis		U (ppm)	Yields (%)		$\frac{^{234}U}{^{238}U}$	$(\frac{^{234}U}{^{238}U})_0$	$\frac{^{230}Th}{^{232}Th}$	$\frac{^{230}Th}{^{234}U}$	AGE (Ka) ± 1σ	Corrected Age ± 1σ
				No.	Location		U	Th						
Ingleborough Cave	76143	5m above floor of Giant's Hall on ledge in mud deposits	6cm deep loose f/st, macro-xilln calcite	-1	basal 2cm	0.07	39	34	1.267	1.450	2.8	0.857	$185.6^{+40.7}_{-30.3}$	$129.3^{+50.1}_{-40.4}$
	76144	Near to pool at end of show cave	15cm deep stalag. boss, laminated, contains detrital layers	-1	basal 3cm	0.37	44	36	0.952	0.951	2.4	0.100	$11.5^{+1.2}_{-1.1}$	4.3±2.2
				-2	top 1cm	0.41	21	22	1.078	1.080	2.7	0.185	$22.2^{+1.2}_{-1.1}$	10.2±2.1
	76145	At end of show cave	49cm long narrow loose stalag. containing many detrital layers and porous calcite	C-1	26-29cm above base	0.95	88	83	0.784	0.777	2.1	0.103	11.9 ± 0.6	3.4±1.1
	77143	In entrance of low crawl at top of aven climb in Giant's Hall	2 blocks separated by detrital layer	A-1	basal 0.5-1.5 cm	0.07	55	9	1.480	1.633	26	0.621	$98.4^{+14.0}_{-12.6}$	
			A = 7cm deep upper f/st block, macro-xilln porous calcite thinly laminated at top and bottom	A-2	top 0.5-1.5cm	0.06	37	43	1.392	1.517	21.6	0.617	$98.2^{+10.0}_{-9,2}$	$93.9^{+11.5}_{-10.7}$
			B = 9.5cm deep lower f/st block. laminated non-porous calcite; clear-white in upper half, well laminated brown below.	B-1	basal 1.5cm	0.12	51	49	1.192	1.273	41	0.702	$125.1^{+8.7}_{-8.1}$	
				B-2	top 1.5cm	0.11	38	8	1.337	1.458	24	0.658	$109.5^{+10.3}_{-9.5}$	
				B-3	middle, 3-4cm above base	0.14	20	42	1.343	1.473	72	0.677	$114.6^{+8.5}_{-7.9}$	
Victoria Cave	76151	F/st block pile in loop passage	3 cm deep piece from f/st block (loose) off middle of pile, white laminated calcite.	-1	basal 1.5cm	0.38	31	23	0.974	-	46	0.954	> 350	
	76152	as 76151	7cm deep f/st from base of (loose) block pile. Opaque brown detrital calcite.	-1	basal 2cm	0.38	22	69	1.006	1.011	3.1	0.869	$219.2^{+44.7}_{-31.6}$	$161.4^{+49.6}_{-36.7}$
	76153	as 76151	loose stalactitic slab on block pile (probably fallen off roof) Brown detrital calcite	-1	top 1cm (youngest)	0.18	22	61	1.301	1.311	3.5	0.162	19.0 ± 1.6	11.4±2.9
	76154	as 76151	6cm deep f/st from base of loose block pile. Clear-brown calcite	-1	top 1cm	0.52	37	46	1.049	1.081	53	0.818	$180.1^{+15.6}_{-13.7}$	
	76155	Near end of fossil phreatic passage leading off back of main entrance passage	4cm deep *in situ* wall veneer of f/st, contains 1 hiatus, clear white calcite	-1	top 1cm (= younger)	0.61	59	41	1.028	-	81	1.009	> 350	
	77150B	*In situ* in laminated clays in entrance passage.	thin f/st veneer covering calcite-cemented mud	-1	piece	0.39	60	68	1.019	-	9.4	1.104	> 350	

Cave Name & Location	Speleothem Number	Location	Speleothem Description	Analysis		U (ppm)	Yields (%)		$\frac{^{234}U}{^{238}U}$	$(\frac{^{234}U}{^{238}U})_o$	$\frac{^{230}Th}{^{232}Th}$	$\frac{^{230}Th}{^{234}U}$	AGE (Ka) ± 1σ	Corrected Age ± 1σ
				No.	Location		U	Th						
Victoria Cave	77151	On east side of Loop Passage, above excavated trench.	Three blocks of f/st A,B,C. A = 8cm deep basal block overlying calcite-cemented mud fragments. Base contains 3cm high stalag. Brown laminated calcite. B = 10.7cm deep middle block, dark brown in lower half clear-white in upper half, no hiatus. White powdery lines separate white calcite in upper half. C = 12cm deep upper block, light-brown calcite below hiatus 3cm from base, brown calcite for rest. Well-laminated throughout. A - B are separated by indistinct hiatus (blocks parted naturally). B - C also parted naturally - no clear hiatus.	A-1	small piece of stalag.	0.36	50	58	1.152	1.270	59	0.875	$204.5^{+34.0}_{-26.3}$	
				A-2	basal 1cm of f/st	0.50	48	60	0.984	0.964	26	0.925	$287.4^{+32.6}_{-25.0}$	
				B-1	basal 3cm	0.43	40	36	1.037	1.082	47	0.935	$281.0^{+43.2}_{-31.0}$	
				B-2	top 1cm	0.45	84	58	1.059	1.125	130	0.927	$264.5^{+29.1}_{-23.1}$	
				C-4	1cm below hiatus	0.41	43	15	1.057	1.114	128	0.914	$250.4^{+28.9}_{-23.0}$	
				C-3	1cm above hiatus	0.46	34	22	1.081	1.137	102	0.836	$187.5^{+12.5}_{-11.3}$	
				C-5	~duplicate of C-3	0.45	35	38	1.112	1.230	118	0.930	$255.3^{+28.1}_{-22.6}$	
				C-1	top 1cm	0.48	58	42	1.081	1.139	56	0.848	$194.6^{+19.3}_{-16.5}$	
				C-2	top 1cm	0.46	46	47	1.020	1.035	> 1000	0.831	$190.8^{+9.2}_{-8.5}$	
	77159	Remanents of fo fossil floor in situ on east wall 5m above present (excavated) floor, 1m below roof level	7cm deep multi-(3) hiatus f/st.	-1	basal 1cm	0.39	85	70	1.104	1.246	24.8	0.969	$307.2^{+53.9}_{-37.3}$	
				-2	top 1cm	0.32	23	25	1.143	1.186	9.0	0.627	$104.0^{+7.5}_{-7.1}$	$92.5^{+9.5}_{-9.0}$
	77230	Overhanging f/st and fill layers On south wall 1.5-4.6m above (excavated) floor	Samples A (base) to H (top) taken A is clear white calcite, 3cm depp. F is 6cm deep f/st-stalactite curtain, brown calcite with detritus layers.	A-1	basal 1cm	1.97	50	5	1.039	-	21	1.103	> 350	
				F-1	basal 1cm	0.35	10	28	1.138	1.276	23	0.933	$252.6^{+55.8}_{-37.5}$	$246.6^{+56.6}_{-38.4}$
	77231	On left of Loop Passage.	5cm long in situ stalag., clear brown non-porous calcite	-1	top 2,5cm	0.50	39	63	0.982	0.965	42	0.889	$242.7^{+26.6}_{-21.3}$	
	77234	In Loop Passage near 2m climb	5cm deep piece of in situ overhanging f/st curtain, brown laminated calcite	-1	top 1.5cm	0.38	10	49	0.947	0.906	12.4	0.848	$213.6^{+31.9}_{-24.4}$	$201.3^{+32.9}_{-25.5}$
	77236	Overlying laminated clays in entrance passage	3cm deep macro-xilln porous f/st	-1	a 3cm piece	0.65	38	55	0.915	-	31	1.156	(> 350) ?	leached ?
	77237	Adjacent to 77236, overlain by black clays apparently in situ	7.5cm deep f/st, light-brown laminated calcite	-1	top 1cm	0.58	50	52	1.001	-	88	-.968	> 350	

Cave Name & Location	Speleothem Number	Location	Speleothem Description	Analysis		U (ppm)	Yields (%)		$\frac{^{234}U}{^{238}U}$	$(\frac{^{234}U}{^{238}U})_o$	$\frac{^{230}Th}{^{232}Th}$	$\frac{^{230}Th}{^{234}U}$	AGE (Ka) ± 1σ	Corrected Age ± 1σ
				No.	Location		U	Th						
Victoria Cave	77238B	Near to 77236, overlies bedrock directly underlies full thickness of laminated clays	up to 8cm deep f/st block, laminated calcite and mud cemented by calcite	-1	∿ middle	1.00	74	56	1.052	-	43	1.006	> 350	
	79000	Excavated from bone layers (Pigyard Museum sample)	clear laminated brown f/st, surrounding rhino tooth	-1	1cm adjacent to tooth	0.62	6	28	1.000	1.000	44	0.610	$102.1^{+12.0}_{-10.8}$	
	79001	as 79000	∿ 8cm deep milky-brown f/st surrounding rhino jaw + teeth	-1	1cm adjacent to teeth	0.50	22	24	1.100	1.132	19.8	0.623	$103.8^{+6.2}_{-5.9}$	$98.7^{+7.5}_{-7.2}$
				-2	1-3cm from teeth	0.40	21	21	1.033	1.048	152	0.691	$126.3^{+9.7}_{-8.9}$	
	79002	as 79000	1cm thick f/st coating, around red deer antler, white calcite with detritus.	-1	1cm piece	0.50	27	27	1.012	1.017	16.2	0.702	$130.7^{+8.8}_{-8.2}$	$123.4^{+10.2}_{-9.5}$
Lost John's Cave, Leck Fell	76160	From boulder choke in R.H. high level pass. in Lyle Cavern.	18cm deep loose laminated f/st non-porous calcite with detrital layers	-2	basal (?) 1cm	0.20	49	31	1.295	1.414	15.9	0.717	$127.5^{+12.6}_{-11.4}$	$120.5^{+14.8}_{-13.4}$
				-3	top (?) 2cm	0.18	47	6	1.283	1.392	15.3	0.702	$123.1^{+29.1}_{-23.4}$	$116.0^{+37.5}_{-32.9}$
	76161	as 76160	17cm long loose stalag, white non-porous calcite	-1	basal 2cm	0.25	62	11	1.273	1.282	0.7	0.106	$12.1^{+5.6}_{-5.3}$	$-15.1^{+14.2}_{-14.8}$
	76164	Embedded in mud deposits on ledge ∿2.5m above stream level in Main Drain (upstream of jnc.)	13cm deep two-coloured f/st, brown non-porous calcite (=top?) white non-porous calcite (=base?)	-1	top 0.5-1cm	3.84	72	54	1.003	1.004	178	0.598	$98.7^{+3.8}_{-3.7}$	
				-2	top 1-2cm	4.31	61	16	0.929	0.905	452	0.612	$104.5^{+6.7}_{-6.3}$	
				-3	basal 2cm	5.68	50	45	0.945	0.926	> 1000	0.620	$106.3^{+4.3}_{-4.1}$	
	76165	near 76164 in situ f/st 2.5m above stream level	many pieces of f/st, white ∿ non-porous calcite	-1	1 piece	9.35	40	33	0.938	0.914	111	0.649	$115.5^{+12.3}_{-11.0}$	
	77162	as 76165	17cm deep piece of in situ f/st ~~white non-porous calcite~~	-1	top 2cm	6.23	48	61	0.944	0.928	127	0.568	$92.0^{+4.3}_{-4.1}$	
				$\overset{**}{-2}$	duplicate split of -1	-	-	-	0.939	0.922	199	-	$\overset{**}{88.8}{}^{+6.8}_{-6.3}$	
				-4	top 2-3cms	7.16	49	60	0.898	0.865	> 1000	0.597	$101.2^{+3.1}_{-3.0}$	
				-3	basal 1cm	7.21	41	48	0.916	0.885	92	0.638	$112.7^{+5.2}_{-5.0}$	
				$\overset{**}{-3b}$	duplicate split of -3	-	-	-	0.882	0.813	> 1000	-	$\overset{**}{165.7}{}^{+18.1}_{-15.1}$	

Cave Name & Location	Speleothem Number	Location	Speleothem Description	Analysis		U (ppm)	Yields (%)		$\frac{^{234}U}{^{238}U}$	$(\frac{^{234}U}{^{238}U})_o$	$\frac{^{230}Th}{^{232}Th}$	$\frac{^{230}Th}{^{234}U}$	AGE (Ka) ± 1σ	Corrected Age ± 1σ
				No.	Location		U	Th						
Sleets Gill Littondale	76172	In main tube towards entrance	piece of fossil stalac.curtain xilln calcite analysed from very porous layers.	-1	0.5cm calcite layer	0.02	55	45	1.067	-	3.8	1.715	-	(leached)
Gavel Pot Leck Fell	76190	Glasfurd's Pass. in well-decorated chamber	89cm long loose stalagmite, jammed under boulders and f/st	-1	basal 2cm	0.57	57	68	1.398	1.415	4.5	0.127	14.7 ± 0.6	10.0±1.1
				-2	top 2cm	0.50	61	35	1.368	1.373	5.4	0.046	5.1 ± 0.6	3.7±1.1
	76191	Glasfurd's Pass. near end.	31cm long loose stalag. contains detrital layers, outside is covered by calcite xtals - pool deposits ?	-2	basal 3-6 cm	0.44	39	12	1.238	1.247	65	0.114	13.1 ± 1.4	
Gaping Gill System	76201	Stump Chamber (near Sand Cavern)	43cm long loose stalag., white non-porous clean calcite.	-1	basal 2cm	2.07	66	52	1.279	1.285	16	0.068	7.6 ± 0.4	6.9 ±0.5
	76202	Mud Hall, on boulder slope	small piece of ∿ 80cm deep block of loose f/st, white-yellow, non-porous calcite	-2	basal 3-5cm	0.46	56	53	1.056	-	40	1.074	> 350	
	76206	Hensler's Upper Passage	2cm thick f/st forming false floor, with mud layers.	-1	a piece	1.81	34	32	1.181	1.204	48	0.333	43.5 ± 1.2	
	76207	Nevada Passage Far Country Series	24cm long loose stalag. with detritus layers and re-solution features on surface	-1	basal 4cm	0.89	50	37	1.290	1.399	76	0.672	$114.2^{+8.5}_{-7.9}$	
				-2	top 4cm	0.30	58	54	1.233	1.340	27	0.735	$135.1^{+15.9}_{-14.0}$	
	76208	Stump Chamber (near Sand Cavern)	25cm long loose stalag., white non-porous calcite	-1	top 1cm	0.42	57	49	1.512	1.515	3.0	0.017	1.9 ± 0.2	1.0±0.4
				-T	top 1cm	0.91	27	31	1.580	1.581	8.3	0.007	0.8 ± 0.2	0.7±0.5
	76209	Sand Cavern overlying varves	16cm long stalag,,white non-porous calcite	-1	basal 1cm	9.38	53	42	1.120	1.120	5.9	0.008	0.8 ± 0.1	0.6±0.1
	76210	Old East Passage near Mud Hall	13cm long loose stalag. on mud, hiatus 1cm below top. White-yellow calcite	-1	basal 1cm	1.39	58	51	1.370	1.412	99	0.303	$38.5^{+1.5}_{-1.4}$	
				-2	top 1cm	2.38	47	16	1.300	1.333	122	0.297	37.7 ± 1.4	
	76211	Old East Pass. near 2m high shelf	2cm thick old scalloped f/st in situ on wall . Contains detritus	-1	a piece	0.39	36	30	1.164	1.334	28	0.938	$252.8^{+29.6}_{-23.6}$	
	77209	as 76211, from under the shelf	5.5cm deep in situ f/st, brown calcite containing detritus	-2	top 1.5cm	0.25	48	33	1.185	1.454	19.8	0.995	$319.1^{+>43.2}_{-43.6}$	$312.2^{+>47.1}_{-45.0}$
	76212	Old East Pass. near shelf	13cm deep loose laminated f/st, contains detrital layers and porous macro-xilln calcite	-2	basal 1cm	2.10	39	11	1.218	1.227	3.6	0.126	14.6 ± 0.7	8.8±1.2
				-3	top 1cm	0.90	46	45	1.274	1.283	6.7	0.107	12.2 ± 0.4	9.6±0.7

Cave Name & Location	Speleo-them Number	Location	Speleothem Description	Analysis		U (ppm)	Yields (%)		$\frac{^{234}U}{^{238}U}$	$(\frac{^{234}U}{^{238}U})_o$	$\frac{^{230}Th}{^{232}Th}$	$\frac{^{230}Th}{^{234}U}$	AGE (Ka) ± 1σ	Corrected Age ± 1σ
				No.	Location		U	Th						
Gaping Gill System	76215	West Chamber	3cm thick stalactite on top of fill (collected by R.R.Glover	-1	a piece	3.92	65	35	0.972	0.972	2.5	0.012	1.4 ± 0.1	0.6 ±0.3
	76216	Old East Pass. on mud bank	9cm long loose stalag., clear white non-porous calcite (RRG)	-1	basal 1cm	8,93	44	40	1.144	1.144	5.5	0.012	1.3 ± 0.1	0.9 ±0.1
	77200	Far East Pass. at aven in N. Craven Pasaage	17cm deep loose f/st, white laminated calcite showing surface re-solution.	-1	top (?) 2cm	0.95	87	77	1.296	1.665	181	0.994	$288.7^{+23.9}_{-20.0}$	
				-2	basal (?) 2.5 cm	1.94	86	46	1.239	-	69	1.032	> 350	
	77201	Old East Pass. in low chamber before Main Chamber	2cm thick loose f/st, overlain by gravel .	-1	piece	1.47	52	58	1.337	1.346	14.6	0.091	10.3 ±0.3	9.3±0.4
	77205	Far East Pass. near end chamber in streamway	12cm long loose stalag., contains hiatus 1cm from top (brown calcite above, white below). Shows surface re-solution features	-1	basal 2cm	1.85	82	68	1.842	1.960	95	0.358	46.4 ±0.9	
				-2	top 1 cm	1.84	66	37	1.858	1.987	28.8	0.379	49.7 ±1.2	
	77210A	as 77205	30cm long loose stalag., contains brownish calcite with many detrital layers and re-solution features on surface	-1	top 2cm	0.44	60	47	1.927	1.956	12	0.097	11.0 ±0.6	9.7±0.9
Newby Moss Cave, Ingleborough	76220	Entrance Pass.	13cm deep, yellow f/st (loose) shows surface re-solution	-1	top (?) 1cm	1.34	76	60	1.257	-	82	1.065	> 350	
Kingsdale Master Cave, Kingsdale	77240	Roof tunnel, near aven *in situ* on roof	piece of f/st chipped off re-solutioned roof-arch	-2	piece	0.20	51	14	1.145	1.359	83	0.989	324.3±>100	
	77241	Roof Tunnel	10cm long *in situ* erodded stalac. with modern straw on tip	-1	1cm below (= older than) hiatus.	0.41	45	23	1.123	1.196	35.2	0.804	$167.7^{+11.4}_{-10.3}$	
	77242	Roof Tunnel, in boulders = below 80' aven	∿ 5cm deep f/st block, macro-xilln calcite	-1	composite piece	1.55	16	15	1.015	1.034	74	0.941	$300.4^{+>70}_{-43.3}$	
	77243	Roof Tunnel near run-in beyond 77240	6cm deep loose f/st block, containing detrital layers and re-solution surface	-1	basal 1.5cm	1.17	35	33	1.053	1.101	73	0.891	$229.6^{+22.7}_{-18.9}$	

b) Stable isotopic data for N.W. England speleothems

Speleothem No.	Analysis No.	Distance along g.l. (cm)	$\delta^{18}O_{c\text{-}PDB}$ (‰)	$\delta^{13}C_{c\text{-}PDB}$ (‰)
76122	122A-1	16.5	-2.21	-1.38
	A-3	9.9	-2.10	-2.19
	A-5	4.4	-3.28	-4.87
	A-6	0.4	-3.28	-4.61
76125	125A-1	15.3	0.23	5.67
	A-2	12.4	-1.11	1.89
	A-3	8.7	-1.36	1.77
	A-4	5.3	-1.04	2.68
	A-5	2.5	-1.87	-0.18
	A-6	0	-1.71	-0.85
76210	210A-1	0	-3.33	-2.87
	A-2	2.9	-3.05	-1.94
	A-3	6.2	-2.88	-1.49
	A-4	8.8	-2.77	-1.28
76190	190A-1	*	-4.35	-7.65
	A-2		-4.25	-7.43
	A-3		-4.53	-8.40
	A-4		-4.84	-8.97
	A-5		-4.47	-8.82
	B-1	0	-4.67	-10.45
	B-2	6.2	-4.59	-9.71
	B-3	11.3	-3.77	-7.34
	B-4	17.1	-4.32	-7.96
	B-5	23.2	-3.25	-5.82
76128	128A-1	0	-3.26	-2.49
	A-2	2.8	-3.35	-0.24
	A-3	5.6	-2.12	3.32
	A-4	7.9	-2.38	0.95
	A-5	10.5	-1.61	5.07
76201	201A-1	0	-3.75	-2.80
	A-2	4.2	-4.55	-3.68
	A-3	8.8	-3.62	-1.43
	A-4	13.2	-3.52	1.23
	A-5	17.6	-2.40	2.93
76142***	142A-1	0	-4.39,-4.80,-4.37, -4.59,-4.21	-10.40
	A-2	3.5 from A-1	-4.39,-4.57,-4.57	-10.65
	A-3	6.0 "	-4.28,-4.07,-4.03	-10.50
	A-4	8.5 "	-3.89,-4.11,-4.07	-9.93
	A-5	0 from A-5	-4.24,-4.30	-10.45
	A-6	3.1 "	-4.15,-4.45,-4.62	-10.59
	A-7	8.3 "	-4.38,-4.66,-4.27	-10.51
	A-8	10.8 "	-4.36,-4.62,-4.32	-10.39
	B-1	0 from B-1	-4.25	-8.79
	B-2	3.2 "	-3.95,-4.06	-8.89
	B-3	6.0 "	-4.58,-4.26	-8.94
	B-4	8.2 "	-4.28	-8.98
	B-5	0 from B-5	-4.44	-9.10
	B-6	5.2 "	-4.40	-9.01
	B-7	7.5 "	-4.25	-9.07
		Distance from base		
77143	143-1	0.6	-4.22,-4.15	-10.71,-10.82
	-2	1.0	-4.19,-4.36,-4.31	-11.25
	-3	1.35	-4.09,-4.26,-4.14	-11.46
	-4	1.7	-4.44,-4.40	-11.41
	-5	2.15	-4.21,-4.15,-4.21	-11.01
	-6	2.6	-4.38,-4.36,-4.49, -4.31	-11.31
	-7	3.0	-4.44,-4.39	-10.87
	-7a	3.5	-4.10,-4.18	-10.94
	-8	4.2	-4.04,-4.14,-4.22, -4.15	-10.65
	-9	4.7	-4.23	-10.92
	-10	5.1	-4.04,-4.14,-4.09	-10.94
	-12	6.1	-4.27,-4.33	-10.20
	-13	6.6	-3.86,-3.88,-3.98, -4.06	-9.76
	-15	7.65	-3.96,-3.99	-9.67
	-16	8.2	-3.96,-3.81,-4.05	-9.86
	-17	8.4	-3.98,-3.70,-3.89, -3.90	-9.86
	-18	8.7	-3.99,-3.91,-3.94	-9.38,-9.83
	-19	9.0	-3.96,-3.69,-3.88	-9.57
	-20	9.4	-3.95,-3.79,-3.95	-9.78

Speleothem No.	Analysis No.	Distance along g.l. (cm)	$\delta^{18}O_{C-PDB}$ (‰)	$\delta^{13}C_{C-PDB}$ (‰)
77151***	151A-1	1.1 from edge	-3.58,-3.54	-8.12
	A-2	3.3 " "	-3.49,-3.49	-8.05
	A-3	5.4 " "	-3.43,-3.40	-8.10
	A-4	7.3 " "	-3.32,-3.47	-8.49
	A-5	9.1 " "	-3.56,-3.53	-8.89
	A-6	1.8 from A-5	-3.88,-4.08, -3.94	-9.22
	A-8	5.2 " "	-3.98,-3.96	-9.90
	151B-1	0 from B-1	-3.82,-3.87	-5.87
	B-2	3.0 " "	-4.33,-4.19	-6.69
	B-3	6.0 " "	-4.18,-4.04	-7.28
	B-4	8.2 " "	-4.20,-4.19	-7.58
	B-5	3.0 from B-4	-4.33,-4.37	-7.66
	B-6	5.3 " "	-4.53,-4.58	-8.01
	B-7	7.4 " "	-4.59,-4.68	-8.00
	151C-1	0 from C-1	-3.31,-3.23	-4.28
	C-2	2.9 " "	-3.80,-3.91	-6.15
	C-3	5.5 " "	-3.46,-3.48	-4.77
	C-4	2.4 from C-3	-3.00,-3.07	-3.96
	C-5	5.2 " "	-3.72,-3.67	-5.28
	151D-2	4.3 from D-1	-4.02,-3.99	-10.63
	D-3	7.1 " "	-4.09,-4.02	-10.87
	D-4	10.8 " "	-4.10,-3.95	-10.55
	D-5	2.3 from D-4	-3.90,-3.60	-9.93
	D-6	3.0 " "	-4.12,-4.01	-10.01
	151E-1	0 from E-1	-4.37,-4.38	-8.61
	E-2	3.4 " "	-4.58,-4.59	-9.38
	E-3	6.5 " "	-4.70,-4.71	-9.37
	E-4	9.3 " "	-4.55,-4.61	-9.35
	E-5	3.8 from E-4	-4.55,-4.60	-9.24
	E-6	6.9 " "	-4.69,-4.79	-9.67
77143***	143D-1	0 from D-1	-4.24,-4.24	-10.61
	D-2	3.6 " "	-4.17	-10.54
	D-3	8.2 " "	-4.41	-10.62
	D-4	12.7 " "	-4.33	-10.78
	D-5	+2.7 from D-6	-4.21	-10.76
	D-6	0 " "	-4.21	-10.62
	D-7	-6.5 " "	-4.10	-10.49
76127	127B-1	0 from B-1	-3.65,-3.61	-0.12
	B-2	2.6 " "	-3.51,-3.49	-0.40
	B-3	5.3 " "	-3.58,-3.66	-0.06
	B-4	2.1 from B-3	-3.58,-3.60	-0.36
	B-5	4.4 " "	-3.72,-3.76	-0.16
	127C-1	0 from C-1	-3.61,-3.61	(+)0.11
	C-2	2.9 " "	-3.88,-3.97	-0.23,-0.33
	C-3	5.4 " "	-3.80,-3.81	-0.17,-0.28
	C-4	+2.7 from C-3	-3.91,-3.66	-0.32,-0.39
	C-5	-1.5 " "	-3.72,-3.72	-0.26
		above base		
	127-1	0.4	-3.28,-3.34	1.37
	-2	1.0	-3.63,-3.57	0.89
	-3	1.7	-3.93,-3.71,-3.92	0.55
	-4	2.4	-3.98,-3.94	-0.14
	-5	3.1	-3.81,-3.90	-0.37
	-6	3.7	-4.00,-3.93	-0.01
	-7	4.4	-3.86.-3.79	-0,40
	-8	5.5	-3.90,-3.96	-0.15
	-9	6.3	-3.87,-3.72,-3.81	-0.57
	-10	7.0	-3.96,-3.83,-3.91	-0.76
	-11	7.6	-3.80,-3.98,-4.02	-0.97
	-12	8.3	-3.90,-3.98	-0.77
	-13	9.2	-3.82,-3.92	-0.73
	-14	9.8	-3.80,-3.88	-1.01
	-15	10.4	-3.80,-3.82	-0.59
	-16	11.0	-3.63,-3.79,-3.76	-0.39
	-17	11.7	-3.55,-3.67,-3.72	-0.44
	-18	12.3	-3.75,-3.80	-0.44
	-19	12.7	-3.67,-3.60	-0.20
	-20	13.8	-3.19,-3.23	0.55
	-21	14.2	-2.69,-2.66	1.93
	-22	14.4	-2.49,-2.67,-2.63	2.49
		from base of block A		
77151	151-1	0	-4.72,-4.70	-7.13
	-2	0.6	-4.59,-4.70	-7.76
	-3	1.2	-4.87,-4.78	-8.46
	-4	1.7	-4.76,-4.83	-8.98
	-5	2.2	-4.61,-4.78,-4.74	-9.02
	-6	2.6	-4.59,-4.54	-8.74

Speleothem No.	Analysis No.	Distance from base of block A (cm)	$^{18}O_{c-PDB}$ (‰)	$^{13}C_{c-PDB}$ (‰)
77151	151-7	3.0	-4.12,-4.28	-8.74
	-8	3.3	-4.42,-4.33	-9.29
	-9	3.7	-4.36,-4.34	-10.15
	-10	4.1	-4.39,-4.43	-10.39
	-11	4.5	-4.34,-4.40	-9.94
	-12	5.0	-4.28,-4.32	-10.39
	-14	5.8	-4.19,-4.07	-10.13
	-15	6.1	-3.97,-3.88	-9.89
	-16	6.4	-4.26,-4.18	-10.44
	-17	6.7	-4.38,-4.33	-10.55
	-18	7.1	-4.45,-4.05	-10.10
	-19	7.4	-3.63,-3.77	-9.59
	-20	7.8	-3.81,-3.85,-3.52	-9.30
	-21A	9.2	-5.10,-5.16	-9.13
	-21N	8.7	-4.93,-5.06	-8.90
	-22	9.7	-5.19	-8.22
	-22N	9.7	-5.15,-5.14	-8.67
	-23	10.4	-5.41,-5.51	-8.83
	-24	11.1	-4.94,-5.02	-7.17
	-25	11.8	-4.39,-4.37	-7.34
	-26	12.3	-4.25,-4.29	-6.82
	-27	12.7	-4.16,-4.22	-8.04
	-28	13.1	-3.93,-3.99	-7.68
	-29	13.3	-3.74,-3.59,-3.63	-6.06
	-30	13.8	-3.78,-3.84	-5.48
	-31	14.3	-3.33,-3.39	-5.10
	-32	14.9	-3.33,-3.41	-4.51
	-33	15.4	-3.12,-3.28,-3.51	-4.72
	-34	16.1	-3.90,-3.85	-6.04
	-35	16.5	-3.35,-3.28,	-4.08
	-36	16.9	-3.51,-3.55	-5.01
	-37	17.4	-3.56,-3.56	-4.93
	-38	17.8	-3.61,-3.62	-4.48
	-39	18.1	-3.95,-4.01	-6.09
	-41	18.8	-3.98,-3.94	-7.27
	-42	19.1	-4.29,-4.32	-7.04
	-43	19.5	-4.33,-4.24	-6.93
	-44	19.8	-4.27,-4.26	-6.81
	-45	20.2	-4.08,-4.06	-6.15
	-46	20.5	-4.31,-4.41	-7.47
	-47	21.0	-4.34,-4.38	-7.24
	-48	21.3	-4.14,-4.16	-6.78
	-49	21.8	-4.18,-4.29	-5.96
	-50	22.3	-5.52,-5.75	-8.28
	-51	22.7	-5.56,-5.48	-7.99
77151	151-52	23.2	-4.70,-4.74	-9.33
	-53	23.7	-4.75,-4.71	-9.12
	-49B	.	-4.54	-7.12
	-54	24.3	-4.60,-4.54	-9.32
	-55	25.0	-4.10,-4.48,-4.40	-9.62
	-56	25.6	-4.42,-4.12,-4.07	-8.88
	-57	26.1	-4.37,-4.45	-9.16
	-58	26.6	-4.23,-4.49,-4.41	-9.42
	-59	27.1	-5.09,-4.99,-4.93	-5.41
	-60	27.6	-4.46,-4.37	-10.59
	-61	28.0	-4.25,-4.02,-4.25	-9.75
	-63	29.1	-3.51,-3.45	-8.78
	-64	29.5	-3.68,-3.81,-3.90	-8.90
	-65	29.8	-4.03,-3.87,-4.03	-10.01
	-66	30.3	-4.29,-4.17	-6.24
	151-21N-1	8.4	-4.90,-4.84	-8.91
	-24A	11.5	-4.66,-4.71	-7.67
	-19-1	7.4	-3.64,-3.68	-8.98
	-20-1	7.8	-3.85,-3.80	-9.65
	-13	5.4	-3.99,-3.93	-9.93
	-20-3	8.3	-3.77,-4.05,-3.92	-9.38
	-20-2	8.0	-3.53,-3.48	-8.97
	-18	7.1	-4.37,-4.33	-10.06
	-22A	10.0	-5.28,-5.21	-9.39
	-62	28.5	-3.95,-3.87	-9.06
	-51A	22.9	-4.78,-4.75	-8.48
	-59A	27.3	-4.49,-4.41	-9.22
	-49A	22.0	-5.11,-4.93,-4.98	-7.77
	-58A	26.7	-4.31,-4.25	-9.25
	-50A	22.5	-5.43,-5.40	-8.39
	-40	18.5	-4.35,-4.33	-8.55
	-23A	10.9	-5.52,-5.47	-8.81
	-67	30.6	-4.87,-4.76	-8.49
	-68	30.9	-4.56,-4.58	-8.19
	-69	31.1	-4.37,-4.43	-8.31
	-70	31.3	-4.25,-4.39,-4.32	-8.82
	-71	31.7	-4.33,-4.33	-8.31
	-72	32.3	-4.22,-4.24	-6.64

APPENDIX 5

a) Sample location, description and radiometric age data for speleothems from Jamaica (described in Chapter 7)

b) List of stable isotope data for speleothems from Jamaica and Bahamas (described in Chapters 7 and 6 respectively)

c) Sample location, description and radiometric age data for speleothems from Grotte St-Elzéar, Québec (described in Chapter 7)

d) Sample location, description and radiometric age data for speleothems from remaining areas (eg. West Virginia, Canadian Rockies, etc.)

abbreviations used :

f/st = flowstone, stalag. = stalagmite
stalac. = stalactite, xilln = crystalline
g.l. = growth layer
* = flowstone, growth layer analysed in two directions

a) Location, description and age data for Jamaica speleothem

Cave Name & Location	Speleothem Number	Location	Speleothem Description	Analysis		U (ppm)	Yields (%)		$\frac{^{234}U}{^{238}U}$	$(\frac{^{234}U}{^{238}U})_o$	$\frac{^{230}Th}{^{232}Th}$	$\frac{^{230}Th}{^{234}U}$	AGE (Ka) ± 1σ	Corrected Age ± 1σ
				No.	Location		U	Th						
Jacksons Bay Cave	75300	*In situ* on wall just beyond Lead-On crawl.	7cm deep dissected fossil f/st yellow clear calcite near top porous, macro-xilln calcite near base.	-3	top 1cm	0.22	62	13	0.906	0.833	25	0.829	$205.6^{+82.3}_{-44.9}$	
				-5	top 1cm	0.28	27	25	0.966	0.926	9.1	0.913	$278.2^{+57.3}_{-37.0}$	$259.7^{+58.4}_{-38.2}$
				-7	basal 1cm	0.36	47	40	1.015	1.027	37	0.835	$193.7^{+25.4}_{-20.6}$	
				-8	top 1cm	0.37	51	13	0.989	0.981	69	0.823	$189.2^{+30.2}_{-23.6}$	
	75301	Coliseum Chamber, on mud.	57cm long loose stalag., well laminated in base and top, middle is re-xillised ?	-1	basal 5cm	0.12	14	7	0.988	0.987	7.7	0.213	$26.0^{+4.7}_{-4.5}$	21.3±8.5
				C-1	27-31cm from base	0.13	36	11	1.092	1.100	7.3	0.227	$27.9^{+12.0}_{-10.8}$	23.6±22.4
				D-4	top 2cm	0.20	37	6	0.937	0.936	> 1000	0.017	$1.9^{+2.9}_{-2.8}$	
Goldings Cave, Auchtembeddie	75320	In entrance passage	29cm long loose stalag. showing re-solution features on outer surface. Contains several detrital layers.	-1	basal 3cm	0.08	60	26	1.034	1.051	8.1	0.735	$142.2^{+25.9}_{-20.9}$	$126.5^{+32.2}_{-27.7}$
				-2	top 2cm	0.09	53	57	1.084	1.106	4.1	0.547	$84.7^{+8.8}_{-8.2}$	$60.8^{+12.4}_{-11.9}$
				-3	∿ 16cm from base	0.06	65	25	0.950	0.913	13.8	0.830	$199.2^{+105.2}_{-51.5}$	$188.5^{+112.6}_{-59.5}$
				-4	∿ 21cm from base	0.08	59	56	0.970	--	2.7	1.073	> 350	
Oxford Cave, Auchtembeddie	75335	Part of cave wall, ∿ 200m inside cave.	7cm deep piece of f/st, deeply-scalloped by re-solution. Non-porous texture.	-3	top 0.5cm	1.06	22	35	1.196	1.304	135	0.788	$156.4^{+10.6}_{-9.8}$	
				-4	basal 0.5cm	0.27	27	11	1.003	1.004	20	0.823	$187.3^{+74.0}_{-43.6}$	$180.4^{+83.1}_{-53.6}$
				-5	basal 0.5-1cm	0.62	38	32	1.100	1.170	47	0.843	$189.8^{+15.4}_{-13.6}$	
Cave River Cave, St.Ann	75341	Gour Passage	23cm long loose stalag. with surface re-solution features, some detrital layers.	-2	basal 1.5cm	0.32	15	36	0.987	0.986	3.4	0.158	18.7 ±2.1	10.9±4.1
				-3	top 2.5cm	0.34	47	23	1.016	1.016	5.3	0.046	5.1 ±0.5	3.7±1.0
				-4	∿ 14cm from base	0.31	17	16	1.017	1.017	6.0	0.073	$8.2^{+3.2}_{-3.1}$	$6.2^{+7.5}_{-7.6}$
	75342	Gour Passage	25cm long loose stalag. contain an inner stalag.	-2	outer 0.5cm at top	0.27	25	12	0.971	0.970	3.3	0.106	12.2± 2.4	6.7±4.7
				-3	as -2	0.30	86	51	0.990	0.989	3.0	0.129	15.0± 0.7	7.9±1.4
Coffee River Cave	75350	In roof of stream passage on fallen block	12cm long *in situ* stalag., contains 1 hiatus	-1	basal 3cm	0.13	75	48	1.056	1.066	4.1	0.407	$56.4^{+4.2}_{-4.1}$	$38.9^{+6.8}_{-6.7}$
				-2	top 1cm	0.05	87	58	1.003	1.003	2.2	0.210	$25.5^{+7.1}_{-6.7}$	$8.7^{+15.0}_{-15.1}$

Cave Name & Location	Speleothem Number	Location	Speleothem Description	Analysis		U (ppm)	Yields (%)		$\frac{^{234}U}{^{238}U}$	$(\frac{^{234}U}{^{238}U})_o$	$\frac{^{230}Th}{^{232}Th}$	$\frac{^{230}Th}{^{234}U}$	AGE (Ka) ± 1σ	Corrected Age ± 1σ
				No.	Location		U	Th						
Coffee River Cave	75351	Attached to fallen block in streamway, not in growth position.	90cm long stalag. containing many detrital layers near base. White non-porous calcite, some re-solution holes near middle.	A-2	3cm above base	0.24	41	44	1.030	1.038	6.8	0.542	$84.3^{+4.9}_{-4.7}$	$70.5^{+6.2}_{-6.0}$
				A-3	5cm from base	0.21	27	21	0.989	0.986	7.0	0.511	$77.7^{+6.2}_{-5.8}$	$65.0^{+7.6}_{-7.3}$
				C-2	∿ 60cm from base	0.09	18	17	1.341	1.395	17.3	0.390	$52.4^{+6.0}_{-5.7}$	$48.8^{+8.3}_{-8.0}$
				-5	∿ 45cm from base	0.10	61	58	1.106	1.125	25	0.425	$59.4^{+3.9}_{-3.8}$	
				D-10	top 2cm	0.16	48	28	0.898	0.880	7.2	0.412	$58.3^{+11.6}_{-10.4}$	$48.3^{+18.5}_{-17.7}$
	75353	Top part of longer stalag. not in growth position in streamway	16cm long piece of stalag., dense white calcite.	-1	basal 3cm	1.96	49	30	1.038	1.040	155	0.136	15.8± 1.1	
				-2	top 1cm	0.19	78	77	1.110	1.117	23	0.166	19.6± 1.6	
Runaway Bay Cave	75371	Donated by J. Lewis, show cave owner	17cm long stalag. white-yellow calcite	-1	basal 5cm	0.03	21	10	0.929	0.884	> 1000	0.786	$173.8^{+223.0}_{-91.2}$	
Hutchinson's Hole	75390	At entrance of side passage near base of hole.	22cm long stalag., in situ, shows surface re-solution features, contains hiatus near top.	-1	basal 3-5cm	0.23	80	64	0.876	0.755	9.1	0.858	$241.8^{+36.3}_{-26.5}$	$222.6^{+36.9}_{-27.3}$
				-2	top 2cm	0.17	54	6	0.949	0.934	> 1000	0.551	$87.8^{+23.3}_{-19.1}$	

b) Stable isotope data for Jamaica and blue hole speleothem

Jamaica

Speleothem No.	Analysis No.	Distance along g.l. (cm)	$\delta^{18}O_{C\text{-}PDB}$ (‰)	$\delta^{13}C_{C\text{-}PDB}$ (‰)
75351	351B-1	0	-1.42	-9.36
	B-2	2.2	-1.18	-9.16
	B-3	5.1	-1.06	-9.10
	B-4	7.9	-0.86	-8.74
	B-5	11.2	-0.60	-8.38
75341	341A-1	0	-4.61	-11.65
	A-2	1.7	-4.52	-11.90
	A-3	3.0	-4.10	-11.50
	A-4	4.0	-4.48	-11.35
	A-5	4.8	-3.87	-10.98
75300*	300A-1	0	-4.09	-9.07
	A-2	3.6 from A-1	-4.26	-9.13
	A-3	7.5 " "	-4.31	-9.38
	A-4	11.7 " "	-4.21	-9.17
	A-5	2.4 from A-5	-3.88	-8.66
	A-6	5.0 " "	-4.20	-9.35
Bahamas				
78033(g.1.)	033-1	0 from -1	-4.42,-4.55	-4.09
	-2	4.4	-4.41,-4.40	-3.63
	-3	9.0	-3.99,-3.97	-2.94
	-4	13.9	-3.88,-3.83,-3.78	-2.63
	-5	17.8	-4.01,-3.92	-2.88
	-6	19.1	-3.68,-3.71	-2.27

c) Location, description and age data for Grotte de Saint-Elzéar speleothem

Cave Name & Location	Speleothem Number	Location	Speleothem Description	Analysis		U (ppm)	Yields (%)		$\frac{^{234}U}{^{238}U}$	$(\frac{^{234}U}{^{238}U})_o$	$\frac{^{230}Th}{^{232}Th}$	$\frac{^{230}Th}{^{234}U}$	AGE (Ka) ± 1σ	Corrected Age ± 1σ
				No.	Location		U	Th						
Grotte de Saint-Elzéar, Bonaventure Québec.	77023	Salle des Ours on surface of breakdown	4cm long loose stalag.	-1	top 1cm	0.06	59	49	2.130	3.118	22	0.991	$223.9^{+30.7}_{-25.0}$	
	77024	as 77023	3cm long stalag., cemented on loose block, appears to be in growth position.	-1	top 1.5cm	0.10	39	28	2.406	3.120	13	0.844	$154.7^{+12.6}_{-11.5}$	$146.3^{+14.4}_{-13.5}$
	77026	as 77023	4cm long loose stalag.	-1	basal 2cm	0.22	76	68	2.289	2.888	14.8	0.783	$135.9^{+7.6}_{-7.2}$	$128.8^{+8.5}_{-8.1}$
	77027	as 77023	6cm long loose stalag.	-1	basal 3cm	0.41	46	65	1.752	2.332	39	0.935	$204.8^{+13.2}_{-12.0}$	
	77029	Grande Salle	7cm long stalag. cemented on block, in growth position (?)	-1	top 3cm	0.07	31	44	1.914	2.218	5.9	0.650	$102.5^{+7.6}_{-7.1}$	$92.5^{+13.5}_{-12.8}$
	77030	as 77029	5cm long stalag., cemented to fallen block, not <u>in situ</u>	-1	top 1cm	0.08	62	29	1.981	2.506	37	0.826	$152.8^{+20.8}_{-18.0}$	
	77040	Salle des Ours in breakdown	12.5cm long loose stalag.	-1	basal 2cm	0.32	81	75	2.490	3.146	65	0.766	$129.9^{+6.2}_{-5.9}$	
				-2	top 3cm	0.12	55	38	2.215	2.776	42	0.779	$135.5^{+9.6}_{-8.9}$	

d) Location, description and age data for speleothem from other areas

Cave Name & Location	Speleo-them Number	Location	Speleothem Description	Analysis No.	Analysis Location	U (ppm)	Yields (%) U	Yields (%) Th	$\frac{^{234}U}{^{238}U}$	$(\frac{^{234}U}{^{238}U})_o$	$\frac{^{230}Th}{^{232}Th}$	$\frac{^{230}Th}{^{234}U}$	AGE (Ka) ± 1σ	Corrected Age ± 1σ
Castleguard Cave, Banff National Park, Alta B.C.	77032	On mud at base of 2nd pitch	∿ 15cm long loose stalag, dense white-yellow calcite.	-1	basal 1cm	2.62	35	29	1.401	-	202	1.080	> 350	
				-2	top 2cm	2.51	71	63	1.362	1.788	274	0.995	$277.8^{+26.1}_{-21.6}$	
Gargantua Cave, Ptolemy Plateau, Crows Nest Alta.-B.C.	72025	Interprovincial Way	15cm piece of large loose stalactite, previously dated by R.S.Harmon.	-5	central core c.f. Harmon analysis	2.91	35	63	1.057	-	77	1.007	> 350	
Norman Bone Cave W.Va.	NBL	In stream near Half-Way Room	49cm long loose stalag. White calcite with some re-solution holes.	-B1	top 5cm	3.40	40	51	1.971	2.260	49	0.613	93.5±4.0	
				-A1	basal 5cm	5.60	24	17	1.917	2.281	23	0.723	121.3±7.7	
	NBS	as NBL	24cm long loose stalag., contains re-solution holes and detrital layers.	-A	top 1cm	0.80	19	43	1.705	2.307	68	0.961	221.4±14.4	
				-B	basal 3cm	0.80	11	24	1.887	-	69	1.140	> 350	leached?
Canadian Hole W.Va.	78042	On dried mud in roof tube of Neasy Strole streamway.	Short stalagmite showing much surface re-solution, clear amber calcite.	-1	composite piece of f/st base.	3.33	41	14	1.712	2.101	> 1000	0.822	$155.3^{+9.0}_{-8.4}$	
Grotte Valerie Nahanni N.W.T.	75037	Buried in lacustrine sediment	brown laminated stalactite boss	-1	outer (=younger) 1cm	27.8	44	37	0.950	-	200	0.961	> 350	
McFails Cave, N.Y.	75032	*In situ* on f/st covered by mud in streamway.	13cm long stalag., clear yellow calcite.	-1	top 1cm	2.23	71	51	2.030	2.139	233	0.289	36.0 ± 1.0	
	75034	*In situ* on mud and gravels 2m above stream	29cm long stalag. , clear yellow calcite in upper part, lower part contains detritus.	-1	top 3cm	4.22	48	57	3.612	3.672	93	0.073	8.2 ± 0.2	
	MCFA 4	Loose on mud bank.	flowstone collected and dated by C.J.Yonge	-	a piece	2.66	36	42	2.673	2.891	38	0.343	43.6 ± 1.2	
Warm Mineral Spring, Fla.	78010	At 15m depth in springs	Massive f/st-stalactite, porous and tufa-like.	-1	a piece	3.47	58	31	0.992	0.992	31	0.110	12.6 ± 0.3	
				-2	a piece	1.91	52	19	1.006	1.006	5.9	0.124	14.4 ± 0.6	10.9±1.1
South Norway	78006	overlying clay breccia	thin f/st veneer	-1	several pieces	0.30	37	77	1.279	1.281	2.5	0.058	6.5 ± 0.6	2.6±1.1
				-2	" "	0.28	28	12	1.207	1.211	0.9	0.069	7.8 ± 1.6	-5.2±4.1
	78007	Buried in gravel	7cm thick f/st, white-yellow	-1	basal 2cm	0.11	43	37	1.114	1.180	9.4	0.791	$162.0^{+20.0}_{-17.0}$	$148.2^{+23.3}_{-20.4}$
Wind Cave South Dakota	76020	-	1cm thick pool encrustation	-1	1cm thickness	3.57	56	5	1.568	-	33	1.099	> 350	